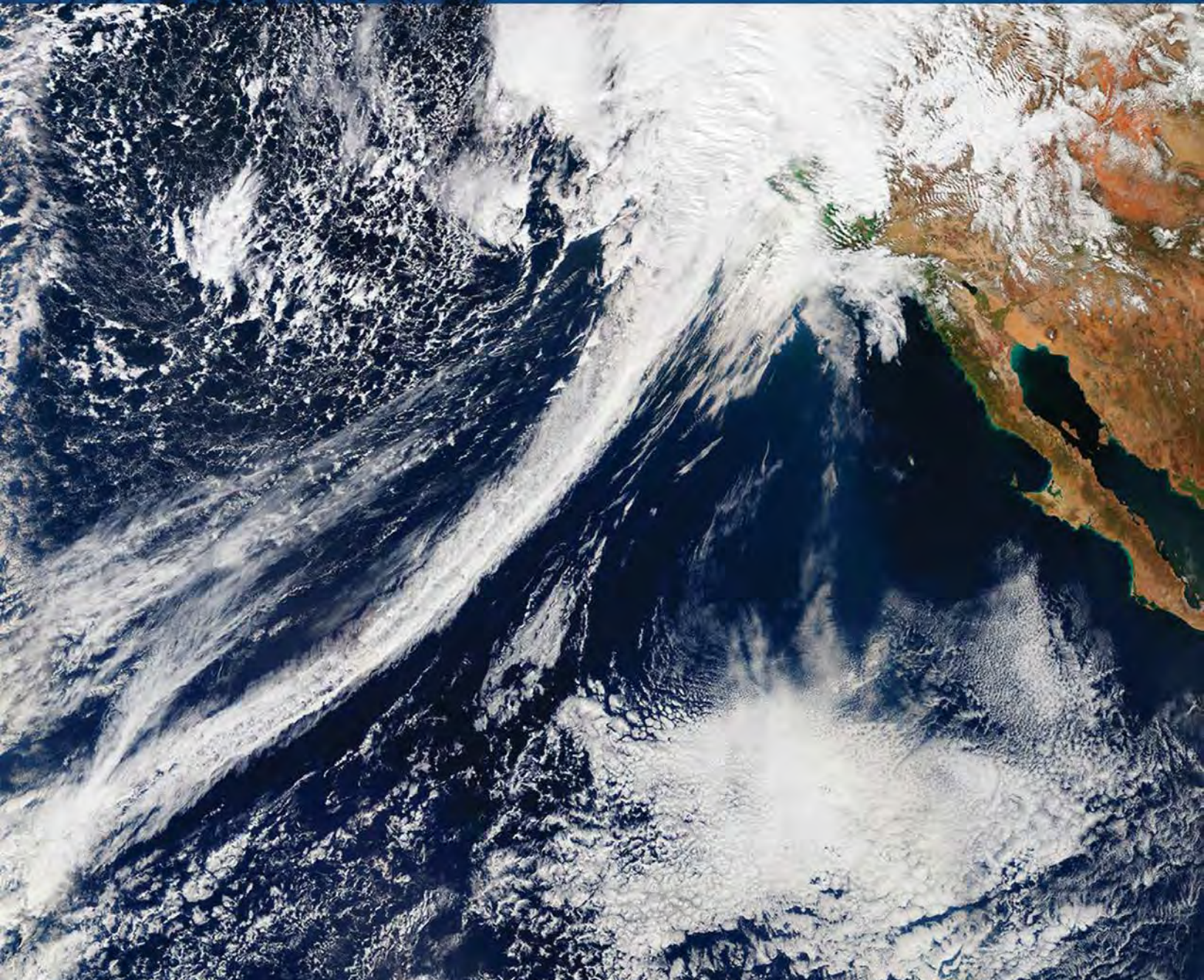




U.S. Global Change
Research Program

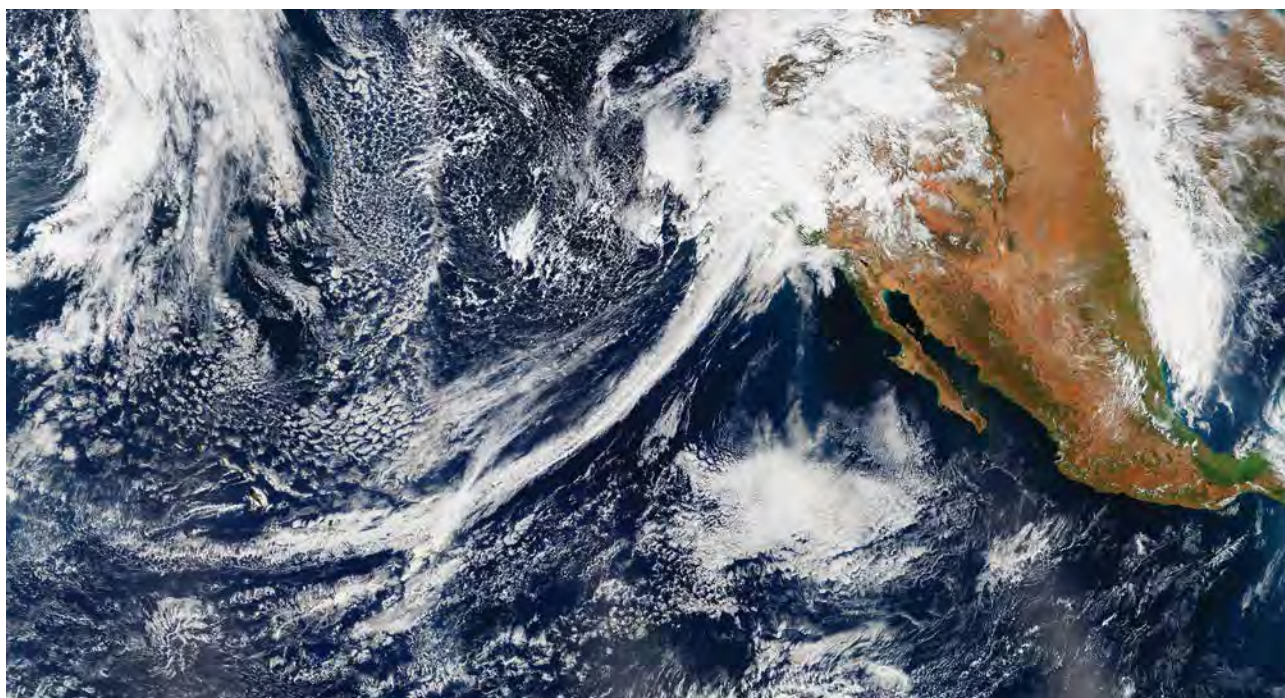
CLIMATE SCIENCE SPECIAL REPORT



Fourth National Climate Assessment | Volume I

CLIMATE SCIENCE

SPECIAL REPORT



Fourth National Climate Assessment | Volume I



U.S. Global Change
Research Program

Available on-line at: <science2017.globalchange.gov>

This document responds to requirements of Section 106 of the U.S. Global Change Research Act of 1990 (P.L. 101-606, <<http://www.globalchange.gov/about/legal-mandate>>). It does not express any regulatory policies of the United States or any of its agencies, or make any findings of fact that could serve as predicates of regulatory action. Agencies must comply with required statutory and regulatory processes before they could rely on any statements in the document or by the USGCRP as basis for regulatory action.

This document was prepared in compliance with Section 515 of the Treasury and General Government Appropriations Act for Fiscal Year 2001 (P.L. 106-554) and information quality guidelines issued by the Department of Commerce / National Oceanic and Atmospheric Administration pursuant to Section 515 (<http://www.cio.noaa.gov/services_programs/info_quality.html>). For purposes of compliance with Section 515, this document is deemed a “highly influential scientific assessment” (HISA). The report graphics follow the ISO 19115 standard which includes the necessary information to achieve reproducibility.

In all cases, permissions were secured by the U.S. Government to use and/or adapt copyrighted material contained in this document. High-resolution art is available at science2017.globalchange.gov/, with accompanying captions providing source and credit information.

First published 2017

Recommended Citation for Report

USGCRP, 2017: *Climate Science Special Report: Fourth National Climate Assessment, Volume I* [Wuebbles, D.J., D.W. Fahey, K.A. Hibbard, D.J. Dokken, B.C. Stewart, and T.K. Maycock (eds.)]. U.S. Global Change Research Program, Washington, DC, USA, 470 pp., doi: 10.7930/J0J964J6.

Image Credit

Front Cover: Atmospheric rivers are relatively long, narrow regions in the atmosphere – like rivers in the sky – that transport most of the water vapor outside of the tropics. When an atmospheric river makes landfall, extreme precipitation and flooding can often result. The cover features a natural-color image of conditions over the northeastern Pacific on 20 February 2017, helping California and the American West emerge from a 5-year drought in stunning fashion. Some parts of California received nearly twice as much rain in a single deluge as normally falls in the preceding 5 months (October–February). The visualization was generated by Jesse Allen (NASA Earth Observatory) using data from the Visible Infrared Imaging Radiometer Suite (VIIRS) on the Suomi National Polar-orbiting Partnership (NPP) satellite.

Chapter Banners: Special thanks to the NASA Earth Observatory team for the non-captioned data products incorporated into chapter titles and web banners throughout the Climate Science Special Report.



CSSR Writing Team

Coordinating Lead Authors

Donald J. Wuebbles, National Science Foundation and
U.S. Global Change Research Program – University
of Illinois

David W. Fahey, NOAA Earth System Research
Laboratory

Kathy A. Hibbard, NASA Headquarters

Lead Authors

Jeff R. Arnold, U.S. Army Corps of Engineers

Benjamin DeAngelo, NOAA Climate Program Office

Sarah Doherty, University of Washington

David R. Easterling, NOAA National Centers for
Environmental Information

James Edmonds, Pacific Northwest National Laboratory

Timothy Hall, NASA Goddard Institute for Space Studies

Katharine Hayhoe, Texas Tech University

Forrest M. Hoffman, Oak Ridge National Laboratory

Radley Horton, Columbia University

Deborah Huntzinger, Northern Arizona University

Libby Jewett, NOAA Ocean Acidification Program

Thomas Knutson, NOAA Geophysical Fluid Dynamics
Lab

Robert E. Kopp, Rutgers University

James P. Kossin, NOAA National Centers for
Environmental Information

Kenneth E. Kunkel, North Carolina State University

Allegra N. LeGrande, NASA Goddard Institute for Space Studies

L. Ruby Leung, Pacific Northwest National Laboratory

Wieslaw Maslowski, Naval Postgraduate School

Carl Mears, Remote Sensing Systems

Judith Perlwitz, NOAA Earth System Research Laboratory

Anastasia Romanou, Columbia University

Benjamin M. Sanderson, National Center for Atmospheric
Research

William V. Sweet, NOAA National Ocean Service

Patrick C. Taylor, NASA Langley Research Center

Robert J. Trapp, University of Illinois at Urbana-Champaign

Russell S. Vose, NOAA National Centers for Environmental
Information

Duane E. Waliser, NASA Jet Propulsion Laboratory

Michael F. Wehner, Lawrence Berkeley National Laboratory

Tristram O. West, DOE Office of Science

Review Editors

Linda O. Mearns, National Center for Atmospheric
Research

Ross J. Salawitch, University of Maryland

Christopher P. Weaver, USEPA

Contributing Authors

Richard Alley, Pennsylvania State University

C. Taylor Armstrong, NOAA Ocean Acidification
Program

John Bruno, University of North Carolina

Shallin Busch, NOAA Ocean Acidification Program

Sarah Champion, North Carolina State University

Imke Durre, NOAA National Centers for Environmental
Information

Dwight Gledhill, NOAA Ocean Acidification Program

Justin Goldstein, U.S. Global Change Research Program
– ICF

Boyin Huang, NOAA National Centers for
Environmental Information

Hari Krishnan, Lawrence Berkeley National Laboratory

Lisa Levin, University of California – San Diego

Frank Muller-Karger, University of South Florida

Alan Rhoades, University of California – Davis

Laura Stevens, North Carolina State University

Liqiang Sun, North Carolina State University

Eugene Takle, Iowa State University

Paul Ullrich, University of California – Davis

Eugene Wahl, NOAA National Centers for Environmental
Information

John Walsh, University of Alaska – Fairbanks

Volume Editors

David J. Dokken, U.S. Global Change Research Program
– ICF

David W. Fahey, National Oceanic and Atmospheric
Administration

Kathy A. Hibbard, National Aeronautics and Space
Administration

Thomas K. Maycock, Cooperative Institute for Climate and
Satellites – North Carolina

Brooke C. Stewart, Cooperative Institute for Climate and
Satellites – North Carolina

Donald J. Wuebbles, National Science Foundation and U.S.
Global Change Research Program – University of Illinois

Science Steering Committee

Benjamin DeAngelo, National Oceanic and Atmospheric
Administration

David W. Fahey, National Oceanic and Atmospheric
Administration

Kathy A. Hibbard, National Aeronautics and Space
Administration

Wayne Higgins, Department of Commerce

Jack Kaye, National Aeronautics and Space Administration

Dorothy Koch, Department of Energy

Russell S. Vose, National Oceanic and Atmospheric
Administration

Donald J. Wuebbles, National Science Foundation and U.S.
Global Change Research Program – University of Illinois

Subcommittee on Global Change Research

Ann Bartuska, Chair, Department of Agriculture

Virginia Burkett, Co-Chair, Department of the Interior

Gerald Geernaert, Vice-Chair, Department of Energy

Michael Kuperberg, Executive Director, U.S. Global
Change Research Program

John Balbus, Department of Health and Human Services

Bill Breed, U.S. Agency for International Development

Pierre Comizzoli, Smithsonian Institution

Wayne Higgins, Department of Commerce

Scott Harper, Department of Defense (Acting)

William Hohenstein, Department of Agriculture

Jack Kaye, National Aeronautics and Space
Administration

Dorothy Koch, Department of Energy

Andrew Miller, U.S. Environmental Protection Agency

David Reidmiller, U.S. Global Change Research Program

Trigg Talley, Department of State

Michael Van Woert, National Science Foundation

Liaison to the Executive Office of the President

Kimberly Miller, Office of Management and Budget

Report Production Team

Bradley Akamine, U.S. Global Change Research Program
– ICF

Jim Biard, Cooperative Institute for Climate and Satellites
– North Carolina

Andrew Buddenberg, Cooperative Institute for Climate
and Satellites – North Carolina

Sarah Champion, Cooperative Institute for Climate and
Satellites – North Carolina

David J. Dokken, U.S. Global Change Research Program
– ICF

Amrutha Elamparathy, U.S. Global Change Research
Program – Straughan Environmental, Inc.

Jennifer Fulford, TeleSolv Consulting

Jessica Griffin, Cooperative Institute for Climate and
Satellites – North Carolina

Kate Johnson, ERT Inc.

Angel Li, Cooperative Institute for Climate and Satellites
– North Carolina

Liz Love-Brotak, NOAA National Centers for
Environmental Information

Thomas K. Maycock, Cooperative Institute for Climate and
Satellites – North Carolina

Deborah Misch, TeleSolv Consulting

Katie Reeves, U.S. Global Change Research Program – ICF

Deborah Riddle, NOAA National Centers for Environmental
Information

Reid Sherman, U.S. Global Change Research Program –
Straughan Environmental, Inc.

Mara Sprain, LAC Group

Laura Stevens, Cooperative Institute for Climate and Satellites –
North Carolina

Brooke C. Stewart, Cooperative Institute for Climate and
Satellites – North Carolina

Liqiang Sun, Cooperative Institute for Climate and Satellites –
North Carolina

Kathryn Tipton, U.S. Global Change Research Program – ICF

Sara Veasey, NOAA National Centers for Environmental
Information

Administrative Lead Agency

Department of Commerce / National Oceanic and Atmospheric Administration

U.S. GLOBAL CHANGE RESEARCH PROGRAM

CLIMATE SCIENCE SPECIAL REPORT (CSSR)

TABLE OF CONTENTS

Front Matter

About This Report	1
Guide to the Report	3
Executive Summary	12

Chapters

1. Our Globally Changing Climate.....	35
2. Physical Drivers of Climate Change	73
3. Detection and Attribution of Climate Change.....	114
4. Climate Models, Scenarios, and Projections	133
5. Large-Scale Circulation and Climate Variability	161
6. Temperature Changes in the United States	185
7. Precipitation Change in the United States	207
8. Droughts, Floods, and Wildfires.....	231
9. Extreme Storms.....	257
10. Changes in Land Cover and Terrestrial Biogeochemistry.....	277
11. Arctic Changes and their Effects on Alaska and the Rest of the United States.....	303
12. Sea Level Rise.....	333
13. Ocean Acidification and Other Ocean Changes	364
14. Perspectives on Climate Change Mitigation.....	393
15. Potential Surprises: Compound Extremes and Tipping Elements.....	411

Appendices

A. Observational Datasets Used in Climate Studies	430
B. Model Weighting Strategy	436
C. Detection and Attribution Methodologies Overview.....	443
D. Acronyms and Units	452
E. Glossary	460



About This Report

As a key part of the Fourth National Climate Assessment (NCA4), the U.S. Global Change Research Program (USGCRP) oversaw the production of this stand-alone report of the state of science relating to climate change and its physical impacts.

The Climate Science Special Report (CSSR) is designed to be an authoritative assessment of the science of climate change, with a focus on the United States, to serve as the foundation for efforts to assess climate-related risks and inform decision-making about responses. In accordance with this purpose, it does not include an assessment of literature on climate change mitigation, adaptation, economic valuation, or societal responses, nor does it include policy recommendations.

As Volume I of NCA4, CSSR serves several purposes, including providing 1) an updated detailed analysis of the findings of how climate change is affecting weather and climate across the United States; 2) an executive summary and other CSSR materials that provide the basis for the discussion of climate science found in the second volume of the NCA4; and 3) foundational information and projections for climate change, including extremes, to improve “end-to-end” consistency in sectoral, regional, and resilience analyses within the second volume. CSSR integrates and evaluates the findings on climate science and discusses the uncertainties associated with these findings. It analyzes current trends in climate change, both human-induced and natural, and projects major trends to the end of this century. As an assessment and analysis of the science, this report provides important input to the development of other parts of NCA4, and their primary focus on the human welfare, societal, economic, and environmental elements of climate change.

Much of this report is written at a level more appropriate for a scientific audience, though the Executive Summary is intended to be accessible to a broader audience.

Report Development, Review, and Approval Process

The National Oceanic and Atmospheric Administration (NOAA) serves as the administrative lead agency for the preparation of NCA4. The CSSR Federal Science Steering Committee (SSC)¹ has representatives from three agencies (NOAA, the National Aeronautics and Space Administration [NASA], and the Department of Energy [DOE]); USGCRP;² and three Coordinating Lead Authors, all of whom were Federal employees during the development of this report. Following a public notice for author nominations in March 2016, the SSC selected the writing team, consisting of scientists representing Federal agencies, national laboratories, universities, and the private sector. Contributing Authors were requested to provide special input to the Lead Authors to help with specific issues of the assessment.

The first Lead Author Meeting was held in Washington, DC, in April 2016, to refine the outline contained in the SSC-endorsed prospectus and to make writing assignments. Over the course of 18 months before final

¹ The CSSR SSC was charged with overseeing the development and production of the report. SSC membership was open to all USGCRP agencies.

² The USGCRP is made up of 13 Federal departments and agencies that carry out research and support the Nation’s response to global change. The USGCRP is overseen by the Subcommittee on Global Change Research (SGCR) of the National Science and Technology Council’s Committee on Environment, Natural Resources, and Sustainability (CENRS), which in turn is overseen by the White House Office of Science and Technology Policy (OSTP). The agencies within USGCRP are the Department of Agriculture, the Department of Commerce (NOAA), the Department of Defense, the Department of Energy, the Department of Health and Human Services, the Department of the Interior, the Department of State, the Department of Transportation, the Environmental Protection Agency, the National Aeronautics and Space Administration, the National Science Foundation, the Smithsonian Institution, and the U.S. Agency for International Development.



publication, seven CSSR drafts were generated, with each successive iteration – from zero- to sixth-order drafts – undergoing additional expert review, as follows: (i) by the writing team itself (13–20 June 2016); (ii) by the SSC convened to oversee report development (29 July–18 August 2016); (iii) by the technical agency representatives (and designees) comprising the Subcommittee on Global Change Research (SGCR, 3–14 October 2016); (iv) by the SSC and technical liaisons again (5–13 December 2016); (v) by the general public during the Public Comment Period (15 December 2016–3 February 2017) and an expert panel convened by the National Academies of Sciences, Engineering, and Medicine (NAS, 21 December 2016–13 March 2017);³ and (vi) by the SGCR again (3–24 May 2017) to confirm the Review Editor conclusions that all public and NAS comments were adequately addressed. In October 2016, an 11-member core writing team was tasked with capturing the most important CSSR key findings and generating an Executive Summary. Two additional Lead Authors Meetings were held after major review milestones to facilitate chapter team deliberations and consistency: 2–4 November 2016 (Boulder, CO) and 21–22 April 2017 (Asheville, NC). Literature cutoff dates were enforced, with all cited material published by June 2017. The fifth-order draft including the Executive Summary was compiled in June 2017, and submitted to the Office of Science and Technology Policy (OSTP). OSTP is responsible for the Federal clearance process prior to final report production and public release. This published report represents the final (sixth-order) draft.

³ Author responses to comments submitted as part of the Public Comment Period and a USGCRP response to the review conducted by NAS can be found on <science2017.globalchange.gov/downloads>.

The Sustained National Climate Assessment

The Climate Science Special Report has been developed as part of the USGCRP's sustained National Climate Assessment (NCA) process. This process facilitates continuous and transparent participation of scientists and stakeholders across regions and sectors, enabling new information and insights to be assessed as they emerge. The Climate Science Special Report is aimed at a comprehensive assessment of the science underlying the changes occurring in Earth's climate system, with a special focus on the United States.

Sources Used in this Report

The findings in this report are based on a large body of scientific, peer-reviewed research, as well as a number of other publicly available sources, including well-established and carefully evaluated observational and modeling datasets. The team of authors carefully reviewed these sources to ensure a reliable assessment of the state of scientific understanding. Each source of information was determined to meet the four parts of the quality assurance guidance provided to authors (following the approach from NCA3): 1) utility, 2) transparency and traceability, 3) objectivity, and 4) integrity and security. Report authors assessed and synthesized information from peer-reviewed journal articles, technical reports produced by Federal agencies, scientific assessments (such as the rigorously-reviewed international assessments from the Intergovernmental Panel on Climate Change,¹ reports of the National Academy of Sciences and its associated National Research Council, and various regional climate impact assessments, conference proceedings, and government statistics (such as population census and energy usage).



Guide to the Report

The following subsections describe the format of the Climate Science Special Report and the overall structure and features of the chapters.

Executive Summary

The Executive Summary describes the major findings from the Climate Science Special Report. It summarizes the overall findings and includes some key figures and additional bullet points covering overarching and especially noteworthy conclusions. The Executive Summary and the majority of the Key Findings are written to be accessible to a wide range of audiences.

Chapters

Key Findings and Traceable Accounts

Each topical chapter includes Key Findings, which are based on the authors' expert judgment of the synthesis of the assessed literature. Each Key Finding includes a confidence statement and, as appropriate, framing of key scientific uncertainties, so as to better support assessment of climate-related risks. (See "Documenting Uncertainty" below).

Each Key Finding is also accompanied by a Traceable Account that documents the supporting evidence, process, and rationale the authors used in reaching these conclusions and provides additional information on sources of uncertainty through confidence and likelihood statements. The Traceable Accounts can be found at the end of each chapter.

Regional Analyses

Throughout the report, the regional analyses of climate changes for the United States are structured on 10 different regions as shown in Figure 1. There are differences from the regions used in the Third National Climate Assessment²: 1) the Great Plains are split into

the Northern Great Plains and Southern Great Plains; and 2) The U.S. islands in the Caribbean are analyzed as a separate region apart from the Southeast.

Chapter Text

Each chapter assesses the state of the science for a particular aspect of the changing climate. The first chapter gives a summary of the global changes occurring in the Earth's climate system. This is followed in Chapter 2 by a summary of the scientific basis for climate change. Chapter 3 gives an overview of the processes used in the detection and attribution of climate change and associated studies using those techniques. Chapter 4 then discusses the scenarios for greenhouse gases and particles and the modeling tools used to study future projections. Chapters 5 through 9 primarily focus on physical changes in climate occurring in the United States, including those projected to occur in the future. Chapter 10 provides a focus on land use change and associated feedbacks on climate. Chapter 11 addresses changes in Alaska in the Arctic, and how the latter affects the United States. Chapters 12 and 13 discuss key issues connected with sea level rise and ocean changes, including ocean acidification, and their potential effects on the United States. Finally, Chapters 14 and 15 discuss some important perspectives on how mitigation activities could affect future changes in climate and provide perspectives on what surprises could be in store for the changing climate beyond the analyses already covered in the rest of the assessment.

Throughout the report, results are presented in United States customary units (e.g., degrees Fahrenheit) as well as in the International System of Units (e.g., degrees Celsius).

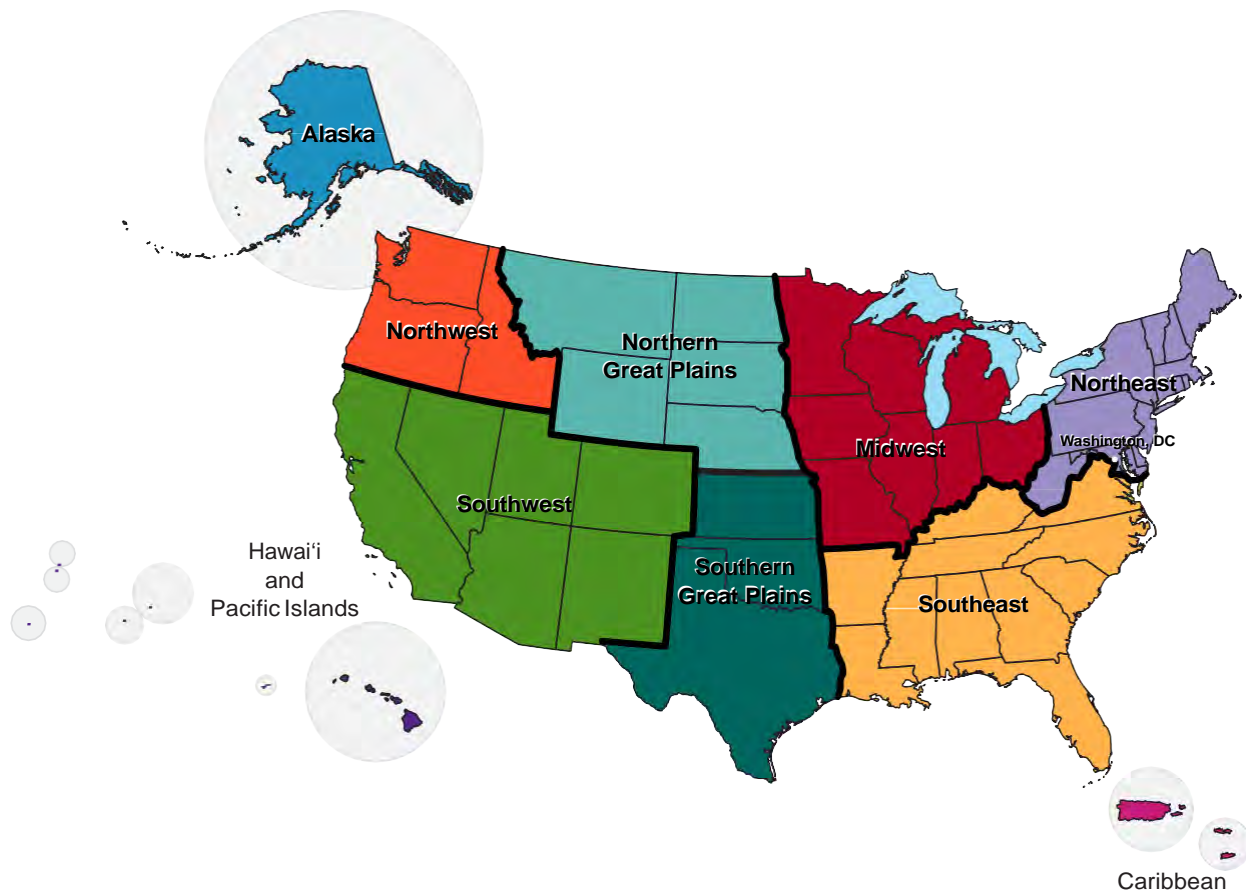


Figure 1. Map of the ten regions of the United States used throughout the Climate Science Special Report. Regions are similar to that used in the Third National Climate Assessment except that 1) the Great Plains are split into the Northern Great Plains and Southern Great Plains, and 2) the Caribbean islands have been split from the Southeast region. (Figure source: adapted from Melillo et al. 2014²).

Reference Time Periods for Graphics

There are many different types of graphics in the Climate Science Special Report. Some of the graphs in this report illustrate historical changes and future trends in climate compared to some reference period, with the choice of this period determined by the purpose of the graph and the availability of data. The scientific community does not have a standard set of reference time periods for assessing the science, and these tend to be chosen differently for different reports and assessments. Some graphics are pulled from other studies using different time periods.

Where graphs were generated for this report (those not based largely on prior publications), they are mostly based on one of two reference

periods. The 1901–1960 reference period is particularly used for graphs that illustrate past changes in climate conditions, whether in observations or in model simulations. This 60-year time period was also used for analyses in the Third National Climate Assessment (NCA3²). The beginning date was chosen because earlier historical observations are generally considered to be less reliable. While a 30-year base period is often used for climate analyses, the choice of 1960 as the ending date of this period was based on past changes in human influences on the climate system. Human-induced forcing exhibited a slow rise during the early part of the last century but then accelerated after 1960. Thus, these graphs highlight observed changes in climate during the period of rapid increase in human-caused



forcing and also reveal how well climate models simulate these observed changes.

Thus, a number of the graphs in the report are able to highlight the recent, more rapid changes relative to the early part of the century (the reference period) and also reveal how well the climate models simulate observed changes. In this report, this time period is used as the base period in most maps of observed trends and all time-varying, area-weighted averages that show both observed and projected quantities. For the observed trends, 1986–2015 is generally chosen as the most recent 30-year period (2016 data was not fully available until late in our development of the assessment).

The other commonly used reference period in this report is 1976–2005. The choice of a 30-year period is chosen to account for natural variations and to have a reasonable sampling in order to estimate likelihoods of trends in extremes. This period is consistent with the World Meteorological Organization’s recommendation for climate statistics. This period is used for graphs that illustrate projected changes simulated by climate models. The purpose of these graphs is to show projected changes compared to a period that allows stakeholders and decision makers to base fundamental planning and decisions on average and extreme climate conditions in a non-stationary climate; thus, a recent available 30-year period was chosen.³ The year 2005 was chosen as an end date because the historical period simulated by the models used in this assessment ends in that year.

For future projections, 30-year periods are again used for consistency. Projections are centered around 2030, 2050, and 2085 with an interval of plus and minus 15 years (for example, results for 2030 cover the period 2015–2045); Most model runs used here only project out to 2100 for future scenarios, but where

possible, results beyond 2100 are shown. Note that these time periods are different than those used in some of the graphics in NCA3. There are also exceptions for graphics that are based on existing publications.

For global results that may be dependent on findings from other assessments (such as those produced by the Intergovernmental Panel on Climate Change, or IPCC), and for other graphics that depend on specific published work, the use of other time periods was also allowed, but an attempt was made to keep them as similar to the selected periods as possible. For example, in the discussion of radiative forcing, the report uses the standard analyses from IPCC for the industrial era (1750 to 2011) (following IPCC 2013a¹). And, of course, the paleoclimatic discussion of past climates goes back much further in time.

Model Results: Past Trends and Projected Futures

The NCA3 included global modeling results from both the CMIP3 (Coupled Model Intercomparison Project, 3rd phase) models used in the 2007 international assessment⁴ and the CMIP5 (Coupled Model Intercomparison Project, Phase 5) models used in the more recent international assessment.¹ Here, the primary resource for this assessment is the more recent global model results and associated downscaled products from CMIP5. The CMIP5 models and the associated downscaled products are discussed in Chapter 4: Projections.

Treatment of Uncertainties: Likelihoods, Confidence, and Risk Framing

Throughout this report’s assessment of the scientific understanding of climate change, the authors have assessed to the fullest extent possible the state-of-the-art understanding of the science resulting from the information in the scientific literature to arrive at a series of findings referred to as Key Findings. The approach used to represent the extent of un-



derstanding represented in the Key Findings is done through two metrics:

- **Confidence** in the validity of a finding based on the type, amount, quality, strength, and consistency of evidence (such as mechanistic understanding, theory, data, models, and expert judgment); the skill, range, and consistency of model projections; and the degree of agreement within the body of literature.
- **Likelihood**, or probability of an effect or impact occurring, is based on measures of uncertainty expressed probabilistically (based on the degree of understanding or knowledge, e.g., resulting from evaluating statistical analyses of observations or model results or on expert judgment).

The terminology used in the report associated with these metrics is shown in Figure 2. This language is based on that used in NCA3,² the IPCC’s Fifth Assessment Report,¹ and most recently the USGCRP Climate and Health assessment.⁵ Wherever used, the confidence and likelihood statements are italicized.

Assessments of confidence in the Key Findings are based on the expert judgment of the author team. Authors provide supporting evidence for each of the chapter’s Key Findings in the Traceable Accounts. Confidence is expressed qualitatively and ranges from low confidence (inconclusive evidence or disagreement among experts) to very high confidence (strong evidence and high consensus) (see Figure 2). Confidence should not be interpreted probabilistically, as it is distinct from statistical likelihood. See chapter 1 in IPCC¹ for further discussion of this terminology.

In this report, likelihood is the chance of occurrence of an effect or impact based on measures of uncertainty expressed probabilis-

tically (based on statistical analysis of observations or model results or on expert judgment). The authors used expert judgment based on the synthesis of the literature assessed to arrive at an estimation of the likelihood that a particular observed effect was related to human contributions to climate change or that a particular impact will occur within the range of possible outcomes. Model uncertainty is an important contributor to uncertainty in climate projections, and includes, but is not restricted to, the uncertainties introduced by errors in the model’s representation of the physical and bio-geochemical processes affecting the climate system as well as in the model’s response to external forcing.¹

Where it is considered justified to report the likelihood of particular impacts within the range of possible outcomes, this report takes a plain-language approach to expressing the expert judgment of the chapter team, based on the best available evidence. For example, an outcome termed “likely” has at least a 66% chance of occurring (a likelihood greater than about 2 of 3 chances); an outcome termed “very likely,” at least a 90% chance (more than 9 out of 10 chances). See Figure 2 for a complete list of the likelihood terminology used in this report.

Traceable Accounts for each Key Finding 1) document the process and rationale the authors used in reaching the conclusions in their Key Finding, 2) provide additional information to readers about the quality of the information used, 3) allow traceability to resources and data, and 4) describe the level of likelihood and confidence in the Key Finding. Thus, the Traceable Accounts represent a synthesis of the chapter author team’s judgment of the validity of findings, as determined through evaluation of evidence and agreement in the scientific literature. The Traceable Accounts also identify areas where data are



Confidence Level	Likelihood
Very High	Virtually Certain
Strong evidence (established theory, multiple sources, consistent results, well documented and accepted methods, etc.), high consensus	99%–100%
High	Extremely Likely
Moderate evidence (several sources, some consistency, methods vary and/or documentation limited, etc.), medium consensus	95%–100%
Medium	Very Likely
Suggestive evidence (a few sources, limited consistency, models incomplete, methods emerging, etc.), competing schools of thought	90%–100%
Low	Likely
Inconclusive evidence (limited sources, extrapolations, inconsistent findings, poor documentation and/or methods not tested, etc.), disagreement or lack of opinions among experts	66%–100%
	About as Likely as Not
	33%–66%
	Unlikely
	0%–33%
	Very Unlikely
	0%–10%
	Extremely Unlikely
	0%–5%
	Exceptionally Unlikely
	0%–1%

Figure 2. Confidence levels and likelihood statements used in the report. (Figure source: adapted from USGCRP 2016⁵ and IPCC 2013¹; likelihoods use the broader range from the IPCC assessment). As an example, regarding “likely,” a 66%–100% probability can be interpreted as a likelihood of greater than 2 out of 3 chances for the statement to be certain or true. Not all likelihoods are used in the report.

limited or emerging. Each Traceable Account includes 1) a description of the evidence base, 2) major uncertainties, and 3) an assessment of confidence based on evidence.

All Key Findings include a description of confidence. Where it is considered scientifically justified to report the likelihood of particular impacts within the range of possible outcomes, Key Findings also include a likelihood designation.

Confidence and likelihood levels are based on the expert judgment of the author team. They determined the appropriate level of confidence or likelihood by assessing the available literature, determining the quality and quantity of available evidence, and evaluating the level of agreement across different studies. Often, the underlying studies provided their own estimates of uncertainty and confidence intervals. When available, these confidence intervals were assessed by the authors in



making their own expert judgments. For specific descriptions of the process by which the author team came to agreement on the Key Findings and the assessment of confidence and likelihood, see the Traceable Accounts in each chapter.

In addition to the use of systematic language to convey confidence and likelihood information, this report attempts to highlight aspects of the science that are most relevant for supporting other parts of the Fourth National Climate Assessment and its analyses of key societal risks posed by climate change. This includes attention to trends and changes in the tails of the probability distribution of future climate change and its proximate impacts (for example, on sea level or temperature and precipitation extremes) and on defining plausible bounds for the magnitude of future changes, since many key risks are disproportionately determined by plausible low-probability, high-consequence outcomes. Therefore, in addition to presenting the expert judgment on the “most likely” range of projected future climate outcomes, where appropriate, this report also provides information on the outcomes

lying outside this range, which nevertheless cannot be ruled out and may therefore be relevant for assessing overall risk. In some cases, this involves an evaluation of the full range of information contained in the ensemble of climate models used for this report, and in other cases this involves the consideration of additional lines of scientific evidence beyond the models.

Complementing this use of risk-focused language and presentation around specific scientific findings in the report, Chapter 15: Potential Surprises provides an overview of potential low probability/high consequence “surprises” resulting from climate change. This includes its analyses of thresholds, also called tipping points, in the climate system and the compounding effects of multiple, interacting climate change impacts whose consequences may be much greater than the sum of the individual impacts. Chapter 15 also highlights critical knowledge gaps that determine the degree to which such high-risk tails and bounding scenarios can be precisely defined, including missing processes and feedbacks.



REFERENCES

1. IPCC, 2013a: *Climate Change 2013: The Physical Science Basis. Contribution of Working Group I to the Fifth Assessment Report of the Intergovernmental Panel on Climate Change*. Cambridge University Press, Cambridge, UK and New York, NY, 1535 pp. <http://www.climatechange2013.org/report/>
2. Melillo, J.M., T.C. Richmond, and G.W. Yohe, eds., 2014a: *Climate Change Impacts in the United States: The Third National Climate Assessment*. U.S. Global Change Research Program: Washington, D.C., 841 pp. <http://dx.doi.org/10.7930/J0Z31WJ2>
3. Arguez, A. and R.S. Vose, 2011: The definition of the standard WMO climate normal: The key to deriving alternative climate normals. *Bulletin of the American Meteorological Society*, **92**, 699-704. <http://dx.doi.org/10.1175/2010BAMS2955.1>
4. IPCC, 2007: *Climate Change 2007: The Physical Science Basis. Contribution of Working Group I to the Fourth Assessment Report of the Intergovernmental Panel on Climate Change*. Solomon, S., D. Qin, M. Manning, Z. Chen, M. Marquis, K.B. Averyt, M. Tignor, and H.L. Miller, Eds. Cambridge University Press, Cambridge, U.K, New York, NY, USA, 996 pp. http://www.ipcc.ch/publications_and_data/publications_ipcc_fourth_assessment_report_wg1_report_the_physical_science_basis.htm
5. USGCRP, 2016: *The Impacts of Climate Change on Human Health in the United States: A Scientific Assessment*. Crimmins, A., J. Balbus, J.L. Gamble, C.B. Beard, J.E. Bell, D. Dodgen, R.J. Eisen, N. Fann, M.D. Hawkins, S.C. Herring, L. Jantarasami, D.M. Mills, S. Saha, M.C. Sarofim, J. Trtanj, and L. Ziska, Eds. U.S. Global Change Research Program, Washington, DC, 312 pp. <http://dx.doi.org/10.7930/J0R49NQX>

Highlights of the U.S. Global Change Research Program

Climate Science Special Report

The climate of the United States is strongly connected to the changing global climate. The statements below highlight past, current, and projected climate changes for the United States and the globe.

Global annually averaged surface air temperature has increased by about 1.8°F (1.0°C) over the last 115 years (1901–2016). **This period is now the warmest in the history of modern civilization.** The last few years have also seen record-breaking, climate-related weather extremes, and the last three years have been the warmest years on record for the globe. These trends are expected to continue over climate timescales.

This assessment concludes, based on extensive evidence, that it is extremely likely that **human activities, especially emissions of greenhouse gases, are the dominant cause of the observed warming since the mid-20th century.** For the warming over the last century, there is no convincing alternative explanation supported by the extent of the observational evidence.

In addition to warming, many other aspects of global climate are changing, primarily in response to human activities. **Thousands of studies conducted by researchers around the world have documented changes in surface, atmospheric, and oceanic temperatures; melting glaciers; diminishing snow cover; shrinking sea ice; rising sea levels; ocean acidification; and increasing atmospheric water vapor.**

For example, **global average sea level has risen by about 7–8 inches** since 1900, with almost half (about 3 inches) of that rise occurring since 1993. Human-caused climate change has made a substantial contribution to this rise since 1900, contributing to a rate of rise that is greater than during any preceding century in at least 2,800 years. Global sea level rise has already affected the United States; **the incidence of daily tidal flooding is accelerating in more than 25 Atlantic and Gulf Coast cities.**

Global average sea levels are expected to continue to rise—by at least several inches in the next 15 years and by 1–4 feet by 2100. A rise of as much as 8 feet by 2100 cannot be ruled out. Sea level rise will be higher than the global average on the East and Gulf Coasts of the United States.

Changes in the characteristics of extreme events are particularly important for human safety, infrastructure, agriculture, water quality and quantity, and natural ecosystems. **Heavy rainfall is increasing in intensity and frequency across the United States and globally and is expected to continue to increase.** The largest observed changes in the United States have occurred in the Northeast.

Heatwaves have become more frequent in the United States since the 1960s, while extreme cold temperatures and cold waves are less frequent. Recent record-setting hot years are projected to become common in the near future for the United States, as annual average temperatures continue to rise. Annual average temperature over the contiguous United States has increased by 1.8°F (1.0°C) for the period 1901–2016; **over the next few decades (2021–2050), annual average temperatures are expected to rise by about 2.5°F for the United States, relative to the recent past (average from 1976–2005), under all plausible future climate scenarios.**

The incidence of large forest fires in the western United States and Alaska has increased since the early 1980s and is projected to further increase in those regions as the climate changes, with profound changes to regional ecosystems.

Annual trends toward earlier spring melt and reduced snowpack are already affecting water resources in the western United States and these trends are expected to continue. Under higher scenarios, and assuming no change to current water resources management, **chronic, long-duration hydrological drought is increasingly possible before the end of this century.**

The magnitude of climate change beyond the next few decades will depend primarily on the amount of greenhouse gases (especially carbon dioxide) emitted globally. Without major reductions in emissions, the increase in annual average global temperature relative to preindustrial times could reach 9°F (5°C) or more by the end of this century. **With significant reductions in emissions, the increase in annual average global temperature could be limited to 3.6°F (2°C) or less.**

The global atmospheric carbon dioxide (CO₂) concentration has now passed 400 parts per million (ppm), a level that last occurred about 3 million years ago, when both global average temperature and sea level were significantly higher than today. Continued growth in CO₂ emissions over this century and beyond would lead to an atmospheric concentration not experienced in tens to hundreds of millions of years. There is broad consensus that the further and the faster the Earth system is pushed towards warming, the greater the risk of unanticipated changes and impacts, some of which are potentially large and irreversible.

The observed increase in carbon emissions over the past 15–20 years has been consistent with higher emissions pathways. **In 2014 and 2015, emission growth rates slowed as economic growth became less carbon-intensive.** Even if this slowing trend continues, however, it is not yet at a rate that would limit global average temperature change to well below 3.6°F (2°C) above preindustrial levels.

Recommended Citation for Chapter

Wuebbles, D.J., D.W. Fahey, K.A. Hibbard, B. DeAngelo, S. Doherty, K. Hayhoe, R. Horton, J.P. Kossin, P.C. Taylor, A.M. Waple, and C.P. Weaver, 2017: Executive summary. In: *Climate Science Special Report: Fourth National Climate Assessment, Volume I* [Wuebbles, D.J., D.W. Fahey, K.A. Hibbard, D.J. Dokken, B.C. Stewart, and T.K. Maycock (eds.)]. U.S. Global Change Research Program, Washington, DC, USA, pp. 12-34, doi: 10.7930/J0DJ5CTG.



Executive Summary

Introduction

New observations and new research have increased our understanding of past, current, and future climate change since the Third U.S. National Climate Assessment (NCA3) was published in May 2014. This Climate Science Special Report (CSSR) is designed to capture that new information and build on the existing body of science in order to summarize the current state of knowledge and provide the scientific foundation for the Fourth National Climate Assessment (NCA4).

Since NCA3, stronger evidence has emerged for continuing, rapid, human-caused warming of the global atmosphere and ocean. This report concludes that “it is *extremely likely* that human influence has been the dominant cause of the observed warming since the mid-20th century. For the warming over the last century, there is no convincing alternative explanation supported by the extent of the observational evidence.”

The last few years have also seen record-breaking, climate-related weather extremes, the three warmest years on record for the globe, and continued decline in arctic sea ice. These trends are expected to continue in the future over climate (multidecadal) timescales. Significant advances have also been made in our understanding of extreme weather events and how they relate to increasing global temperatures and associated climate changes. Since 1980, the cost of extreme events for the United States has exceeded \$1.1 trillion; therefore, better understanding of the frequency and severity of these events in the context of a changing climate is warranted.

Periodically taking stock of the current state of knowledge about climate change and putting new weather extremes, changes in sea ice, increases in ocean temperatures, and ocean acidification into context ensures that rigorous, scientifically-based information is available to inform dialogue and decisions at every level. This climate science report serves as the climate science foundation of the NCA4 and is generally intended for those who have a technical background in climate science. In this Executive Summary, gray boxes present highlights of the main report. These are followed by related points and selected figures providing more scientific details. The summary material on each topic presents the most salient points of chapter findings and therefore represents only a subset of the report’s content. For more details, the reader is referred to the individual chapters. This report discusses climate trends and findings at several scales: global, nationwide for the United States, and for ten specific U.S. regions (shown in Figure 1 in the Guide to the Report). A statement of scientific confidence also follows each point in the Executive Summary. The confidence scale is described in the Guide to the Report. At the end of the Executive Summary and in Chapter 1: Our Globally Changing Climate, there is also a summary box highlighting the most notable advances and topics since NCA3 and since the 2013 Intergovernmental Panel on Climate Change (IPCC) Fifth Assessment Report.

Global and U.S. Temperatures Continue to Rise

Long-term temperature observations are among the most consistent and widespread evidence of a warming planet. Temperature (and, above all, its local averages and extremes) affects agricultural productivity, energy use, human health, water resources, infrastructure, natural ecosystems, and many other essential aspects of society and the natural environment. Recent data add to the weight of evidence for rapid global-scale warming, the dominance of human causes, and the expected continuation of increasing temperatures, including more record-setting extremes. (Ch. 1)

Changes in Observed and Projected Global Temperature

The global, long-term, and unambiguous warming trend has continued during recent years. Since the last National Climate Assessment was published, 2014 became the warmest year on record globally; 2015 surpassed 2014 by a wide margin; and 2016 surpassed 2015. Sixteen of the warmest years on record for the globe occurred in the last 17 years (1998 was the exception). (Ch. 1; Fig. ES.1)

- Global annual average temperature (as calculated from instrumental records over both land and oceans) has increased by more than 1.2°F (0.65°C) for the period 1986–2016 relative to 1901–1960; the linear regression change over the entire period from 1901–2016 is 1.8°F (1.0°C) (*very high confidence*; Fig. ES.1). Longer-term climate records over past centuries and millennia indicate that average temperatures in recent decades over much of the world have been much higher, and have risen faster during this time period than at any time in the past 1,700 years or more, the time period for which the global distribution of surface temperatures can be reconstructed (*high confidence*). (Ch. 1)

Global Temperatures Continue to Rise

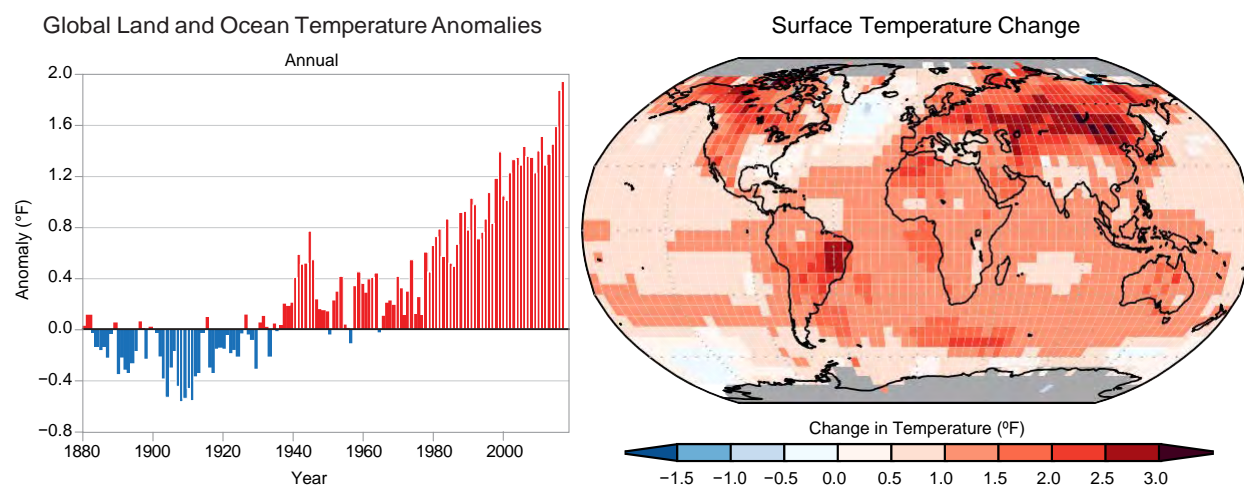


Figure ES.1: (left) Global annual average temperature has increased by more than 1.2°F (0.7°C) for the period 1986–2016 relative to 1901–1960. Red bars show temperatures that were above the 1901–1960 average, and blue bars indicate temperatures below the average. (right) Surface temperature change (in °F) for the period 1986–2016 relative to 1901–1960. Gray indicates missing data. *From Figures 1.2. and 1.3 in Chapter 1.*

- Many lines of evidence demonstrate that it is *extremely likely* that human influence has been the dominant cause of the observed warming since the mid-20th century. Over the last century, there are no convincing alternative explanations supported by the extent of the observational evidence. Solar output changes and internal natural variability can only contribute marginally to the observed changes in climate over the last century, and there is no convincing evidence for natural cycles in the observational record that could explain the observed changes in climate. (*Very high confidence*) (Ch. 1)
- The *likely* range of the human contribution to the global mean temperature increase over the period 1951–2010 is 1.1° to 1.4°F (0.6° to 0.8°C), and the central estimate of the observed warming of 1.2°F (0.65°C) lies within this range (*high confidence*). This translates to a *likely* human contribution of 92%–123% of the observed 1951–2010 change. The *likely* contributions of natural forcing and internal variability to global temperature change over that period are minor (*high confidence*). (Ch. 3; Fig. ES.2)
- Natural variability, including El Niño events and other recurring patterns of ocean–atmosphere interactions, impact temperature and precipitation, especially regionally, over timescales of months to years. The global influence of natural variability, however, is limited to a small fraction of observed climate trends over decades. (*Very high confidence*) (Ch. 1)

Human Activities Are the Primary Driver of Recent Global Temperature Rise

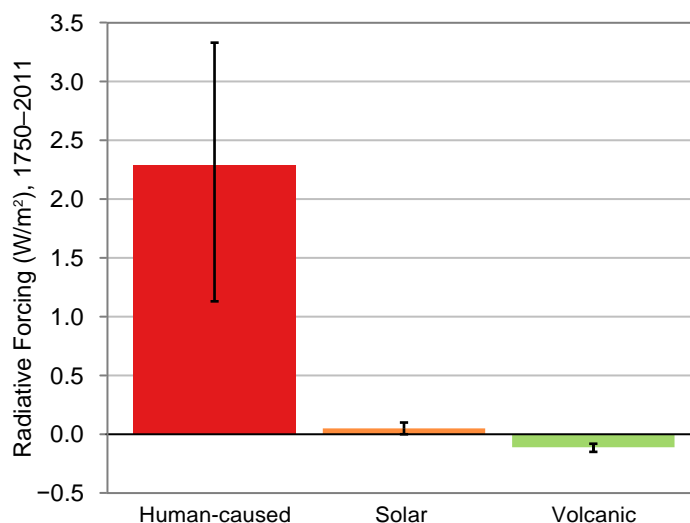


Figure ES.2: Global annual average radiative forcing change from 1750 to 2011 due to human activities, changes in total solar irradiance, and volcanic emissions. Black bars indicate the uncertainty in each. Radiative forcing is a measure of the influence a factor (such as greenhouse gas emissions) has in changing the global balance of incoming and outgoing energy. Radiative forcings greater than zero (positive forcings) produce climate warming; forcings less than zero (negative forcings) produce climate cooling. Over this time period, solar forcing has oscillated on approximately an 11-year cycle between -0.11 and $+0.19$ W/m^2 . Radiative forcing due to volcanic emissions is always negative (cooling) and can be very large immediately following significant eruptions but is short-lived. Over the industrial era, the largest volcanic forcing followed the eruption of Mt. Tambora in 1815 (-11.6 W/m^2). This forcing declined to -4.5 W/m^2 in 1816, and to near-zero by 1820. Forcing due to human activities, in contrast, has become increasingly positive (warming) since about 1870, and has grown at an accelerated rate since about 1970. There are also natural variations in temperature and other climate variables which operate on annual to decadal timescales. This natural variability contributes very little to climate trends over decades and longer. *Simplified from Figure 2.6 in Chapter 2. See Chapter 2 for more details.*

- Global climate is projected to continue to change over this century and beyond. The magnitude of climate change beyond the next few decades will depend primarily on the amount of greenhouse (heat-trapping) gases emitted globally and on the remaining uncertainty in the sensitivity of Earth's climate to those emissions (*very high confidence*). With significant reductions in the emissions of greenhouse gases, the global annually averaged temperature rise could be limited to 3.6°F (2°C) or less. Without major reductions in these emissions, the increase in annual average global temperatures relative to preindustrial times could reach 9°F (5°C) or more by the end of this century. (Ch. 1; Fig. ES.3)
- If greenhouse gas concentrations were stabilized at their current level, existing concentrations would commit the world to at least an additional 1.1°F (0.6°C) of warming over this century relative to the last few decades (*high confidence* in continued warming, *medium confidence* in amount of warming). (Ch. 4)



Scenarios Used in this Assessment

Projections of future climate conditions use a range of plausible future scenarios. Consistent with previous practice, this assessment relies on scenarios generated for the Intergovernmental Panel on Climate Change (IPCC). The IPCC completed its last assessment in 2013–2014, and its projections were based on updated scenarios, namely four “representative concentration pathways” (RCPs). The RCP scenarios are numbered according to changes in radiative forcing in 2100 relative to preindustrial conditions: +2.6, +4.5, +6.0 and +8.5 watts per square meter (W/m^2). Radiative forcing is a measure of the influence a factor (such as greenhouse gas emissions) has in changing the global balance of incoming and outgoing energy. Absorption by greenhouse gases (GHGs) of infrared energy radiated from the surface leads to warming of the surface and atmosphere. Though multiple emissions pathways could lead to the same 2100 radiative forcing value, an associated pathway of CO_2 and other human-caused emissions of greenhouse gases, aerosols, and air pollutants has been selected for each RCP. RCP8.5 implies a future with continued high emissions growth, whereas the other RCPs represent different pathways of mitigating emissions. Figure ES.3 shows these emissions pathways and the corresponding projected changes in global temperature.

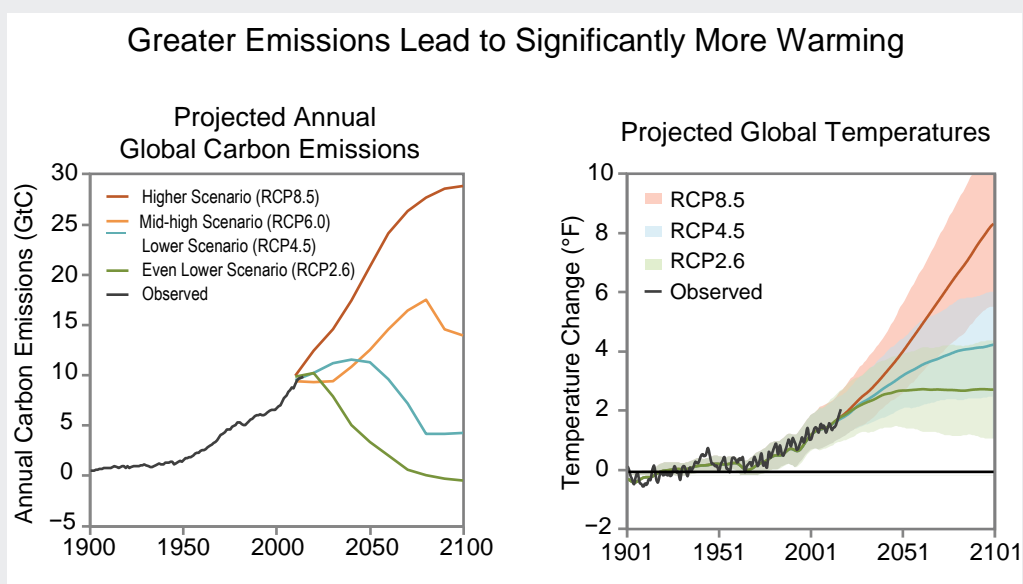


Figure ES.3: The two panels above show annual historical and a range of plausible future carbon emissions in units of gigatons of carbon (GtC) per year (left) and the historical observed and future temperature change that would result for a range of future scenarios relative to the 1901–1960 average, based on the central estimate (lines) and a range (shaded areas, two standard deviations) as simulated by the full suite of CMIP5 global climate models (right). By 2081–2100, the projected range in global mean temperature change is 1.1°–4.3°F under the even lower scenario (RCP2.6; 0.6°–2.4°C, green), 2.4°–5.9°F under the lower scenario (RCP4.5; 1.3°–3.3°C, blue), 3.0°–6.8°F under the mid-high scenario (RCP6.0; 1.6°–3.8°C, not shown) and 5.0°–10.2°F under the higher scenario (RCP8.5; 2.8°–5.7°C, orange). See the main report for more details on these scenarios and implications. *Based on Figure 4.1 in Chapter 4.*

Changes in Observed and Projected U.S. Temperature

Annual average temperature over the contiguous United States has increased by 1.8°F (1.0°C) for the period 1901–2016 and is projected to continue to rise. (*Very high confidence*). (Ch. 6; Fig. ES.4)

- Annual average temperature over the contiguous United States has increased by 1.2°F (0.7°C) for the period 1986–2016 relative to 1901–1960 and by 1.8°F (1.0°C) based on a linear regression for the period 1901–2016 (*very high confidence*). Surface and satellite data are consistent in their depiction of rapid warming since 1979 (*high confidence*). Paleo-temperature evidence shows that recent decades are the warmest of the past 1,500 years (*medium confidence*). (Ch. 6)
- Annual average temperature over the contiguous United States is projected to rise (*very high confidence*). Increases of about 2.5°F (1.4°C) are projected for the period 2021–2050 relative to the average from 1976–2005 in all RCP scenarios, implying recent record-setting years may be “common” in the next few decades (*high confidence*). Much larger rises are projected by late century (2071–2100): 2.8°–7.3°F (1.6°–4.1°C) in a lower scenario (RCP4.5) and 5.8°–11.9°F (3.2°–6.6°C) in a higher scenario (RCP8.5) (*high confidence*). (Ch. 6; Fig. ES.4)
- In the United States, the urban heat island effect results in daytime temperatures 0.9°–7.2°F (0.5°–4.0°C) higher and nighttime temperatures 1.8°–4.5°F (1.0°–2.5°C) higher in urban areas than in rural areas, with larger temperature differences in humid regions (primarily in the eastern United States) and in cities with larger and denser populations. The urban heat island effect will strengthen in the future as the structure and spatial extent as well as population density of urban areas change and grow (*high confidence*). (Ch. 10)

Significantly More Warming Occurs Under Higher Greenhouse Gas Concentration Scenarios

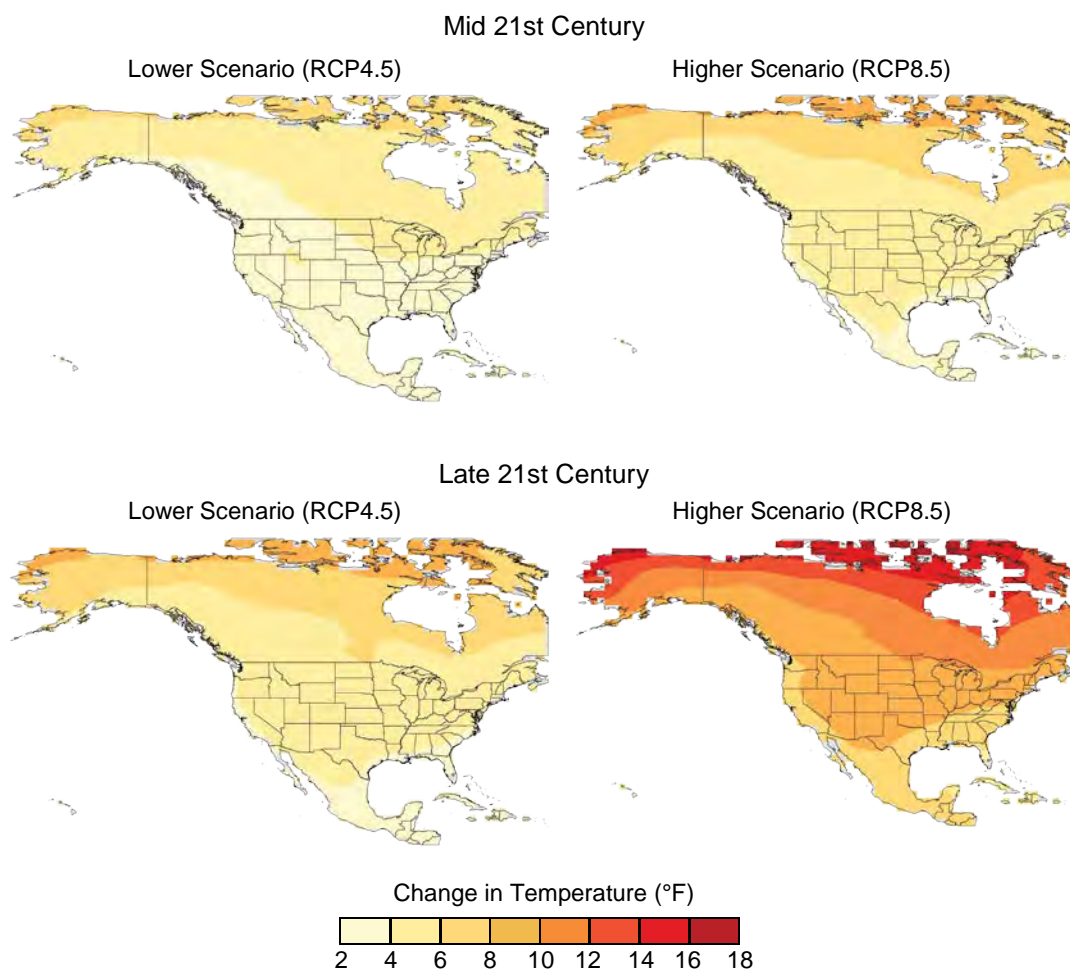


Figure ES.4: These maps show the projected changes in annual average temperatures for mid- and late-21st century for two future pathways. Changes are the differences between the average projected temperatures for mid-century (2036–2065; top), and late-century (2070–2099; bottom), and those observed for the near-present (1976–2005). See *Figure 6.7 in Chapter 6* for more details.

Many Temperature and Precipitation Extremes Are Becoming More Common

Temperature and precipitation extremes can affect water quality and availability, agricultural productivity, human health, vital infrastructure, iconic ecosystems and species, and the likelihood of disasters. Some extremes have already become more frequent, intense, or of longer duration, and many extremes are expected to continue to increase or worsen, presenting substantial challenges for built, agricultural, and natural systems. Some storm types such as hurricanes, tornadoes, and winter storms are also exhibiting changes that have been linked to climate change, although the current state of the science does not yet permit detailed understanding.

Observed Changes in Extremes

There have been marked changes in temperature extremes across the contiguous United States. The number of high temperature records set in the past two decades far exceeds the number of low temperature records. (*Very high confidence*) (Ch. 6, Fig. ES.5)

- The frequency of cold waves has decreased since the early 1900s, and the frequency of heat waves has increased since the mid-1960s (the Dust Bowl era of the 1930s remains the peak period for extreme heat in the United States). (*Very high confidence*). (Ch. 6)
- The frequency and intensity of extreme heat and heavy precipitation events are increasing in most continental regions of the world (*very high confidence*). These trends are consistent with expected physical responses to a warming climate. Climate model studies are also consistent with these trends, although models tend to underestimate the observed trends, especially for the increase in extreme precipitation events (*very high confidence* for temperature, *high confidence* for extreme precipitation). (Ch. 1)

Record Warm Daily Temperatures Are Occurring More Often

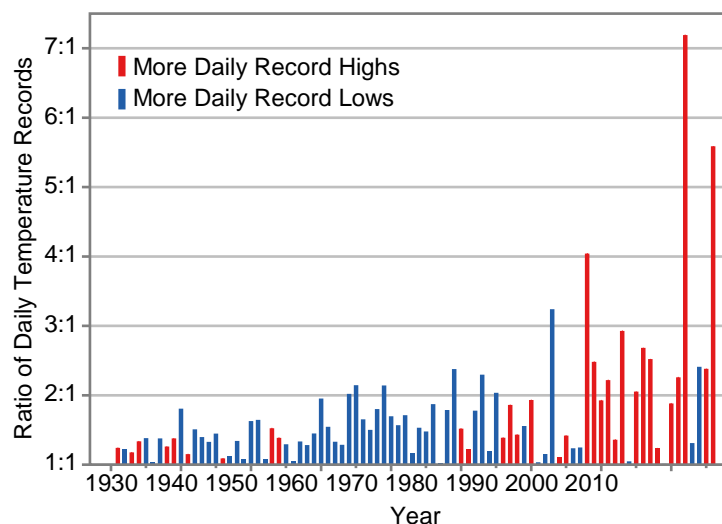


Figure ES.5: Observed changes in the occurrence of record-setting daily temperatures in the contiguous United States. Red bars indicate a year with more daily record highs than daily record lows, while blue bars indicate a year with more record lows than highs. The height of the bar indicates the ratio of record highs to lows (red) or of record lows to highs (blue). For example, a ratio of 2:1 for a blue bar means that there were twice as many record daily lows as daily record highs that year. (Figure source: NOAA/NCEI). From Figure 6.5 in Chapter 6.

Heavy precipitation events in most parts of the United States have increased in both intensity and frequency since 1901 (*high confidence*). There are important regional differences in trends, with the largest increases occurring in the northeastern United States (*high confidence*). (Ch. 7; Fig. ES.6)

Extreme Precipitation Has Increased Across Much of the United States

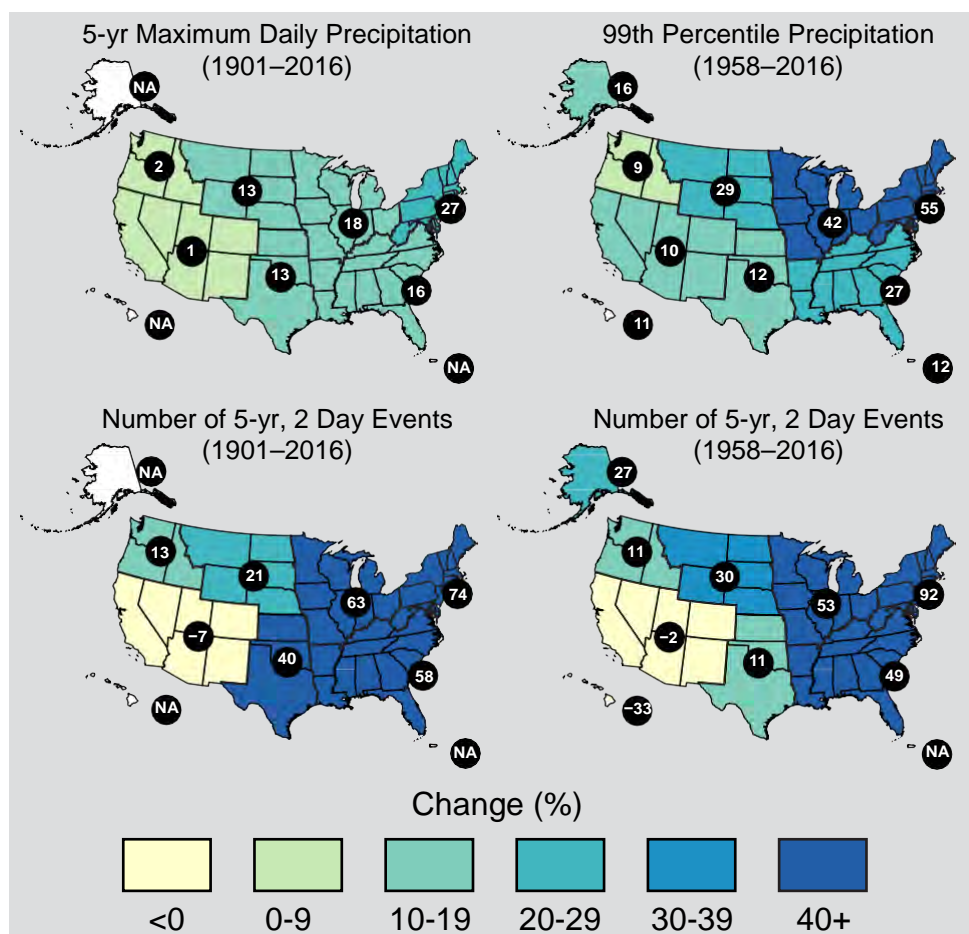


Figure ES.6: These maps show the percentage change in several metrics of extreme precipitation by NCA4 region, including (upper left) the maximum daily precipitation in consecutive 5-year periods; (upper right) the amount of precipitation falling in daily events that exceed the 99th percentile of all non-zero precipitation days (top 1% of all daily precipitation events); (lower left) the number of 2-day events with a precipitation total exceeding the largest 2-day amount that is expected to occur, on average, only once every 5 years, as calculated over 1901–2016; and (lower right) the number of 2-day events with a precipitation total exceeding the largest 2-day amount that is expected to occur, on average, only once every 5 years, as calculated over 1958–2016. The number in each black circle is the percent change over the entire period, either 1901–2016 or 1958–2016. Note that Alaska and Hawai'i are not included in the 1901–2016 maps owing to a lack of observations in the earlier part of the 20th century. (Figure source: CICS-NC / NOAA NCEI). Based on figure 7.4 in Chapter 7.

- Recent droughts and associated heat waves have reached record intensity in some regions of the United States; however, by geographical scale and duration, the Dust Bowl era of the 1930s remains the benchmark drought and extreme heat event in the historical record. (*Very high confidence*) (Ch. 8)
- Northern Hemisphere spring snow cover extent, North America maximum snow depth, snow water equivalent in the western United States, and extreme snowfall years in the southern and western United States have all declined, while extreme snowfall years in parts of the northern United States have increased. (*Medium confidence*). (Ch. 7)
- There has been a trend toward earlier snowmelt and a decrease in snowstorm frequency on the southern margins of climatologically snowy areas (*medium confidence*). Winter storm tracks have shifted northward since 1950 over the Northern Hemisphere (*medium confidence*). Potential linkages between the frequency and intensity of severe winter storms in the United States and accelerated warming in the Arctic have been postulated, but they are complex, and, to some extent, contested, and confidence in the connection is currently *low*. (Ch. 9)
- Tornado activity in the United States has become more variable, particularly over the 2000s, with a decrease in the number of days per year with tornadoes and an increase in the number of tornadoes on these days (*medium confidence*). Confidence in past trends for hail and severe thunderstorm winds, however, is *low* (Ch. 9)

Projected Changes in Extremes

- The frequency and intensity of extreme high temperature events are *virtually certain* to increase in the future as global temperature increases (*high confidence*). Extreme precipitation events will *very likely* continue to increase in frequency and intensity throughout most of the world (*high confidence*). Observed and projected trends for some other types of extreme events, such as floods, droughts, and severe storms, have more variable regional characteristics. (Ch. 1)

Extreme temperatures in the contiguous United States are projected to increase even more than average temperatures (*very high confidence*). (Ch. 6)

- Both extremely cold days and extremely warm days are expected to become warmer. Cold waves are predicted to become less intense while heat waves will become more intense. The number of days below freezing is projected to decline while the number above 90°F will rise. (*Very high confidence*) (Ch. 6)
- The frequency and intensity of heavy precipitation events in the United States are projected to continue to increase over the 21st century (*high confidence*). There are, however, important regional and seasonal differences in projected changes in total precipitation: the northern United States, including Alaska, is projected to receive more precipitation in the winter and spring, and parts of the southwestern United States are projected to receive less precipitation in the winter and spring (*medium confidence*). (Ch. 7)

- The frequency and severity of landfalling “atmospheric rivers” on the U.S. West Coast (narrow streams of moisture that account for 30%–40% of the typical snowpack and annual precipitation in the region and are associated with severe flooding events) will increase as a result of increasing evaporation and resulting higher atmospheric water vapor that occurs with increasing temperature. (*Medium confidence*) (Ch. 9)
- Projections indicate large declines in snowpack in the western United States and shifts to more precipitation falling as rain than snow in the cold season in many parts of the central and eastern United States (*high confidence*). (Ch. 7)
- Substantial reductions in western U.S. winter and spring snowpack are projected as the climate warms. Earlier spring melt and reduced snow water equivalent have been formally attributed to human-induced warming (*high confidence*) and will *very likely* be exacerbated as the climate continues to warm (*very high confidence*). Under higher scenarios, and assuming no change to current water resources management, chronic, long-duration hydrological drought is increasingly possible by the end of this century (*very high confidence*). (Ch. 8)

Future decreases in surface soil moisture from human activities over most of the United States are likely as the climate warms under the higher scenarios. (*Medium confidence*) (Ch. 8)

- The human effect on recent major U.S. droughts is complicated. Little evidence is found for a human influence on observed precipitation deficits, but much evidence is found for a human influence on surface soil moisture deficits due to increased evapotranspiration caused by higher temperatures. (*High confidence*) (Ch. 8)
- The incidence of large forest fires in the western United States and Alaska has increased since the early 1980s (*high confidence*) and is projected to further increase in those regions as the climate warms, with profound changes to certain ecosystems (*medium confidence*). (Ch. 8)
- Both physics and numerical modeling simulations generally indicate an increase in tropical cyclone intensity in a warmer world, and the models generally show an increase in the number of very intense tropical cyclones. For Atlantic and eastern North Pacific hurricanes and western North Pacific typhoons, increases are projected in precipitation rates (*high confidence*) and intensity (*medium confidence*). The frequency of the most intense of these storms is projected to increase in the Atlantic and western North Pacific (*low confidence*) and in the eastern North Pacific (*medium confidence*). (Ch. 9)

Box ES.1: The Connected Climate System: Distant Changes Affect the United States

Weather conditions and the ways they vary across regions and over the course of the year are influenced, in the United States as elsewhere, by a range of factors, including local conditions (such as topography and urban heat islands), global trends (such as human-caused warming), and global and regional circulation patterns, including cyclical and chaotic patterns of natural variability within the climate system. For example, during an El Niño year, winters across the southwestern United States are typically wetter than average, and global temperatures are higher than average. During a La Niña year, conditions across the southwestern United States are typically dry, and there tends to be a lowering of global temperatures (Fig. ES.7).

El Niño is not the only repeating pattern of natural variability in the climate system. Other important patterns include the North Atlantic Oscillation (NAO)/Northern Annular Mode (NAM), which particularly affects conditions on the U.S. East Coast, and the North Pacific Oscillation (NPO) and Pacific North American Pattern (PNA), which especially affect conditions in Alaska and the U.S. West Coast. These patterns are closely linked to other atmospheric circulation phenomena like the position of the jet streams. Changes in the occurrence of these patterns or their properties have contributed to recent U.S. temperature and precipitation trends (*medium confidence*) although *confidence is low* regarding the size of the role of human activities in these changes. (Ch. 5)

Understanding the full scope of human impacts on climate requires a global focus because of the interconnected nature of the climate system. For example, the climate of the Arctic and the climate of the continental United States are connected through atmospheric circulation patterns. While the Arctic may seem remote to most Americans, the climatic effects of perturbations to arctic sea ice, land ice, surface temperature, snow cover, and permafrost affect the amount of warming, sea level change, carbon cycle impacts, and potentially even weather patterns in the lower 48 states. The Arctic is warming at a rate approximately twice as fast as the global average and, if it continues to warm at the same rate, Septembers will be nearly ice-free in the Arctic Ocean sometime between now and the 2040s (see Fig. ES.10). The important influence of arctic climate change on Alaska is apparent; the influence of arctic changes on U.S. weather over the coming decades remains an open question with the potential for significant impact. (Ch. 11)

Changes in the Tropics can also impact the rest of the globe, including the United States. There is growing evidence that the Tropics have expanded poleward by about 70 to 200 miles in each hemisphere over the period 1979–2009, with an accompanying shift of the subtropical dry zones, midlatitude jets, and storm tracks (*medium to high confidence*). Human activities have played a role in the change (*medium confidence*), although confidence is presently low regarding the magnitude of the human contribution relative to natural variability (Ch. 5).

(continued on next page)

Box ES.1 (continued)

Large-Scale Patterns of Natural Variability Affect U.S. Climate

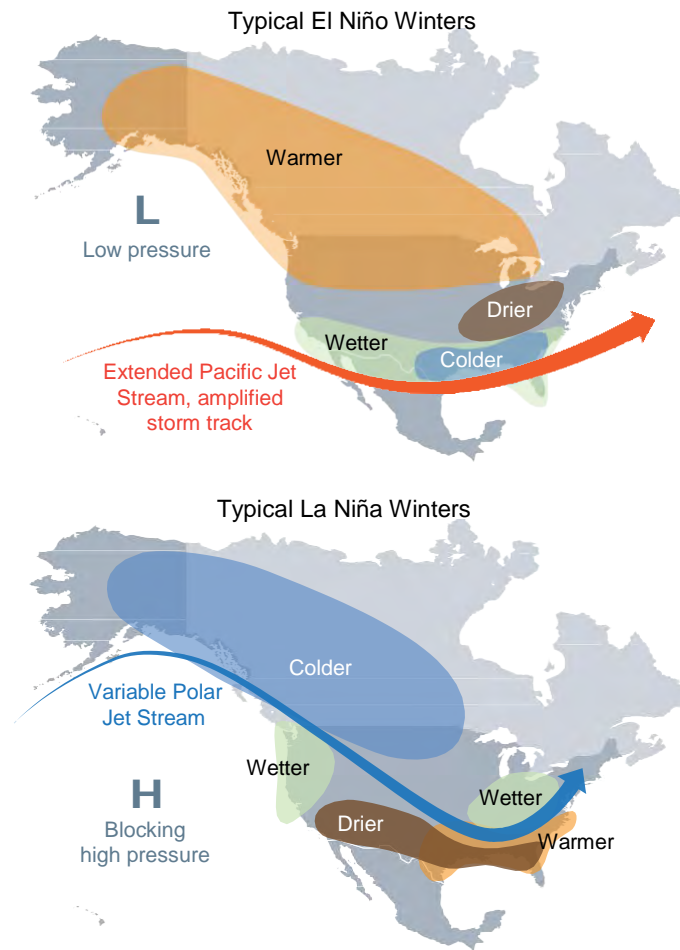


Figure ES.7: This figure illustrates the typical January–March weather anomalies and atmospheric circulation during moderate to strong (top) El Niño and (bottom) La Niña. These influences over the United States often occur most strongly during the cold season. *From Figure 5.2 in Chapter 5.*

Oceans Are Rising, Warming, and Becoming More Acidic

Oceans occupy two-thirds of the planet's surface and host unique ecosystems and species, including those important for global commercial and subsistence fishing. Understanding climate impacts on the ocean and the ocean's feedbacks to the climate system is critical for a comprehensive understanding of current and future changes in climate.

Global Ocean Heat

The world's oceans have absorbed about 93% of the excess heat caused by greenhouse gas warming since the mid-20th century, making them warmer and altering global and regional climate feedbacks. (*Very high confidence*) (Ch. 13)

- Ocean heat content has increased at all depths since the 1960s and surface waters have warmed by about $1.3^{\circ} \pm 0.1^{\circ}\text{F}$ ($0.7^{\circ} \pm 0.08^{\circ}\text{C}$) per century globally since 1900 to 2016. Under higher scenarios, a global increase in average sea surface temperature of $4.9^{\circ} \pm 1.3^{\circ}\text{F}$ ($2.7^{\circ} \pm 0.7^{\circ}\text{C}$) is projected by 2100. (*Very high confidence*). (Ch. 13)

Global and Regional Sea Level Rise

Global mean sea level (GMSL) has risen by about 7–8 inches (about 16–21 cm) since 1900, with about 3 of those inches (about 7 cm) occurring since 1993 (*very high confidence*). (Ch. 12)

- Human-caused climate change has made a substantial contribution to GMSL rise since 1900 (*high confidence*), contributing to a rate of rise that is greater than during any preceding century in at least 2,800 years (*medium confidence*). (Ch. 12; Fig. ES.8)
- Relative to the year 2000, GMSL is *very likely* to rise by 0.3–0.6 feet (9–18 cm) by 2030, 0.5–1.2 feet (15–38 cm) by 2050, and 1.0–4.3 feet (30–130 cm) by 2100 (*very high confidence* in lower bounds; *medium confidence* in upper bounds for 2030 and 2050; *low confidence* in upper bounds for 2100). Future emissions pathways have little effect on projected GMSL rise in the first half of the century, but significantly affect projections for the second half of the century (*high confidence*). (Ch. 12)

Recent Sea Level Rise Fastest for Over 2,000 Years

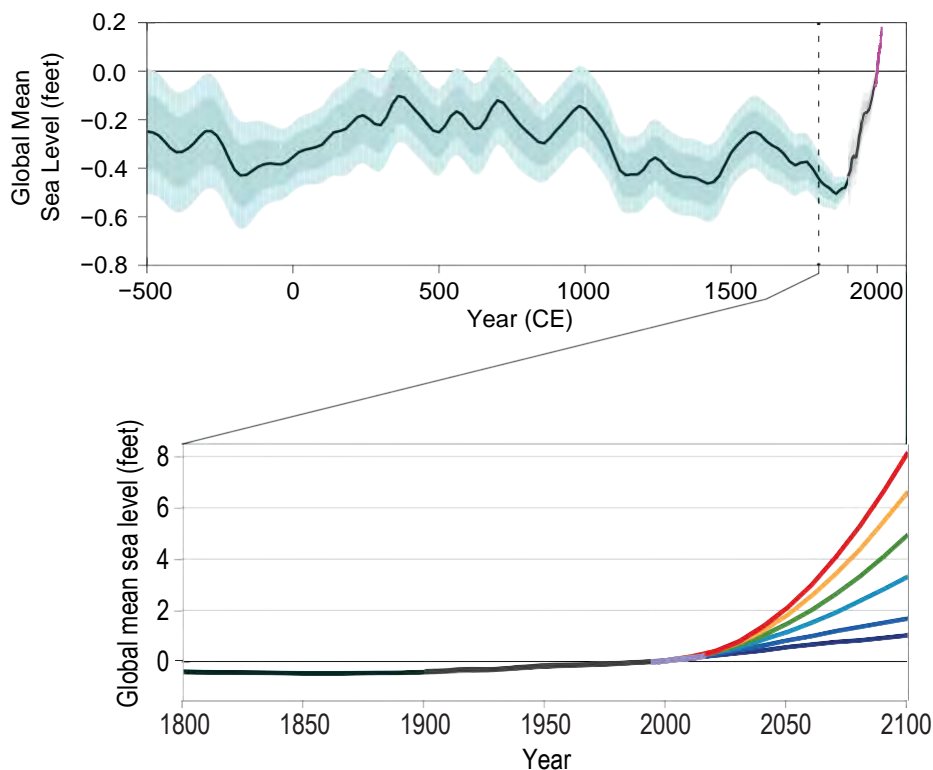


Figure ES.8: The top panel shows observed and reconstructed mean sea level for the last 2,500 years. The bottom panel shows projected mean sea level for six future scenarios. The six scenarios—spanning a range designed to inform a variety of decision makers—extend from a low scenario, consistent with continuation of the rate of sea level rise over the last quarter century, to an extreme scenario, assuming rapid mass loss from the Antarctic ice sheet. Note that the range on the vertical axis in the bottom graph is approximately ten times greater than in the top graph. *Based on Figure 12.2 and 12.4 in Chapter 12. See the main report for more details.*

- Emerging science regarding Antarctic ice sheet stability suggests that, for higher scenarios, a GMSL rise exceeding 8 feet (2.4 m) by 2100 is physically possible, although the probability of such an extreme outcome cannot currently be assessed. Regardless of emission pathway, it is *extremely likely* that GMSL rise will continue beyond 2100 (*high confidence*). (Ch. 12)
- Relative sea level rise in this century will vary along U.S. coastlines due, in part, to changes in Earth’s gravitational field and rotation from melting of land ice, changes in ocean circulation, and vertical land motion (*very high confidence*). For almost all future GMSL rise scenarios, relative sea level rise is *likely* to be greater than the global average in the U.S. Northeast and the western Gulf of Mexico. In intermediate and low GMSL rise scenarios, relative sea level rise is *likely* to be less than the global average in much of the Pacific Northwest and Alaska. For high GMSL rise scenarios, relative sea level rise is *likely* to be higher than the global average along all U.S. coastlines outside Alaska. Almost all U.S. coastlines experience more than global mean sea level rise in response to Antarctic ice loss, and thus would be particularly affected under extreme GMSL rise scenarios involving substantial Antarctic mass loss (*high confidence*). (Ch. 12)

Coastal Flooding

- As sea levels have risen, the number of tidal floods each year that cause minor impacts (also called “nuisance floods”) have increased 5- to 10-fold since the 1960s in several U.S. coastal cities (*very high confidence*). Rates of increase are accelerating in over 25 Atlantic and Gulf Coast cities (*very high confidence*). Tidal flooding will continue increasing in depth, frequency, and extent this century (*very high confidence*). (Ch. 12)

“Nuisance Flooding” Increases Across the United States

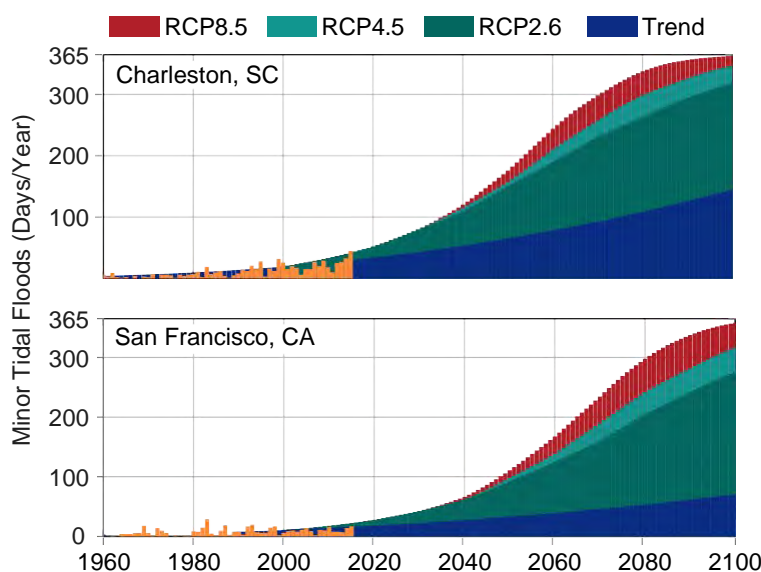


Figure ES. 9: Annual occurrences of tidal floods (days per year), also called sunny-day or nuisance flooding, have increased for some U.S. coastal cities. The figure shows historical exceedances (orange bars) for two of the locations—Charleston, SC and San Francisco, CA—and future projections through 2100. The projections are based upon the continuation of the historical trend (blue) and under median RCP2.6, 4.5 and 8.5 conditions. *From Figure 12.5, Chapter 12.*

- Assuming storm characteristics do not change, sea level rise will increase the frequency and extent of extreme flooding associated with coastal storms, such as hurricanes and nor’easters (*very high confidence*). A projected increase in the intensity of hurricanes in the North Atlantic (*medium confidence*) could increase the probability of extreme flooding along most of the U.S. Atlantic and Gulf Coast states beyond what would be projected based solely on relative sea level rise. However, there is *low confidence* in the projected increase in frequency of intense Atlantic hurricanes, and the associated flood risk amplification, and flood effects could be offset or amplified by such factors, such as changes in overall storm frequency or tracks. (Ch.12; Fig. ES. 9)

Global Ocean Circulation

- The potential slowing of the Atlantic meridional overturning circulation (AMOC; of which the Gulf Stream is one component)—as a result of increasing ocean heat content and freshwater-driven buoyancy changes—could have dramatic climate feedbacks as the ocean absorbs less heat and CO₂ from the atmosphere. This slowing would also affect the climates of

North America and Europe. Any slowing documented to date cannot be directly tied to human-caused forcing, primarily due to lack of adequate observational data and to challenges in modeling ocean circulation changes. Under a higher scenario (RCP8.5), models show that the AMOC weakens over the 21st century (*low confidence*). (Ch. 13)

Global and Regional Ocean Acidification

The world's oceans are currently absorbing more than a quarter of the CO₂ emitted to the atmosphere annually from human activities, making them more acidic (*very high confidence*), with potential detrimental impacts to marine ecosystems. (Ch. 13)

- Higher-latitude systems typically have a lower buffering capacity against changing acidity, exhibiting seasonally corrosive conditions sooner than low-latitude systems. The rate of acidification is unparalleled in at least the past 66 million years (*medium confidence*). Under the higher scenario (RCP8.5), the global average surface ocean acidity is projected to increase by 100% to 150% (*high confidence*). (Ch. 13)
- Acidification is regionally greater than the global average along U.S. coastal systems as a result of upwelling (e.g., in the Pacific Northwest) (*high confidence*), changes in freshwater inputs (e.g., in the Gulf of Maine) (*medium confidence*), and nutrient input (e.g., in urbanized estuaries) (*high confidence*). (Ch. 13)

Ocean Oxygen

- Increasing sea surface temperatures, rising sea levels, and changing patterns of precipitation, winds, nutrients, and ocean circulation are contributing to overall declining oxygen concentrations at intermediate depths in various ocean locations and in many coastal areas. Over the last half century, major oxygen losses have occurred in inland seas, estuaries, and in the coastal and open ocean (*high confidence*). Ocean oxygen levels are projected to decrease by as much as 3.5% under the higher scenario (RCP8.5) by 2100 relative to preindustrial values (*high confidence*). (Ch. 13)

Climate Change in Alaska and across the Arctic Continues to Outpace Global Climate Change

Residents of Alaska are on the front lines of climate change. Crumbling buildings, roads, and bridges and eroding shorelines are commonplace. Accelerated melting of multiyear sea ice cover, mass loss from the Greenland Ice Sheet, reduced snow cover, and permafrost thawing are stark examples of the rapid changes occurring in the Arctic. Furthermore, because elements of the climate system are interconnected (see Box ES.1), changes in the Arctic influence climate conditions outside the Arctic.

Arctic Temperature Increases

Annual average near-surface air temperatures across Alaska and the Arctic have increased over the last 50 years at a rate more than twice as fast as the global average temperature. (*Very high confidence*) (Ch. 11)

- Rising Alaskan permafrost temperatures are causing permafrost to thaw and become more discontinuous; this process releases additional carbon dioxide and methane resulting in additional warming (*high confidence*). The overall magnitude of the permafrost-carbon feedback is uncertain (Ch.2); however, it is clear that these emissions have the potential to compromise the ability to limit global temperature increases. (Ch. 11)
- Atmospheric circulation patterns connect the climates of the Arctic and the contiguous United States. Evidenced by recent record warm temperatures in the Arctic and emerging science, the midlatitude circulation has influenced observed arctic temperatures and sea ice (*high confidence*). However, confidence is low regarding whether or by what mechanisms observed arctic warming may have influenced the midlatitude circulation and weather patterns over the continental United States. The influence of arctic changes on U.S. weather over the coming decades remains an open question with the potential for significant impact. (Ch. 11)

Arctic Land Ice Loss

- Arctic land ice loss observed in the last three decades continues, in some cases accelerating (*very high confidence*). It is *virtually certain* that Alaska glaciers have lost mass over the last 50 years, with each year since 1984 showing an annual average ice mass less than the previous year. Over the satellite record, average ice mass loss from Greenland was -269 Gt per year between April 2002 and April 2016, accelerating in recent years (*high confidence*). (Ch.11)

Arctic Sea Ice Loss

Since the early 1980s, annual average arctic sea ice has decreased in extent between 3.5% and 4.1% per decade, has become thinner by between 4.3 and 7.5 feet, and is melting at least 15 more days each year. September sea ice extent has decreased between 10.7% and 15.9% per decade. (*Very high confidence*) (Ch. 11)

- Arctic sea ice loss is expected to continue through the 21st century, *very likely* resulting in nearly sea ice-free late summers by the 2040s (*very high confidence*). (Ch. 11)
- It is *very likely* that human activities have contributed to observed arctic surface temperature warming, sea ice loss, glacier mass loss, and northern hemisphere snow extent decline (*high confidence*). (Ch. 11)

Multiyear Sea Ice Has Declined Dramatically

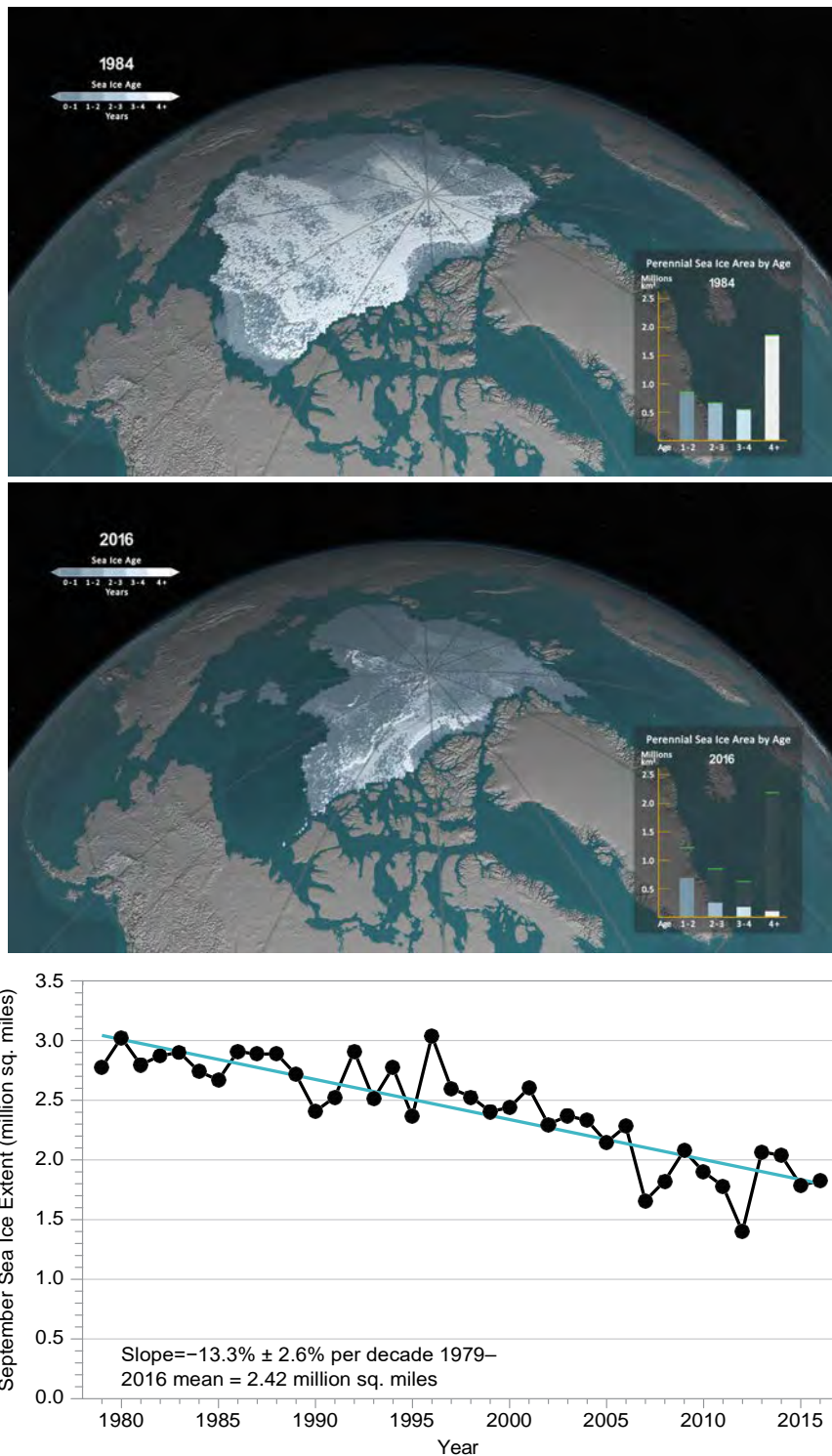


Figure ES.10: September sea ice extent and age shown for (top) 1984 and (middle) 2016, illustrating significant reductions in sea ice extent and age (thickness). The bar graph in the lower right of each panel illustrates the sea ice area (unit: million km²) covered within each age category (> 1 year), and the green bars represent the maximum extent for each age range during the record. The year 1984 is representative of September sea ice characteristics during the 1980s. The years 1984 and 2016 are selected as endpoints in the time series; a movie of the complete time series is available at <http://svs.gsfc.nasa.gov/cgi-bin/details.cgi?aid=4489>. (bottom) The satellite-era arctic sea ice areal extent trend from 1979 to 2016 for September (unit: million mi²). From Figure 11.1 in Chapter 11.

Limiting Globally Averaged Warming to 2°C (3.6°F) Will Require Major Reductions in Emissions

Human activities are now the dominant cause of the observed trends in climate. For that reason, future climate projections are based on scenarios of how human activities will continue to affect the climate over the remainder of this century and beyond (see Sidebar: Scenarios Used in this Assessment). There remains significant uncertainty about future emissions due to changing economic, political, and demographic factors. For that reason, this report quantifies possible climate changes for a broad set of plausible future scenarios through the end of the century. (Ch. 2, 4, 10, 14)

The observed increase in global carbon emissions over the past 15–20 years has been consistent with higher scenarios (e.g., RCP8.5) (*very high confidence*). In 2014 and 2015, emission growth rates slowed as economic growth became less carbon-intensive (*medium confidence*). Even if this slowing trend continues, however, it is not yet at a rate that would limit the increase in the global average temperature to well below 3.6°F (2°C) above preindustrial levels (*high confidence*). (Ch. 4)

- Global mean atmospheric carbon dioxide (CO₂) concentration has now passed 400 ppm, a level that last occurred about 3 million years ago, when global average temperature and sea level were significantly higher than today (*high confidence*). Continued growth in CO₂ emissions over this century and beyond would lead to an atmospheric concentration not experienced in tens of millions of years (*medium confidence*). The present-day emissions rate of nearly 10 GtC per year suggests that there is no climate analog for this century any time in at least the last 50 million years (*medium confidence*). (Ch. 4)
- Warming and associated climate effects from CO₂ emissions persist for decades to millennia. In the near-term, changes in climate are determined by past and present greenhouse gas emissions modified by natural variability. Reducing net emissions of CO₂ is necessary to limit near-term climate change and long-term warming. Other greenhouse gases (e.g., methane) and black carbon aerosols exert stronger warming effects than CO₂ on a per ton basis, but they do not persist as long in the atmosphere (Ch. 2); therefore, mitigation of non-CO₂ species contributes substantially to near-term cooling benefits but cannot be relied upon for ultimate stabilization goals. (*Very high confidence*) (Ch. 14)

Choices made today will determine the magnitude of climate change risks beyond the next few decades. (Ch. 4, 14)

- Stabilizing global mean temperature to less than 3.6°F (2°C) above preindustrial levels requires substantial reductions in net global CO₂ emissions prior to 2040 relative to present-day values and likely requires net emissions to become zero or possibly negative later in the century. After accounting for the temperature effects of non-CO₂ species, cumulative global CO₂ emissions must stay below about 800 GtC in order to provide a two-thirds likelihood of preventing 3.6°F (2°C) of

warming. Given estimated cumulative emissions since 1870, no more than approximately 230 GtC may be emitted in the future in order to remain under this temperature limit. Assuming global emissions are equal to or greater than those consistent with the RCP4.5 scenario, this cumulative carbon threshold would be exceeded in approximately two decades. (Ch. 14)

- Achieving global greenhouse gas emissions reductions before 2030 consistent with targets and actions announced by governments in the lead up to the 2015 Paris climate conference would hold open the possibility of meeting the long-term temperature goal of limiting global warming to 3.6°F (2°C) above preindustrial levels, whereas there would be virtually no chance if net global emissions followed a pathway well above those implied by country announcements. Actions in the announcements are, by themselves, insufficient to meet a 3.6°F (2°C) goal; the likelihood of achieving that depends strongly on the magnitude of global emissions reductions after 2030. (*High confidence*) (Ch. 14)
- Climate intervention or geoengineering strategies such as solar radiation management are measures that attempt to limit or reduce global temperature increases. Further assessments of the technical feasibilities, costs, risks, co-benefits, and governance challenges of climate intervention or geoengineering strategies, which are as yet unproven at scale, are a necessary step before judgments about the benefits and risks of these approaches can be made with high confidence. (*High confidence*) (Ch. 14)
- In recent decades, land-use and land-cover changes have turned the terrestrial biosphere (soil and plants) into a net “sink” for carbon (drawing down carbon from the atmosphere), and this sink has steadily increased since 1980 (*high confidence*). Because of the uncertainty in the trajectory of land cover, the possibility of the land becoming a net carbon source cannot be excluded (*very high confidence*). (Ch. 10)

There is a Significant Possibility for Unanticipated Changes

Humanity’s effect on the Earth system, through the large-scale combustion of fossil fuels and widespread deforestation and the resulting release of carbon dioxide (CO₂) into the atmosphere, as well as through emissions of other greenhouse gases and radiatively active substances from human activities, is unprecedented. There is significant potential for humanity’s effect on the planet to result in unanticipated surprises and a broad consensus that the further and faster the Earth system is pushed towards warming, the greater the risk of such surprises.

There are at least two types of potential surprises: *compound events*, where multiple extreme climate events occur simultaneously or sequentially (creating greater overall impact), and *critical threshold* or *tipping point events*, where some threshold is crossed in the climate system (that leads to large impacts). The probability of such surprises – some of which may be abrupt and/or irreversible – as well as other more predictable but difficult-to-manage impacts, increases as the influence of human activities on the climate system increases. (Ch. 15)

Unanticipated and difficult or impossible-to-manage changes in the climate system are possible throughout the next century as critical thresholds are crossed and/or multiple climate-related extreme events occur simultaneously. (Ch. 15)

- Positive feedbacks (self-reinforcing cycles) within the climate system have the potential to accelerate human-induced climate change and even shift the Earth's climate system, in part or in whole, into new states that are very different from those experienced in the recent past (for example, ones with greatly diminished ice sheets or different large-scale patterns of atmosphere or ocean circulation). Some feedbacks and potential state shifts can be modeled and quantified; others can be modeled or identified but not quantified; and some are probably still unknown. (*Very high confidence* in the potential for state shifts and in the incompleteness of knowledge about feedbacks and potential state shifts). (Ch. 15)
- The physical and socioeconomic impacts of compound extreme events (such as simultaneous heat and drought, wildfires associated with hot and dry conditions, or flooding associated with high precipitation on top of snow or waterlogged ground) can be greater than the sum of the parts (*very high confidence*). Few analyses consider the spatial or temporal correlation between extreme events. (Ch. 15)
- While climate models incorporate important climate processes that can be well quantified, they do not include all of the processes that can contribute to feedbacks (Ch. 2), compound extreme events, and abrupt and/or irreversible changes. For this reason, future changes outside the range projected by climate models cannot be ruled out (*very high confidence*). Moreover, the systematic tendency of climate models to underestimate temperature change during warm paleoclimates suggests that climate models are more likely to underestimate than to overestimate the amount of long-term future change (*medium confidence*). (Ch. 15)



Box ES.2: A Summary of Advances Since NCA3

Advances in scientific understanding and scientific approach, as well as developments in global policy, have occurred since NCA3. A detailed summary of these advances can be found at the end of Chapter 1: Our Globally Changing Climate. Highlights of what aspects are either especially strengthened or are emerging in the current findings include

- **Detection and attribution:** Significant advances have been made in the attribution of the human influence for individual climate and weather extreme events since NCA3. (Chapters 3, 6, 7, 8).
- **Atmospheric circulation and extreme events:** The extent to which atmospheric circulation in the midlatitudes is changing or is projected to change, possibly in ways not captured by current climate models, is a new important area of research. (Chapters 5, 6, 7).
- **Increased understanding of specific types of extreme events:** How climate change may affect specific types of extreme events in the United States is another key area where scientific understanding has advanced. (Chapter 9).
- **High-resolution global climate model simulations:** As computing resources have grown, multidecadal simulations of global climate models are now being conducted at horizontal resolutions on the order of 15 miles (25 km) that provide more realistic characterization of intense weather systems, including hurricanes. (Chapter 9).
- **Oceans and coastal waters:** Ocean acidification, warming, and oxygen loss are all increasing, and scientific understanding of the severity of their impacts is growing. Both oxygen loss and acidification may be magnified in some U.S. coastal waters relative to the global average, raising the risk of serious ecological and economic consequences. (Chapters 2, 13).
- **Local sea level change projections:** For the first time in the NCA process, sea level rise projections incorporate geographic variation based on factors such as local land subsidence, ocean currents, and changes in Earth's gravitational field. (Chapter 12).
- **Accelerated ice-sheet loss:** New observations from many different sources confirm that ice-sheet loss is accelerating. Combining observations with simultaneous advances in the physical understanding of ice sheets leads to the conclusion that up to 8.5 feet of global sea level rise is possible by 2100 under a higher scenario (RCP8.5), up from 6.6 feet in NCA3. (Chapter 12).
- **Low sea-ice areal extent:** The annual arctic sea ice extent minimum for 2016 relative to the long-term record was the second lowest on record. The arctic sea ice minimums in 2014 and 2015 were also amongst the lowest on record. Since 1981, the sea ice minimum has decreased by 13.3% per decade, more than 46% over the 35 years. The annual arctic sea ice maximum in March 2017 was the lowest maximum areal extent on record. (Chapter 11).
- **Potential surprises:** Both large-scale state shifts in the climate system (sometimes called “tipping points”) and compound extremes have the potential to generate unanticipated climate surprises. The further the Earth system departs from historical climate forcings, and the more the climate changes, the greater the potential for these surprises. (Chapter 15).
- **Mitigation:** This report discusses some important aspects of climate science that are relevant to long-term temperature goals and different mitigation scenarios, including those implied by government announcements for the Paris Agreement. (Chapters 4, 14).



1

Our Globally Changing Climate

KEY FINDINGS

1. The global climate continues to change rapidly compared to the pace of the natural variations in climate that have occurred throughout Earth's history. Trends in globally averaged temperature, sea level rise, upper-ocean heat content, land-based ice melt, arctic sea ice, depth of seasonal permafrost thaw, and other climate variables provide consistent evidence of a warming planet. These observed trends are robust and have been confirmed by multiple independent research groups around the world. (*Very high confidence*)
2. The frequency and intensity of extreme heat and heavy precipitation events are increasing in most continental regions of the world (*very high confidence*). These trends are consistent with expected physical responses to a warming climate. Climate model studies are also consistent with these trends, although models tend to underestimate the observed trends, especially for the increase in extreme precipitation events (*very high confidence* for temperature, *high confidence* for extreme precipitation). The frequency and intensity of extreme high temperature events are *virtually certain* to increase in the future as global temperature increases (*high confidence*). Extreme precipitation events will *very likely* continue to increase in frequency and intensity throughout most of the world (*high confidence*). Observed and projected trends for some other types of extreme events, such as floods, droughts, and severe storms, have more variable regional characteristics.
3. Many lines of evidence demonstrate that it is *extremely likely* that human influence has been the dominant cause of the observed warming since the mid-20th century. Formal detection and attribution studies for the period 1951 to 2010 find that the observed global mean surface temperature warming lies in the middle of the range of likely human contributions to warming over that same period. We find no convincing evidence that natural variability can account for the amount of global warming observed over the industrial era. For the period extending over the last century, there are no convincing alternative explanations supported by the extent of the observational evidence. Solar output changes and internal variability can only contribute marginally to the observed changes in climate over the last century, and we find no convincing evidence for natural cycles in the observational record that could explain the observed changes in climate. (*Very high confidence*)
4. Global climate is projected to continue to change over this century and beyond. The magnitude of climate change beyond the next few decades will depend primarily on the amount of greenhouse (heat-trapping) gases emitted globally and on the remaining uncertainty in the sensitivity of Earth's climate to those emissions (*very high confidence*). With significant reductions in the emissions of greenhouse gases, the global annually averaged temperature rise could be limited to 3.6°F (2°C) or less. Without major reductions in these emissions, the increase in annual average global temperatures relative to preindustrial times could reach 9°F (5°C) or more by the end of this century (*high confidence*).

(continued on next page)

KEY FINDINGS *(continued)*

5. Natural variability, including El Niño events and other recurring patterns of ocean–atmosphere interactions, impact temperature and precipitation, especially regionally, over months to years. The global influence of natural variability, however, is limited to a small fraction of observed climate trends over decades. *(Very high confidence)*
6. Longer-term climate records over past centuries and millennia indicate that average temperatures in recent decades over much of the world have been much higher, and have risen faster during this time period, than at any time in the past 1,700 years or more, the time period for which the global distribution of surface temperatures can be reconstructed. *(High confidence)*

Recommended Citation for Chapter

Wuebbles, D.J., D.R. Easterling, K. Hayhoe, T. Knutson, R.E. Kopp, J.P. Kossin, K.E. Kunkel, A.N. LeGrande, C. Mears, W.V. Sweet, P.C. Taylor, R.S. Vose, and M.F. Wehner, 2017: Our globally changing climate. In: *Climate Science Special Report: Fourth National Climate Assessment, Volume I* [Wuebbles, D.J., D.W. Fahey, K.A. Hibbard, D.J. Dokken, B.C. Stewart, and T.K. Maycock (eds.)]. U.S. Global Change Research Program, Washington, DC, USA, pp. 35-72, doi: 10.7930/J08S4N35.

1.1 Introduction

Since the Third U.S. National Climate Assessment (NCA3) was published in May 2014, new observations along multiple lines of evidence have strengthened the conclusion that Earth’s climate is changing at a pace and in a pattern not explainable by natural influences. While this report focuses especially on observed and projected future changes for the United States, it is important to understand those changes in the global context (this chapter).

The world has warmed over the last 150 years, especially over the last six decades, and that warming has triggered many other changes to Earth’s climate. Evidence for a changing climate abounds, from the top of the atmosphere to the depths of the oceans. Thousands of studies conducted by tens of thousands of scientists around the world have documented changes in surface, atmospheric, and oceanic temperatures; melting glaciers; disappearing snow cover; shrinking sea ice; rising sea level; and an increase in atmospheric water vapor.

Rainfall patterns and storms are changing, and the occurrence of droughts is shifting.

Many lines of evidence demonstrate that human activities, especially emissions of greenhouse gases, are primarily responsible for the observed climate changes in the industrial era, especially over the last six decades (see attribution analysis in Ch. 3: Detection and Attribution). Formal detection and attribution studies for the period 1951 to 2010 find that the observed global mean surface temperature warming lies in the middle of the range of likely human contributions to warming over that same period. The Intergovernmental Panel on Climate Change concluded that it is extremely likely that human influence has been the dominant cause of the observed warming since the mid-20th century.¹ Over the last century, there are no alternative explanations supported by the evidence that are either credible or that can contribute more than marginally to the observed patterns. There is no convincing evidence that natural variability can account for the amount of and the pattern of global warming

observed over the industrial era.^{2,3,4,5} Solar flux variations over the last six decades have been too small to explain the observed changes in climate.^{6,7,8} There are no apparent natural cycles in the observational record that can explain the recent changes in climate (e.g., PAGES 2k Consortium 2013;⁹ Marcott et al. 2013;¹⁰ Otto-Bliesner et al. 2016¹¹). In addition, natural cycles within Earth’s climate system can only redistribute heat; they cannot be responsible for the observed increase in the overall heat content of the climate system.¹² Any explanations for the observed changes in climate must be grounded in understood physical mechanisms, appropriate in scale, and consistent in timing and direction with the long-term observed trends. Known human activities quite reasonably explain what has happened without the need for other factors. Internal variability and forcing factors other than human activities cannot explain what is happening, and there are no suggested factors, even speculative ones, that can explain the timing or magnitude and that would somehow cancel out the role of human factors.^{3,13} The science underlying this evidence, along with the observed and projected changes in climate, is discussed in later chapters, starting with the basis for a human influence on climate in Chapter 2: Physical Drivers of Climate Change.

Throughout this report, we also analyze projections of future changes in climate. As discussed in Chapter 4, beyond the next few decades, the magnitude of climate change depends primarily on cumulative emissions of greenhouse gases and aerosols and the sensitivity of the climate system to those emissions. Predicting how climate will change in future decades is a different scientific issue from predicting weather a few weeks from now. Local weather is short term, with limited predictability, and is determined by the complicated movement and interaction of high pressure and low pressure systems in the atmosphere; thus, it is difficult to forecast day-to-day

changes beyond about two weeks into the future. Climate, on the other hand, is the statistics of weather – meaning not just average values but also the prevalence and intensity of extremes – as observed over a period of decades. Climate emerges from the interaction, over time, of rapidly changing local weather and more slowly changing regional and global influences, such as the distribution of heat in the oceans, the amount of energy reaching Earth from the sun, and the composition of the atmosphere. See Chapter 4: Projections and later chapters for more on climate projections.

Throughout this report, we include many findings that further strengthen or add to the understanding of climate change relative to those found in NCA3 and other assessments of the science. Several of these are highlighted in an “Advances Since NCA3” box at the end of this chapter.

1.2 Indicators of a Globally Changing Climate

Highly diverse types of direct measurements made on land, sea, and in the atmosphere over many decades have allowed scientists to conclude with high confidence that global mean temperature is increasing. Observational datasets for many other climate variables support the conclusion with high confidence that the global climate is changing (also see EPA 2016¹⁴).^{15,16} Figure 1.1 depicts several of the observational indicators that demonstrate trends consistent with a warming planet over the last century. Temperatures in the lower atmosphere and ocean have increased, as have near-surface humidity and sea level. Not only has ocean heat content increased dramatically (Figure 1.1), but more than 90% of the energy gained in the combined ocean-atmosphere system over recent decades has gone into the ocean.^{17,18} Five different observational datasets show the heat content of the oceans is increasing.



Indicators of Warming from Multiple Datasets

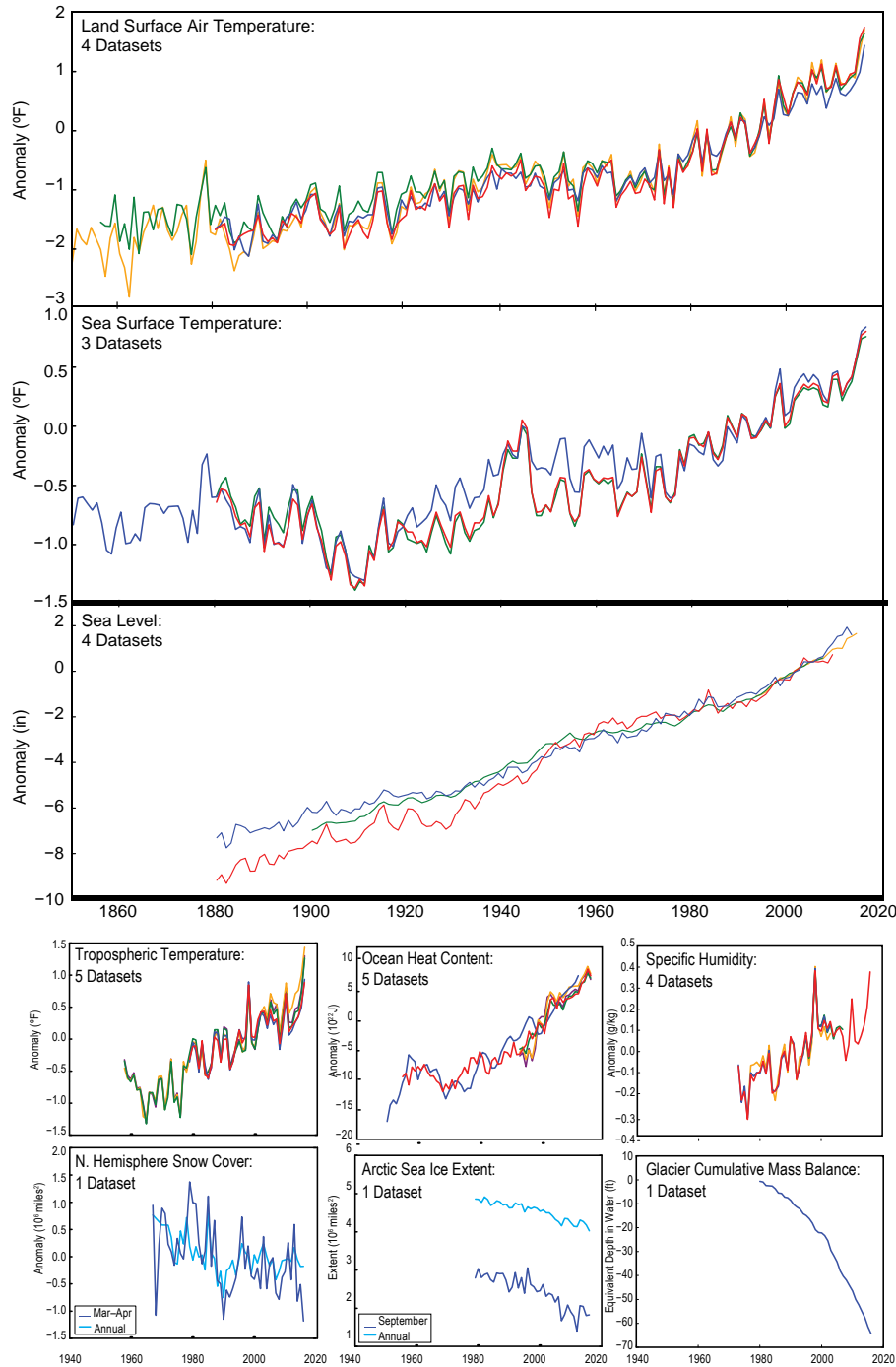


Figure 1.1: This image shows observations globally from nine different variables that are key indicators of a warming climate. The indicators (listed below) all show long-term trends that are consistent with global warming. In parentheses are the number of datasets shown in each graph, the length of time covered by the combined datasets and their anomaly reference period (where applicable), and the direction of the trend: land surface air temperature (4 datasets, 1850–2016 relative to 1976–2005, increase); sea surface temperature (3 datasets, 1850–2016 relative to 1976–2005, increase); sea level (4 datasets, 1880–2014 relative to 1996–2005, increase); tropospheric temperature (5 datasets, 1958–2016 relative to 1981–2005, increase); ocean heat content, upper 700m (5 datasets, 1950–2016 relative to 1996–2005, increase); specific humidity (4 datasets, 1973–2016 relative to 1980–2003, increase); Northern Hemisphere snow cover, March–April and annual (1 dataset, 1967–2016 relative to 1976–2005, decrease); arctic sea ice extent, September and annual (1 dataset, 1979–2016, decrease); glacier cumulative mass balance (1 dataset, 1980–2016, decrease). More information on the datasets can be found in the accompanying metadata. (Figure source: NOAA NCEI and CICS-NC, updated from Melillo et al. 2014;¹⁴⁴ Blunden and Arndt 2016¹⁵).

Basic physics tells us that a warmer atmosphere can hold more water vapor; this is exactly what is measured from satellite data. At the same time, a warmer world means higher evaporation rates and major changes to the hydrological cycle (e.g., Kundzewicz 2008;¹⁹ IPCC 2013¹), including increases in the prevalence of torrential downpours. In addition, arctic sea ice, mountain glaciers, and Northern Hemisphere spring snow cover have all decreased. The relatively small increase in Antarctic sea ice in the 15-year period from 2000 through early 2016 appears to be best explained as being due to localized natural variability (see e.g., Meehl et al. 2016;¹⁶ Ramsayer 2014²⁰); while possibly also related to natural variability, the 2017 Antarctic sea ice minimum reached in early March was the lowest measured since reliable records began in 1979. The vast majority of the glaciers in the world are losing mass at significant rates. The two largest ice sheets on our planet—on the land masses of Greenland and Antarctica—are shrinking.

Many other indicators of the changing climate have been determined from other observations—for example, changes in the growing season and the allergy season (see e.g., EPA 2016;¹⁴ USGCRP 2017²¹). In general, the indicators demonstrate continuing changes in climate since the publication of NCA3. As with temperature, independent researchers have analyzed each of these indicators and come to the same conclusion: all of these changes paint a consistent and compelling picture of a warming planet.

1.3 Trends in Global Temperatures

Global annual average temperature (as calculated from instrumental records over both land and oceans; used interchangeably with global average temperature in the discussion below) has increased by more than 1.2°F (0.7°C) for the period 1986–2016 relative to

1901–1960 (Figure 1.2); see Vose et al.²² for discussion on how global annual average temperature is derived by scientists. The linear regression change over the entire period from 1901–2016 is 1.8°F (1.0°C). Global average temperature is not expected to increase smoothly over time in response to the human warming influences, because the warming trend is superimposed on natural variability associated with, for example, the El Niño/La Niña ocean-heat oscillations and the cooling effects of particles emitted by volcanic eruptions. Even so, 16 of the 17 warmest years in the instrumental record (since the late 1800s) occurred in the period from 2001 to 2016 (1998 was the exception). Global average temperature for 2016 has now surpassed 2015 by a small amount as the warmest year on record. The year 2015 far surpassed 2014 by 0.29°F (0.16°C), four times greater than the difference between 2014 and the next warmest year, 2010.²³ Three of the four warmest years on record have occurred since the analyses through 2012 were reported in NCA3.

A strong El Niño contributed to 2015's record warmth.¹⁵ Though an even more powerful El Niño occurred in 1998, the global temperature in that year was significantly lower (by 0.49°F [0.27°C]) than that in 2015. This suggests that human-induced warming now has a stronger influence on the occurrence of record temperatures than El Niño events. In addition, the El Niño/La Niña cycle may itself be affected by the human influence on Earth's climate system.^{3,24} It is the complex interaction of natural sources of variability with the continuously growing human warming influence that is now shaping Earth's weather and, as a result, its climate.

Globally, the persistence of the warming over the past 60 years far exceeds what can be accounted for by natural variability alone.¹ That does not mean, of course, that natural sources



Global Land and Ocean Temperature Anomalies

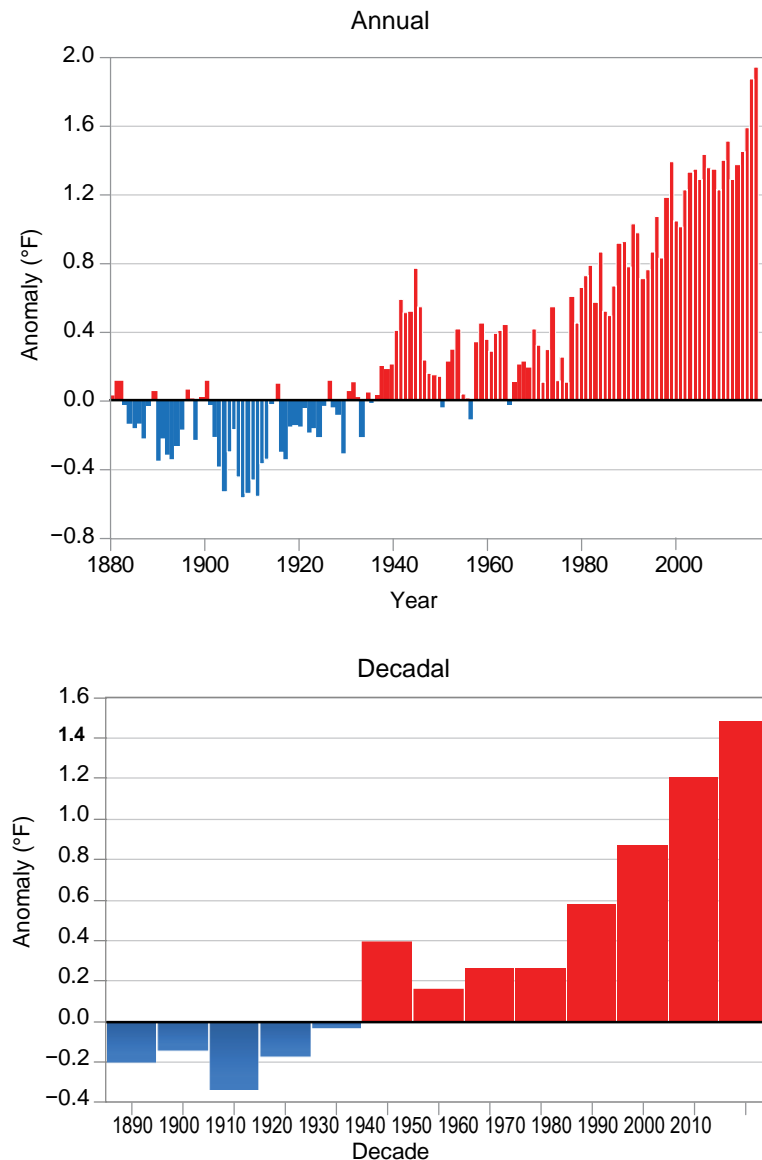


Figure 1.2: Top: Global annual average temperatures (as measured over both land and oceans) for 1880–2016 relative to the reference period of 1901–1960; red bars indicate temperatures above the average over 1901–1960, and blue bars indicate temperatures below the average. Global annual average temperature has increased by more than 1.2°F (0.7°C) for the period 1986–2016 relative to 1901–1960. While there is a clear long-term global warming trend, some years do not show a temperature increase relative to the previous year, and some years show greater changes than others. These year-to-year fluctuations in temperature are mainly due to natural sources of variability, such as the effects of El Niños, La Niñas, and volcanic eruptions. Based on the NCEI (NOAAGlobalTemp) dataset (updated from Vose et al.²²) Bottom: Global average temperature averaged over decadal periods (1886–1895, 1896–1905, ..., 1996–2005, except for the 11 years in the last period, 2006–2016). Horizontal label indicates midpoint year of decadal period. Every decade since 1966–1975 has been warmer than the previous decade. (Figure source: [top] adapted from NCEI 2016,²³ [bottom] NOAA NCEI and CICS-NC).

of variability have become insignificant. They can be expected to continue to contribute a degree of “bumpiness” in the year-to-year global average temperature trajectory, as well as exert influences on the average rate of warming that can last a decade or more (see Box 1.1).^{25, 26, 27}

Warming during the first half of the 1900s occurred mostly in the Northern Hemisphere.²⁸ Recent decades have seen greater warming in response to accelerating increases in green-

house gas concentrations, particularly at high northern latitudes, and over land as compared to the ocean (see Figure 1.3). In general, winter is warming faster than summer (especially in northern latitudes). Also, nights are warming faster than days.^{29, 30} There is also some evidence of faster warming at higher elevations.³¹

Most ocean areas around Earth are warming (see Ch. 13: Ocean Changes). Even in the absence of significant ice melt, the ocean is expected to warm more slowly given its larger

Surface Temperature Change

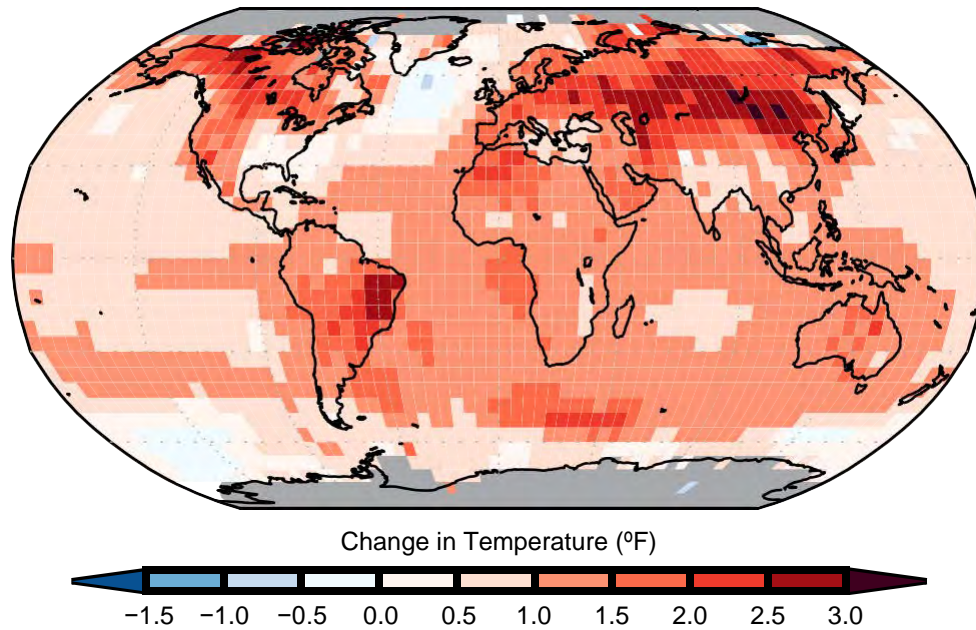


Figure 1.3: Surface temperature change (in °F) for the period 1986–2015 relative to 1901–1960 from the NOAA National Centers for Environmental Information’s (NCEI) surface temperature product. For visual clarity, statistical significance is not depicted on this map. Changes are generally significant (at the 90% level) over most land and ocean areas. Changes are not significant in parts of the North Atlantic Ocean, the South Pacific Ocean, and the southeastern United States. There is insufficient data in the Arctic Ocean and Antarctica for computing long-term changes (those sections are shown in gray because no trend can be derived). The relatively coarse resolution ($5.0^\circ \times 5.0^\circ$) of these maps does not capture the finer details associated with mountains, coastlines, and other small-scale effects (see Ch. 6: Temperature Changes for a focus on the United States). (Figure source: updated from Vose et al. 2012²²).

heat capacity, leading to land–ocean differences in warming (as seen in Figure 1.3). As a result, the climate for land areas often responds more rapidly than the ocean areas, even though the forcing driving a change in climate occurs equally over land and the oceans.¹ A few regions, such as the North Atlantic Ocean, have experienced cooling over the last century, though these areas have warmed over recent decades. Regional climate variability is important to determining potential effects of climate change on the ocean circulation (e.g., Hurrell and Deser 2009;³² Hoegh-Guldberg et al. 2014³³) as are the effects of the increasing freshwater in the North Atlantic from melting of sea and land ice.³⁴

Figure 1.4 shows the projected changes in globally averaged temperature for a range of future pathways that vary from assuming strong continued dependence on fossil fuels in energy and transportation systems over the 21st century (the high scenario is Representative Concentration Pathway 8.5, or RCP8.5) to assuming major emissions reduction (the even lower scenario, RCP2.6). Chapter 4: Projections describes the future scenarios and the models of Earth’s climate system being used to quantify the impact of human choices and natural variability on future climate. These analyses also suggest that global surface temperature increases for the end of the 21st century are *very likely* to exceed 1.5°C (2.7°F) relative to the 1850–1900 average for all projections, with the exception of the lowest part of the uncertainty range for RCP2.6.^{1, 35, 36, 37}

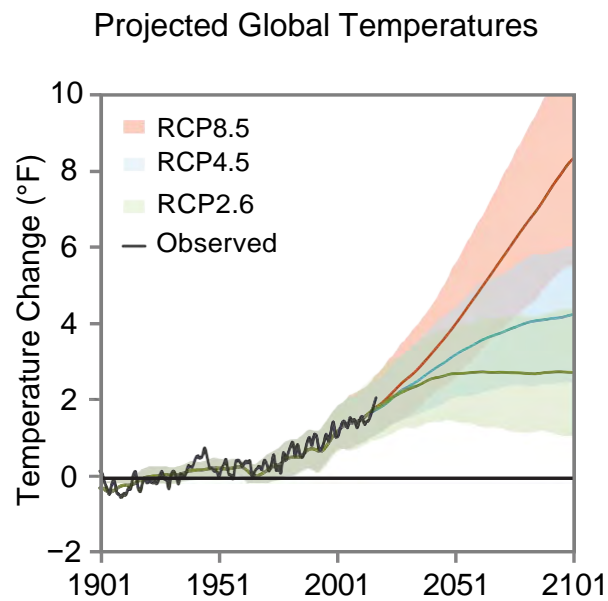


Figure 1.4: Multimodel simulated time series from 1900 to 2100 for the change in global annual mean surface temperature relative to 1901–1960 for a range of the Representative Concentration Pathways (RCPs; see Ch. 4: Projections for more information). These scenarios account for the uncertainty in future emissions from human activities (as analyzed with the 20+ models from around the world used in the most recent international assessment¹). The mean (solid lines) and associated uncertainties (shading, showing ± 2 standard deviations [5%–95%] across the distribution of individual models based on the average over 2081–2100) are given for all of the RCP scenarios as colored vertical bars. The numbers of models used to calculate the multimodel means are indicated. (Figure source: adapted from Walsh et al. 2014²⁰¹).

Box 1.1: Was there a “Hiatus” in Global Warming?

Natural variability in the climate system leads to year-to-year and decade-to-decade changes in global mean temperature. For short enough periods of time, this variability can lead to temporary slowdowns or even reversals in the globally-averaged temperature increase. Focusing on overly short periods can lead to incorrect conclusions about longer-term changes. Over the past decade, such a slowdown led to numerous assertions about a “hiatus” (a period of zero or negative temperature trend) in global warming over the previous 1.5 decades, which is not found when longer periods are analyzed (see Figure 1.5).³⁸ Thus the surface and tropospheric temperature records do not support the assertion that long-term (time periods of 25 years or longer) global warming has ceased or substantially slowed,^{39,40} a conclusion further reinforced by recently updated and improved datasets.^{26, 41, 42, 43}

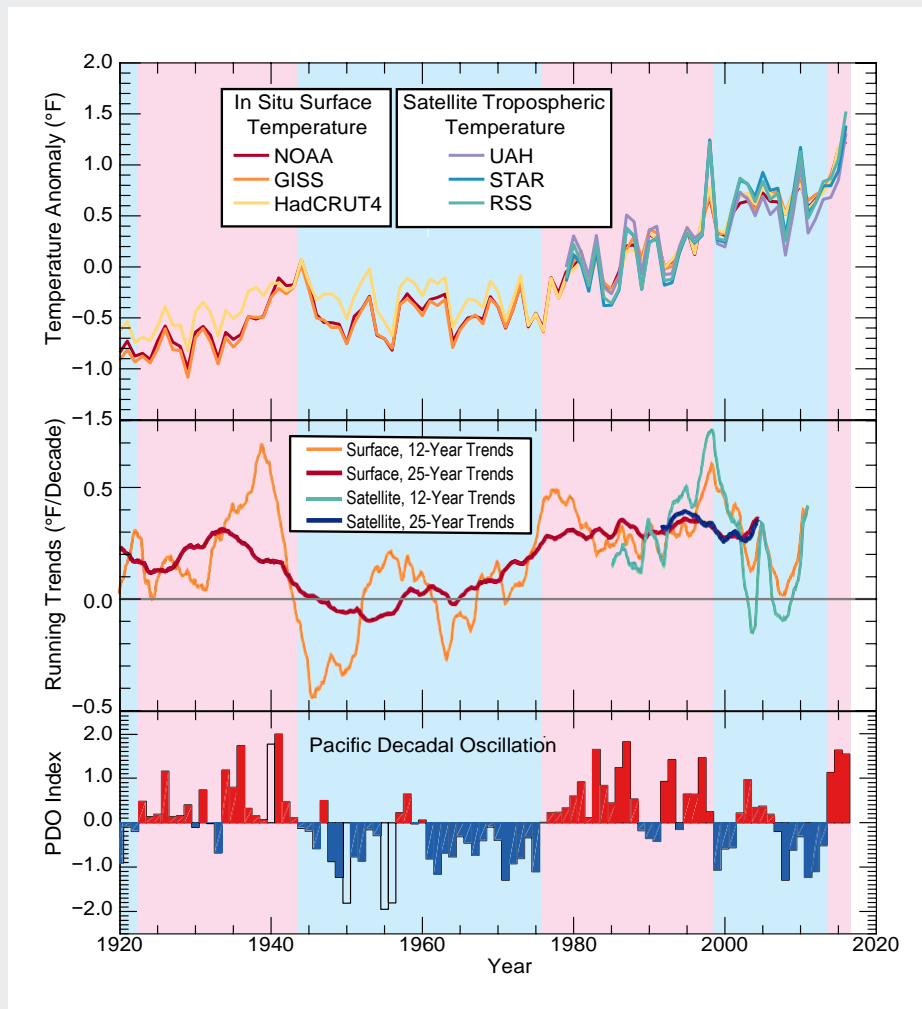


Figure 1.5: Panel A shows the annual mean temperature anomalies relative to a 1901–1960 baseline for global mean surface temperature and global mean tropospheric temperature. Short-term variability is superposed on a long-term warming signal, particularly since the 1960s. Panel B shows the linear trend of short (12-year) and longer (25-year) overlapping periods plotted at the time of the center of the trend period. For the longer period, trends are positive and nearly constant since about 1975. Panel C shows the annual mean Pacific Decadal Oscillation (PDO) index. Short-term temperature trends show a marked tendency to be lower during periods of generally negative PDO index, shown by the blue shading. (Figure source: adapted and updated from Trenberth 2015³ and Santer et al. 2017;³⁸ Panel B, © American Meteorological Society. Used with permission.)

(continued on next page)

Box 1.1 (continued)

For the 15 years following the 1997–1998 El Niño–Southern Oscillation (ENSO) event, the observed rate of temperature increase was smaller than the underlying long-term increasing trend on 30-year climate time scales,⁴⁴ even as other measures of global warming such as ocean heat content (see Ch. 13: Ocean Changes) and arctic sea ice extent (see Ch. 12: Sea Level Rise) continued to change.⁴⁵ Variation in the rate of warming on this time scale is not unexpected and can be the result of long-term internal variability in the climate system, or short-term changes in climate forcings such as aerosols or solar irradiance. Temporary periods similar or larger in magnitude to the current slowdown have occurred earlier in the historical record.

Even though such slowdowns are not unexpected, the slowdown of the early 2000s has been used as informal evidence to cast doubt on the accuracy of climate projections from CMIP5 models, since the measured rate of warming in all surface and tropospheric temperature datasets from 2000 to 2014 was less than expected given the results of the CMIP3 and CMIP5 historical climate simulations.³⁸ Thus, it is important to explore a physical explanation of the recent slowdown and to identify the relative contributions of different factors.

Numerous studies have investigated the role of natural modes of variability and how they affected the flow of energy in the climate system of the post-2000 period.^{16, 46, 47, 48, 49} For the 2000–2013 time period, they find

- In the Pacific Ocean, a number of interrelated features, including cooler than expected tropical ocean surface temperatures, stronger than normal trade winds, and a shift to the cool phase of the Pacific Decadal Oscillation (PDO) led to cooler than expected surface temperatures in the Eastern Tropical Pacific, a region that has been shown to have an influence on global-scale climate.⁴⁹
- For most of the world’s oceans, heat was transferred from the surface into the deeper ocean,^{46, 47, 50, 51} causing a reduction in surface warming worldwide.
- Other studies attributed part of the cause of the measurement/model discrepancy to natural fluctuations in radiative forcings, such as volcanic aerosols, stratospheric water vapor, or solar output.^{52, 53, 54, 55, 56}

When comparing model predictions with measurements, it is important to note that the CMIP5 runs used an assumed representation of these factors for time periods after 2000, possibly leading to errors, especially in the year-to-year simulation of internal variability in the oceans. It is *very likely* that the early 2000s slowdown was caused by a combination of short-term variations in forcing and internal variability in the climate system, though the relative contribution of each is still an area of active research .

Although 2014 already set a new high in globally averaged temperature record up to that time, in 2015–2016, the situation changed dramatically. A switch of the PDO to the positive phase, combined with a strong El Niño event during the fall and winter of 2015–2016, led to months of record-breaking globally averaged temperatures in both the surface and satellite temperature records (see Figure 1.5),³ bringing observed temperature trends into better agreement with model expectations (see Figure 1.6).

(continued on next page)



Box 1.1 (continued)

On longer time scales, observed temperature changes and model simulations are more consistent. The observed temperature changes on longer time scales have also been attributed to anthropogenic causes with high confidence (see Ch. 3: Detection and Attribution for further discussion).⁶ The pronounced globally averaged surface temperature record of 2015 and 2016 appear to make recent observed temperature changes more consistent with model simulations—including with CMIP5 projections that were (notably) developed in advance of occurrence of the 2015–2016 observed anomalies (Figure 1.6). A second important point illustrated by Figure 1.6 is the broad overall agreement between observations and models on the century time scale, which is robust to the shorter-term variations in trends in the past decade or so. Continued global warming and the frequent setting of new high global mean temperature records or near-records is consistent with expectations based on model projections of continued anthropogenic forcing toward warmer global mean conditions.

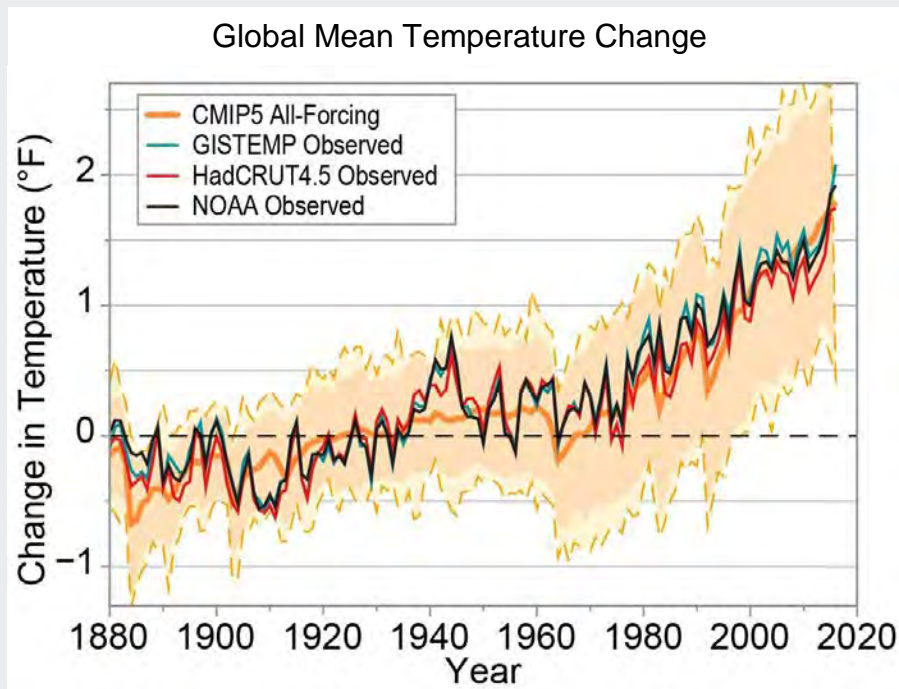


Figure 1.6: Comparison of global mean temperature anomalies (°F) from observations (through 2016) and the CMIP5 multimodel ensemble (through 2016), using the reference period 1901–1960. The CMIP5 multimodel ensemble (orange range) is constructed from blended surface temperature (ocean regions) and surface air temperature (land regions) data from the models, masked where observations are not available in the GISTEMP dataset.²⁷ The importance of using blended model data is shown in Richardson et al.⁴² The thick solid orange curve is the model ensemble mean, formed from the ensemble across 36 models of the individual model ensemble means. The shaded region shows the \pm two standard deviation range of the individual ensemble member annual means from the 36 CMIP5 models. The dashed lines show the range from maximum to minimum values for each year among these ensemble members. The sources for the three observational indices are: HadCRUT4.5 (red): <http://www.metoffice.gov.uk/hadobs/hadcrut4/data/current/download.html>; NOAA (black): <https://www.ncdc.noaa.gov/monitoring-references/faq/anomalies.php>; and GISTEMP (blue): https://data.giss.nasa.gov/pub/gistemp/gistemp1200_ERSSTv4.nc. (NOAA and HadCRUT4 downloaded on Feb. 15, 2017; GISTEMP downloaded on Feb. 10, 2017). (Figure source: adapted from Knutson et al. 2016²⁷).

1.4 Trends in Global Precipitation

Annual averaged precipitation across global land areas exhibits a slight rise (that is not statistically significant because of a lack of data coverage early in the record) over the past century (see Figure 1.7) along with ongoing increases in atmospheric moisture levels. Inter-annual and interdecadal variability is clearly found in all precipitation evaluations, owing to factors such as the North Atlantic Oscillation (NAO) and ENSO—note that precipitation reconstructions are updated operationally by NOAA NCEI on a monthly basis.^{57,58}

The hydrological cycle and the amount of global mean precipitation is primarily controlled by the atmosphere's energy budget and its interactions with clouds.⁵⁹ The amount of global mean precipitation also changes as a result of a mix of fast and slow atmospheric responses to the changing climate.⁶⁰ In the long term, increases in tropospheric radiative effects from increasing amounts of atmospheric CO₂ (i.e., increasing CO₂ leads to greater energy absorbed by the atmosphere and

re-emitted to the surface, with the additional transport to the atmosphere coming by convection) must be balanced by increased latent heating, resulting in precipitation increases of approximately 0.55% to 0.72% per °F (1% to 3% per °C).^{1, 61} Global atmospheric water vapor should increase by about 6%–7% per °C of warming based on the Clausius–Clapeyron relationship (see Ch. 2: Physical Drivers of Climate Change); satellite observations of changes in precipitable water over oceans have been detected at about this rate and attributed to human-caused changes in the atmosphere.⁶² Similar observed changes in land-based measurements have also been attributed to the changes in climate from greenhouse gases.⁶³

Earlier studies suggested a climate change pattern of wet areas getting wetter and dry areas getting drier (e.g., Greve et al. 2014⁶⁴). While Hadley Cell expansion should lead to more drying in the subtropics, the poleward shift of storm tracks should lead to enhanced wet regions. While this high/low rainfall behavior appears to be valid over ocean areas,

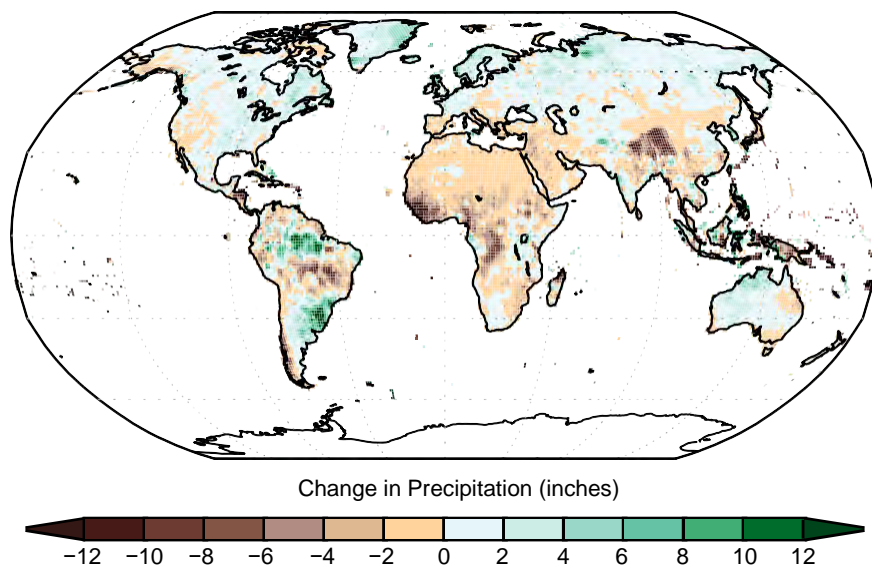


Figure 1.7: Surface annually averaged precipitation change (in inches) for the period 1986–2015 relative to 1901–1960. The data is from long-term stations, so precipitation changes over the ocean and Antarctica cannot be evaluated. The trends are not considered to be statistically significant because of a lack of data coverage early in the record. The relatively coarse resolution ($0.5^\circ \times 0.5^\circ$) of these maps does not capture the finer details associated with mountains, coastlines, and other small-scale effects. (Figure source: NOAA NCEI and CICS-NC).

changes over land are more complicated. The wet versus dry pattern in observed precipitation has only been attributed for the zonal mean^{65,66} and not regionally due to the large amount of spatial variation in precipitation changes as well as significant natural variability. The detected signal in zonal mean precipitation is largest in the Northern Hemisphere, with decreases in the subtropics and increases at high latitudes. As a result, the observed increase (about 5% since the 1950s^{67,68}) in annual averaged arctic precipitation have been detected and attributed to human activities.⁶⁹

1.5 Trends in Global Extreme Weather Events

A change in the frequency, duration, and/or magnitude of extreme weather events is one of the most important consequences of a warming climate. In statistical terms, a small shift in the mean of a weather variable, with or without this shift occurring in concert with a change in the shape of its probability distribution, can cause a large change in the probability of a value relative to an extreme threshold (see Figure 1.8 in IPCC 2013¹).⁷⁰ Examples include extreme high temperature events and heavy precipitation events. Some of the other extreme events, such as intense tropical cyclones, midlatitude cyclones, lightning, and hail and tornadoes associated with thunderstorms can occur as more isolated events and generally have more limited temporal and spatial observational datasets, making it more difficult to study their long-term trends. Detecting trends in the frequency and intensity of extreme weather events is challenging.⁷¹ The most intense events are rare by definition, and observations may be incomplete and suffer from reporting biases. Further discussion on trends and projections of extreme events for the United States can be found in Chapters 6–9 and 11.

An emerging area in the science of detection and attribution has been the attribution of

extreme weather and climate events. Extreme event attribution generally addresses the question of whether climate change has altered the odds of occurrence of an extreme event like one just experienced. Attribution of extreme weather events under a changing climate is now an important and highly visible aspect of climate science. As discussed in a recent National Academy of Sciences (NAS) report,⁷² the science of event attribution is rapidly advancing, including the understanding of the mechanisms that produce extreme events and the development of methods that are used for event attribution. Several other reports and papers have reviewed the topic of extreme event attribution.^{73,74,75} This report briefly reviews extreme event attribution methodologies in practice (Ch. 3: Detection and Attribution) and provides a number of examples within the chapters on various climate phenomena (especially relating to the United States in Chapters 6–9).

Extreme Heat and Cold

The frequency of multiday heat waves and extreme high temperatures at both daytime and nighttime hours is increasing over many of the global land areas.¹ There are increasing areas of land throughout our planet experiencing an excess number of daily highs above given thresholds (for example, the 90th percentile), with an approximate doubling of the world's land area since 1998 with 30 extreme heat days per year.⁷⁶ At the same time, frequencies of cold waves and extremely low temperatures are decreasing over the United States and much of the earth. In the United States, the number of record daily high temperatures has been about double the number of record daily low temperatures in the 2000s,⁷⁷ and much of the United States has experienced decreases of 5%–20% per decade in cold wave frequency.^{1,75}

The enhanced radiative forcing caused by greenhouse gases has a direct influence on



heat extremes by shifting distributions of daily temperature.⁷⁸ Recent work indicates changes in atmospheric circulation may also play a significant role (see Ch. 5: Circulation and Variability). For example, a recent study found that increasing anticyclonic circulations partially explain observed trends in heat events over North America and Eurasia, among other effects.⁷⁹ Observed changes in circulation may also be the result of human influences on climate, though this is still an area of active research.

Extreme Precipitation

A robust consequence of a warming climate is an increase in atmospheric water vapor, which exacerbates precipitation events under similar meteorological conditions, meaning that when rainfall occurs, the amount of rain falling in that event tends to be greater. As a result, what in the past have been considered to be extreme precipitation events are becoming more frequent.^{1, 80, 81, 82} On a global scale, the observational annual-maximum daily precipitation has increased by 8.5% over the last 110 years; global climate models also derive an increase in extreme precipitation globally but tend to underestimate the rate of the observed increase.^{80, 82, 83} Extreme precipitation events are increasing in frequency globally over both wet and dry regions.⁸² Although more spatially heterogeneous than heat extremes, numerous studies have found increases in precipitation extremes on many regions using a variety of methods and threshold definitions,⁸⁴ and those increases can be attributed to human-caused changes to the atmosphere.^{85, 86} Finally, extreme precipitation associated with tropical cyclones (TCs) is expected to increase in the future,⁸⁷ but current trends are not clear.⁸⁴

The impact of extreme precipitation trends on flooding globally is complex because additional factors like soil moisture and changes in land cover are important.⁸⁸ Globally, due to

limited data, there is low confidence for any significant current trends in river-flooding associated with climate change,⁸⁹ but the magnitude and intensity of river flooding is projected to increase in the future.⁹⁰ More on flooding trends in the United States is in Chapter 8: Droughts, Floods, and Wildfires.

Tornadoes and Thunderstorms

Increasing air temperature and moisture increase the risk of extreme convection, and there is evidence for a global increase in severe thunderstorm conditions.⁹¹ Strong convection, along with wind shear, represents favorable conditions for tornadoes. Thus, there is reason to expect increased tornado frequency and intensity in a warming climate.⁹² Inferring current changes in tornado activity is hampered by changes in reporting standards, and trends remain highly uncertain (see Ch. 9: Extreme Storms).⁸⁴

Winter Storms

Winter storm tracks have shifted slightly northward (by about 0.4 degrees latitude) in recent decades over the Northern Hemisphere.⁹³ More generally, extratropical cyclone activity is projected to change in complex ways under future climate scenarios, with increases in some regions and seasons and decreases in others. There are large model-to-model differences among CMIP5 climate models, with some models underestimating the current cyclone track density.^{94, 95}

Enhanced arctic warming (arctic amplification), due in part to sea ice loss, reduces lower tropospheric meridional temperature gradients, diminishing baroclinicity (a measure of how misaligned the gradient of pressure is from the gradient of air density) – an important energy source for extratropical cyclones. At the same time, upper-level meridional temperature gradients will increase due to a warming tropical upper troposphere and a cooling high-latitude lower stratosphere.





While these two effects counteract each other with respect to a projected change in midlatitude storm tracks, the simulations indicate that the magnitude of arctic amplification may modulate some aspects (e.g., jet stream position, wave extent, and blocking frequency) of the circulation in the North Atlantic region in some seasons.⁹⁶

Tropical Cyclones

Detection and attribution of trends in past tropical cyclone (TC) activity is hampered by uncertainties in the data collected prior to the satellite era and by uncertainty in the relative contributions of natural variability and anthropogenic influences. Theoretical arguments and numerical modeling simulations support an expectation that radiative forcing by greenhouse gases and anthropogenic aerosols can affect TC activity in a variety of ways, but robust formal detection and attribution for past observed changes has not yet been realized. Since the IPCC AR5,¹ there is new evidence that the locations where tropical cyclones reach their peak intensity have migrated poleward in both the Northern and Southern Hemispheres, in concert with the independently measured expansion of the tropics.⁹⁷ In the western North Pacific, this migration has substantially changed the tropical cyclone hazard exposure patterns in the region and appears to have occurred outside of the historically measured modes of regional natural variability.⁹⁸

Whether global trends in high-intensity tropical cyclones are already observable is a topic of active debate. Some research suggests positive trends,^{99,100} but significant uncertainties remain (see Ch. 9: Extreme Storms).¹⁰⁰ Other studies have suggested that aerosol pollution has masked the increase in TC intensity expected otherwise from enhanced greenhouse warming.^{101,102}

Tropical cyclone intensities are expected to increase with warming, both on average and at the high end of the scale, as the range of achievable intensities expands, so that the most intense storms will exceed the intensity of any in the historical record.¹⁰² Some studies have projected an overall increase in tropical cyclone activity.¹⁰³ However, studies with high-resolution models are giving a different result. For example, a high-resolution dynamical downscaling study of global TC activity under the lower scenario (RCP4.5) projects an increased occurrence of the highest-intensity tropical cyclones (Saffir–Simpson Categories 4 and 5), along with a reduced overall tropical cyclone frequency, though there are considerable basin-to-basin differences.⁸⁷ Chapter 9: Extreme Storms covers more on extreme storms affecting the United States.

1.6 Global Changes in Land Processes

Changes in regional land cover have had important effects on climate, while climate change also has important effects on land cover (also see Ch. 10: Land Cover).¹ In some cases, there are changes in land cover that are both consequences of and influences on global climate change (e.g., declines in land ice and snow cover, thawing permafrost, and insect damage to forests).

Northern Hemisphere snow cover extent has decreased, especially in spring, primarily due to earlier spring snowmelt (by about 0.2 million square miles [0.5 million square km]^{104,105}), and this decrease since the 1970s is at least partially driven by anthropogenic influences.¹⁰⁶ Snow cover reductions, especially in the Arctic region in summer, have led to reduced seasonal albedo.¹⁰⁷

While global-scale trends in drought are uncertain due to insufficient observations, regional trends indicate increased frequency and intensity of drought and aridification on land cover in the Mediterranean^{108,109} and West

Africa^{110, 111} and decreased frequency and intensity of droughts in central North America¹¹² and northwestern Australia.^{110, 111, 113}

Anthropogenic land-use changes, such as deforestation and growing cropland extent, have increased the global land surface albedo, resulting in a small cooling effect. Effects of other land-use changes, including modifications of surface roughness, latent heat flux, river runoff, and irrigation, are difficult to quantify, but may offset the direct land-use albedo changes.^{114, 115}

Globally, land-use change since 1750 has been typified by deforestation, driven by the growth in intensive farming and urban development. Global land-use change is estimated to have released 190 ± 65 GtC (gigatonnes of carbon) through 2015.^{116, 117} Over the same period, cumulative fossil fuel and industrial emissions are estimated to have been 410 ± 20 GtC, yielding total anthropogenic emissions of 600 ± 70 GtC, of which cumulative land-use change emissions were about 32%.^{116, 117} Tropical deforestation is the dominant driver of land-use change emissions, estimated at 0.1–1.7 GtC per year, primarily from biomass burning. Global deforestation emissions of about 3 GtC per year are compensated by around 2 GtC per year of forest regrowth in some regions, mainly from abandoned agricultural land.^{118, 119}

Natural terrestrial ecosystems are gaining carbon through uptake of CO₂ by enhanced photosynthesis due to higher CO₂ levels, increased nitrogen deposition, and longer growing seasons in mid- and high latitudes. Anthropogenic atmospheric CO₂ absorbed by land ecosystems is stored as organic matter in live biomass (leaves, stems, and roots), dead biomass (litter and woody debris), and soil carbon.

Many studies have documented a lengthening growing season, primarily due to the changing climate,^{120, 121, 122, 123} and elevated CO₂ is expected to further lengthen the growing season in places where the length is water limited.¹²⁴ In addition, a recent study has shown an overall increase in greening of Earth in vegetated regions,¹²⁵ while another has demonstrated evidence that the greening of Northern Hemisphere extratropical vegetation is attributable to anthropogenic forcings, particularly rising atmospheric greenhouse gas levels.¹²⁶ However, observations^{127, 128, 129} and models^{130, 131, 132} indicate that nutrient limitations and land availability will constrain future land carbon sinks.

Modifications to the water, carbon, and biogeochemical cycles on land result in both positive and negative feedbacks to temperature increases.^{114, 133, 134} Snow and ice albedo feedbacks are positive, leading to increased temperatures with loss of snow and ice extent. While land ecosystems are expected to have a net positive feedback due to reduced natural sinks of CO₂ in a warmer world, anthropogenically increased nitrogen deposition may reduce the magnitude of the net feedback.^{131, 135, 136} Increased temperature and reduced precipitation increase wildfire risk and susceptibility of terrestrial ecosystems to pests and disease, with resulting feedbacks on carbon storage. Increased temperature and precipitation, particularly at high latitudes, drives up soil decomposition, which leads to increased CO₂ and CH₄ (methane) emissions.^{137, 138, 139, 140, 141, 142, 143} While some of these feedbacks are well known, others are not so well quantified and yet others remain unknown; the potential for surprise is discussed further in Chapter 15: Potential Surprises.



1.7 Global Changes in Sea Ice, Glaciers, and Land Ice

Since NCA3,¹⁴⁴ there have been significant advances in the understanding of changes in the cryosphere. Observations continue to show declines in arctic sea ice extent and thickness, Northern Hemisphere snow cover, and the volume of mountain glaciers and continental ice sheets.^{1, 145, 146, 147, 148, 149} Evidence suggests in many cases that the net loss of mass from the global cryosphere is accelerating indicating significant climate feedbacks and societal consequences.^{150, 151, 152, 153, 154, 155}

Arctic sea ice areal extent, thickness, and volume have declined since 1979.^{1, 146, 147, 148, 156} The annual arctic sea ice extent minimum for 2016 relative to the long-term record was the second lowest (2012 was the lowest) (<http://nsidc.org/arcticseaicenews/>). The arctic sea ice minimum extents in 2014 and 2015 were also among the lowest on record. Annually averaged arctic sea ice extent has decreased by 3.5%–4.1% per decade since 1979 with much larger reductions in summer and fall.^{1, 146, 148, 157} For example, September sea ice extent decreased by 13.3% per decade between 1979 and 2016. At the same time, September multi-year sea ice has melted faster than perennial sea ice (13.5% ± 2.5% and 11.5% ± 2.1% per decade, respectively, relative to the 1979–2012 average) corresponding to 4–7.5 feet (1.3–2.3 meter) declines in winter sea ice thickness.^{1, 156} October 2016 serves as a recent example of the observed lengthening of the arctic sea ice melt season marking the slowest recorded arctic sea ice growth rate for that month.^{146, 158, 159} The annual arctic sea ice maximum in March 2017 was the lowest maximum areal extent on record (<http://nsidc.org/arcticseaicenews/>).

While current generation climate models project a nearly ice-free Arctic Ocean in late summer by mid-century, they still simulate weaker reductions in volume and extent than

observed, suggesting that projected changes are too conservative.^{1, 147, 160, 161} See Chapter 11: Arctic Changes for further discussion of the implications of changes in the Arctic.

In contrast to the Arctic, sea ice extent around Antarctica has increased since 1979 by 1.2% to 1.8% per decade.¹ Strong regional differences in the sea ice growth rates are found around Antarctica but most regions (about 75%) show increases over the last 30 years.¹⁶² The gain in antarctic sea ice is much smaller than the decrease in arctic sea ice. Changes in wind patterns, ice–ocean feedbacks, and freshwater flux have contributed to antarctic sea ice growth.^{162, 163, 164, 165}

Since the NCA3,¹⁴⁴ the Gravity Recovery and Climate Experiment (GRACE) constellation (e.g., Velicogna and Wahr 2013¹⁶⁶) has provided a record of gravimetric land ice measurements, advancing knowledge of recent mass loss from the global cryosphere. These measurements indicate that mass loss from the Antarctic Ice Sheet, Greenland Ice Sheet, and mountain glaciers around the world continues accelerating in some cases.^{151, 152, 154, 155, 167, 168} The annually averaged ice mass from 37 global reference glaciers has decreased every year since 1984, a decline expected to continue even if climate were to stabilize.^{1, 153, 169, 170}

Ice sheet dynamics in West Antarctica are characterized by land ice that transitions to coastal and marine ice sheet systems. Recent observed rapid mass loss from West Antarctica's floating ice shelves is attributed to increased glacial discharge rates due to diminishing ice shelves from the surrounding ocean becoming warmer.^{171, 172} Recent evidence suggests that the Amundsen Sea sector is expected to disintegrate entirely^{151, 168, 172} raising sea level by at least 1.2 meters (about 4 feet) and potentially an additional foot or more on top of current sea level rise projections during



this century (see Section 1.2.7 and Ch. 12: Sea Level Rise for further details).¹⁷³ The potential for unanticipated rapid ice sheet melt and/or disintegration is discussed further in Chapter 15: Potential Surprises.

Over the last decade, the Greenland Ice Sheet mass loss has accelerated, losing 244 ± 6 Gt per year on average between January 2003 and May 2013.^{1, 155, 174, 175} The portion of the Greenland Ice Sheet experiencing annual melt has increased since 1980 including significant events.^{1, 176, 177, 178} A recent example, an unprecedented 98.6% of the Greenland Ice Sheet surface experienced melt on a single day in July 2012.^{179, 180} Encompassing this event, GRACE data indicate that Greenland lost 562 Gt of mass between April 2012 and April 2013—more than double the average annual mass loss.

In addition, permafrost temperatures and active layer thicknesses have increased across much of the Arctic (also see Ch. 11: Arctic Changes).^{1, 181, 182} Rising permafrost temperatures causing permafrost to thaw and become more discontinuous raises concerns about potential emissions of carbon dioxide and methane.¹ The potentially large contribution of carbon and methane emissions from permafrost and the continental shelf in the Arctic to overall warming is discussed further in Chapter 15: Potential Surprises.

1.8 Global Changes in Sea Level

Statistical analyses of tide gauge data indicate that global mean sea level has risen about 8–9 inches (20–23 cm) since 1880, with a rise rate of approximately 0.5–0.6 inches/decade from 1901 to 1990 (about 12–15 mm/decade; also see Ch. 12: Sea Level Rise).^{183, 184} However, since the early 1990s, both tide gauges and satellite altimeters have recorded a faster rate of sea level rise of about 1.2 inches/decade (approximately 3 cm/decade),^{183, 184, 185} resulting in

about 3 inches (about 8 cm) of the global rise since the early 1990s. Nearly two-thirds of the sea level rise measured since 2005 has resulted from increases in ocean mass, primarily from land-based ice melt; the remaining one-third of the rise is in response to changes in density from increasing ocean temperatures.¹⁸⁶

Global sea level rise and its regional variability forced by climatic and ocean circulation patterns are contributing to significant increases in annual tidal-flood frequencies, which are measured by NOAA tide gauges and associated with minor infrastructure impacts to date; along some portions of the U.S. coast, frequency of the impacts from such events appears to be accelerating (also see Ch. 12: Sea-Level Rise).^{187, 188}

Future projections show that by 2100, global mean sea level is *very likely* to rise by 1.6–4.3 feet (0.5–1.3 m) under the higher scenario (RCP8.5), 1.1–3.1 feet (0.35–0.95 m) under a lower scenario (RCP4.5), and 0.8–2.6 feet (0.24–0.79 m) under an even lower scenario (RCP2.6) (see Ch. 4: Projections for a description of the scenarios).¹⁸⁹ Sea level will not rise uniformly around the coasts of the United States and its oversea territories. Local sea level rise is *likely* to be greater than the global average along the U.S. Atlantic and Gulf Coasts and less than the global average in most of the Pacific Northwest. Emerging science suggests these projections may be underestimates, particularly for higher scenarios; a global mean sea level rise exceeding 8 feet (2.4 m) by 2100 cannot be excluded (see Ch. 12: Sea Level Rise), and even higher amounts are possible as a result of marine ice sheet instability (see Ch. 15: Potential Surprises). We have updated the global sea level rise scenarios for 2100 of Parris et al.¹⁹⁰ accordingly,¹⁹¹ and also extended to year 2200 in Chapter 12: Sea Level Rise. The scenarios are regionalized to better match the decision context needed for local risk framing purposes.



1.9 Recent Global Changes Relative to Paleoclimates

Paleoclimate records demonstrate long-term natural variability in the climate and overlap the records of the last two millennia, referred to here as the “Common Era.” Before the emissions of greenhouse gases from fossil fuels and other human-related activities became a major factor over the last few centuries, the strongest drivers of climate during the last few thousand years had been volcanoes and land-use change (which has both albedo and greenhouse gas emissions effects).¹⁹² Based on a number of proxies for temperature (for example, from tree rings, fossil pollen, corals, ocean and lake sediments, and ice cores), temperature records are available for the last 2,000 years on hemispherical and continental scales (Figures 1.8 and 1.9).^{9,193} High-resolution temperature records for North America extend back less than half of this period, with temperatures in the early parts of the Common Era inferred from analyses of pollen and other archives. For this era, there is a general cooling trend, with a relatively rapid increase in temperature over the last 150–200 years (Figure 1.9,). For context, global annual averaged temperatures for 1986–2015 are likely much higher, and appear to have risen at a more rapid rate during the last 3 decades, than any similar period possibly over the past 2,000 years or longer (IPCC¹ makes a similar statement, but for the last 1,400 years because of data quality issues before that time).

Global temperatures of the magnitude observed recently (and projected for the rest of this century) are related to very different forcings than past climates, but studies of past climates suggest that such global temperatures were *likely* last observed during the Eemian period – the last interglacial – 125,000 years ago; at that time, global temperatures were, at their peak, about 1.8°F–3.6°F (1°C–2°C) warmer than preindustrial temperatures.¹⁹⁴ Coincident with these higher temperatures, sea levels during that period were about 16–30 feet (6–9 meters) higher than modern levels^{195,196} (for further discussion on sea levels in the past, see Ch. 12: Sea Level Rise).

Modeling studies suggest that the Eemian period warming can be explained in part by the hemispheric changes in solar insolation from orbital forcing as a result of cyclic changes in the shape of Earth’s orbit around the sun (e.g., Kaspar et al. 2005¹⁹⁷), even though greenhouse gas concentrations were similar to preindustrial levels. Equilibrium climate with modern greenhouse gas concentrations (about 400 ppm CO₂) most recently occurred 3 million years ago during the Pliocene. During the warmest parts of this period, global temperatures were 5.4°F–7.2°F (3°C–4°C) higher than today, and sea levels were about 82 feet (25 meters) higher.¹⁹⁸



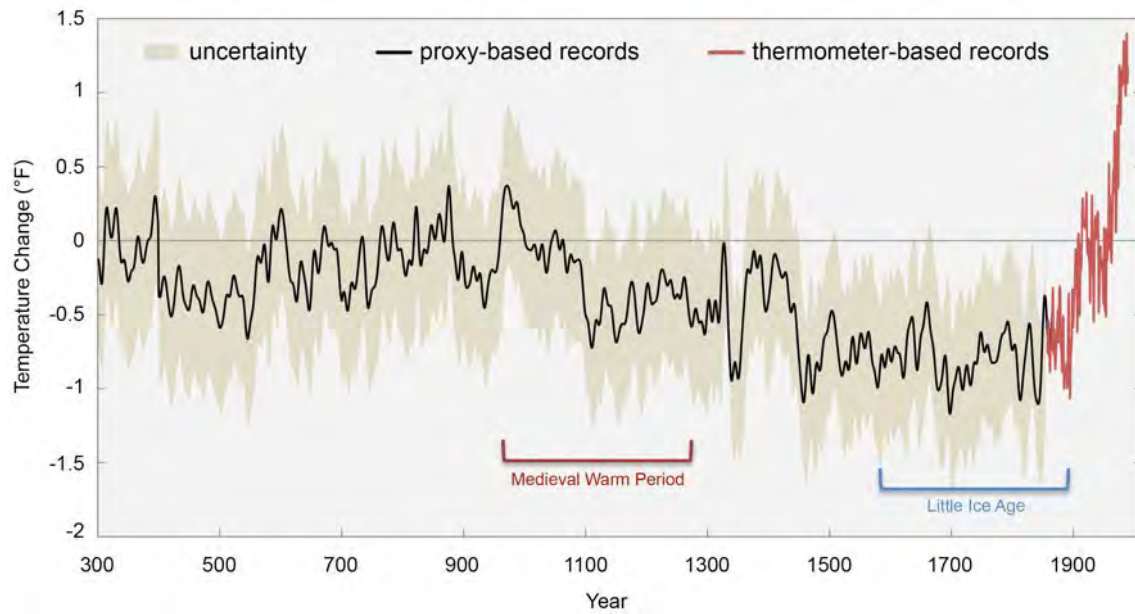


Figure 1.8: Changes in the temperature of the Northern Hemisphere from surface observations (in red) and from proxies (in black; uncertainty range represented by shading) relative to 1961–1990 average temperature. If this graph were plotted relative to 1901–1960 instead of 1961–1990, the temperature changes would be 0.47°F (0.26°C) higher. These analyses suggest that current temperatures are higher than seen in the Northern Hemisphere, and likely globally, in at least the last 1,700 years, and that the last decade (2006–2015) was the warmest decade on record. (Figure source: adapted from Mann et al. 2008¹⁹³).

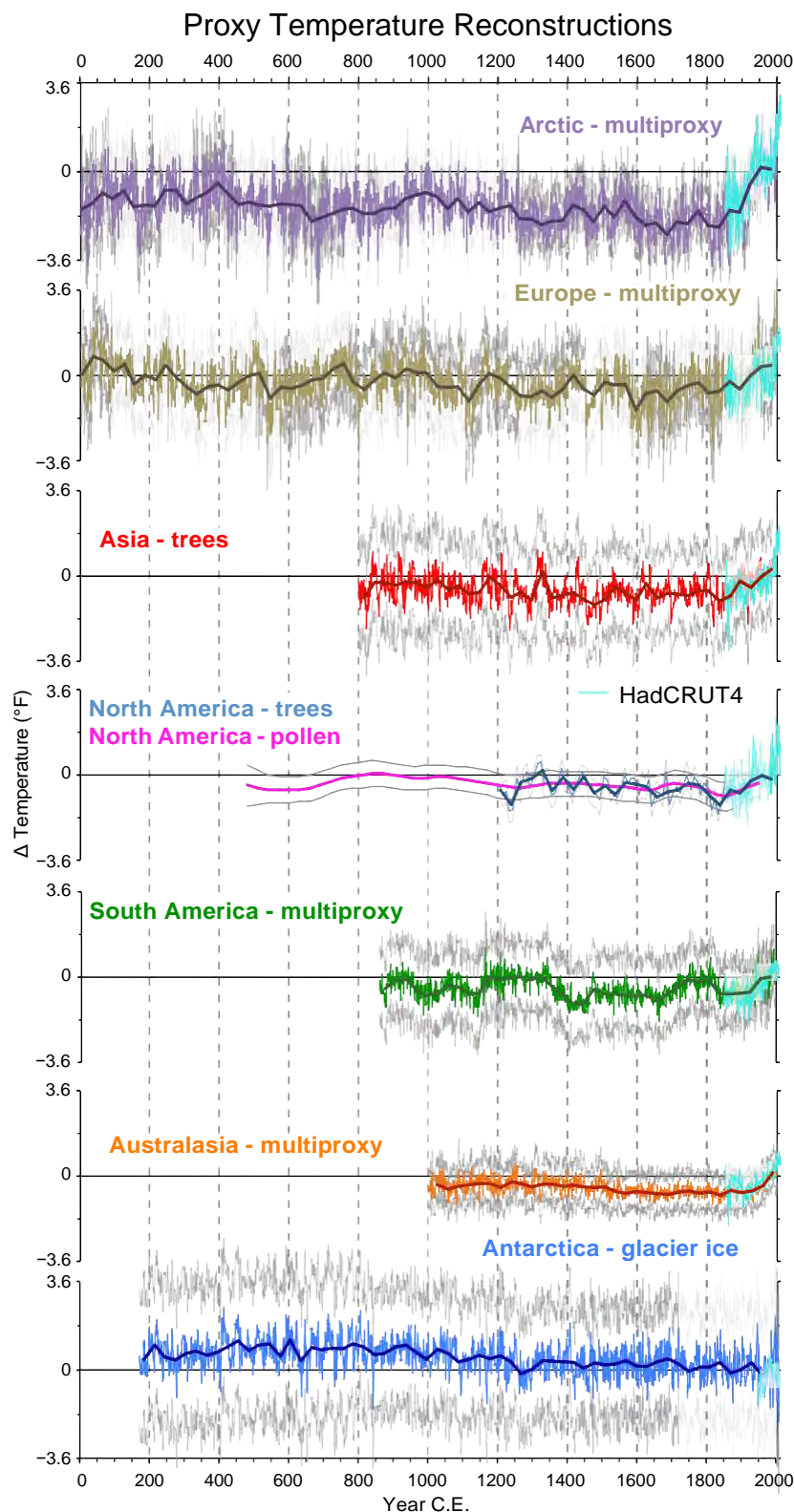


Figure 1.9: Proxy temperatures reconstructions for the seven regions of the PAGES 2k Network. Temperature anomalies are relative to the 1961–1990 reference period. If this graph were plotted relative to 1901–1960 instead of 1961–1990, the temperature changes would be 0.47°F (0.26°C) higher. Gray lines around expected-value estimates indicate uncertainty ranges as defined by each regional group (see PAGES 2k Consortium⁹ and related Supplementary Information). Note that the changes in temperature over the last century tend to occur at a much faster rate than found in the previous time periods. The teal values are from the HadCRUT4 surface observation record for land and ocean for the 1800s to 2000.²⁰² (Figure source: adapted from PAGES 2k Consortium 2013⁹).

Box 1.2: Advances Since NCA3

This assessment reflects both advances in scientific understanding and approach since NCA3, as well as global policy developments. Highlights of what aspects are either especially strengthened or are emerging in the findings include

- *Spatial downscaling*: Projections of climate changes are downscaled to a finer resolution than the original global climate models using the Localized Constructed Analogs (LOCA) empirical statistical downscaling model. The downscaling generates temperature and precipitation on a 1/16th degree latitude/longitude grid for the contiguous United States. LOCA, one of the best statistical downscaling approaches, produces downscaled estimates using a multi-scale spatial matching scheme to pick appropriate analog days from observations (Chapters 4, 6, 7).
- *Risk-based framing*: Highlighting aspects of climate science most relevant to assessment of key societal risks are included more here than in prior national climate assessments. This approach allows for emphasis of possible outcomes that, while relatively unlikely to occur or characterized by high uncertainty, would be particularly consequential, and thus associated with large risks (Chapters 6, 7, 8, 9, 12, 15).
- *Detection and attribution*: Significant advances have been made in the attribution of the human influence for individual climate and weather extreme events since NCA3. This assessment contains extensive discussion of new and emerging findings in this area (Chapters 3, 6, 7, 8).
- *Atmospheric circulation and extreme events*: The extent to which atmospheric circulation in the midlatitudes is changing or is projected to change, possibly in ways not captured by current climate models, is a new important area of research. While still in its formative stages, this research is critically important because of the implications of such changes for climate extremes including extended cold air outbreaks, long-duration heat waves, and changes in storms and drought patterns (Chapters 5, 6, 7).
- *Increased understanding of specific types of extreme events*: How climate change may affect specific types of extreme events in the United States is another key area where scientific understanding has advanced. For example, this report highlights how intense flooding associated with atmospheric rivers could increase dramatically as the atmosphere and oceans warm or how tornadoes could be concentrated into a smaller number of high-impact days over the average severe weather season (Chapter 9).
- *Model weighting*: For the first time, maps and plots of climate projections will not show a straight average of all available climate models. Rather, each model is given a weight based on their 1) historical performance relative to observations and 2) independence relative to other models. Although this is a more accurate way of representing model output, it does not significantly alter the key findings: the weighting produces very similar trends and spatial patterns to the equal-weighting-of-models approach used in prior assessments (Chapters 4, 6, 7, Appendix B).
- *High-resolution global climate model simulations*: As computing resources have grown, multidecadal simulations of global climate models are now being conducted at horizontal resolutions on the order of 15 miles (25 km) that provide more realistic characterization of intense weather systems, including hurricanes. Even the limited number of high-resolution models currently available have increased confidence in projections of extreme weather (Chapter 9).



Box 1.2 (continued)

- *The so-called “global warming hiatus”*: Since NCA3, many studies have investigated causes for the reported slowdown in the rate of increase in near-surface global mean temperature from roughly 2000 through 2013. The slowdown, which ended with the record warmth in 2014–2016, is understood to have been caused by a combination of internal variability, mostly in the heat exchange between the ocean and the atmosphere, and short-term variations in external forcing factors, both human and natural. On longer time scales, relevant to human-induced climate change, there is no hiatus, and the planet continues to warm at a steady pace as predicted by basic atmospheric physics and the well-documented increase in heat-trapping gases (Chapter 1).
- *Oceans and coastal waters*: Ocean acidification, warming, and oxygen loss are all increasing, and scientific understanding of the severity of their impacts is growing. Both oxygen loss and acidification may be magnified in some U.S. coastal waters relative to the global average, raising the risk of serious ecological and economic consequences. There is some evidence, still highly uncertain, that the Atlantic Meridional Circulation (AMOC), sometimes referred to as the ocean’s conveyor belt, may be slowing down (Chapters 2, 13).
- *Local sea level change projections*: For the first time in the NCA process, sea level rise projections incorporate geographic variation based on factors such as local land subsidence, ocean currents, and changes in Earth’s gravitational field (Chapter 12).
- *Accelerated ice-sheet loss*: New observations from many different sources confirm that ice-sheet loss is accelerating. Combining observations with simultaneous advances in the physical understanding of ice sheets, scientists are now concluding that up to 8.5 feet of global sea level rise is possible by 2100 under a higher scenario, up from 6.6 feet in NCA3 (Chapter 12).
- *Low sea-ice areal extent*: The annual arctic sea ice extent minimum for 2016 relative to the long-term record was the second lowest on record. The arctic sea ice minimums in 2014 and 2015 were also amongst the lowest on record. Since 1981, the sea ice minimum has decreased by 13.3% per decade, more than 46% over the 35 years. The annual arctic sea ice maximum in March 2017 was the lowest maximum areal extent on record. (Chapter 11).
- *Potential surprises*: Both large-scale state shifts in the climate system (sometimes called “tipping points”) and compound extremes have the potential to generate unanticipated surprises. The further Earth system departs from historical climate forcings, and the more the climate changes, the greater the potential for these surprises. For the first time in the NCA process we include an extended discussion of these potential surprises (Chapter 15).
- *Mitigation*: This report discusses some important aspects of climate science that are relevant to long-term temperature goals and different mitigation scenarios, including those implied by government announcements for the Paris Agreement. (Chapters 4, 14).



TRACEABLE ACCOUNTS

Key Finding 1

The global climate continues to change rapidly compared to the pace of the natural variations in climate that have occurred throughout Earth's history. Trends in globally averaged temperature, sea level rise, upper-ocean heat content, land-based ice melt, arctic sea ice, depth of seasonal permafrost thaw, and other climate variables provide consistent evidence of a warming planet. These observed trends are robust and have been confirmed by multiple independent research groups around the world.

Description of evidence base

The Key Finding and supporting text summarize extensive evidence documented in the climate science literature. Similar to statements made in previous national (NCA3)¹⁴⁴ and international¹ assessments.

Evidence for changes in global climate arises from multiple analyses of data from in-situ, satellite, and other records undertaken by many groups over several decades. These observational datasets are used throughout this chapter and are discussed further in Appendix 1 (e.g., updates of prior uses of these datasets by Vose et al. 2012;²² Karl et al. 2015²⁶). Changes in the mean state have been accompanied by changes in the frequency and nature of extreme events (e.g., Kunkel and Frankson 2015;⁸¹ Donat et al. 2016⁸²). A substantial body of analysis comparing the observed changes to a broad range of climate simulations consistently points to the necessity of invoking human-caused changes to adequately explain the observed climate system behavior. The influence of human impacts on the climate system has also been observed in a number of individual climate variables (attribution studies are discussed in Ch. 3: Detection and Attribution and in other chapters).

Major uncertainties

Key remaining uncertainties relate to the precise magnitude and nature of changes at global, and particularly regional, scales, and especially for extreme events and our ability to observe these changes at sufficient resolution and to simulate and attribute such changes using climate models. Innovative new approaches to

instigation and maintenance of reference quality observation networks such as the U.S. Climate Reference Network (<http://www.ncei.noaa.gov/crn/>), enhanced climate observational and data analysis capabilities, and continued improvements in climate modeling all have the potential to reduce uncertainties.

Assessment of confidence based on evidence and agreement, including short description of nature of evidence and level of agreement

There is *very high confidence* that global climate is changing and this change is apparent across a wide range of observations, given the evidence base and remaining uncertainties. All observational evidence is consistent with a warming climate since the late 1800s. There is *very high confidence* that the global climate change of the past 50 years is primarily due to human activities, given the evidence base and remaining uncertainties.¹ Recent changes have been consistently attributed in large part to human factors across a very broad range of climate system characteristics.

Summary sentence or paragraph that integrates the above information

The key message and supporting text summarizes extensive evidence documented in the climate science peer-reviewed literature. The trends described in NCA3 have continued and our understanding of the observations related to climate and the ability to evaluate the many facets of the climate system have increased substantially.

Key Finding 2

The frequency and intensity of extreme heat and heavy precipitation events are increasing in most continental regions of the world (*very high confidence*). These trends are consistent with expected physical responses to a warming climate. Climate model studies are also consistent with these trends, although models tend to underestimate the observed trends, especially for the increase in extreme precipitation events (*very high confidence* for temperature, *high confidence* for extreme precipitation). The frequency and intensity of extreme high temperature events are *virtually certain* to



increase in the future as global temperature increases (*high confidence*). Extreme precipitation events will *very likely* continue to increase in frequency and intensity throughout most of the world (*high confidence*). Observed and projected trends for some other types of extreme events, such as floods, droughts, and severe storms, have more variable regional characteristics.

Description of evidence base

The Key Finding and supporting text summarizes extensive evidence documented in the climate science literature and are similar to statements made in previous national (NCA3)¹⁴⁴ and international¹ assessments. The analyses of past trends and future projections in extreme events and the fact that models tend to underestimate the observed trends are also well substantiated through more recent peer-reviewed literature as well.^{75, 76, 81, 82, 83, 88, 90, 199}

Major uncertainties

Key remaining uncertainties relate to the precise magnitude and nature of changes at global, and particularly regional, scales, and especially for extreme events and our ability to simulate and attribute such changes using climate models. Innovative new approaches to climate data analysis, continued improvements in climate modeling, and instigation and maintenance of reference quality observation networks such as the U.S. Climate Reference Network (<http://www.nci.noaa.gov/crn/>) all have the potential to reduce uncertainties.

Assessment of confidence based on evidence and agreement, including short description of nature of evidence and level of agreement

There is *very high confidence* for the statements about past extreme changes in temperature and precipitation and *high confidence* for future projections, based on the observational evidence and physical understanding, that there are major trends in extreme events and significant projected changes for the future.

Summary sentence or paragraph that integrates the above information

The Key Finding and supporting text summarizes extensive evidence documented in the climate science

peer-reviewed literature. The trends for extreme events that were described in the NCA3 and IPCC assessments have continued, and our understanding of the data and ability to evaluate the many facets of the climate system have increased substantially.

Key Finding 3

Many lines of evidence demonstrate that it is *extremely likely* that human influence has been the dominant cause of the observed warming since the mid-20th century. Formal detection and attribution studies for the period 1951 to 2010 find that the observed global mean surface temperature warming lies in the middle of the range of likely human contributions to warming over that same period. We find no convincing evidence that natural variability can account for the amount of global warming observed over the industrial era. For the period extending over the last century, there are no convincing alternative explanations supported by the extent of the observational evidence. Solar output changes and internal variability can only contribute marginally to the observed changes in climate over the last century, and we find no convincing evidence for natural cycles in the observational record that could explain the observed changes in climate. (*Very high confidence*)

Description of evidence base

The Key Finding and supporting text summarizes extensive evidence documented in the climate science literature and are similar to statements made in previous national (NCA3)¹⁴⁴ and international¹ assessments. The human effects on climate have been well documented through many papers in the peer-reviewed scientific literature (e.g., see Ch. 2: Physical Drivers of Climate Change and Ch. 3: Detection and Attribution for more discussion of supporting evidence).

Major uncertainties

Key remaining uncertainties relate to the precise magnitude and nature of changes at global, and particularly regional, scales, and especially for extreme events and our ability to simulate and attribute such changes using climate models. The exact effects from land use changes relative to the effects from greenhouse gas emissions need to be better understood.



Assessment of confidence based on evidence and agreement, including short description of nature of evidence and level of agreement

There is *very high confidence* for a major human influence on climate.

Summary sentence or paragraph that integrates the above information

The key message and supporting text summarizes extensive evidence documented in the climate science peer-reviewed literature. The analyses described in the NCA3 and IPCC assessments support our findings, and new observations and modeling studies have further substantiated these conclusions.

Key Finding 4

Global climate is projected to continue to change over this century and beyond. The magnitude of climate change beyond the next few decades will depend primarily on the amount of greenhouse (heat-trapping) gases emitted globally and on the remaining uncertainty in the sensitivity of Earth's climate to those emissions (*very high confidence*). With significant reductions in the emissions of greenhouse gases, the global annually averaged temperature rise could be limited to 3.6°F (2°C) or less. Without major reductions in these emissions, the increase in annual average global temperatures relative to preindustrial times could reach 9°F (5°C) or more by the end of this century (*high confidence*).

Description of evidence base

The Key Finding and supporting text summarizes extensive evidence documented in the climate science literature and are similar to statements made in previous national (NCA3)¹⁴⁴ and international¹ assessments. The projections for future climate have been well documented through many papers in the peer-reviewed scientific literature (e.g., see Ch. 4: Projections for descriptions of the scenarios and the models used).

Major uncertainties

Key remaining uncertainties relate to the precise magnitude and nature of changes at global, and particularly regional, scales, and especially for extreme events and our ability to simulate and attribute such changes using

climate models. Of particular importance are remaining uncertainties in the understanding of feedbacks in the climate system, especially in ice–albedo and cloud cover feedbacks. Continued improvements in climate modeling to represent the physical processes affecting Earth's climate system are aimed at reducing uncertainties. Monitoring and observation programs also can help improve the understanding needed to reduce uncertainties.

Assessment of confidence based on evidence and agreement, including short description of nature of evidence and level of agreement

There is *very high confidence* for continued changes in climate and *high confidence* for the levels shown in the Key Finding.

Summary sentence or paragraph that integrates the above information

The Key Finding and supporting text summarizes extensive evidence documented in the climate science peer-reviewed literature. The projections that were described in the NCA3 and IPCC assessments support our findings, and new modeling studies have further substantiated these conclusions.

Key Finding 5

Natural variability, including El Niño events and other recurring patterns of ocean–atmosphere interactions, impact temperature and precipitation, especially regionally, over months to years. The global influence of natural variability, however, is limited to a small fraction of observed climate trends over decades.

Description of evidence base

The Key Finding and supporting text summarizes extensive evidence documented in the climate science literature and are similar to statements made in previous national (NCA3)¹⁴⁴ and international¹ (IPCC 2013) assessments. The role of natural variability in climate trends has been extensively discussed in the peer-reviewed literature (e.g., Karl et al. 2015;²⁶ Rahmstorf et al. 2015;³⁴ Lewandowsky et al. 2016;³⁹ Mears and Wentz 2016;⁴¹ Trenberth et al. 2014;²⁰⁰ Santer et al. 2017^{38, 40, 68}).



Major uncertainties

Uncertainties still exist in the precise magnitude and nature of the full effects of individual ocean cycles and other aspects of natural variability on the climate system. Increased emphasis on monitoring should reduce this uncertainty significantly over the next few decades.

Assessment of confidence based on evidence and agreement, including short description of nature of evidence and level of agreement

There is *very high confidence*, affected to some degree by limitations in the observational record, that the role of natural variability on future climate change is limited.

Summary sentence or paragraph that integrates the above information

The Key Finding and supporting text summarizes extensive evidence documented in the climate science peer-reviewed literature. There has been an extensive increase in the understanding of the role of natural variability on the climate system over the last few decades, including a number of new findings since NCA3.

Key Finding 6

Longer-term climate records over past centuries and millennia indicate that average temperatures in recent decades over much of the world have been much higher, and have risen faster during this time period, than at any time in the past 1,700 years or more, the time period for which the global distribution of surface temperatures can be reconstructed.

Description of evidence base

The Key Finding and supporting text summarizes extensive evidence documented in the climate science literature and are similar to statements made in previous national (NCA3)¹⁴⁴ and international¹ assessments. There are many recent studies of the paleoclimate leading to this conclusion including those cited in the report (e.g., Mann et al. 2008;¹⁹³ PAGE 2k Consortium 2013⁹).

Major uncertainties

Despite the extensive increase in knowledge in the last few decades, there are still many uncertainties in understanding the hemispheric and global changes in climate over Earth's history, including that of the last few millennia. Additional research efforts in this direction can help reduce those uncertainties.

Assessment of confidence based on evidence and agreement, including short description of nature of evidence and level of agreement

There is *high confidence* for current temperatures to be higher than they have been in at least 1,700 years and perhaps much longer.

Summary sentence or paragraph that integrates the above information

The Key Finding and supporting text summarizes extensive evidence documented in the climate science peer-reviewed literature. There has been an extensive increase in the understanding of past climates on our planet, including a number of new findings since NCA3.



REFERENCES

1. IPCC, 2013: *Climate Change 2013: The Physical Science Basis. Contribution of Working Group I to the Fifth Assessment Report of the Intergovernmental Panel on Climate Change*. Cambridge University Press, Cambridge, UK and New York, NY, 1535 pp. <http://www.climatechange2013.org/report/>
2. Trenberth, K.E. and J.T. Fasullo, 2013: An apparent hiatus in global warming? *Earth's Future*, **1**, 19-32. <http://dx.doi.org/10.1002/2013EF000165>
3. Trenberth, K.E., 2015: Has there been a hiatus? *Science*, **349**, 691-692. <http://dx.doi.org/10.1126/science.aac9225>
4. Marotzke, J. and P.M. Forster, 2015: Forcing, feedback and internal variability in global temperature trends. *Nature*, **517**, 565-570. <http://dx.doi.org/10.1038/nature14117>
5. Lehmann, J., D. Coumou, and K. Frieler, 2015: Increased record-breaking precipitation events under global warming. *Climatic Change*, **132**, 501-515. <http://dx.doi.org/10.1007/s10584-015-1434-y>
6. Bindoff, N.L., P.A. Stott, K.M. AchutaRao, M.R. Allen, N. Gillett, D. Gutzler, K. Hansingo, G. Hegerl, Y. Hu, S. Jain, I.I. Mokhov, J. Overland, J. Perlwitz, R. Sebbi, and X. Zhang, 2013: Detection and attribution of climate change: From global to regional. *Climate Change 2013: The Physical Science Basis. Contribution of Working Group I to the Fifth Assessment Report of the Intergovernmental Panel on Climate Change*. Stocker, T.F., D. Qin, G.-K. Plattner, M. Tignor, S.K. Allen, J. Boschung, A. Nauels, Y. Xia, V. Bex, and P.M. Midgley, Eds. Cambridge University Press, Cambridge, United Kingdom and New York, NY, USA, 867-952. <http://www.climatechange2013.org/report/full-report/>
7. Schurer, A.P., S.F.B. Tett, and G.C. Hegerl, 2014: Small influence of solar variability on climate over the past millennium. *Nature Geoscience*, **7**, 104-108. <http://dx.doi.org/10.1038/ngeo2040>
8. Kopp, G., 2014: An assessment of the solar irradiance record for climate studies. *Journal of Space Weather and Space Climate*, **4**, A14. <http://dx.doi.org/10.1051/swsc/2014012>
9. PAGES 2K Consortium, 2013: Continental-scale temperature variability during the past two millennia. *Nature Geoscience*, **6**, 339-346. <http://dx.doi.org/10.1038/ngeo1797>
10. Marcott, S.A., J.D. Shakun, P.U. Clark, and A.C. Mix, 2013: A reconstruction of regional and global temperature for the past 11,300 years. *Science*, **339**, 1198-1201. <http://dx.doi.org/10.1126/science.1228026>
11. Otto-Bliesner, B.L., E.C. Brady, J. Fasullo, A. Jahn, L. Landrum, S. Stevenson, N. Rosenbloom, A. Mai, and G. Strand, 2016: Climate Variability and Change since 850 CE: An Ensemble Approach with the Community Earth System Model. *Bulletin of the American Meteorological Society*, **97**, 735-754. <http://dx.doi.org/10.1175/bams-d-14-00233.1>
12. Church, J.A., N.J. White, L.F. Konikow, C.M. Domingues, J.G. Cogley, E. Rignot, J.M. Gregory, M.R. van den Broeke, A.J. Monaghan, and I. Velicogna, 2011: Revisiting the Earth's sea-level and energy budgets from 1961 to 2008. *Geophysical Research Letters*, **38**, L18601. <http://dx.doi.org/10.1029/2011GL048794>
13. Anderson, B.T., J.R. Knight, M.A. Ringer, J.-H. Yoon, and A. Cherchi, 2012: Testing for the possible influence of unknown climate forcings upon global temperature increases from 1950 to 2000. *Journal of Climate*, **25**, 7163-7172. <http://dx.doi.org/10.1175/jcli-d-11-00645.1>
14. EPA, 2016: *Climate Change Indicators in the United States*, 2016. 4th edition. EPA 430-R-16-004. U.S. Environmental Protection Agency, Washington, D.C., 96 pp. https://www.epa.gov/sites/production/files/2016-08/documents/climate_indicators_2016.pdf
15. Blunden, J. and D.S. Arndt, 2016: State of the climate in 2015. *Bulletin of the American Meteorological Society*, **97**, Si-S275. <http://dx.doi.org/10.1175/2016BAMS-StateoftheClimate.1>
16. Meehl, G.A., A. Hu, B.D. Santer, and S.-P. Xie, 2016: Contribution of the Interdecadal Pacific Oscillation to twentieth-century global surface temperature trends. *Nature Climate Change*, **6**, 1005-1008. <http://dx.doi.org/10.1038/nclimate3107>
17. Johnson, G.C., J.M. Lyman, J. Antonov, N. Bindoff, T. Boyer, C.M. Domingues, S.A. Good, M. Ishii, and J.K. Willis, 2015: Ocean heat content [in "State of the Climate in 2014"]. *Bulletin of the American Meteorological Society*, **96** (7), S64-S66, S68. <http://dx.doi.org/10.1175/2014BAMSStateoftheClimate.1>
18. Rhein, M., S.R. Rintoul, S. Aoki, E. Campos, D. Chambers, R.A. Feely, S. Gulev, G.C. Johnson, S.A. Josey, A. Kostianoy, C. Mauritzen, D. Roemmich, L.D. Talley, and F. Wang, 2013: Observations: Ocean. *Climate Change 2013: The Physical Science Basis. Contribution of Working Group I to the Fifth Assessment Report of the Intergovernmental Panel on Climate Change*. Stocker, T.F., D. Qin, G.-K. Plattner, M. Tignor, S.K. Allen, J. Boschung, A. Nauels, Y. Xia, V. Bex, and P.M. Midgley, Eds. Cambridge University Press, Cambridge, United Kingdom and New York, NY, USA, 255-316. <http://www.climatechange2013.org/report/full-report/>



19. Kundzewicz, Z.W., 2008: Climate change impacts on the hydrological cycle. *Ecohydrology & Hydrobiology*, **8**, 195-203. <http://dx.doi.org/10.2478/v10104-009-0015-y>
20. Ramsayer, K., 2014: Antarctic sea ice reaches new record maximum. <https://www.nasa.gov/content/goddard/antarctic-sea-ice-reaches-new-record-maximum>
21. USGCRP, 2017: [National Climate Assessment] Indicators. U.S. Global Change Research Program. <http://www.globalchange.gov/browse/indicators>
22. Vose, R.S., D. Arndt, V.F. Banzon, D.R. Easterling, B. Gleason, B. Huang, E. Kearns, J.H. Lawrimore, M.J. Menne, T.C. Peterson, R.W. Reynolds, T.M. Smith, C.N. Williams, and D.L. Wuertz, 2012: NOAA's merged land-ocean surface temperature analysis. *Bulletin of the American Meteorological Society*, **93**, 1677-1685. <http://dx.doi.org/10.1175/BAMS-D-11-00241.1>
23. NCEI, 2016: Climate at a Glance: Global Temperature Anomalies. http://www.ncdc.noaa.gov/cag/time-series/global/globe/land_ocean/ytd/12/1880-2015
24. Steinman, B.A., M.B. Abbott, M.E. Mann, N.D. Stansell, and B.P. Finney, 2012: 1,500 year quantitative reconstruction of winter precipitation in the Pacific Northwest. *Proceedings of the National Academy of Sciences*, **109**, 11619-11623. <http://dx.doi.org/10.1073/pnas.1201083109>
25. Deser, C., R. Knutti, S. Solomon, and A.S. Phillips, 2012: Communication of the role of natural variability in future North American climate. *Nature Climate Change*, **2**, 775-779. <http://dx.doi.org/10.1038/nclimate1562>
26. Karl, T.R., A. Arguez, B. Huang, J.H. Lawrimore, J.R. McMahon, M.J. Menne, T.C. Peterson, R.S. Vose, and H.-M. Zhang, 2015: Possible artifacts of data biases in the recent global surface warming hiatus. *Science*, **348**, 1469-1472. <http://dx.doi.org/10.1126/science.aaa5632>
27. Knutson, T.R., R. Zhang, and L.W. Horowitz, 2016: Prospects for a prolonged slowdown in global warming in the early 21st century. *Nature Communications*, **7**, 13676. <http://dx.doi.org/10.1038/ncomms13676>
28. Delworth, T.L. and T.R. Knutson, 2000: Simulation of early 20th century global warming. *Science*, **287**, 2246-2250. <http://dx.doi.org/10.1126/science.287.5461.2246>
29. Alexander, L.V., X. Zhang, T.C. Peterson, J. Caesar, B. Gleason, A.M.G. Klein Tank, M. Haylock, D. Collins, B. Trewin, F. Rahimzadeh, A. Tagipour, K. Rupa Kumar, J. Revadekar, G. Griffiths, L. Vincent, D.B. Stephenson, J. Burn, E. Aguilar, M. Brunet, M. Taylor, M. New, P. Zhai, M. Rusticucci, and J.L. Vazquez-Aguirre, 2006: Global observed changes in daily climate extremes of temperature and precipitation. *Journal of Geophysical Research*, **111**, D05109. <http://dx.doi.org/10.1029/2005JD006290>
30. Davy, R., I. Esau, A. Chernokulsky, S. Outten, and S. Zilitinkevich, 2016: Diurnal asymmetry to the observed global warming. *International Journal of Climatology*, **37**, 79-93. <http://dx.doi.org/10.1002/joc.4688>
31. Mountain Research Initiative, 2015: Elevation-dependent warming in mountain regions of the world. *Nature Climate Change*, **5**, 424-430. <http://dx.doi.org/10.1038/nclimate2563>
32. Hurrell, J.W. and C. Deser, 2009: North Atlantic climate variability: The role of the North Atlantic oscillation. *Journal of Marine Systems*, **78**, 28-41. <http://dx.doi.org/10.1016/j.jmarsys.2008.11.026>
33. Hoegh-Guldberg, O., R. Cai, E.S. Poloczanska, P.G. Brewer, S. Sundby, K. Hilmi, V.J. Fabry, and S. Jung, 2014: The Ocean. *Climate Change 2014: Impacts, Adaptation, and Vulnerability. Part B: Regional Aspects. Contribution of Working Group II to the Fifth Assessment Report of the Intergovernmental Panel of Climate Change*. Barros, V.R., C.B. Field, D.J. Dokken, M.D. Mastrandrea, K.J. Mach, T.E. Bilir, M. Chatterjee, K.L. Ebi, Y.O. Estrada, R.C. Genova, B. Girma, E.S. Kissel, A.N. Levy, S. MacCracken, P.R. Mastrandrea, and L.L. White, Eds. Cambridge University Press, Cambridge, United Kingdom and New York, NY, USA, 1655-1731. http://www.ipcc.ch/pdf/assessment-report/ar5/wg2/WGIIAR5-Chap30_FINAL.pdf
34. Rahmstorf, S., J.E. Box, G. Feulner, M.E. Mann, A. Robinson, S. Rutherford, and E.J. Schaffernicht, 2015: Exceptional twentieth-century slowdown in Atlantic Ocean overturning circulation. *Nature Climate Change*, **5**, 475-480. <http://dx.doi.org/10.1038/nclimate2554>
35. Knutti, R., J. Rogelj, J. Sedlacek, and E.M. Fischer, 2016: A scientific critique of the two-degree climate change target. *Nature Geoscience*, **9**, 13-18. <http://dx.doi.org/10.1038/ngeo2595>
36. Peters, G.P., R.M. Andrew, T. Boden, J.G. Canadell, P. Ciais, C. Le Quere, G. Marland, M.R. Raupach, and C. Wilson, 2013: The challenge to keep global warming below 2°C. *Nature Climate Change*, **3**, 4-6. <http://dx.doi.org/10.1038/nclimate1783>
37. Schellnhuber, H.J., S. Rahmstorf, and R. Winkelman, 2016: Why the right climate target was agreed in Paris. *Nature Climate Change*, **6**, 649-653. <http://dx.doi.org/10.1038/nclimate3013>



38. Santer, B.D., S. Solomon, G. Pallotta, C. Mears, S. Po-Chedley, Q. Fu, F. Wentz, C.-Z. Zou, J. Painter, I. Cvijanovic, and C. Bonfils, 2017: Comparing tropospheric warming in climate models and satellite data. *Journal of Climate*, **30**, 373-392. <http://dx.doi.org/10.1175/JCLI-D-16-0333.1>
39. Lewandowsky, S., J.S. Risbey, and N. Oreskes, 2016: The “pause” in global warming: Turning a routine fluctuation into a problem for science. *Bulletin of the American Meteorological Society*, **97**, 723-733. <http://dx.doi.org/10.1175/BAMS-D-14-00106.1>
40. Santer, B.D., S. Solomon, F.J. Wentz, Q. Fu, S. Po-Chedley, C. Mears, J.F. Painter, and C. Bonfils, 2017: Tropospheric warming over the past two decades. *Scientific Reports*, **7**, 2336. <http://dx.doi.org/10.1038/s41598-017-02520-7>
41. Mears, C.A. and F.J. Wentz, 2016: Sensitivity of satellite-derived tropospheric temperature trends to the diurnal cycle adjustment. *Journal of Climate*, **29**, 3629-3646. <http://dx.doi.org/10.1175/JCLI-D-15-0744.1>
42. Richardson, M., K. Cowtan, E. Hawkins, and M.B. Stolpe, 2016: Reconciled climate response estimates from climate models and the energy budget of Earth. *Nature Climate Change*, **6**, 931-935. <http://dx.doi.org/10.1038/nclimate3066>
43. Hausfather, Z., K. Cowtan, D.C. Clarke, P. Jacobs, M. Richardson, and R. Rohde, 2017: Assessing recent warming using instrumentally homogeneous sea surface temperature records. *Science Advances*, **3**, e1601207. <http://dx.doi.org/10.1126/sciadv.1601207>
44. Fyfe, J.C., G.A. Meehl, M.H. England, M.E. Mann, B.D. Santer, G.M. Flato, E. Hawkins, N.P. Gillett, S.-P. Xie, Y. Kosaka, and N.C. Swart, 2016: Making sense of the early-2000s warming slowdown. *Nature Climate Change*, **6**, 224-228. <http://dx.doi.org/10.1038/nclimate2938>
45. Benestad, R.E., 2017: A mental picture of the greenhouse effect. *Theoretical and Applied Climatology*, **128**, 679-688. <http://dx.doi.org/10.1007/s00704-016-1732-y>
46. Balmaseda, M.A., K.E. Trenberth, and E. Källén, 2013: Distinctive climate signals in reanalysis of global ocean heat content. *Geophysical Research Letters*, **40**, 1754-1759. <http://dx.doi.org/10.1002/grl.50382>
47. England, M.H., S. McGregor, P. Spence, G.A. Meehl, A. Timmermann, W. Cai, A.S. Gupta, M.J. McPhaden, A. Purich, and A. Santoso, 2014: Recent intensification of wind-driven circulation in the Pacific and the ongoing warming hiatus. *Nature Climate Change*, **4**, 222-227. <http://dx.doi.org/10.1038/nclimate2106>
48. Meehl, G.A., J.M. Arblaster, J.T. Fasullo, A. Hu, and K.E. Trenberth, 2011: Model-based evidence of deep-ocean heat uptake during surface-temperature hiatus periods. *Nature Climate Change*, **1**, 360-364. <http://dx.doi.org/10.1038/nclimate1229>
49. Kosaka, Y. and S.-P. Xie, 2013: Recent global-warming hiatus tied to equatorial Pacific surface cooling. *Nature*, **501**, 403-407. <http://dx.doi.org/10.1038/nature12534>
50. Chen, X. and K.-K. Tung, 2014: Varying planetary heat sink led to global-warming slowdown and acceleration. *Science*, **345**, 897-903. <http://dx.doi.org/10.1126/science.1254937>
51. Nieves, V., J.K. Willis, and W.C. Patzert, 2015: Recent hiatus caused by decadal shift in Indo-Pacific heating. *Science*, **349**, 532-535. <http://dx.doi.org/10.1126/science.aaa4521>
52. Solomon, S., K.H. Rosenlof, R.W. Portmann, J.S. Daniel, S.M. Davis, T.J. Sanford, and G.-K. Plattner, 2010: Contributions of stratospheric water vapor to decadal changes in the rate of global warming. *Science*, **327**, 1219-1223. <http://dx.doi.org/10.1126/science.1182488>
53. Schmidt, G.A., D.T. Shindell, and K. Tsigaridis, 2014: Reconciling warming trends. *Nature Geoscience*, **7**, 158-160. <http://dx.doi.org/10.1038/ngeo2105>
54. Huber, M. and R. Knutti, 2014: Natural variability, radiative forcing and climate response in the recent hiatus reconciled. *Nature Geoscience*, **7**, 651-656. <http://dx.doi.org/10.1038/ngeo2228>
55. Ridley, D.A., S. Solomon, J.E. Barnes, V.D. Burlakov, T. Deshler, S.I. Dolgii, A.B. Herber, T. Nagai, R.R. Neely, A.V. Nevzorov, C. Ritter, T. Sakai, B.D. Santer, M. Sato, A. Schmidt, O. Uchino, and J.P. Vernier, 2014: Total volcanic stratospheric aerosol optical depths and implications for global climate change. *Geophysical Research Letters*, **41**, 7763-7769. <http://dx.doi.org/10.1002/2014GL061541>
56. Santer, B.D., C. Bonfils, J.F. Painter, M.D. Zelinka, C. Mears, S. Solomon, G.A. Schmidt, J.C. Fyfe, J.N.S. Cole, L. Nazarenko, K.E. Taylor, and F.J. Wentz, 2014: Volcanic contribution to decadal changes in tropospheric temperature. *Nature Geoscience*, **7**, 185-189. <http://dx.doi.org/10.1038/ngeo2098>
57. Becker, A., P. Finger, A. Meyer-Christoffer, B. Rudolf, K. Schamm, U. Schneider, and M. Ziese, 2013: A description of the global land-surface precipitation data products of the Global Precipitation Climatology Centre with sample applications including centennial (trend) analysis from 1901-present. *Earth System Science Data*, **5**, 71-99. <http://dx.doi.org/10.5194/essd-5-71-2013>
58. Adler, R.F., G.J. Huffman, A. Chang, R. Ferraro, P.-P. Xie, J. Janowiak, B. Rudolf, U. Schneider, S. Curtis, D. Bolvin, A. Gruber, J. Susskind, P. Arkin, and E. Nelkin, 2003: The version-2 Global Precipitation Climatology Project (GPCP) monthly precipitation analysis (1979-present). *Journal of Hydrometeorology*, **4**, 1147-1167. [http://dx.doi.org/10.1175/1525-7541\(2003\)004<1147:TVG-PCP>2.0.CO;2](http://dx.doi.org/10.1175/1525-7541(2003)004<1147:TVG-PCP>2.0.CO;2)



59. Allen, M.R. and W.J. Ingram, 2002: Constraints on future changes in climate and the hydrologic cycle. *Nature*, **419**, 224-232. <http://dx.doi.org/10.1038/nature01092>
60. Collins, M., R. Knutti, J. Arblaster, J.-L. Dufresne, T. Fichefet, P. Friedlingstein, X. Gao, W.J. Gutowski, T. Johns, G. Krinner, M. Shongwe, C. Tebaldi, A.J. Weaver, and M. Wehner, 2013: Long-term climate change: Projections, commitments and irreversibility. *Climate Change 2013: The Physical Science Basis. Contribution of Working Group I to the Fifth Assessment Report of the Intergovernmental Panel on Climate Change*. Stocker, T.F., D. Qin, G.-K. Plattner, M. Tignor, S.K. Allen, J. Boschung, A. Nauels, Y. Xia, V. Bex, and P.M. Midgley, Eds. Cambridge University Press, Cambridge, United Kingdom and New York, NY, USA, 1029-1136. <http://www.climatechange2013.org/report/full-report/>
61. Held, I.M. and B.J. Soden, 2006: Robust responses of the hydrological cycle to global warming. *Journal of Climate*, **19**, 5686-5699. <http://dx.doi.org/10.1175/jcli3990.1>
62. Santer, B.D., C. Mears, F.J. Wentz, K.E. Taylor, P.J. Gleckler, T.M.L. Wigley, T.P. Barnett, J.S. Boyle, W. Brüggemann, N.P. Gillett, S.A. Klein, G.A. Meehl, T. Nozawa, D.W. Pierce, P.A. Stott, W.M. Washington, and M.F. Wehner, 2007: Identification of human-induced changes in atmospheric moisture content. *Proceedings of the National Academy of Sciences*, **104**, 15248-15253. <http://dx.doi.org/10.1073/pnas.0702872104>
63. Willett, K.M., D.J. Philip, W.T. Peter, and P.G. Nathan, 2010: A comparison of large scale changes in surface humidity over land in observations and CMIP3 general circulation models. *Environmental Research Letters*, **5**, 025210. <http://dx.doi.org/10.1088/1748-9326/5/2/025210>
64. Greve, P., B. Orlowsky, B. Mueller, J. Sheffield, M. Reichstein, and S.I. Seneviratne, 2014: Global assessment of trends in wetting and drying over land. *Nature Geoscience*, **7**, 716-721. <http://dx.doi.org/10.1038/ngeo2247>
65. Zhang, X., F.W. Zwiers, G.C. Hegerl, F.H. Lambert, N.P. Gillett, S. Solomon, P.A. Stott, and T. Nozawa, 2007: Detection of human influence on twentieth-century precipitation trends. *Nature*, **448**, 461-465. <http://dx.doi.org/10.1038/nature06025>
66. Marvel, K. and C. Bonfils, 2013: Identifying external influences on global precipitation. *Proceedings of the National Academy of Sciences*, **110**, 19301-19306. <http://dx.doi.org/10.1073/pnas.1314382110>
67. Walsh, J.E., J.E. Overland, P.Y. Groisman, and B. Rudolf, 2011: Ongoing climate change in the Arctic. *Ambio*, **40**, 6-16. <http://dx.doi.org/10.1007/s13280-011-0211-z>
68. Vihma, T., J. Screen, M. Tjernström, B. Newton, X. Zhang, V. Popova, C. Deser, M. Holland, and T. Prowse, 2016: The atmospheric role in the Arctic water cycle: A review on processes, past and future changes, and their impacts. *Journal of Geophysical Research Biogeosciences*, **121**, 586-620. <http://dx.doi.org/10.1002/2015JG003132>
69. Min, S.-K., X. Zhang, and F. Zwiers, 2008: Human-induced Arctic moistening. *Science*, **320**, 518-520. <http://dx.doi.org/10.1126/science.1153468>
70. Katz, R.W. and B.G. Brown, 1992: Extreme events in a changing climate: Variability is more important than averages. *Climatic Change*, **21**, 289-302. <http://dx.doi.org/10.1007/bf00139728>
71. Sardeshmukh, P.D., G.P. Compo, and C. Penland, 2015: Need for caution in interpreting extreme weather statistics. *Journal of Climate*, **28**, 9166-9187. <http://dx.doi.org/10.1175/JCLI-D-15-0020.1>
72. NAS, 2016: *Attribution of Extreme Weather Events in the Context of Climate Change*. The National Academies Press, Washington, DC, 186 pp. <http://dx.doi.org/10.17226/21852>
73. Hulme, M., 2014: Attributing weather extremes to 'climate change'. *Progress in Physical Geography*, **38**, 499-511. <http://dx.doi.org/10.1177/0309133314538644>
74. Stott, P., 2016: How climate change affects extreme weather events. *Science*, **352**, 1517-1518. <http://dx.doi.org/10.1126/science.aaf7271>
75. Easterling, D.R., K.E. Kunkel, M.F. Wehner, and L. Sun, 2016: Detection and attribution of climate extremes in the observed record. *Weather and Climate Extremes*, **11**, 17-27. <http://dx.doi.org/10.1016/j.wace.2016.01.001>
76. Seneviratne, S.I., M.G. Donat, B. Mueller, and L.V. Alexander, 2014: No pause in the increase of hot temperature extremes. *Nature Climate Change*, **4**, 161-163. <http://dx.doi.org/10.1038/nclimate2145>
77. Meehl, G.A., C. Tebaldi, G. Walton, D. Easterling, and L. McDaniel, 2009: Relative increase of record high maximum temperatures compared to record low minimum temperatures in the US. *Geophysical Research Letters*, **36**, L23701. <http://dx.doi.org/10.1029/2009GL040736>
78. Min, S.-K., X. Zhang, F. Zwiers, H. Shiogama, Y.-S. Tung, and M. Wehner, 2013: Multimodel detection and attribution of extreme temperature changes. *Journal of Climate*, **26**, 7430-7451. <http://dx.doi.org/10.1175/JCLI-D-12-00551.1>
79. Horton, D.E., N.C. Johnson, D. Singh, D.L. Swain, B. Rajaratnam, and N.S. Diffenbaugh, 2015: Contribution of changes in atmospheric circulation patterns to extreme temperature trends. *Nature*, **522**, 465-469. <http://dx.doi.org/10.1038/nature14550>



80. Asadih, B. and N.Y. Krakauer, 2015: Global trends in extreme precipitation: climate models versus observations. *Hydrology and Earth System Sciences*, **19**, 877-891. <http://dx.doi.org/10.5194/hess-19-877-2015>
81. Kunkel, K.E. and R.M. Frankson, 2015: Global land surface extremes of precipitation: Data limitations and trends. *Journal of Extreme Events*, **02**, 1550004. <http://dx.doi.org/10.1142/S2345737615500049>
82. Donat, M.G., A.L. Lowry, L.V. Alexander, P.A. Ogorman, and N. Maher, 2016: More extreme precipitation in the world's dry and wet regions. *Nature Climate Change*, **6**, 508-513. <http://dx.doi.org/10.1038/nclimate2941>
83. Fischer, E.M. and R. Knutti, 2016: Observed heavy precipitation increase confirms theory and early models. *Nature Climate Change*, **6**, 986-991. <http://dx.doi.org/10.1038/nclimate3110>
84. Kunkel, K.E., T.R. Karl, H. Brooks, J. Kossin, J. Lawrimore, D. Arndt, L. Bosart, D. Changnon, S.L. Cutter, N. Doesken, K. Emanuel, P.Y. Groisman, R.W. Katz, T. Knutson, J. O'Brien, C.J. Paciorek, T.C. Peterson, K. Redmond, D. Robinson, J. Trapp, R. Vose, S. Weaver, M. Wehner, K. Wolter, and D. Wuebbles, 2013: Monitoring and understanding trends in extreme storms: State of knowledge. *Bulletin of the American Meteorological Society*, **94**, 499-514. <http://dx.doi.org/10.1175/BAMS-D-11-00262.1>
85. Min, S.K., X. Zhang, F.W. Zwiers, and G.C. Hegerl, 2011: Human contribution to more-intense precipitation extremes. *Nature*, **470**, 378-381. <http://dx.doi.org/10.1038/nature09763>
86. Zhang, X., H. Wan, F.W. Zwiers, G.C. Hegerl, and S.-K. Min, 2013: Attributing intensification of precipitation extremes to human influence. *Geophysical Research Letters*, **40**, 5252-5257. <http://dx.doi.org/10.1002/grl.51010>
87. Knutson, T.R., J.J. Sirutis, M. Zhao, R.E. Tuleya, M. Bender, G.A. Vecchi, G. Villarini, and D. Chavas, 2015: Global projections of intense tropical cyclone activity for the late twenty-first century from dynamical downscaling of CMIP5/RCP4.5 scenarios. *Journal of Climate*, **28**, 7203-7224. <http://dx.doi.org/10.1175/JCLI-D-15-0129.1>
88. Berghuijs, W.R., R.A. Woods, C.J. Hutton, and M. Sivapalan, 2016: Dominant flood generating mechanisms across the United States. *Geophysical Research Letters*, **43**, 4382-4390. <http://dx.doi.org/10.1002/2016GL068070>
89. Kundzewicz, Z.W., S. Kanae, S.I. Seneviratne, J. Handmer, N. Nicholls, P. Peduzzi, R. Mechler, L.M. Bouwer, N. Arnell, K. Mach, R. Muir-Wood, G.R. Brakenridge, W. Kron, G. Benito, Y. Honda, K. Takahashi, and B. Sherstyukov, 2014: Flood risk and climate change: Global and regional perspectives. *Hydrological Sciences Journal*, **59**, 1-28. <http://dx.doi.org/10.1080/02626667.2013.857411>
90. Arnell, N.W. and S.N. Gosling, 2016: The impacts of climate change on river flood risk at the global scale. *Climatic Change*, **134**, 387-401. <http://dx.doi.org/10.1007/s10584-014-1084-5>
91. Sander, J., J.F. Eichner, E. Faust, and M. Steuer, 2013: Rising variability in thunderstorm-related U.S. losses as a reflection of changes in large-scale thunderstorm forcing. *Weather, Climate, and Society*, **5**, 317-331. <http://dx.doi.org/10.1175/WCAS-D-12-00023.1>
92. Diffenbaugh, N.S., M. Scherer, and R.J. Trapp, 2013: Robust increases in severe thunderstorm environments in response to greenhouse forcing. *Proceedings of the National Academy of Sciences*, **110**, 16361-16366. <http://dx.doi.org/10.1073/pnas.1307758110>
93. Bender, F.A.-M., V. Ramanathan, and G. Tselioudis, 2012: Changes in extratropical storm track cloudiness 1983-2008: Observational support for a poleward shift. *Climate Dynamics*, **38**, 2037-2053. <http://dx.doi.org/10.1007/s00382-011-1065-6>
94. Chang, E.K.M., 2013: CMIP5 projection of significant reduction in extratropical cyclone activity over North America. *Journal of Climate*, **26**, 9903-9922. <http://dx.doi.org/10.1175/JCLI-D-13-00209.1>
95. Colle, B.A., Z. Zhang, K.A. Lombardo, E. Chang, P. Liu, and M. Zhang, 2013: Historical evaluation and future prediction of eastern North American and western Atlantic extratropical cyclones in the CMIP5 models during the cool season. *Journal of Climate*, **26**, 6882-6903. <http://dx.doi.org/10.1175/JCLI-D-12-00498.1>
96. Barnes, E.A. and L.M. Polvani, 2015: CMIP5 projections of Arctic amplification, of the North American/North Atlantic circulation, and of their relationship. *Journal of Climate*, **28**, 5254-5271. <http://dx.doi.org/10.1175/JCLI-D-14-00589.1>
97. Kossin, J.P., K.A. Emanuel, and G.A. Vecchi, 2014: The poleward migration of the location of tropical cyclone maximum intensity. *Nature*, **509**, 349-352. <http://dx.doi.org/10.1038/nature13278>
98. Kossin, J.P., K.A. Emanuel, and S.J. Camargo, 2016: Past and projected changes in western North Pacific tropical cyclone exposure. *Journal of Climate*, **29**, 5725-5739. <http://dx.doi.org/10.1175/JCLI-D-16-0076.1>
99. Elsner, J.B., J.P. Kossin, and T.H. Jagger, 2008: The increasing intensity of the strongest tropical cyclones. *Nature*, **455**, 92-95. <http://dx.doi.org/10.1038/nature07234>
100. Kossin, J.P., T.L. Olander, and K.R. Knapp, 2013: Trend analysis with a new global record of tropical cyclone intensity. *Journal of Climate*, **26**, 9960-9976. <http://dx.doi.org/10.1175/JCLI-D-13-00262.1>



101. Wang, C., L. Zhang, S.-K. Lee, L. Wu, and C.R. Mechoso, 2014: A global perspective on CMIP5 climate model biases. *Nature Climate Change*, **4**, 201-205. <http://dx.doi.org/10.1038/nclimate2118>
102. Sobel, A.H., S.J. Camargo, T.M. Hall, C.-Y. Lee, M.K. Tippett, and A.A. Wing, 2016: Human influence on tropical cyclone intensity. *Science*, **353**, 242-246. <http://dx.doi.org/10.1126/science.aaf6574>
103. Emanuel, K.A., 2013: Downscaling CMIP5 climate models shows increased tropical cyclone activity over the 21st century. *Proceedings of the National Academy of Sciences*, **110**, 12219-12224. <http://dx.doi.org/10.1073/pnas.1301293110>
104. NSIDC, 2017: SOTC (State of the Cryosphere): Northern Hemisphere Snow. National Snow and Ice Data Center. https://nsidc.org/cryosphere/sotc/snow_extent.html
105. Kunkel, K.E., D.A. Robinson, S. Champion, X. Yin, T. Estilow, and R.M. Frankson, 2016: Trends and extremes in Northern Hemisphere snow characteristics. *Current Climate Change Reports*, **2**, 65-73. <http://dx.doi.org/10.1007/s40641-016-0036-8>
106. Rupp, D.E., P.W. Mote, N.L. Bindoff, P.A. Stott, and D.A. Robinson, 2013: Detection and attribution of observed changes in Northern Hemisphere spring snow cover. *Journal of Climate*, **26**, 6904-6914. <http://dx.doi.org/10.1175/JCLI-D-12-00563.1>
107. Callaghan, T.V., M. Johansson, R.D. Brown, P.Y. Groisman, N. Labba, V. Radionov, R.S. Bradley, S. Blangy, O.N. Bulygina, T.R. Christensen, J.E. Colman, R.L.H. Essery, B.C. Forbes, M.C. Forchhammer, V.N. Golubev, R.E. Honrath, G.P. Juday, A.V. Meshcherskaya, G.K. Phoenix, J. Pomeroy, A. Rautio, D.A. Robinson, N.M. Schmidt, M.C. Serreze, V.P. Shevchenko, A.I. Shiklomanov, A.B. Shmakin, P. Sköld, M. Sturm, M.-k. Woo, and E.F. Wood, 2011: Multiple effects of changes in Arctic snow cover. *Ambio*, **40**, 32-45. <http://dx.doi.org/10.1007/s13280-011-0213-x>
108. Sousa, P.M., R.M. Trigo, P. Aizpurua, R. Nieto, L. Gimeno, and R. Garcia-Herrera, 2011: Trends and extremes of drought indices throughout the 20th century in the Mediterranean. *Natural Hazards and Earth System Sciences*, **11**, 33-51. <http://dx.doi.org/10.5194/nhess-11-33-2011>
109. Hoerling, M., M. Chen, R. Dole, J. Eischeid, A. Kumar, J.W. Nielsen-Gammon, P. Pegion, J. Perlwitz, X.-W. Quan, and T. Zhang, 2013: Anatomy of an extreme event. *Journal of Climate*, **26**, 2811-2832. <http://dx.doi.org/10.1175/JCLI-D-12-00270.1>
110. Sheffield, J., E.F. Wood, and M.L. Roderick, 2012: Little change in global drought over the past 60 years. *Nature*, **491**, 435-438. <http://dx.doi.org/10.1038/nature11575>
111. Dai, A., 2013: Increasing drought under global warming in observations and models. *Nature Climate Change*, **3**, 52-58. <http://dx.doi.org/10.1038/nclimate1633>
112. Peterson, T.C., R.R. Heim, R. Hirsch, D.P. Kaiser, H. Brooks, N.S. Diffenbaugh, R.M. Dole, J.P. Giannantonio, K. Guirguis, T.R. Karl, R.W. Katz, K. Kunkel, D. Lettenmaier, G.J. McCabe, C.J. Paciorek, K.R. Ryberg, S. Schubert, V.B.S. Silva, B.C. Stewart, A.V. Vecchia, G. Villarini, R.S. Vose, J. Walsh, M. Wehner, D. Wollock, K. Wolter, C.A. Woodhouse, and D. Wuebbles, 2013: Monitoring and understanding changes in heat waves, cold waves, floods and droughts in the United States: State of knowledge. *Bulletin of the American Meteorological Society*, **94**, 821-834. <http://dx.doi.org/10.1175/BAMS-D-12-00066.1>
113. Jones, D.A., W. Wang, and R. Fawcett, 2009: High-quality spatial climate data-sets for Australia. *Australian Meteorological and Oceanographic Journal*, **58**, 233-248. <http://dx.doi.org/10.22499/2.5804.003>
114. Bonan, G.B., 2008: Forests and climate change: Forcings, feedbacks, and the climate benefits of forests. *Science*, **320**, 1444-1449. <http://dx.doi.org/10.1126/science.1155121>
115. de Noblet-Ducoudré, N., J.-P. Boisier, A. Pitman, G.B. Bonan, V. Brovkin, F. Cruz, C. Delire, V. Gayler, B.J.J.M.v.d. Hurk, P.J. Lawrence, M.K.v.d. Molen, C. Müller, C.H. Reick, B.J. Strengers, and A. Voldoire, 2012: Determining robust impacts of land-use-induced land cover changes on surface climate over North America and Eurasia: Results from the first set of LUCID experiments. *Journal of Climate*, **25**, 3261-3281. <http://dx.doi.org/10.1175/JCLI-D-11-00338.1>
116. Le Quéré, C., R. Moriarty, R.M. Andrew, J.G. Canadell, S. Sitch, J.I. Korsbakken, P. Friedlingstein, G.P. Peters, R.J. Andres, T.A. Boden, R.A. Houghton, J.I. House, R.F. Keeling, P. Tans, A. Arneeth, D.C.E. Bakker, L. Barbero, L. Bopp, J. Chang, F. Chevallier, L.P. Chini, P. Ciais, M. Fader, R.A. Feely, T. Gkritzalis, I. Harris, J. Hauck, T. Ilyina, A.K. Jain, E. Kato, V. Kitidis, K. Klein Goldewijk, C. Koven, P. Landschützer, S.K. Lauvset, N. Lefèvre, A. Lenton, I.D. Lima, N. Metz, F. Millero, D.R. Munro, A. Murata, J.E.M.S. Nabel, S. Nakaoka, Y. Nojiri, K. O'Brien, A. Olsen, T. Ono, F.F. Pérez, B. Pfeil, D. Pierrot, B. Poulter, G. Rehder, C. Rödenbeck, S. Saito, U. Schuster, J. Schwinger, R. Séférian, T. Steinhoff, B.D. Stocker, A.J. Sutton, T. Takahashi, B. Tilbrook, I.T. van der Laan-Luijkx, G.R. van der Werf, S. van Heuven, D. Vandemark, N. Viovy, A. Wiltshire, S. Zaehle, and N. Zeng, 2015: Global carbon budget 2015. *Earth System Science Data*, **7**, 349-396. <http://dx.doi.org/10.5194/essd-7-349-2015>



117. Le Quéré, C., R.M. Andrew, J.G. Canadell, S. Sitch, J.I. Korsbakken, G.P. Peters, A.C. Manning, T.A. Boden, P.P. Tans, R.A. Houghton, R.F. Keeling, S. Alin, O.D. Andrews, P. Anthoni, L. Barbero, L. Bopp, F. Chevallier, L.P. Chini, P. Ciais, K. Currie, C. Delire, S.C. Doney, P. Friedlingstein, T. Gkritzalis, I. Harris, J. Hauck, V. Haverd, M. Hoppema, K. Klein Goldewijk, A.K. Jain, E. Kato, A. Körtzinger, P. Landschützer, N. Lefèvre, A. Lenton, S. Liener, D. Lombardozzi, J.R. Melton, N. Metz, F. Miller, P.M.S. Monteiro, D.R. Munro, J.E.M.S. Nabel, S.I. Nakaoka, K. O'Brien, A. Olsen, A.M. Omar, T. Ono, D. Pierrot, B. Poulter, C. Rödenbeck, J. Salisbury, U. Schuster, J. Schwinger, R. Séférian, I. Skjelvan, B.D. Stocker, A.J. Sutton, T. Takahashi, H. Tian, B. Tilbrook, I.T. van der Laan-Luijk, G.R. van der Werf, N. Viovy, A.P. Walker, A.J. Wiltshire, and S. Zaehle, 2016: Global carbon budget 2016. *Earth System Science Data*, **8**, 605-649. <http://dx.doi.org/10.5194/essd-8-605-2016>
118. Houghton, R.A., J.I. House, J. Pongratz, G.R. van der Werf, R.S. DeFries, M.C. Hansen, C. Le Quéré, and N. Ramankutty, 2012: Carbon emissions from land use and land-cover change. *Biogeosciences*, **9**, 5125-5142. <http://dx.doi.org/10.5194/bg-9-5125-2012>
119. Pan, Y., R.A. Birdsey, J. Fang, R. Houghton, P.E. Kauppi, W.A. Kurz, O.L. Phillips, A. Shvidenko, S.L. Lewis, J.G. Canadell, P. Ciais, R.B. Jackson, S.W. Pacala, A.D. McGuire, S. Piao, A. Rautiainen, S. Sitch, and D. Hayes, 2011: A large and persistent carbon sink in the world's forests. *Science*, **333**, 988-993. <http://dx.doi.org/10.1126/science.1201609>
120. Myneni, R.B., C.D. Keeling, C.J. Tucker, G. Asrar, and R.R. Nemani, 1997: Increased plant growth in the northern high latitudes from 1981 to 1991. *Nature*, **386**, 698-702. <http://dx.doi.org/10.1038/386698a0>
121. Menzel, A., T.H. Sparks, N. Estrella, E. Koch, A. Aasa, R. Ahas, K. Alm-Kübler, P. Bissolli, O.G. Braslavská, A. Briede, F.M. Chmielewski, Z. Crepinsek, Y. Curnel, Å. Dahl, C. Defila, A. Donnelly, Y. Filella, K. Jatzak, F. Mäge, A. Mestre, Ø. Nordli, J. Peñuelas, P. Pirinen, V. Remišvá, H. Scheffinger, M. Striz, A. Susnik, A.J.H. Van Vliet, F.-E. Wielgolaski, S. Zach, and A.N.A. Züst, 2006: European phenological response to climate change matches the warming pattern. *Global Change Biology*, **12**, 1969-1976. <http://dx.doi.org/10.1111/j.1365-2486.2006.01193.x>
122. Schwartz, M.D., R. Ahas, and A. Aasa, 2006: Onset of spring starting earlier across the Northern Hemisphere. *Global Change Biology*, **12**, 343-351. <http://dx.doi.org/10.1111/j.1365-2486.2005.01097.x>
123. Kim, Y., J.S. Kimball, K. Zhang, and K.C. McDonald, 2012: Satellite detection of increasing Northern Hemisphere non-frozen seasons from 1979 to 2008: Implications for regional vegetation growth. *Remote Sensing of Environment*, **121**, 472-487. <http://dx.doi.org/10.1016/j.rse.2012.02.014>
124. Reyes-Fox, M., H. Steltzer, M.J. Trlica, G.S. McMaster, A.A. Andales, D.R. LeCain, and J.A. Morgan, 2014: Elevated CO₂ further lengthens growing season under warming conditions. *Nature*, **510**, 259-262. <http://dx.doi.org/10.1038/nature13207>
125. Zhu, Z., S. Piao, R.B. Myneni, M. Huang, Z. Zeng, J.G. Canadell, P. Ciais, S. Sitch, P. Friedlingstein, A. Arneth, C. Cao, L. Cheng, E. Kato, C. Koven, Y. Li, X. Lian, Y. Liu, R. Liu, J. Mao, Y. Pan, S. Peng, J. Penuelas, B. Poulter, T.A.M. Pugh, B.D. Stocker, N. Viovy, X. Wang, Y. Wang, Z. Xiao, H. Yang, S. Zaehle, and N. Zeng, 2016: Greening of the Earth and its drivers. *Nature Climate Change*, **6**, 791-795. <http://dx.doi.org/10.1038/nclimate3004>
126. Mao, J., A. Ribes, B. Yan, X. Shi, P.E. Thornton, R. Seferian, P. Ciais, R.B. Myneni, H. Douville, S. Piao, Z. Zhu, R.E. Dickinson, Y. Dai, D.M. Ricciuto, M. Jin, F.M. Hoffman, B. Wang, M. Huang, and X. Lian, 2016: Human-induced greening of the northern extratropical land surface. *Nature Climate Change*, **6**, 959-963. <http://dx.doi.org/10.1038/nclimate3056>
127. Finzi, A.C., D.J.P. Moore, E.H. DeLucia, J. Lichter, K.S. Hofmockel, R.B. Jackson, H.-S. Kim, R. Matamala, H.R. McCarthy, R. Oren, J.S. Pippen, and W.H. Schlesinger, 2006: Progressive nitrogen limitation of ecosystem processes under elevated CO₂ in a warm-temperate forest. *Ecology*, **87**, 15-25. <http://dx.doi.org/10.1890/04-1748>
128. Palmroth, S., R. Oren, H.R. McCarthy, K.H. Johnsen, A.C. Finzi, J.R. Butnor, M.G. Ryan, and W.H. Schlesinger, 2006: Aboveground sink strength in forests controls the allocation of carbon below ground and its [CO₂]-induced enhancement. *Proceedings of the National Academy of Sciences*, **103**, 19362-19367. <http://dx.doi.org/10.1073/pnas.0609492103>
129. Norby, R.J., J.M. Warren, C.M. Iversen, B.E. Medlyn, and R.E. McMurtrie, 2010: CO₂ enhancement of forest productivity constrained by limited nitrogen availability. *Proceedings of the National Academy of Sciences*, **107**, 19368-19373. <http://dx.doi.org/10.1073/pnas.1006463107>
130. Sokolov, A.P., D.W. Kicklighter, J.M. Melillo, B.S. Felzer, C.A. Schlosser, and T.W. Cronin, 2008: Consequences of considering carbon-nitrogen interactions on the feedbacks between climate and the terrestrial carbon cycle. *Journal of Climate*, **21**, 3776-3796. <http://dx.doi.org/10.1175/2008JCLI2038.1>
131. Thornton, P.E., S.C. Doney, K. Lindsay, J.K. Moore, N. Mahowald, J.T. Randerson, I. Fung, J.F. Lamarque, J.J. Feddema, and Y.H. Lee, 2009: Carbon-nitrogen interactions regulate climate-carbon cycle feedbacks: Results from an atmosphere-ocean general circulation model. *Biogeosciences*, **6**, 2099-2120. <http://dx.doi.org/10.5194/bg-6-2099-2009>



132. Zaehle, S. and A.D. Friend, 2010: Carbon and nitrogen cycle dynamics in the O-CN land surface model: 1. Model description, site-scale evaluation, and sensitivity to parameter estimates. *Global Biogeochemical Cycles*, **24**, GB1005. <http://dx.doi.org/10.1029/2009GB003521>
133. Betts, R.A., O. Boucher, M. Collins, P.M. Cox, P.D. Falloon, N. Gedney, D.L. Hemming, C. Huntingford, C.D. Jones, D.M.H. Sexton, and M.J. Webb, 2007: Projected increase in continental runoff due to plant responses to increasing carbon dioxide. *Nature*, **448**, 1037-1041. <http://dx.doi.org/10.1038/nature06045>
134. Bernier, P.Y., R.L. Desjardins, Y. Karimi-Zindashty, D. Worth, A. Beaudoin, Y. Luo, and S. Wang, 2011: Boreal lichen woodlands: A possible negative feedback to climate change in eastern North America. *Agricultural and Forest Meteorology*, **151**, 521-528. <http://dx.doi.org/10.1016/j.agrformet.2010.12.013>
135. Churkina, G., V. Brovkin, W. von Bloh, K. Trusilova, M. Jung, and F. Dentener, 2009: Synergy of rising nitrogen depositions and atmospheric CO₂ on land carbon uptake moderately offsets global warming. *Global Biogeochemical Cycles*, **23**, GB4027. <http://dx.doi.org/10.1029/2008GB003291>
136. Zaehle, S., P. Friedlingstein, and A.D. Friend, 2010: Terrestrial nitrogen feedbacks may accelerate future climate change. *Geophysical Research Letters*, **37**, L01401. <http://dx.doi.org/10.1029/2009GL041345>
137. Page, S.E., F. Siegert, J.O. Rieley, H.-D.V. Boehm, A. Jaya, and S. Limin, 2002: The amount of carbon released from peat and forest fires in Indonesia during 1997. *Nature*, **420**, 61-65. <http://dx.doi.org/10.1038/nature01131>
138. Ciais, P., M. Reichstein, N. Viovy, A. Granier, J. Ogee, V. Allard, M. Aubinet, N. Buchmann, C. Bernhofer, A. Carrara, F. Chevallier, N. De Noblet, A.D. Friend, P. Friedlingstein, T. Grunwald, B. Heinesch, P. Keronen, A. Knohl, G. Krinner, D. Loustau, G. Manca, G. Matteucci, F. Miglietta, J.M. Ourcival, D. Papale, K. Pilegaard, S. Rambal, G. Seufert, J.F. Soussana, M.J. Sanz, E.D. Schulze, T. Vesala, and R. Valentini, 2005: Europe-wide reduction in primary productivity caused by the heat and drought in 2003. *Nature*, **437**, 529-533. <http://dx.doi.org/10.1038/nature03972>
139. Chambers, J.Q., J.I. Fisher, H. Zeng, E.L. Chapman, D.B. Baker, and G.C. Hurtt, 2007: Hurricane Katrina's carbon footprint on U.S. Gulf Coast forests. *Science*, **318**, 1107-1107. <http://dx.doi.org/10.1126/science.1148913>
140. Kurz, W.A., G. Stinson, G.J. Rampley, C.C. Dymond, and E.T. Neilson, 2008: Risk of natural disturbances makes future contribution of Canada's forests to the global carbon cycle highly uncertain. *Proceedings of the National Academy of Sciences*, **105**, 1551-1555. <http://dx.doi.org/10.1073/pnas.0708133105>
141. Clark, D.B., D.A. Clark, and S.F. Oberbauer, 2010: Annual wood production in a tropical rain forest in NE Costa Rica linked to climatic variation but not to increasing CO₂. *Global Change Biology*, **16**, 747-759. <http://dx.doi.org/10.1111/j.1365-2486.2009.02004.x>
142. van der Werf, G.R., J.T. Randerson, L. Giglio, G.J. Collatz, M. Mu, P.S. Kasibhatla, D.C. Morton, R.S. DeFries, Y. Jin, and T.T. van Leeuwen, 2010: Global fire emissions and the contribution of deforestation, savanna, forest, agricultural, and peat fires (1997–2009). *Atmospheric Chemistry and Physics*, **10**, 11707-11735. <http://dx.doi.org/10.5194/acp-10-11707-2010>
143. Lewis, S.L., P.M. Brando, O.L. Phillips, G.M.F. van der Heijden, and D. Nepstad, 2011: The 2010 Amazon drought. *Science*, **331**, 554-554. <http://dx.doi.org/10.1126/science.1200807>
144. Melillo, J.M., T.C. Richmond, and G.W. Yohe, eds., 2014: *Climate Change Impacts in the United States: The Third National Climate Assessment*. U.S. Global Change Research Program: Washington, D.C., 841 pp. <http://dx.doi.org/10.7930/J0Z31WJ2>
145. Derksen, C. and R. Brown, 2012: Spring snow cover extent reductions in the 2008–2012 period exceeding climate model projections. *Geophysical Research Letters*, **39**, L19504. <http://dx.doi.org/10.1029/2012gl053387>
146. Stroeve, J., A. Barrett, M. Serreze, and A. Schweiger, 2014: Using records from submarine, aircraft and satellites to evaluate climate model simulations of Arctic sea ice thickness. *The Cryosphere*, **8**, 1839-1854. <http://dx.doi.org/10.5194/tc-8-1839-2014>
147. Stroeve, J.C., T. Markus, L. Boisvert, J. Miller, and A. Barrett, 2014: Changes in Arctic melt season and implications for sea ice loss. *Geophysical Research Letters*, **41**, 1216-1225. <http://dx.doi.org/10.1002/2013GL058951>
148. Comiso, J.C. and D.K. Hall, 2014: Climate trends in the Arctic as observed from space. *Wiley Interdisciplinary Reviews: Climate Change*, **5**, 389-409. <http://dx.doi.org/10.1002/wcc.277>
149. Derksen, D., R. Brown, L. Mudryk, and K. Loujus, 2015: [The Arctic] Terrestrial snow cover [in "State of the Climate in 2014"]. *Bulletin of the American Meteorological Society*, **96** (12), S133-S135. <http://dx.doi.org/10.1175/2015BAMSStateoftheClimate.1>
150. Rignot, E., I. Velicogna, M.R. van den Broeke, A. Monaghan, and J.T.M. Lenaerts, 2011: Acceleration of the contribution of the Greenland and Antarctic ice sheets to sea level rise. *Geophysical Research Letters*, **38**, L05503. <http://dx.doi.org/10.1029/2011GL046583>
151. Rignot, E., J. Mouginot, M. Morlighem, H. Seroussi, and B. Scheuchl, 2014: Widespread, rapid grounding line retreat of Pine Island, Thwaites, Smith, and Kohler Glaciers, West Antarctica, from 1992 to 2011. *Geophysical Research Letters*, **41**, 3502-3509. <http://dx.doi.org/10.1002/2014GL060140>



152. Williams, S.D.P., P. Moore, M.A. King, and P.L. Whitehouse, 2014: Revisiting GRACE Antarctic ice mass trends and accelerations considering autocorrelation. *Earth and Planetary Science Letters*, **385**, 12-21. <http://dx.doi.org/10.1016/j.epsl.2013.10.016>
153. Zemp, M., H. Frey, I. Gärtner-Roer, S.U. Nussbaumer, M. Hoelzle, F. Paul, W. Haeberli, F. Denzinger, A.P. Ahlström, B. Anderson, S. Bajracharya, C. Baroni, L.N. Braun, B.E. Cáceres, G. Casassa, G. Cobos, L.R. Dávila, H. Delgado Granados, M.N. Demuth, L. Espizua, A. Fischer, K. Fujita, B. Gadek, A. Ghazanfar, J.O. Hagen, P. Holmlund, N. Karimi, Z. Li, M. Pelto, P. Pitte, V.V. Popovnin, C.A. Portocarrero, R. Prinz, C.V. Sangewar, I. Severskiy, O. Sigurðsson, A. Soruco, R. Usabaliyev, and C. Vincent, 2015: Historically unprecedented global glacier decline in the early 21st century. *Journal of Glaciology*, **61**, 745-762. <http://dx.doi.org/10.3189/2015JG15J017>
154. Seo, K.-W., C.R. Wilson, T. Scambos, B.-M. Kim, D.E. Waliser, B. Tian, B.-H. Kim, and J. Eom, 2015: Surface mass balance contributions to acceleration of Antarctic ice mass loss during 2003–2013. *Journal of Geophysical Research Solid Earth*, **120**, 3617-3627. <http://dx.doi.org/10.1002/2014JB011755>
155. Harig, C. and F.J. Simons, 2016: Ice mass loss in Greenland, the Gulf of Alaska, and the Canadian Archipelago: Seasonal cycles and decadal trends. *Geophysical Research Letters*, **43**, 3150-3159. <http://dx.doi.org/10.1002/2016GL067759>
156. Perovich, D., S. Gerlnad, S. Hendricks, W. Meier, M. Nicolaus, and M. Tschudi, 2015: [The Arctic] Sea ice cover [in “State of the Climate in 2014”]. *Bulletin of the American Meteorological Society*, **96** (12), S145-S146. <http://dx.doi.org/10.1175/2015BAMSStateoftheClimate.1>
157. Stroeve, J.C., M.C. Serreze, M.M. Holland, J.E. Kay, J. Malanik, and A.P. Barrett, 2012: The Arctic’s rapidly shrinking sea ice cover: A research synthesis. *Climatic Change*, **110**, 1005-1027. <http://dx.doi.org/10.1007/s10584-011-0101-1>
158. Parkinson, C.L., 2014: Spatially mapped reductions in the length of the Arctic sea ice season. *Geophysical Research Letters*, **41**, 4316-4322. <http://dx.doi.org/10.1002/2014GL060434>
159. NSIDC, 2016: Sluggish Ice Growth in the Arctic. Arctic Sea Ice News and Analysis, National Snow and Ice Data Center. <http://nsidc.org/arcticseaicenews/2016/11/sluggish-ice-growth-in-the-arctic/>
160. Stroeve, J.C., V. Kattsov, A. Barrett, M. Serreze, T. Pavlova, M. Holland, and W.N. Meier, 2012: Trends in Arctic sea ice extent from CMIP5, CMIP3 and observations. *Geophysical Research Letters*, **39**, L16502. <http://dx.doi.org/10.1029/2012GL052676>
161. Zhang, R. and T.R. Knutson, 2013: The role of global climate change in the extreme low summer Arctic sea ice extent in 2012 [in “Explaining Extreme Events of 2012 from a Climate Perspective”]. *Bulletin of the American Meteorological Society*, **94** (9), S23-S26. <http://dx.doi.org/10.1175/BAMS-D-13-00085.1>
162. Zunz, V., H. Goosse, and F. Massonnet, 2013: How does internal variability influence the ability of CMIP5 models to reproduce the recent trend in Southern Ocean sea ice extent? *The Cryosphere*, **7**, 451-468. <http://dx.doi.org/10.5194/tc-7-451-2013>
163. Eisenman, I., W.N. Meier, and J.R. Norris, 2014: A spurious jump in the satellite record: Has Antarctic sea ice expansion been overestimated? *The Cryosphere*, **8**, 1289-1296. <http://dx.doi.org/10.5194/tc-8-1289-2014>
164. Pauling, A.G., C.M. Bitz, I.J. Smith, and P.J. Langhorne, 2016: The response of the Southern Ocean and Antarctic sea ice to freshwater from ice shelves in an Earth system model. *Journal of Climate*, **29**, 1655-1672. <http://dx.doi.org/10.1175/JCLI-D-15-0501.1>
165. Meehl, G.A., J.M. Arblaster, C.M. Bitz, C.T.Y. Chung, and H. Teng, 2016: Antarctic sea-ice expansion between 2000 and 2014 driven by tropical Pacific decadal climate variability. *Nature Geoscience*, **9**, 590-595. <http://dx.doi.org/10.1038/ngeo2751>
166. Velicogna, I. and J. Wahr, 2013: Time-variable gravity observations of ice sheet mass balance: Precision and limitations of the GRACE satellite data. *Geophysical Research Letters*, **40**, 3055-3063. <http://dx.doi.org/10.1002/grl.50527>
167. Harig, C. and F.J. Simons, 2015: Accelerated West Antarctic ice mass loss continues to outpace East Antarctic gains. *Earth and Planetary Science Letters*, **415**, 134-141. <http://dx.doi.org/10.1016/j.epsl.2015.01.029>
168. Joughin, I., B.E. Smith, and B. Medley, 2014: Marine ice sheet collapse potentially under way for the Thwaites Glacier Basin, West Antarctica. *Science*, **344**, 735-738. <http://dx.doi.org/10.1126/science.1249055>
169. Pelto, M.S., 2015: [Global Climate] Alpine glaciers [in “State of the Climate in 2014”]. *Bulletin of the American Meteorological Society*, **96** (12), S19-S20. <http://dx.doi.org/10.1175/2015BAMSStateoftheClimate.1>
170. Mengel, M., A. Levermann, K. Frieler, A. Robinson, B. Marzeion, and R. Winkelmann, 2016: Future sea level rise constrained by observations and long-term commitment. *Proceedings of the National Academy of Sciences*, **113**, 2597-2602. <http://dx.doi.org/10.1073/pnas.1500515113>
171. Jenkins, A., P. Dutrioux, S.S. Jacobs, S.D. McPhail, J.R. Perrett, A.T. Webb, and D. White, 2010: Observations beneath Pine Island Glacier in West Antarctica and implications for its retreat. *Nature Geoscience*, **3**, 468-472. <http://dx.doi.org/10.1038/ngeo890>



172. Feldmann, J. and A. Levermann, 2015: Collapse of the West Antarctic Ice Sheet after local destabilization of the Amundsen Basin. *Proceedings of the National Academy of Sciences*, **112**, 14191-14196. <http://dx.doi.org/10.1073/pnas.1512482112>
173. DeConto, R.M. and D. Pollard, 2016: Contribution of Antarctica to past and future sea-level rise. *Nature*, **531**, 591-597. <http://dx.doi.org/10.1038/nature17145>
174. Harig, C. and F.J. Simons, 2012: Mapping Greenland's mass loss in space and time. *Proceedings of the National Academy of Sciences*, **109**, 19934-19937. <http://dx.doi.org/10.1073/pnas.1206785109>
175. Jacob, T., J. Wahr, W.T. Pfeffer, and S. Swenson, 2012: Recent contributions of glaciers and ice caps to sea level rise. *Nature*, **482**, 514-518. <http://dx.doi.org/10.1038/nature10847>
176. Tedesco, M., X. Fettweis, M.R.v.d. Broeke, R.S.W.v.d. Wal, C.J.P.P. Smeets, W.J.v.d. Berg, M.C. Serreze, and J.E. Box, 2011: The role of albedo and accumulation in the 2010 melting record in Greenland. *Environmental Research Letters*, **6**, 014005. <http://dx.doi.org/10.1088/1748-9326/6/1/014005>
177. Fettweis, X., M. Tedesco, M. van den Broeke, and J. Ettema, 2011: Melting trends over the Greenland ice sheet (1958–2009) from spaceborne microwave data and regional climate models. *The Cryosphere*, **5**, 359-375. <http://dx.doi.org/10.5194/tc-5-359-2011>
178. Tedesco, M., E. Box, J. Cappelen, R.S. Fausto, X. Fettweis, K. Hansen, T. Mote, C.J.P.P. Smeets, D.V. As, R.S.W.V.d. Wal, and J. Wahr, 2015: [The Arctic] Greenland ice sheet [in "State of the Climate in 2014"]. *Bulletin of the American Meteorological Society*, **96** (12), S137-S139. <http://dx.doi.org/10.1175/2015BAMS-StateoftheClimate.1>
179. Nghiem, S.V., D.K. Hall, T.L. Mote, M. Tedesco, M.R. Albert, K. Keegan, C.A. Shuman, N.E. DiGirolamo, and G. Neumann, 2012: The extreme melt across the Greenland ice sheet in 2012. *Geophysical Research Letters*, **39**, L20502. <http://dx.doi.org/10.1029/2012GL053611>
180. Tedesco, M., X. Fettweis, T. Mote, J. Wahr, P. Alexander, J.E. Box, and B. Wouters, 2013: Evidence and analysis of 2012 Greenland records from spaceborne observations, a regional climate model and reanalysis data. *The Cryosphere*, **7**, 615-630. <http://dx.doi.org/10.5194/tc-7-615-2013>
181. Romanovsky, V.E., S.L. Smith, H.H. Christiansen, N.I. Shiklomanov, D.A. Streletskiy, D.S. Drozdov, G.V. Malkova, N.G. Oberman, A.L. Kholodov, and S.S. Marchenko, 2015: [The Arctic] Terrestrial permafrost [in "State of the Climate in 2014"]. *Bulletin of the American Meteorological Society*, **96** (12), S139-S141. <http://dx.doi.org/10.1175/2015BAMSStateoftheClimate.1>
182. Shiklomanov, N.E., D.A. Streletskiy, and F.E. Nelson, 2012: Northern Hemisphere component of the global Circumpolar Active Layer Monitory (CALM) program. In *Proceedings of the 10th International Conference on Permafrost*, Salekhard, Russia. Kane, D.L. and K.M. Hinkel, Eds., 377-382. http://research.iarc.uaf.edu/NICOP/proceedings/10th/TICOP_vol1.pdf
183. Church, J.A. and N.J. White, 2011: Sea-level rise from the late 19th to the early 21st century. *Surveys in Geophysics*, **32**, 585-602. <http://dx.doi.org/10.1007/s10712-011-9119-1>
184. Hay, C.C., E. Morrow, R.E. Kopp, and J.X. Mitrovica, 2015: Probabilistic reanalysis of twentieth-century sea-level rise. *Nature*, **517**, 481-484. <http://dx.doi.org/10.1038/nature14093>
185. Nerem, R.S., D.P. Chambers, C. Choe, and G.T. Mitchum, 2010: Estimating mean sea level change from the TOPEX and Jason altimeter missions. *Marine Geodesy*, **33**, 435-446. <http://dx.doi.org/10.1080/01490419.2010.491031>
186. Merrifield, M.A., P. Thompson, E. Leuliette, G.T. Mitchum, D.P. Chambers, S. Jevrejeva, R.S. Nerem, M. Menéndez, W. Sweet, B. Hamlington, and J.J. Marra, 2015: [Global Oceans] Sea level variability and change [in "State of the Climate in 2014"]. *Bulletin of the American Meteorological Society*, **96** (12), S82-S85. <http://dx.doi.org/10.1175/2015BAMSStateoftheClimate.1>
187. Ezer, T. and L.P. Atkinson, 2014: Accelerated flooding along the U.S. East Coast: On the impact of sea-level rise, tides, storms, the Gulf Stream, and the North Atlantic Oscillations. *Earth's Future*, **2**, 362-382. <http://dx.doi.org/10.1002/2014EF000252>
188. Sweet, W.V. and J. Park, 2014: From the extreme to the mean: Acceleration and tipping points of coastal inundation from sea level rise. *Earth's Future*, **2**, 579-600. <http://dx.doi.org/10.1002/2014EF000272>
189. Kopp, R.E., R.M. Horton, C.M. Little, J.X. Mitrovica, M. Oppenheimer, D.J. Rasmussen, B.H. Strauss, and C. Tebaldi, 2014: Probabilistic 21st and 22nd century sea-level projections at a global network of tide-gauge sites. *Earth's Future*, **2**, 383-406. <http://dx.doi.org/10.1002/2014EF000239>
190. Parris, A., P. Bromirski, V. Burkett, D. Cayan, M. Culver, J. Hall, R. Horton, K. Knuuti, R. Moss, J. Obeyesekere, A. Sallenger, and J. Weiss, 2012: Global Sea Level Rise Scenarios for the United States National Climate Assessment. National Oceanic and Atmospheric Administration, Silver Spring, MD. 37 pp. http://scenarios.globalchange.gov/sites/default/files/NOAA_SLR_r3_0.pdf



191. Sweet, W.V., R.E. Kopp, C.P. Weaver, J. Obeysekera, R.M. Horton, E.R. Thieler, and C. Zervas, 2017: Global and Regional Sea Level Rise Scenarios for the United States. National Oceanic and Atmospheric Administration, National Ocean Service, Silver Spring, MD. 75 pp. https://tidesandcurrents.noaa.gov/publications/techrpt83_Global_and_Regional_SLR_Scenarios_for_the_US_final.pdf
192. Schmidt, G.A., J.H. Jungclaus, C.M. Ammann, E. Bard, P. Braconnot, T.J. Crowley, G. Delaygue, F. Joos, N.A. Krivova, R. Muscheler, B.L. Otto-Bliesner, J. Pongratz, D.T. Shindell, S.K. Solanki, F. Steinhilber, and L.E.A. Vieira, 2011: Climate forcing reconstructions for use in PMIP simulations of the last millennium (v1.0). *Geoscientific Model Development*, **4**, 33-45. <http://dx.doi.org/10.5194/gmd-4-33-2011>
193. Mann, M.E., Z. Zhang, M.K. Hughes, R.S. Bradley, S.K. Miller, S. Rutherford, and F. Ni, 2008: Proxy-based reconstructions of hemispheric and global surface temperature variations over the past two millennia. *Proceedings of the National Academy of Sciences*, **105**, 13252-13257. <http://dx.doi.org/10.1073/pnas.0805721105>
194. Turney, C.S.M. and R.T. Jones, 2010: Does the Agulhas Current amplify global temperatures during super-interglacials? *Journal of Quaternary Science*, **25**, 839-843. <http://dx.doi.org/10.1002/jqs.1423>
195. Dutton, A. and K. Lambeck, 2012: Ice volume and sea level during the Last Interglacial. *Science*, **337**, 216-219. <http://dx.doi.org/10.1126/science.1205749>
196. Kopp, R.E., F.J. Simons, J.X. Mitrovica, A.C. Maloof, and M. Oppenheimer, 2009: Probabilistic assessment of sea level during the last interglacial stage. *Nature*, **462**, 863-867. <http://dx.doi.org/10.1038/nature08686>
197. Kaspar, F., N. Kühl, U. Cubasch, and T. Litt, 2005: A model-data comparison of European temperatures in the Eemian interglacial. *Geophysical Research Letters*, **32**, L11703. <http://dx.doi.org/10.1029/2005GL022456>
198. Haywood, A.M., D.J. Hill, A.M. Dolan, B.L. Otto-Bliesner, F. Bragg, W.L. Chan, M.A. Chandler, C. Contoux, H.J. Dowsett, A. Jost, Y. Kamae, G. Lohmann, D.J. Lunt, A. Abe-Ouchi, S.J. Pickering, G. Ramstein, N.A. Rosenbloom, U. Salzmann, L. Sohl, C. Stepanek, H. Ueda, Q. Yan, and Z. Zhang, 2013: Large-scale features of Pliocene climate: Results from the Pliocene Model Intercomparison Project. *Climate of the Past*, **9**, 191-209. <http://dx.doi.org/10.5194/cp-9-191-2013>
199. Wuebbles, D., G. Meehl, K. Hayhoe, T.R. Karl, K. Kunkel, B. Santer, M. Wehner, B. Colle, E.M. Fischer, R. Fu, A. Goodman, E. Janssen, V. Kharin, H. Lee, W. Li, L.N. Long, S.C. Olsen, Z. Pan, A. Seth, J. Sheffield, and L. Sun, 2014: CMIP5 climate model analyses: Climate extremes in the United States. *Bulletin of the American Meteorological Society*, **95**, 571-583. <http://dx.doi.org/10.1175/BAMS-D-12-00172.1>
200. Trenberth, K.E., A. Dai, G. van der Schrier, P.D. Jones, J. Barichivich, K.R. Briffa, and J. Sheffield, 2014: Global warming and changes in drought. *Nature Climate Change*, **4**, 17-22. <http://dx.doi.org/10.1038/nclimate2067>
201. Walsh, J., D. Wuebbles, K. Hayhoe, J. Kossin, K. Kunkel, G. Stephens, P. Thorne, R. Vose, M. Wehner, J. Willis, D. Anderson, S. Doney, R. Feely, P. Hennon, V. Kharin, T. Knutson, F. Landerer, T. Lenton, J. Kennedy, and R. Somerville, 2014: Ch. 2: Our changing climate. *Climate Change Impacts in the United States: The Third National Climate Assessment*. Melillo, J.M., T.C. Richmond, and G.W. Yohe, Eds. U.S. Global Change Research Program, Washington, D.C., 19-67. <http://dx.doi.org/10.7930/J0KW5CXT>
202. Jones, P.D., D.H. Lister, T.J. Osborn, C. Harpham, M. Salmon, and C.P. Morice, 2012: Hemispheric and large-scale land surface air temperature variations: An extensive revision and an update to 2010. *Journal of Geophysical Research*, **117**, D05127. <http://dx.doi.org/10.1029/2011JD017139>





2

Physical Drivers of Climate Change

KEY FINDINGS

1. Human activities continue to significantly affect Earth's climate by altering factors that change its radiative balance. These factors, known as radiative forcings, include changes in greenhouse gases, small airborne particles (aerosols), and the reflectivity of the Earth's surface. In the industrial era, human activities have been, and are increasingly, the dominant cause of climate warming. The increase in radiative forcing due to these activities has far exceeded the relatively small net increase due to natural factors, which include changes in energy from the sun and the cooling effect of volcanic eruptions. (*Very high confidence*)
2. Aerosols caused by human activity play a profound and complex role in the climate system through radiative effects in the atmosphere and on snow and ice surfaces and through effects on cloud formation and properties. The combined forcing of aerosol-radiation and aerosol-cloud interactions is negative (cooling) over the industrial era (*high confidence*), offsetting a substantial part of greenhouse gas forcing, which is currently the predominant human contribution. The magnitude of this offset, globally averaged, has declined in recent decades, despite increasing trends in aerosol emissions or abundances in some regions (*medium to high confidence*).
3. The interconnected Earth-atmosphere-ocean system includes a number of positive and negative feedback processes that can either strengthen (positive feedback) or weaken (negative feedback) the system's responses to human and natural influences. These feedbacks operate on a range of time scales from very short (essentially instantaneous) to very long (centuries). Global warming by net radiative forcing over the industrial era includes a substantial amplification from these feedbacks (approximately a factor of three) (*high confidence*). While there are large uncertainties associated with some of these feedbacks, the net feedback effect over the industrial era has been positive (amplifying warming) and will continue to be positive in coming decades (*very high confidence*).

Recommended Citation for Chapter

Fahey, D.W., S.J. Doherty, K.A. Hibbard, A. Romanou, and P.C. Taylor, 2017: Physical drivers of climate change. In: *Climate Science Special Report: Fourth National Climate Assessment, Volume I* [Wuebbles, D.J., D.W. Fahey, K.A. Hibbard, D.J. Dokken, B.C. Stewart, and T.K. Maycock (eds.)]. U.S. Global Change Research Program, Washington, DC, USA, pp. 73-113, doi: 10.7930/J0513WCR.

2.0 Introduction

Earth's climate is undergoing substantial change due to anthropogenic activities (Ch. 1: Our Globally Changing Climate). Understanding the causes of past and present climate change and confidence in future projected changes depend directly on our ability to understand and model the physical drivers of climate change.¹ Our understanding is challenged by the complexity and interconnectedness of the components of the climate system (that is, the atmosphere, land, ocean, and cryosphere). This chapter lays out the foundation of climate change by describing its physical drivers, which are primarily associat-

ed with atmospheric composition (gases and aerosols) and cloud effects. We describe the principle radiative forcings and the variety of feedback responses which serve to amplify these forcings.

2.1 Earth's Energy Balance and the Greenhouse Effect

The temperature of the Earth system is determined by the amounts of incoming (short-wavelength) and outgoing (both short- and long-wavelength) radiation. In the modern era, radiative fluxes are well-constrained by satellite measurements (Figure 2.1). About a third (29.4%) of incoming, short-wavelength

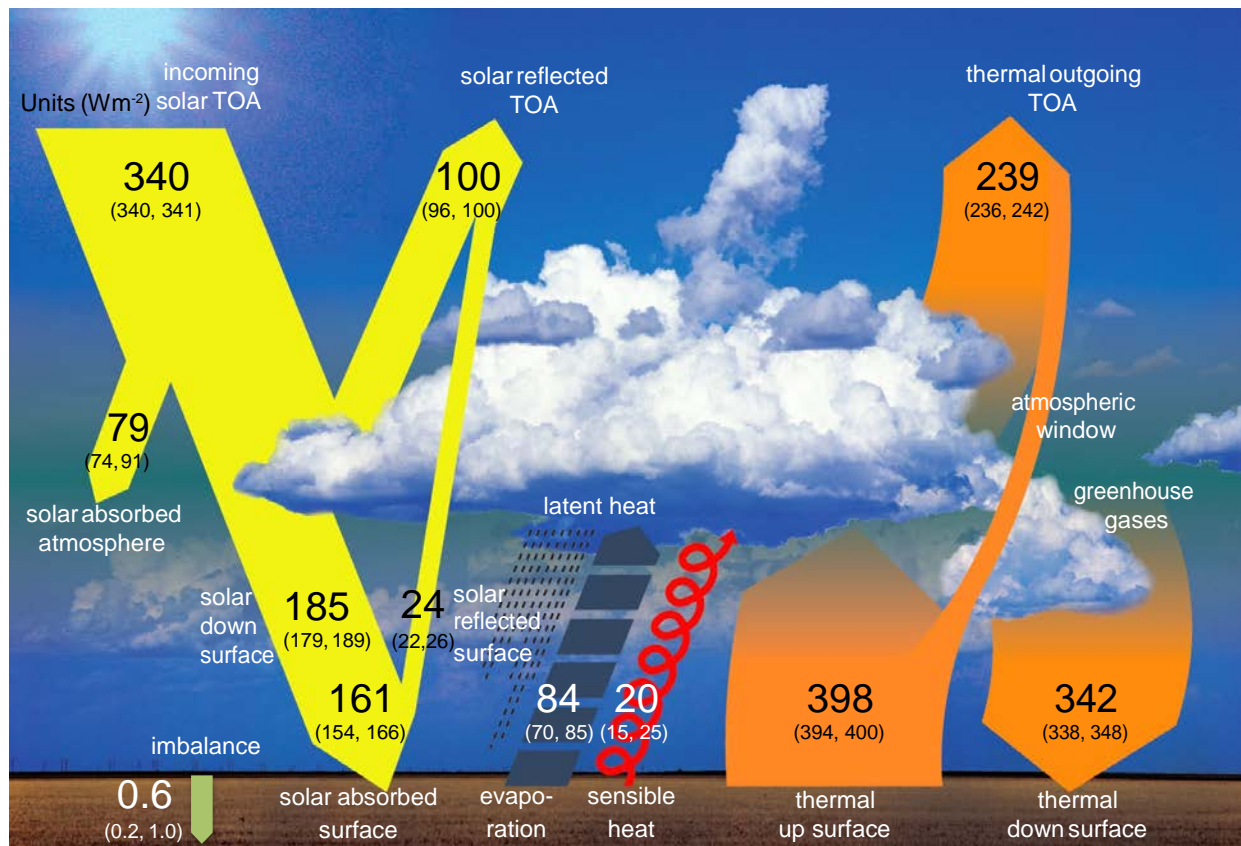


Figure 2.1: Global mean energy budget of Earth under present-day climate conditions. Numbers state magnitudes of the individual energy fluxes in watts per square meter (W/m²) averaged over Earth's surface, adjusted within their uncertainty ranges to balance the energy budgets of the atmosphere and the surface. Numbers in parentheses attached to the energy fluxes cover the range of values in line with observational constraints. Fluxes shown include those resulting from feedbacks. Note the net imbalance of 0.6 W/m² in the global mean energy budget. The observational constraints are largely provided by satellite-based observations, which have directly measured solar and infrared fluxes at the top of the atmosphere over nearly the whole globe since 1984.^{217, 218} More advanced satellite-based measurements focusing on the role of clouds in Earth's radiative fluxes have been available since 1998.^{219, 220} Top of Atmosphere (TOA) reflected solar values given here are based on observations 2001–2010; TOA outgoing longwave is based on 2005–2010 observations. (Figure source: Hartmann et al. 2013,²²¹ Figure 2-11; © IPCC, used with permission).

energy from the sun is reflected back to space, and the remainder is absorbed by Earth's system. The fraction of sunlight scattered back to space is determined by the reflectivity (albedo) of clouds, land surfaces (including snow and ice), oceans, and particles in the atmosphere. The amount and albedo of clouds, snow cover, and ice cover are particularly strong determinants of the amount of sunlight reflected back to space because their albedos are much higher than that of land and oceans.

In addition to reflected sunlight, Earth loses energy through infrared (long-wavelength) radiation from the surface and atmosphere. Absorption by greenhouse gases (GHGs) of infrared energy radiated from the surface leads to warming of the surface and atmosphere. Figure 2.1 illustrates the importance of greenhouse gases in the energy balance of Earth's system. The naturally occurring GHGs in Earth's atmosphere—principally water vapor and carbon dioxide—keep the near-surface air temperature about 60°F (33°C) warmer than it would be in their absence, assuming albedo is held constant.² Geothermal heat from Earth's interior, direct heating from energy production, and frictional heating through tidal flows also contribute to the amount of energy available for heating Earth's surface and atmosphere, but their total contribution is an extremely small fraction (< 0.1%) of that due to net solar (shortwave) and infrared (long-wave) radiation (e.g., see Davies and Davies 2010;³ Flanner 2009;⁴ Munk and Wunsch 1998,⁵ where these forcings are quantified).

Thus, Earth's equilibrium temperature in the modern era is controlled by a short list of factors: incoming sunlight, absorbed and reflected sunlight, emitted infrared radiation, and infrared radiation absorbed and re-emitted in the atmosphere, primarily by GHGs. Changes in these factors affect Earth's radiative balance and therefore its climate, including

but not limited to the average, near-surface air temperature. Anthropogenic activities have changed Earth's radiative balance and its albedo by adding GHGs, particles (aerosols), and aircraft contrails to the atmosphere, and through land-use changes. Changes in the radiative balance (or forcings) produce changes in temperature, precipitation, and other climate variables through a complex set of physical processes, many of which are coupled (Figure 2.2). These changes, in turn, trigger feedback processes which can further amplify and/or dampen the changes in radiative balance (Sections 2.5 and 2.6).

In the following sections, the principal components of the framework shown in Figure 2.2 are described. Climate models are structured to represent these processes; climate models and their components and associated uncertainties, are discussed in more detail in Chapter 4: Projections.

The processes and feedbacks connecting changes in Earth's radiative balance to a climate response (Figure 2.2) operate on a large range of time scales. Reaching an equilibrium temperature distribution in response to anthropogenic activities takes decades or longer because some components of Earth's system—in particular the oceans and cryosphere—are slow to respond due to their large thermal masses and the long time scale of circulation between the ocean surface and the deep ocean. Of the substantial energy gained in the combined ocean-atmosphere system over the previous four decades, over 90% of it has gone into ocean warming (see Box 3.1 Figure 1 of Rhein et al. 2013).⁶ Even at equilibrium, internal variability in Earth's climate system causes limited annual- to decadal-scale variations in regional temperatures and other climate parameters that do not contribute to long-term trends. For example, it is *likely* that natural variability has contributed between



Simplified Conceptual Framework of the Climate System

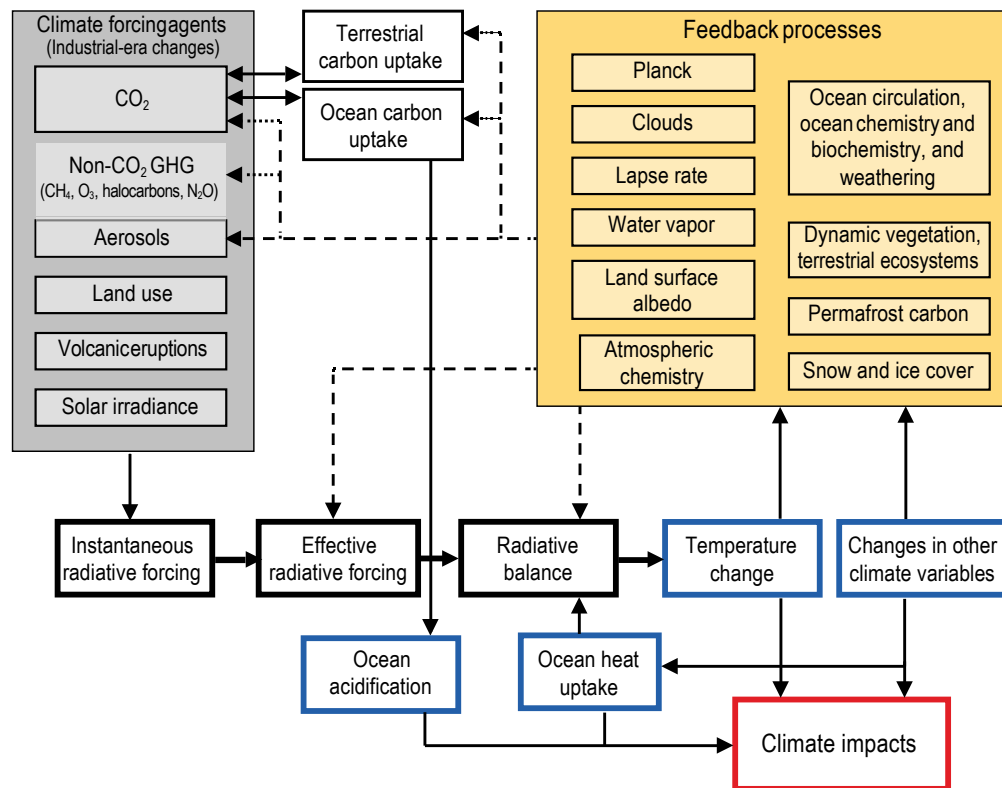


Figure 2.2: Simplified conceptual modeling framework for the climate system as implemented in many climate models (Ch. 4: Projections). Modeling components include forcing agents, feedback processes, carbon uptake processes, and radiative forcing and balance. The lines indicate physical interconnections (solid lines) and feedback pathways (dashed lines). Principal changes (blue boxes) lead to climate impacts (red box) and feedbacks. (Figure source: adapted from Knutti and Rugenstein 2015⁸²).

–0.18°F (–0.1°C) and 0.18°F (0.1°C) to changes in surface temperatures from 1951 to 2010; by comparison, anthropogenic GHGs have *likely* contributed between 0.9°F (0.5°C) and 2.3°F (1.3°C) to observed surface warming over this same period.⁷ Due to these longer time scale responses and natural variability, changes in Earth’s radiative balance are not realized immediately as changes in climate, and even in equilibrium there will always be variability around mean conditions.

2.2 Radiative Forcing (RF) and Effective Radiative Forcing (ERF)

Radiative forcing (RF) is widely used to quantify a radiative imbalance in Earth’s atmosphere resulting from either natural changes or anthropogenic activities over the industrial

era. It is expressed as a change in net radiative flux (W/m^2) either at the tropopause or top of the atmosphere,⁸ with the latter nominally defined at 20 km altitude to optimize observation/model comparisons.⁹ The instantaneous RF is defined as the immediate change in net radiative flux following a change in a climate driver. RF can also be calculated after allowing different types of system response: for example, after allowing stratospheric temperatures to adjust, after allowing both stratospheric and surface temperature to adjust, or after allowing temperatures to adjust everywhere (the equilibrium RF) (Figure 8.1 of Myhre et al. 2013⁸).

In this report, we follow the Intergovernmental Panel on Climate Change (IPCC) recom-

mendation that the RF caused by a forcing agent be evaluated as the net radiative flux change at the tropopause after stratospheric temperatures have adjusted to a new radiative equilibrium while assuming all other variables (for example, temperatures and cloud cover) are held fixed (Box 8.1 of Myhre et al. 2013⁸). A change that results in a net increase in the downward flux (shortwave plus longwave) constitutes a positive RF, normally resulting in a warming of the surface and/or atmosphere and potential changes in other climate parameters. Conversely, a change that yields an increase in the net upward flux constitutes a negative RF, leading to a cooling of the surface and/or atmosphere and potential changes in other climate parameters.

RF serves as a metric to compare present, past, or future perturbations to the climate system (e.g., Boer and Yu 2003;¹⁰ Gillett et al. 2004;¹¹ Matthews et al. 2004;¹² Meehl et al. 2004;¹³ Jones et al. 2007;¹⁴ Mahajan et al. 2013;¹⁵ Shiogama et al. 2013¹⁶). For clarity and consistency, RF calculations require that a time period be defined over which the forcing occurs. Here, this period is the industrial era, defined as beginning in 1750 and extending to 2011, unless otherwise noted. The 2011 end date is that adopted by the CMIP5 calculations, which are the basis of RF evaluations by the IPCC.⁸

A refinement of the RF concept introduced in the latest IPCC assessment¹⁷ is the use of effective radiative forcing (ERF). ERF for a climate driver is defined as its RF plus rapid adjustment(s) to that RF.⁸ These rapid adjustments occur on time scales much shorter than, for example, the response of ocean temperatures. For an important subset of climate drivers, ERF is more reliably correlated with the climate response to the forcing than is RF; as such, it is an increasingly used metric when discussing forcing. For atmospheric components, ERF includes rapid adjustments due

to direct warming of the troposphere, which produces horizontal temperature variations, variations in the vertical lapse rate, and changes in clouds and vegetation, and it includes the microphysical effects of aerosols on cloud lifetime. Rapid changes in land surface properties (temperature, snow and ice cover, and vegetation) are also included. Not included in ERF are climate responses driven by changes in sea surface temperatures or sea ice cover. For forcing by aerosols in snow (Section 2.3.2), ERF includes the effects of direct warming of the snowpack by particulate absorption (for example, snow-grain size changes). Changes in all of these parameters in response to RF are quantified in terms of their impact on radiative fluxes (for example, albedo) and included in the ERF. The largest differences between RF and ERF occur for forcing by light-absorbing aerosols because of their influence on clouds and snow (Section 2.3.2). For most non-aerosol climate drivers, the differences between RF and ERF are small.

2.3 Drivers of Climate Change over the Industrial Era

Climate drivers of significance over the industrial era include both those associated with anthropogenic activity and, to a lesser extent, those of natural origin. The only significant natural climate drivers in the industrial era are changes in solar irradiance, volcanic eruptions, and the El Niño–Southern Oscillation. Natural emissions and sinks of GHGs and tropospheric aerosols have varied over the industrial era but have not contributed significantly to RF. The effects of cosmic rays on cloud formation have been studied, but global radiative effects are not considered significant.¹⁸ There are other known drivers of natural origin that operate on longer time scales (for example, changes in Earth’s orbit [Milankovitch cycles] and changes in atmospheric CO₂ via chemical weathering of rock). Anthropogenic drivers can be divided into a



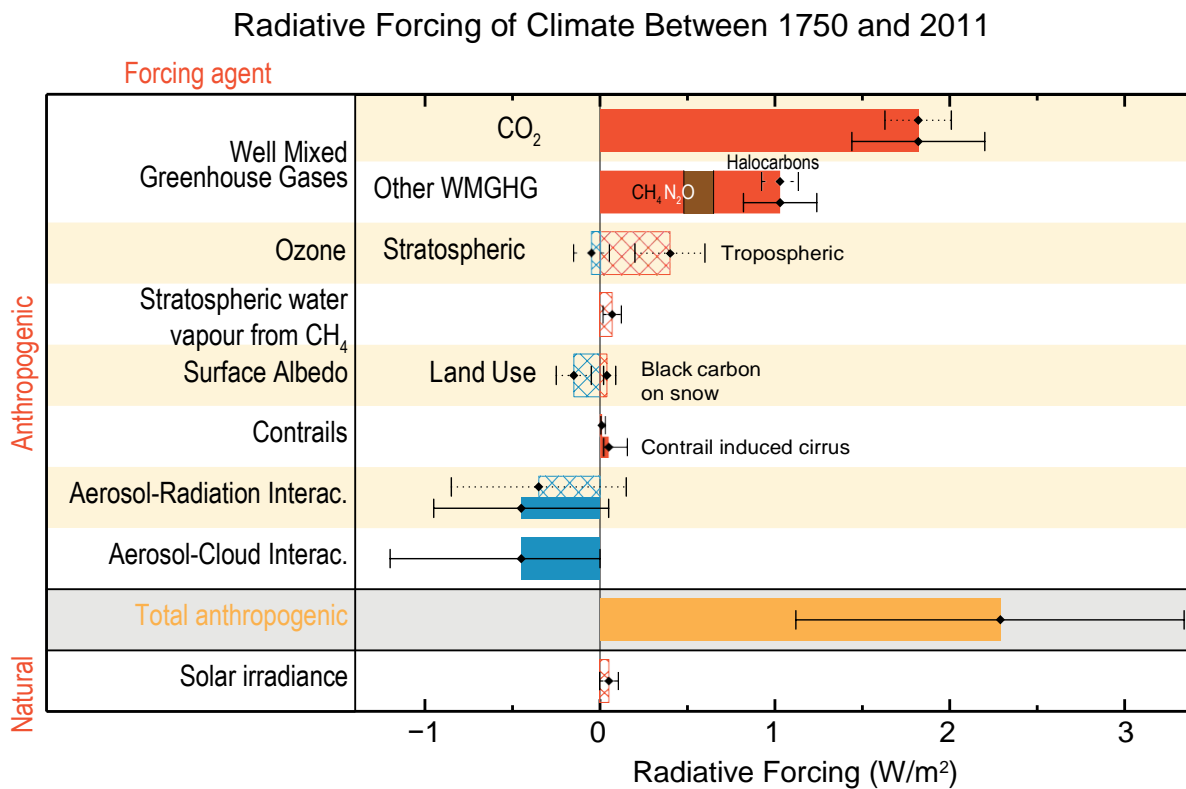


Figure 2.3: Bar chart for radiative forcing (RF; hatched) and effective radiative forcing (ERF; solid) for the period 1750–2011, where the total ERF is derived from the Intergovernmental Panel on Climate Change’s Fifth Assessment Report. Uncertainties (5% to 95% confidence range) are given for RF (dotted lines) and ERF (solid lines). Volcanic forcing is not shown because this forcing is intermittent, exerting forcing over only a few years for eruptions during the industrial era; the net forcing over the industrial era is negligible. (Figure source: Myhre et al. 2013,⁸ Figure 8-15; © IPCC, used with permission).

number of categories, including well-mixed greenhouse gases (WMGHGs), short-lived climate forcers (SLCFs, which include methane, some hydrofluorocarbons [HFCs], ozone, and aerosols), contrails, and changes in albedo (for example, land-use changes). Some WMGHGs are also considered SLCFs (for example, methane). Figures 2.3–2.7 summarize features of the principal climate drivers in the industrial era. Each is described briefly in the following.

2.3.1 Natural Drivers

Solar Irradiance

Changes in solar irradiance directly impact the climate system because the irradiance is Earth’s primary energy source.¹⁹ In the industrial era, the largest variations in total solar irradiance follow an 11-year cycle.^{20, 21} Direct solar observations have been available since

1978,²² though proxy indicators of solar cycles are available back to the early 1600s.²³ Although these variations amount to only 0.1% of the total solar output of about 1360 W/m²,²⁴ relative variations in irradiance at specific wavelengths can be much larger (tens of percent). Spectral variations in solar irradiance are highest at near-ultraviolet (UV) and shorter wavelengths,²⁵ which are also the most important wavelengths for driving changes in ozone.^{26, 27} By affecting ozone concentrations, variations in total and spectral solar irradiance induce discernible changes in atmospheric heating and changes in circulation.^{21, 28, 29} The relationships between changes in irradiance and changes in atmospheric composition, heating, and dynamics are such that changes in total solar irradiance are not directly correlated with the resulting radiative flux changes.^{26, 30, 31}

The IPCC estimate of the RF due to changes in total solar irradiance over the industrial era is 0.05 W/m^2 (range: 0.0 to 0.10 W/m^2).⁸ This forcing does not account for radiative flux changes resulting from changes in ozone driven by changes in the spectral irradiance. Understanding of the links between changes in spectral irradiance, ozone concentrations, heating rates, and circulation changes has recently improved using, in particular, satellite data starting in 2002 that provide solar spectral irradiance measurements through the UV²⁶ along with a series of chemistry–climate modeling studies.^{26, 27, 32, 33, 34} At the regional scale, circulation changes driven by solar spectral irradiance variations may be significant for some locations and seasons but are poorly quantified.²⁸ Despite remaining uncertainties, there is *very high confidence* that solar radiance-induced changes in RF are small relative to RF from anthropogenic GHGs over the industrial era (Figure 2.3).⁸

Volcanoes

Most volcanic eruptions are minor events with the effects of emissions confined to the troposphere and only lasting for weeks to months. In contrast, explosive volcanic eruptions inject substantial amounts of sulfur dioxide (SO_2) and ash into the stratosphere, which lead to significant short-term climate effects (Myhre et al. 2013,⁸ and references therein). SO_2 oxidizes to form sulfuric acid (H_2SO_4) which condenses, forming new particles or adding mass to preexisting particles, thereby substantially enhancing the attenuation of sunlight transmitted through the stratosphere (that is, increasing aerosol optical depth). These aerosols increase Earth’s albedo by scattering sunlight back to space, creating a negative RF that cools the planet.^{35, 36} The RF persists for the lifetime of aerosol in the stratosphere, which is a few years, far exceeding that in the troposphere (about a week). The oceans respond to a negative volcanic RF through cooling and chang-

es in ocean circulation patterns that last for decades after major eruptions (for example, Mt. Tambora in 1815).^{37, 38, 39, 40} In addition to the direct RF, volcanic aerosol heats the stratosphere, altering circulation patterns, and depletes ozone by enhancing surface reactions, which further changes heating and circulation. The resulting impacts on advective heat transport can be larger than the temperature impacts of the direct forcing.³⁶ Aerosol from both explosive and non-explosive eruptions also affects the troposphere through changes in diffuse radiation and through aerosol–cloud interactions. It has been proposed that major eruptions might “fertilize” the ocean with sufficient iron to affect phytoplankton production and, therefore, enhance the ocean carbon sink.⁴¹ Volcanoes also emit CO_2 and water vapor, although in small quantities relative to other emissions. At present, conservative estimates of annual CO_2 emissions from volcanoes are less than 1% of CO_2 emissions from all anthropogenic activities.⁴² The magnitude of volcanic effects on climate depends on the number and strength of eruptions, the latitude of injection and, for ocean temperature and circulation impacts, the timing of the eruption relative to ocean temperature and circulation patterns.^{39, 40}

Volcanic eruptions represent the largest natural forcing within the industrial era. In the last millennium, eruptions caused several multiyear, transient episodes of negative RF of up to several W/m^2 (Figure 2.6). The RF of the last major volcanic eruption, Mt. Pinatubo in 1991, decayed to negligible values later in the 1990s, with the temperature signal lasting about twice as long due to the effects of changes in ocean heat uptake.³⁷ A net volcanic RF has been omitted from the drivers of climate change in the industrial era in Figure 2.3 because the value from multiple, episodic eruptions is negligible compared with the other climate drivers. While future explosive



volcanic eruptions have the potential to again alter Earth's climate for periods of several years, predictions of occurrence, intensity, and location remain elusive. If a sufficient number of non-explosive eruptions occur over an extended time period in the future, average changes in tropospheric composition or circulation could yield a significant RF.³⁶

2.3.2 Anthropogenic Drivers

Principal Well-mixed Greenhouse Gases (WMGHGs)

The principal WMGHGs are carbon dioxide (CO₂), methane (CH₄), and nitrous oxide

(N₂O). With atmospheric lifetimes of a decade to a century or more, these gases have modest-to-small regional variabilities and are circulated and mixed around the globe to yield small interhemispheric gradients. The atmospheric abundances and associated radiative forcings of WMGHGs have increased substantially over the industrial era (Figures 2.4–2.6). Contributions from natural sources of these constituents are accounted for in the industrial-era RF calculations shown in Figure 2.6.

CO₂ has substantial global sources and sinks (Figure 2.7). CO₂ emission sources have grown

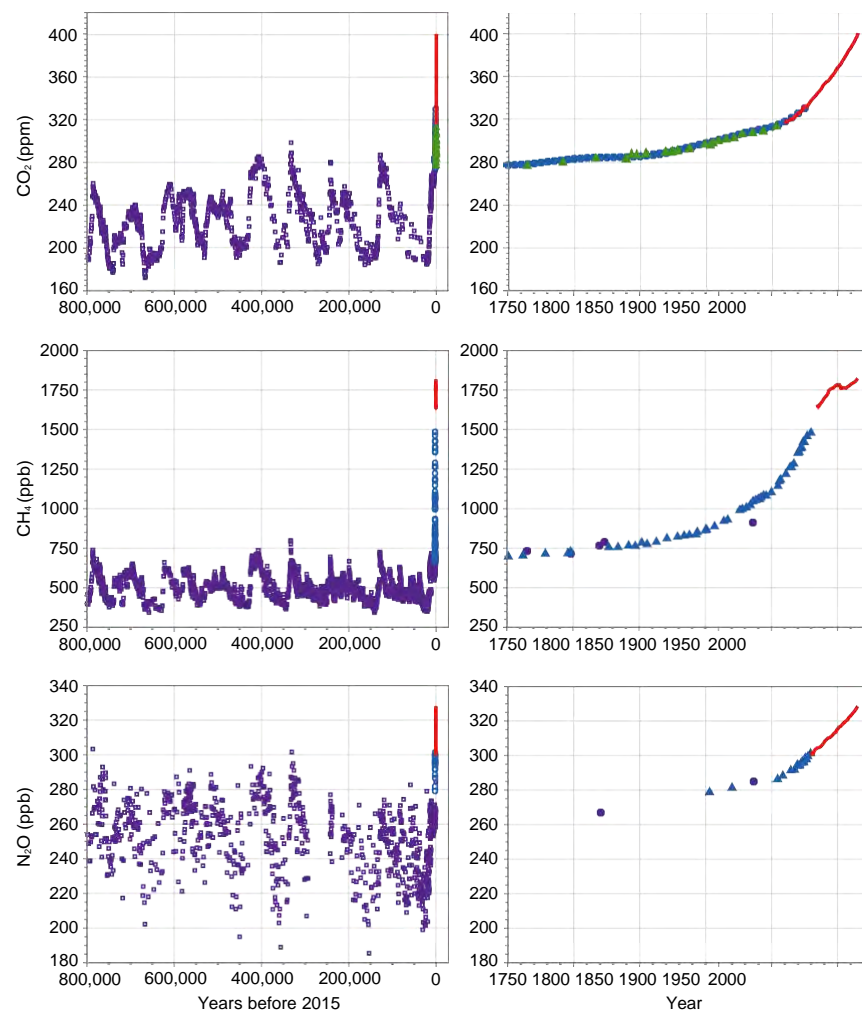


Figure 2.4: Atmospheric concentrations of CO₂ (top), CH₄ (middle), and N₂O (bottom) over the last 800,000 years (left panels) and for 1750–2015 (right panels). Measurements are shown from ice cores (symbols with different colors for different studies) and for direct atmospheric measurements (red lines). (Adapted from IPCC 2007,⁸⁸ Figure SPM.1, © IPCC, used with permission; data are from <https://www.epa.gov/climate-indicators/climate-change-indicators-atmospheric-concentrations-greenhouse-gases>).

in the industrial era primarily from fossil fuel combustion (that is, coal, gas, and oil), cement manufacturing, and land-use change from activities such as deforestation.⁴³ Carbonation of finished cement products is a sink of atmospheric CO₂, offsetting a substantial fraction (0.43) of the industrial-era emissions from

cement production.⁴⁴ A number of processes act to remove CO₂ from the atmosphere, including uptake in the oceans, residual land uptake, and rock weathering. These combined processes yield an effective atmospheric lifetime for emitted CO₂ of many decades to millennia, far greater than any other major

Radiative Forcing of Well-mixed Greenhouse Gases

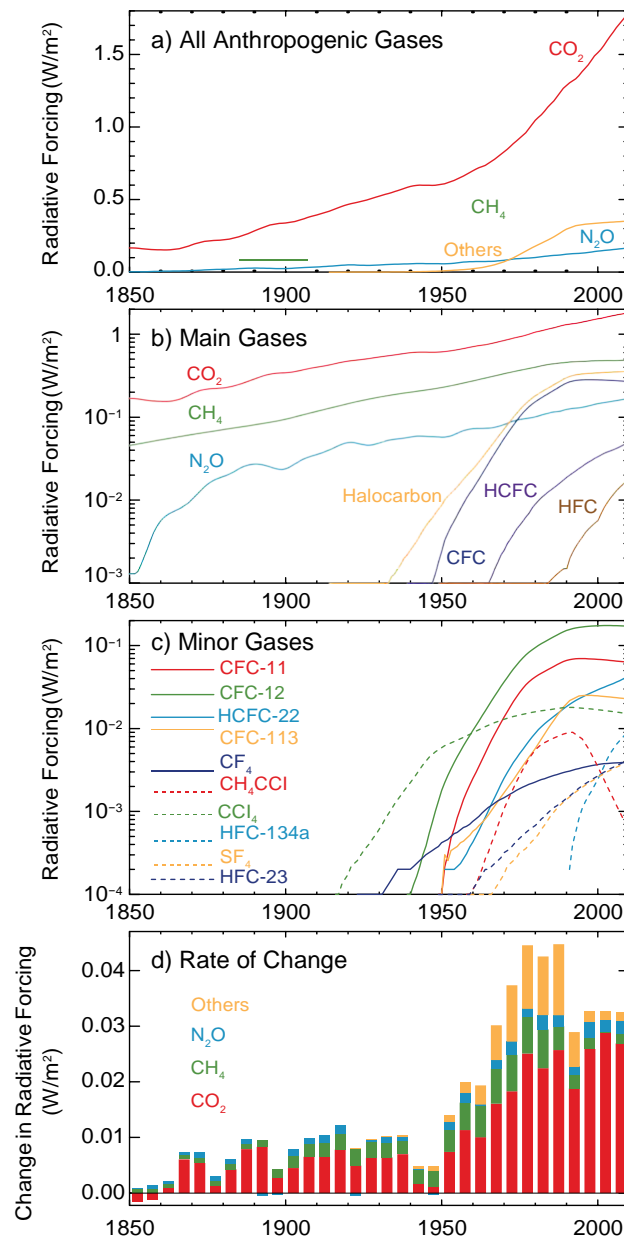


Figure 2.5: (a) Radiative forcing (RF) from the major WMGHGs and groups of halocarbons (Others) from 1850 to 2011; (b) the data in (a) with a logarithmic scale; (c) RFs from the minor WMGHGs from 1850 to 2011 (logarithmic scale); (d) the annual rate of change ($[W/m^2]/year$) in forcing from the major WMGHGs and halocarbons from 1850 to 2011. (Figure source: Myhre et al. 2013,⁸ Figure 8-06; © IPCC, used with permission).

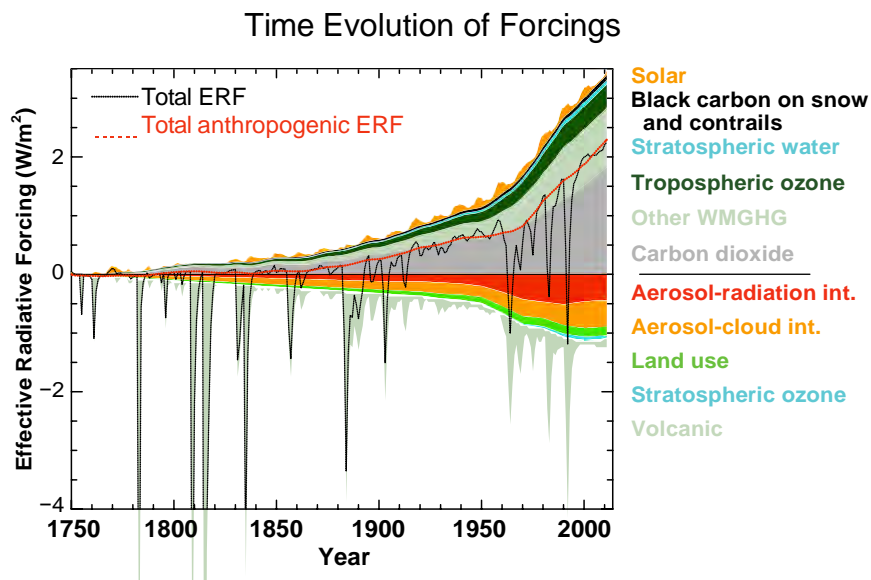


Figure 2.6: Time evolution in effective radiative forcings (ERFs) across the industrial era for anthropogenic and natural forcing mechanisms. The terms contributing to cumulative totals of positive and negative ERF are shown with colored regions. The terms are labeled in order on the right-hand side with positive ERFs above the zero line and negative ERFs below the zero line. The forcings from black-carbon-on-snow and contrail terms are grouped together into a single term in the plot. Also shown are the cumulative sum of all forcings (Total; black dashed line) and of anthropogenic-only forcings (Total Anthropogenic; red dashed line). Uncertainties in 2011 ERF values are shown in the original figure (Myhre et al. 2013,⁸ Figure 8-18). See the Intergovernmental Panel on Climate Change Fifth Assessment Report (IPCC AR5) Supplementary Material Table 8.SM.8⁸ for further information on the forcing time evolutions. Forcing numbers are provided in Annex II of IPCC AR5. The total anthropogenic forcing was 0.57 (0.29 to 0.85) W/m^2 in 1950, 1.25 (0.64 to 1.86) W/m^2 in 1980, and 2.29 (1.13 to 3.33) W/m^2 in 2011. (Figure source: Myhre et al. 2013,⁸ Figure 8-18; © IPCC, used with permission).

GHG. Seasonal variations in CO_2 atmospheric concentrations occur in response to seasonal changes in photosynthesis in the biosphere, and to a lesser degree to seasonal variations in anthropogenic emissions. In addition to fossil fuel reserves, there are large natural reservoirs of carbon in the oceans, in vegetation and soils, and in permafrost.

In the industrial era, the CO_2 atmospheric growth rate has been exponential (Figure 2.4), with the increase in atmospheric CO_2 approximately twice that absorbed by the oceans. Over at least the last 50 years, CO_2 has shown the largest annual RF increases among all GHGs (Figures 2.4 and 2.5). The global average CO_2 concentration has increased by 40% over the industrial era, increasing from 278 parts per million (ppm) in 1750 to 390 ppm in 2011;⁴³ it now exceeds 400 ppm (as of 2016) (<http://www.esrl.noaa.gov/gmd/ccgg/trends/>). CO_2 has been chosen as the refer-

ence in defining the global warming potential (GWP) of other GHGs and climate agents. The GWP of a GHG is the integrated RF over a specified time period (for example, 100 years) from the emission of a given mass of the GHG divided by the integrated RF from the same mass emission of CO_2 .

The global mean methane concentration and RF have also grown substantially in the industrial era (Figures 2.4 and 2.5). Methane is a stronger GHG than CO_2 for the same emission mass and has a shorter atmospheric lifetime of about 12 years. Methane also has indirect climate effects through induced changes in CO_2 , stratospheric water vapor, and ozone.⁴⁵ The 100-year GWP of methane is 28–36, depending on whether oxidation into CO_2 is included and whether climate-carbon feedbacks are accounted for; its 20-year GWP is even higher (84–86) (Myhre et al. 2013⁸ Table 8.7). With a current global mean value near 1840 parts per

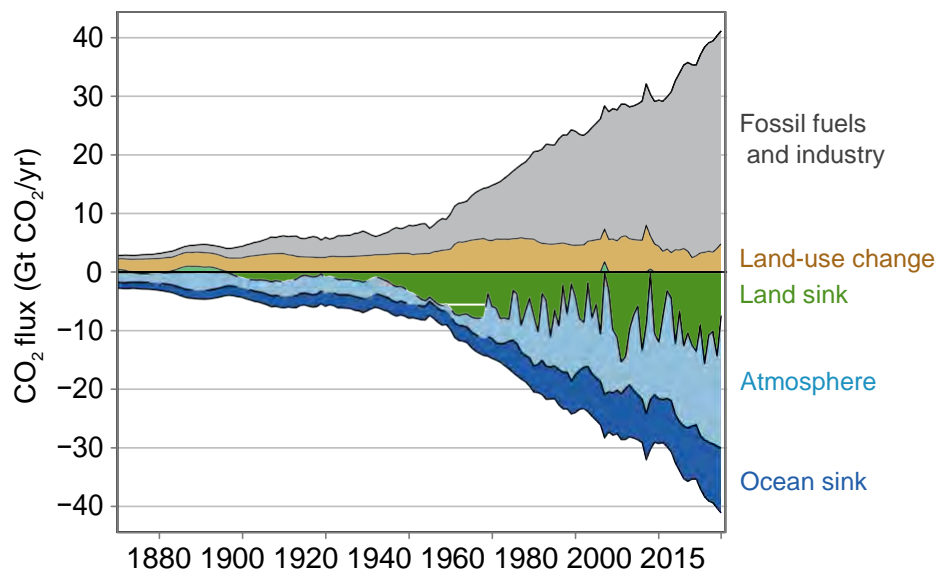


Figure 2.7: CO₂ sources and sinks (GtCO₂/yr) over the period 1870–2015. The partitioning of atmospheric emissions among the atmosphere, land, and ocean is shown as equivalent negative emissions in the lower panel; of these, the land and ocean terms are sinks of atmospheric CO₂. CO₂ emissions from net land-use changes are mainly from deforestation. The atmospheric CO₂ growth rate is derived from atmospheric observations and ice core data. The ocean CO₂ sink is derived from a combination of models and observations. The land sink is the residual of the other terms in a balanced CO₂ budget and represents the sink of anthropogenic CO₂ in natural land ecosystems. These terms only represent changes since 1750 and do not include natural CO₂ fluxes (for example, from weathering and outgassing from lakes and rivers). (Figure source: Le Quéré et al. 2016,¹³⁵ Figure 3).

billion by volume (ppb), the methane concentration has increased by a factor of about 2.5 over the industrial era. The annual growth rate for methane has been more variable than that for CO₂ and N₂O over the past several decades, and has occasionally been negative for short periods.

Methane emissions, which have a variety of natural and anthropogenic sources, totaled 556 ± 56 Tg CH₄ in 2011 based on top-down analyses, with about 60% from anthropogenic sources.⁴³ The methane budget is complicated by the variety of natural and anthropogenic sources and sinks that influence its atmospheric concentration. These include the global abundance of the hydroxyl radical (OH), which controls the methane atmospheric lifetime; changes in large-scale anthropogenic activities such as mining, natural gas extraction, animal husbandry, and agricultural practices; and natural wetland emissions (Table 6.8, Ciais et al. 2013⁴³). The remaining uncertainty in the cause(s) of the approximately 20-year

negative trend in the methane annual growth rate starting in the mid-1980s and the rapid increases in the annual rate in the last decade (Figure 2.4) reflect the complexity of the methane budget.^{43, 46, 47}

Growth rates in the global mean nitrous oxide (N₂O) concentration and RF over the industrial era are smaller than for CO₂ and methane (Figures 2.4 and 2.5). N₂O is emitted in the nitrogen cycle in natural ecosystems and has a variety of anthropogenic sources, including the use of synthetic fertilizers in agriculture, motor vehicle exhaust, and some manufacturing processes. The current global value near 330 ppb reflects steady growth over the industrial era with average increases in recent decades of 0.75 ppb per year (Figure 2.4).⁴³ Fertilization in global food production is responsible for about 80% of the growth rate. Anthropogenic sources account for approximately 40% of the annual N₂O emissions of 17.9 (8.1 to 30.7) TgN.⁴³ N₂O has an atmospheric lifetime of about 120 years and a GWP in the

range 265–298 (Myhre et al. 2013⁸ Table 8.7). The primary sink of N₂O is photochemical destruction in the stratosphere, which produces nitrogen oxides (NO_x) that catalytically destroy ozone (e.g., Skiba and Rees 2014⁴⁸). Small indirect climate effects, such as the response of stratospheric ozone, are generally not included in the N₂O RF.

N₂O is a component of the larger global budget of total reactive nitrogen (N) comprising N₂O, ammonia (NH₃), and nitrogen oxides (NO_x) and other compounds. Significant uncertainties are associated with balancing this budget over oceans and land while accounting for deposition and emission processes.⁴³ ⁴⁹ Furthermore, changes in climate parameters such as temperature, moisture, and CO₂ concentrations are expected to affect the N₂O budget in the future, and perhaps atmospheric concentrations.

Other Well-mixed Greenhouse Gases

Other WMGHGs include several categories of synthetic (i.e., manufactured) gases, including chlorofluorocarbons (CFCs), halons, hydrochlorofluorocarbons (HCFCs), hydrofluorocarbons (HFCs), perfluorocarbons (PFCs), and sulfur hexafluoride (SF₆), collectively known as halocarbons. Natural sources of these gases in the industrial era are small compared to anthropogenic sources. Important examples are the expanded use of CFCs as refrigerants and in other applications beginning in the mid-20th century. The atmospheric abundances of principal CFCs began declining in the 1990s after their regulation under the Montreal Protocol as substances that deplete stratospheric ozone (Figure 2.5). All of these gases are GHGs covering a wide range of GWPs, atmospheric concentrations, and trends. PFCs, SF₆, and HFCs are in the basket of gases covered under the United Nations Framework Convention on Climate Change. The United States joined other countries in proposing that

HFCs be controlled as a WMGHGs under the Montreal Protocol because of their large projected future abundances.⁵⁰ In October 2016, the Montreal Protocol adopted an amendment to phase down global HFC production and consumption, avoiding emissions equivalent to approximately 105 Gt CO₂ by 2100 based on earlier projections.⁵⁰ The atmospheric growth rates of some halocarbon concentrations are significant at present (for example, SF₆ and HFC-134a), although their RF contributions remain small (Figure 2.5).

Water Vapor

Water vapor in the atmosphere acts as a powerful natural GHG, significantly increasing Earth's equilibrium temperature. In the stratosphere, water vapor abundances are controlled by transport from the troposphere and from oxidation of methane. Increases in methane from anthropogenic activities therefore increase stratospheric water vapor, producing a positive RF (e.g., Solomon et al. 2010;⁵¹ Hegglin et al. 2014⁵²). Other less-important anthropogenic sources of stratospheric water vapor are hydrogen oxidation,⁵³ aircraft exhaust,^{54, 55} and explosive volcanic eruptions.⁵⁶

In the troposphere, the amount of water vapor is controlled by temperature.⁵⁷ Atmospheric circulation, especially convection, limits the buildup of water vapor in the atmosphere such that the water vapor from direct emissions, for example by combustion of fossil fuels or by large power plant cooling towers, does not accumulate in the atmosphere but actually offsets water vapor that would otherwise evaporate from the surface. Direct changes in atmospheric water vapor are negligible in comparison to the indirect changes caused by temperature changes resulting from radiative forcing. As such, changes in tropospheric water vapor are considered a feedback in the climate system (see Section 2.6.1 and Figure 2.2). As increasing GHG concentrations warm



the atmosphere, tropospheric water vapor concentrations increase, thereby amplifying the warming effect.⁵⁷

Ozone

Ozone is a naturally occurring GHG in the troposphere and stratosphere and is produced and destroyed in response to a variety of anthropogenic and natural emissions. Ozone abundances have high spatial and temporal variability due to the nature and variety of the production, loss, and transport processes controlling ozone abundances, which adds complexity to the ozone RF calculations. In the global troposphere, emissions of methane, NO_x, carbon monoxide (CO), and non-methane volatile organic compounds (VOCs) form ozone photochemically both near and far downwind of these precursor source emissions, leading to regional and global positive RF contributions (e.g., Dentener et al. 2005⁵⁸). Stratospheric ozone is destroyed photochemically in reactions involving the halogen species chlorine and bromine. Halogens are released in the stratosphere from the decomposition of some halocarbons emitted at the surface as a result of natural processes and human activities.⁵⁹ Stratospheric ozone depletion, which is most notable in the polar regions, yields a net negative RF.⁸

Aerosols

Atmospheric aerosols are perhaps the most complex and most uncertain component of forcing due to anthropogenic activities.⁸ Aerosols have diverse natural and anthropogenic sources, and emissions from these sources interact in non-linear ways.⁶⁰ Aerosol types are categorized by composition; namely, sulfate, black carbon, organic, nitrate, dust, and sea salt. Individual particles generally include a mix of these components due to chemical and physical transformations of aerosols and aerosol precursor gases following emission. Aerosol tropospheric lifetimes are days to

weeks due to the general hygroscopic nature of primary and secondary particles and the ubiquity of cloud and precipitation systems in the troposphere. Particles that act as cloud condensation nuclei (CCN) or are scavenged by cloud droplets are removed from the troposphere in precipitation. The heterogeneity of aerosol sources and locations combined with short aerosol lifetimes leads to the high spatial and temporal variabilities observed in the global aerosol distribution and their associated forcings.

Aerosols from anthropogenic activities influence RF in three primary ways: through aerosol–radiation interactions, through aerosol–cloud interactions, and through albedo changes from absorbing-aerosol deposition on snow and ice.⁶⁰ RF from aerosol–radiation interactions, also known as the aerosol “direct effect,” involves absorption and scattering of longwave and shortwave radiation. RF from aerosol–cloud interactions, also known as the cloud albedo “indirect effect,” results from changes in cloud droplet number and size due to changes in aerosol (cloud condensation nuclei) number and composition. The RF for the global net aerosol–radiation and aerosol–cloud interaction is negative.⁸ However, the RF is not negative for all aerosol types. Light-absorbing aerosols, such as black carbon, absorb sunlight, producing a positive RF. This absorption warms the atmosphere; on net, this response is assessed to increase cloud cover and therefore increase planetary albedo (the “semi-direct” effect). This “rapid response” lowers the ERF of atmospheric black carbon by approximately 15% relative to its RF from direct absorption alone.⁶¹ ERF for aerosol–cloud interactions includes this rapid adjustment for absorbing aerosol (that is, the cloud response to atmospheric heating) and it includes cloud lifetime effects (for example, glaciation and thermodynamic effects).⁶⁰ Light-absorbing aerosols also affect climate when present in surface snow by



lowering surface albedo, yielding a positive RF (e.g., Flanner et al. 2009⁶²). For black carbon deposited on snow, the ERF is a factor of three higher than the RF because of positive feedbacks that reduce snow albedo and accelerate snow melt (e.g., Flanner et al. 2009;⁶² Bond et al. 2013⁶¹). There is *very high confidence* that the RF from snow and ice albedo is positive.⁶¹

Land Surface

Land-cover changes (LCC) due to anthropogenic activities in the industrial era have changed the land surface brightness (albedo), principally through deforestation and afforestation. There is strong evidence that these changes have increased Earth's global surface albedo, creating a negative (cooling) RF of $-0.15 \pm 0.10 \text{ W/m}^2$.⁸ In specific regions, however, LCC has lowered surface albedo producing a positive RF (for example, through afforestation and pasture abandonment). In addition to the direct radiative forcing through albedo changes, LCC also have indirect forcing effects on climate, such as altering carbon cycles and altering dust emissions through effects on the hydrologic cycle. These effects are generally not included in the direct LCC RF calculations and are instead included in the net GHG and aerosol RFs over the industrial era. These indirect forcings may be of opposite sign to that of the direct LCC albedo forcing and may constitute a significant fraction of industrial-era RF driven by human activities.⁶³ Some of these effects, such as alteration of the carbon cycle, constitute climate feedbacks (Figure 2.2) and are discussed more extensively in Chapter 10: Land Cover. The increased use of satellite observations to quantify LCC has resulted in smaller negative LCC RF values (e.g., Ju and Masek 2016⁶⁴). In areas with significant irrigation, surface temperatures and precipitation are affected by a change in energy partitioning from sensible to latent heating. Direct RF due to irrigation is generally small and can be positive or nega-

tive, depending on the balance of longwave (surface cooling or increases in water vapor) and shortwave (increased cloudiness) effects.⁶⁵

Contrails

Line-shaped (linear) contrails are a special type of cirrus cloud that forms in the wake of jet-engine aircraft operating in the mid- to upper troposphere under conditions of high ambient humidity. Persistent contrails, which can last for many hours, form when ambient humidity conditions are supersaturated with respect to ice. As persistent contrails spread and drift with the local winds after formation, they lose their linear features, creating additional cirrus cloudiness that is indistinguishable from background cloudiness. Contrails and contrail cirrus are additional forms of cirrus cloudiness that interact with solar and thermal radiation to provide a global net positive RF and thus are visible evidence of an anthropogenic contribution to climate change.⁶⁶

2.4 Industrial-era Changes in Radiative Forcing Agents

The IPCC best-estimate values of present day RFs and ERFs from principal anthropogenic and natural climate drivers are shown in Figure 2.3 and in Table 2.1. The past changes in the industrial era leading up to present day RF are shown for anthropogenic gases in Figure 2.5 and for all climate drivers in Figure 2.6.

The combined figures have several striking features. First, there is a large range in the magnitudes of RF terms, with contrails, stratospheric ozone, black carbon on snow, and stratospheric water vapor being small fractions of the largest term (CO_2). The sum of ERFs from CO_2 and non- CO_2 GHGs, tropospheric ozone, stratospheric water, contrails, and black carbon on snow shows a gradual increase from 1750 to the mid-1960s and accelerated annual growth in the subsequent 50 years (Figure 2.6). The sum of aerosol effects, strato-



Table 2.1. Global mean RF and ERF values in 2011 for the industrial era. ^a

Radiative Forcing Term	Radiative forcing (W/m ²)	Effective radiative forcing (W/m ²) ^b
Well-mixed greenhouse gases (CO ₂ , CH ₄ , N ₂ O, and halocarbons)	+2.83 (2.54 to 3.12)	+2.83 (2.26 to 3.40)
Tropospheric ozone	+0.40 (0.20 to 0.60)	
Stratospheric ozone	-0.05 (-0.15 to +0.05)	
Stratospheric water vapor from CH ₄	+0.07 (+0.02 to +0.12)	
Aerosol–radiation interactions	-0.35 (-0.85 to +0.15)	-0.45 (-0.95 to +0.05)
Aerosol–cloud interactions	Not quantified	-0.45 (-1.2 to 0.0)
Surface albedo (land use)	-0.15 (-0.25 to -0.05)	
Surface albedo (black carbon aerosol on snow and ice)	+0.04 (+0.02 to +0.09)	
Contrails	+0.01 (+0.005 to +0.03)	
Combined contrails and contrail-induced cirrus	Not quantified	+0.05 (0.02 to 0.15)
Total anthropogenic	Not quantified	+2.3 (1.1 to 3.3)
Solar irradiance	+0.05 (0.0 to +0.10)	

^aFrom IPCC⁸

^bRF is a good estimate of ERF for most forcing agents except black carbon on snow and ice and aerosol–cloud interactions.

spheric ozone depletion, and land use show a monotonically increasing cooling trend for the first two centuries of the depicted time series. During the past several decades, however, this combined cooling trend has leveled off due to reductions in the emissions of aerosols and aerosol precursors, largely as a result of legislation designed to improve air quality.^{67,68} In contrast, the volcanic RF reveals its episodic, short-lived characteristics along with large values that at times dominate the total RF. Changes in total solar irradiance over the industrial era are dominated by the 11-year solar cycle and other short-term variations. The solar irradiance RF between 1745 and 2005 is 0.05 (range of 0.0–0.1) W/m²,⁸ a very small fraction of total anthropogenic forcing in 2011. The large relative uncertainty derives from inconsistencies among solar models, which all rely on proxies of solar irradiance to fit the industrial era. In total, ERF has increased substantially in the industrial era, driven almost completely by anthropogenic activities, with

annual growth in ERF notably higher after the mid-1960s.

The principal anthropogenic activities that have increased ERF are those that increase net GHG emissions. The atmospheric concentrations of CO₂, CH₄, and N₂O are higher now than they have been in at least the past 800,000 years.⁶⁹ All have increased monotonically over the industrial era (Figure 2.4), and are now 40%, 250%, and 20%, respectively, above their preindustrial concentrations as reflected in the RF time series in Figure 2.5. Tropospheric ozone has increased in response to growth in precursor emissions in the industrial era. Emissions of synthetic GHGs have grown rapidly beginning in the mid-20th century, with many bringing halogens to the stratosphere and causing ozone depletion in subsequent decades. Aerosol RF effects are a sum over aerosol–radiation and aerosol–cloud interactions; this RF has increased in the industrial era due to increased emissions of aerosol and

aerosol precursors (Figure 2.6). These global aerosol RF trends average across disparate trends at the regional scale. The recent leveling off of global aerosol concentrations is the result of declines in many regions that were driven by enhanced air quality regulations, particularly starting in the 1980s (e.g., Philipona et al. 2009;⁷⁰ Liebensperger et al. 2012;⁷¹ Wild 2016⁷²). These declines are partially offset by increasing trends in other regions, such as much of Asia and possibly the Arabian Peninsula.^{73, 74, 75} In highly polluted regions, negative aerosol RF may fully offset positive GHG RF, in contrast to global annual averages in which positive GHG forcing fully offsets negative aerosol forcing (Figures 2.3 and 2.6).

2.5 The Complex Relationship between Concentrations, Forcing, and Climate Response

Climate changes occur in response to ERFs, which generally include certain rapid responses to the underlying RF terms (Figure 2.2). Responses within Earth's system to forcing can act to either amplify (positive feedback) or reduce (negative feedback) the original forcing. These feedbacks operate on a range of time scales, from days to centuries. Thus, in general, the full climate impact of a given forcing is not immediately realized. Of interest are the climate response at a given point in time under continuously evolving forcings and the total climate response realized for a given forcing. A metric for the former, which approximates near-term climate change from a GHG forcing, is the transient climate response (TCR), defined as the change in global mean surface temperature when the atmospheric CO₂ concentration has doubled in a scenario of concentration increasing at 1% per year. The latter is given by the equilibrium climate sensitivity (ECS), defined as the change at equilibrium in annual and global mean surface temperature following a doubling of the atmospheric CO₂ concentration.⁷⁶ TCR is more

representative of near-term climate change from a GHG forcing. To estimate ECS, climate model runs have to simulate thousands of years in order to allow sufficient time for ocean temperatures to reach equilibrium.

In the IPCC's Fifth Assessment Report, ECS is assessed to be a factor of 1.5 or more greater than the TCR (ECS is 2.7°F to 8.1°F [1.5°C to 4.5°C] and TCR is 1.8°F to 4.5°F [1.0°C to 2.5°C]⁷⁶), exemplifying that longer time-scale feedbacks are both significant and positive. Confidence in the model-based TCR and ECS values is increased by their agreement, within respective uncertainties, with other methods of calculating these metrics (Box 12.2 of Collins et al. 2013)⁷⁷. The alternative methods include using reconstructed temperatures from paleoclimate archives, the forcing/response relationship from past volcanic eruptions, and observed surface and ocean temperature changes over the industrial era.⁷⁷

While TCR and ECS are defined specifically for the case of doubled CO₂, the climate sensitivity factor, λ , more generally relates the equilibrium surface temperature response (ΔT) to a constant forcing (ERF) as given by $\Delta T = \lambda \text{ERF}$.^{76, 78} The λ factor is highly dependent on feedbacks within Earth's system; all feedbacks are quantified themselves as radiative forcings, since each one acts by affecting Earth's albedo or its greenhouse effect. Models in which feedback processes are more positive (that is, more strongly amplify warming) tend to have a higher climate sensitivity (see Figure 9.43 of Flato et al.⁷⁶). In the absence of feedbacks, λ would be equal to 0.54°F/(W/m²) (0.30°C/[W/m²]). The magnitude of λ for ERF over the industrial era varies across models, but in all cases λ is greater than 0.54°F/(W/m²), indicating the sum of all climate feedbacks tends to be positive. Overall, the global warming response to ERF includes a substantial amplification from feedbacks, with a



model mean λ of $0.86^\circ\text{F}/(\text{W}/\text{m}^2)$ ($0.48^\circ\text{C}/[\text{W}/\text{m}^2]$) with a 90% uncertainty range of $\pm 0.23^\circ\text{F}/(\text{W}/\text{m}^2)$ ($\pm 0.13^\circ\text{C}/[\text{W}/\text{m}^2]$) (as derived from climate sensitivity parameter in Table 9.5 of Flato et al.⁷⁶ combined with methodology of Bony et al.⁷⁹). Thus, there is *high confidence* that the response of Earth's system to the industrial-era net positive forcing is to amplify that forcing (Figure 9.42 of Flato et al.⁷⁶).

The models used to quantify λ account for the near-term feedbacks described below (Section 2.6.1), though with mixed levels of detail regarding feedbacks to atmospheric composition. Feedbacks to the land and ocean carbon sink, land albedo and ocean heat uptake, most of which operate on longer time scales (Section 2.6.2), are currently included on only a limited basis, or in some cases not at all, in climate models. Climate feedbacks are the largest source of uncertainty in quantifying climate sensitivity;⁷⁶ namely, the responses of clouds, the carbon cycle, ocean circulation and, to a lesser extent, land and sea ice to surface temperature and precipitation changes.

The complexity of mapping forcings to climate responses on a global scale is enhanced by geographic and seasonal variations in these forcings and responses, driven in part by similar variations in anthropogenic emissions and concentrations. Studies show that the spatial pattern and timing of climate responses are not always well correlated with the spatial pattern and timing of a radiative forcing, since adjustments within the climate system can determine much of the response (e.g., Shindell and Faluvegi 2009;⁸⁰ Crook and Forster 2011;⁸¹ Knutti and Rugenstein 2015⁸²). The RF patterns of short-lived climate drivers with inhomogeneous source distributions, such as aerosols, tropospheric ozone, contrails, and land cover change, are leading examples of highly inhomogeneous forcings. Spatial and temporal variability in aerosol and

aerosol precursor emissions is enhanced by in-atmosphere aerosol formation and chemical transformations, and by aerosol removal in precipitation and surface deposition. Even for relatively uniformly distributed species (for example, WMOGHGs), RF patterns are less homogenous than their concentrations. The RF of a uniform CO_2 distribution, for example, depends on latitude and cloud cover.⁸³ With the added complexity and variability of regional forcings, the global mean RFs are known with more confidence than the regional RF patterns. Forcing feedbacks in response to spatially variable forcings also have variable geographic and temporal patterns.

Quantifying the relationship between spatial RF patterns and regional and global climate responses in the industrial era is difficult because it requires distinguishing forcing responses from the inherent internal variability of the climate system, which acts on a range of time scales. The ability to test the accuracy of modeled responses to forcing patterns is limited by the sparsity of long-term observational records of regional climate variables. As a result, there is generally *very low confidence* in our understanding of the qualitative and quantitative forcing-response relationships at the regional scale. However, there is *medium to high confidence* in other features, such as aerosol effects altering the location of the Inter Tropical Convergence Zone (ITCZ) and the positive feedback to reductions of snow and ice and albedo changes at high latitudes.^{8,60}

2.6 Radiative-forcing Feedbacks

2.6.1 Near-term Feedbacks

Planck Feedback

When the temperatures of Earth's surface and atmosphere increase in response to RF, more infrared radiation is emitted into the lower atmosphere; this serves to restore radiative balance at the tropopause. This radiative feedback, defined as the Planck feedback, only



partially offsets the positive RF while triggering other feedbacks that affect radiative balance. The Planck feedback magnitude is $-3.20 \pm 0.04 \text{ W/m}^2$ per 1.8°F (1°C) of warming and is the strongest and primary stabilizing feedback in the climate system.⁸⁴

Water Vapor and Lapse Rate Feedbacks

Warmer air holds more moisture (water vapor) than cooler air – about 7% more per degree Celsius – as dictated by the Clausius–Clapeyron relationship.⁸⁵ Thus, as global temperatures increase, the total amount of water vapor in the atmosphere increases, adding further to greenhouse warming – a positive feedback – with a mean value derived from a suite of atmosphere/ocean global climate models (AOGCM) of $1.6 \pm 0.3 \text{ W/m}^2$ per 1.8°F (1°C) of warming (Table 9.5 of Flato et al. 2013).⁷⁶ The water vapor feedback is responsible for more than doubling the direct climate warming from CO_2 emissions alone.^{57, 79, 84, 86} Observations confirm that global tropospheric water vapor has increased commensurate with measured warming (FAQ 3.2 and its Figure 1a in IPCC 2013).¹⁷ Interannual variations and trends in stratospheric water vapor, while influenced by tropospheric abundances, are controlled largely by tropopause temperatures and dynamical processes.⁸⁷ Increases in tropospheric water vapor have a larger warming effect in the upper troposphere (where it is cooler) than in the lower troposphere, thereby decreasing the rate at which temperatures decrease with altitude (the lapse rate). Warmer temperatures aloft increase outgoing infrared radiation – a negative feedback – with a mean value derived from the same AOGCM suite of $-0.6 \pm 0.4 \text{ W/m}^2$ per 1.8°F (1°C) warming. These feedback values remain largely unchanged between recent IPCC assessments.¹⁷ ⁸⁸ Recent advances in both observations and models have increased confidence that the net effect of the water vapor and lapse rate feedbacks is a significant positive RF.⁷⁶

Cloud Feedbacks

An increase in cloudiness has two direct impacts on radiative fluxes: first, it increases scattering of sunlight, which increases Earth's albedo and cools the surface (the shortwave cloud radiative effect); second, it increases trapping of infrared radiation, which warms the surface (the longwave cloud radiative effect). A decrease in cloudiness has the opposite effects. Clouds have a relatively larger shortwave effect when they form over dark surfaces (for example, oceans) than over higher albedo surfaces, such as sea ice and deserts. For clouds globally, the shortwave cloud radiative effect is about -50 W/m^2 , and the longwave effect is about $+30 \text{ W/m}^2$, yielding a net cooling influence.^{89, 90} The relative magnitudes of both effects vary with cloud type as well as with location. For low-altitude, thick clouds (for example, stratus and stratocumulus) the shortwave radiative effect dominates, so they cause a net cooling. For high-altitude, thin clouds (for example, cirrus) the longwave effect dominates, so they cause a net warming (e.g., Hartmann et al. 1992;⁹¹ Chen et al. 2000⁹²). Therefore, an increase in low clouds is a negative feedback to RF, while an increase in high clouds is a positive feedback. The potential magnitude of cloud feedbacks is large compared with global RF (see Section 2.4). Cloud feedbacks also influence natural variability within the climate system and may amplify atmospheric circulation patterns and the El Niño–Southern Oscillation.⁹³

The net radiative effect of cloud feedbacks is positive over the industrial era, with an assessed value of $+0.27 \pm 0.42 \text{ W/m}^2$ per 1.8°F (1°C) warming.⁸⁴ The net cloud feedback can be broken into components, where the longwave cloud feedback is positive ($+0.24 \pm 0.26 \text{ W/m}^2$ per 1.8°F [1°C] warming) and the shortwave feedback is near-zero ($+0.14 \pm 0.40 \text{ W/m}^2$ per 1.8°F [1°C] warming⁸⁴), though the two do not add linearly. The value of the



shortwave cloud feedback shows a significant sensitivity to computation methodology.^{84, 94}
⁹⁵Uncertainty in cloud feedback remains the largest source of inter-model differences in calculated climate sensitivity.^{60, 84}

Snow, Ice, and Surface Albedo

Snow and ice are highly reflective to solar radiation relative to land surfaces and the ocean. Loss of snow cover, glaciers, ice sheets, or sea ice resulting from climate warming lowers Earth's surface albedo. The losses create the snow-albedo feedback because subsequent increases in absorbed solar radiation lead to further warming as well as changes in turbulent heat fluxes at the surface.⁹⁶ For seasonal snow, glaciers, and sea ice, a positive albedo feedback occurs where light-absorbing aerosols are deposited to the surface, darkening the snow and ice and accelerating the loss of snow and ice mass (e.g., Hansen and Nazarenko 2004;⁹⁷ Jacobson 2004;⁹⁸ Flanner et al. 2009;⁶² Skeie et al. 2011;⁹⁹ Bond et al. 2013;⁶¹ Yang et al. 2015¹⁰⁰).

For ice sheets (for example, on Antarctica and Greenland – see Ch. 11: Arctic Changes), the positive radiative feedback is further amplified by dynamical feedbacks on ice-sheet mass loss. Specifically, since continental ice shelves limit the discharge rates of ice sheets into the ocean; any melting of the ice shelves accelerates the discharge rate, creating a positive feedback on the ice-stream flow rate and total mass loss (e.g., Holland et al. 2008;¹⁰¹ Schoof 2010;¹⁰² Rignot et al. 2010;¹⁰³ Joughin et al. 2012¹⁰⁴). Warming oceans also lead to accelerated melting of basal ice (ice at the base of a glacier or ice sheet) and subsequent ice-sheet loss (e.g., Straneo et al. 2013;¹⁰⁵ Thoma et al. 2015;¹⁰⁶ Alley et al. 2016;¹⁰⁷ Silvano et al. 2016¹⁰⁸). Feedbacks related to ice sheet dynamics occur on longer time scales than other feedbacks – many centuries or longer. Significant ice-sheet melt can also lead to changes in

freshwater input to the oceans, which in turn can affect ocean temperatures and circulation, ocean-atmosphere heat exchange and moisture fluxes, and atmospheric circulation.⁶⁹

The complete contribution of ice-sheet feedbacks on time scales of millennia are not generally included in CMIP5 climate simulations. These slow feedbacks are also not thought to change in proportion to global mean surface temperature change, implying that the apparent climate sensitivity changes with time, making it difficult to fully understand climate sensitivity considering only the industrial age. This slow response increases the likelihood for tipping points, as discussed further in Chapter 15: Potential Surprises.

The surface-albedo feedback is an important influence on interannual variations in sea ice as well as on long-term climate change. While there is a significant range in estimates of the snow-albedo feedback, it is assessed as positive,^{84, 109, 110} with a best estimate of 0.27 ± 0.06 W/m² per 1.8°F (1°C) of warming globally. Within the cryosphere, the surface-albedo feedback is most effective in polar regions;^{94, 111} there is also evidence that polar surface-albedo feedbacks might influence the tropical climate as well.¹¹²

Changes in sea ice can also influence arctic cloudiness. Recent work indicates that arctic clouds have responded to sea ice loss in fall but not summer.^{113, 114, 115, 116, 117} This has important implications for future climate change, as an increase in summer clouds could offset a portion of the amplifying surface-albedo feedback, slowing down the rate of arctic warming.

Atmospheric Composition

Climate change alters the atmospheric abundance and distribution of some radiatively active species by changing natural emissions,



atmospheric photochemical reaction rates, atmospheric lifetimes, transport patterns, or deposition rates. These changes in turn alter the associated ERFs, forming a feedback.^{118, 119, 120} Atmospheric composition feedbacks occur through a variety of processes. Important examples include climate-driven changes in temperature and precipitation that affect 1) natural sources of NO_x from soils and lightning and VOC sources from vegetation, all of which affect ozone abundances;^{120, 121, 122} 2) regional aridity, which influences surface dust sources as well as susceptibility to wildfires; and 3) surface winds, which control the emission of dust from the land surface and the emissions of sea salt and dimethyl sulfide—a natural precursor to sulfate aerosol—from the ocean surface.

Climate-driven ecosystem changes that alter the carbon cycle potentially impact atmospheric CO₂ and CH₄ abundances (Section 2.6.2). Atmospheric aerosols affect clouds and precipitation rates, which in turn alter aerosol removal rates, lifetimes, and atmospheric abundances. Longwave radiative feedbacks and climate-driven circulation changes also alter stratospheric ozone abundance.¹²³ Investigation of these and other composition-climate interactions is an active area of research (e.g., John et al. 2012;¹²⁴ Pacifico et al. 2012;¹²⁵ Morgenstern et al. 2013;¹²⁶ Holmes et al. 2013;¹²⁷ Naik et al. 2013;¹²⁸ Voulgarakis et al. 2013;¹²⁹ Isaksen et al. 2014;¹³⁰ Dietmuller et al. 2014;¹³¹ Banerjee et al. 2014¹³²). While understanding of key processes is improving, atmospheric composition feedbacks are absent or limited in many global climate modeling studies used to project future climate, though this is rapidly changing.¹³³ For some composition-climate feedbacks involving shorter-lived constituents, the net effects may be near zero at the global scale while significant at local to regional scales (e.g., Raes et al. 2010;¹²⁰ Han et al. 2013¹³⁴).

2.6.2 Long-term Feedbacks

Terrestrial Ecosystems and Climate Change Feedbacks

The cycling of carbon through the climate system is an important long-term climate feedback that affects atmospheric CO₂ concentrations. The global mean atmospheric CO₂ concentration is determined by emissions from burning fossil fuels, wildfires, and permafrost thaw balanced against CO₂ uptake by the oceans and terrestrial biosphere (Figures 2.2 and 2.7).^{43, 135} During the past decade, just less than a third of anthropogenic CO₂ has been taken up by the terrestrial environment, and another quarter by the oceans (Le Quéré et al.¹³⁵ Table 8) through photosynthesis and through direct absorption by ocean surface waters. The capacity of the land to continue uptake of CO₂ is uncertain and depends on land-use management and on responses of the biosphere to climate change (see Ch. 10: Land Cover). Altered uptake rates affect atmospheric CO₂ abundance, forcing, and rates of climate change. Such changes are expected to evolve on the decadal and longer time scale, though abrupt changes are possible.

Significant uncertainty exists in quantification of carbon-cycle feedbacks, with large differences in the assumed characteristics of the land carbon-cycle processes in current models. Ocean carbon-cycle changes in future climate scenarios are also highly uncertain. Both of these contribute significant uncertainty to longer-term (century-scale) climate projections. Basic principles of carbon cycle dynamics in terrestrial ecosystems suggest that increased atmospheric CO₂ concentrations can directly enhance plant growth rates and, therefore, increase carbon uptake (the “CO₂ fertilization” effect), nominally sequestering much of the added carbon from fossil-fuel combustion (e.g., Wenzel et al. 2016¹³⁶). However, this effect is variable; sometimes plants acclimate so that higher CO₂ concentrations



no longer enhance growth (e.g., Franks et al. 2013¹³⁷). In addition, CO₂ fertilization is often offset by other factors limiting plant growth, such as water and or nutrient availability and temperature and incoming solar radiation that can be modified by changes in vegetation structure. Large-scale plant mortality through fire, soil moisture drought, and/or temperature changes also impact successional processes that contribute to reestablishment and revegetation (or not) of disturbed ecosystems, altering the amount and distribution of plants available to uptake CO₂. With sufficient disturbance, it has been argued that forests could, on net, turn into a source rather than a sink of CO₂.¹³⁸

Climate-induced changes in the horizontal (for example, landscape to biome) and vertical (soils to canopy) structure of terrestrial ecosystems also alter the physical surface roughness and albedo, as well as biogeochemical (carbon and nitrogen) cycles and biophysical evapotranspiration and water demand. Combined, these responses constitute climate feedbacks by altering surface albedo and atmospheric GHG abundances. Drivers of these changes in terrestrial ecosystems include changes in the biophysical growing season, altered seasonality, wildfire patterns, and multiple additional interacting factors (Ch. 10: Land Cover).

Accurate determination of future CO₂ stabilization scenarios depends on accounting for the significant role that the land biosphere plays in the global carbon cycle and feedbacks between climate change and the terrestrial carbon cycle.¹³⁹ Earth System Models (ESMs) are increasing the representation of terrestrial carbon cycle processes, including plant photosynthesis, plant and soil respiration and decomposition, and CO₂ fertilization, with the latter based on the assumption that an increased atmospheric CO₂ concentration provides more substrate for photosynthesis

and productivity. Recent advances in ESMs are beginning to account for other important factors such as nutrient limitations.^{140, 141, 142} ESMs that do include carbon-cycle feedbacks appear, on average, to overestimate terrestrial CO₂ uptake under the present-day climate^{143, 144} and underestimate nutrient limitations to CO₂ fertilization.¹⁴² The sign of the land carbon-cycle feedback through 2100 remains unclear in the newest generation of ESMs.^{142, 145, 146} Eleven CMIP5 ESMs forced with the same CO₂ emissions scenario – one consistent with RCP8.5 concentrations – produce a range of 795 to 1145 ppm for atmospheric CO₂ concentration in 2100. The majority of the ESMs (7 out of 11) simulated a CO₂ concentration larger (by 44 ppm on average) than their equivalent non-interactive carbon cycle counterpart.¹⁴⁶ This difference in CO₂ equates to about 0.4°F (0.2°C) more warming by 2100. The inclusion of carbon-cycle feedbacks does not alter the lower-end bound on climate sensitivity, but, in most climate models, inclusion pushes the upper bound higher.¹⁴⁶

Ocean Chemistry, Ecosystem, and Circulation Changes

The ocean plays a significant role in climate change by playing a critical role in controlling the amount of GHGs (including CO₂, water vapor, and N₂O) and heat in the atmosphere (Figure 2.7). To date most of the net energy increase in the climate system from anthropogenic RF is in the form of ocean heat (see Box 3.1 Figure 1 of Rhein et al. 2013).⁶ This additional heat is stored predominantly (about 60%) in the upper 700 meters of the ocean (see Ch. 12: Sea Level Rise and Ch. 13: Ocean Changes).¹⁴⁷ Ocean warming and climate-driven changes in ocean stratification and circulation alter oceanic biological productivity and therefore CO₂ uptake; combined, these feedbacks affect the rate of warming from radiative forcing.



Marine ecosystems take up CO₂ from the atmosphere in the same way that plants do on land. About half of the global net primary production (NPP) is by marine plants (approximately 50 ± 28 GtC/year^{148, 149, 150}). Phytoplankton NPP supports the biological pump, which transports 2–12 GtC/year of organic carbon to the deep sea,^{151, 152} where it is sequestered away from the atmospheric pool of carbon for 200–1,500 years. Since the ocean is an important carbon sink, climate-driven changes in NPP represent an important feedback because they potentially change atmospheric CO₂ abundance and forcing.

There are multiple links between RF-driven changes in climate, physical changes to the ocean, and feedbacks to ocean carbon and heat uptake. Changes in ocean temperature, circulation, and stratification driven by climate change alter phytoplankton NPP. Absorption of CO₂ by the ocean also increases its acidity, which can also affect NPP and therefore the carbon sink (see Ch. 13: Ocean Changes for a more detailed discussion of ocean acidification).

In addition to being an important carbon sink, the ocean dominates the hydrological cycle, since most surface evaporation and rainfall occur over the ocean.^{153, 154} The ocean component of the water vapor feedback derives from the rate of evaporation, which depends on surface wind stress and ocean temperature. Climate warming from radiative forcing also is associated with intensification of the water cycle (Ch. 7: Precipitation Change). Over decadal time scales the surface ocean salinity has increased in areas of high salinity, such as the subtropical gyres, and decreased in areas of low salinity, such as the Warm Pool region (see Ch. 13: Ocean Changes).^{155, 156} This increase in stratification in select regions and mixing in other regions are feedback processes because

they lead to altered patterns of ocean circulation, which impacts uptake of anthropogenic heat and CO₂.

Increased stratification inhibits surface mixing, high-latitude convection, and deep-water formation, thereby potentially weakening ocean circulations, in particular the Atlantic Meridional Overturning Circulation (AMOC) (see also Ch. 13: Ocean Changes).^{157, 158} Reduced deep-water formation and slower overturning are associated with decreased heat and carbon sequestration at greater depths. Observational evidence is mixed regarding whether the AMOC has slowed over the past decades to century (see Sect. 13.2.1 of Ch. 13: Ocean Changes). Future projections show that the strength of AMOC may significantly decrease as the ocean warms and freshens and as upwelling in the Southern Ocean weakens due to the storm track moving poleward (see also Ch. 13: Ocean Changes).¹⁵⁹ Such a slowdown of the ocean currents will impact the rate at which the ocean absorbs CO₂ and heat from the atmosphere.

Increased ocean temperatures also accelerate ice sheet melt, particularly for the Antarctic Ice Sheet where basal sea ice melting is important relative to surface melting due to colder surface temperatures.¹⁶⁰ For the Greenland Ice Sheet, submarine melting at tidewater margins is also contributing to volume loss.¹⁶¹ In turn, changes in ice sheet melt rates change cold- and freshwater inputs, also altering ocean stratification. This affects ocean circulation and the ability of the ocean to absorb more GHGs and heat.¹⁶² Enhanced sea ice export to lower latitudes gives rise to local salinity anomalies (such as the Great Salinity Anomaly¹⁶³) and therefore to changes in ocean circulation and air-sea exchanges of momentum, heat, and freshwater, which in turn affect the atmospheric distribution of heat and GHGs.



Remote sensing of sea surface temperature and chlorophyll as well as model simulations and sediment records suggest that global phytoplankton NPP may have increased recently as a consequence of decadal-scale natural climate variability, such as the El Niño–Southern Oscillation, which promotes vertical mixing and upwelling of nutrients.^{150, 164, 165} Analyses of longer trends, however, suggest that phytoplankton NPP has decreased by about 1% per year over the last 100 years.^{166, 167, 168} The latter results, although controversial,¹⁶⁹ are the only studies of the global rate of change over this period. In contrast, model simulations show decreases of only 6.6% in NPP and 8% in the biological pump over the last five decades.¹⁷⁰ Total NPP is complex to model, as there are still areas of uncertainty on how multiple physical factors affect phytoplankton growth, grazing, and community composition, and as certain phytoplankton species are more efficient at carbon export.^{171, 172} As a result, model uncertainty is still significant in NPP projections.¹⁷³ While there are variations across climate model projections, there is good agreement that in the future there will be increasing stratification, decreasing NPP, and a decreasing sink of CO₂ to the ocean via biological activity.¹⁷² Overall, compared to the 1990s, in 2090 total NPP is expected to decrease by 2%–16% and export production (that is, particulate flux to the deep ocean) could decline by 7%–18% under the higher scenario (RCP8.5).¹⁷² Consistent with this result, carbon cycle feedbacks in the ocean were positive (that is, higher CO₂ concentrations leading to a lower rate of CO₂ sequestration to the ocean, thereby accelerating the growth of atmospheric CO₂ concentrations) across the suite of CMIP5 models.

Permafrost and Hydrates

Permafrost and methane hydrates contain large stores of methane and (for permafrost) carbon in the form of organic materials, mostly at northern high latitudes. With warming, this organic material can thaw, making previously frozen

organic matter available for microbial decomposition, releasing CO₂ and methane to the atmosphere, providing additional radiative forcing and accelerating warming. This process defines the permafrost–carbon feedback. Combined data and modeling studies suggest that this feedback is *very likely* positive.^{174, 175, 176} This feedback was not included in recent IPCC projections but is an active area of research. Meeting stabilization or mitigation targets in the future will require limits on total GHG abundances in the atmosphere. Accounting for additional permafrost–carbon release reduces the amount of anthropogenic emissions that can occur and still meet these limits.¹⁷⁷

The permafrost–carbon feedback in the higher scenario (RCP8.5; Section 1.2.2 and Figure 1.4) contributes 120 ± 85 Gt of additional carbon by 2100; this represents 6% of the total anthropogenic forcing for 2100 and corresponds to a global temperature increase of +0.52° ± 0.38°F (+0.29° ± 0.21°C).¹⁷⁴ Considering the broader range of forcing scenarios (Figure 1.4), it is *likely* that the permafrost–carbon feedback increases carbon emissions between 2% and 11% by 2100. A key feature of the permafrost feedback is that, once initiated, it will continue for an extended period because emissions from decomposition occur slowly over decades and longer. In the coming few decades, enhanced plant growth at high latitudes and its associated CO₂ sink¹⁴⁵ are expected to partially offset the increased emissions from permafrost thaw;^{174, 176} thereafter, decomposition will dominate uptake. Recent evidence indicates that permafrost thaw is occurring faster than expected; poorly understood deep-soil carbon decomposition and ice wedge processes *likely* contribute.^{178, 179} Chapter 11: Arctic Changes includes a more detailed discussion of permafrost and methane hydrates in the Arctic. Future changes in permafrost emissions and the potential for even greater emissions from methane hydrates in the continental shelf are discussed further in Chapter 15: Potential Surprises.



TRACEABLE ACCOUNTS

Key Finding 1

Human activities continue to significantly affect Earth's climate by altering factors that change its radiative balance. These factors, known as radiative forcings, include changes in greenhouse gases, small airborne particles (aerosols), and the reflectivity of Earth's surface. In the industrial era, human activities have been, and are increasingly, the dominant cause of climate warming. The increase in radiative forcing due to these activities has far exceeded the relatively small net increase due to natural factors, which include changes in energy from the sun and the cooling effect of volcanic eruptions. (*Very high confidence*)

Description of evidence base

The Key Finding and supporting text summarizes extensive evidence documented in the climate science literature, including in previous national (NCA3)¹⁸⁰ and international¹⁷ assessments. The assertion that Earth's climate is controlled by its radiative balance is a well-established physical property of the planet. Quantification of the changes in Earth's radiative balance come from a combination of observations and calculations. Satellite data are used directly to observe changes in Earth's outgoing visible and infrared radiation. Since 2002, observations of incoming sunlight include both total solar irradiance and solar spectral irradiance.²⁶ Extensive in situ and remote sensing data are used to quantify atmospheric concentrations of radiative forcing agents (greenhouse gases [e.g., Ciais et al. 2013;⁴³ Le Quéré et al. 2016¹³⁵] and aerosols [e.g., Bond et al. 2013;⁶¹ Boucher et al. 2013;⁶⁰ Myhre et al. 2013;⁹ Jiao et al. 2014;¹⁸¹ Tsigaridis et al. 2014;¹⁸² Koffi et al. 2016¹⁸³]) and changes in land cover,^{64, 184, 185} as well as the relevant properties of these agents (for example, aerosol microphysical and optical properties). Climate models are constrained by these observed concentrations and properties. Concentrations of long-lived greenhouse gases in particular are well-quantified with observations because of their relatively high spatial homogeneity. Climate model calculations of radiative forcing by greenhouse gases and aerosols are supported by observations of radiative fluxes from the surface, from

airborne research platforms, and from satellites. Both direct observations and modeling studies show large, explosive eruptions affect climate parameters for years to decades.^{36, 186} Over the industrial era, radiative forcing by volcanoes has been episodic and currently does not contribute significantly to forcing trends. Observations indicate a positive but small increase in solar input over the industrial era.^{8, 22, 23} Relatively higher variations in solar input at shorter (UV) wavelengths²⁵ may be leading to indirect changes in Earth's radiative balance through their impact on ozone concentrations that are larger than the radiative impact of changes in total solar irradiance,^{21, 26, 27, 28, 29} but these changes are also small in comparison to anthropogenic greenhouse gas and aerosol forcing.⁸ The finding of an increasingly strong positive forcing over the industrial era is supported by observed increases in atmospheric temperatures (see Ch. 1: Our Globally Changing Climate) and by observed increases in ocean temperatures (Ch. 1: Our Globally Changing Climate and Ch. 13: Ocean Changes). The attribution of climate change to human activities is supported by climate models, which are able to reproduce observed temperature trends when RF from human activities is included and considerably deviate from observed trends when only natural forcings are included (Ch. 3: Detection and Attribution, Figure 3.1).

Major uncertainties

The largest source of uncertainty in radiative forcing (both natural and anthropogenic) over the industrial era is quantifying forcing by aerosols. This finding is consistent across previous assessments (e.g., IPCC 2007;⁸⁸ IPCC 2013¹⁷). The major uncertainties associated with aerosol forcing is discussed below in the Traceable Accounts for Key Finding 2.

Recent work has highlighted the potentially larger role of variations in UV solar irradiance, versus total solar irradiance, in solar forcing. However, this increase in solar forcing uncertainty is not sufficiently large to reduce confidence that anthropogenic activities dominate industrial-era forcing.



Assessment of confidence based on evidence and agreement, including short description of nature of evidence and level of agreement

There is *very high confidence* that anthropogenic radiative forcing exceeds natural forcing over the industrial era based on quantitative assessments of known radiative forcing components. Assessments of the natural forcings of solar irradiance changes and volcanic activity show with *very high confidence* that both forcings are small over the industrial era relative to total anthropogenic forcing. Total anthropogenic forcing is assessed to have become larger and more positive during the industrial era, while natural forcings show no similar trend.

Summary sentence or paragraph that integrates the above information

This key finding is consistent with that in the IPCC Fourth Assessment Report (AR4)⁸⁸ and Fifth Assessment Report (AR5);¹⁷ namely, anthropogenic radiative forcing is positive (climate warming) and substantially larger than natural forcing from variations in solar input and volcanic emissions. Confidence in this finding has increased from AR4 to AR5, as anthropogenic GHG forcings have continued to increase, whereas solar forcing remains small and volcanic forcing near-zero over decadal time scales.

Key Finding 2

Aerosols caused by human activity play a profound and complex role in the climate system through radiative effects in the atmosphere and on snow and ice surfaces and through effects on cloud formation and properties. The combined forcing of aerosol–radiation and aerosol–cloud interactions is negative (cooling) over the industrial era (*high confidence*), offsetting a substantial part of greenhouse gas forcing, which is currently the predominant human contribution. The magnitude of this offset, globally averaged, has declined in recent decades, despite increasing trends in aerosol emissions or abundances in some regions. (*Medium to high confidence*)

Description of evidence base

The Key Finding and supporting text summarize extensive evidence documented in the climate science literature, including in previous national (NCA3)¹⁸⁰ and international¹⁷ assessments. Aerosols affect Earth’s albedo by directly interacting with solar radiation (scattering and absorbing sunlight) and by affecting cloud properties (albedo and lifetime).

Fundamental physical principles show how atmospheric aerosols scatter and absorb sunlight (aerosol–radiation interaction), and thereby directly reduce incoming solar radiation reaching the surface. Extensive in situ and remote sensing data are used to measure emission of aerosols and aerosol precursors from specific source types, the concentrations of aerosols in the atmosphere, aerosol microphysical and optical properties, and, via remote sensing, their direct impacts on radiative fluxes. Atmospheric models used to calculate aerosol forcings are constrained by these observations (see Key Finding 1).

In addition to their direct impact on radiative fluxes, aerosols also act as cloud condensation nuclei. Aerosol–cloud interactions are more complex, with a strong theoretical basis supported by observational evidence. Multiple observational and modeling studies have concluded that increasing the number of aerosols in the atmosphere increases cloud albedo and lifetime, adding to the negative forcing (aerosol–cloud microphysical interactions) (e.g., Twohy 2005;¹⁸⁷ Lohmann and Feichter 2005;¹⁸⁸ Quaas et al. 2009;¹⁸⁹ Rosenfeld et al. 2014¹⁹⁰). Particles that absorb sunlight increase atmospheric heating; if they are sufficiently absorbing, the net effect of scattering plus absorption is a positive radiative forcing. Only a few source types (for example, from diesel engines) produce aerosols that are sufficiently absorbing that they have a positive radiative forcing.⁶¹ Modeling studies, combined with observational inputs, have investigated the thermodynamic response to aerosol absorption in the atmosphere. Averaging over aerosol locations relative to the clouds and other factors, the resulting changes in cloud properties represent a



negative forcing, offsetting approximately 15% of the positive radiative forcing from heating by absorbing aerosols (specifically, black carbon).⁶¹

Modeling and observational evidence both show that annually averaged global aerosol ERF increased until the 1980s and since then has flattened or slightly declined,^{191,192,193,194} driven by the introduction of stronger air quality regulations (Smith and Bond 2014; Fiore et al. 2015). In one recent study,¹⁹⁵ global mean aerosol RF has become less negative since IPCC AR5,⁸ due to a combination of declining sulfur dioxide emissions (which produce negative RF) and increasing black carbon emissions (which produce positive RF). Within these global trends there are significant regional variations (e.g., Mao et al. 2014¹⁹⁶), driven by both changes in aerosol abundance and changes in the relative contributions of primarily light-scattering and light-absorbing aerosols.^{68,195} In Europe and North America, aerosol ERF has significantly declined (become less negative) since the 1980s.^{70, 71, 197, 198, 199, 200} In contrast, observations show significant increases in aerosol abundances over India,^{201,202} and these increases are expected to continue into the near future.²⁰³ Several modeling and observational studies point to aerosol ERF for China peaking around 1990,^{204, 205, 206} though in some regions of China aerosol abundances and ERF have continued to increase.²⁰⁶ The suite of scenarios used for future climate projection (i.e., the scenarios shown in Ch. 1: Our Globally Changing Climate, Figure 1.4) includes emissions for aerosols and aerosol precursors. Across this range of scenarios, globally averaged ERF of aerosols is expected to decline (become less negative) in the coming decades,^{67,192} reducing the current aerosol offset to the increasing RF from GHGs.

Major uncertainties

Aerosol–cloud interactions are the largest source of uncertainty in both aerosol and total anthropogenic radiative forcing. These include the microphysical effects of aerosols on clouds and changes in clouds that result from the rapid response to absorption of sunlight by aerosols. This finding, consistent across previous assessments (e.g., Forster et al. 2007;²⁰⁷ Myhre et al. 2013⁸), is due to poor understanding of how both natural and

anthropogenic aerosol emissions have changed and how changing aerosol concentrations and composition affect cloud properties (albedo and lifetime).^{60,208} From a theoretical standpoint, aerosol–cloud interactions are complex, and using observations to isolate the effects of aerosols on clouds is complicated by the fact that other factors (for example, the thermodynamic state of the atmosphere) also strongly influence cloud properties. Further, changes in aerosol properties and the atmospheric thermodynamic state are often correlated and interact in non-linear ways.²⁰⁹

Assessment of confidence based on evidence and agreement, including short description of nature of evidence and level of agreement

There is *very high confidence* that aerosol radiative forcing is negative on a global, annually averaged basis, *medium confidence* in the magnitude of the aerosol RF, *high confidence* that aerosol ERF is also, on average, negative, and *low to medium confidence* in the magnitude of aerosol ERF. Lower confidence in the magnitude of aerosol ERF is due to large uncertainties in the effects of aerosols on clouds. Combined, we assess a *high level of confidence* that aerosol ERF is negative and sufficiently large to be substantially offsetting positive GHG forcing. Improvements in the quantification of emissions, in observations (from both surface-based networks and satellites), and in modeling capability give *medium to high confidence* in the finding that aerosol forcing trends are decreasing in recent decades.

Summary sentence or paragraph that integrates the above information

This key finding is consistent with the findings of IPCC AR5⁸ that aerosols constitute a negative radiative forcing. While significant uncertainty remains in the quantification of aerosol ERF, we assess with *high confidence* that aerosols offset about half of the positive forcing by anthropogenic CO₂ and about a third of the forcing by all well-mixed anthropogenic GHGs. The fraction of GHG forcing that is offset by aerosols has been decreasing over recent decades, as aerosol forcing has leveled off while GHG forcing continues to increase.



Key Finding 3

The interconnected Earth–atmosphere–ocean climate system includes a number of positive and negative feedback processes that can either strengthen (positive feedback) or weaken (negative feedback) the system’s responses to human and natural influences. These feedbacks operate on a range of time scales from very short (essentially instantaneous) to very long (centuries). Global warming by net radiative forcing over the industrial era includes a substantial amplification from these feedbacks (approximately a factor of three) (*high confidence*). While there are large uncertainties associated with some of these feedbacks, the net feedback effect over the industrial era has been positive (amplifying warming) and will continue to be positive in coming decades. (*Very high confidence*)

Description of evidence base

The variety of climate system feedbacks all depend on fundamental physical principles and are known with a range of uncertainties. The Planck feedback is based on well-known radiative transfer models. The largest positive feedback is the water vapor feedback, which derives from the dependence of vapor pressure on temperature. There is *very high confidence* that this feedback is positive, approximately doubling the direct forcing due to CO₂ emissions alone. The lapse rate feedback derives from thermodynamic principles. There is *very high confidence* that this feedback is negative and partially offsets the water vapor feedback. The water vapor and lapse-rate feedbacks are linked by the fact that both are driven by increases in atmospheric water vapor with increasing temperature. Estimates of the magnitude of these two feedbacks have changed little across recent assessments.^{60, 210} The snow- and ice-albedo feedback is positive in sign, with the magnitude of the feedback dependent in part on the time scale of interest.^{109, 110} The assessed strength of this feedback has also not changed significantly since IPCC 2007.⁸⁸ Cloud feedbacks modeled using microphysical principles are either positive or negative, depending on the sign of the change in clouds with warming (increase or decrease) and the type of cloud that changes (low or high clouds). Recent international assessments^{60, 210} and a separate feedback assessment⁸⁴ all give best

estimates of the cloud feedback as net positive. Feedback via changes in atmospheric composition is not well-quantified but is expected to be small relative to water-vapor-plus-lapse-rate, snow, and cloud feedbacks at the global scale.¹²⁰ Carbon cycle feedbacks through changes in the land biosphere are currently of uncertain sign and have asymmetric uncertainties: they might be small and negative but could also be large and positive.¹³⁸ Recent best estimates of the ocean carbon-cycle feedback are that it is positive with significant uncertainty that includes the possibility of a negative feedback for present-day CO₂ levels.^{170, 211} The permafrost–carbon feedback is *very likely* positive, and as discussed in Chapter 15: Potential Surprises, could be a larger positive feedback in the longer term. Thus, in the balance of multiple negative and positive feedback processes, the preponderance of evidence is that positive feedback processes dominate the overall radiative forcing feedback from anthropogenic activities.

Major uncertainties

Uncertainties in cloud feedbacks are the largest source of uncertainty in the net climate feedback (and therefore climate sensitivity) on the decadal to century time scale.^{60, 84} This results from the fact that cloud feedbacks can be either positive or negative, depending not only on the direction of change (more or less cloud) but also on the type of cloud affected and, to a lesser degree, the location of the cloud.⁸⁴ On decadal and longer time scales, the biological and physical responses of the ocean and land to climate change, and the subsequent changes in land and oceanic sinks of CO₂, contribute significant uncertainty to the net climate feedback (Ch. 13: Ocean Changes). Changes in the Brewer–Dobson atmospheric circulation driven by climate change and subsequent effects on stratosphere–troposphere coupling also contribute to climate feedback uncertainty.^{77, 212, 213, 214, 215, 216}

Assessment of confidence based on evidence and agreement, including short description of nature of evidence and level of agreement

There is *high confidence* that the net effect of all feedback processes in the climate system is positive, thereby amplifying warming. This confidence is based on



consistency across multiple assessments, including IPCC AR5 (IPCC 2013¹⁷ and references therein), of the magnitude of, in particular, the largest feedbacks in the climate system, two of which (water vapor feedback and snow/ice albedo feedback) are definitively positive in sign. While significant increases in low cloud cover with climate warming would be a large negative feedback to warming, modeling and observational studies do not support the idea of increases, on average, in low clouds with climate warming.

Summary sentence or paragraph that integrates the above information

The net effect of all identified feedbacks to forcing is positive based on the best current assessments and therefore amplifies climate warming. Feedback uncertainties, which are large for some processes, are included in these assessments. The various feedback processes operate on different time scales with carbon cycle and snow– and ice–albedo feedbacks operating on longer timelines than water vapor, lapse rate, cloud, and atmospheric composition feedbacks.



REFERENCES

1. Clark, P.U., J.D. Shakun, S.A. Marcott, A.C. Mix, M. Eby, S. Kulp, A. Levermann, G.A. Milne, P.L. Pfister, B.D. Santer, D.P. Schrag, S. Solomon, T.F. Stocker, B.H. Strauss, A.J. Weaver, R. Winkelmann, D. Archer, E. Bard, A. Goldner, K. Lambeck, R.T. Pierrehumbert, and G.-K. Plattner, 2016: Consequences of twenty-first-century policy for multi-millennial climate and sea-level change. *Nature Climate Change*, **6**, 360-369. <http://dx.doi.org/10.1038/nclimate2923>
2. Lacis, A.A., G.A. Schmidt, D. Rind, and R.A. Ruedy, 2010: Atmospheric CO₂: Principal control knob governing Earth's temperature. *Science*, **330**, 356-359. <http://dx.doi.org/10.1126/science.1190653>
3. Davies, J.H. and D.R. Davies, 2010: Earth's surface heat flux. *Solid Earth*, **1**, 5-24. <http://dx.doi.org/10.5194/se-1-5-2010>
4. Flanner, M.G., 2009: Integrating anthropogenic heat flux with global climate models. *Geophysical Research Letters*, **36**, L02801. <http://dx.doi.org/10.1029/2008gl036465>
5. Munk, W. and C. Wunsch, 1998: Abyssal recipes II: Energetics of tidal and wind mixing. *Deep Sea Research Part I: Oceanographic Research Papers*, **45**, 1977-2010. [http://dx.doi.org/10.1016/S0967-0637\(98\)00070-3](http://dx.doi.org/10.1016/S0967-0637(98)00070-3)
6. Rhein, M., S.R. Rintoul, S. Aoki, E. Campos, D. Chambers, R.A. Feely, S. Gulev, G.C. Johnson, S.A. Josey, A. Kostianoy, C. Mauritzen, D. Roemmich, L.D. Talley, and F. Wang, 2013: Observations: Ocean. *Climate Change 2013: The Physical Science Basis. Contribution of Working Group I to the Fifth Assessment Report of the Intergovernmental Panel on Climate Change*. Stocker, T.F., D. Qin, G.-K. Plattner, M. Tignor, S.K. Allen, J. Boschung, A. Nauels, Y. Xia, V. Bex, and P.M. Midgley, Eds. Cambridge University Press, Cambridge, United Kingdom and New York, NY, USA, 255-316. <http://www.climatechange2013.org/report/full-report/>
7. Bindoff, N.L., P.A. Stott, K.M. AchutaRao, M.R. Allen, N. Gillett, D. Gutzler, K. Hansingo, G. Hegerl, Y. Hu, S. Jain, I.I. Mokhov, J. Overland, J. Perlwitz, R. Sebbani, and X. Zhang, 2013: Detection and attribution of climate change: From global to regional. *Climate Change 2013: The Physical Science Basis. Contribution of Working Group I to the Fifth Assessment Report of the Intergovernmental Panel on Climate Change*. Stocker, T.F., D. Qin, G.-K. Plattner, M. Tignor, S.K. Allen, J. Boschung, A. Nauels, Y. Xia, V. Bex, and P.M. Midgley, Eds. Cambridge University Press, Cambridge, United Kingdom and New York, NY, USA, 867-952. <http://www.climatechange2013.org/report/full-report/>
8. Myhre, G., D. Shindell, F.-M. Bréon, W. Collins, J. Fuglestvedt, J. Huang, D. Koch, J.-F. Lamarque, D. Lee, B. Mendoza, T. Nakajima, A. Robock, G. Stephens, T. Takemura, and H. Zhang, 2013: Anthropogenic and natural radiative forcing. *Climate Change 2013: The Physical Science Basis. Contribution of Working Group I to the Fifth Assessment Report of the Intergovernmental Panel on Climate Change*. Stocker, T.F., D. Qin, G.-K. Plattner, M. Tignor, S.K. Allen, J. Boschung, A. Nauels, Y. Xia, V. Bex, and P.M. Midgley, Eds. Cambridge University Press, Cambridge, United Kingdom and New York, NY, USA, 659-740. <http://www.climatechange2013.org/report/full-report/>
9. Loeb, N.G., S. Kato, and B.A. Wielicki, 2002: Defining top-of-the-atmosphere flux reference level for earth radiation budget studies. *Journal of Climate*, **15**, 3301-3309. [http://dx.doi.org/10.1175/1520-0442\(2002\)015<3301:dtotaf>2.0.co;2](http://dx.doi.org/10.1175/1520-0442(2002)015<3301:dtotaf>2.0.co;2)
10. Boer, G. and B. Yu, 2003: Climate sensitivity and response. *Climate Dynamics*, **20**, 415-429. <http://dx.doi.org/10.1007/s00382-002-0283-3>
11. Gillett, N.P., M.F. Wehner, S.F.B. Tett, and A.J. Weaver, 2004: Testing the linearity of the response to combined greenhouse gas and sulfate aerosol forcing. *Geophysical Research Letters*, **31**, L14201. <http://dx.doi.org/10.1029/2004GL020111>
12. Matthews, H.D., A.J. Weaver, K.J. Meissner, N.P. Gillett, and M. Eby, 2004: Natural and anthropogenic climate change: Incorporating historical land cover change, vegetation dynamics and the global carbon cycle. *Climate Dynamics*, **22**, 461-479. <http://dx.doi.org/10.1007/s00382-004-0392-2>
13. Meehl, G.A., W.M. Washington, C.M. Ammann, J.M. Arblaster, T.M.L. Wigley, and C. Tebaldi, 2004: Combinations of natural and anthropogenic forcings in twentieth-century climate. *Journal of Climate*, **17**, 3721-3727. [http://dx.doi.org/10.1175/1520-0442\(2004\)017<3721:CONAAF>2.0.CO;2](http://dx.doi.org/10.1175/1520-0442(2004)017<3721:CONAAF>2.0.CO;2)
14. Jones, A., J.M. Haywood, and O. Boucher, 2007: Aerosol forcing, climate response and climate sensitivity in the Hadley Centre climate model. *Journal of Geophysical Research*, **112**, D20211. <http://dx.doi.org/10.1029/2007JD008688>
15. Mahajan, S., K.J. Evans, J.J. Hack, and J.E. Truesdale, 2013: Linearity of climate response to increases in black carbon aerosols. *Journal of Climate*, **26**, 8223-8237. <http://dx.doi.org/10.1175/JCLI-D-12-00715.1>
16. Shiogama, H., D.A. Stone, T. Nagashima, T. Nozawa, and S. Emori, 2013: On the linear additivity of climate forcing-response relationships at global and continental scales. *International Journal of Climatology*, **33**, 2542-2550. <http://dx.doi.org/10.1002/joc.3607>



17. IPCC, 2013: *Climate Change 2013: The Physical Science Basis. Contribution of Working Group I to the Fifth Assessment Report of the Intergovernmental Panel on Climate Change*. Cambridge University Press, Cambridge, UK and New York, NY, 1535 pp. <http://www.climatechange2013.org/report/>
18. Krissansen-Totton, J. and R. Davies, 2013: Investigation of cosmic ray–cloud connections using MISR. *Geophysical Research Letters*, **40**, 5240-5245. <http://dx.doi.org/10.1002/grl.50996>
19. Lean, J., 1997: The sun's variable radiation and its relevance for earth. *Annual Review of Astronomy and Astrophysics*, **35**, 33-67. <http://dx.doi.org/10.1146/annurev.astro.35.1.33>
20. Fröhlich, C. and J. Lean, 2004: Solar radiative output and its variability: Evidence and mechanisms. *The Astronomy and Astrophysics Review*, **12**, 273-320. <http://dx.doi.org/10.1007/s00159-004-0024-1>
21. Gray, L.J., J. Beer, M. Geller, J.D. Haigh, M. Lockwood, K. Matthes, U. Cubasch, D. Fleitmann, G. Harrison, L. Hood, J. Luterbacher, G.A. Meehl, D. Shindell, B. van Geel, and W. White, 2010: Solar influences on climate. *Reviews of Geophysics*, **48**, RG4001. <http://dx.doi.org/10.1029/2009RG000282>
22. Kopp, G., 2014: An assessment of the solar irradiance record for climate studies. *Journal of Space Weather and Space Climate*, **4**, A14. <http://dx.doi.org/10.1051/swsc/2014012>
23. Kopp, G., N. Krivova, C.J. Wu, and J. Lean, 2016: The impact of the revised sunspot record on solar irradiance reconstructions. *Solar Physics*, **291**, 2951-1965. <http://dx.doi.org/10.1007/s11207-016-0853-x>
24. Kopp, G. and J.L. Lean, 2011: A new, lower value of total solar irradiance: Evidence and climate significance. *Geophysical Research Letters*, **38**, L01706. <http://dx.doi.org/10.1029/2010GL045777>
25. Floyd, L.E., J.W. Cook, L.C. Herring, and P.C. Crane, 2003: SUSIM'S 11-year observational record of the solar UV irradiance. *Advances in Space Research*, **31**, 2111-2120. [http://dx.doi.org/10.1016/S0273-1177\(03\)00148-0](http://dx.doi.org/10.1016/S0273-1177(03)00148-0)
26. Ermolli, I., K. Matthes, T. Dudok de Wit, N.A. Krivova, K. Tourpali, M. Weber, Y.C. Unruh, L. Gray, U. Langematz, P. Pilewskie, E. Rozanov, W. Schmutz, A. Shapiro, S.K. Solanki, and T.N. Woods, 2013: Recent variability of the solar spectral irradiance and its impact on climate modelling. *Atmospheric Chemistry and Physics*, **13**, 3945-3977. <http://dx.doi.org/10.5194/acp-13-3945-2013>
27. Bolduc, C., M.S. Bourqui, and P. Charbonneau, 2015: A comparison of stratospheric photochemical response to different reconstructions of solar ultraviolet radiative variability. *Journal of Atmospheric and Solar-Terrestrial Physics*, **132**, 22-32. <http://dx.doi.org/10.1016/j.jastp.2015.06.008>
28. Lockwood, M., 2012: Solar influence on global and regional climates. *Surveys in Geophysics*, **33**, 503-534. <http://dx.doi.org/10.1007/s10712-012-9181-3>
29. Seppälä, A., K. Matthes, C.E. Randall, and I.A. Mironova, 2014: What is the solar influence on climate? Overview of activities during CAWSES-II. *Progress in Earth and Planetary Science*, **1**, 1-12. <http://dx.doi.org/10.1186/s40645-014-0024-3>
30. Xu, J. and A.M. Powell, 2013: What happened to surface temperature with sunspot activity in the past 130 years? *Theoretical and Applied Climatology*, **111**, 609-622. <http://dx.doi.org/10.1007/s00704-012-0694-y>
31. Gao, F.-L., L.-R. Tao, G.-M. Cui, J.-L. Xu, and T.-C. Hua, 2015: The influence of solar spectral variations on global radiative balance. *Advances in Space Research*, **55**, 682-687. <http://dx.doi.org/10.1016/j.asr.2014.10.028>
32. Swartz, W.H., R.S. Stolarski, L.D. Oman, E.L. Fleming, and C.H. Jackman, 2012: Middle atmosphere response to different descriptions of the 11-yr solar cycle in spectral irradiance in a chemistry-climate model. *Atmospheric Chemistry and Physics*, **12**, 5937-5948. <http://dx.doi.org/10.5194/acp-12-5937-2012>
33. Chiodo, G., D.R. Marsh, R. Garcia-Herrera, N. Calvo, and J.A. García, 2014: On the detection of the solar signal in the tropical stratosphere. *Atmospheric Chemistry and Physics*, **14**, 5251-5269. <http://dx.doi.org/10.5194/acp-14-5251-2014>
34. Dhomse, S.S., M.P. Chipperfield, W. Feng, W.T. Ball, Y.C. Unruh, J.D. Haigh, N.A. Krivova, S.K. Solanki, and A.K. Smith, 2013: Stratospheric O₃ changes during 2001–2010: The small role of solar flux variations in a chemical transport model. *Atmospheric Chemistry and Physics*, **13**, 10113-10123. <http://dx.doi.org/10.5194/acp-13-10113-2013>
35. Andronova, N.G., E.V. Rozanov, F. Yang, M.E. Schlesinger, and G.L. Stenichkov, 1999: Radiative forcing by volcanic aerosols from 1850 to 1994. *Journal of Geophysical Research*, **104**, 16807-16826. <http://dx.doi.org/10.1029/1999JD900165>
36. Robock, A., 2000: Volcanic eruptions and climate. *Reviews of Geophysics*, **38**, 191-219. <http://dx.doi.org/10.1029/1998RG000054>
37. Stenichkov, G., T.L. Delworth, V. Ramaswamy, R.J. Stouffer, A. Wittenberg, and F. Zeng, 2009: Volcanic signals in oceans. *Journal of Geophysical Research*, **114**, D16104. <http://dx.doi.org/10.1029/2008JD011673>
38. Otterå, O.H., M. Bentsen, H. Drange, and L. Suo, 2010: External forcing as a metronome for Atlantic multidecadal variability. *Nature Geoscience*, **3**, 688-694. <http://dx.doi.org/10.1038/ngeo955>



39. Zanchettin, D., C. Timmreck, H.-F. Graf, A. Rubino, S. Lorenz, K. Lohmann, K. Krüger, and J.H. Jungclauss, 2012: Bi-decadal variability excited in the coupled ocean-atmosphere system by strong tropical volcanic eruptions. *Climate Dynamics*, **39**, 419-444. <http://dx.doi.org/10.1007/s00382-011-1167-1>
40. Zhang, D., R. Blender, and K. Fraedrich, 2013: Volcanoes and ENSO in millennium simulations: Global impacts and regional reconstructions in East Asia. *Theoretical and Applied Climatology*, **111**, 437-454. <http://dx.doi.org/10.1007/s00704-012-0670-6>
41. Langmann, B., 2014: On the role of climate forcing by volcanic sulphate and volcanic ash. *Advances in Meteorology*, **2014**, 17. <http://dx.doi.org/10.1155/2014/340123>
42. Gerlach, T., 2011: Volcanic versus anthropogenic carbon dioxide. *Eos, Transactions, American Geophysical Union*, **92**, 201-202. <http://dx.doi.org/10.1029/2011EO240001>
43. Ciais, P., C. Sabine, G. Bala, L. Bopp, V. Brovkin, J. Canadell, A. Chhabra, R. DeFries, J. Galloway, M. Heimann, C. Jones, C. Le Quéré, R.B. Myneni, S. Piao, and P. Thornton, 2013: Carbon and other biogeochemical cycles. *Climate Change 2013: The Physical Science Basis. Contribution of Working Group I to the Fifth Assessment Report of the Intergovernmental Panel on Climate Change*. Stocker, T.F., D. Qin, G.-K. Plattner, M. Tignor, S.K. Allen, J. Boschung, A. Nauels, Y. Xia, V. Bex, and P.M. Midgley, Eds. Cambridge University Press, Cambridge, United Kingdom and New York, NY, USA, 465-570. <http://www.climatechange2013.org/report/full-report/>
44. Xi, F., S.J. Davis, P. Ciais, D. Crawford-Brown, D. Guan, C. Pade, T. Shi, M. Syddall, J. Lv, L. Ji, L. Bing, J. Wang, W. Wei, K.-H. Yang, B. Lagerblad, I. Galan, C. Andrade, Y. Zhang, and Z. Liu, 2016: Substantial global carbon uptake by cement carbonation. *Nature Geoscience*, **9**, 880-883. <http://dx.doi.org/10.1038/ngeo2840>
45. Lelieveld, J. and P.J. Crutzen, 1992: Indirect chemical effects of methane on climate warming. *Nature*, **355**, 339-342. <http://dx.doi.org/10.1038/355339a0>
46. Saunio, M., R.B. Jackson, P. Bousquet, B. Poulter, and J.G. Canadell, 2016: The growing role of methane in anthropogenic climate change. *Environmental Research Letters*, **11**, 120207. <http://dx.doi.org/10.1088/1748-9326/11/12/120207>
47. Nisbet, E.G., E.J. Dlugokencky, M.R. Manning, D. Lowry, R.E. Fisher, J.L. France, S.E. Michel, J.B. Miller, J.W.C. White, B. Vaughn, P. Bousquet, J.A. Pyle, N.J. Warwick, M. Cain, R. Brownlow, G. Zazzeri, M. Lanoisellé, A.C. Manning, E. Gloor, D.E.J. Worthly, E.G. Brunke, C. Labuschagne, E.W. Wolff, and A.L. Ganesan, 2016: Rising atmospheric methane: 2007-2014 growth and isotopic shift. *Global Biogeochemical Cycles*, **30**, 1356-1370. <http://dx.doi.org/10.1002/2016GB005406>
48. Skiba, U.M. and R.M. Rees, 2014: Nitrous oxide, climate change and agriculture. *CAB Reviews*, **9**, 7. <http://dx.doi.org/10.1079/PAVSNR20149010>
49. Fowler, D., M. Coyle, U. Skiba, M.A. Sutton, J.N. Cape, S. Reis, L.J. Sheppard, A. Jenkins, B. Grizzetti, J.N. Galloway, P. Vitousek, A. Leach, A.F. Bouwman, K. Butterbach-Bahl, F. Dentener, D. Stevenson, M. Amann, and M. Voss, 2013: The global nitrogen cycle in the twenty-first century. *Philosophical Transactions of the Royal Society B: Biological Sciences*, **368**, 20130164. <http://dx.doi.org/10.1098/rstb.2013.0164>
50. Velders, G.J.M., D.W. Fahey, J.S. Daniel, S.O. Andersen, and M. McFarland, 2015: Future atmospheric abundances and climate forcings from scenarios of global and regional hydrofluorocarbon (HFC) emissions. *Atmospheric Environment*, **123**, Part A, 200-209. <http://dx.doi.org/10.1016/j.atmosenv.2015.10.071>
51. Solomon, S., K.H. Rosenlof, R.W. Portmann, J.S. Daniel, S.M. Davis, T.J. Sanford, and G.-K. Plattner, 2010: Contributions of stratospheric water vapor to decadal changes in the rate of global warming. *Science*, **327**, 1219-1223. <http://dx.doi.org/10.1126/science.1182488>
52. Hegglin, M.I., D.A. Plummer, T.G. Shepherd, J.F. Scinocca, J. Anderson, L. Froidevaux, B. Funke, D. Hurst, A. Rozanov, J. Urban, T. von Clarmann, K.A. Walker, H.J. Wang, S. Tegtmeier, and K. Weigel, 2014: Vertical structure of stratospheric water vapour trends derived from merged satellite data. *Nature Geoscience*, **7**, 768-776. <http://dx.doi.org/10.1038/ngeo2236>
53. le Texier, H., S. Solomon, and R.R. Garcia, 1988: The role of molecular hydrogen and methane oxidation in the water vapour budget of the stratosphere. *Quarterly Journal of the Royal Meteorological Society*, **114**, 281-295. <http://dx.doi.org/10.1002/qj.49711448002>
54. Rosenlof, K.H., S.J. Oltmans, D. Kley, J.M. Russell, E.W. Chiou, W.P. Chu, D.G. Johnson, K.K. Kelly, H.A. Michelsen, G.E. Nedoluha, E.E. Remsburg, G.C. Toon, and M.P. McCormick, 2001: Stratospheric water vapor increases over the past half-century. *Geophysical Research Letters*, **28**, 1195-1198. <http://dx.doi.org/10.1029/2000GL012502>
55. Morris, G.A., J.E. Rosenfield, M.R. Schoeberl, and C.H. Jackman, 2003: Potential impact of subsonic and supersonic aircraft exhaust on water vapor in the lower stratosphere assessed via a trajectory model. *Journal of Geophysical Research*, **108**, 4103. <http://dx.doi.org/10.1029/2002JD002614>
56. Löffler, M., S. Brinkop, and P. Jöckel, 2016: Impact of major volcanic eruptions on stratospheric water vapour. *Atmospheric Chemistry and Physics*, **16**, 6547-6562. <http://dx.doi.org/10.5194/acp-16-6547-2016>
57. Held, I.M. and B.J. Soden, 2000: Water vapor feedback and global warming. *Annual Review of Energy and the Environment*, **25**, 441-475. <http://dx.doi.org/10.1146/annurev.energy.25.1.441>



58. Dentener, F., D. Stevenson, J. Cofala, R. Mechler, M. Amann, P. Bergamaschi, F. Raes, and R. Derwent, 2005: The impact of air pollutant and methane emission controls on tropospheric ozone and radiative forcing: CTM calculations for the period 1990-2030. *Atmospheric Chemistry and Physics*, **5**, 1731-1755. <http://dx.doi.org/10.5194/acp-5-1731-2005>
59. WMO, 2014: Scientific Assessment of Ozone Depletion: 2014. World Meteorological Organization Geneva, Switzerland. 416 pp. <http://www.esrl.noaa.gov/csd/assessments/ozone/2014/>
60. Boucher, O., D. Randall, P. Artaxo, C. Bretherton, G. Feingold, P. Forster, V.-M. Kerminen, Y. Kondo, H. Liao, U. Lohmann, P. Rasch, S.K. Satheesh, S. Sherwood, B. Stevens, and X.Y. Zhang, 2013: Clouds and aerosols. *Climate Change 2013: The Physical Science Basis. Contribution of Working Group I to the Fifth Assessment Report of the Intergovernmental Panel on Climate Change*. Stocker, T.F., D. Qin, G.-K. Plattner, M. Tignor, S.K. Allen, J. Boschung, A. Nauels, Y. Xia, V. Bex, and P.M. Midgley, Eds. Cambridge University Press, Cambridge, United Kingdom and New York, NY, USA, 571-658. <http://www.climatechange2013.org/report/full-report/>
61. Bond, T.C., S.J. Doherty, D.W. Fahey, P.M. Forster, T. Berntsen, B.J. DeAngelo, M.G. Flanner, S. Ghan, B. Kärcher, D. Koch, S. Kinne, Y. Kondo, P.K. Quinn, M.C. Sarofim, M.G. Schultz, M. Schulz, C. Venkataraman, H. Zhang, S. Zhang, N. Bellouin, S.K. Guttikunda, P.K. Hopke, M.Z. Jacobson, J.W. Kaiser, Z. Klimont, U. Lohmann, J.P. Schwarz, D. Shindell, T. Storelvmo, S.G. Warren, and C.S. Zender, 2013: Bounding the role of black carbon in the climate system: A scientific assessment. *Journal of Geophysical Research Atmospheres*, **118**, 5380-5552. <http://dx.doi.org/10.1002/jgrd.50171>
62. Flanner, M.G., C.S. Zender, P.G. Hess, N.M. Mahowald, T.H. Painter, V. Ramanathan, and P.J. Rasch, 2009: Springtime warming and reduced snow cover from carbonaceous particles. *Atmospheric Chemistry and Physics*, **9**, 2481-2497. <http://dx.doi.org/10.5194/acp-9-2481-2009>
63. Ward, D.S., N.M. Mahowald, and S. Kloster, 2014: Potential climate forcing of land use and land cover change. *Atmospheric Chemistry and Physics*, **14**, 12701-12724. <http://dx.doi.org/10.5194/acp-14-12701-2014>
64. Ju, J. and J.G. Masek, 2016: The vegetation greenness trend in Canada and US Alaska from 1984-2012 Landsat data. *Remote Sensing of Environment*, **176**, 1-16. <http://dx.doi.org/10.1016/j.rse.2016.01.001>
65. Cook, B.I., S.P. Shukla, M.J. Puma, and L.S. Nazarenko, 2015: Irrigation as an historical climate forcing. *Climate Dynamics*, **44**, 1715-1730. <http://dx.doi.org/10.1007/s00382-014-2204-7>
66. Burkhardt, U. and B. Kärcher, 2011: Global radiative forcing from contrail cirrus. *Nature Climate Change*, **1**, 54-58. <http://dx.doi.org/10.1038/nclimate1068>
67. Smith, S.J. and T.C. Bond, 2014: Two hundred fifty years of aerosols and climate: The end of the age of aerosols. *Atmospheric Chemistry and Physics*, **14**, 537-549. <http://dx.doi.org/10.5194/acp-14-537-2014>
68. Fiore, A.M., V. Naik, and E.M. Leibensperger, 2015: Air quality and climate connections. *Journal of the Air & Waste Management Association*, **65**, 645-686. <http://dx.doi.org/10.1080/10962247.2015.1040526>
69. Masson-Delmotte, V., M. Schulz, A. Abe-Ouchi, J. Beer, A. Ganopolski, J.F. González Rouco, E. Jansen, K. Lambeck, J. Luterbacher, T. Naish, T. Osborn, B. Otto-Bliesner, T. Quinn, R. Ramesh, M. Rojas, X. Shao, and A. Timmermann, 2013: Information from paleoclimate archives. *Climate Change 2013: The Physical Science Basis. Contribution of Working Group I to the Fifth Assessment Report of the Intergovernmental Panel on Climate Change*. Stocker, T.F., D. Qin, G.-K. Plattner, M. Tignor, S.K. Allen, J. Boschung, A. Nauels, Y. Xia, V. Bex, and P.M. Midgley, Eds. Cambridge University Press, Cambridge, United Kingdom and New York, NY, USA, 383-464. <http://www.climatechange2013.org/report/full-report/>
70. Philipona, R., K. Behrens, and C. Ruckstuhl, 2009: How declining aerosols and rising greenhouse gases forced rapid warming in Europe since the 1980s. *Geophysical Research Letters*, **36**, L02806. <http://dx.doi.org/10.1029/2008GL036350>
71. Leibensperger, E.M., L.J. Mickley, D.J. Jacob, W.T. Chen, J.H. Seinfeld, A. Nenes, P.J. Adams, D.G. Streets, N. Kumar, and D. Rind, 2012: Climatic effects of 1950-2050 changes in US anthropogenic aerosols - Part 1: Aerosol trends and radiative forcing. *Atmospheric Chemistry and Physics*, **12**, 3333-3348. <http://dx.doi.org/10.5194/acp-12-3333-2012>
72. Wild, M., 2016: Decadal changes in radiative fluxes at land and ocean surfaces and their relevance for global warming. *Wiley Interdisciplinary Reviews: Climate Change*, **7**, 91-107. <http://dx.doi.org/10.1002/wcc.372>
73. Hsu, N.C., R. Gautam, A.M. Sayer, C. Bettenhausen, C. Li, M.J. Jeong, S.C. Tsay, and B.N. Holben, 2012: Global and regional trends of aerosol optical depth over land and ocean using SeaWiFS measurements from 1997 to 2010. *Atmospheric Chemistry and Physics*, **12**, 8037-8053. <http://dx.doi.org/10.5194/acp-12-8037-2012>



74. Chin, M., T. Diehl, Q. Tan, J.M. Prospero, R.A. Kahn, L.A. Remer, H. Yu, A.M. Sayer, H. Bian, I.V. Geogdzhayev, B.N. Holben, S.G. Howell, B.J. Huebert, N.C. Hsu, D. Kim, T.L. Kucsera, R.C. Levy, M.I. Mishchenko, X. Pan, P.K. Quinn, G.L. Schuster, D.G. Streets, S.A. Strode, O. Torres, and X.P. Zhao, 2014: Multi-decadal aerosol variations from 1980 to 2009: A perspective from observations and a global model. *Atmospheric Chemistry and Physics*, **14**, 3657-3690. <http://dx.doi.org/10.5194/acp-14-3657-2014>
75. Lynch, P., J.S. Reid, D.L. Westphal, J. Zhang, T.F. Hogan, E.J. Hyer, C.A. Curtis, D.A. Hegg, Y. Shi, J.R. Campbell, J.I. Rubin, W.R. Sessions, F.J. Turk, and A.L. Walker, 2016: An 11-year global gridded aerosol optical thickness reanalysis (v1.0) for atmospheric and climate sciences. *Geoscientific Model Development*, **9**, 1489-1522. <http://dx.doi.org/10.5194/gmd-9-1489-2016>
76. Flato, G., J. Marotzke, B. Abiodun, P. Braconnot, S.C. Chou, W. Collins, P. Cox, F. Driouech, S. Emori, V. Eyring, C. Forest, P. Gleckler, E. Guilyardi, C. Jakob, V. Kattsov, C. Reason, and M. Rummukainen, 2013: Evaluation of climate models. *Climate Change 2013: The Physical Science Basis. Contribution of Working Group I to the Fifth Assessment Report of the Intergovernmental Panel on Climate Change*. Stocker, T.F., D. Qin, G.-K. Plattner, M. Tignor, S.K. Allen, J. Boschung, A. Nauels, Y. Xia, V. Bex, and P.M. Midgley, Eds. Cambridge University Press, Cambridge, United Kingdom and New York, NY, USA, 741-866. <http://www.climatechange2013.org/report/full-report/>
77. Collins, M., R. Knutti, J. Arblaster, J.-L. Dufresne, T. Fichefet, P. Friedlingstein, X. Gao, W.J. Gutowski, T. Johns, G. Krinner, M. Shongwe, C. Tebaldi, A.J. Weaver, and M. Wehner, 2013: Long-term climate change: Projections, commitments and irreversibility. *Climate Change 2013: The Physical Science Basis. Contribution of Working Group I to the Fifth Assessment Report of the Intergovernmental Panel on Climate Change*. Stocker, T.F., D. Qin, G.-K. Plattner, M. Tignor, S.K. Allen, J. Boschung, A. Nauels, Y. Xia, V. Bex, and P.M. Midgley, Eds. Cambridge University Press, Cambridge, United Kingdom and New York, NY, USA, 1029-1136. <http://www.climatechange2013.org/report/full-report/>
78. Knutti, R. and G.C. Hegerl, 2008: The equilibrium sensitivity of the Earth's temperature to radiation changes. *Nature Geoscience*, **1**, 735-743. <http://dx.doi.org/10.1038/ngeo337>
79. Bony, S., R. Colman, V.M. Kattsov, R.P. Allan, C.S. Bretherton, J.-L. Dufresne, A. Hall, S. Hallegatte, M.M. Holland, W. Ingram, D.A. Randall, B.J. Soden, G. Tselioudis, and M.J. Webb, 2006: How well do we understand and evaluate climate change feedback processes? *Journal of Climate*, **19**, 3445-3482. <http://dx.doi.org/10.1175/JCLI3819.1>
80. Shindell, D. and G. Faluvegi, 2009: Climate response to regional radiative forcing during the twentieth century. *Nature Geoscience*, **2**, 294-300. <http://dx.doi.org/10.1038/ngeo473>
81. Crook, J.A. and P.M. Forster, 2011: A balance between radiative forcing and climate feedback in the modeled 20th century temperature response. *Journal of Geophysical Research*, **116**, D17108. <http://dx.doi.org/10.1029/2011JD015924>
82. Knutti, R. and M.A.A. Rugenstein, 2015: Feedbacks, climate sensitivity and the limits of linear models. *Philosophical Transactions of the Royal Society A: Mathematical, Physical and Engineering Sciences*, **373**, 20150146. <http://dx.doi.org/10.1098/rsta.2015.0146>
83. Ramanathan, V., M.S. Lian, and R.D. Cess, 1979: Increased atmospheric CO₂: Zonal and seasonal estimates of the effect on the radiation energy balance and surface temperature. *Journal of Geophysical Research*, **84**, 4949-4958. <http://dx.doi.org/10.1029/JC084iC08p04949>
84. Vial, J., J.-L. Dufresne, and S. Bony, 2013: On the interpretation of inter-model spread in CMIP5 climate sensitivity estimates. *Climate Dynamics*, **41**, 3339-3362. <http://dx.doi.org/10.1007/s00382-013-1725-9>
85. Allen, M.R. and W.J. Ingram, 2002: Constraints on future changes in climate and the hydrologic cycle. *Nature*, **419**, 224-232. <http://dx.doi.org/10.1038/nature01092>
86. Soden, B.J. and I.M. Held, 2006: An assessment of climate feedbacks in coupled ocean-atmosphere models. *Journal of Climate*, **19**, 3354-3360. <http://dx.doi.org/10.1175/JCLI3799.1>
87. Dessler, A.E., M.R. Schoeberl, T. Wang, S.M. Davis, K.H. Rosenlof, and J.P. Vernier, 2014: Variations of stratospheric water vapor over the past three decades. *Journal of Geophysical Research Atmospheres*, **119**, 12,588-12,598. <http://dx.doi.org/10.1002/2014JD021712>
88. IPCC, 2007: *Climate Change 2007: The Physical Science Basis. Contribution of Working Group I to the Fourth Assessment Report of the Intergovernmental Panel on Climate Change*. Solomon, S., D. Qin, M. Manning, Z. Chen, M. Marquis, K.B. Averyt, M. Tignor, and H.L. Miller, Eds. Cambridge University Press, Cambridge, U.K, New York, NY, USA, 996 pp. http://www.ipcc.ch/publications_and_data/publications_ipcc_fourth_assessment_report_wg1_report_the_physical_science_basis.htm
89. Loeb, N.G., B.A. Wielicki, D.R. Doelling, G.L. Smith, D.F. Keyes, S. Kato, N. Manalo-Smith, and T. Wong, 2009: Toward optimal closure of the Earth's top-of-atmosphere radiation budget. *Journal of Climate*, **22**, 748-766. <http://dx.doi.org/10.1175/2008JCLI2637.1>



90. Sohn, B.J., T. Nakajima, M. Satoh, and H.S. Jang, 2010: Impact of different definitions of clear-sky flux on the determination of longwave cloud radiative forcing: NICAM simulation results. *Atmospheric Chemistry and Physics*, **10**, 11641-11646. <http://dx.doi.org/10.5194/acp-10-11641-2010>
91. Hartmann, D.L., M.E. Ockert-Bell, and M.L. Michelsen, 1992: The effect of cloud type on Earth's energy balance: Global analysis. *Journal of Climate*, **5**, 1281-1304. [http://dx.doi.org/10.1175/1520-0442\(1992\)005<1281:teocto>2.0.co;2](http://dx.doi.org/10.1175/1520-0442(1992)005<1281:teocto>2.0.co;2)
92. Chen, T., W.B. Rossow, and Y. Zhang, 2000: Radiative effects of cloud-type variations. *Journal of Climate*, **13**, 264-286. [http://dx.doi.org/10.1175/1520-0442\(2000\)013<0264:reoctv>2.0.co;2](http://dx.doi.org/10.1175/1520-0442(2000)013<0264:reoctv>2.0.co;2)
93. Rädel, G., T. Mauritsen, B. Stevens, D. Dommenges, D. Matei, K. Bellomo, and A. Clement, 2016: Amplification of El Niño by cloud longwave coupling to atmospheric circulation. *Nature Geoscience*, **9**, 106-110. <http://dx.doi.org/10.1038/ngeo2630>
94. Taylor, P.C., R.G. Ellingson, and M. Cai, 2011: Geographical distribution of climate feedbacks in the NCAR CCSM3.0. *Journal of Climate*, **24**, 2737-2753. <http://dx.doi.org/10.1175/2010JCLI3788.1>
95. Klocke, D., J. Quaas, and B. Stevens, 2013: Assessment of different metrics for physical climate feedbacks. *Climate Dynamics*, **41**, 1173-1185. <http://dx.doi.org/10.1007/s00382-013-1757-1>
96. Sejas, S.A., M. Cai, A. Hu, G.A. Meehl, W. Washington, and P.C. Taylor, 2014: Individual feedback contributions to the seasonality of surface warming. *Journal of Climate*, **27**, 5653-5669. <http://dx.doi.org/10.1175/JCLI-D-13-00658.1>
97. Hansen, J. and L. Nazarenko, 2004: Soot climate forcing via snow and ice albedos. *Proceedings of the National Academy of Sciences of the United States of America*, **101**, 423-428. <http://dx.doi.org/10.1073/pnas.2237157100>
98. Jacobson, M.Z., 2004: Climate response of fossil fuel and biofuel soot, accounting for soot's feedback to snow and sea ice albedo and emissivity. *Journal of Geophysical Research*, **109**, D21201. <http://dx.doi.org/10.1029/2004JD004945>
99. Skeie, R.B., T. Berntsen, G. Myhre, C.A. Pedersen, J. Ström, S. Gerland, and J.A. Ogren, 2011: Black carbon in the atmosphere and snow, from pre-industrial times until present. *Atmospheric Chemistry and Physics*, **11**, 6809-6836. <http://dx.doi.org/10.5194/acp-11-6809-2011>
100. Yang, S., B. Xu, J. Cao, C.S. Zender, and M. Wang, 2015: Climate effect of black carbon aerosol in a Tibetan Plateau glacier. *Atmospheric Environment*, **111**, 71-78. <http://dx.doi.org/10.1016/j.atmosenv.2015.03.016>
101. Holland, D.M., R.H. Thomas, B. de Young, M.H. Ribergaard, and B. Lyberth, 2008: Acceleration of Jakobshavn Isbrae triggered by warm subsurface ocean waters. *Nature Geoscience*, **1**, 659-664. <http://dx.doi.org/10.1038/ngeo316>
102. Schoof, C., 2010: Ice-sheet acceleration driven by melt supply variability. *Nature*, **468**, 803-806. <http://dx.doi.org/10.1038/nature09618>
103. Rignot, E., M. Koppes, and I. Velicogna, 2010: Rapid submarine melting of the calving faces of West Greenland glaciers. *Nature Geoscience*, **3**, 187-191. <http://dx.doi.org/10.1038/ngeo765>
104. Joughin, I., R.B. Alley, and D.M. Holland, 2012: Ice-sheet response to oceanic forcing. *Science*, **338**, 1172-1176. <http://dx.doi.org/10.1126/science.1226481>
105. Straneo, F. and P. Heimbach, 2013: North Atlantic warming and the retreat of Greenland's outlet glaciers. *Nature*, **504**, 36-43. <http://dx.doi.org/10.1038/nature12854>
106. Thoma, M., J. Determann, K. Grosfeld, S. Goeller, and H.H. Hellmer, 2015: Future sea-level rise due to projected ocean warming beneath the Filchner Ronne Ice Shelf: A coupled model study. *Earth and Planetary Science Letters*, **431**, 217-224. <http://dx.doi.org/10.1016/j.epsl.2015.09.013>
107. Alley, K.E., T.A. Scambos, M.R. Siegfried, and H.A. Fricker, 2016: Impacts of warm water on Antarctic ice shelf stability through basal channel formation. *Nature Geoscience*, **9**, 290-293. <http://dx.doi.org/10.1038/ngeo2675>
108. Silvano, A., S.R. Rintoul, and L. Herraiz-Borreguero, 2016: Ocean-ice shelf interaction in East Antarctica. *Oceanography*, **29**, 130-143. <http://dx.doi.org/10.5670/oceanog.2016.105>
109. Hall, A. and X. Qu, 2006: Using the current seasonal cycle to constrain snow albedo feedback in future climate change. *Geophysical Research Letters*, **33**, L03502. <http://dx.doi.org/10.1029/2005GL025127>
110. Fernandes, R., H. Zhao, X. Wang, J. Key, X. Qu, and A. Hall, 2009: Controls on Northern Hemisphere snow albedo feedback quantified using satellite Earth observations. *Geophysical Research Letters*, **36**, L21702. <http://dx.doi.org/10.1029/2009GL040057>
111. Winton, M., 2006: Surface albedo feedback estimates for the AR4 climate models. *Journal of Climate*, **19**, 359-365. <http://dx.doi.org/10.1175/JCLI3624.1>
112. Hall, A., 2004: The role of surface albedo feedback in climate. *Journal of Climate*, **17**, 1550-1568. [http://dx.doi.org/10.1175/1520-0442\(2004\)017<1550:TROSAF>2.0.CO;2](http://dx.doi.org/10.1175/1520-0442(2004)017<1550:TROSAF>2.0.CO;2)



113. Kay, J.E. and A. Gettelman, 2009: Cloud influence on and response to seasonal Arctic sea ice loss. *Journal of Geophysical Research*, **114**, D18204. <http://dx.doi.org/10.1029/2009JD011773>
114. Kay, J.E., K. Raeder, A. Gettelman, and J. Anderson, 2011: The boundary layer response to recent Arctic sea ice loss and implications for high-latitude climate feedbacks. *Journal of Climate*, **24**, 428-447. <http://dx.doi.org/10.1175/2010JCLI3651.1>
115. Kay, J.E. and T. L'Ecuyer, 2013: Observational constraints on Arctic Ocean clouds and radiative fluxes during the early 21st century. *Journal of Geophysical Research Atmospheres*, **118**, 7219-7236. <http://dx.doi.org/10.1002/jgrd.50489>
116. Pistone, K., I. Eisenman, and V. Ramanathan, 2014: Observational determination of albedo decrease caused by vanishing Arctic sea ice. *Proceedings of the National Academy of Sciences*, **111**, 3322-3326. <http://dx.doi.org/10.1073/pnas.1318201111>
117. Taylor, P.C., S. Kato, K.-M. Xu, and M. Cai, 2015: Covariance between Arctic sea ice and clouds within atmospheric state regimes at the satellite footprint level. *Journal of Geophysical Research Atmospheres*, **120**, 12656-12678. <http://dx.doi.org/10.1002/2015JD023520>
118. Liao, H., Y. Zhang, W.-T. Chen, F. Raes, and J.H. Seinfeld, 2009: Effect of chemistry-aerosol-climate coupling on predictions of future climate and future levels of tropospheric ozone and aerosols. *Journal of Geophysical Research*, **114**, D10306. <http://dx.doi.org/10.1029/2008JD010984>
119. Unger, N., S. Menon, D.M. Koch, and D.T. Shindell, 2009: Impacts of aerosol-cloud interactions on past and future changes in tropospheric composition. *Atmospheric Chemistry and Physics*, **9**, 4115-4129. <http://dx.doi.org/10.5194/acp-9-4115-2009>
120. Raes, F., H. Liao, W.-T. Chen, and J.H. Seinfeld, 2010: Atmospheric chemistry-climate feedbacks. *Journal of Geophysical Research*, **115**, D12121. <http://dx.doi.org/10.1029/2009JD013300>
121. Tai, A.P.K., L.J. Mickley, C.L. Heald, and S. Wu, 2013: Effect of CO₂ inhibition on biogenic isoprene emission: Implications for air quality under 2000 to 2050 changes in climate, vegetation, and land use. *Geophysical Research Letters*, **40**, 3479-3483. <http://dx.doi.org/10.1002/grl.50650>
122. Yue, X., L.J. Mickley, J.A. Logan, R.C. Hudman, M.V. Martin, and R.M. Yantosca, 2015: Impact of 2050 climate change on North American wildfire: consequences for ozone air quality. *Atmospheric Chemistry and Physics*, **15**, 10033-10055. <http://dx.doi.org/10.5194/acp-15-10033-2015>
123. Nowack, P.J., N. Luke Abraham, A.C. Maycock, P. Braesicke, J.M. Gregory, M.M. Joshi, A. Osprey, and J.A. Pyle, 2015: A large ozone-circulation feedback and its implications for global warming assessments. *Nature Climate Change*, **5**, 41-45. <http://dx.doi.org/10.1038/nclimate2451>
124. John, J.G., A.M. Fiore, V. Naik, L.W. Horowitz, and J.P. Dunne, 2012: Climate versus emission drivers of methane lifetime against loss by tropospheric OH from 1860-2100. *Atmospheric Chemistry and Physics*, **12**, 12021-12036. <http://dx.doi.org/10.5194/acp-12-12021-2012>
125. Pacifico, F., G.A. Folberth, C.D. Jones, S.P. Harrison, and W.J. Collins, 2012: Sensitivity of biogenic isoprene emissions to past, present, and future environmental conditions and implications for atmospheric chemistry. *Journal of Geophysical Research*, **117**, D22302. <http://dx.doi.org/10.1029/2012JD018276>
126. Morgenstern, O., G. Zeng, N. Luke Abraham, P.J. Telford, P. Braesicke, J.A. Pyle, S.C. Hardiman, F.M. O'Connor, and C.E. Johnson, 2013: Impacts of climate change, ozone recovery, and increasing methane on surface ozone and the tropospheric oxidizing capacity. *Journal of Geophysical Research Atmospheres*, **118**, 1028-1041. <http://dx.doi.org/10.1029/2012JD018382>
127. Holmes, C.D., M.J. Prather, O.A. Søvde, and G. Myhre, 2013: Future methane, hydroxyl, and their uncertainties: Key climate and emission parameters for future predictions. *Atmospheric Chemistry and Physics*, **13**, 285-302. <http://dx.doi.org/10.5194/acp-13-285-2013>
128. Naik, V., A. Voulgarakis, A.M. Fiore, L.W. Horowitz, J.F. Lamarque, M. Lin, M.J. Prather, P.J. Young, D. Bergmann, P.J. Cameron-Smith, I. Cionni, W.J. Collins, S.B. Dalsøren, R. Doherty, V. Eyring, G. Faluvegi, G.A. Folberth, B. Josse, Y.H. Lee, I.A. MacKenzie, T. Nagashima, T.P.C. van Noije, D.A. Plummer, M. Righi, S.T. Rumbold, R. Skeie, D.T. Shindell, D.S. Stevenson, S. Strode, K. Sudo, S. Szopa, and G. Zeng, 2013: Preindustrial to present-day changes in tropospheric hydroxyl radical and methane lifetime from the Atmospheric Chemistry and Climate Model Intercomparison Project (ACCMIP). *Atmospheric Chemistry and Physics*, **13**, 5277-5298. <http://dx.doi.org/10.5194/acp-13-5277-2013>
129. Voulgarakis, A., V. Naik, J.F. Lamarque, D.T. Shindell, P.J. Young, M.J. Prather, O. Wild, R.D. Field, D. Bergmann, P. Cameron-Smith, I. Cionni, W.J. Collins, S.B. Dalsøren, R.M. Doherty, V. Eyring, G. Faluvegi, G.A. Folberth, L.W. Horowitz, B. Josse, I.A. MacKenzie, T. Nagashima, D.A. Plummer, M. Righi, S.T. Rumbold, D.S. Stevenson, S.A. Strode, K. Sudo, S. Szopa, and G. Zeng, 2013: Analysis of present day and future OH and methane lifetime in the ACCMIP simulations. *Atmospheric Chemistry and Physics*, **13**, 2563-2587. <http://dx.doi.org/10.5194/acp-13-2563-2013>



130. Isaksen, I., T. Bernsten, S. Dalsøren, K. Eleftheratos, Y. Orsolini, B. Rognerud, F. Stordal, O. Søvde, C. Zerefos, and C. Holmes, 2014: Atmospheric ozone and methane in a changing climate. *Atmosphere*, **5**, 518. <http://dx.doi.org/10.3390/atmos5030518>
131. Dietmüller, S., M. Ponater, and R. Sausen, 2014: Interactive ozone induces a negative feedback in CO₂-driven climate change simulations. *Journal of Geophysical Research Atmospheres*, **119**, 1796-1805. <http://dx.doi.org/10.1002/2013JD020575>
132. Banerjee, A., A.T. Archibald, A.C. Maycock, P. Telford, N.L. Abraham, X. Yang, P. Braesicke, and J.A. Pyle, 2014: Lightning NO_x a key chemistry-climate interaction: Impacts of future climate change and consequences for tropospheric oxidising capacity. *Atmospheric Chemistry and Physics*, **14**, 9871-9881. <http://dx.doi.org/10.5194/acp-14-9871-2014>
133. ACC-MIP, 2017: Atmospheric Chemistry and Climate MIP. WCRP Working Group on Coupled Modeling. <https://www.wcrp-climate.org/modelling-wgcm-mip-catalogue/modelling-wgcm-mips-2/226-modelling-wgcm-acc-mip>
134. Han, Z., J. Li, W. Guo, Z. Xiong, and W. Zhang, 2013: A study of dust radiative feedback on dust cycle and meteorology over East Asia by a coupled regional climate-chemistry-aerosol model. *Atmospheric Environment*, **68**, 54-63. <http://dx.doi.org/10.1016/j.atmosenv.2012.11.032>
135. Le Quéré, C., R.M. Andrew, J.G. Canadell, S. Sitch, J.I. Korsbakken, G.P. Peters, A.C. Manning, T.A. Boden, P.P. Tans, R.A. Houghton, R.F. Keeling, S. Alin, O.D. Andrews, P. Anthoni, L. Barbero, L. Bopp, F. Chevallier, L.P. Chini, P. Ciais, K. Currie, C. Delire, S.C. Doney, P. Friedlingstein, T. Gkritzalis, I. Harris, J. Hauck, V. Haverd, M. Hoppema, K. Klein Goldewijk, A.K. Jain, E. Kato, A. Körtzinger, P. Landschützer, N. Lefèvre, A. Lenton, S. Lienert, D. Lombardozzi, J.R. Melton, N. Metz, F. Miller, P.M.S. Monteiro, D.R. Munro, J.E.M.S. Nabel, S.I. Nakaoka, K. O'Brien, A. Olsen, A.M. Omar, T. Ono, D. Pierrot, B. Poulter, C. Rödenbeck, J. Salisbury, U. Schuster, J. Schwinger, R. Séférian, I. Skjelvan, B.D. Stocker, A.J. Sutton, T. Takahashi, H. Tian, B. Tilbrook, I.T. van der Laan-Luijk, G.R. van der Werf, N. Viovy, A.P. Walker, A.J. Wiltshire, and S. Zaehle, 2016: Global carbon budget 2016. *Earth System Science Data*, **8**, 605-649. <http://dx.doi.org/10.5194/essd-8-605-2016>
136. Wenzel, S., P.M. Cox, V. Eyring, and P. Friedlingstein, 2016: Projected land photosynthesis constrained by changes in the seasonal cycle of atmospheric CO₂. *Nature*, **538**, 499-501. <http://dx.doi.org/10.1038/nature19772>
137. Franks, P.J., M.A. Adams, J.S. Amthor, M.M. Barbour, J.A. Berry, D.S. Ellsworth, G.D. Farquhar, O. Ghanoun, J. Lloyd, N. McDowell, R.J. Norby, D.T. Tissue, and S. von Caemmerer, 2013: Sensitivity of plants to changing atmospheric CO₂ concentration: From the geological past to the next century. *New Phytologist*, **197**, 1077-1094. <http://dx.doi.org/10.1111/nph.12104>
138. Seppälä, R., 2009: A global assessment on adaptation of forests to climate change. *Scandinavian Journal of Forest Research*, **24**, 469-472. <http://dx.doi.org/10.1080/02827580903378626>
139. Hibbard, K.A., G.A. Meehl, P.M. Cox, and P. Friedlingstein, 2007: A strategy for climate change stabilization experiments. *Eos, Transactions, American Geophysical Union*, **88**, 217-221. <http://dx.doi.org/10.1029/2007EO200002>
140. Thornton, P.E., J.-F. Lamarque, N.A. Rosenbloom, and N.M. Mahowald, 2007: Influence of carbon-nitrogen cycle coupling on land model response to CO₂ fertilization and climate variability. *Global Biogeochemical Cycles*, **21**, GB4018. <http://dx.doi.org/10.1029/2006GB002868>
141. Brzostek, E.R., J.B. Fisher, and R.P. Phillips, 2014: Modeling the carbon cost of plant nitrogen acquisition: Mycorrhizal trade-offs and multipath resistance uptake improve predictions of retranslocation. *Journal of Geophysical Research Biogeosciences*, **119**, 1684-1697. <http://dx.doi.org/10.1002/2014JG002660>
142. Wieder, W.R., C.C. Cleveland, W.K. Smith, and K. Todd-Brown, 2015: Future productivity and carbon storage limited by terrestrial nutrient availability. *Nature Geoscience*, **8**, 441-444. <http://dx.doi.org/10.1038/ngeo2413>
143. Anav, A., P. Friedlingstein, M. Kidston, L. Bopp, P. Ciais, P. Cox, C. Jones, M. Jung, R. Myneni, and Z. Zhu, 2013: Evaluating the land and ocean components of the global carbon cycle in the CMIP5 earth system models. *Journal of Climate*, **26**, 6801-6843. <http://dx.doi.org/10.1175/jcli-d-12-00417.1>
144. Smith, W.K., S.C. Reed, C.C. Cleveland, A.P. Ballantyne, W.R.L. Anderegg, W.R. Wieder, Y.Y. Liu, and S.W. Running, 2016: Large divergence of satellite and Earth system model estimates of global terrestrial CO₂ fertilization. *Nature Climate Change*, **6**, 306-310. <http://dx.doi.org/10.1038/nclimate2879>
145. Friedlingstein, P., P. Cox, R. Betts, L. Bopp, W.v. Bloh, V. Brovkin, P. Cadule, S. Doney, M. Eby, I. Fung, G. Bala, J. John, C. Jones, F. Joos, T. Kato, M. Kawamiya, W. Knorr, K. Lindsay, H.D. Matthews, T. Raddatz, P. Rayner, C. Reick, E. Roeckner, K.-G. Schnitzler, R. Schnur, K. Strassmann, A.J. Weaver, C. Yoshikawa, and N. Zeng, 2006: Climate-carbon cycle feedback analysis: Results from the C⁴MIP model intercomparison. *Journal of Climate*, **19**, 3337-3353. <http://dx.doi.org/10.1175/JCLI3800.1>



146. Friedlingstein, P., M. Meinshausen, V.K. Arora, C.D. Jones, A. Anav, S.K. Liddicoat, and R. Knutti, 2014: Uncertainties in CMIP5 climate projections due to carbon cycle feedbacks. *Journal of Climate*, **27**, 511-526. <http://dx.doi.org/10.1175/JCLI-D-12-00579.1>
147. Johnson, G.C., J.M. Lyman, T. Boyer, C.M. Domingues, M. Ishii, R. Killick, D. Monselesan, and S.E. Wijffels, 2016: [Global Oceans] Ocean heat content [in "State of the Climate in 2015"]. *Bulletin of the American Meteorological Society*, **97**, S66-S70. <http://dx.doi.org/10.1175/2016BAMSStateoftheClimate.1>
148. Falkowski, P.G., M.E. Katz, A.H. Knoll, A. Quigg, J.A. Raven, O. Schofield, and F.J.R. Taylor, 2004: The evolution of modern eukaryotic phytoplankton. *Science*, **305**, 354-360. <http://dx.doi.org/10.1126/science.1095964>
149. Carr, M.-E., M.A.M. Friedrichs, M. Schmeltz, M. Noguchi Aita, D. Antoine, K.R. Arrigo, I. Asanuma, O. Aumont, R. Barber, M. Behrenfeld, R. Bidigare, E.T. Buitenhuis, J. Campbell, A. Ciotti, H. Dierssen, M. Dowell, J. Dunne, W. Esaias, B. Gentili, W. Gregg, S. Groom, N. Hoepffner, J. Ishizaka, T. Kameda, C. Le Quéré, S. Lohrenz, J. Marra, F. Mélin, K. Moore, A. Morel, T.E. Reddy, J. Ryan, M. Scardi, T. Smyth, K. Turpie, G. Tilstone, K. Waters, and Y. Yamanaka, 2006: A comparison of global estimates of marine primary production from ocean color. *Deep Sea Research Part II: Topical Studies in Oceanography*, **53**, 741-770. <http://dx.doi.org/10.1016/j.dsr2.2006.01.028>
150. Chavez, F.P., M. Messié, and J.T. Pennington, 2011: Marine primary production in relation to climate variability and change. *Annual Review of Marine Science*, **3**, 227-260. <http://dx.doi.org/10.1146/annurev.marine.010908.163917>
151. Doney, S.C., 2010: The growing human footprint on coastal and open-ocean biogeochemistry. *Science*, **328**, 1512-6. <http://dx.doi.org/10.1126/science.1185198>
152. Passow, U. and C.A. Carlson, 2012: The biological pump in a high CO₂ world. *Marine Ecology Progress Series*, **470**, 249-271. <http://dx.doi.org/10.3354/meps09985>
153. Trenberth, K.E., P.D. Jones, P. Ambenje, R. Bojariu, D. Easterling, A.K. Tank, D. Parker, F. Rahimzadeh, J.A. Renwick, M. Rusticucci, B. Soden, and P. Zhai, 2007: Observations: Surface and atmospheric climate change. *Climate Change 2007: The Physical Science Basis. Contribution of Working Group I to the Fourth Assessment Report of the Intergovernmental Panel on Climate Change*. Solomon, S., D. Qin, M. Manning, Z. Chen, M. Marquis, K.B. Averyt, M. Tignor, and H.L. Miller, Eds. Cambridge University Press, Cambridge, United Kingdom and New York, NY, USA. http://www.ipcc.ch/publications_and_data/ar4/wg1/en/ch3.html
154. Schanze, J.J., R.W. Schmitt, and L.L. Yu, 2010: The global oceanic freshwater cycle: A state-of-the-art quantification. *Journal of Marine Research*, **68**, 569-595. <http://dx.doi.org/10.1357/002224010794657164>
155. Durack, P.J. and S.E. Wijffels, 2010: Fifty-year trends in global ocean salinities and their relationship to broad-scale warming. *Journal of Climate*, **23**, 4342-4362. <http://dx.doi.org/10.1175/2010jcli3377.1>
156. Good, P., J.M. Gregory, J.A. Lowe, and T. Andrews, 2013: Abrupt CO₂ experiments as tools for predicting and understanding CMIP5 representative concentration pathway projections. *Climate Dynamics*, **40**, 1041-1053. <http://dx.doi.org/10.1007/s00382-012-1410-4>
157. Andrews, T., J.M. Gregory, M.J. Webb, and K.E. Taylor, 2012: Forcing, feedbacks and climate sensitivity in CMIP5 coupled atmosphere-ocean climate models. *Geophysical Research Letters*, **39**, L09712. <http://dx.doi.org/10.1029/2012GL051607>
158. Kostov, Y., K.C. Armour, and J. Marshall, 2014: Impact of the Atlantic meridional overturning circulation on ocean heat storage and transient climate change. *Geophysical Research Letters*, **41**, 2108-2116. <http://dx.doi.org/10.1002/2013GL058998>
159. Rahmstorf, S., J.E. Box, G. Feulner, M.E. Mann, A. Robinson, S. Rutherford, and E.J. Schaffernicht, 2015: Exceptional twentieth-century slowdown in Atlantic Ocean overturning circulation. *Nature Climate Change*, **5**, 475-480. <http://dx.doi.org/10.1038/nclimate2554>
160. Rignot, E. and R.H. Thomas, 2002: Mass balance of polar ice sheets. *Science*, **297**, 1502-1506. <http://dx.doi.org/10.1126/science.1073888>
161. van den Broeke, M., J. Bamber, J. Ettema, E. Rignot, E. Schrama, W.J. van de Berg, E. van Meijgaard, I. Velicogna, and B. Wouters, 2009: Partitioning recent Greenland mass loss. *Science*, **326**, 984-986. <http://dx.doi.org/10.1126/science.1178176>
162. Enderlin, E.M. and G.S. Hamilton, 2014: Estimates of iceberg submarine melting from high-resolution digital elevation models: Application to Sermilik Fjord, East Greenland. *Journal of Glaciology*, **60**, 1084-1092. <http://dx.doi.org/10.3189/2014jog14j085>
163. Gelderloos, R., F. Straneo, and C.A. Katsman, 2012: Mechanisms behind the temporary shutdown of deep convection in the Labrador Sea: Lessons from the great salinity anomaly years 1968-71. *Journal of Climate*, **25**, 6743-6755. <http://dx.doi.org/10.1175/jcli-d-11-00549.1>
164. Bidigare, R.R., F. Chai, M.R. Landry, R. Lukas, C.C.S. Hannides, S.J. Christensen, D.M. Karl, L. Shi, and Y. Chao, 2009: Subtropical ocean ecosystem structure changes forced by North Pacific climate variations. *Journal of Plankton Research*, **31**, 1131-1139. <http://dx.doi.org/10.1093/plankt/fbp064>



165. Zhai, P.-W., Y. Hu, C.A. Hostetler, B. Cairns, R.A. Ferrare, K.D. Knobelspiesse, D.B. Jossset, C.R. Trepte, P.L. Lucker, and J. Chowdhary, 2013: Uncertainty and interpretation of aerosol remote sensing due to vertical inhomogeneity. *Journal of Quantitative Spectroscopy and Radiative Transfer*, **114**, 91-100. <http://dx.doi.org/10.1016/j.jqsrt.2012.08.006>
166. Behrenfeld, M.J., R.T. O'Malley, D.A. Siegel, C.R. McClain, J.L. Sarmiento, G.C. Feldman, A.J. Milligan, P.G. Falkowski, R.M. Letelier, and E.S. Boss, 2006: Climate-driven trends in contemporary ocean productivity. *Nature*, **444**, 752-755. <http://dx.doi.org/10.1038/nature05317>
167. Boyce, D.G., M.R. Lewis, and B. Worm, 2010: Global phytoplankton decline over the past century. *Nature*, **466**, 591-596. <http://dx.doi.org/10.1038/nature09268>
168. Capotondi, A., M.A. Alexander, N.A. Bond, E.N. Curchitser, and J.D. Scott, 2012: Enhanced upper ocean stratification with climate change in the CMIP3 models. *Journal of Geophysical Research*, **117**, C04031. <http://dx.doi.org/10.1029/2011JC007409>
169. Rykaczewski, R.R. and J.P. Dunne, 2011: A measured look at ocean chlorophyll trends. *Nature*, **472**, E5-E6. <http://dx.doi.org/10.1038/nature09952>
170. Laufkötter, C., M. Vogt, N. Gruber, M. Aita-Noguchi, O. Aumont, L. Bopp, E. Buitenhuis, S.C. Doney, J. Dunne, T. Hashioka, J. Hauck, T. Hirata, J. John, C. Le Quéré, I.D. Lima, H. Nakano, R. Seferian, I. Totterdell, M. Vichi, and C. Völker, 2015: Drivers and uncertainties of future global marine primary production in marine ecosystem models. *Biogeosciences*, **12**, 6955-6984. <http://dx.doi.org/10.5194/bg-12-6955-2015>
171. Jin, X., N. Gruber, J.P. Dunne, J.L. Sarmiento, and R.A. Armstrong, 2006: Diagnosing the contribution of phytoplankton functional groups to the production and export of particulate organic carbon, CaCO₃, and opal from global nutrient and alkalinity distributions. *Global Biogeochemical Cycles*, **20**, GB2015. <http://dx.doi.org/10.1029/2005GB002532>
172. Fu, W., J.T. Randerson, and J.K. Moore, 2016: Climate change impacts on net primary production (NPP) and export production (EP) regulated by increasing stratification and phytoplankton community structure in the CMIP5 models. *Biogeosciences*, **13**, 5151-5170. <http://dx.doi.org/10.5194/bg-13-5151-2016>
173. Frölicher, T.L., K.B. Rodgers, C.A. Stock, and W.W.L. Cheung, 2016: Sources of uncertainties in 21st century projections of potential ocean ecosystem stressors. *Global Biogeochemical Cycles*, **30**, 1224-1243. <http://dx.doi.org/10.1002/2015GB005338>
174. Schaefer, K., H. Lantuit, E.R. Vladimirov, E.A.G. Schuur, and R. Witt, 2014: The impact of the permafrost carbon feedback on global climate. *Environmental Research Letters*, **9**, 085003. <http://dx.doi.org/10.1088/1748-9326/9/8/085003>
175. Koven, C.D., E.A.G. Schuur, C. Schädel, T.J. Bohn, E.J. Burke, G. Chen, X. Chen, P. Ciais, G. Grosse, J.W. Harden, D.J. Hayes, G. Hugelius, E.E. Jafarov, G. Krinner, P. Kuhry, D.M. Lawrence, A.H. MacDougall, S.S. Marchenko, A.D. McGuire, S.M. Natali, D.J. Nicolsky, D. Olefeldt, S. Peng, V.E. Romanovsky, K.M. Schaefer, J. Strauss, C.C. Treat, and M. Turetsky, 2015: A simplified, data-constrained approach to estimate the permafrost carbon-climate feedback. *Philosophical Transactions of the Royal Society A: Mathematical, Physical and Engineering Sciences*, **373**, 20140423. <http://dx.doi.org/10.1098/rsta.2014.0423>
176. Schuur, E.A.G., A.D. McGuire, C. Schadel, G. Grosse, J.W. Harden, D.J. Hayes, G. Hugelius, C.D. Koven, P. Kuhry, D.M. Lawrence, S.M. Natali, D. Olefeldt, V.E. Romanovsky, K. Schaefer, M.R. Turetsky, C.C. Treat, and J.E. Vonk, 2015: Climate change and the permafrost carbon feedback. *Nature*, **520**, 171-179. <http://dx.doi.org/10.1038/nature14338>
177. González-Eguino, M. and M.B. Neumann, 2016: Significant implications of permafrost thawing for climate change control. *Climatic Change*, **136**, 381-388. <http://dx.doi.org/10.1007/s10584-016-1666-5>
178. Koven, C.D., D.M. Lawrence, and W.J. Riley, 2015: Permafrost carbon-climate feedback is sensitive to deep soil carbon decomposability but not deep soil nitrogen dynamics. *Proceedings of the National Academy of Sciences*, **112**, 3752-3757. <http://dx.doi.org/10.1073/pnas.1415123112>
179. Liljedahl, A.K., J. Boike, R.P. Daanen, A.N. Fedorov, G.V. Frost, G. Grosse, L.D. Hinzman, Y. Iijima, J.C. Jorgenson, N. Matveyeva, M. Necsoiu, M.K. Reynolds, V.E. Romanovsky, J. Schulla, K.D. Tape, D.A. Walker, C.J. Wilson, H. Yabuki, and D. Zona, 2016: Pan-Arctic ice-wedge degradation in warming permafrost and its influence on tundra hydrology. *Nature Geoscience*, **9**, 312-318. <http://dx.doi.org/10.1038/ngeo2674>
180. Melillo, J.M., T.C. Richmond, and G.W. Yohe, eds., 2014: *Climate Change Impacts in the United States: The Third National Climate Assessment*. U.S. Global Change Research Program: Washington, D.C., 841 pp. <http://dx.doi.org/10.7930/J0Z31WJ2>
181. Jiao, C., M.G. Flanner, Y. Balkanski, S.E. Bauer, N. Bellouin, T.K. Berntsen, H. Bian, K.S. Carslaw, M. Chin, N. De Luca, T. Diehl, S.J. Ghan, T. Iversen, A. Kirkevåg, D. Koch, X. Liu, G.W. Mann, J.E. Penner, G. Pitari, M. Schulz, Ø. Seland, R.B. Skeie, S.D. Steenrod, P. Stier, T. Takemura, K. Tsigaridis, T. van Noije, Y. Yun, and K. Zhang, 2014: An AeroCom assessment of black carbon in Arctic snow and sea ice. *Atmospheric Chemistry and Physics*, **14**, 2399-2417. <http://dx.doi.org/10.5194/acp-14-2399-2014>



182. Tsigaridis, K., N. Daskalakis, M. Kanakidou, P.J. Adams, P. Artaxo, R. Bahadur, Y. Balkanski, S.E. Bauer, N. Bellouin, A. Benedetti, T. Bergman, T.K. Berntsen, J.P. Beukes, H. Bian, K.S. Carslaw, M. Chin, G. Curci, T. Diehl, R.C. Easter, S.J. Ghan, S.L. Gong, A. Hodzic, C.R. Hoyle, T. Iversen, S. Jathar, J.L. Jimenez, J.W. Kaiser, A. Kirkevåg, D. Koch, H. Kokkola, Y.H. Lee, G. Lin, X. Liu, G. Luo, X. Ma, G.W. Mann, N. Mihalopoulos, J.J. Morcrette, J.F. Müller, G. Myhre, S. Myriokefalitakis, N.L. Ng, D. O'Donnell, J.E. Penner, L. Pozzoli, K.J. Pringle, L.M. Russell, M. Schulz, J. Sciare, Ø. Seland, D.T. Shindell, S. Sillman, R.B. Skeie, D. Spracklen, T. Stavrakou, S.D. Steenrod, T. Takemura, P. Tiitta, S. Tilmes, H. Tost, T. van Noije, P.G. van Zyl, K. von Salzen, F. Yu, Z. Wang, Z. Wang, R.A. Zaveri, H. Zhang, K. Zhang, Q. Zhang, and X. Zhang, 2014: The AeroCom evaluation and intercomparison of organic aerosol in global models. *Atmospheric Chemistry and Physics*, **14**, 10845-10895. <http://dx.doi.org/10.5194/acp-14-10845-2014>
183. Koffi, B., M. Schulz, F.-M. Bréon, F. Dentener, B.M. Steensen, J. Griesfeller, D. Winker, Y. Balkanski, S.E. Bauer, N. Bellouin, T. Berntsen, H. Bian, M. Chin, T. Diehl, R. Easter, S. Ghan, D.A. Hauglustaine, T. Iversen, A. Kirkevåg, X. Liu, U. Lohmann, G. Myhre, P. Rasch, Ø. Seland, R.B. Skeie, S.D. Steenrod, P. Stier, J. Tackett, T. Takemura, K. Tsigaridis, M.R. Vuolo, J. Yoon, and K. Zhang, 2016: Evaluation of the aerosol vertical distribution in global aerosol models through comparison against CALIOP measurements: AeroCom phase II results. *Journal of Geophysical Research Atmospheres*, **121**, 7254-7283. <http://dx.doi.org/10.1002/2015JD024639>
184. Zhu, Z., S. Piao, R.B. Myneni, M. Huang, Z. Zeng, J.G. Canadell, P. Ciais, S. Sitch, P. Friedlingstein, A. Arneth, C. Cao, L. Cheng, E. Kato, C. Koven, Y. Li, X. Lian, Y. Liu, R. Liu, J. Mao, Y. Pan, S. Peng, J. Penuelas, B. Poulter, T.A.M. Pugh, B.D. Stocker, N. Viovy, X. Wang, Y. Wang, Z. Xiao, H. Yang, S. Zaehle, and N. Zeng, 2016: Greening of the Earth and its drivers. *Nature Climate Change*, **6**, 791-795. <http://dx.doi.org/10.1038/nclimate3004>
185. Mao, J., A. Ribes, B. Yan, X. Shi, P.E. Thornton, R. Seferian, P. Ciais, R.B. Myneni, H. Douville, S. Piao, Z. Zhu, R.E. Dickinson, Y. Dai, D.M. Ricciuto, M. Jin, F.M. Hoffman, B. Wang, M. Huang, and X. Lian, 2016: Human-induced greening of the northern extratropical land surface. *Nature Climate Change*, **6**, 959-963. <http://dx.doi.org/10.1038/nclimate3056>
186. Raible, C.C., S. Brönnimann, R. Auchmann, P. Brohan, T.L. Frölicher, H.-F. Graf, P. Jones, J. Luterbacher, S. Muthers, R. Neukom, A. Robock, S. Self, A. Sudrajat, C. Timmreck, and M. Wegmann, 2016: Tambora 1815 as a test case for high impact volcanic eruptions: Earth system effects. *Wiley Interdisciplinary Reviews: Climate Change*, **7**, 569-589. <http://dx.doi.org/10.1002/wcc.407>
187. Twohy, C.H., M.D. Petters, J.R. Snider, B. Stevens, W. Tahnk, M. Wetzel, L. Russell, and F. Burnet, 2005: Evaluation of the aerosol indirect effect in marine stratocumulus clouds: Droplet number, size, liquid water path, and radiative impact. *Journal of Geophysical Research*, **110**, D08203. <http://dx.doi.org/10.1029/2004JD005116>
188. Lohmann, U. and J. Feichter, 2005: Global indirect aerosol effects: A review. *Atmospheric Chemistry and Physics*, **5**, 715-737. <http://dx.doi.org/10.5194/acp-5-715-2005>
189. Quaas, J., Y. Ming, S. Menon, T. Takemura, M. Wang, J.E. Penner, A. Gettelman, U. Lohmann, N. Bellouin, O. Boucher, A.M. Sayer, G.E. Thomas, A. McComiskey, G. Feingold, C. Hoose, J.E. Kristjánsson, X. Liu, Y. Balkanski, L.J. Donner, P.A. Ginoux, P. Stier, B. Grandey, J. Feichter, I. Sednev, S.E. Bauer, D. Koch, R.G. Grainger, Kirkev, aring, A. g. T. Iversen, Ø. Seland, R. Easter, S.J. Ghan, P.J. Rasch, H. Morrison, J.F. Lamarque, M.J. Iacono, S. Kinne, and M. Schulz, 2009: Aerosol indirect effects – general circulation model intercomparison and evaluation with satellite data. *Atmospheric Chemistry and Physics*, **9**, 8697-8717. <http://dx.doi.org/10.5194/acp-9-8697-2009>
190. Rosenfeld, D., M.O. Andreae, A. Asmi, M. Chin, G. de Leeuw, D.P. Donovan, R. Kahn, S. Kinne, N. Kivekäs, M. Kulmala, W. Lau, K.S. Schmidt, T. Suni, T. Wagner, M. Wild, and J. Quaas, 2014: Global observations of aerosol–cloud–precipitation–climate interactions. *Reviews of Geophysics*, **52**, 750-808. <http://dx.doi.org/10.1002/2013RG000441>
191. Wild, M., 2009: Global dimming and brightening: A review. *Journal of Geophysical Research*, **114**, D00D16. <http://dx.doi.org/10.1029/2008JD011470>
192. Szopa, S., Y. Balkanski, M. Schulz, S. Bekki, D. Cugnet, A. Fortems-Cheiney, S. Turquety, A. Cozic, C. Déandreis, D. Hauglustaine, A. Idelkadi, J. Lathière, F. Lefevre, M. Marchand, R. Vuolo, N. Yan, and J.-L. Dufresne, 2013: Aerosol and ozone changes as forcing for climate evolution between 1850 and 2100. *Climate Dynamics*, **40**, 2223-2250. <http://dx.doi.org/10.1007/s00382-012-1408-y>
193. Stjern, C.W. and J.E. Kristjánsson, 2015: Contrasting influences of recent aerosol changes on clouds and precipitation in Europe and East Asia. *Journal of Climate*, **28**, 8770-8790. <http://dx.doi.org/10.1175/jcli-d-14-00837.1>
194. Wang, Y., J.H. Jiang, and H. Su, 2015: Atmospheric responses to the redistribution of anthropogenic aerosols. *Journal of Geophysical Research Atmospheres*, **120**, 9625-9641. <http://dx.doi.org/10.1002/2015JD023665>



195. Myhre, G., W. Aas, R. Cherian, W. Collins, G. Faluvegi, M. Flanner, P. Forster, Ø. Hodnebrog, Z. Klimont, M.T. Lund, J. Mülmenstädt, C. Lund Myhre, D. Olivie, M. Prather, J. Quaas, B.H. Samset, J.L. Schnell, M. Schulz, D. Shindell, R.B. Skeie, T. Takemura, and S. Tsyro, 2017: Multi-model simulations of aerosol and ozone radiative forcing due to anthropogenic emission changes during the period 1990–2015. *Atmospheric Chemistry and Physics*, **17**, 2709–2720. <http://dx.doi.org/10.5194/acp-17-2709-2017>
196. Mao, K.B., Y. Ma, L. Xia, W.Y. Chen, X.Y. Shen, T.J. He, and T.R. Xu, 2014: Global aerosol change in the last decade: An analysis based on MODIS data. *Atmospheric Environment*, **94**, 680–686. <http://dx.doi.org/10.1016/j.atmosenv.2014.04.053>
197. Marmer, E., B. Langmann, H. Fagerli, and V. Vestreng, 2007: Direct shortwave radiative forcing of sulfate aerosol over Europe from 1900 to 2000. *Journal of Geophysical Research*, **112**, D23S17. <http://dx.doi.org/10.1029/2006JD008037>
198. Murphy, D.M., J.C. Chow, E.M. Leibensperger, W.C. Malm, M. Pitchford, B.A. Schichtel, J.G. Watson, and W.H. White, 2011: Decreases in elemental carbon and fine particle mass in the United States. *Atmospheric Chemistry and Physics*, **11**, 4679–4686. <http://dx.doi.org/10.5194/acp-11-4679-2011>
199. Kühn, T., A.I. Partanen, A. Laakso, Z. Lu, T. Bergman, S. Mikkonen, H. Kokkola, H. Korhonen, P. Räisänen, D.G. Streets, S. Romakkaniemi, and A. Laaksonen, 2014: Climate impacts of changing aerosol emissions since 1996. *Geophysical Research Letters*, **41**, 4711–4718. <http://dx.doi.org/10.1002/2014GL060349>
200. Turnock, S.T., D.V. Spracklen, K.S. Carslaw, G.W. Mann, M.T. Woodhouse, P.M. Forster, J. Haywood, C.E. Johnson, M. Dalvi, N. Bellouin, and A. Sanchez-Lorenzo, 2015: Modelled and observed changes in aerosols and surface solar radiation over Europe between 1960 and 2009. *Atmospheric Chemistry and Physics*, **15**, 9477–9500. <http://dx.doi.org/10.5194/acp-15-9477-2015>
201. Babu, S.S., M.R. Manoj, K.K. Moorthy, M.M. Gogoi, V.S. Nair, S.K. Kompalli, S.K. Satheesh, K. Niranjana, K. Ramagopal, P.K. Bhuyan, and D. Singh, 2013: Trends in aerosol optical depth over Indian region: Potential causes and impact indicators. *Journal of Geophysical Research Atmospheres*, **118**, 11,794–11,806. <http://dx.doi.org/10.1002/2013JD020507>
202. Krishna Moorthy, K., S. Suresh Babu, M.R. Manoj, and S.K. Satheesh, 2013: Buildup of aerosols over the Indian Region. *Geophysical Research Letters*, **40**, 1011–1014. <http://dx.doi.org/10.1002/grl.50165>
203. Pietikäinen, J.P., K. Kupiainen, Z. Klimont, R. Makkonen, H. Korhonen, R. Karinkanta, A.P. Hyvärinen, N. Karvosenoja, A. Laaksonen, H. Lihavainen, and V.M. Kerminen, 2015: Impacts of emission reductions on aerosol radiative effects. *Atmospheric Chemistry and Physics*, **15**, 5501–5519. <http://dx.doi.org/10.5194/acp-15-5501-2015>
204. Streets, D.G., C. Yu, Y. Wu, M. Chin, Z. Zhao, T. Hayasaka, and G. Shi, 2008: Aerosol trends over China, 1980–2000. *Atmospheric Research*, **88**, 174–182. <http://dx.doi.org/10.1016/j.atmosres.2007.10.016>
205. Li, J., Z. Han, and Z. Xie, 2013: Model analysis of long-term trends of aerosol concentrations and direct radiative forcings over East Asia. *Tellus B*, **65**, 20410. <http://dx.doi.org/10.3402/tellusb.v65i0.20410>
206. Wang, Y., Y. Yang, S. Han, Q. Wang, and J. Zhang, 2013: Sunshine dimming and brightening in Chinese cities (1955–2011) was driven by air pollution rather than clouds. *Climate Research*, **56**, 11–20. <http://dx.doi.org/10.3354/cr01139>
207. Forster, P., V. Ramaswamy, P. Artaxo, T. Berntsen, R. Betts, D.W. Fahey, J. Haywood, J. Lean, D.C. Lowe, G. Myhre, J. Nganga, R. Prinn, G. Raga, M. Schulz, and R. Van Dorland, 2007: Ch. 2: Changes in atmospheric constituents and in radiative forcing. *Climate Change 2007: The Physical Science Basis. Contribution of Working Group I to the Fourth Assessment Report (AR4) of the Intergovernmental Panel on Climate Change*. Solomon, S., D. Qin, M. Manning, Z. Chen, M. Marquis, K.B. Averyt, M. Tignor, and H.L. Miller, Eds. Cambridge University Press, Cambridge, UK. http://www.ipcc.ch/publications_and_data/ar4/wg1/en/ch2.html
208. Carslaw, K.S., L.A. Lee, C.L. Reddington, K.J. Pringle, A. Rap, P.M. Forster, G.W. Mann, D.V. Spracklen, M.T. Woodhouse, L.A. Regayre, and J.R. Pierce, 2013: Large contribution of natural aerosols to uncertainty in indirect forcing. *Nature*, **503**, 67–71. <http://dx.doi.org/10.1038/nature12674>
209. Stevens, B. and G. Feingold, 2009: Untangling aerosol effects on clouds and precipitation in a buffered system. *Nature*, **461**, 607–613. <http://dx.doi.org/10.1038/nature08281>
210. Randall, D.A., R.A. Wood, S. Bony, R. Colman, T. Fichefet, J. Fyfe, V. Kattsov, A. Pitman, J. Shukla, J. Srinivasan, R.J. Stouffer, A. Sumi, and K.E. Taylor, 2007: Ch. 8: Climate models and their evaluation. *Climate Change 2007: The Physical Science Basis. Contribution of Working Group I to the Fourth Assessment Report of the Intergovernmental Panel on Climate Change*. Solomon, S., D. Qin, M. Manning, Z. Chen, M. Marquis, K.B. Averyt, M. Tignor, and H.L. Miller, Eds. Cambridge University Press, Cambridge, United Kingdom and New York, NY, USA, 589–662. www.ipcc.ch/pdf/assessment-report/ar4/wg1/ar4-wg1-chapter8.pdf



211. Steinacher, M., F. Joos, T.L. Frölicher, L. Bopp, P. Cadule, V. Cocco, S.C. Doney, M. Gehlen, K. Lindsay, and J.K. Moore, 2010: Projected 21st century decrease in marine productivity: A multi-model analysis. *Biogeosciences*, **7**, 979-1005. <http://dx.doi.org/10.5194/bg-7-979-2010>
212. Hauglustaine, D.A., J. Lathière, S. Szopa, and G.A. Folberth, 2005: Future tropospheric ozone simulated with a climate-chemistry-biosphere model. *Geophysical Research Letters*, **32**, L24807. <http://dx.doi.org/10.1029/2005GL024031>
213. Jiang, X., S.J. Eichelberger, D.L. Hartmann, R. Shia, and Y.L. Yung, 2007: Influence of doubled CO₂ on ozone via changes in the Brewer-Dobson circulation. *Journal of the Atmospheric Sciences*, **64**, 2751-2755. <http://dx.doi.org/10.1175/jas3969.1>
214. Li, F., J. Austin, and J. Wilson, 2008: The strength of the Brewer-Dobson circulation in a changing climate: Coupled chemistry-climate model simulations. *Journal of Climate*, **21**, 40-57. <http://dx.doi.org/10.1175/2007jcli1663.1>
215. Shepherd, T.G. and C. McLandress, 2011: A robust mechanism for strengthening of the Brewer-Dobson circulation in response to climate change: Critical-layer control of subtropical wave breaking. *Journal of the Atmospheric Sciences*, **68**, 784-797. <http://dx.doi.org/10.1175/2010jas3608.1>
216. McLandress, C., T.G. Shepherd, M.C. Reader, D.A. Plummer, and K.P. Shine, 2014: The climate impact of past changes in halocarbons and CO₂ in the tropical UTLS region. *Journal of Climate*, **27**, 8646-8660. <http://dx.doi.org/10.1175/jcli-d-14-00232.1>
217. Barkstrom, B.R., 1984: The Earth Radiation Budget Experiment (ERBE). *Bulletin of the American Meteorological Society*, **65**, 1170-1185. [http://dx.doi.org/10.1175/1520-0477\(1984\)065<1170:terbe>2.0.co;2](http://dx.doi.org/10.1175/1520-0477(1984)065<1170:terbe>2.0.co;2)
218. Smith, G.L., B.R. Barkstrom, E.F. Harrison, R.B. Lee, and B.A. Wielicki, 1994: Radiation budget measurements for the eighties and nineties. *Advances in Space Research*, **14**, 81-84. [http://dx.doi.org/10.1016/0273-1177\(94\)90351-4](http://dx.doi.org/10.1016/0273-1177(94)90351-4)
219. Wielicki, B.A., E.F. Harrison, R.D. Cess, M.D. King, and D.A. Randall, 1995: Mission to planet Earth: Role of clouds and radiation in climate. *Bulletin of the American Meteorological Society*, **76**, 2125-2153. [http://dx.doi.org/10.1175/1520-0477\(1995\)076<2125:mtpero>2.0.co;2](http://dx.doi.org/10.1175/1520-0477(1995)076<2125:mtpero>2.0.co;2)
220. Wielicki, B.A., B.R. Barkstrom, E.F. Harrison, R.B. Lee, III, G.L. Smith, and J.E. Cooper, 1996: Clouds and the Earth's Radiant Energy System (CERES): An Earth observing system experiment. *Bulletin of the American Meteorological Society*, **77**, 853-868. [http://dx.doi.org/10.1175/1520-0477\(1996\)077<0853:ca-tere>2.0.co;2](http://dx.doi.org/10.1175/1520-0477(1996)077<0853:ca-tere>2.0.co;2)
221. Hartmann, D.L., A.M.G. Klein Tank, M. Rusticucci, L.V. Alexander, S. Brönnimann, Y. Charabi, F.J. Dentener, E.J. Dlugokencky, D.R. Easterling, A. Kaplan, B.J. Soden, P.W. Thorne, M. Wild, and P.M. Zhai, 2013: Observations: Atmosphere and surface. *Climate Change 2013: The Physical Science Basis. Contribution of Working Group I to the Fifth Assessment Report of the Intergovernmental Panel on Climate Change*. Stocker, T.F., D. Qin, G.-K. Plattner, M. Tignor, S.K. Allen, J. Boschung, A. Nauels, Y. Xia, V. Bex, and P.M. Midgley, Eds. Cambridge University Press, Cambridge, United Kingdom and New York, NY, USA, 159-254. <http://www.climatechange2013.org/report/full-report/>





3

Detection and Attribution of Climate Change

KEY FINDINGS

1. The *likely* range of the human contribution to the global mean temperature increase over the period 1951–2010 is 1.1° to 1.4°F (0.6° to 0.8°C), and the central estimate of the observed warming of 1.2°F (0.65°C) lies within this range (*high confidence*). This translates to a *likely* human contribution of 93%–123% of the observed 1951–2010 change. It is *extremely likely* that more than half of the global mean temperature increase since 1951 was caused by human influence on climate (*high confidence*). The *likely* contributions of natural forcing and internal variability to global temperature change over that period are minor (*high confidence*).
2. The science of event attribution is rapidly advancing through improved understanding of the mechanisms that produce extreme events and the marked progress in development of methods that are used for event attribution (*high confidence*).

Recommended Citation for Chapter

Knutson, T., J.P. Kossin, C. Mears, J. Perlwitz, and M.F. Wehner, 2017: Detection and attribution of climate change. In: *Climate Science Special Report: Fourth National Climate Assessment, Volume I* [Wuebbles, D.J., D.W. Fahey, K.A. Hibbard, D.J. Dokken, B.C. Stewart, and T.K. Maycock (eds.)]. U.S. Global Change Research Program, Washington, DC, USA, pp. 114-132, doi: 10.7930/J01834ND.

3.1 Introduction

Detection and attribution of climate change involves assessing the causes of observed changes in the climate system through systematic comparison of climate models and observations using various statistical methods. Detection and attribution studies are important for a number of reasons. For example, such studies can help determine whether a human influence on climate variables (for example, temperature) can be distinguished from natural variability. Detection and attribution studies can help evaluate whether model simulations are consistent with observed trends or other changes in the climate system. Results from detection and attribution studies

can inform decision making on climate policy and adaptation.

There are several general types of detection and attribution studies, including: attribution of trends or long-term changes in climate variables; attribution of changes in extremes; attribution of weather or climate events; attribution of climate-related impacts; and the estimation of climate sensitivity using observational constraints. Paleoclimate proxies can also be useful for detection and attribution studies, particularly to provide a longer-term perspective on climate variability as a baseline on which to compare recent climate changes of the past century or so (for example, see Figure

12.2 from Ch. 12: Sea Level Rise). Detection and attribution studies can be done at various scales, from global to regional.

Since the Intergovernmental Panel on Climate Change (IPCC) Fifth Assessment Report (AR5) chapter on detection and attribution¹ and the Third National Climate Assessment (NCA³²), the science of detection and attribution has advanced, with a major scientific question being the issue of attribution of extreme events.^{3, 4, 5, 6} Therefore, the methods used in this developing area of the science are briefly reviewed in Appendix C: Detection and Attribution Methods, along with a brief overview of the various general detection and attribution methodologies, including some recent developments in these areas. Detection and attribution of changes in extremes in general presents a number of challenges,⁷ including limitations of observations, models, statistical methods, process understanding for extremes, and uncertainties about the natural variability of extremes. Although the present report does not focus on climate impacts on ecosystems or human systems, a relatively new and developing area of detection and attribution science (reviewed in Stone et al. 2013⁸), concerns detecting and attributing the impacts of climate change on natural or human systems. Many new developments in detection and attribution science have been fostered by the International Detection and Attribution Group (IDAG; <http://www.image.ucar.edu/idag/> and <http://www.clivar.org/clivar-panels/etccdi/idag/international-detection-attribution-group-idag>) which is an international group of scientists who have collaborated since 1995 on “assessing and reducing uncertainties in the estimates of climate change.”

In the remainder of this chapter, we review highlights of detection and attribution science, particularly key attribution findings for the rise in global mean temperature. However, as

this is a U.S.-focused assessment, the report as a whole will focus more on the detection and attribution findings for particular regional phenomena (for example, regional temperature, precipitation) or at least global-scale phenomena that are directly affecting the United States (for example, sea level rise). Most of these findings are contained in the individual phenomena chapters, rather than in this general overview chapter on detection and attribution. We provide summary links to the chapters where particular detection and attribution findings are presented in more detail.

3.2 Detection and Attribution of Global Temperature Changes

The concept of detection and attribution is illustrated in Figure 3.1, which shows a very simple example of detection and attribution of global mean temperature. While more powerful pattern-based detection and attribution methods (discussed later), and even greater use of time averaging, can result in much stronger statements about detection and attribution, the example in Figure 3.1 serves to illustrate the general concept. In the figure, observed global mean temperature anomalies (relative to a 1901–1960 baseline) are compared with anomalies from historical simulations of CMIP5 models. The spread of different individual model simulations (the blue and orange shading) arises both from differences between the models in their responses to the different specified climate forcing agents (natural and anthropogenic) and from internal (unforced) climate variability. Observed annual temperatures after about 1980 are shown to be inconsistent with models that include only natural forcings (blue shading) and are consistent with the model simulations that include both anthropogenic and natural forcing (orange shading). This implies that the observed global warming is attributable in large part to anthropogenic forcing. A key aspect of a detection and attribution finding will be the



Global Mean Temperature Change

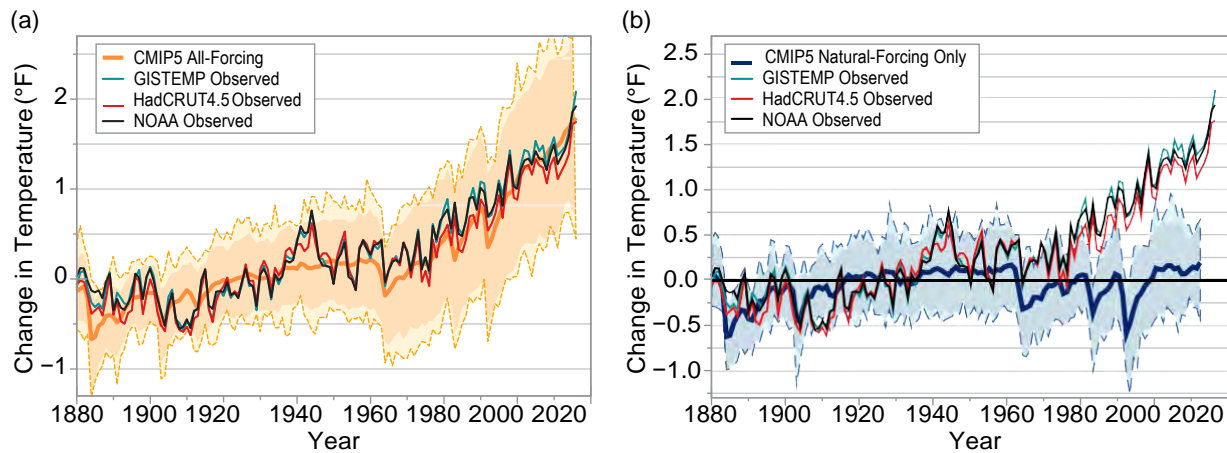


Figure 3.1: Comparison of observed global mean temperature anomalies from three observational datasets to CMIP5 climate model historical experiments using: (a) anthropogenic and natural forcings combined, or (b) natural forcings only. In (a) the thick orange curve is the CMIP5 grand ensemble mean across 36 models while the orange shading and outer dashed lines depict the ± 2 standard deviation and absolute ranges of annual anomalies across all individual simulations of the 36 models. Model data are a masked blend of surface air temperature over land regions and sea surface temperature over ice-free ocean regions to be more consistent with observations than using surface air temperature alone. All time series ($^{\circ}\text{F}$) are referenced to a 1901–1960 baseline value. The simulations in (a) have been extended from 2006 through 2016 using projections under the higher scenario (RCP8.5). (b) As in (a) but the blue curves and shading are based on 18 CMIP5 models using natural forcings only. See legends to identify observational datasets. Observations after about 1980 are shown to be inconsistent with the natural forcing-only models (indicating detectable warming) and also consistent with the models that include both anthropogenic and natural forcing, implying that the warming is attributable in part to anthropogenic forcing according to the models. (Figure source: adapted from Melillo et al.² and Knutson et al.¹⁹).

assessment of the adequacy of the models and observations used for these conclusions, as discussed and assessed in Flato et al.,⁹ Bindoff et al.,¹ and IPCC.¹⁰

The detection and attribution of global temperature change to human causes has been one of the most important and visible findings over the course of the past global climate change scientific assessments by the IPCC. The first IPCC report¹¹ concluded that a human influence on climate had not yet been detected, but judged that “the unequivocal detection of the enhanced greenhouse effect from observations is not likely for a decade or more.” The second IPCC report¹² concluded that “the balance of evidence suggests a discernible human influence on climate.” The third IPCC report¹³ strengthened this conclusion to: “most of the observed warming over the last 50 years is likely to have been due to the increase of greenhouse gas concentrations.” The fourth

IPCC report¹⁴ further strengthened the conclusion to: “Most of the observed increase in global average temperatures since the mid-20th century is very likely due to the observed increase in anthropogenic greenhouse gas concentrations.” The fifth IPCC report¹⁰ further strengthened this to: “It is extremely likely that more than half of the observed increase in global average surface temperature from 1951 to 2010 was caused by the anthropogenic increase in greenhouse gas concentrations and other anthropogenic forcings together.” These increasingly confident statements have resulted from scientific advances, including better observational datasets, improved models and detection/attribution methods, and improved estimates of climate forcings. Importantly, the continued long-term warming of the global climate system since the time of the first IPCC report and the broad-scale agreement of the spatial pattern of observed temperature changes with climate model projections of

greenhouse gas-induced changes as published in the late 1980s (e.g., Stouffer and Manabe 2017¹⁵) give more confidence in the attribution of observed warming since 1951 as being due primarily to human activity.

The IPCC AR5 presented an updated assessment of detection and attribution research at the global to regional scale¹ which is briefly summarized here. Key attribution assessment results from IPCC AR5 for global mean temperature are summarized in Figure 3.2, which shows assessed *likely* ranges and midpoint estimates for several factors contributing to increases in global mean temperature. According to Bindoff et al.,¹ the *likely* range of the anthropogenic contribution to global mean temperature increases over 1951–2010 was 0.6° to 0.8°C (1.1° to 1.4°F), compared with the

observed warming 5th to 95th percentile range of 0.59° to 0.71°C (1.1° to 1.3°F). The estimated *likely* contribution ranges for natural forcing and internal variability were both much smaller (–0.1° to 0.1°C, or –0.2° to 0.2°F) than the observed warming. The confidence intervals that encompass the *extremely likely* range for the anthropogenic contribution are wider than the *likely* range. Using these wider confidence limits, the lower limit of attributable warming contribution range still lies above 50% of the observed warming rate, and thus Bindoff et al.¹ concluded that it is *extremely likely* that more than half of the global mean temperature increase since 1951 was caused by human influence on climate. This assessment concurs with the Bindoff et al.¹ assessment of attributable warming and cooling influences.

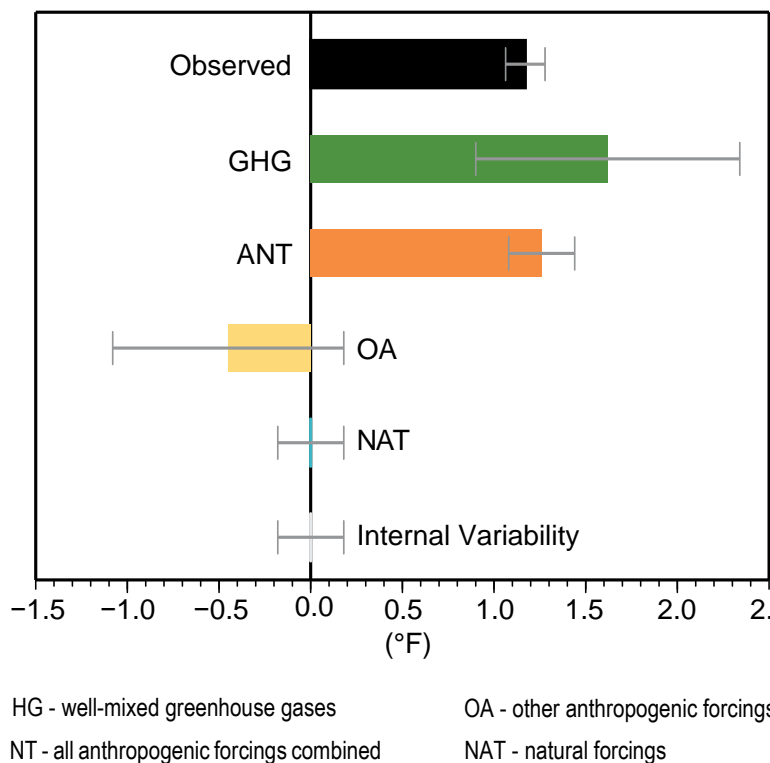


Figure 3.2: Observed global mean temperature trend (black bar) and attributable warming or cooling influences of anthropogenic and natural forcings over 1951–2010. Observations are from HadCRUT4, along with observational uncertainty (5% to 95%) error bars.⁶² Likely ranges (bar-whisker plots) and midpoint values (colored bars) for attributable forcings are from IPCC AR5.¹ GHG refers to well-mixed greenhouse gases, OA to other anthropogenic forcings, NAT to natural forcings, and ANT to all anthropogenic forcings combined. Likely ranges are broader for contributions from well-mixed greenhouse gases and for other anthropogenic forcings, assessed separately, than for the contributions from all anthropogenic forcings combined, as it is more difficult to quantitatively constrain the separate contributions of the various anthropogenic forcing agents. (Figure source: redrawn from Bindoff et al.,¹ © IPCC. Used with permission.)

Apart from formal detection attribution studies such as those underlying the results above, which use global climate model output and pattern-based regression methods, anthropogenic influences on global mean temperature can also be estimated using simpler empirical models, such as multiple linear regression/energy balance models (e.g., Canty et al. 2013¹⁶; Zhou and Tung 2013¹⁷). For example, Figure 3.3 illustrates how the global mean surface temperature changes since the late 1800s can be decomposed into components linearly related to several forcing variables (anthropogenic forcing, solar variability, volcanic forcing, plus an internal variability component, here related to El Niño–Southern Oscillation). Using this approach, Canty et al.¹⁶ also infer a substantial contribution of anthropogenic forcing to the rise in global mean temperature since the late 1800s. Stern and Kaufmann¹⁸ use another method—Granger causality tests—and again infer that “human activity is partially responsible for the observed rise in global temperature and that this rise in temperature also has an effect on the global carbon cycle.” They also conclude that anthropogenic sulfate aerosol effects may only be about half as large as inferred in a number of previous studies.

Multi-century to multi-millennial-scale climate model integrations with unchanging external forcing provide a means of estimating potential contributions of internal climate variability to observed trends. Bindoff et al.¹ conclude, based on multimodel assessments, that the likely range contribution of internal variability to observed trends over 1951–2010 is about $\pm 0.2^\circ\text{F}$, compared to the observed warming of about 1.2°F over that period. A recent 5,200-year integration of the CMIP5 model having apparently the largest global mean temperature variability among CMIP5 models shows rare instances of multidecadal global warming approaching the observed 1951–2010 warming trend.¹⁹ However, even that most

extreme model cannot simulate century-scale warming trends from internal variability that approach the observed global mean warming over the past century. According to a multimodel analysis of observed versus CMIP5 modeled global temperature trends (Knutson et al. 2013²⁰, Fig. 7a), the modeled natural fluctuations (forced plus internal) would need to be larger by about a factor of three for even an unusual natural variability episode (95th percentile) to approach the observed trend since 1900. Thus, using present models there is no known source of internal climate variability that can reproduce the observed warming over the past century without including strong positive forcing from anthropogenic greenhouse gas emissions (Figure 3.1). The modeled century-scale trend due to natural forcings (solar and volcanic) is also minor (Figure 3.1), so that, using present models, there is no known source of natural variability that can reproduce the observed global warming over the past century. One study²¹ comparing paleoclimate data with models concluded that current climate models may substantially underestimate regional sea surface temperature variability on multidecadal to multi-centennial timescales, especially at low latitudes. The causes of this apparent discrepancy—whether due to data issues, external forcings/response, or simulated internal variability issues—and its implications for simulations of global temperature variability in climate models remain unresolved. Since Laepple and Huybers²¹ is a single paleoclimate-based study and focuses on regional, not global mean, temperature variability, we have consequently not modified our conclusions regarding global temperature attribution from those contained in Bindoff et al.,¹ although further research on this issue is warranted. In summary, we are not aware of any convincing evidence that natural variability alone could have accounted for the amount and timing of global warming that was observed over the industrial era.



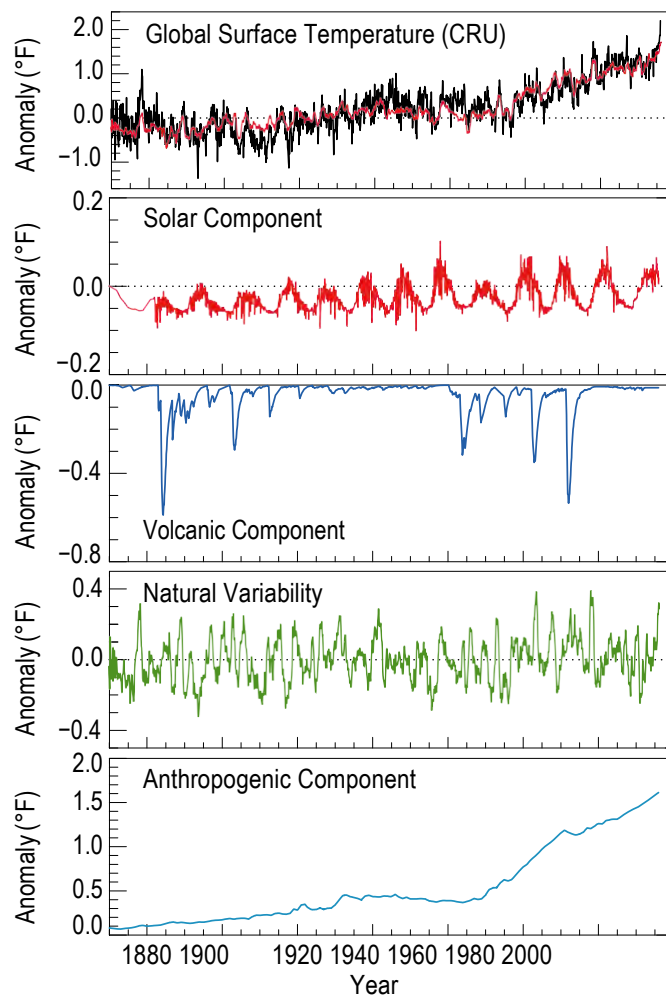


Figure 3.3: Estimates of the contributions of several forcing factors and internal variability to global mean temperature change since 1870, based on an empirical approach using multiple linear regression and energy balance models. The top panel shows global temperature anomalies ($^{\circ}\text{F}$) from the observations⁶² in black with the multiple linear regression result in red (1901–1960 base period). The lower four panels show the estimated contribution to global mean temperature anomalies from four factors: solar variability; volcanic eruptions; internal variability related to El Niño/Southern Oscillation; and anthropogenic forcing. The anthropogenic contribution includes a warming component from greenhouse gases concentrations and a cooling component from anthropogenic aerosols. (Figure source: adapted from Canty et al.¹⁶).

While most detection and attribution studies focus on changes in temperature and other variables in the historical record since about 1860 or later, some studies relevant to detection and attribution focus on changes over much longer periods. For example, geological and tide-based reconstructions of global mean sea level (Ch. 12: Sea Level Rise, Figure 12.2b) suggest that the rate of sea level rise in the last century was faster than during any century over the past ~2,800 years. As an example, for Northern Hemisphere annual mean temperatures, Schurer et al.²² use detection and attribution fingerprinting methods along with

paleoclimate reconstructions and millennial-scale climate model simulations from eight models to explore causes for temperature variations from 850 AD to the present, including the Medieval Climate Anomaly (MCA, around 900 to 1200 AD) and the Little Ice Age (LIA, around 1450 to 1800 AD). They conclude that solar variability and volcanic eruptions were the main causal factors for changes in Northern Hemisphere temperatures from 1400 to 1900, but that greenhouse gas changes of uncertain origin apparently contributed to the cool conditions during 1600–1800. Their study provides further support for previous IPCC

report conclusions (e.g., IPCC 2007¹⁴) that internal variability alone was extremely unlikely to have been the cause of the recent observed 50- and 100-year warming trends. Andres and Peltier²³ also inferred from millennial-scale climate model simulations that volcanoes, solar variability, greenhouse gases, and orbital variations all contributed significantly to the transition from the MCA to the LIA.

An active and important area of climate research that involves detection and attribution science is the estimation of global climate sensitivity, based on past observational constraints. An important measure of climate sensitivity, with particular relevance for climate projections over the coming decades, is the transient climate response (TCR), defined as the rise in global mean surface temperature at the time of CO₂ doubling for a 1% per year transient increase of atmospheric CO₂. (Equilibrium climate sensitivity is discussed in Ch. 2: Physical Drivers of Climate Change). The TCR of the climate system has an estimated range of 0.9° to 2.0°C (1.6° to 3.6°F) and 0.9° to 2.5°C (1.6° to 4.5°F), according to two recent assessments (Otto et al.²⁴ and Lewis and Curry²⁵, respectively). Marvel et al.²⁶ suggest, based on experiments with a single climate model, that after accounting for the different efficacies of various historical climate forcing agents, the TCR could be adjusted upward from the Otto et al.²⁴ and Lewis and Curry²⁵ estimates. Richardson et al.²⁷ report a best estimate for TCR of 1.66°C (2.99 °F), with a 5% to 95% confidence range of 1.0° to 3.3°C (1.8° to 5.9°F). Furthermore, Richardson et al. conclude that the earlier studies noted above may underestimate TCR because the surface temperature dataset they used undersamples rapidly warming regions due to limited coverage and because surface water warms less than surface air. Gregory et al.²⁸ note, within CMIP5 models, that the TCR to the second doubling of CO₂ (that is, from doubling to quadrupling)

is 40% higher than that for the first doubling. They explore the various physical reasons for this finding and conclude this may also lead to an underestimate of TCR in the empirical observation-based studies. In summary, estimation of TCR from observations continues to be an active area of research with considerable remaining uncertainties, as discussed above. Even the low-end estimates for TCR cited above from some recent studies (about 0.9°C or 1.6°F) imply that the climate will continue to warm substantially if atmospheric CO₂ concentrations continue to increase over the coming century as projected under a number of future scenarios.

3.3 Detection and Attribution with a United States Regional Focus

Detection and attribution at regional scales is generally more challenging than at the global scale for a number of reasons. At the regional scale, the magnitude of natural variability swings are typically larger than for global means. If the climate change signal is similar in magnitude at the regional and global scales, this makes it more difficult to detect anthropogenic climate changes at the regional scale. Furthermore, there is less spatial pattern information at the regional scale that can be used to distinguish contributions from various forcings. Other forcings that have typically received less attention than greenhouse gases, such as land-use change, could be more important at regional scales than globally.²⁹ Also, simulated internal variability at regional scales may be less reliable than at global scales (Bindoff et al.¹). While detection and attribution of changes in extremes (including at the regional scale) presents a number of key challenges,⁷ previous studies (e.g., Zwiers et al. 2011³⁰) have demonstrated how detection and attribution methods, combined with generalized extreme value distributions, can be used to detect a human influence on extreme temperatures at the regional scale, including over North America.



In IPCC AR5,¹ which had a broader global focus than this report, attributable human contributions were reported for warming over all continents except Antarctica. Changes in daily temperature extremes throughout the world; ocean surface and subsurface temperature and salinity sea level pressure patterns; arctic sea ice loss; northern hemispheric snow cover decrease; global mean sea level rise; and ocean acidification were all associated with human activity in AR5.¹ IPCC AR5 also reported medium confidence in anthropogenic contributions to increased atmospheric specific humidity, zonal mean precipitation over Northern Hemisphere mid to high latitudes, and intensification of heavy precipitation over land regions. IPCC AR5 had weaker attribution conclusions than IPCC AR4 on some phenomena, including tropical cyclone and drought changes.

Although the present assessment follows most of the IPCC AR5 conclusions on detection and attribution of relevance to the United States, we make some additional attribution assessment statements in the relevant chapters of this report. Among the notable detection and attribution-relevant findings in this report are the following (refer to the listed chapters for further details):

- Ch. 5: Circulation and Variability: The tropics have expanded poleward by about 70 to 200 miles in each hemisphere over the period 1979–2009, with an accompanying shift of the subtropical dry zones, midlatitude jets, and storm tracks (*medium to high confidence*). Human activities have played a role in this change (*medium confidence*), although confidence is presently *low* regarding the magnitude of the human contribution relative to natural variability.
- Ch. 6: Temperature Change: Detectable anthropogenic warming since 1901 has

occurred over the western and northern regions of the contiguous United States according to observations and CMIP5 models (*medium confidence*), although over the southeastern United States there has been no detectable warming trend since 1901. The combined influence of natural and anthropogenic forcings on temperature *extremes* have been detected over large subregions of North America (*medium confidence*).

- Ch. 7: Precipitation Change: For the continental United States, there is *high confidence* in the detection of extreme precipitation increases, while there is *low confidence* in attributing the extreme precipitation changes purely to anthropogenic forcing. There is stronger evidence for a human contribution (*medium confidence*) when taking into account process-based understanding (for example, increased water vapor in a warmer atmosphere).
- Ch. 8: Drought, Floods, and Wildfire: While by some measures drought has decreased over much of the continental United States in association with long-term increases in precipitation, neither the precipitation increases nor inferred drought decreases have been confidently attributed to anthropogenic forcing. Detectable changes—a mix of increases and decreases—in some classes of flood frequency have occurred in parts of the United States, although attribution studies have not established a robust connection between increased riverine flooding and human-induced climate change. There is *medium confidence* for a human-caused climate change contribution to increased forest fire activity in Alaska in recent decades and *low to medium confidence* for a detectable human climate change contribution in the western United States.



- Ch. 9: Extreme Storms: There is broad agreement in the literature that human factors (greenhouse gases and aerosols) have had a measurable impact on the observed oceanic and atmospheric variability in the North Atlantic, and there is *medium confidence* that this has contributed to the observed increase in Atlantic hurricane activity since the 1970s. There is no consensus on the relative magnitude of human and natural influences on past changes in hurricane activity.
- Ch. 10: Land Cover: Modifications to land use and land cover due to human activities produce changes in surface albedo, latent and sensible heat, and atmospheric aerosol and greenhouse gas concentrations, accounting for an estimated $40\% \pm 16\%$ of the human-caused global radiative forcing from 1850 to 2010 (*high confidence*).
- Ch. 11: Arctic Changes: It is *very likely* that human activities have contributed to observed arctic surface temperature warming, sea ice loss, glacier mass loss, and Northern Hemisphere snow extent decline (*high confidence*).
- Ch. 12: Sea Level Rise: Human-caused climate change has made a substantial contribution to global mean sea level rise since 1900 (*high confidence*), contributing to a rate of rise that is greater than during any preceding century in at least 2,800 years (*medium confidence*).
- Ch. 13: Ocean Changes: The world's oceans have absorbed about 93% of the excess heat caused by greenhouse warming since the mid-20th Century. The world's oceans are currently absorbing more than a quarter of the carbon dioxide emitted to the atmosphere annually from human activities, making them more acidic (*very high confidence*).

3.4 Extreme Event Attribution

Since the IPCC AR5 and NCA3,² the attribution of extreme weather and climate events has been an emerging area in the science of detection and attribution. Attribution of extreme weather events under a changing climate is now an important and highly visible aspect of climate science. As discussed in the recent National Academy of Sciences report,⁵ the science of event attribution is rapidly advancing, including the understanding of the mechanisms that produce extreme events and the rapid progress in development of methods used for event attribution.

When an extreme weather event occurs, the question is often asked: was this event caused by climate change? A generally more appropriate framing for the question is whether climate change has altered the odds of occurrence of an extreme event like the one just experienced. Extreme event attribution studies to date have generally been concerned with answering the latter question. In recent developments, Hannart et al.³¹ discuss the application of causal theory to event attribution, including discussion of conditions under which stronger causal statements can be made, in principle, based on theory of causality and distinctions between necessary and sufficient causality.

Several recent studies, including NAS,⁵ have reviewed aspects of extreme event attribution.^{3,4,6} Hulme⁴ and NAS⁵ discuss the motivations for scientists to be pursuing extreme event attribution, including the need to inform risk management and adaptation planning. Hulme⁴ categorizes event attribution studies/statements into general types, including those based on: physical reasoning, statistical analysis of time series, fraction of attributable risk (FAR) estimation (discussed in the Appendix), or those that rely on the philosophical argument that there are no longer any purely



natural weather events. The NAS⁵ report outlines two general approaches to event attribution: 1) using observations to estimate a change in probability of magnitude of events, or 2) using model simulations to compare an event in the current climate versus that in a hypothetical “counterfactual” climate not influenced by human activities. As discussed by Trenberth et al.,³² Shepherd,³³ and Horton et al.,³⁴ an ingredients-based or conditional attribution approach can also be used, when one examines the impact of certain environmental changes (for example, greater atmospheric moisture) on the character of an extreme event using model experiments, all else being equal. Further discussion of methodologies is given in Appendix C.

Examples of extreme event attribution studies are numerous. Many are cited by Hulme,⁴ NAS,⁵ Easterling et al.,³ and there are many further examples in an annual collection of studies of extreme events of the previous year, published in the *Bulletin of the American Meteorological Society*.^{35, 36, 37, 38, 39}

While an extensive review of extreme event attribution is beyond the scope of this report, particularly given the recent publication of several assessments or review papers on the topic, some general findings from the more comprehensive NAS⁵ report are summarized here:

- Confidence in attribution findings of anthropogenic influence is greatest for extreme events that are related to an aspect of temperature, followed by hydrological drought and heavy precipitation, with little or no confidence for severe convective storms or extratropical storms.
- Event attribution is more reliable when based on sound physical principles, consistent evidence from observations, and

numerical models that can replicate the event.

- Statements about attribution are sensitive to the way the questions are posed (that is, framing).
- Assumptions used in studies must be clearly stated and uncertainties estimated in order for a clear, unambiguous interpretation of an event attribution to be possible.

The NAS report noted that uncertainties about the roles of low-frequency natural variability and confounding factors (for example, the effects of dams on flooding) could be sources of difficulties in event attribution studies. In addition, the report noted that attribution conclusions would be more robust in cases where observed changes in the event being examined are consistent with expectations from model-based attribution studies. The report endorsed the need for more research to improve understanding of a number of important aspects of event attribution studies, including physical processes, models and their capabilities, natural variability, reliable long-term observational records, statistical methods, confounding factors, and future projections of the phenomena of interest.

As discussed in Appendix C: Detection and Attribution Methodologies, confidence is typically lower for an attribution-without-detection statement than for an attribution statement accompanied by an established, detectable anthropogenic influence (for example, a detectable and attributable long-term trend or increase in variability) for the phenomenon itself. An example of the former would be stating that a change in the probability or magnitude of a heat wave in the southeastern United States was attributable to rising greenhouse gases, because there has not been a detectable



century-scale trend in either temperature or temperature variability in this region (e.g., Ch. 6: Temperature Change; Knutson et al. 2013²⁰).

To our knowledge, no extreme weather event observed to date has been found to have zero probability of occurrence in a preindustrial climate, according to climate model simulations. Therefore, the causes of attributed extreme events are a combination of natural variations in the climate system compounded (or alleviated) by the anthropogenic change to the climate system. Event attribution statements quantify the relative contribution of these human and natural causal factors. In the future, as the climate change signal gets stronger compared to natural variability, humans may experience weather events which are essentially impossible to simulate in a preindustrial climate. This is already becoming the case at large time and spatial scales, where for example the record global mean surface temperature anomaly observed in 2016 (relative to a 1901–1960 baseline) is essentially impossible for global climate models to reproduce under preindustrial climate forcing conditions (for example, see Figure 3.1).

The European heat wave of 2003⁴⁰ and Australia’s extreme temperatures and heat indices of 2013 (e.g., Arblaster et al. 2014⁴¹; King et al. 2014⁴²; Knutson et al. 2014⁴³; Lewis and Karoly 2014⁴⁴; Perkins et al. 2014⁴⁵) are examples of extreme weather or climate events where relatively strong evidence for a human contribution to the event has been found. Similarly, in the United States, the science of event attribution for weather and climate extreme events has been actively pursued since the NCA3. For example, for the case of the recent California drought, investigators have attempted to determine, using various methods discussed in this chapter, whether human-caused climate change contributed to the event (see discussion in Ch. 8: Droughts, Floods, and Wildfires).

As an example, illustrating different methods of attribution for an event in the United States, Hoerling et al.⁴⁶ concluded that the 2011 Texas heat wave/meteorological drought was primarily caused by antecedent and concurrent negative rainfall anomalies due mainly to natural variability and the La Niña conditions at the time of the event, but with a relatively small (not detected) warming contribution from anthropogenic forcing. The anthropogenic contribution nonetheless doubled the chances of reaching a new temperature record in 2011 compared to the 1981–2010 reference period, according to their study. Rupp et al.,⁴⁷ meanwhile, concluded that extreme heat events in Texas were about 20 times more likely for 2008 La Niña conditions than similar conditions during the 1960s. This pair of studies illustrates how the framing of the attribution question can matter. For example, the studies used different baseline reference periods to determine the magnitude of anomalies, which can also affect quantitative conclusions, since using an earlier baseline period typically results in larger magnitude anomalies (in a generally warming climate). The Hoerling et al. analysis focused on both what caused most of the magnitude of the anomalies as well as changes in probability of the event, whereas Rupp et al. focused on the changes in the probability of the event. Otto et al.⁴⁸ showed for the case of the Russian heat wave of 2010 how a different focus of attribution (fraction of anomaly explained vs. change in probability of occurrence over a threshold) can give seemingly conflicting results, yet have no real fundamental contradiction. In the illustrative case for the 2011 Texas heat/drought, we conclude that there is *medium* confidence that anthropogenic forcing contributed to the heat wave, both in terms of a small contribution to the anomaly magnitude and a significant increase in the probability of occurrence of the event.



In this report, we do not assess or compile all individual weather or climate extreme events for which an attributable anthropogenic climate change has been claimed in a published study, as there are now many such studies that provide this information. Some event attribution-related studies that focus on the United States are discussed in more detail in Chapters 6–9, which primarily examine phenomena such as precipitation extremes, droughts, floods, severe storms, and temperature extremes. For example, as discussed in Chapter 6: Temperature Change (Table 6.3), a number of extreme temperature events (warm anomalies) in the United States have been partly attributed to anthropogenic influence on climate.



Traceable Accounts

Key Finding 1

The *likely* range of the human contribution to the global mean temperature increase over the period 1951–2010 is 1.1° to 1.4°F (0.6° to 0.8°C), and the central estimate of the observed warming of 1.2°F (0.65°C) lies within this range (*high confidence*). This translates to a *likely* human contribution of 93%–123% of the observed 1951–2010 change. It is *extremely likely* that more than half of the global mean temperature increase since 1951 was caused by human influence on climate (*high confidence*). The *likely* contributions of natural forcing and internal variability to global temperature change over that period are minor (*high confidence*).

Description of evidence base

This Key Finding summarizes key detection and attribution evidence documented in the climate science literature and in the IPCC AR5,¹ and references therein. The Key Finding is essentially the same as the summary assessment of IPCC AR5.

According to Bindoff et al.,¹ the *likely* range of the anthropogenic contribution to global mean temperature increases over 1951–2010 was 1.1° to 1.4°F (0.6° to 0.8°C), compared with the observed warming 5th to 95th percentile range of 1.1° to 1.3°F (0.59° to 0.71°C). The estimated likely contribution ranges for natural forcing and internal variability were both much smaller (–0.2° to 0.2°F, or –0.1° to 0.1°C) than the observed warming. The confidence intervals that encompass the *extremely likely* range for the anthropogenic contribution are wider than the *likely* range, but nonetheless allow for the conclusion that it is *extremely likely* that more than half of the global mean temperature increase since 1951 was caused by human influence on climate (*high confidence*).

The attribution of temperature increases since 1951 is based largely on the detection and attribution analyses of Gillett et al.,⁴⁹ Jones et al.,⁵⁰ and consideration of Ribes and Terray,⁵¹ Huber and Knutti,⁵² Wigley and Santer,⁵³ and IPCC AR4.⁵⁴ The IPCC finding receives further support from alternative approaches, such as multiple linear regression/energy balance modeling¹⁶ and

a new methodological approach to detection and attribution that uses additive decomposition and hypothesis testing,⁵⁵ which infer similar attributable warming results. Individual study results used to derive the IPCC finding are summarized in Figure 10.4 of Bindoff et al.,¹ which also assesses model dependence by comparing results obtained from several individual CMIP5 models. The estimated potential influence of internal variability is based on Knutson et al.²⁰ and Huber and Knutti,⁵² with consideration of the above references. Moreover, simulated global temperature multidecadal variability is assessed to be adequate,¹ with *high confidence* that models reproduce global and Northern Hemisphere temperature variability across a range of timescales.⁹ Further support for these assessments comes from assessments of paleoclimate data⁵⁶ and increased confidence in physical understanding and models of the climate system.^{10,15} A more detailed traceable account is contained in Bindoff et al.¹ Post-IPCC AR5 supporting evidence includes additional analyses showing the unusual nature of observed global warming since the late 1800s compared to simulated internal climate variability,¹⁹ and the recent occurrence of new record high global mean temperatures are consistent with model projections of continued warming on multidecadal scales (for example, Figure 3.1).

Major uncertainties

As discussed in the main text, estimation of the transient climate response (TCR), defined as the global mean surface temperature change at the time of CO₂ doubling in a 1% per year CO₂ transient increase experiment, continues to be an active area of research with considerable remaining uncertainties. Some detection attribution methods use model-based methods together with observations to attempt to infer scaling magnitudes of the forced responses based on regression methods (that is, they do not use the models' climate sensitivities directly). However, if climate models are significantly more sensitive to CO₂ increases than the real world, as suggested by the studies of Otto et al.²⁴ and Lewis and Curry²⁵ (though see differing conclusions from other studies in the main text), this could lead to an overestimate of attributable warming esti-



mates, at least as obtained using some detection and attribution methods. In any case, it is important to better constrain the TCR to have higher confidence in general in attributable warming estimates obtained using various methods.

The global temperature change since 1951 attributable to anthropogenic forcings other than greenhouse gases has a wide estimated *likely* range (-1.1° to $+0.2^{\circ}\text{F}$ in Fig. 3.1). This wide range is largely due to the considerable uncertainty of estimated total radiative forcing due to aerosols (i.e., the direct effect combined with the effects of aerosols on clouds⁵⁷). Although more of the relevant physical processes are being included in models, confidence in these model representations remains low.⁵⁸ In detection/attribution studies there are substantial technical challenges in quantifying the separate attributable contributions to temperature change from greenhouse gases and aerosols.¹ Finally, there is a range of estimates of the potential contributions of internal climate variability, and some sources of uncertainty around modeled estimates (e.g., Laepple and Huybers 2014²¹). However, current CMIP5 multimodel estimates (*likely* range of $\pm 0.2^{\circ}\text{F}$, or 0.1°C , over 60 years) would have to increase by a factor of about three for even half of the observed 60-year trend to lie within a revised *likely* range of potential internal variability (e.g., Knutson et al. 2013;²⁰ Huber and Knutti 2012⁵²). Recently, Knutson et al.¹⁹ examined a 5,000-year integration of the CMIP5 model having the strongest internal multidecadal variability among 25 CMIP5 models they examined. While the internal variability within this strongly varying model can on rare occasions produce 60-year warmings approaching that observed from 1951–2010, even this most extreme model did not produce any examples of centennial-scale internal variability warming that could match the observed global warming since the late 1800s, even in a 5,000-year integration.

Assessment of confidence based on evidence and agreement, including short description of nature of evidence and level of agreement

There is *very high confidence* that global temperature has been increasing and that anthropogenic forcings have played a major role in the increase observed over

the past 60 years, with strong evidence from several studies using well-established detection and attribution techniques. There is *high confidence* that the role of internal variability is minor, as the CMIP5 climate models as a group simulate only a minor role for internal variability over the past 60 years, and the models have been assessed by IPCC AR5 as adequate for the purpose of estimating the potential role of internal variability.

If appropriate, estimate likelihood of impact or consequence, including short description of basis of estimate

The amount of historical warming attributable to anthropogenic forcing has a very high likelihood of consequence, as it is related to the amount of future warming to be expected under various emission scenarios, and the impacts of global warming are generally larger for higher warming rates and higher warming amounts.

Summary sentence or paragraph that integrates the above information

Detection and attribution studies, climate models, observations, paleoclimate data, and physical understanding lead to *high confidence (extremely likely)* that more than half of the observed global mean warming since 1951 was caused by humans, and *high confidence* that internal climate variability played only a minor role (and possibly even a negative contribution) in the observed warming since 1951. The key message and supporting text summarizes extensive evidence documented in the peer-reviewed detection and attribution literature, including in the IPCC AR5.

Key Finding 2

The science of event attribution is rapidly advancing through improved understanding of the mechanisms that produce extreme events and the marked progress in development of methods that are used for event attribution (*high confidence*).

Description of evidence base

This Key Finding paraphrases a conclusion of the National Academy of Sciences report⁵ on attribution of extreme weather events in the context of climate change. That report discusses advancements in event attribu-



tion in more detail than possible here due to space limitations. Weather and climate science in general continue to seek improved physical understanding of extreme weather events. One aspect of improved understanding is the ability to more realistically simulate extreme weather events in models, as the models embody current physical understanding in a simulation framework that can be tested on sample cases. NAS⁵ provides references to studies that evaluate weather and climate models used to simulated extreme events in a climate context. Such models can include coupled climate models (e.g., Taylor et al. 2012;⁵⁹ Flato et al. 2013⁹), atmospheric models with specified sea surface temperatures, regional models for dynamical downscaling, weather forecasting models, or statistical downscaling models. Appendix C includes a brief description of the evolving set of methods used for event attribution, discussed in more detail in references such as NAS,⁵ Hulme,⁴ Trenberth et al.,³² Shepherd,³³ Horton et al.,³⁴ Hannart,⁶⁰ and Hannart et al.^{31, 61} Most of this methodology as applied to extreme weather and climate event attribution, has evolved since the European heat wave study of Stott et al.⁴⁰

Major uncertainties

While the science of event attribution is rapidly advancing, studies of individual events will typically contain caveats. In some cases, attribution statements are made without a clear detection of an anthropogenic influence on observed occurrences of events similar to the one in question, so that there is reliance on models to assess probabilities of occurrence. In such cases there will typically be uncertainties in the model-based estimations of the anthropogenic influence, in the estimation of the influence of natural variability on the event's occurrence, and even in the observational records related to the event (e.g., long-term records of hurricane occurrence). Despite these uncertainties in individual attribution studies, the science of event attribution is advancing through increased physical understanding and development of new methods of attribution and evaluation of models.

Assessment of confidence based on evidence and agreement, including short description of nature of evidence and level of agreement

There is *very high confidence* that weather and climate science are advancing in their understanding of the physical mechanisms that produce extreme events. For example, hurricane track forecasts have improved in part due to improved models. There is *high confidence* that new methods being developed will help lead to further advances in the science of event attribution.

If appropriate, estimate likelihood of impact or consequence, including short description of basis of estimate

Improving science of event attribution has a high likelihood of impact, as it is one means by which scientists can better understand the relationship between occurrence of extreme events and long-term climate change. A further impact will be the improved ability to communicate this information to the public and to policymakers for various uses, including improved adaptation planning.^{4,5}

Summary sentence or paragraph that integrates the above information

Owing to the improved physical understanding of extreme weather and climate events as the science in these fields progress, and owing to the high promise of newly developed methods for exploring the roles of different influences on occurrence of extreme events, there is *high confidence* that the science of event attribution is rapidly advancing.



References

1. Bindoff, N.L., P.A. Stott, K.M. AchutaRao, M.R. Allen, N. Gillett, D. Gutzler, K. Hansingo, G. Hegerl, Y. Hu, S. Jain, I.I. Mokhov, J. Overland, J. Perlwitz, R. Sebbari, and X. Zhang, 2013: Detection and attribution of climate change: From global to regional. *Climate Change 2013: The Physical Science Basis. Contribution of Working Group I to the Fifth Assessment Report of the Intergovernmental Panel on Climate Change*. Stocker, T.F., D. Qin, G.-K. Plattner, M. Tignor, S.K. Allen, J. Boschung, A. Nauels, Y. Xia, V. Bex, and P.M. Midgley, Eds. Cambridge University Press, Cambridge, United Kingdom and New York, NY, USA, 867-952. <http://www.climatechange2013.org/report/full-report/>
2. Melillo, J.M., T.C. Richmond, and G.W. Yohe, eds., 2014: *Climate Change Impacts in the United States: The Third National Climate Assessment*. U.S. Global Change Research Program: Washington, D.C., 841 pp. <http://dx.doi.org/10.7930/J0Z31WJ2>
3. Easterling, D.R., K.E. Kunkel, M.F. Wehner, and L. Sun, 2016: Detection and attribution of climate extremes in the observed record. *Weather and Climate Extremes*, **11**, 17-27. <http://dx.doi.org/10.1016/j.wace.2016.01.001>
4. Hulme, M., 2014: Attributing weather extremes to 'climate change'. *Progress in Physical Geography*, **38**, 499-511. <http://dx.doi.org/10.1177/0309133314538644>
5. NAS, 2016: *Attribution of Extreme Weather Events in the Context of Climate Change*. The National Academies Press, Washington, DC, 186 pp. <http://dx.doi.org/10.17226/21852>
6. Stott, P., 2016: How climate change affects extreme weather events. *Science*, **352**, 1517-1518. <http://dx.doi.org/10.1126/science.aaf7271>
7. Zwiers, F.W., L.V. Alexander, G.C. Hegerl, T.R. Knutson, J.P. Kossin, P. Naveau, N. Nicholls, C. Schär, S.I. Seneviratne, and X. Zhang, 2013: Climate extremes: Challenges in estimating and understanding recent changes in the frequency and intensity of extreme climate and weather events. *Climate Science for Serving Society: Research, Modeling and Prediction Priorities*. Asrar, G.R. and J.W. Hurrell, Eds. Springer Netherlands, Dordrecht, 339-389. http://dx.doi.org/10.1007/978-94-007-6692-1_13
8. Stone, D., M. Auffhammer, M. Carey, G. Hansen, C. Huggel, W. Cramer, D. Lobell, U. Molau, A. Solow, L. Tibig, and G. Yohe, 2013: The challenge to detect and attribute effects of climate change on human and natural systems. *Climatic Change*, **121**, 381-395. <http://dx.doi.org/10.1007/s10584-013-0873-6>
9. Flato, G., J. Marotzke, B. Abiodun, P. Braconnot, S.C. Chou, W. Collins, P. Cox, F. Driouech, S. Emori, V. Eyring, C. Forest, P. Gleckler, E. Guilyardi, C. Jakob, V. Kattsov, C. Reason, and M. Rummukainen, 2013: Evaluation of climate models. *Climate Change 2013: The Physical Science Basis. Contribution of Working Group I to the Fifth Assessment Report of the Intergovernmental Panel on Climate Change*. Stocker, T.F., D. Qin, G.-K. Plattner, M. Tignor, S.K. Allen, J. Boschung, A. Nauels, Y. Xia, V. Bex, and P.M. Midgley, Eds. Cambridge University Press, Cambridge, United Kingdom and New York, NY, USA, 741-866. <http://www.climatechange2013.org/report/full-report/>
10. IPCC, 2013: *Climate Change 2013: The Physical Science Basis. Contribution of Working Group I to the Fifth Assessment Report of the Intergovernmental Panel on Climate Change*. Cambridge University Press, Cambridge, UK and New York, NY, 1535 pp. <http://www.climatechange2013.org/report/>
11. IPCC, 1990: *Climate Change: The IPCC Scientific Assessment*. Houghton, J.T., G.J. Jenkins, and J.J. Ephraums, Eds. Cambridge University Press, Cambridge, United Kingdom and New York, NY, USA, 212 pp.
12. IPCC, 1996: *Climate Change 1995: The Science of Climate Change. Contribution of Working Group I to the Second Assessment Report of the Intergovernmental Panel on Climate Change*. Houghton, J.T., L.G. Meira Filho, B.A. Callander, N. Harris, A. Kattenberg, and K. Maskell, Eds. Cambridge University Press, Cambridge, United Kingdom and New York, NY, USA, 584 pp.
13. IPCC, 2001: *Climate Change 2001: The Scientific Basis. Contribution of Working Group I to the Third Assessment Report of the Intergovernmental Panel on Climate Change*. Houghton, J.T., Y. Ding, D.J. Griggs, M. Noquer, P.J. van der Linden, X. Dai, K. Maskell, and C.A. Johnson, Eds. Cambridge University Press, Cambridge, United Kingdom and New York, NY, USA, 881 pp.
14. IPCC, 2007: *Climate Change 2007: The Physical Science Basis. Contribution of Working Group I to the Fourth Assessment Report of the Intergovernmental Panel on Climate Change*. Solomon, S., D. Qin, M. Manning, Z. Chen, M. Marquis, K.B. Averyt, M. Tignor, and H.L. Miller, Eds. Cambridge University Press, Cambridge, U.K, New York, NY, USA, 996 pp. http://www.ipcc.ch/publications_and_data/publications_ipcc_fourth_assessment_report_wg1_report_the_physical_science_basis.htm
15. Stouffer, R.J. and S. Manabe, 2017: Assessing temperature pattern projections made in 1989. *Nature Climate Change*, **7**, 163-165. <http://dx.doi.org/10.1038/nclimate3224>
16. Canty, T., N.R. Mascioli, M.D. Smarte, and R.J. Salawitch, 2013: An empirical model of global climate - Part 1: A critical evaluation of volcanic cooling. *Atmospheric Chemistry and Physics*, **13**, 3997-4031. <http://dx.doi.org/10.5194/acp-13-3997-2013>

17. Zhou, J. and K.-K. Tung, 2013: Deducing multidecadal anthropogenic global warming trends using multiple regression analysis. *Journal of the Atmospheric Sciences*, **70**, 3-8. <http://dx.doi.org/10.1175/jas-d-12-0208.1>
18. Stern, D.I. and R.K. Kaufmann, 2014: Anthropogenic and natural causes of climate change. *Climatic Change*, **122**, 257-269. <http://dx.doi.org/10.1007/s10584-013-1007-x>
19. Knutson, T.R., R. Zhang, and L.W. Horowitz, 2016: Prospects for a prolonged slowdown in global warming in the early 21st century. *Nature Communications*, **7**, 13676. <http://dx.doi.org/10.1038/ncomms13676>
20. Knutson, T.R., F. Zeng, and A.T. Wittenberg, 2013: Multimodel assessment of regional surface temperature trends: CMIP3 and CMIP5 twentieth-century simulations. *Journal of Climate*, **26**, 8709-8743. <http://dx.doi.org/10.1175/JCLI-D-12-00567.1>
21. Laepple, T. and P. Huybers, 2014: Ocean surface temperature variability: Large model–data differences at decadal and longer periods. *Proceedings of the National Academy of Sciences*, **111**, 16682-16687. <http://dx.doi.org/10.1073/pnas.1412077111>
22. Schurer, A.P., G.C. Hegerl, M.E. Mann, S.F.B. Tett, and S.J. Phipps, 2013: Separating forced from chaotic climate variability over the past millennium. *Journal of Climate*, **26**, 6954-6973. <http://dx.doi.org/10.1175/jcli-d-12-00826.1>
23. Andres, H.J. and W.R. Peltier, 2016: Regional influences of natural external forcings on the transition from the Medieval Climate Anomaly to the Little Ice Age. *Journal of Climate*, **29**, 5779-5800. <http://dx.doi.org/10.1175/jcli-d-15-0599.1>
24. Otto, A., F.E.L. Otto, O. Boucher, J. Church, G. Hegerl, P.M. Forster, N.P. Gillett, J. Gregory, G.C. Johnson, R. Knutti, N. Lewis, U. Lohmann, J. Marotzke, G. Myhre, D. Shindell, B. Stevens, and M.R. Allen, 2013: Energy budget constraints on climate response. *Nature Geoscience*, **6**, 415-416. <http://dx.doi.org/10.1038/ngeo1836>
25. Lewis, N. and J.A. Curry, 2015: The implications for climate sensitivity of AR5 forcing and heat uptake estimates. *Climate Dynamics*, **45**, 1009-1023. <http://dx.doi.org/10.1007/s00382-014-2342-y>
26. Marvel, K., G.A. Schmidt, R.L. Miller, and L.S. Nazarenko, 2016: Implications for climate sensitivity from the response to individual forcings. *Nature Climate Change*, **6**, 386-389. <http://dx.doi.org/10.1038/nclimate2888>
27. Richardson, M., K. Cowtan, E. Hawkins, and M.B. Stolpe, 2016: Reconciled climate response estimates from climate models and the energy budget of Earth. *Nature Climate Change*, **6**, 931-935. <http://dx.doi.org/10.1038/nclimate3066>
28. Gregory, J.M., T. Andrews, and P. Good, 2015: The inconstancy of the transient climate response parameter under increasing CO₂. *Philosophical Transactions of the Royal Society A: Mathematical, Physical and Engineering Sciences*, **373**, 20140417. <http://dx.doi.org/10.1098/rsta.2014.0417>
29. Pielke Sr., R.A., R. Mahmood, and C. McAlpine, 2016: Land's complex role in climate change. *Physics Today*, **69**, 40-46. <http://dx.doi.org/10.1063/PT.3.3364>
30. Zwiers, F.W., X.B. Zhang, and Y. Feng, 2011: Anthropogenic influence on long return period daily temperature extremes at regional scales. *Journal of Climate*, **24**, 881-892. <http://dx.doi.org/10.1175/2010jcli3908.1>
31. Hannart, A., J. Pearl, F.E.L. Otto, P. Naveau, and M. Ghil, 2016: Causal counterfactual theory for the attribution of weather and climate-related events. *Bulletin of the American Meteorological Society*, **97**, 99-110. <http://dx.doi.org/10.1175/bams-d-14-00034.1>
32. Trenberth, K.E., J.T. Fasullo, and T.G. Shepherd, 2015: Attribution of climate extreme events. *Nature Climate Change*, **5**, 725-730. <http://dx.doi.org/10.1038/nclimate2657>
33. Shepherd, T.G., 2016: A common framework for approaches to extreme event attribution. *Current Climate Change Reports*, **2**, 28-38. <http://dx.doi.org/10.1007/s40641-016-0033-y>
34. Horton, R.M., J.S. Mankin, C. Lesk, E. Coffel, and C. Raymond, 2016: A review of recent advances in research on extreme heat events. *Current Climate Change Reports*, **2**, 242-259. <http://dx.doi.org/10.1007/s40641-016-0042-x>
35. Herring, S.C., A. Hoell, M.P. Hoerling, J.P. Kossin, C.J. Schreck III, and P.A. Stott, 2016: Explaining Extreme Events of 2015 from a Climate Perspective. *Bulletin of the American Meteorological Society*, **97**, S1-S145. <http://dx.doi.org/10.1175/BAMS-ExplainingExtremeEvents2015.1>
36. Herring, S.C., M.P. Hoerling, J.P. Kossin, T.C. Peterson, and P.A. Stott, 2015: Explaining Extreme Events of 2014 from a Climate Perspective. *Bulletin of the American Meteorological Society*, **96**, S1-S172. <http://dx.doi.org/10.1175/BAMS-ExplainingExtremeEvents2014.1>
37. Herring, S.C., M.P. Hoerling, T.C. Peterson, and P.A. Stott, 2014: Explaining Extreme Events of 2013 from a Climate Perspective. *Bulletin of the American Meteorological Society*, **95**, S1-S104. <http://dx.doi.org/10.1175/1520-0477-95.9.s1.1>
38. Peterson, T.C., M.P. Hoerling, P.A. Stott, and S.C. Herring, 2013: Explaining Extreme Events of 2012 from a Climate Perspective. *Bulletin of the American Meteorological Society*, **94**, S1-S74. <http://dx.doi.org/10.1175/bams-d-13-00085.1>



39. Peterson, T.C., P.A. Stott, and S. Herring, 2012: Explaining extreme events of 2011 from a climate perspective. *Bulletin of the American Meteorological Society*, **93**, 1041-1067. <http://dx.doi.org/10.1175/BAMS-D-12-00021.1>
40. Stott, P.A., D.A. Stone, and M.R. Allen, 2004: Human contribution to the European heatwave of 2003. *Nature*, **432**, 610-614. <http://dx.doi.org/10.1038/nature03089>
41. Arblaster, J.M., E.-P. Lim, H.H. Hendon, B.C. Trewin, M.C. Wheeler, G. Liu, and K. Braganza, 2014: Understanding Australia's hottest September on record [in "Explaining Extreme Events of 2013 from a Climate Perspective"]. *Bulletin of the American Meteorological Society*, **95** (9), S37-S41. <http://dx.doi.org/10.1175/1520-0477-95.9.S1.1>
42. King, A.D., D.J. Karoly, M.G. Donat, and L.V. Alexander, 2014: Climate change turns Australia's 2013 Big Dry into a year of record-breaking heat [in "Explaining Extreme Events of 2013 from a Climate Perspective"]. *Bulletin of the American Meteorological Society*, **95** (9), S41-S45. <http://dx.doi.org/10.1175/1520-0477-95.9.S1.1>
43. Knutson, T.R., F. Zeng, and A.T. Wittenberg, 2014: Multimodel assessment of extreme annual-mean warm anomalies during 2013 over regions of Australia and the western tropical Pacific [in "Explaining Extreme Events of 2013 from a Climate Perspective"]. *Bulletin of the American Meteorological Society*, **95** (9), S26-S30. <http://dx.doi.org/10.1175/1520-0477-95.9.S1.1>
44. Lewis, S. and D.J. Karoly, 2014: The role of anthropogenic forcing in the record 2013 Australia-wide annual and spring temperatures [in "Explaining Extreme Events of 2013 from a Climate Perspective"]. *Bulletin of the American Meteorological Society*, **95** (9), S31-S33. <http://dx.doi.org/10.1175/1520-0477-95.9.S1.1>
45. Perkins, S.E., S.C. Lewis, A.D. King, and L.V. Alexander, 2014: Increased simulated risk of the hot Australian summer of 2012/13 due to anthropogenic activity as measured by heat wave frequency and intensity [in "Explaining Extreme Events of 2013 from a Climate Perspective"]. *Bulletin of the American Meteorological Society*, **95** (9), S34-S37. <http://dx.doi.org/10.1175/1520-0477-95.9.S1.1>
46. Hoerling, M., M. Chen, R. Dole, J. Eischeid, A. Kumar, J.W. Nielsen-Gammon, P. Pegion, J. Perlwitz, X.-W. Quan, and T. Zhang, 2013: Anatomy of an extreme event. *Journal of Climate*, **26**, 2811-2832. <http://dx.doi.org/10.1175/JCLI-D-12-00270.1>
47. Rupp, D.E., P.W. Mote, N. Massey, C.J. Rye, R. Jones, and M.R. Allen, 2012: Did human influence on climate make the 2011 Texas drought more probable? [in "Explaining Extreme Events of 2011 from a Climate Perspective"]. *Bulletin of the American Meteorological Society*, **93**, 1052-1054. <http://dx.doi.org/10.1175/BAMS-D-12-00021.1>
48. Otto, F.E.L., N. Massey, G.J. van Oldenborgh, R.G. Jones, and M.R. Allen, 2012: Reconciling two approaches to attribution of the 2010 Russian heat wave. *Geophysical Research Letters*, **39**, L04702. <http://dx.doi.org/10.1029/2011GL050422>
49. Gillett, N.P., J.C. Fyfe, and D.E. Parker, 2013: Attribution of observed sea level pressure trends to greenhouse gas, aerosol, and ozone changes. *Geophysical Research Letters*, **40**, 2302-2306. <http://dx.doi.org/10.1002/grl.50500>
50. Jones, G.S., P.A. Stott, and N. Christidis, 2013: Attribution of observed historical near surface temperature variations to anthropogenic and natural causes using CMIP5 simulations. *Journal of Geophysical Research*, **118**, 4001-4024. <http://dx.doi.org/10.1002/jgrd.50239>
51. Ribes, A. and L. Terray, 2013: Application of regularised optimal fingerprinting to attribution. Part II: Application to global near-surface temperature. *Climate Dynamics*, **41**, 2837-2853. <http://dx.doi.org/10.1007/s00382-013-1736-6>
52. Huber, M. and R. Knutti, 2012: Anthropogenic and natural warming inferred from changes in Earth's energy balance. *Nature Geoscience*, **5**, 31-36. <http://dx.doi.org/10.1038/ngeo1327>
53. Wigley, T.M.L. and B.D. Santer, 2013: A probabilistic quantification of the anthropogenic component of twentieth century global warming. *Climate Dynamics*, **40**, 1087-1102. <http://dx.doi.org/10.1007/s00382-012-1585-8>
54. Hegerl, G.C., F.W. Zwiers, P. Braconnot, N.P. Gillett, Y. Luo, J.A.M. Orsini, N. Nicholls, J.E. Penner, and P.A. Stott, 2007: Understanding and attributing climate change. *Climate Change 2007: The Physical Science Basis. Contribution of Working Group I to the Fourth Assessment Report of the Intergovernmental Panel on Climate Change*. Solomon, S., D. Qin, M. Manning, Z. Chen, M. Marquis, K.B. Averyt, M. Tignor, and H.L. Miller, Eds. Cambridge University Press, Cambridge, United Kingdom and New York, NY, USA, 663-745. http://www.ipcc.ch/publications_and_data/ar4/wg1/en/ch9.html
55. Ribes, A., F.W. Zwiers, J.-M. Azaïs, and P. Naveau, 2017: A new statistical approach to climate change detection and attribution. *Climate Dynamics*, **48**, 367-386. <http://dx.doi.org/10.1007/s00382-016-3079-6>



56. Masson-Delmotte, V., M. Schulz, A. Abe-Ouchi, J. Beer, A. Ganopolski, J.F. González Rouco, E. Jansen, K. Lambeck, J. Luterbacher, T. Naish, T. Osborn, B. Otto-Bliesner, T. Quinn, R. Ramesh, M. Rojas, X. Shao, and A. Timmermann, 2013: Information from paleoclimate archives. *Climate Change 2013: The Physical Science Basis. Contribution of Working Group I to the Fifth Assessment Report of the Intergovernmental Panel on Climate Change*. Stocker, T.F., D. Qin, G.-K. Plattner, M. Tignor, S.K. Allen, J. Boschung, A. Nauels, Y. Xia, V. Bex, and P.M. Midgley, Eds. Cambridge University Press, Cambridge, United Kingdom and New York, NY, USA, 383–464. <http://www.climatechange2013.org/report/full-report/>
57. Myhre, G., D. Shindell, F.-M. Bréon, W. Collins, J. Fuglestvedt, J. Huang, D. Koch, J.-F. Lamarque, D. Lee, B. Mendoza, T. Nakajima, A. Robock, G. Stephens, T. Takemura, and H. Zhang, 2013: Anthropogenic and natural radiative forcing. *Climate Change 2013: The Physical Science Basis. Contribution of Working Group I to the Fifth Assessment Report of the Intergovernmental Panel on Climate Change*. Stocker, T.F., D. Qin, G.-K. Plattner, M. Tignor, S.K. Allen, J. Boschung, A. Nauels, Y. Xia, V. Bex, and P.M. Midgley, Eds. Cambridge University Press, Cambridge, United Kingdom and New York, NY, USA, 659–740. <http://www.climatechange2013.org/report/full-report/>
58. Boucher, O., D. Randall, P. Artaxo, C. Bretherton, G. Feingold, P. Forster, V.-M. Kerminen, Y. Kondo, H. Liao, U. Lohmann, P. Rasch, S.K. Satheesh, S. Sherwood, B. Stevens, and X.Y. Zhang, 2013: Clouds and aerosols. *Climate Change 2013: The Physical Science Basis. Contribution of Working Group I to the Fifth Assessment Report of the Intergovernmental Panel on Climate Change*. Stocker, T.F., D. Qin, G.-K. Plattner, M. Tignor, S.K. Allen, J. Boschung, A. Nauels, Y. Xia, V. Bex, and P.M. Midgley, Eds. Cambridge University Press, Cambridge, United Kingdom and New York, NY, USA, 571–658. <http://www.climatechange2013.org/report/full-report/>
59. Taylor, K.E., R.J. Stouffer, and G.A. Meehl, 2012: An overview of CMIP5 and the experiment design. *Bulletin of the American Meteorological Society*, **93**, 485–498. <http://dx.doi.org/10.1175/BAMS-D-11-00094.1>
60. Hannart, A., 2016: Integrated optimal fingerprinting: Method description and illustration. *Journal of Climate*, **29**, 1977–1998. <http://dx.doi.org/10.1175/jcli-d-14-00124.1>
61. Hannart, A., A. Carrasi, M. Bocquet, M. Ghil, P. Naveau, M. Pulido, J. Ruiz, and P. Tandeo, 2016: DADA: Data assimilation for the detection and attribution of weather and climate-related events. *Climate Change*, **136**, 155–174. <http://dx.doi.org/10.1007/s10584-016-1595-3>
62. Morice, C.P., J.J. Kennedy, N.A. Rayner, and P.D. Jones, 2012: Quantifying uncertainties in global and regional temperature change using an ensemble of observational estimates: The HadCRUT4 dataset. *Journal of Geophysical Research*, **117**, D08101. <http://dx.doi.org/10.1029/2011JD017187>





4

Climate Models, Scenarios, and Projections

KEY FINDINGS

1. If greenhouse gas concentrations were stabilized at their current level, existing concentrations would commit the world to at least an additional 1.1°F (0.6°C) of warming over this century relative to the last few decades (*high confidence* in continued warming, *medium confidence* in amount of warming).
2. Over the next two decades, global temperature increase is projected to be between 0.5°F and 1.3°F (0.3°–0.7°C) (*medium confidence*). This range is primarily due to uncertainties in natural sources of variability that affect short-term trends. In some regions, this means that the trend may not be distinguishable from natural variability (*high confidence*).
3. Beyond the next few decades, the magnitude of climate change depends primarily on cumulative emissions of greenhouse gases and aerosols and the sensitivity of the climate system to those emissions (*high confidence*). Projected changes range from 4.7°–8.6°F (2.6°–4.8°C) under the higher scenario (RCP8.5) to 0.5°–1.3°F (0.3°–1.7°C) under the much lower scenario (RCP2.6), for 2081–2100 relative to 1986–2005 (*medium confidence*).
4. Global mean atmospheric carbon dioxide (CO₂) concentration has now passed 400 ppm, a level that last occurred about 3 million years ago, when global average temperature and sea level were significantly higher than today (*high confidence*). Continued growth in CO₂ emissions over this century and beyond would lead to an atmospheric concentration not experienced in tens of millions of years (*medium confidence*). The present-day emissions rate of nearly 10 GtC per year suggests that there is no climate analog for this century any time in at least the last 50 million years (*medium confidence*).
5. The observed increase in global carbon emissions over the past 15–20 years has been consistent with higher scenarios (*very high confidence*). In 2014 and 2015, emission growth rates slowed as economic growth has become less carbon-intensive (*medium confidence*). Even if this trend continues, however, it is not yet at a rate that would limit the increase in the global average temperature to well below 3.6°F (2°C) above preindustrial levels (*high confidence*).
6. Combining output from global climate models and dynamical and statistical downscaling models using advanced averaging, weighting, and pattern scaling approaches can result in more relevant and robust future projections. For some regions, sectors, and impacts, these techniques are increasing the ability of the scientific community to provide guidance on the use of climate projections for quantifying regional-scale changes and impacts (*medium to high confidence*).

Recommended Citation for Chapter

Hayhoe, K., J. Edmonds, R.E. Kopp, A.N. LeGrande, B.M. Sanderson, M.F. Wehner, and D.J. Wuebbles, 2017: Climate models, scenarios, and projections. In: *Climate Science Special Report: Fourth National Climate Assessment, Volume I* [Wuebbles, D.J., D.W. Fahey, K.A. Hibbard, D.J. Dokken, B.C. Stewart, and T.K. Maycock (eds.)]. U.S. Global Change Research Program, Washington, DC, USA, pp. 133-160, doi: 10.7930/J0WH2N54.

4.1 The Human Role in Future Climate

The Earth's climate, past and future, is not static; it changes in response to both natural and anthropogenic drivers (see Ch. 2: Physical Drivers of Climate Change). Human emissions of carbon dioxide (CO₂), methane (CH₄), and other greenhouse gases now overwhelm the influence of natural drivers on the external forcing of Earth's climate (see Ch. 3: Detection and Attribution). Climate change (see Ch. 1: Our Globally Changing Climate) and ocean acidification (see Ch. 13: Ocean Changes) are already occurring due to the buildup of atmospheric CO₂ from human emissions in the industrial era.^{1,2}

Even if existing concentrations could be immediately stabilized, temperature would continue to increase by an estimated 1.1°F (0.6°C) over this century, relative to 1980–1999.³ This is because of the long timescale over which some climate feedbacks act (Ch. 2: Physical Drivers of Climate Change). Over the next few decades, concentrations are projected to increase and the resulting global temperature increase is projected to range from 0.5°F to 1.3°F (0.3°C to 0.7°C). This range depends on natural variability, on emissions of short-lived species such as CH₄ and black carbon that contribute to warming, and on emissions of sulfur dioxide (SO₂) and other aerosols that have a net cooling effect (Ch. 2: Physical Drivers of Climate Change). The role of emission reductions of non-CO₂ gases and aerosols in achieving various global temperature targets is discussed in Chapter 14: Mitigation.

Over the past 15–20 years, the growth rate in atmospheric carbon emissions from human activities has increased from 1.5 to 2 parts per million (ppm) per year due to increasing carbon emissions from human activities that track the rate projected under higher scenarios, in large part due to growing contributions from developing economies.^{4,5,6} One possible

analog for the rapid pace of change occurring today is the relatively abrupt warming of 9°–14°F (5°–8°C) that occurred during the Paleocene-Eocene Thermal Maximum (PETM), approximately 55–56 million years ago.^{7,8,9,10} However, emissions today are nearly 10 GtC per year. During the PETM, the rate of maximum sustained carbon release was less than 1.1 GtC per year, with significant differences in both background conditions and forcing relative to today. This suggests that there is no precise past analog any time in the last 66 million years for the conditions occurring today.^{10,11}

Since 2014, growth rates of global carbon emissions have declined, a trend cautiously attributed to declining coal use in China, despite large uncertainties in emissions reporting.^{12,13} Economic growth is becoming less carbon-intensive, as both developed and emerging economies begin to phase out coal and transition to natural gas and renewable, non-carbon energy.^{14,15}

Beyond the next few decades, the magnitude of future climate change will be primarily a function of future carbon emissions and the response of the climate system to those emissions. This chapter describes the scenarios that provide the basis for the range of future projections presented in this report: from those consistent with continued increases in greenhouse gas emissions, to others that can only be achieved by various levels of emission reductions (see Ch. 14: Mitigation). This chapter also describes the models used to quantify projected changes at the global to regional scale and how it is possible to estimate the range in potential climate change—as determined by climate sensitivity, which is the response of global temperature to a natural or anthropogenic forcing (see Ch. 2: Physical Drivers of Climate Change)—that would result from a given scenario.³



4.2 Future Scenarios

Climate projections are typically presented for a range of plausible pathways, scenarios, or targets that capture the relationships between human choices, emissions, concentrations, and temperature change. Some scenarios are consistent with continued dependence on fossil fuels, while others can only be achieved by deliberate actions to reduce emissions. The resulting range reflects the uncertainty inherent in quantifying human activities (including technological change) and their influence on climate.

The first Intergovernmental Panel on Climate Change Assessment Report (IPCC FAR) in 1990 discussed three types of scenarios: equilibrium scenarios, in which CO₂ concentration was fixed; transient scenarios, in which CO₂ concentration increased by a fixed percentage each year over the duration of the scenario; and four brand-new Scientific Assessment (SA90) emission scenarios based on World Bank population projections.¹⁶ Today, that original portfolio has expanded to encompass a wide variety of time-dependent or transient scenarios that project how population, energy sources, technology, emissions, atmospheric concentrations, radiative forcing, and/or global temperature change over time.

Other scenarios are simply expressed in terms of an end-goal or target, such as capping cumulative carbon emissions at a specific level or stabilizing global temperature at or below a certain threshold such as 3.6°F (2°C), a goal that is often cited in a variety of scientific and policy discussions, most recently the Paris Agreement.¹⁷ To stabilize climate at any particular temperature level, however, it is not enough to halt the growth in annual carbon emissions. Global net carbon emissions will eventually need to reach zero³ and negative emissions may be needed for a greater-than-50% chance of limiting warming

below 3.6°F (2°C) (see also Ch. 14: Mitigation for a discussion of negative emissions).¹⁸

Finally, some scenarios, like the “commitment” scenario in Key Finding 1 and the fixed-CO₂ equilibrium scenarios described above, continue to explore hypothetical questions such as, “what would the world look like, long-term, if humans were able to stabilize atmospheric CO₂ concentration at a given level?” This section describes the different types of scenarios used today and their relevance to assessing impacts and informing policy targets.

4.2.1 Emissions Scenarios, Representative Concentration Pathways, and Shared Socioeconomic Pathways

The standard sets of time-dependent scenarios used by the climate modeling community as input to global climate model simulations provide the basis for the majority of the future projections presented in IPCC assessment reports and U.S. National Climate Assessments (NCAs). Developed by the integrated assessment modeling community, these sets of standard scenarios have become more comprehensive with each new generation, as the original SA90 scenarios¹⁹ were replaced by the IS92 emission scenarios of the 1990s,²⁰ which were in turn succeeded by the Special Report on Emissions Scenarios in 2000 (SRES)²¹ and by the Representative Concentration Pathways in 2010 (RCPs).²²

SA90, IS92, and SRES are all emission-based scenarios. They begin with a set of storylines that were based on population projections initially. By SRES, they had become much more complex, laying out a consistent picture of demographics, international trade, flow of information and technology, and other social, technological, and economic characteristics of future worlds. These assumptions were then fed through socioeconomic and Integrated As-



assessment Models (IAMs) to derive emissions. For SRES, the use of various IAMs resulted in multiple emissions scenarios corresponding to each storyline; however, one scenario for each storyline was selected as the representative “marker” scenario to be used as input to global models to calculate the resulting atmospheric concentrations, radiative forcing, and climate change for the higher A1fi (fossil-intensive), mid-high A2, mid-low B2, and lower B1 storylines. IS92-based projections were used in the IPCC Second and Third Assessment Reports (SAR and TAR)^{23, 24} and the first NCA.²⁵ Projections based on SRES scenarios were used in the second and third NCAs^{26, 27} as well as the IPCC TAR and Fourth Assessment Reports (AR4).^{24, 28}

The most recent set of time-dependent scenarios, RCPs, builds on these two decades of scenario development. However, RCPs differ from previous sets of standard scenarios in at least four important ways. First, RCPs are not emissions scenarios; they are radiative forcing scenarios. Each scenario is tied to one value: the change in radiative forcing at the tropopause by 2100 relative to preindustrial levels. The four RCPs are numbered according to the change in radiative forcing by 2100: +2.6, +4.5, +6.0 and +8.5 watts per square meter (W/m²).^{29, 30, 31, 32}

The second difference is that, starting from these radiative forcing values, IAMs are used to work backwards to derive a range of emissions trajectories and corresponding policies and technological strategies for each RCP that would achieve the same ultimate impact on radiative forcing. From the multiple emissions pathways that could lead to the same 2100 radiative forcing value, an associated pathway of annual carbon dioxide and other anthropogenic emissions of greenhouse gases, aerosols, air pollutants, and other short-lived species has been selected for each RCP to use as input to future climate model simulations

(e.g., Meinshausen et al. 2011;³³ Cubasch et al. 2013³⁴). In addition, RCPs provide climate modelers with gridded trajectories of land use and land cover.

A third difference between the RCPs and previous scenarios is that while none of the SRES scenarios included a scenario with explicit policies and measures to limit climate forcing, all of the three lower RCP scenarios (2.6, 4.5, and 6.0) are climate-policy scenarios. At the higher end of the range, the RCP8.5 scenario corresponds to a future where carbon dioxide and methane emissions continue to rise as a result of fossil fuel use, albeit with significant declines in emission growth rates over the second half of the century (Figure 4.1), significant reduction in aerosols, and modest improvements in energy intensity and technology.³² Atmospheric carbon dioxide levels for RCP8.5 are similar to those of the SRES A1FI scenario: they rise from current-day levels of 400 up to 936 ppm by the end of this century. CO₂-equivalent levels (including emissions of other non-CO₂ greenhouse gases, aerosols, and other substances that affect climate) reach more than 1200 ppm by 2100, and global temperature is projected to increase by 5.4°–9.9°F (3°–5.5°C) by 2100 relative to the 1986–2005 average. RCP8.5 reflects the upper range of the open literature on emissions, but is not intended to serve as an upper limit on possible emissions nor as a business-as-usual or reference scenario for the other three scenarios.

Under the lower scenarios (RCP4.5 and RCP2.6),^{29, 30} atmospheric CO₂ levels remain below 550 and 450 ppm by 2100, respectively. Emissions of other substances are also lower; by 2100, CO₂-equivalent concentrations that include all emissions from human activities reach 580 ppm under RCP4.5 and 425 ppm under RCP2.6. RCP4.5 is similar to SRES B1, but the RCP2.6 scenario is much lower than any SRES scenario because it includes the option of using policies to achieve net negative carbon dioxide



emissions before the end of the century, while SRES scenarios do not. RCP-based projections were used in the most recent IPCC Fifth Assessment Report (AR5)³ and the third NCA²⁷ and are used in this fourth NCA as well.

Within the RCP family, individual scenarios have not been assigned a formal likelihood. Higher-numbered scenarios correspond to higher emissions and a larger and more rapid global temperature change (Figure 4.1); the range of values covered by the scenarios was chosen to reflect the then-current range in the open literature. Since the choice of scenario constrains the magnitudes of future changes, most assessments (including this one; see Ch. 6: Temperature Change) quantify future change and corresponding impacts under a range of future scenarios that reflect the uncertainty in the consequences of human choices over the coming century.

Fourth, a broad range of socioeconomic scenarios were developed independently from the RCPs and a subset of these were constrained, using emissions limitations policies consistent with their underlying storylines, to create five Shared Socioeconomic Pathways (SSPs) with climate forcing that matches the RCP values. This pairing of SSPs and RCPs is designed to

meet the needs of the impacts, adaptation, and vulnerability (IAV) communities, enabling them to couple alternative socioeconomic scenarios with the climate scenarios developed using RCPs to explore the socioeconomic challenges to climate mitigation and adaptation.³⁵ The five SSPs consist of SSP1 (“Sustainability”; low challenges to mitigation and adaptation), SSP2 (“Middle of the Road”; middle challenges to mitigation and adaptation), SSP3 (“Regional Rivalry”; high challenges to mitigation and adaptation), SSP4 (“Inequality”; low challenges to mitigation, high challenges to adaptation), and SSP5 (“Fossil-fueled Development”; high challenges to mitigation, low challenges to adaptation). Each scenario has an underlying SSP narrative, as well as consistent assumptions regarding demographics, urbanization, economic growth, and technology development. Only SSP5 produces a reference scenario that is consistent with RCP8.5; climate forcing in the other SSPs’ reference scenarios that don’t include climate policy remains below 8.5 W/m². In addition, the nature of SSP3 makes it impossible for that scenario to produce a climate forcing as low as 2.6 W/m². While new research is under way to explore scenarios that limit climate forcing to 2.0 W/m², neither the RCPs nor the SSPs have produced scenarios in that range.



Emissions, Concentrations, and Temperature Projections

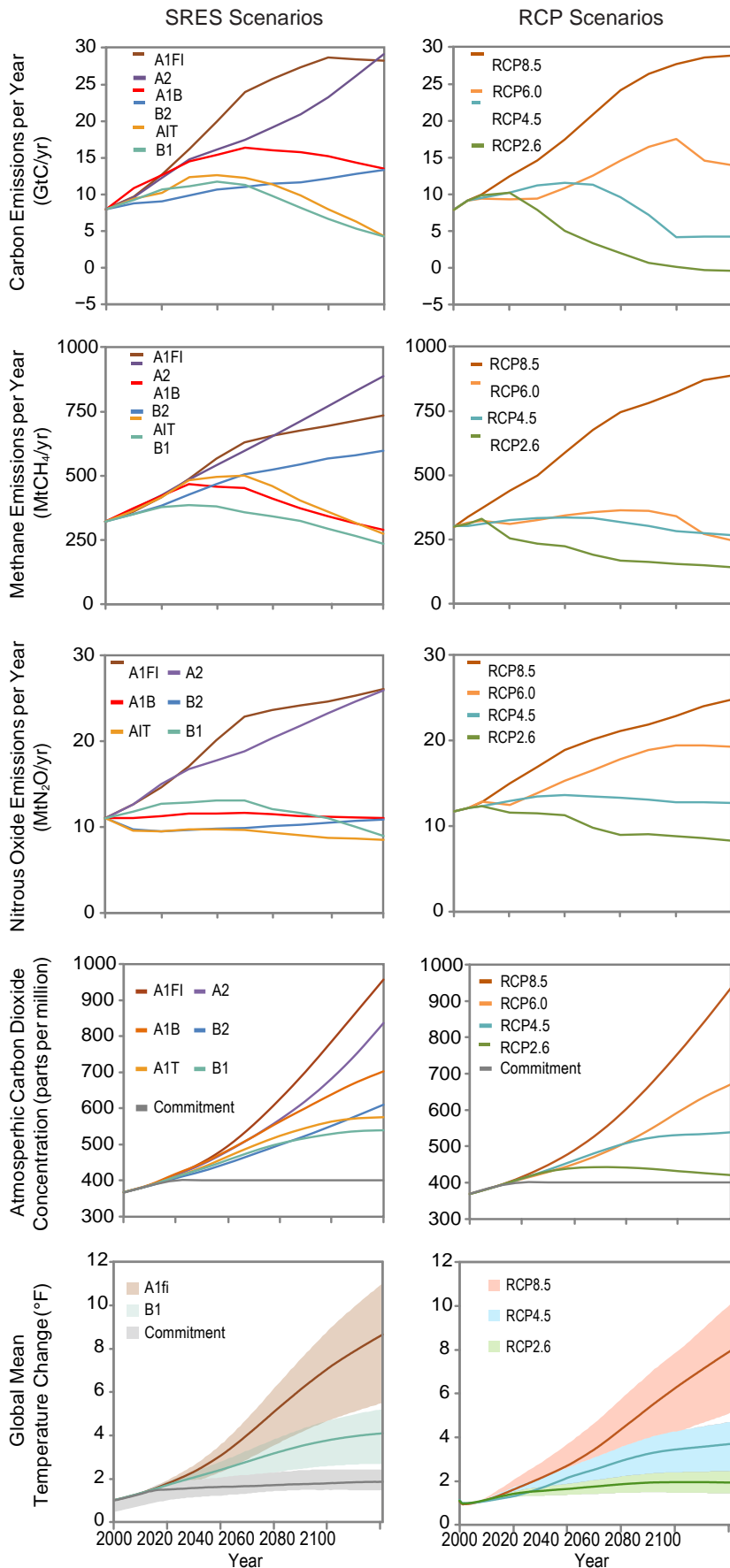


Figure 4.1: The climate projections used in this report are based on the 2010 Representative Concentration Pathways (RCP, right). They are largely consistent with scenarios used in previous assessments, the 2000 Special Report on Emission Scenarios (SRES, left). This figure compares SRES and RCP annual carbon emissions (GtC per year, first row), annual methane emissions (MtCH₄ per year, second row), annual nitrous oxide emissions (MtN₂O per year, third row), carbon dioxide concentration in the atmosphere (ppm, fourth row), and global mean temperature change relative to 1900–1960 as simulated by CMIP3 models for the SRES scenarios and CMIP5 models for the RCP scenarios (°F, fifth row). Note that global mean temperature from SRES A1FI simulations are only available from four global climate models. (Data from IPCC-DDC, IIASA, CMIP3, and CMIP5).



4.2.2 Alternative Scenarios

The emissions and radiative forcing scenarios described above include a component of time: how much will climate change, and by when? Ultimately, however, the magnitude of human-induced climate change depends less on the year-to-year emissions than it does on the net amount of carbon, or cumulative carbon, emitted into the atmosphere. The lower the atmospheric concentrations of CO₂, the greater the chance that eventual global temperature change will not reach the high end temperature projections, or possibly remain below 3.6°F (2°C) relative to preindustrial levels.

Cumulative carbon targets offer an alternative approach to expressing a goal designed to limit global temperature to a certain level. As discussed in Chapter 14: Mitigation, it is possible to quantify the expected amount of carbon that can be emitted globally in order to meet a specific global warming target such as 3.6°F (2°C) or even 2.7°F (1.5°C)—although if current carbon emission rates of just under 10 GtC per year were to continue, the lower target would be reached in a matter of years. The higher target would be reached in a matter of decades (see Ch. 14: Mitigation).

Under a lower scenario (RCP4.5), global temperature change is more likely than not to exceed 3.6°F (2°C),^{3,36} whereas under the even lower scenario (RCP2.6), it is likely to remain below 3.6°F (2°C).^{3,37} While new research is under way to explore scenarios consistent with limiting climate forcing to 2.0 W/m², a level consistent with limiting global mean surface temperature change to 2.7°F (1.5°C), neither the RCPs nor the SSPs have produced scenarios that allow for such a small amount of temperature change (see also Ch. 14: Mitigation).³⁷

Future projections are most commonly summarized for a given future scenario (for example, RCP8.5 or 4.5) over a range of future

climatological time periods (for example, temperature change in 2040–2079 or 2070–2099 relative to 1980–2009). While this approach has the advantage of developing projections for a specific time horizon, uncertainty in future projections is relatively high, incorporating both the uncertainty due to multiple scenarios as well as uncertainty regarding the response of the climate system to human emissions. These uncertainties increase the further out in time the projections go. Using these same transient, scenario-based simulations, however, it is possible to analyze the projected changes for a given global mean temperature (GMT) threshold by extracting a time slice (typically 20 years) centered around the point in time at which that change is reached (Figure 4.2).

Derived GMT scenarios offer a way for the public and policymakers to understand the impacts for any given temperature threshold, as many physical changes and impacts have been shown to scale with global mean surface temperature, including shifts in average precipitation, extreme heat, runoff, drought risk, wildfire, temperature-related crop yield changes, and even risk of coral bleaching (e.g., NRC 2011;³⁸ Collins et al. 2013;³ Frieler et al. 2013;³⁹ Swain and Hayhoe 2015⁴⁰). They also allow scientists to highlight the effect of global mean temperature on projected regional change by de-emphasizing the uncertainty due to both climate sensitivity and future scenarios.^{40, 41} This approach is less useful for those impacts that vary based on rate of change, such as species migrations, or where equilibrium changes are very different from transient effects, such as sea level rise.

Pattern scaling techniques⁴² are based on a similar assumption to GMT scenarios, namely that large-scale patterns of regional change will scale with global temperature change. These techniques can be used to quantify regional projections for scenarios that are not



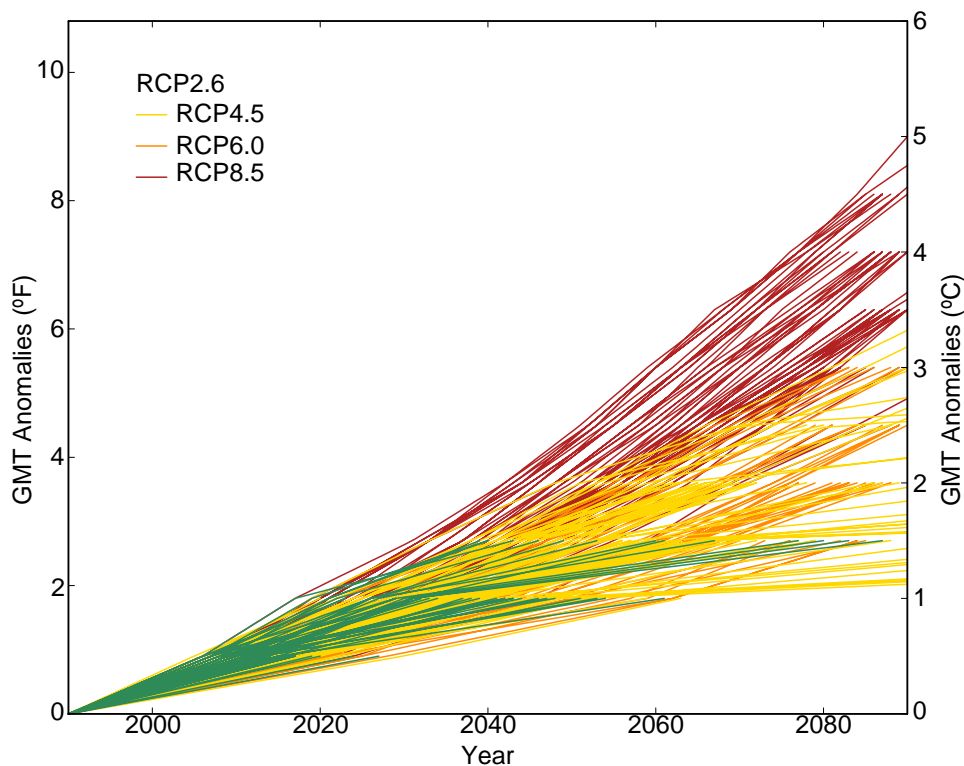


Figure 4.2: Global mean temperature anomalies (°F) relative to 1976–2005 for four RCP scenarios, 2.6 (green), 4.5 (yellow), 6.0 (orange), and 8.5 (red). Each line represents an individual simulation from the CMIP5 archive. Every RCP-based simulation with annual or monthly temperature outputs available was used here. The values shown here were calculated in 0.5°C increments; since not every simulation reaches the next 0.5°C increment before end of century, many lines terminate before 2100. (Figure source: adapted from Swain and Hayhoe 2015⁴⁰).

readily available in preexisting databases of global climate model simulations, including changes in both mean and extremes (e.g., Fix et al. 2016⁴³). A comprehensive assessment both confirms and constrains the validity of applying pattern scaling to quantify climate response to a range of projected future changes.⁴⁴ For temperature-based climate targets, these pattern scaling frames or GMT scenarios offer the basis for more consistent comparisons across studies examining regional change or potential risks and impacts.

4.2.3 Analogs from the Paleoclimate Record

Most CMIP5 simulations project transient changes in climate through 2100; a few simulations extend to 2200, 2300, or beyond. However, as discussed in Chapter 2: Physical Drivers of Climate Change, the long-term impact of human activities on the carbon cycle

and Earth’s climate over the next few decades and for the remainder of this century can only be assessed by considering changes that occur over multiple centuries and even millennia.³⁸

In the past, there have been several examples of “hothouse” climates where carbon dioxide concentrations and/or global mean temperatures were similar to preindustrial, current, or plausible future levels. These periods are sometimes referenced as analogs, albeit imperfect and incomplete, of future climate (e.g., Crowley 1990¹⁰), though comparing climate model simulations to geologic reconstructions of temperature and carbon dioxide during these periods suggests that today’s global climate models tend to underestimate the magnitude of change in response to higher CO₂ (see Ch. 15: Potential Surprises).

The last interglacial period, approximately 125,000 years ago, is known as the Eemian. During that time, CO₂ concentration was similar to preindustrial concentrations, around 280 ppm.⁴⁵ Global mean temperature was approximately 1.8°–3.6°F (1°–2°C) higher than preindustrial temperatures,^{46, 47} although the poles were significantly warmer^{48, 49} and sea level was 6 to 9 meters (20 to 30 feet) higher than today.⁵⁰ During the Pliocene, approximately 3 million years ago, long-term CO₂ concentration was similar to today's, around 400 ppm⁵¹ – although this level was sustained over long periods of time, whereas today the global CO₂ concentration is increasing rapidly. At that time, global mean temperature was approximately 3.6°–6.3°F (2°–3.5°C) above preindustrial, and sea level was somewhere between 66 ± 33 feet (20 ± 10 meters) higher than today.^{52, 53, 54}

Under the higher scenario (RCP8.5), CO₂ concentrations are projected to reach 936 ppm by 2100. During the Eocene, 35 to 55 million years ago, CO₂ levels were between 680 and 1260 ppm, or somewhere between two and a half to four and a half times higher than preindustrial levels.⁵⁵ If Eocene conditions are used as an analog, this suggests that if the CO₂ concentrations projected to occur under the RCP8.5 scenario by 2100 were sustained over long periods of time, global temperatures would be approximately 9°–14°F (5°–8°C) above preindustrial temperatures.⁵⁶ During the Eocene, there were no permanent land-based ice sheets; Antarctic glaciation did not begin until approximately 34 million years ago.⁵⁷ Calibrating sea level rise models against past climate suggests that, under the RCP8.5 scenario, Antarctica could contribute 3 feet (1 meter) of sea level rise by 2100 and 50 feet (15 meters) by 2500.⁵⁸ If atmospheric CO₂ were sustained at levels approximately two to three times above preindustrial for tens of thousands of years, it is estimated that Greenland

and Antarctic ice sheets could melt entirely,⁵⁹ resulting in approximately 215 feet (65 meters) of sea level rise.⁶⁰

4.3 Modeling Tools

Using transient scenarios such as SRES and RCP as input, global climate models (GCMs) produce trajectories of future climate change, including global and regional changes in temperature, precipitation, and other physical characteristics of the climate system (see also Ch. 6: Temperature Change and Ch. 7: Precipitation Change).^{3, 61} The resolution of global models has increased significantly since IPCC FAR.¹⁹ However, even the latest experimental high-resolution simulations, at 15–30 miles (25–50 km) per gridbox, are unable to simulate all of the important fine-scale processes occurring at regional to local scales. Instead, downscaling methods are often used to correct systematic biases, or offsets relative to observations, in global projections and translate them into the higher-resolution information typically required for impact assessments.

Dynamical downscaling with regional climate models (RCMs) directly simulates the response of regional climate processes to global change, while empirical statistical downscaling models (ESDMs) tend to be more flexible and computationally efficient. Comparing the ability of dynamical and statistical methods to reproduce observed climate shows that the relative performance of the two approaches depends on the assessment criteria.⁶² Although dynamical and statistical methods can be combined into a hybrid framework, many assessments still tend to rely on one or the other type of downscaling, where the choice is based on the needs of the assessment. The projections shown in this report, for example, are either based on the original GCM simulations or on simulations that have been statistically downscaled using the LOcalized Constructed Analogs method (LOCA).⁶³ This section describes the global climate models



used today, briefly summarizes their development over the past few decades, and explains the general characteristics and relative strengths and weaknesses of the dynamical and statistical downscaling.

4.3.1 Global Climate Models

Global climate models are mathematical frameworks that were originally built on fundamental equations of physics. They account for the conservation of energy, mass, and momentum and how these are exchanged among different components of the climate system. Using these fundamental relationships, GCMs are able to simulate many important aspects of Earth's climate: large-scale patterns of temperature and precipitation, general characteristics of storm tracks and extratropical cyclones, and observed changes in global mean temperature and ocean heat content as a result of human emissions.⁶⁴

The complexity of climate models has grown over time, as they incorporate additional components of Earth's climate system (Figure 4.3). For example, GCMs were previously referred to as "general circulation models" when they included only the physics needed to simulate the general circulation of the atmosphere. Today, global climate models simulate many more aspects of the climate system: atmospheric chemistry and aerosols, land surface interactions including soil and vegetation, land and sea ice, and increasingly even an interactive carbon cycle and/or biogeochemistry. Models that include this last component are also referred to as Earth system models (ESMs).

In addition to expanding the number of processes in the models and improving the treatment of existing processes, the total number of GCMs and the average horizontal spatial resolution of the models have increased over time, as computers become more powerful, and with each successive version of the World Cli-

mate Research Programme's (WCRP's) Coupled Model Intercomparison Project (CMIP). CMIP5 provides output from over 50 GCMs with spatial resolutions ranging from about 30 to 200 miles (50 to 300 km) per horizontal size and variable vertical resolution on the order of hundreds of meters in the troposphere or lower atmosphere.

It is often assumed that higher-resolution, more complex, and more up-to-date models will perform better and/or produce more robust projections than previous-generation models. However, a large body of research comparing CMIP3 and CMIP5 simulations concludes that, although the spatial resolution of CMIP5 has improved relative to CMIP3, the overall improvement in performance is relatively minor. For certain variables, regions, and seasons, there is some improvement; for others, there is little difference or even sometimes degradation in performance, as greater complexity does not necessarily imply improved performance.^{65, 66, 67, 68} CMIP5 simulations do show modest improvement in model ability to simulate ENSO,⁶⁹ some aspects of cloud characteristics,⁷⁰ and the rate of arctic sea ice loss,⁷¹ as well as greater consensus regarding projected drying in the southwestern United States and Mexico.⁶⁸

Projected changes in hurricane rainfall rates and the reduction in tropical storm frequency are similar, but CMIP5-based projections of increases in the frequency of the strongest hurricanes are generally smaller than CMIP3-based projections.⁷² On the other hand, many studies find little to no significant difference in large-scale patterns of changes in both mean and extreme temperature and precipitation from CMIP3 to CMIP5.^{65, 68, 73,} ⁷⁴ Also, CMIP3 simulations are driven by SRES scenarios, while CMIP5 simulations are driven by RCP scenarios. Although some scenarios have comparable CO₂ concentration pathways (Figure 4.1), differences in non-CO₂ species and aerosols



A Climate Modeling Timeline (When Various Components Became Commonly Used)

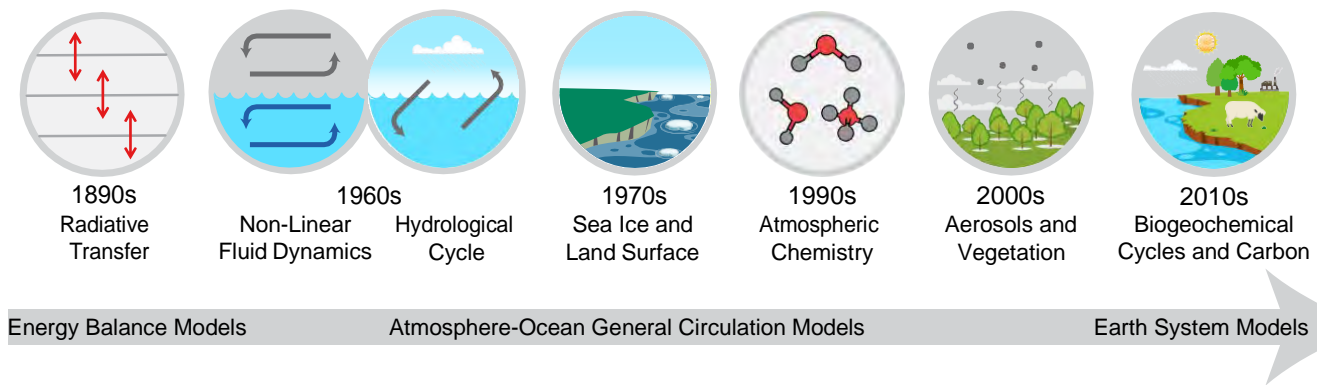


Figure 4.3: As scientific understanding of climate has evolved over the last 120 years, increasing amounts of physics, chemistry, and biology have been incorporated into calculations and, eventually, models. This figure shows when various processes and components of the climate system became regularly included in scientific understanding of global climate calculations and, over the second half of the century as computing resources became available, formalized in global climate models.

could be responsible for some of the differences between the simulations.⁶⁸ In NCA3, projections were based on simulations from both CMIP3 and CMIP5. In this report, future projections are based on CMIP5 alone.

GCMs are constantly being expanded to include more physics, chemistry, and, increasingly, even the biology and biogeochemistry at work in the climate system (Figure 4.3). Interactions within and between the various components of the climate system result in positive and negative feedbacks that can act to enhance or dampen the effect of human emissions on the climate system. The extent to which models explicitly resolve or incorporate these processes determines their climate sensitivity, or response to external forcing (see Ch. 2: Physical Drivers of Climate Change, Section 2.5 on climate sensitivity, and Ch. 15: Potential Surprises on the importance of processes not included in present-day GCMs).

Confidence in the usefulness of the future projections generated by global climate models is based on multiple factors. These include the fundamental nature of the physical processes they represent, such as radiative transfer or geophysical fluid dynamics, which can be

tested directly against measurements or theoretical calculations to demonstrate that model approximations are valid (e.g., IPCC 1990¹⁹). They also include the vast body of literature dedicated to evaluating and assessing model abilities to simulate observed features of the earth system, including large-scale modes of natural variability, and to reproduce their net response to external forcing that captures the interaction of many processes which produce observable climate system feedbacks (e.g., Flato et al. 2013⁶⁴). There is no better framework for integrating our knowledge of the physical processes in a complex coupled system like Earth's climate.

Given their complexities, GCMs typically build on previous generations and therefore many models are not fully independent from each other. Many share both ideas and model components or code, complicating the interpretation of multimodel ensembles that often are assumed to be independent.^{75, 76} Consideration of the independence of different models is one of the key pieces of information going into the weighting approach used in this report (see Appendix B: Weighting Strategy).

4.3.2 Regional Climate Models

Dynamical downscaling models are often referred to as regional climate models, since they include many of the same physical processes that make up a global climate model, but simulate these processes at higher spatial resolution over smaller regions, such as the western or eastern United States (Figure 4.4).⁷⁷ Most RCM simulations use GCM fields from pre-computed global simulations as boundary conditions. This approach allows RCMs to draw from a broad set of GCM simulations, such as CMIP5, but does not allow for possible two-way feedbacks and interactions between the regional and global scales. Dynamical downscaling can also be conducted interactively through nesting a higher-resolution regional grid or model into a global model during a simulation. Both approaches directly simulate the dynamics of the regional climate system, but only the second allows for two-way interactions between regional and global change.

RCMs are computationally intensive, providing a broad range of output variables that resolve regional climate features important for assessing climate impacts. The size of individual grid cells can be as fine as 0.6 to 1.2 miles (1 to 2 km) per gridbox in some studies, but more commonly range from about 6 to 30 miles (10 to 50 km). At smaller spatial scales, and for specific variables and areas with complex terrain, such as coastlines or mountains, regional climate models have been shown to add value.⁷⁸ As model resolution increases, RCMs are also able to explicitly resolve some processes that are parameterized in global models. For example, some models with spatial scales below 2.5 miles (4 km) are able to dispense with the parameterization of convective precipitation, a significant source of error and uncertainty in coarser models.⁷⁹ RCMs can also incorporate changes in land use, land cover, or hydrology into local climate at spatial scales relevant to planning and decision-making at the regional level.

Despite the differences in resolution, RCMs are still subject to many of the same types of uncertainty as GCMs. Even the highest-resolution RCM cannot explicitly model physical processes that occur at even smaller scales than the model is able to resolve; instead, parameterizations are required. Similarly, RCMs might not include a process or an interaction that is not yet well understood, even if it is able to be resolved at the spatial scale of the model. One additional source of uncertainty unique to RCMs arises from the fact that at their boundaries RCMs require output from GCMs to provide large-scale circulation such as winds, temperature, and moisture; the degree to which the driving GCM correctly captures large-scale circulation and climate will affect the performance of the RCM.⁸⁰ RCMs can be evaluated by directly comparing their output to observations; although this process can be challenging and time-consuming, it is often necessary to quantify the appropriate level of confidence that can be placed in their output.⁷⁷

Studies have also highlighted the importance of large ensemble simulations when quantifying regional change.⁸¹ However, due to their computational demand, extensive ensembles of RCM-based projections are rare. The largest ensembles of RCM simulations for North America are hosted by the North American Regional Climate Change Assessment Program (NARCCAP) and the North American CORDEX project (NA-CORDEX). These simulations are useful for examining patterns of change over North America and providing a broad suite of surface and upper-air variables to characterize future impacts. Since these ensembles are based on four simulations from four CMIP3 GCMs for a mid-high SRES scenario (NARCCAP) and six CMIP5 GCMs for two RCP scenarios (NA-CORDEX), they do not encompass the full range of uncertainty in future projections due to human activities, natural variability, and climate sensitivity.



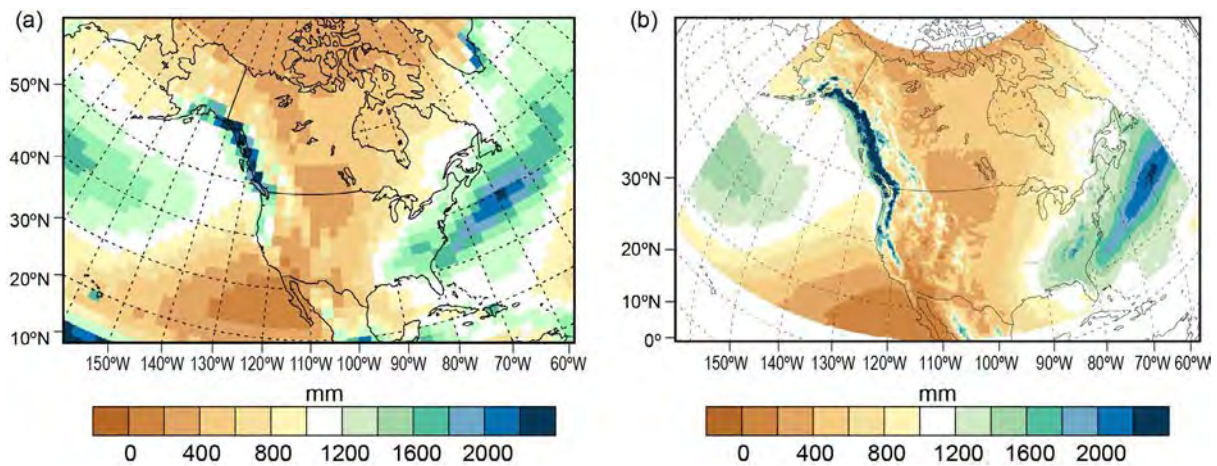


Figure 4.4: CMIP5 global climate models typically operate at coarser horizontal spatial scales on the order of 30 to 200 miles (50 to 300 km), while regional climate models have much finer resolutions, on the order of 6 to 30 miles (10 to 50 km). This figure compares annual average precipitation (in millimeters) for the historical period 1979–2008 using (a) a resolution of 250 km or 150 miles with (b) a resolution of 15 miles or 25 km to illustrate the importance of spatial scale in resolving key topographical features, particularly along the coasts and in mountainous areas. In this case, both simulations are by the GFDL HIRAM, an experimental high-resolution model. (Figure source: adapted from Dixon et al. 2016⁸⁶).

4.3.3 Empirical Statistical Downscaling Models

Empirical statistical downscaling models (ESDMs) combine GCM output with historical observations to translate large-scale predictors or patterns into high-resolution projections at the scale of observations. The observations used in an ESDM can range from individual weather stations to gridded datasets. As output, ESDMs can generate a range of products, from large grids to analyses optimized for a specific location, variable, or decision-context.

Statistical techniques are varied, from the simple difference or delta approaches used in the first NCA (subtracting historical simulated values from future values, and adding the resulting delta to historical observations)²⁵ to the parametric quantile mapping approach used in NCA2 and 3.^{26, 27, 82} Even more complex clustering and advanced mathematical modeling techniques can rival dynamical downscaling in their demand for computational resources (e.g., Vrac et al. 2007⁸³).

Statistical models are generally flexible and less computationally demanding than RCMs. A number of databases using a variety of

methods, including the LOcalized Constructed Analogs method (LOCA), provide statistically downscaled projections for a continuous period from 1960 to 2100 using a large ensemble of global models and a range of higher and lower future scenarios to capture uncertainty due to human activities. ESDMs are also effective at removing biases in historical simulated values, leading to a good match between the average (multidecadal) statistics of observed and statistically downscaled climate at the spatial scale and over the historical period of the observational data used to train the statistical model. Unless methods can simultaneously downscale multiple variables, however, statistical downscaling carries the risk of altering some of the physical interdependences between variables. ESDMs are also limited in that they require observational data as input; the longer and more complete the record, the greater the confidence that the ESDM is being trained on a representative sample of climatic conditions for that location. Application of ESDMs to remote locations with sparse temporal and/or spatial records is challenging, though in many cases reanalysis⁸⁴ or even monthly satellite data⁸⁵ can be used in lieu of

in situ observations. Lack of data availability can also limit the use of ESDMs in applications that require more variables than temperature and precipitation. Finally, statistical models are based on the key assumption that the relationship between large-scale weather systems and local climate or the spatial pattern of surface climate will remain stationary over the time horizon of the projections. This assumption may not hold if climate change alters local feedback processes that affect these relationships.

ESDMs can be evaluated in three different ways, each of which provides useful insight into model performance.⁷⁷ First, the model's goodness-of-fit can be quantified by comparing downscaled simulations for the historical period with the identical observations used to train the model. Second, the generalizability of the model can be determined by comparing downscaled historical simulations with observations from a different time period than was used to train the model; this is often accomplished via cross-validation. Third and most importantly, the stationarity of the model can be evaluated through a "perfect model" experiment using coarse-resolution GCM simulations to generate future projections, then comparing these with high-resolution GCM simulations for the same future time period. Initial analyses using the perfect model approach have demonstrated that the assumption of stationarity can vary significantly by ESDM method, by quantile, and by the time scale (daily or monthly) of the GCM input.⁸⁶

ESDMs are best suited for analyses that require a broad range of future projections of standard, near-surface variables such as temperature and precipitation, at the scale of observations that may already be used for planning purposes. If the study needs to evaluate the full range of projected changes pro-

vided by multiple models and scenarios, then statistical downscaling may be more appropriate than dynamical downscaling. However, even within statistical downscaling, selecting an appropriate method for any given study depends on the questions being asked (see Kotamarthi et al. 2016⁷⁷ for further discussion on selection of appropriate downscaling methods). This report uses projections generated by LOCA,⁶³ which spatially matches model-simulated days, past and future, to analogs from observations.

4.3.4 Averaging, Weighting, and Selection of Global Models

The results of individual climate model simulations using the same inputs can differ from each other over shorter time scales ranging from several years to several decades.^{87, 88} These differences are the result of normal, natural variability, as well as the various ways models characterize various small-scale processes. Although decadal predictability is an active research area,⁸⁹ the timing of specific natural variations is largely unpredictable beyond several seasons. For this reason, multimodel simulations are generally averaged to remove the effects of randomly occurring natural variations from long-term trends and make it easier to discern the impact of external drivers, both human and natural, on Earth's climate. Multimodel averaging is typically the last stage in any analysis, used to prepare figures showing projected changes in quantities such as annual or seasonal temperature or precipitation (see Ch. 6: Temperature Change and Ch. 7: Precipitation Change). While the effect of averaging on the systematic errors depends on the extent to which models have similar errors or offsetting errors, there is growing recognition of the value of large ensembles of climate model simulations in addressing uncertainty in both natural variability and scientific modeling (e.g., Deser et al. 2012⁸⁷).



Previous assessments have used a simple average to calculate the multimodel ensemble. This approach implicitly assumes each climate model is independent from the others and of equal ability. Neither of these assumptions, however, are completely valid. Some models share many components with other models in the CMIP5 archive, whereas others have been developed largely in isolation.^{75,76} Also, some models are more successful than others at replicating observed climate and trends over the past century, at simulating the large-scale dynamical features responsible for creating or affecting the average climate conditions over a certain region, such as the Arctic or the Caribbean (e.g., Wang et al. 2007;⁹⁰ Wang et al. 2014;⁹¹ Ryu and Hayhoe 2014⁹²), or at simulating past climates with very different states than present day.⁹³ Evaluation of the success of a specific model often depends on the variable or metric being considered in the analysis, with some models performing better than others for certain regions or variables. However, all future simulations agree that both global and regional temperatures will increase over this century in response to increasing emissions of greenhouse gases from human activities.

Can more sophisticated weighting or model selection schemes improve the quality of future projections? In the past, model weights were often based on historical performance; yet performance varies by region and variable, and may not equate to improved future projections.⁶⁵ For example, ranking GCMs based on their average biases in temperature gives a very different result than when the same models are ranked based on their ability to simulate observed temperature trends.⁹⁴ ⁹⁵ If GCMs are weighted in a way that does not accurately capture the true uncertainty in regional change, the result can be less robust than an equally-weighted mean.⁹⁶ Although the intent of weighting models is to increase

the robustness of the projections, by giving lesser weight to outliers a weighting scheme may increase the risk of underestimating the range of uncertainty, a tendency that has already been noted in multi-model ensembles (see Ch. 15: Potential Surprises).

Despite these challenges, for the first time in an official U.S. Global Change Research Program report, this assessment uses model weighting to refine future climate change projections (see also Appendix B: Weighting Strategy).⁹⁷ The weighting approach is unique: it takes into account the interdependence of individual climate models as well as their relative abilities in simulating North American climate. Understanding of model history, together with the fingerprints of particular model biases, has been used to identify model pairs that are not independent. In this report, model independence and selected global and North American model quality metrics are considered in order to determine the weighting parameters.⁹⁷ Evaluation of this approach shows improved performance of the weighted ensemble over the Arctic, a region where model-based trends often differ from observations, but little change in global-scale temperature response and in other regions where modeled and observed trends are similar, although there are small regional differences in the statistical significance of projected changes. The choice of metric used to evaluate models has very little effect on the independence weighting, and some moderate influence on the skill weighting if only a small number of variables are used to assess model quality. Because a large number of variables are combined to produce a comprehensive “skill metric,” the metric is not highly sensitive to any single variable. All multimodel figures in this report use the approach described in Appendix B: Weighting Strategy.



4.4 Uncertainty in Future Projections

The timing and magnitude of projected future climate change is uncertain due to the ambiguity introduced by human choices (as discussed in Section 4.2), natural variability, and scientific uncertainty,^{87,98,99} which includes uncertainty in both scientific modeling and climate sensitivity (see Ch. 2: Physical Drivers of Climate Change). Confidence in projections of specific aspects of future climate change increases if formal detection and attribution analyses (Ch. 3: Detection and Attribution) indicate that an observed change has been influenced by human activities, and the projection is consistent with attribution. However, in many cases, especially at the regional scales considered in this assessment, a human-forced response may not yet have emerged from the noise of natural climate variability but may be expected to in the future (e.g., Hawkins and Sutton 2009⁹⁸, 2011⁹⁹). In such cases, confidence in such “projections without attribution” may still be significant under higher scenarios, if the relevant physical mechanisms of change are well understood.

Scientific uncertainty encompasses multiple factors. The first is parametric uncertainty – the ability of GCMs to simulate processes that occur on spatial or temporal scales smaller than they can resolve. The second is structural uncertainty – whether GCMs include and accurately represent all the important physical processes occurring on scales they can resolve. Structural uncertainty can arise because a process is not yet recognized – such as “tipping points” or mechanisms of abrupt change – or because it is known but is not yet understood well enough to be modeled accurately – such as dynamical mechanisms that are important to melting ice sheets (see Ch. 15: Potential Surprises). The third is climate sensitivity – a measure of the response of the planet to increasing levels of CO₂, which is formally defined in Chapter 2: Physical Drivers of Cli-

mate Change as the equilibrium temperature change resulting from a doubling of CO₂ levels in the atmosphere relative to preindustrial levels. Various lines of evidence constrain the likely value of climate sensitivity to between 2.7°F and 8.1°F (1.5°C and 4.5°C;¹⁰⁰ see Ch. 2: Physical Drivers of Climate Change for further discussion).

Which of these sources of uncertainty – human, natural, and scientific – is most important depends on the time frame and the variable considered. As future scenarios diverge (Figure 4.1), so too do projected changes in global and regional temperatures.⁹⁸ Uncertainty in the magnitude and sign of projected changes in precipitation and other aspects of climate is even greater. The processes that lead to precipitation happen at scales smaller than what can be resolved by even high-resolution models, requiring significant parameterization. Precipitation also depends on many large-scale aspects of climate, including atmospheric circulation, storm tracks, and moisture convergence. Due to the greater level of complexity associated with modeling precipitation, scientific uncertainty tends to dominate in precipitation projections throughout the entire century, affecting both the magnitude and sometimes (depending on location) the sign of the projected change in precipitation.⁹⁹

Over the next few decades, the greater part of the range or uncertainty in projected global and regional change will be the result of a combination of natural variability (mostly related to uncertainty in specifying the initial conditions of the state of the ocean)⁸⁸ and scientific limitations in our ability to model and understand the Earth’s climate system (Figure 4.5, Ch. 5: Circulation & Variability). Differences in future scenarios, shown in orange in Figure 4.5, represent the difference between scenarios, or human activity. Over the short term, this uncertainty is relatively small. As time progresses, however,



differences in various possible future pathways become larger and the delayed ocean response to these differences begins to be realized. By about 2030, the human source of uncertainty becomes increasingly important in determining the magnitude and patterns of future global warming. Even though natural variability will continue

to occur, most of the difference between present and future climates will be determined by choices that society makes today and over the next few decades. The further out in time we look, the greater the influence of these human choices are on the magnitude of future warming.

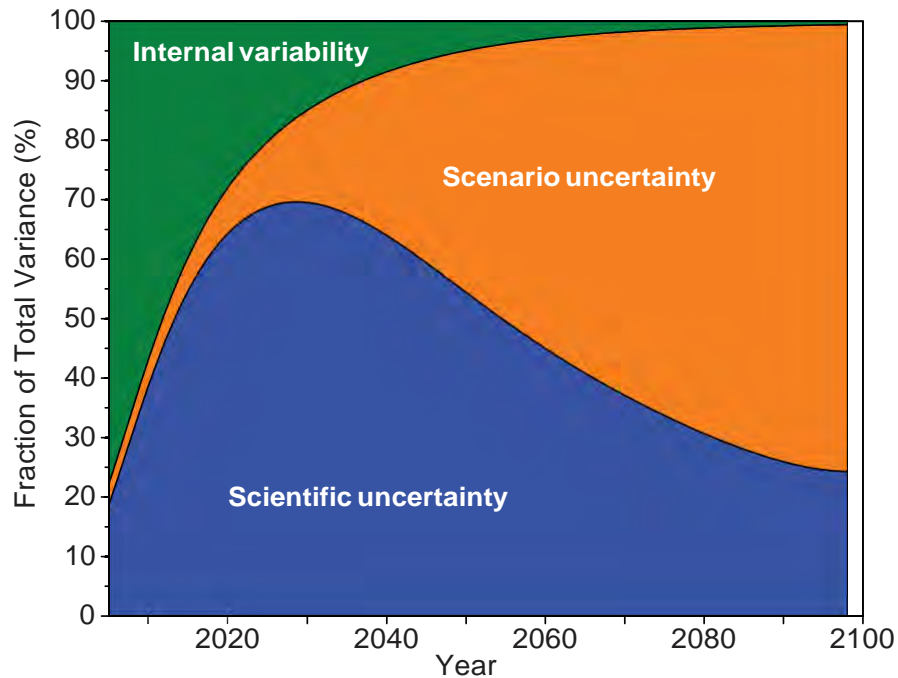


Figure 4.5: The fraction of total variance in decadal mean surface air temperature predictions explained by the three components of total uncertainty is shown for the lower 48 states (similar results are seen for Hawai'i and Alaska, not shown). Orange regions represent human or scenario uncertainty, blue regions represent scientific uncertainty, and green regions represent the internal variability component. As the size of the region is reduced, the relative importance of internal variability increases. In interpreting this figure, it is important to remember that it shows the fractional sources of uncertainty. Total uncertainty increases as time progresses. (Figure source: adapted from Hawkins and Sutton 2009⁹⁸).

TRACEABLE ACCOUNTS

Key Finding 1

If greenhouse gas concentrations were stabilized at their current level, existing concentrations would commit the world to at least an additional 1.1°F (0.6°C) of warming over this century relative to the last few decades (*high confidence* in continued warming, *medium confidence* in amount of warming).

Description of evidence base

The basic physics underlying the impact of human emissions on global climate, and the role of climate sensitivity in moderating the impact of those emissions on global temperature, has been documented since the 1800s in a series of peer-reviewed journal articles that is summarized in a collection titled, “The Warming Papers: The Scientific Foundation for the Climate Change Forecast”.¹⁰¹

The estimate of committed warming at constant atmospheric concentrations is based on IPCC AR5 WG1, Chapter 12, section 12.5.2,³ page 1103 which is in turn derived from AR4 WG1, Chapter 10, section 10.7.1,²⁸ page 822.

Major uncertainties

The uncertainty in projected change under a commitment scenario is low and primarily the result of uncertainty in climate sensitivity. This key finding describes a hypothetical scenario that assumes all human-caused emissions cease and the Earth system responds only to what is already in the atmosphere.

Assessment of confidence based on evidence and agreement, including short description of nature of evidence and level of agreement

The statement has *high confidence* in the sign of future change and *medium confidence* in the amount of warming, based on the estimate of committed warming at constant atmospheric concentrations from Collins et al.³ based on Meehl et al.²⁸ for a hypothetical scenario where concentrations in the atmosphere were fixed at a known level.

Summary sentence or paragraph that integrates the above information

The key finding is based on the basic physical principles of radiative transfer that have been well established for decades to centuries; the amount of estimated warming for this hypothetical scenario is derived from Collins et al.³ which is in turn based on Meehl et al.²⁸ using CMIP3 models.

Key Finding 2

Over the next two decades, global temperature increase is projected to be between 0.5°F and 1.3°F (0.3°–0.7°C) (*medium confidence*). This range is primarily due to uncertainties in natural sources of variability that affect short-term trends. In some regions, this means that the trend may not be distinguishable from natural variability (*high confidence*).

Description of evidence base

The estimate of projected near-term warming under continued emissions of carbon dioxide and other greenhouse gases and aerosols was obtained directly from IPCC AR5 WG1.⁶¹

The statement regarding the sources of uncertainty in near-term projections and regional uncertainty is based on Hawkins and Sutton^{98, 99} and Deser et al.^{87, 88}

Major uncertainties

As stated in the key finding, natural variability is the primary uncertainty in quantifying the amount of global temperature change over the next two decades.

Assessment of confidence based on evidence and agreement, including short description of nature of evidence and level of agreement

The first statement regarding projected warming over the next two decades has *medium confidence* in the amount of warming due to the uncertainties described in the key finding. The second statement has *high confidence*, as the literature strongly supports the statement that natural variability is the primary source of uncertainty over time scales of years to decades.^{87, 88, 89}



Summary sentence or paragraph that integrates the above information

The estimated warming presented in this Key Finding is based on calculations reported by Kirtman et al.⁶¹ The key finding that natural variability is the most important uncertainty over the near-term is based on multiple peer reviewed publications.

Key Finding 3

Beyond the next few decades, the magnitude of climate change depends primarily on cumulative emissions of greenhouse gases and aerosols and the sensitivity of the climate system to those emissions (*high confidence*). Projected changes range from 4.7°–8.6°F (2.6°–4.8°C) under the higher scenario (RCP8.5) to 0.5°–1.3°F (0.3°–1.7°C) under the much lower scenario (RCP2.6), for 2081–2100 relative to 1986–2005 (*medium confidence*).

Description of evidence base

The estimate of projected long-term warming under continued emissions of carbon dioxide and other greenhouse gases and aerosols under the RCP scenario was obtained directly from IPCC AR5 WG1.³

All credible climate models assessed in Chapter 9 of the IPCC WG1 AR5⁶⁴ from the simplest to the most complex respond with elevated global mean temperature, the simplest indicator of climate change, when atmospheric concentrations of greenhouse gases increase. It follows then that an emissions pathway that tracks or exceeds the higher scenario (RCP8.5) would lead to larger amounts of climate change.

The statement regarding the sources of uncertainty in long-term projections is based on Hawkins and Sutton.^{98,99}

Major uncertainties

As stated in the key finding, the magnitude of climate change over the long term is uncertain due to human emissions of greenhouse gases and climate sensitivity.

Assessment of confidence based on evidence and agreement, including short description of nature of evidence and level of agreement

The first statement regarding additional warming and its dependence on human emissions and climate sensitivity has *high confidence*, as understanding of the radiative properties of greenhouse gases and the existence of both positive and negative feedbacks in the climate system is basic physics, dating to the 19th century. The second has *medium confidence* in the specific magnitude of warming, due to the uncertainties described in the key finding.

Summary sentence or paragraph that integrates the above information

The estimated warming presented in this key finding is based on calculations reported by Collins et al.³ The key finding that human emissions and climate sensitivity are the most important sources of uncertainty over the long-term is based on both basic physics regarding the radiative properties of greenhouse gases, as well as a large body of peer reviewed publications.

Key Finding 4

Global mean atmospheric carbon dioxide (CO₂) concentration has now passed 400 ppm, a level that last occurred about 3 million years ago, when global average temperature and sea level were significantly higher than today (*high confidence*). Continued growth in CO₂ emissions over this century and beyond would lead to an atmospheric concentration not experienced in tens of millions of years (*medium confidence*). The present-day emissions rate of nearly 10 GtC per year suggests that there is no climate analog for this century any time in at least the last 50 million years (*medium confidence*).

Description of evidence base

The key finding is based on a large body of research including Crowley,¹⁰ Schneider et al.,⁴⁵ Lunt et al.,⁴⁶ Otto-Bleisner et al.,⁴⁷ NEEM,⁴⁸ Jouzel et al.,⁴⁹ Dutton et al.,⁵³ Seki et al.,⁵¹ Haywood et al.,⁵² Miller et al.,⁵⁴ Royer,⁵⁶ Bowen et al.,⁷ Kirtland Turner et al.,⁸ Penman et al.,⁹ Zeebe et al.,¹¹ and summarized in NRC³⁸ and Masson-Delmotte et al.¹⁰²

Major uncertainties

The largest uncertainty is the measurement of past sea



level, given the contributions of not only changes in land ice mass, but also in solid earth, mantle, isostatic adjustments, etc. that occur on timescales of millions of years. This uncertainty increases the further back in time we go; however, the signal (and forcing) size is also much greater. There are also associated uncertainties in precise quantification of past global mean temperature and carbon dioxide levels. There is uncertainty in the age models used to determine rates of change and coincidence of response at shorter, sub-millennial timescales.

Assessment of confidence based on evidence and agreement, including short description of nature of evidence and level of agreement

High confidence in the likelihood statement that past global mean temperature and sea level rise were higher with similar or higher CO₂ concentrations is based on Masson-Delmotte et al.¹⁰² in IPCC AR5. *Medium confidence* that no precise analog exists in 66 million years is based on Zeebe et al.¹¹ as well as the larger body of literature summarized in Masson-Delmotte et al.¹⁰²

Summary sentence or paragraph that integrates the above information

The key finding is based on a vast body of literature that summarizes the results of observations, paleoclimate analyses, and paleoclimate modeling over the past 50 years and more.

Key Finding 5

The observed increase in global carbon emissions over the past 15–20 years has been consistent with higher scenarios (*very high confidence*). In 2014 and 2015, emission growth rates slowed as economic growth has become less carbon-intensive (*medium confidence*). Even if this trend continues, however, it is not yet at a rate that would limit the increase in the global average temperature to well below 3.6°F (2°C) above preindustrial levels (*high confidence*).

Description of Evidence Base

Observed emissions for 2014 and 2015 and estimated emissions for 2016 suggest a decrease in the growth rate and possibly even emissions of carbon; this shift is attributed primarily to decreased coal use in China although with significant uncertainty as noted in the

references in the text. This statement is based on Tans and Keeling 2017;⁴ Raupach et al. 2007;⁵ Le Quéré et al. 2009;⁶ Jackson et al. 2016;¹² Korsbakken et al. 2016¹³ and personal communication with Le Quéré (2017).

The statement that the growth rate of carbon dioxide increased over the past 15–20 years is based on the data available here: <https://www.esrl.noaa.gov/gmd/ccgg/trends/gr.html>

The evidence that actual emission rates track or exceed the higher scenario (RCP8.5) is as follows. The actual emission of CO₂ from fossil fuel consumption and concrete manufacture over the period 2005–2014 is 90.11 Pg.¹⁰⁴ The emissions consistent with RCP8.5 over the same period assuming linear trends between years 2000, 2005, 2010, and 2020 in the specification is 99.24 Pg.

Actual emissions:

<http://www.globalcarbonproject.org/> and Le Quéré et al.¹⁰³

Emissions consistent with RCP8.5

<http://tntcat.iiasa.ac.at:8787/RcpDb/dsd?Action=html-page&page=compare>

The numbers for fossil fuel and industrial emissions (RCP) compared to fossil fuel and cement emissions (observed) in units of GtC are

	RCP8.5	Actual	Difference
2005	7.97	8.23	0.26
2006	8.16	8.53	0.36
2007	8.35	8.78	0.42
2008	8.54	8.96	0.42
2009	8.74	8.87	0.14
2010	8.93	9.21	0.28
2011	9.19	9.54	0.36
2012	9.45	9.69	0.24
2013	9.71	9.82	0.11
2014	9.97	9.89	-0.08
2015	10.23	9.90	-0.34
total	99.24	101.41	2.18



Major Uncertainties

None

Assessment of confidence based on evidence and agreement, including short description of nature of evidence and level of agreement

Very high confidence in increasing emissions over the last 20 years and *high confidence* in the fact that recent emission trends will not be sufficient to avoid 3.6°F (2°C). *Medium confidence* in recent findings that the growth rate is slowing. Climate change scales with the amount of anthropogenic greenhouse gas in the atmosphere. If emissions exceed those consistent with RCP8.5, the likely range of changes in temperatures and climate variables will be larger than projected.

Summary sentence or paragraph that integrates the above information

The key finding is based on basic physics relating emissions to concentrations, radiative forcing, and resulting change in global mean temperature, as well as on IEA data on national emissions as reported in the peer-reviewed literature.

Key Finding 6

Combining output from global climate models and dynamical and statistical downscaling models using advanced averaging, weighting, and pattern scaling approaches can result in more relevant and robust future projections. For some regions, sectors, and impacts, these techniques are increasing the ability of the scientific community to provide guidance on the use of climate projections for quantifying regional-scale changes and impacts (*medium to high confidence*).

Description of evidence base

The contribution of weighting and pattern scaling to improving the robustness of multimodel ensemble projections is described and quantified by a large body of literature as summarized in the text, including Sanderson et al.⁷⁶ and Knutti et al.⁹⁷ The state of the art of dynamical and statistical downscaling and the scientific community's ability to provide guidance regarding the application of climate projections to regional impact

assessments is summarized in Kotamarthi et al.⁷⁷ and supported by Feser et al.⁷⁸ and Prein et al.⁷⁹

Major uncertainties

Regional climate models are subject to the same structural and parametric uncertainties as global models, as well as the uncertainty due to incorporating boundary conditions. The primary source of error in application of empirical statistical downscaling methods is inappropriate application, followed by stationarity.

Assessment of confidence based on evidence and agreement, including short description of nature of evidence and level of agreement

Advanced weighting techniques have significantly improved over previous Bayesian approaches; confidence in their ability to improve the robustness of multimodel ensembles, while currently rated as *medium*, is likely to grow in coming years. Downscaling has evolved significantly over the last decade and is now broadly viewed as a robust source for high-resolution climate projections that can be used as input to regional impact assessments.

Summary sentence or paragraph that integrates the above information

Scientific understanding of climate projections, downscaling, multimodel ensembles, and weighting has evolved significantly over the last decades to the extent that appropriate methods are now broadly viewed as robust sources for climate projections that can be used as input to regional impact assessments.



REFERENCES

1. Hartmann, D.L., A.M.G. Klein Tank, M. Rusticucci, L.V. Alexander, S. Brönnimann, Y. Charabi, F.J. Dentener, E.J. Dlugokencky, D.R. Easterling, A. Kaplan, B.J. Soden, P.W. Thorne, M. Wild, and P.M. Zhai, 2013: Observations: Atmosphere and surface. *Climate Change 2013: The Physical Science Basis. Contribution of Working Group I to the Fifth Assessment Report of the Intergovernmental Panel on Climate Change*. Stocker, T.F., D. Qin, G.-K. Plattner, M. Tignor, S.K. Allen, J. Boschung, A. Nauels, Y. Xia, V. Bex, and P.M. Midgley, Eds. Cambridge University Press, Cambridge, United Kingdom and New York, NY, USA, 159–254. <http://www.climatechange2013.org/report/full-report/>
2. Rhein, M., S.R. Rintoul, S. Aoki, E. Campos, D. Chambers, R.A. Feely, S. Gulev, G.C. Johnson, S.A. Josey, A. Kostianoy, C. Mauritzen, D. Roemmich, L.D. Talley, and F. Wang, 2013: Observations: Ocean. *Climate Change 2013: The Physical Science Basis. Contribution of Working Group I to the Fifth Assessment Report of the Intergovernmental Panel on Climate Change*. Stocker, T.F., D. Qin, G.-K. Plattner, M. Tignor, S.K. Allen, J. Boschung, A. Nauels, Y. Xia, V. Bex, and P.M. Midgley, Eds. Cambridge University Press, Cambridge, United Kingdom and New York, NY, USA, 255–316. <http://www.climatechange2013.org/report/full-report/>
3. Collins, M., R. Knutti, J. Arblaster, J.-L. Dufresne, T. Fichefet, P. Friedlingstein, X. Gao, W.J. Gutowski, T. Johns, G. Krinner, M. Shongwe, C. Tebaldi, A.J. Weaver, and M. Wehner, 2013: Long-term climate change: Projections, commitments and irreversibility. *Climate Change 2013: The Physical Science Basis. Contribution of Working Group I to the Fifth Assessment Report of the Intergovernmental Panel on Climate Change*. Stocker, T.F., D. Qin, G.-K. Plattner, M. Tignor, S.K. Allen, J. Boschung, A. Nauels, Y. Xia, V. Bex, and P.M. Midgley, Eds. Cambridge University Press, Cambridge, United Kingdom and New York, NY, USA, 1029–1136. <http://www.climatechange2013.org/report/full-report/>
4. Tans, P. and R. Keeling, 2017: Trends in Atmospheric Carbon Dioxide. Annual Mean Growth Rate of CO₂ at Mauna Loa. NOAA Earth System Research Laboratory. <https://www.esrl.noaa.gov/gmd/ccgg/trends/gr.html>
5. Raupach, M.R., G. Marland, P. Ciais, C. Le Quéré, J.G. Canadell, G. Klepper, and C.B. Field, 2007: Global and regional drivers of accelerating CO₂ emissions. *Proceedings of the National Academy of Sciences*, **104**, 10288–10293. <http://dx.doi.org/10.1073/pnas.0700609104>
6. Le Quéré, C., M.R. Raupach, J.G. Canadell, G. Marland, L. Bopp, P. Ciais, T.J. Conway, S.C. Doney, R.A. Feely, P. Foster, P. Friedlingstein, K. Gurney, R.A. Houghton, J.I. House, C. Huntingford, P.E. Levy, M.R. Lomas, J. Majkut, N. Metz, J.P. Ometto, G.P. Peters, I.C. Prentice, J.T. Randerson, S.W. Running, J.L. Sarmiento, U. Schuster, S. Sitch, T. Takahashi, N. Viovy, G.R. van der Werf, and F.I. Woodward, 2009: Trends in the sources and sinks of carbon dioxide. *Nature Geoscience*, **2**, 831–836. <http://dx.doi.org/10.1038/ngeo689>
7. Bowen, G.J., B.J. Maibauer, M.J. Kraus, U. Rohl, T. Westerhold, A. Steimke, P.D. Gingerich, S.L. Wing, and W.C. Clyde, 2015: Two massive, rapid releases of carbon during the onset of the Palaeocene-Eocene thermal maximum. *Nature Geoscience*, **8**, 44–47. <http://dx.doi.org/10.1038/ngeo2316>
8. Kirtland Turner, S., P.F. Sexton, C.D. Charles, and R.D. Norris, 2014: Persistence of carbon release events through the peak of early Eocene global warmth. *Nature Geoscience*, **7**, 748–751. <http://dx.doi.org/10.1038/ngeo2240>
9. Penman, D.E., B. Hönisch, R.E. Zeebe, E. Thomas, and J.C. Zachos, 2014: Rapid and sustained surface ocean acidification during the Paleocene-Eocene Thermal Maximum. *Paleoceanography*, **29**, 357–369. <http://dx.doi.org/10.1002/2014PA002621>
10. Crowley, T.J., 1990: Are there any satisfactory geologic analogs for a future greenhouse warming? *Journal of Climate*, **3**, 1282–1292. [http://dx.doi.org/10.1175/1520-0442\(1990\)003<1282:atasga>2.0.co;2](http://dx.doi.org/10.1175/1520-0442(1990)003<1282:atasga>2.0.co;2)
11. Zeebe, R.E., A. Ridgwell, and J.C. Zachos, 2016: Anthropogenic carbon release rate unprecedented during the past 66 million years. *Nature Geoscience*, **9**, 325–329. <http://dx.doi.org/10.1038/ngeo2681>
12. Jackson, R.B., J.G. Canadell, C. Le Quere, R.M. Andrew, J.I. Korsbakken, G.P. Peters, and N. Nakićenovic, 2016: Reaching peak emissions. *Nature Climate Change*, **6**, 7–10. <http://dx.doi.org/10.1038/nclimate2892>
13. Korsbakken, J.I., G.P. Peters, and R.M. Andrew, 2016: Uncertainties around reductions in China's coal use and CO₂ emissions. *Nature Climate Change*, **6**, 687–690. <http://dx.doi.org/10.1038/nclimate2963>
14. IEA, 2016: Decoupling of global emissions and economic growth confirmed. International Energy Agency, March 16. <https://www.iea.org/newsroomandevents/pressreleases/2016/march/decoupling-of-global-emissions-and-economic-growth-confirmed.html>
15. Green, F. and N. Stern, 2016: China's changing economy: Implications for its carbon dioxide emissions. *Climate Policy*, **17**, 423–442. <http://dx.doi.org/10.1080/14693062.2016.1156515>



16. Bretherton, F., K. Bryan, J. Woods, J. Hansen, M. Hoffert, X. Jiang, S. Manabe, G. Meehl, S. Raper, D. Rind, M. Schlesinger, R. Stouffer, T. Volk, and T. Wigley, 1990: Time-dependent greenhouse-gas-induced climate change. *Climate Change: The IPCC Scientific Assessment Report prepared for Intergovernmental Panel on Climate Change by Working Group I* Houghton, J.T., G.J. Jenkins, and J.J. Ephraums, Eds. Cambridge University Press, Cambridge, United Kingdom and New York, NY, USA, 173-193. https://www.ipcc.ch/publications_and_data/publications_ipcc_first_assessment_1990_wg1.shtml
17. UNFCCC, 2015: Paris Agreement. United Nations Framework Convention on Climate Change, [Bonn, Germany]. 25 pp. http://unfccc.int/files/essential_background/convention/application/pdf/english_paris_agreement.pdf
18. Smith, P., S.J. Davis, F. Creutzig, S. Fuss, J. Minx, B. Gabrielle, E. Kato, R.B. Jackson, A. Cowie, E. Kriegler, D.P. van Vuuren, J. Rogelj, P. Ciais, J. Milne, J.G. Canadell, D. McCollum, G. Peters, R. Andrew, V. Krey, G. Shrestha, P. Friedlingstein, T. Gasser, A. Grubler, W.K. Heidug, M. Jonas, C.D. Jones, F. Kraxner, E. Littleton, J. Lowe, J.R. Moreira, N. Nakicenovic, M. Obersteiner, A. Patwardhan, M. Rogner, E. Rubin, A. Sharifi, A. Torvanger, Y. Yamagata, J. Edmonds, and C. Yongsung, 2016: Biophysical and economic limits to negative CO₂ emissions. *Nature Climate Change*, 6, 42-50. <http://dx.doi.org/10.1038/nclimate2870>
19. IPCC, 1990: *Climate Change: The IPCC Scientific Assessment*. Houghton, J.T., G.J. Jenkins, and J.J. Ephraums, Eds. Cambridge University Press, Cambridge, United Kingdom and New York, NY, USA, 212 pp. https://www.ipcc.ch/publications_and_data/publications_ipcc_first_assessment_1990_wg1.shtml
20. Leggett, J., W.J. Pepper, R.J. Swart, J. Edmonds, L.G.M. Filho, I. Mintzer, M.X. Wang, and J. Watson, 1992: Emissions scenarios for the IPCC: An update. *Climate Change 1992: The Supplementary Report to the IPCC Scientific Assessment*. Houghton, J.T., B.A. Callander, and S.K. Varney, Eds. Cambridge University Press, Cambridge, United Kingdom, New York, NY, USA, and Victoria, Australia, 73-95. https://www.ipcc.ch/ipccreports/1992%20IPCC%20Supplement/IPCC_Suppl_Report_1992_wg_I/ipcc_wg_I_1992_suppl_report_section_a3.pdf
21. Nakicenovic, N., J. Alcamo, G. Davis, B.d. Vries, J. Fenhann, S. Gaffin, K. Gregory, A. Grübler, T.Y. Jung, T. Kram, E.L.L. Rovere, L. Michaelis, S. Mori, T. Morita, W. Pepper, H. Pitcher, L. Price, K. Riahi, A. Roehrl, H.-H. Rogner, A. Sankovski, M. Schlesinger, P. Shukla, S. Smith, R. Swart, S.v. Rooijen, N. Victor, and Z. Dadi, 2000: IPCC Special Report on Emissions Scenarios. Nakicenovic, N. and R. Swart (Eds.). Cambridge University Press. <http://www.ipcc.ch/ipccreports/sres/emission/index.php?idp=0>
22. Moss, R.H., J.A. Edmonds, K.A. Hibbard, M.R. Manning, S.K. Rose, D.P. van Vuuren, T.R. Carter, S. Emori, M. Kainuma, T. Kram, G.A. Meehl, J.F.B. Mitchell, N. Nakicenovic, K. Riahi, S.J. Smith, R.J. Stouffer, A.M. Thomson, J.P. Weyant, and T.J. Wilbanks, 2010: The next generation of scenarios for climate change research and assessment. *Nature*, 463, 747-756. <http://dx.doi.org/10.1038/nature08823>
23. Kattenberg, A., F. Giorgi, H. Grassl, G. Meehl, J. Mitchell, R. Stouffer, T. Tokioka, A. Weaver, and T. Wigley, 1996: Climate models - projections of future climate. *Climate Change 1995: The Science of Climate Change. Contribution of Working Group I to the Second Assessment Report of the Intergovernmental Panel on Climate Change*. Houghton, J.T., L.G. Meira Filho, B.A. Callander, N. Harris, A. Kattenberg, and K. Maskell, Eds. Cambridge University Press, Cambridge, United Kingdom and New York, NY, USA, 285-358. https://www.ipcc.ch/ipccreports/sar/wg_I/ipcc_sar_wg_I_full_report.pdf
24. Cubasch, U., G. Meehl, G. Boer, R. Stouffer, M. Dix, A. Noda, C. Senior, S. Raper, and K. Yap, 2001: Projections of future climate change. *Climate Change 2001: The Scientific Basis. Contribution of Working Group I to the Third Assessment Report of the Intergovernmental Panel on Climate Change*. Houghton, J.T., Y. Ding, D.J. Griggs, M. Noquer, P.J. van der Linden, X. Dai, K. Maskell, and C.A. Johnson, Eds. Cambridge University Press, Cambridge, United Kingdom and New York, NY, USA, 525-582. <https://www.ipcc.ch/ipccreports/tar/wg1/pdf/TAR-09.PDF>
25. NASTI, 2001: Climate Change Impacts on the United States: The Potential Consequences of Climate Variability and Change, Report for the US Global Change Research Program. U.S. Global Climate Research Program, National Assessment Synthesis Team, Cambridge, UK. 620 pp. <http://www.globalchange.gov/browse/reports/climate-change-impacts-united-states-potential-consequences-climate-variability-and-3>
26. Karl, T.R., J.T. Melillo, and T.C. Peterson, eds., 2009: *Global Climate Change Impacts in the United States*. Cambridge University Press: New York, NY, 189 pp. <http://downloads.globalchange.gov/usimpacts/pdfs/climate-impacts-report.pdf>
27. Melillo, J.M., T.C. Richmond, and G.W. Yohe, eds., 2014: *Climate Change Impacts in the United States: The Third National Climate Assessment*. U.S. Global Change Research Program: Washington, D.C., 841 pp. <http://dx.doi.org/10.7930/JOZ31WJ2>



28. Meehl, G.A., T.F. Stocker, W.D. Collins, P. Friedlingstein, A.T. Gaye, J.M. Gregory, A. Kitoh, R. Knutti, J.M. Murphy, A. Noda, S.C.B. Raper, I.G. Watterson, A.J. Weaver, and Z.-C. Zhao, 2007: Ch. 10: Global climate projections. *Climate Change 2007: The Physical Science Basis: Contribution of Working Group I to the Fourth Assessment Report of the Intergovernmental Panel on Climate Change*. Solomon, S., D. Qin, M. Manning, Z. Chen, M. Marquis, K.B. Averyt, M. Tignor, and H.L. Miller, Eds. Cambridge University Press, Cambridge, UK and New York, NY, 747-845. <http://www.ipcc.ch/pdf/assessment-report/ar4/wg1/ar4-wg1-chapter10.pdf>
29. van Vuuren, D.P., S. Deetman, M.G.J. den Elzen, A. Hof, M. Isaac, K. Klein Goldewijk, T. Kram, A. Mendoza Beltran, E. Stehfest, and J. van Vliet, 2011: RCP2.6: Exploring the possibility to keep global mean temperature increase below 2°C. *Climatic Change*, **109**, 95-116. <http://dx.doi.org/10.1007/s10584-011-0152-3>
30. Thomson, A.M., K.V. Calvin, S.J. Smith, G.P. Kyle, A. Volke, P. Patel, S. Delgado-Arias, B. Bond-Lamberty, M.A. Wise, and L.E. Clarke, 2011: RCP4.5: A pathway for stabilization of radiative forcing by 2100. *Climatic Change*, **109**, 77-94. <http://dx.doi.org/10.1007/s10584-011-0151-4>
31. Masui, T., K. Matsumoto, Y. Hijioka, T. Kinoshita, T. Nozawa, S. Ishiwatari, E. Kato, P.R. Shukla, Y. Yamagata, and M. Kainuma, 2011: An emission pathway for stabilization at 6 Wm⁻² radiative forcing. *Climatic Change*, **109**, 59. <http://dx.doi.org/10.1007/s10584-011-0150-5>
32. Riahi, K., S. Rao, V. Krey, C. Cho, V. Chirkov, G. Fischer, G. Kindermann, N. Nakicenovic, and P. Rafaj, 2011: RCP 8.5—A scenario of comparatively high greenhouse gas emissions. *Climatic Change*, **109**, 33-57. <http://dx.doi.org/10.1007/s10584-011-0149-y>
33. Meinshausen, M., S.J. Smith, K. Calvin, J.S. Daniel, M.L.T. Kainuma, J.-F. Lamarque, K. Matsumoto, S.A. Montzka, S.C.B. Raper, K. Riahi, A. Thomson, G.J.M. Velders, and D.P.P. van Vuuren, 2011: The RCP greenhouse gas concentrations and their extensions from 1765 to 2300. *Climatic Change*, **109**, 213-241. <http://dx.doi.org/10.1007/s10584-011-0156-z>
34. Cubasch, U., D. Wuebbles, D. Chen, M.C. Facchini, D. Frame, N. Mahowald, and J.-G. Winther, 2013: Introduction. *Climate Change 2013: The Physical Science Basis. Contribution of Working Group I to the Fifth Assessment Report of the Intergovernmental Panel on Climate Change*. Stocker, T.F., D. Qin, G.-K. Plattner, M. Tignor, S.K. Allen, J. Boschung, A. Nauels, Y. Xia, V. Bex, and P.M. Midgley, Eds. Cambridge University Press, Cambridge, United Kingdom and New York, NY, USA, 119-158. <http://www.climatechange2013.org/report/full-report/>
35. O'Neill, B.C., E. Kriegler, K. Riahi, K.L. Ebi, S. Hallegatte, T.R. Carter, R. Mathur, and D.P. van Vuuren, 2014: A new scenario framework for climate change research: The concept of shared socioeconomic pathways. *Climatic Change*, **122**, 387-400. <http://dx.doi.org/10.1007/s10584-013-0905-2>
36. IIASA, 2016: RCP Database. Version 2.0.5. International Institute for Applied Systems Analysis. <https://tntcat.iiasa.ac.at/RcpDb/dsd?Action=html-page&page=compare>
37. Sanderson, B.M., B.C. O'Neill, and C. Tebaldi, 2016: What would it take to achieve the Paris temperature targets? *Geophysical Research Letters*, **43**, 7133-7142. <http://dx.doi.org/10.1002/2016GL069563>
38. NRC, 2011: *Climate Stabilization Targets: Emissions, Concentrations, and Impacts over Decades to Millennia*. National Research Council. The National Academies Press, Washington, D.C., 298 pp. <http://dx.doi.org/10.17226/12877>
39. Frieler, K., M. Meinshausen, A. Golly, M. Mengel, K. Lebek, S.D. Donner, and O. Hoegh-Guldberg, 2013: Limiting global warming to 2°C is unlikely to save most coral reefs. *Nature Climate Change*, **3**, 165-170. <http://dx.doi.org/10.1038/nclimate1674>
40. Swain, S. and K. Hayhoe, 2015: CMIP5 projected changes in spring and summer drought and wet conditions over North America. *Climate Dynamics*, **44**, 2737-2750. <http://dx.doi.org/10.1007/s00382-014-2255-9>
41. Herger, N., B.M. Sanderson, and R. Knutti, 2015: Improved pattern scaling approaches for the use in climate impact studies. *Geophysical Research Letters*, **42**, 3486-3494. <http://dx.doi.org/10.1002/2015GL063569>
42. Mitchell, T.D., 2003: Pattern scaling: An examination of the accuracy of the technique for describing future climates. *Climatic Change*, **60**, 217-242. <http://dx.doi.org/10.1023/a:1026035305597>
43. Fix, M.J., D. Cooley, S.R. Sain, and C. Tebaldi, 2016: A comparison of U.S. precipitation extremes under RCP8.5 and RCP4.5 with an application of pattern scaling. *Climatic Change*, **First online**, 1-13. <http://dx.doi.org/10.1007/s10584-016-1656-7>
44. Tebaldi, C. and J.M. Arblaster, 2014: Pattern scaling: Its strengths and limitations, and an update on the latest model simulations. *Climatic Change*, **122**, 459-471. <http://dx.doi.org/10.1007/s10584-013-1032-9>
45. Schneider, R., J. Schmitt, P. Köhler, F. Joos, and H. Fischer, 2013: A reconstruction of atmospheric carbon dioxide and its stable carbon isotopic composition from the penultimate glacial maximum to the last glacial inception. *Climate of the Past*, **9**, 2507-2523. <http://dx.doi.org/10.5194/cp-9-2507-2013>



46. Lunt, D.J., T. Dunkley Jones, M. Heinemann, M. Huber, A. LeGrande, A. Winguth, C. Loptson, J. Marotzke, C.D. Roberts, J. Tindall, P. Valdes, and C. Winguth, 2012: A model-data comparison for a multi-model ensemble of early Eocene atmosphere-ocean simulations: EoMIP. *Climate of the Past*, **8**, 1717-1736. <http://dx.doi.org/10.5194/cp-8-1717-2012>
47. Otto-Bliesner, B.L., N. Rosenbloom, E.J. Stone, N.P. McKay, D.J. Lunt, E.C. Brady, and J.T. Overpeck, 2013: How warm was the last interglacial? New model-data comparisons. *Philosophical Transactions of the Royal Society A: Mathematical, Physical and Engineering Sciences*, **371**, 20130097. <http://dx.doi.org/10.1098/rsta.2013.0097>
48. NEEM, 2013: Eemian interglacial reconstructed from a Greenland folded ice core. *Nature*, **493**, 489-494. <http://dx.doi.org/10.1038/nature11789>
49. Jouzel, J., V. Masson-Delmotte, O. Cattani, G. Dreyfus, S. Falourd, G. Hoffmann, B. Minster, J. Nouet, J.M. Barnola, J. Chappellaz, H. Fischer, J.C. Gallet, S. Johnsen, M. Leuenberger, L. Loulergue, D. Luethi, H. Oerter, F. Parrenin, G. Raisbeck, D. Raynaud, A. Schilt, J. Schwander, E. Selmo, R. Souchez, R. Spahni, B. Stauffer, J.P. Steffensen, B. Stenni, T.F. Stocker, J.L. Tison, M. Werner, and E.W. Wolff, 2007: Orbital and millennial Antarctic climate variability over the past 800,000 years. *Science*, **317**, 793-796. <http://dx.doi.org/10.1126/science.1141038>
50. Kopp, R.E., F.J. Simons, J.X. Mitrovica, A.C. Maloof, and M. Oppenheimer, 2009: Probabilistic assessment of sea level during the last interglacial stage. *Nature*, **462**, 863-867. <http://dx.doi.org/10.1038/nature08686>
51. Seki, O., G.L. Foster, D.N. Schmidt, A. Mackensen, K. Kawamura, and R.D. Pancost, 2010: Alkenone and boron-based Pliocene pCO₂ records. *Earth and Planetary Science Letters*, **292**, 201-211. <http://dx.doi.org/10.1016/j.epsl.2010.01.037>
52. Haywood, A.M., D.J. Hill, A.M. Dolan, B.L. Otto-Bliesner, F. Bragg, W.L. Chan, M.A. Chandler, C. Contoux, H.J. Dowsett, A. Jost, Y. Kamae, G. Lohmann, D.J. Lunt, A. Abe-Ouchi, S.J. Pickering, G. Ramstein, N.A. Rosenbloom, U. Salzmann, L. Sohl, C. Stepanek, H. Ueda, Q. Yan, and Z. Zhang, 2013: Large-scale features of Pliocene climate: Results from the Pliocene Model Intercomparison Project. *Climate of the Past*, **9**, 191-209. <http://dx.doi.org/10.5194/cp-9-191-2013>
53. Dutton, A., A.E. Carlson, A.J. Long, G.A. Milne, P.U. Clark, R. DeConto, B.P. Horton, S. Rahmstorf, and M.E. Raymo, 2015: Sea-level rise due to polar ice-sheet mass loss during past warm periods. *Science*, **349**, aaa4019. <http://dx.doi.org/10.1126/science.aaa4019>
54. Miller, K.G., J.D. Wright, J.V. Browning, A. Kulpecz, M. Kominz, T.R. Naish, B.S. Cramer, Y. Rosenthal, W.R. Peltier, and S. Sosdian, 2012: High tide of the warm Pliocene: Implications of global sea level for Antarctic deglaciation. *Geology*, **40**, 407-410. <http://dx.doi.org/10.1130/g32869.1>
55. Jagniecki, E.A., T.K. Lowenstein, D.M. Jenkins, and R.V. Demicco, 2015: Eocene atmospheric CO₂ from the nahcolite proxy. *Geology*, **43**, 1075-1078. <http://dx.doi.org/10.1130/g36886.1>
56. Royer, D.L., 2014: 6.11 - Atmospheric CO₂ and O₂ during the Phanerozoic: Tools, patterns, and impacts. *Treatise on Geochemistry (Second Edition)*. Holland, H.D. and K.K. Turekian, Eds. Elsevier, Amsterdam, Netherlands, 251-267. <http://dx.doi.org/10.1016/B978-0-08-095975-7.01311-5>
57. Pagani, M., M. Huber, Z. Liu, S.M. Bohaty, J. Henderiks, W. Sijp, S. Krishnan, and R.M. DeConto, 2011: The role of carbon dioxide during the onset of Antarctic glaciation. *Science*, **334**, 1261-1264. <http://dx.doi.org/10.1126/science.1203909>
58. DeConto, R.M. and D. Pollard, 2016: Contribution of Antarctica to past and future sea-level rise. *Nature*, **531**, 591-597. <http://dx.doi.org/10.1038/nature17145>
59. Gasson, E., D.J. Lunt, R. DeConto, A. Goldner, M. Heinemann, M. Huber, A.N. LeGrande, D. Pollard, N. Sahoo, M. Siddall, A. Winguth, and P.J. Valdes, 2014: Uncertainties in the modelled CO₂ threshold for Antarctic glaciation. *Climate of the Past*, **10**, 451-466. <http://dx.doi.org/10.5194/cp-10-451-2014>
60. Vaughan, D.G., J.C. Comiso, I. Allison, J. Carrasco, G. Kaser, R. Kwok, P. Mote, T. Murray, F. Paul, J. Ren, E. Rignot, O. Solomina, K. Steffen, and T. Zhang, 2013: Observations: Cryosphere. *Climate Change 2013: The Physical Science Basis. Contribution of Working Group I to the Fifth Assessment Report of the Intergovernmental Panel on Climate Change*. Stocker, T.F., D. Qin, G.-K. Plattner, M. Tignor, S.K. Allen, J. Boschung, A. Nauels, Y. Xia, V. Bex, and P.M. Midgley, Eds. Cambridge University Press, Cambridge, United Kingdom and New York, NY, USA, 317-382. <http://www.climatechange2013.org/report/full-report/>
61. Kirtman, B., S.B. Power, J.A. Adedoyin, G.J. Boer, R. Bojariu, I. Camilloni, F.J. Doblas-Reyes, A.M. Fiore, M. Kimoto, G.A. Meehl, M. Prather, A. Sarr, C. Schär, R. Sutton, G.J. van Oldenborgh, G. Vecchi, and H.J. Wang, 2013: Near-term climate change: Projections and predictability. *Climate Change 2013: The Physical Science Basis. Contribution of Working Group I to the Fifth Assessment Report of the Intergovernmental Panel on Climate Change*. Stocker, T.F., D. Qin, G.-K. Plattner, M. Tignor, S.K. Allen, J. Boschung, A. Nauels, Y. Xia, V. Bex, and P.M. Midgley, Eds. Cambridge University Press, Cambridge, UK and New York, NY, USA, 953-1028. <http://www.climatechange2013.org/report/full-report/>



62. Vaittinada Ayar, P., M. Vrac, S. Bastin, J. Carreau, M. Déqué, and C. Gallardo, 2016: Intercomparison of statistical and dynamical downscaling models under the EURO- and MED-CORDEX initiative framework: Present climate evaluations. *Climate Dynamics*, **46**, 1301-1329. <http://dx.doi.org/10.1007/s00382-015-2647-5>
63. Pierce, D.W., D.R. Cayan, and B.L. Thrasher, 2014: Statistical downscaling using Localized Constructed Analogs (LOCA). *Journal of Hydrometeorology*, **15**, 2558-2585. <http://dx.doi.org/10.1175/jhm-d-14-0082.1>
64. Flato, G., J. Marotzke, B. Abiodun, P. Braconnot, S.C. Chou, W. Collins, P. Cox, F. Driouech, S. Emori, V. Eyring, C. Forest, P. Gleckler, E. Guilyardi, C. Jakob, V. Kattsov, C. Reason, and M. Rummukainen, 2013: Evaluation of climate models. *Climate Change 2013: The Physical Science Basis. Contribution of Working Group I to the Fifth Assessment Report of the Intergovernmental Panel on Climate Change*. Stocker, T.F., D. Qin, G.-K. Plattner, M. Tignor, S.K. Allen, J. Boschung, A. Nauels, Y. Xia, V. Bex, and P.M. Midgley, Eds. Cambridge University Press, Cambridge, United Kingdom and New York, NY, USA, 741-866. <http://www.climatechange2013.org/report/full-report/>
65. Knutti, R. and J. Sedláček, 2013: Robustness and uncertainties in the new CMIP5 climate model projections. *Nature Climate Change*, **3**, 369-373. <http://dx.doi.org/10.1038/nclimate1716>
66. Kumar, D., E. Kodra, and A.R. Ganguly, 2014: Regional and seasonal intercomparison of CMIP3 and CMIP5 climate model ensembles for temperature and precipitation. *Climate Dynamics*, **43**, 2491-2518. <http://dx.doi.org/10.1007/s00382-014-2070-3>
67. Sheffield, J., A.P. Barrett, B. Colle, D.N. Fernando, R. Fu, K.L. Geil, Q. Hu, J. Kinter, S. Kumar, B. Langenbrunner, K. Lombardo, L.N. Long, E. Maloney, A. Mariotti, J.E. Meyerson, K.C. Mo, J.D. Neelin, S. Nigam, Z. Pan, T. Ren, A. Ruiz-Barradas, Y.L. Serra, A. Seth, J.M. Thibeault, J.C. Stroeve, Z. Yang, and L. Yin, 2013: North American climate in CMIP5 experiments. Part I: Evaluation of historical simulations of continental and regional climatology. *Journal of Climate*, **26**, 9209-9245. <http://dx.doi.org/10.1175/jcli-d-12-00592.1>
68. Sheffield, J., A. Barrett, D. Barrie, S.J. Camargo, E.K.M. Chang, B. Colle, D.N. Fernando, R. Fu, K.L. Geil, Q. Hu, X. Jiang, N. Johnson, K.B. Karnauskas, S.T. Kim, J. Kinter, S. Kumar, B. Langenbrunner, K. Lombardo, L.N. Long, E. Maloney, A. Mariotti, J.E. Meyerson, K.C. Mo, J.D. Neelin, S. Nigam, Z. Pan, T. Ren, A. Ruiz-Barradas, R. Seager, Y.L. Serra, A. Seth, D.-Z. Sun, J.M. Thibeault, J.C. Stroeve, C. Wang, S.-P. Xie, Z. Yang, L. Yin, J.-Y. Yu, T. Zhang, and M. Zhao, 2014: Regional Climate Processes and Projections for North America: CMIP3/CMIP5 Differences, Attribution and Outstanding Issues. NOAA Technical Report OAR CPO-2. NOAA Climate Program Office, Silver Spring, MD. 47 pp. <http://dx.doi.org/10.7289/V5D-B7ZRC>
69. Bellenger, H., E. Guilyardi, J. Leloup, M. Lengaigne, and J. Vialard, 2014: ENSO representation in climate models: From CMIP3 to CMIP5. *Climate Dynamics*, **42**, 1999-2018. <http://dx.doi.org/10.1007/s00382-013-1783-z>
70. Lauer, A. and K. Hamilton, 2013: Simulating clouds with global climate models: A comparison of CMIP5 results with CMIP3 and satellite data. *Journal of Climate*, **26**, 3823-3845. <http://dx.doi.org/10.1175/jcli-d-12-00451.1>
71. Wang, M. and J.E. Overland, 2012: A sea ice free summer Arctic within 30 years: An update from CMIP5 models. *Geophysical Research Letters*, **39**, L18501. <http://dx.doi.org/10.1029/2012GL052868>
72. Knutson, T.R., J.J. Sirutis, G.A. Vecchi, S. Garner, M. Zhao, H.-S. Kim, M. Bender, R.E. Tuleya, I.M. Held, and G. Villarini, 2013: Dynamical downscaling projections of twenty-first-century Atlantic hurricane activity: CMIP3 and CMIP5 model-based scenarios. *Journal of Climate*, **27**, 6591-6617. <http://dx.doi.org/10.1175/jcli-d-12-00539.1>
73. Kharin, V.V., F.W. Zwiers, X. Zhang, and M. Wehner, 2013: Changes in temperature and precipitation extremes in the CMIP5 ensemble. *Climatic Change*, **119**, 345-357. <http://dx.doi.org/10.1007/s10584-013-0705-8>
74. Sun, L., K.E. Kunkel, L.E. Stevens, A. Buddenberg, J.G. Dobson, and D.R. Easterling, 2015: Regional Surface Climate Conditions in CMIP3 and CMIP5 for the United States: Differences, Similarities, and Implications for the U.S. National Climate Assessment. NOAA Technical Report NESDIS 144. National Oceanic and Atmospheric Administration, National Environmental Satellite, Data, and Information Service, 111 pp. <http://dx.doi.org/10.7289/V5RB72KG>
75. Knutti, R., D. Masson, and A. Gettelman, 2013: Climate model genealogy: Generation CMIP5 and how we got there. *Geophysical Research Letters*, **40**, 1194-1199. <http://dx.doi.org/10.1002/grl.50256>



76. Sanderson, B.M., R. Knutti, and P. Caldwell, 2015: A representative democracy to reduce interdependency in a multimodel ensemble. *Journal of Climate*, **28**, 5171-5194. <http://dx.doi.org/10.1175/JCLI-D-14-00362.1>
77. Kotamarthi, R., L. Mearns, K. Hayhoe, C. Castro, and D. Wuebbles, 2016: Use of Climate Information for Decision-Making and Impact Research. U.S. Department of Defense, Strategic Environment Research and Development Program Report, 55 pp. <http://dx.doi.org/10.13140/RG.2.1.1986.0085>
78. Feser, F., B. Rockel, H.v. Storch, J. Winterfeldt, and M. Zahn, 2011: Regional climate models add value to global model data: A review and selected examples. *Bulletin of the American Meteorological Society*, **92**, 1181-1192. <http://dx.doi.org/10.1175/2011BAMS3061.1>
79. Prein, A.F., W. Langhans, G. Fossier, A. Ferrone, N. Ban, K. Goergen, M. Keller, M. Tölle, O. Gutjahr, F. Feser, E. Brisson, S. Kollet, J. Schmidli, N.P.M. van Lipzig, and R. Leung, 2015: A review on regional convection-permitting climate modeling: Demonstrations, prospects, and challenges. *Reviews of Geophysics*, **53**, 323-361. <http://dx.doi.org/10.1002/2014RG000475>
80. Wang, Y., L.R. Leung, J.L. McGregor, D.-K. Lee, W.-C. Wang, Y. Ding, and F. Kimura, 2004: Regional climate modeling: Progress, challenges, and prospects. *Journal of the Meteorological Society of Japan. Series II*, **82**, 1599-1628. <http://dx.doi.org/10.2151/jmsj.82.1599>
81. Xie, S.-P., C. Deser, G.A. Vecchi, M. Collins, T.L. Delworth, A. Hall, E. Hawkins, N.C. Johnson, C. Cassou, A. Giannini, and M. Watanabe, 2015: Towards predictive understanding of regional climate change. *Nature Climate Change*, **5**, 921-930. <http://dx.doi.org/10.1038/nclimate2689>
82. Stoner, A.M.K., K. Hayhoe, X. Yang, and D.J. Wuebbles, 2012: An asynchronous regional regression model for statistical downscaling of daily climate variables. *International Journal of Climatology*, **33**, 2473-2494. <http://dx.doi.org/10.1002/joc.3603>
83. Vrac, M., M. Stein, and K. Hayhoe, 2007: Statistical downscaling of precipitation through nonhomogeneous stochastic weather typing. *Climate Research*, **34**, 169-184. <http://dx.doi.org/10.3354/cr00696>
84. Brands, S., J.M. Gutiérrez, S. Herrera, and A.S. Cofiño, 2012: On the use of reanalysis data for downscaling. *Journal of Climate*, **25**, 2517-2526. <http://dx.doi.org/10.1175/jcli-d-11-00251.1>
85. Thrasher, B., J. Xiong, W. Wang, F. Melton, A. Michaelis, and R. Nemani, 2013: Downscaled climate projections suitable for resource management. *Eos, Transactions, American Geophysical Union*, **94**, 321-323. <http://dx.doi.org/10.1002/2013EO370002>
86. Dixon, K.W., J.R. Lanzante, M.J. Nath, K. Hayhoe, A. Stoner, A. Radhakrishnan, V. Balaji, and C.F. Gaitán, 2016: Evaluating the stationarity assumption in statistically downscaled climate projections: Is past performance an indicator of future results? *Climatic Change*, **135**, 395-408. <http://dx.doi.org/10.1007/s10584-016-1598-0>
87. Deser, C., A. Phillips, V. Bourdette, and H. Teng, 2012: Uncertainty in climate change projections: The role of internal variability. *Climate Dynamics*, **38**, 527-546. <http://dx.doi.org/10.1007/s00382-010-0977-x>
88. Deser, C., R. Knutti, S. Solomon, and A.S. Phillips, 2012: Communication of the role of natural variability in future North American climate. *Nature Climate Change*, **2**, 775-779. <http://dx.doi.org/10.1038/nclimate1562>
89. Deser, C., A.S. Phillips, M.A. Alexander, and B.V. Smoliak, 2014: Projecting North American climate over the next 50 years: Uncertainty due to internal variability. *Journal of Climate*, **27**, 2271-2296. <http://dx.doi.org/10.1175/JCLI-D-13-00451.1>
90. Wang, M., J.E. Overland, V. Kattsov, J.E. Walsh, X. Zhang, and T. Pavlova, 2007: Intrinsic versus forced variation in coupled climate model simulations over the Arctic during the twentieth century. *Journal of Climate*, **20**, 1093-1107. <http://dx.doi.org/10.1175/JCLI4043.1>
91. Wang, C., L. Zhang, S.-K. Lee, L. Wu, and C.R. Mechoso, 2014: A global perspective on CMIP5 climate model biases. *Nature Climate Change*, **4**, 201-205. <http://dx.doi.org/10.1038/nclimate2118>
92. Ryu, J.-H. and K. Hayhoe, 2014: Understanding the sources of Caribbean precipitation biases in CMIP3 and CMIP5 simulations. *Climate Dynamics*, **42**, 3233-3252. <http://dx.doi.org/10.1007/s00382-013-1801-1>
93. Braconnot, P., S.P. Harrison, M. Kageyama, P.J. Bartlein, V. Masson-Delmotte, A. Abe-Ouchi, B. Otto-Bliesner, and Y. Zhao, 2012: Evaluation of climate models using palaeoclimatic data. *Nature Climate Change*, **2**, 417-424. <http://dx.doi.org/10.1038/nclimate1456>
94. Jun, M., R. Knutti, and D.W. Nychka, 2008: Local eigenvalue analysis of CMIP3 climate model errors. *Tellus A*, **60**, 992-1000. <http://dx.doi.org/10.1111/j.1600-0870.2008.00356.x>
95. Giorgi, F. and E. Coppola, 2010: Does the model regional bias affect the projected regional climate change? An analysis of global model projections. *Climatic Change*, **100**, 787-795. <http://dx.doi.org/10.1007/s10584-010-9864-z>
96. Weigel, A.P., R. Knutti, M.A. Liniger, and C. Appenzeller, 2010: Risks of model weighting in multimodel climate projections. *Journal of Climate*, **23**, 4175-4191. <http://dx.doi.org/10.1175/2010jcli3594.1>



97. Knutti, R., J. Sedláček, B.M. Sanderson, R. Lorenz, E.M. Fischer, and V. Eyring, 2017: A climate model projection weighting scheme accounting for performance and interdependence. *Geophysical Research Letters*, **44**, 1909-1918. <http://dx.doi.org/10.1002/2016GL072012>
98. Hawkins, E. and R. Sutton, 2009: The potential to narrow uncertainty in regional climate predictions. *Bulletin of the American Meteorological Society*, **90**, 1095-1107. <http://dx.doi.org/10.1175/2009BAMS2607.1>
99. Hawkins, E. and R. Sutton, 2011: The potential to narrow uncertainty in projections of regional precipitation change. *Climate Dynamics*, **37**, 407-418. <http://dx.doi.org/10.1007/s00382-010-0810-6>
100. IPCC, 2013: Summary for policymakers. *Climate Change 2013: The Physical Science Basis. Contribution of Working Group I to the Fifth Assessment Report of the Intergovernmental Panel on Climate Change*. Stocker, T.F., D. Qin, G.-K. Plattner, M. Tignor, S.K. Allen, J. Boschung, A. Nauels, Y. Xia, V. Bex, and P.M. Midgley, Eds. Cambridge University Press, Cambridge, United Kingdom and New York, NY, USA, 1-30. <http://www.climatechange2013.org/report/>
101. Archer, D. and R. Pierrehumbert, eds., 2011: *The Warming Papers: The Scientific Foundation for the Climate Change Forecast*. Wiley-Blackwell: Oxford, UK, 432 pp. <http://www.wiley.com/WileyCDA/WileyTitle/productCd-1405196165.html>
102. Masson-Delmotte, V., M. Schulz, A. Abe-Ouchi, J. Beer, A. Ganopolski, J.F. González Rouco, E. Jansen, K. Lambeck, J. Luterbacher, T. Naish, T. Osborn, B. Otto-Bliesner, T. Quinn, R. Ramesh, M. Rojas, X. Shao, and A. Timmermann, 2013: Information from paleoclimate archives. *Climate Change 2013: The Physical Science Basis. Contribution of Working Group I to the Fifth Assessment Report of the Intergovernmental Panel on Climate Change*. Stocker, T.F., D. Qin, G.-K. Plattner, M. Tignor, S.K. Allen, J. Boschung, A. Nauels, Y. Xia, V. Bex, and P.M. Midgley, Eds. Cambridge University Press, Cambridge, United Kingdom and New York, NY, USA, 383-464. <http://www.climatechange2013.org/report/full-report/>
103. Le Quéré, C., R. Moriarty, R.M. Andrew, J.G. Canadell, S. Sitch, J.I. Korsbakken, P. Friedlingstein, G.P. Peters, R.J. Andres, T.A. Boden, R.A. Houghton, J.I. House, R.F. Keeling, P. Tans, A. Arneeth, D.C.E. Bakker, L. Barbero, L. Bopp, J. Chang, F. Chevallier, L.P. Chini, P. Ciais, M. Fader, R.A. Feely, T. Gkritzalis, I. Harris, J. Hauck, T. Ilyina, A.K. Jain, É. Kato, V. Kitidis, K. Klein Goldewijk, C. Koven, P. Landschützer, S.K. Lauvset, N. Lefèvre, A. Lenton, I.D. Lima, N. Metz, F. Millero, D.R. Munro, A. Murata, J.E.M.S. Nabel, S. Nakaoka, Y. Nojiri, K. O'Brien, A. Olsen, T. Ono, F.F. Pérez, B. Pfeil, D. Pierrot, B. Poulter, G. Rehder, C. Rödenbeck, S. Saito, U. Schuster, J. Schwinger, R. Séférian, T. Steinhoff, B.D. Stocker, A.J. Sutton, T. Takahashi, B. Tilbrook, I.T. van der Laan-Luijkx, G.R. van der Werf, S. van Heuven, D. Vandemark, N. Viovy, A. Wiltshire, S. Zaehle, and N. Zeng, 2015: Global carbon budget 2015. *Earth System Science Data*, **7**, 349-396. <http://dx.doi.org/10.5194/essd-7-349-2015>





5

Large-Scale Circulation and Climate Variability

KEY FINDINGS

1. The tropics have expanded poleward by about 70 to 200 miles in each hemisphere over the period 1979–2009, with an accompanying shift of the subtropical dry zones, midlatitude jets, and storm tracks (*medium to high confidence*). Human activities have played a role in this change (*medium confidence*), although confidence is presently *low* regarding the magnitude of the human contribution relative to natural variability.
2. Recurring patterns of variability in large-scale atmospheric circulation (such as the North Atlantic Oscillation and Northern Annular Mode) and the atmosphere–ocean system (such as El Niño–Southern Oscillation) cause year-to-year variations in U.S. temperatures and precipitation (*high confidence*). Changes in the occurrence of these patterns or their properties have contributed to recent U.S. temperature and precipitation trends (*medium confidence*), although confidence is *low* regarding the size of the

Recommended Citation for Chapter

Perlwitz, J., T. Knutson, J.P. Kossin, and A.N. LeGrande, 2017: Large-scale circulation and climate variability. In: *Climate Science Special Report: Fourth National Climate Assessment, Volume I* [Wuebbles, D.J., D.W. Fahey, K.A. Hibbard, D.J. Dokken, B.C. Stewart, and T.K. Maycock (eds.)]. U.S. Global Change Research Program, Washington, DC, USA, pp. 161-184, doi: 10.7930/J0RV0KVQ.

5.1 Introduction

The causes of regional climate trends cannot be understood without considering the impact of variations in large-scale atmospheric circulation and an assessment of the role of internally generated climate variability. There are contributions to regional climate trends from changes in large-scale latitudinal circulation, which is generally organized into three cells in each hemisphere—Hadley cell, Ferrell cell and Polar cell—and which determines the location of subtropical dry zones and midlatitude jet streams (Figure 5.1). These circulation cells are expected to shift poleward during warmer periods,^{1,2,3,4} which could result in poleward shifts in precipitation patterns, affecting natural ecosystems, agriculture, and water resources.^{5,6}

In addition, regional climate can be strongly affected by non-local responses to recurring patterns (or modes) of variability of the atmospheric circulation or the coupled atmosphere–ocean system. These modes of variability represent preferred spatial patterns and their temporal variation. They account for gross features in variance and for teleconnections which describe climate links between geographically separated regions. Modes of variability are often described as a product of a spatial climate pattern and an associated climate index time series that are identified based on statistical methods like Principal Component Analysis (PC analysis), which is also called Empirical Orthogonal Function Analysis (EOF analysis), and cluster analysis.

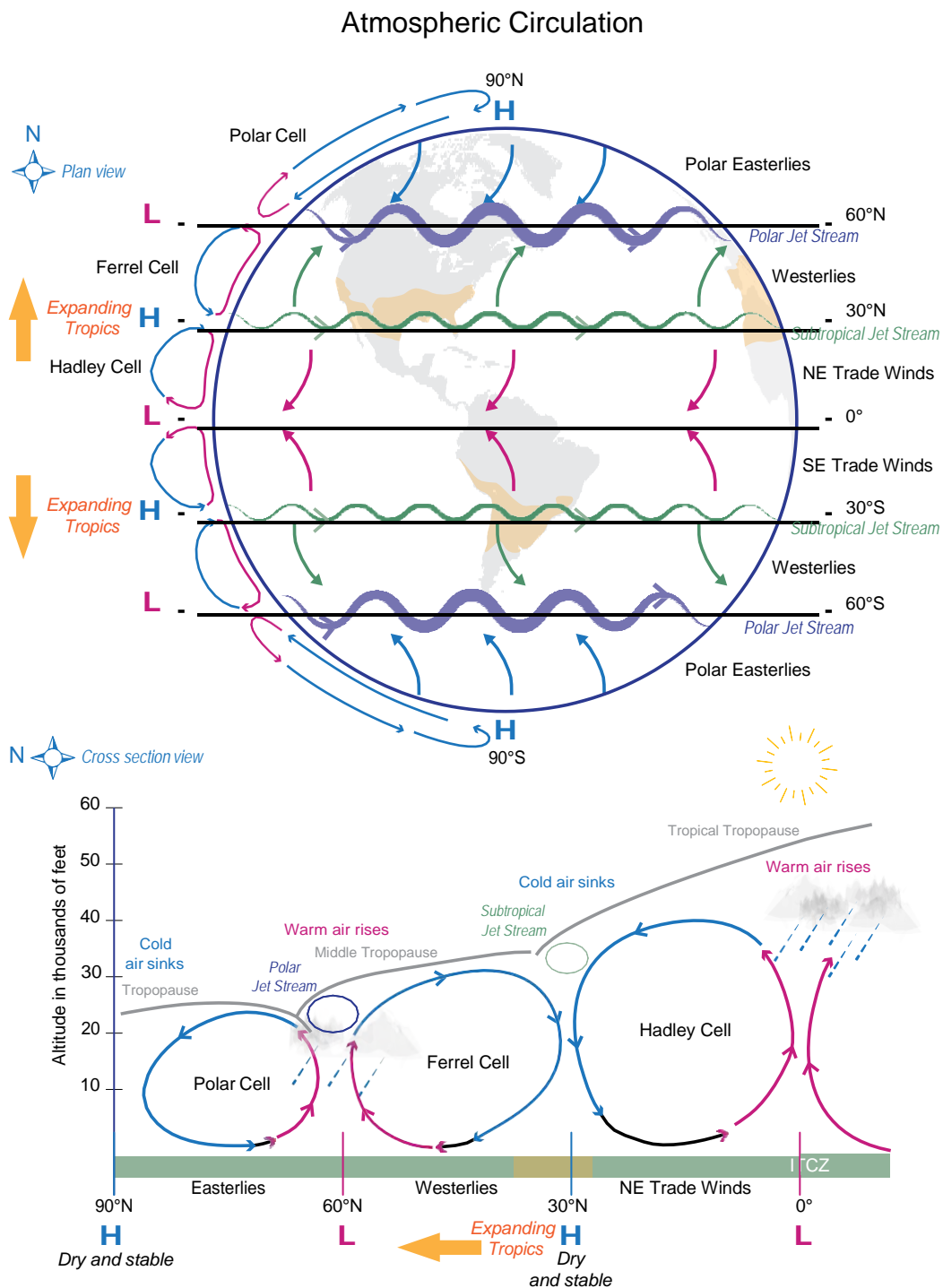


Figure 5.1: (top) Plan and (bottom) cross-section schematic view representations of the general circulation of the atmosphere. Three main circulations exist between the equator and poles due to solar heating and Earth's rotation: 1) **Hadley cell** – Low-latitude air moves toward the equator. Due to solar heating, air near the equator rises vertically and moves poleward in the upper atmosphere. 2) **Ferrel cell** – A midlatitude mean atmospheric circulation cell. In this cell, the air flows poleward and eastward near the surface and equatorward and westward at higher levels. 3) **Polar cell** – Air rises, diverges, and travels toward the poles. Once over the poles, the air sinks, forming the polar highs. At the surface, air diverges outward from the polar highs. Surface winds in the polar cell are easterly (polar easterlies). A high pressure band is located at about 30° N/S latitude, leading to dry/hot weather due to descending air motion (subtropical dry zones are indicated in orange in the schematic views). Expanding tropics (indicted by orange arrows) are associated with a poleward shift of the subtropical dry zones. A low pressure band is found at 50°–60° N/S, with rainy and stormy weather in relation to the polar jet stream bands of strong westerly wind in the upper levels of the atmosphere. (Figure source: adapted from NWS 2016¹⁷⁷).

On intraseasonal to interannual time scales, the climate of the United States is strongly affected by modes of atmospheric circulation variability like the North Atlantic Oscillation (NAO)/Northern Annular Mode (NAM), North Pacific Oscillation (NPO), and Pacific/North American Pattern (PNA).^{7, 8, 9} These modes are closely linked to other atmospheric circulation phenomena like blocking and quasi-stationary wave patterns and jet streams that can lead to weather and climate extremes.¹⁰ On an interannual time scale, coupled atmosphere–ocean phenomena like El Niño–Southern Oscillation (ENSO) have a prominent effect.¹¹ On longer time scales, U.S. climate anomalies are linked to slow variations of sea surface temperature related to the Pacific Decadal Oscillation (PDO) and the Atlantic Multidecadal Oscillation (AMO).^{12, 13, 14}

These modes of variability can affect the local-to-regional climate response to external forcing in various ways. The climate response may be altered by the forced response of these existing, recurring modes of variability.¹⁵ Further, the structure and strength of regional temperature and precipitation impacts of these recurring modes of variability may be modified due to a change in the background climate.¹⁶ Modes of internal variability of the climate system also contribute to observed decadal and multidecadal temperature and precipitation trends on local to regional scales, masking possible systematic changes due to an anthropogenic influence.¹⁷ However, there are still large uncertainties in our understanding of the impact of human-induced climate change on atmospheric circulation.^{4, 18} Furthermore, the confidence in any specific projected change in ENSO variability in the 21st century remains *low*.¹⁹

5.2 Modes of Variability: Past and Projected Changes

5.2.1 Width of the Tropics and Global Circulation

Evidence continues to mount for an expansion of the tropics over the past several decades, with a poleward expansion of the Hadley cell and an associated poleward shift of the subtropical dry zones and storm tracks in each hemisphere.^{5, 20, 21, 22, 23, 24, 25, 26, 27, 28, 29} The rate of expansion is uncertain and depends on the metrics and data sources that are used. Recent estimates of the widening of the global tropics for the period 1979–2009 range between 1° and 3° latitude (between about 70 and 200 miles) in each hemisphere, an average trend of between approximately 0.5° and 1.0° per decade.²⁶ While the roles of increasing greenhouse gases in both hemispheres,^{4, 30} stratospheric ozone depletion in the Southern Hemisphere,³¹ and anthropogenic aerosols in the Northern Hemisphere^{32, 33} have been implicated as contributors to the observed expansion, there is uncertainty in the relative contributions of natural and anthropogenic factors, and natural variability may currently be dominating.^{23, 34, 35}

Most of the previous work on tropical expansion to date has focused on zonally averaged changes. There are only a few recent studies that diagnose regional characteristics of tropical expansion. The findings depend on analysis methods and datasets. For example, a northward expansion of the tropics in most regions of the Northern Hemisphere, including the Eastern Pacific with impact on drying in the American Southwest, is found based on diagnosing outgoing longwave radiation.³⁶ However, other studies do not find a significant poleward expansion of the tropics over the Eastern Pacific and North America.^{37, 38} Thus, while some studies associate the observed drying of the U.S. Southwest with the poleward expansion of the tropics,^{5, 39} regional impacts of the observed zonally averaged changes in the width of the tropics are not understood.



Due to human-induced greenhouse gas increases, the Hadley cell is *likely* to widen in the future, with an accompanying poleward shift in the subtropical dry zones, midlatitude jets, and storm tracks.^{2, 4, 5, 40, 41, 42, 43} Large uncertainties remain in projected changes in non-zonal to regional circulation components and related changes in precipitation patterns.^{18, 40, 44, 45} Uncertainties in projected changes in midlatitude jets are also related to the projected rate of arctic amplification and variations in the stratospheric polar vortex. Both factors could shift the midlatitude jet equatorward, especially in the North Atlantic region.^{46, 47, 48, 49}

5.2.2 El Niño–Southern Oscillation

El Niño–Southern Oscillation (ENSO) is a main source of climate variability, with a two- to seven-year timescale, originating from coupled ocean–atmosphere interactions in the tropical Pacific. Major ENSO events affect weather patterns over many parts of the globe through atmospheric teleconnections. ENSO strongly affects precipitation and temperature in the United States with impacts being most pronounced during the cold season (Figure 5.2).^{11, 50, 51, 52, 53} A cooling trend of the tropical Pacific Ocean that resembles La Niña conditions contributed to drying in southwestern North America from 1979 to 2006⁵⁴ and is found to explain most of the decrease in heavy daily precipitation events in the southern United States from 1979 to 2013.⁵⁵

El Niño teleconnections are modulated by the location of maximum anomalous tropical Pacific sea surface temperatures (SST). Eastern Pacific (EP) El Niño events affect winter temperatures primarily over the Great Lakes, Northeast, and Southwest, while Central Pacific (CP) events influence temperatures primarily over the northwestern and southeastern United States.⁵⁶ The CP El Niño also enhances the drying effect, but weakens the wetting effect, typically produced by traditional EP El Niño events on U.S. winter

precipitation.⁵⁷ It is not clear whether observed decadal-scale modulations of ENSO properties, including an increase in ENSO amplitude⁵⁸ and an increase in frequency of CP El Niño events,^{59, 60} are due to internal variability or anthropogenic forcing. Uncertainties in both the diagnosed distinct U.S. climate effects of EP and CP events and causes for the decadal scale changes result from the limited sample size of observed ENSO events in each category^{61, 62} and the relatively short record of the comprehensive observations (since late 1970s) that would allow the investigation of ENSO-related coupled atmosphere–ocean feedbacks.¹⁹ Furthermore, unforced global climate model simulations show that decadal to centennial modulations of ENSO can be generated without any change in external forcing.⁶³ A model study based on large, single-model ensembles of atmospheric and coupled atmosphere–ocean models finds that external radiative forcing resulted in an atmospheric teleconnection pattern that is independent of ENSO-like variations during the 1979–2014 period and is characterized by a hemisphere-scale increasing trend in heights.⁵³

The representation of ENSO in climate models has improved from CMIP3 to CMIP5 models, especially in relation to ENSO amplitude.^{64, 65} However, CMIP5 models still cannot capture the seasonal timing of ENSO events.⁶⁶ Furthermore, they still exhibit errors in simulating key atmospheric feedbacks, and the improvement in ENSO amplitudes might therefore result from error compensations.⁶⁴ Limited observational records and the nonstationarity of tropical Pacific teleconnections to North America on multidecadal time scales pose challenges for evaluating teleconnections between ENSO and U.S. climate in coupled atmosphere–ocean models.^{61, 67} For a given SST forcing, however, the atmospheric component of CMIP5 models simulate the sign of the precipitation change over the southern section of North America.⁶⁸



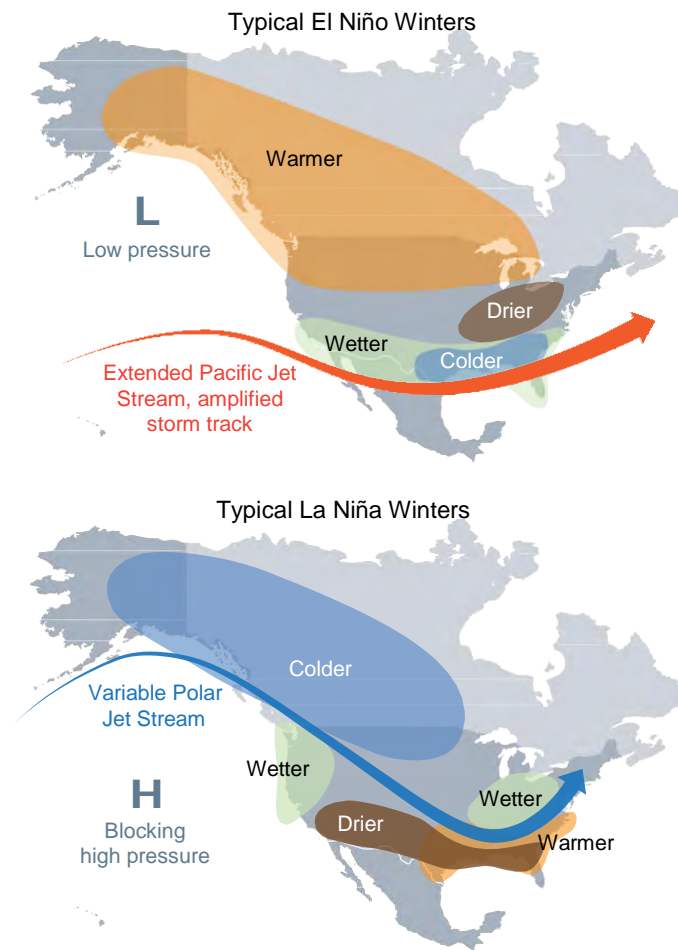


Figure 5.2: El Niño- and La Niña-related winter features over North America. Shown are typical January to March weather anomalies and atmospheric circulation during moderate to strong El Niño and La Niña conditions: (top) During El Niño, there is a tendency for a strong jet stream and storm track across the southern part of the United States. The southern tier of Alaska and the U.S. Pacific Northwest tend to be warmer than average, whereas the southern tier of United States tends to be cooler and wetter than average. (bottom) During La Niña, there is a tendency of a very wave-like jet stream flow over the United States and Canada, with colder and stormier than average conditions across the North and warmer and less stormy conditions across the South. (Figure source: adapted from Lindsey 2016¹⁷⁸).

Climate projections suggest that ENSO will remain a primary mode of natural climate variability in the 21st century.¹⁹ Climate models do not agree, however, on projected changes in the intensity or spatial pattern of ENSO.¹⁹ This uncertainty is related to a model dependence of simulated changes in the zonal gradient of tropical Pacific sea surface temperature in a warming climate.¹⁹ Model studies suggest an eastward shift of ENSO-induced teleconnection patterns due to greenhouse gas-induced climate change.^{69, 70, 71, 72} However, the impact of such a shift on ENSO-induced climate anomalies in the United States is not well understood.^{72, 73}

In summary, there is *high confidence* that, in the 21st century, ENSO will remain a main source of climate variability over the United States on seasonal to interannual timescales. There is *low confidence* for a specific projected change in ENSO variability.

5.2.3 Extra-tropical Modes of Variability and Phenomena

North Atlantic Oscillation and Northern Annular Mode

The North Atlantic Oscillation (NAO), the leading recurring mode of variability in the extratropical North Atlantic region, describes an opposing pattern of sea level pressure

between the Atlantic subtropical high and the Iceland/Arctic low. Variations in the NAO are accompanied by changes in the location and intensity of the Atlantic midlatitude storm track and blocking activity that affect climate over the North Atlantic and surrounding continents. A negative NAO phase is related to anomalously cold conditions and an enhanced number of cold outbreaks in the eastern United States, while a strong positive phase of the NAO tends to be associated with above-normal temperatures in this region.^{7, 74} The positive phase of the NAO is associated with increased precipitation frequency and positive daily rainfall anomalies, including extreme daily precipitation anomalies in the northeastern United States.^{75, 76}

The Northern Annular Mode/Arctic Oscillation (NAM/AO) is closely related to the NAO. It describes a similar out-of-phase pressure variation between mid- and high latitudes but on a hemispheric rather than regional scale.^{77, 78} The time series of the NAO and NAM/AO are highly correlated, with persistent NAO and NAM/AO events being indistinguishable.^{79, 80}

The wintertime NAO/NAM index exhibits pronounced variability on multidecadal time scales, with an increase from the 1960s to the 1990s, a shift to a more negative phase since the 1990s due to a series of winters like 2009–2010 and 2010–2011 (which had exceptionally low index values), and a return to more positive values after 2011.³⁰ Decadal scale temperature trends in the eastern United States, including occurrences of cold outbreaks during recent years, are linked to these changes in the NAO/NAM.^{81, 82, 83, 84}

The NAO's influence on the ocean occurs through changes in heat content, gyre circulations, mixed layer depth, salinity, high-latitude deep water formation, and sea ice cov-

er.^{7, 85} Climate model simulations show that multidecadal variations in the NAO induce multidecadal variations in the strength of the Atlantic Meridional Overturning Circulation (AMOC) and poleward ocean heat transport in the Atlantic, extending to the Arctic, with potential impacts on recent arctic sea ice loss and Northern Hemisphere warming.⁸⁵ However, other model simulations suggest that the NAO and recent changes in Northern Hemisphere climate were affected by recent variations in the AMOC,⁸⁶ for which enhanced freshwater discharge from the Greenland Ice Sheet (GrIS) may have been a contributing cause.⁸⁷

Climate models are widely analyzed for their ability to simulate the spatial patterns of the NAO/NAM and their relationship to temperature and precipitation anomalies over the United States.^{9, 65, 88} Climate models reproduce the broad spatial and temporal features of the NAO, although there are large differences among the individual models in the location of the NAO centers of action and their average magnitude. These differences affect the agreement between observed and simulated climate anomalies related to the NAO.^{9, 65} Climate models tend to have a NAM pattern that is more annular than observed,^{65, 88} resulting in a strong bias in the Pacific center of the NAM. As a result, temperature anomalies over the northwestern United States associated with the NAM in most models are of opposite sign compared to observation.⁸⁸ Biases in the model representation of NAO/NAM features are linked to limited abilities of general circulation models to reproduce dynamical processes, including atmospheric blocking,⁸⁹ troposphere-stratosphere coupling,⁹⁰ and climatological stationary waves.^{90, 91}

The CMIP5 models on average simulate a progressive shift of the NAO/NAM towards the positive phase due to human-induced climate change.⁹² However, the spread between model



simulations is larger than the projected multimodel increase,¹⁹ and there are uncertainties related to future scenarios.⁹ Furthermore, it is found that shifts between preferred periods of positive and negative NAO phase will continue to occur similar to those observed in the past.^{19, 93} There is no consensus on the location of changes of NAO centers among the global climate models under future warming scenarios.⁹ Uncertainties in future projections of the NAO/NAM in some seasons are linked to model spread in projected future arctic warming^{46, 47} (Ch. 11: Arctic Changes) and to how models resolve stratospheric processes.^{19, 94}

In summary, while it is *likely* that the NAO/NAM index will become slightly more positive (on average) due to increases in GHGs, there is *low confidence* in temperature and precipitation changes over the United States related to such variations in the NAO/NAM.

North Pacific Oscillation/West Pacific Oscillation

The North Pacific Oscillation (NPO) is a recurring mode of variability in the extratropical North Pacific region and is characterized by a north-south seesaw in sea level pressure. Effects of NPO on U.S. hydroclimate and marginal ice zone extent in the arctic seas have been reported.⁸

The NPO is linked to tropical sea surface temperature variability. Specifically, NPO contributes to the excitation of ENSO events via the “Seasonal Footprinting Mechanism”.⁹⁵ In turn, warm events in the central tropical Pacific Ocean are suggested to force an NPO-like circulation pattern.⁹⁷ There is *low confidence* in future projections of the NPO due to the small number of modeling studies as well as the finding that many climate models do not properly simulate the observed linkages between the NPO and tropical sea surface temperature variability.^{19, 98}

Pacific/North American Pattern

The Pacific/North American (PNA) pattern is the leading recurring mode of internal atmospheric variability over the North Pacific and the North American continent, especially during the cold season. It describes a quadrupole pattern of mid-tropospheric height anomalies, with anomalies of similar sign located over the subtropical northeastern Pacific and northwestern North America and of the opposite sign centered over the Gulf of Alaska and the southeastern United States. The PNA pattern is associated with strong fluctuations in the strength and location of the East Asian jet stream. The positive phase of the PNA pattern is associated with above average temperatures over the western and northwestern United States, and below average temperatures across the south-central and southeastern United States, including an enhanced occurrence of extreme cold temperatures.^{9, 99, 100} Significant negative correlation between the PNA and winter precipitation over the Ohio River Valley has been documented.^{9, 99, 101} The PNA is related to ENSO events¹⁰² and also serves as a bridge linking ENSO and NAO variability.¹⁰³

Climate models are able to reasonably represent the atmospheric circulation and climate anomalies associated with the PNA pattern. However, individual models exhibit differences compared to the observed relationship, due to displacements of the simulated PNA centers of action and offsets in their magnitudes.⁹ Climate models do not show consistent location changes of the PNA centers due to increases in GHGs.^{9, 72} Therefore, there is *low confidence* for projected changes in the PNA and the association with temperature and precipitation variations over the United States.

Blocking and Quasi-Stationary Waves

Anomalous atmospheric flow patterns in the extratropics that remain in place for an ex-



tended period of time (for example, blocking and quasi-stationary Rossby waves) – and thus affect a region with similar weather conditions like rain or clear sky for several days to weeks – can lead to flooding, drought, heat waves, and cold waves.^{10, 104, 105} Specifically, blocking describes large-scale, persistent high pressure systems that interrupt the typical westerly flow, while planetary waves (Rossby waves) describe large-scale meandering of the atmospheric jet stream.

A persistent pattern of high pressure in the circulation off the West Coast of the United States has been associated with the recent multiyear California drought^{106, 107, 108} (Ch. 8: Droughts, Floods, and Wildfire). Blocking in the Alaskan region, which is enhanced during La Niña winters (Figure 5.2),¹⁰⁹ is associated with higher temperatures in western Alaska but shift to lower mean and extreme surface temperatures from the Yukon southward to the southern Plains.¹¹⁰ The anomalously cold winters of 2009–2010 and 2010–2011 in the United States are linked to the blocked (or negative) phase of the NAO.¹¹¹ Stationary Rossby wave patterns may have contributed to the North American temperature extremes during summers like 2011.¹¹² It has been suggested that arctic amplification has already led to weakened westerly winds and hence more slowly moving and amplified wave patterns and enhanced occurrence of blocking^{113, 114} (Ch. 11: Arctic Changes). While some studies suggest an observed increase in the metrics of these persistent circulation patterns,^{113, 115} other studies suggest that observed changes are small compared to atmospheric internal variability.^{116, 117, 118}

A decrease of blocking frequency with climate change is found in CMIP3, CMIP5, and higher-resolution models.^{19, 119, 120} Climate models robustly project a change in Northern Hemisphere winter quasi-stationary wave fields

that are linked to a wetting of the North American West Coast,^{45, 121, 122} due to a strengthening of the zonal mean westerlies in the subtropical upper troposphere. However, CMIP5 models still underestimate observed blocking activity in the North Atlantic sector while they tend to overestimate activity in the North Pacific, although with a large intermodel spread.¹⁹ Most climate models also exhibit biases in the representation of relevant stationary waves.⁴⁴

In summary, there is *low confidence* in projected changes in atmospheric blocking and winter-time quasi-stationary waves. Therefore, our confidence is *low* on the association between observed and projected changes in weather and climate extremes over the United States and variations in these persistent atmospheric circulation patterns.

5.2.4 Modes of Variability on Decadal to Multidecadal Time Scales

Pacific Decadal Oscillation (PDO) / Interdecadal Pacific Oscillation (IPO)

The Pacific Decadal Oscillation (PDO) was first introduced by Mantua et al. 1997¹²³ as the leading empirical orthogonal function of North Pacific (20°–70°N) monthly averaged sea surface temperature anomalies.¹⁴ Interdecadal Pacific Oscillation (IPO) refers to the same phenomenon and is based on Pacific-wide sea surface temperatures. PDO/IPO lacks a characteristic timescale and represents a combination of physical processes that span the tropics and extratropics, including both remote tropical forcing and local North Pacific atmosphere–ocean interactions.¹⁴ Consequently, PDO-related variations in temperature and precipitation in the United States are very similar to (and indeed may be caused by) variations associated with ENSO and the strength of the Aleutian low (North Pacific Index, NPI), as shown in Figure 5.3. A PDO-related temperature variation in Alaska is also apparent.^{124, 125}



Cold Season Relationship between Climate Indices and Precipitation/Temperature Anomalies

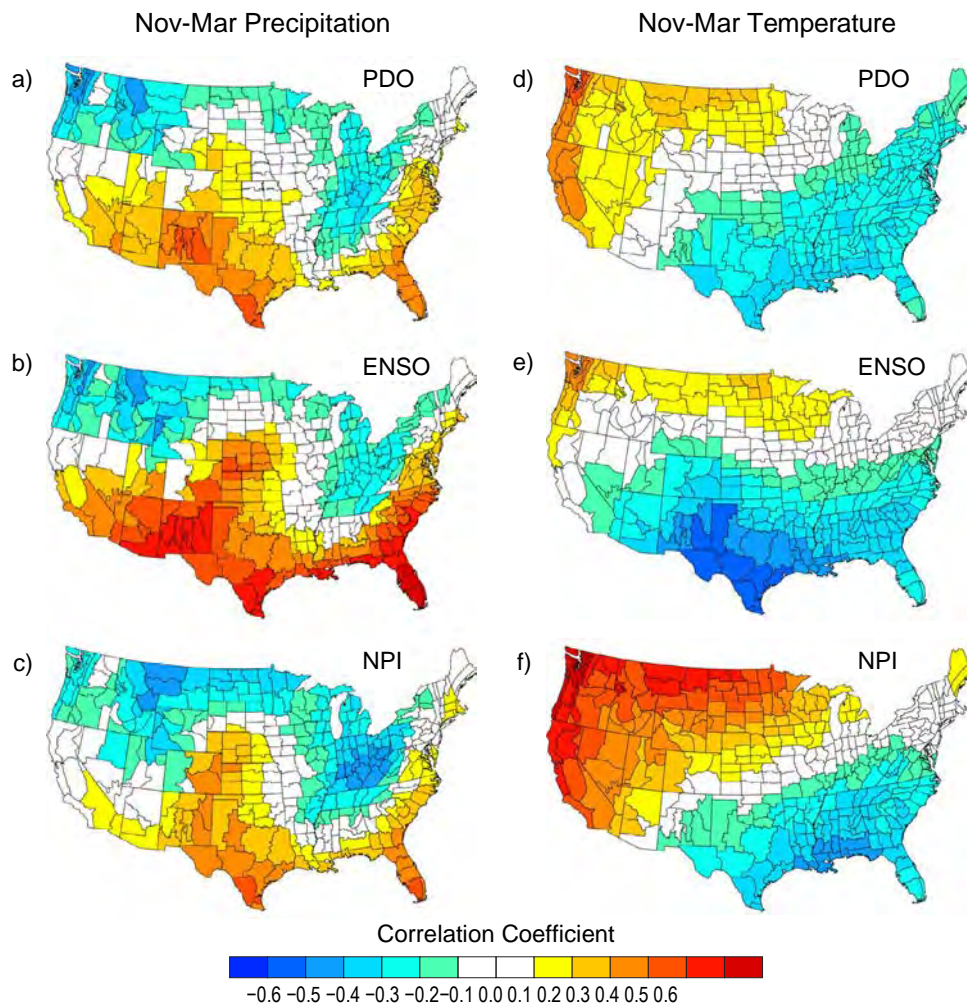


Figure 5.3: Cold season relationship between climate indices and U.S. precipitation and temperature anomalies determined from U.S. climate division data,¹⁷⁹ for the years 1901–2014. November–March mean U.S. precipitation anomalies correlated with (a) the Pacific Decadal Oscillation (PDO) index, (b) the El Niño–Southern Oscillation (ENSO) index, and (c) the North Pacific Index (NPI). November–March U.S. temperature anomalies correlated with (d) the PDO index, (e) the ENSO index, and (f) the NPI. United States temperature and precipitation related to the Pacific Decadal Oscillation are very similar to (and indeed may be caused by) variations associated with ENSO and the Aleutian low strength (North Pacific Index). (Figure source: Newman et al. 2016¹⁴; ©American Meteorological Society, used with permission).

The PDO does not show a long-term trend either in SST reconstructions or in the ensemble mean of historical CMIP3 and CMIP5 simulations.¹⁴ Emerging science suggests that externally forced natural and anthropogenic factors have contributed to the observed PDO-like variability. For example, a model study finds that the observed PDO phase is affected by large volcanic events and the variability in incoming solar radiation.¹²⁶ Aerosols from anthropogenic sources could change the

temporal variability of the North Pacific SST through modifications of the atmospheric circulation.^{127, 128} Furthermore, some studies show that periods with near-zero warming trends of global mean temperature and periods of accelerated temperatures could result from the interplay between internally generated PDO/IPO-like temperature variations in the tropical Pacific Ocean and greenhouse gas-induced ocean warming.^{129, 130}

Future changes in the spatial and temporal characteristics of PDO/IPO are uncertain. Based on CMIP3 models, one study finds that most of these models do not exhibit significant changes,⁹⁸ while another study points out that the PDO/IPO becomes weaker and more frequent by the end of the 21st century in some models.¹³¹ Furthermore, future changes in ENSO variability, which strongly contributes to the PDO/IPO,¹³² are also uncertain (Section 5.2.2). Therefore, there is *low confidence* in projected future changes in the PDO/IPO.

Atlantic Multidecadal Variability (AMV) / Atlantic Multidecadal Oscillation (AMO)

The North Atlantic Ocean region exhibits coherent multidecadal variability that exerts measurable impacts on regional climate for variables such as U.S. precipitation^{12, 133, 134, 135} and Atlantic hurricane activity.^{13, 136, 137, 138, 139, 140} This observed Atlantic multidecadal variability, or AMV, is generally understood to be driven by a combination of internal and external factors.^{12, 141, 142, 143, 144, 145, 146, 147, 148} The AMV manifests in SST variability and patterns as well as synoptic-scale variability of atmospheric conditions. The internal part of the observed AMV is often referred to as the Atlantic Multidecadal Oscillation (AMO) and is putatively driven by changes in the strength of the Atlantic Meridional Overturning Circulation (AMOC).^{142, 143, 149, 150} It is important to understand the distinction between the AMO, which is often assumed to be natural (because of its putative relationship with natural AMOC variability), and AMV, which simply represents the observed multidecadal variability as a whole.

The relationship between observed AMV and the AMOC has recently been called into question and arguments have been made that AMV can occur in the absence of the AMOC via stochastic forcing of the ocean by coherent atmospheric circulation variability, but this is

presently a topic of debate.^{151, 152, 153, 154} Despite the ongoing debates, it is generally acknowledged that observed AMV, as a whole, represents a complex conflation of natural internal variability of the AMOC, natural red-noise stochastic forcing of the ocean by the atmosphere,¹⁴⁶ natural external variability from volcanic events^{155, 156} and mineral aerosols,¹⁵⁷ and anthropogenic forcing from greenhouse gases and pollution aerosols.^{158, 159, 160, 161}

As also discussed in Chapter 9: Extreme Storms (in the context of Atlantic hurricanes), determining the relative contributions of each mechanism to the observed multidecadal variability in the Atlantic is presently an active area of research and debate, and no consensus has yet been reached.^{146, 161, 162, 163, 164, 165, 166} Still, despite the level of disagreement about the relative magnitude of human influences (particularly whether natural or anthropogenic factors are dominating), there is broad agreement in the literature of the past decade or so that human factors have had a measurable impact on the observed AMV. Furthermore, the AMO, as measured by indices constructed from environmental data (e.g., Enfield et al. 2001¹²), is generally based on detrended SST data and is then, by construction, segregated from the century-scale linear SST trends that are likely forced by increasing greenhouse gas concentrations. In particular, removal of a linear trend is not expected to account for all of the variability forced by changes in sulfate aerosol concentrations that have occurred over the past century. In this case, increasing sulfate aerosols are argued to cause cooling of Atlantic SST, thus offsetting the warming caused by increasing greenhouse gas concentration. After the Clean Air Act and Amendments of the 1970s, however, a steady reduction of sulfate aerosols is argued to have caused SST warming that compounds the warming from the ongoing increases in greenhouse gas concentrations.^{160, 161} This combination of greenhouse



gas and sulfate aerosol forcing, by itself, can lead to Atlantic multidecadal SST variability that would not be removed by removing a linear trend.¹⁵⁵

In summary, it is unclear what the statistically derived AMO indices represent, and it is not readily supportable to treat AMO index variability as tacitly representing natural variability, nor is it clear that the observed AMV is truly oscillatory in nature.¹⁶⁷ There is a physical basis for treating the AMOC as oscillatory (via thermohaline circulation arguments),¹⁶⁸ but there is no expectation of true oscillatory behavior in the hypothesized external forcing agents for the remaining variability. Detrending the SST data used to construct the AMO indices may partially remove the century-scale trends forced by increasing greenhouse gas concentrations, but it is not adequate for removing multidecadal variability forced by aerosol concentration variability. There is evidence that natural AMOC variability has been occurring for hundreds of years,^{149, 169, 170, 171, 172} and this has apparently played some role in the observed AMV as a whole, but a growing body of evidence shows that external factors, both natural and anthropogenic, have played a substantial additional role in the past century.

5.3 Quantifying the Role of Internal Variability on Past and Future U.S. Climate Trends

The role of internal variability in masking trends is substantially increased on regional and local scales relative to the global scale, and in the extratropics relative to the tropics (Ch. 4: Projections). Approaches have been developed to better quantify the externally forced and internally driven contributions to observed and future climate trends and variability and further separate these contributions into thermodynamically and dynamically driven factors.¹⁷ Specifically, large “initial

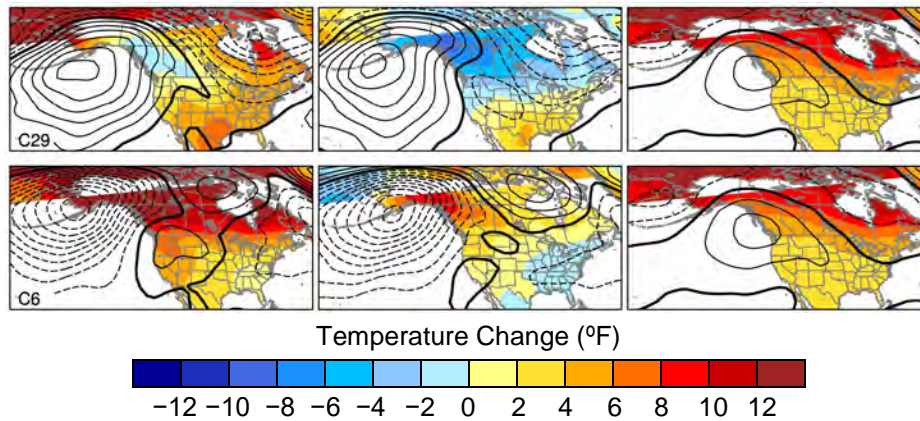
condition” climate model ensembles with 30 ensemble members and more^{93, 173, 174} and long control runs¹⁷⁵ have been shown to be useful tools to characterize uncertainties in climate change projections at local/regional scales.

North American temperature and precipitation trends on timescales of up to a few decades are strongly affected by intrinsic atmospheric circulation variability.^{17, 173} For example, it is estimated that internal circulation trends account for approximately one-third of the observed wintertime warming over North America during the past 50 years. In a few areas, such as the central Rocky Mountains and far western Alaska, internal dynamics have offset the warming trend by 10%–30%.¹⁷ Natural climate variability superimposed upon forced climate change will result in a large range of possible trends for surface air temperature and precipitation in the United States over the next 50 years (Figure 5.4).¹⁷³

Climate models are evaluated with respect to their proper simulation of internal decadal variability. Comparing observed and simulated variability estimates at timescales longer than 10 years suggest that models tend to overestimate the internal variability in the northern extratropics, including over the continental United States, but underestimate it over much of the tropics and subtropical ocean regions.^{93, 176} Such biases affect signal-to-noise estimates of regional scale climate change response and thus assessment of internally driven contributions to regional/local trends.



a) Winter surface air temperature and sea level pressure



b) Winter precipitation and sea level pressure

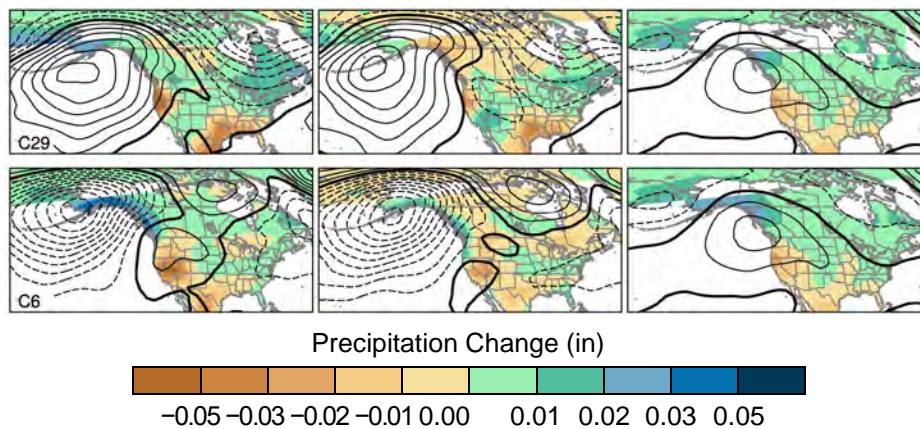


Figure 5.4: (left) Total 2010–2060 winter trends decomposed into (center) internal and (right) forced components for two contrasting CCSM3 ensemble members (runs 29 and 6) for (a) surface air temperature [color shading; °F/(51 years)] and sea level pressure (SLP; contours) and (b) precipitation [color shading; inches per day/(51 years)] and SLP (contours). SLP contour interval is 1 hPa/(51 years), with solid (dashed) contours for positive (negative) values; the zero contour is thickened. The same climate model (CCSM3) simulates a large range of possible trends in North American climate over the 2010–2060 period because of the influence of internal climate variability superposed upon forced climate trends. (Figure source: adapted from Deser et al. 2014;¹⁷³ © American Meteorological Society, used with permission).

TRACEABLE ACCOUNTS

Key Finding 1

The tropics have expanded poleward by about 70 to 200 miles in each hemisphere over the period 1979–2009, with an accompanying shift of the subtropical dry zones, midlatitude jets, and storm tracks (*medium to high confidence*). Human activities have played a role in this change (*medium confidence*), although confidence is presently *low* regarding the magnitude of the human contribution relative to natural variability

Description of evidence base

The Key Finding is supported by statements of the Intergovernmental Panel on Climate Change’s Fifth Assessment Report²⁴ and a large number of more recent studies that examined the magnitude of the observed tropical widening and various causes.^{5, 20, 22, 23, 25, 26, 27, 28, 29, 31} Additional evidence for an impact of greenhouse gas increases on the widening of the tropical belt and poleward shifts of the midlatitude jets is provided by the diagnosis of CMIP5 simulations.^{4, 40} There is emerging evidence for an impact of anthropogenic aerosols on the tropical expansion in the Northern Hemisphere.³² Recent studies provide new evidence on the significance of internal variability on recent changes in the tropical width.^{23, 34, 35}

Major uncertainties

The rate of observed expansion of tropics depends on which metric is used. The linkages between different metrics are not fully explored. Uncertainties also result from the utilization of reanalysis to determine trends and from limited observational records of free atmosphere circulation, precipitation, and evaporation. The dynamical mechanisms behind changes in the width of the tropical belt (e.g., tropical–extratropical interactions and baroclinic eddies) are not fully understood. There is also a limited understanding of how various climate forcings, such as anthropogenic aerosols, affect the width of tropics. The coarse horizontal and vertical resolution of global climate models may limit the ability of these models to properly resolve latitudinal changes in the atmospheric circulation. Limited observational records affect the ability to accurately estimate

the contribution of natural decadal to multi-decadal variability on observed expansion of the tropics.

Assessment of confidence based on evidence and agreement, including short description of nature of evidence and level of agreement

Medium to high confidence that the tropics and related features of the global circulation have expanded poleward is based upon the results of a large number of observational studies, using a wide variety of metrics and data sets, which reach similar conclusions. A large number of studies utilizing modeling of different complexity and theoretical considerations provide compounding evidence that human activities, including increases in greenhouse gases, ozone depletion, and anthropogenic aerosols, contributed to the observed poleward expansion of the tropics. Climate models forced with these anthropogenic drivers cannot explain the observed magnitude of tropical expansion and some studies suggest a possibly large contribution of internal variability. These multiple lines of evidence lead to the conclusion of *medium confidence* that human activities contributed to observed expansion of the tropics.

Summary sentence or paragraph that integrates the above information

The tropics have expanded poleward in each hemisphere over the period 1979–2009 (*medium to high confidence*) as shown by a large number of studies using a variety of metrics, observations and reanalysis. Modeling studies and theoretical considerations illustrate that human activities, including increases in greenhouse gases, ozone depletion, and anthropogenic aerosols, cause a widening of the tropics. There is *medium confidence* that human activities have contributed to the observed poleward expansion, taking into account uncertainties in the magnitude of observed trends and a possible large contribution of natural climate variability.

Key Finding 2

Recurring patterns of variability in large-scale atmospheric circulation (such as the North Atlantic Oscilla-



tion and Northern Annular Mode) and the atmosphere–ocean system (such as El Niño–Southern Oscillation) cause year-to-year variations in U.S. temperatures and precipitation (*high confidence*). Changes in the occurrence of these patterns or their properties have contributed to recent U.S. temperature and precipitation trends (*medium confidence*), although confidence is *low* regarding the size of the role of human activities in these changes.

Description of evidence base

The Key Finding is supported by a large number of studies that diagnose recurring patterns of variability and their changes, as well as their impact on climate over the United States. Regarding year-to-year variations, a large number of studies based on models and observations show statistically significant associations between North Atlantic Oscillation/Northern Annular Mode and United States temperature and precipitation,^{7, 9, 74, 75, 76, 88} as well as El Niño–Southern Oscillation and related U.S. climate teleconnections.^{11, 50, 51, 52, 53, 56, 57} Regarding recent decadal trends, several studies provide evidence for concurrent changes in the North Atlantic Oscillation/Northern Annular Mode and climate anomalies over the United States.^{81, 82, 83, 84} Modeling studies provide evidence for a linkage between cooling trends of the tropical Pacific Ocean that resemble La Niña and precipitation changes in the southern United States.^{54, 55} Several studies describe a decadal modification of ENSO.^{58, 59, 60, 63} Modeling evidence is provided that such decadal modifications can be due to internal variability.⁶³ Climate models are widely analyzed for their ability to simulate recurring patterns of variability and teleconnections over the United States.^{9, 64, 65, 68, 88, 98} Climate model projections are also widely analyzed to diagnose the impact of human activities on NAM/NAO, ENSO teleconnections, and other recurring modes of variability associated with climate anomalies.^{9, 19, 72, 92}

Major uncertainties

A key uncertainty is related to limited observational records and our capability to properly simulate climate variability on decadal to multidecadal timescales, as well as to properly simulate recurring patterns of climate variability, underlying physical mechanisms, and

associated variations in temperature and precipitation over the United States.

Assessment of confidence based on evidence and agreement, including short description of nature of evidence and level of agreement

There is *high confidence* that preferred patterns of variability affect U.S. temperature on a year-to-year timescale, based on a large number of studies that diagnose observational data records and long simulations. There is *medium confidence* that changes in the occurrence of these patterns or their properties have contributed to recent U.S. temperature and precipitation trends. Several studies agree on a linkage between decadal changes in the NAO/NAM and climate trends over the United States, and there is some modeling evidence for a linkage between a La Niña-like cooling trend over the tropical Pacific and precipitation changes in the southwestern United States. There is no robust evidence for observed decadal changes in the properties of ENSO and related United States climate impacts. Confidence is *low* regarding the size of the role of human influences in these changes because models do not agree on the impact of human activity on preferred patterns of variability or because projected changes are small compared to internal variability.

Summary sentence or paragraph that integrates the above information

Recurring modes of variability strongly affect temperature and precipitation over the United States on interannual timescales (*high confidence*) as supported by a very large number of observational and modeling studies. Changes in some recurring patterns of variability have contributed to recent trends in U.S. temperature and precipitation (*medium confidence*). The causes of these changes are uncertain due to the limited observational record and because models exhibit some difficulties simulating these recurring patterns of variability and their underlying physical mechanisms.



References

1. Frierson, D.M.W., J. Lu, and G. Chen, 2007: Width of the Hadley cell in simple and comprehensive general circulation models. *Geophysical Research Letters*, **34**, L18804. <http://dx.doi.org/10.1029/2007GL031115>
2. Mbengue, C. and T. Schneider, 2017: Storm-track shifts under climate change: Toward a mechanistic understanding using baroclinic mean available potential energy. *Journal of the Atmospheric Sciences*, **74**, 93-110. <http://dx.doi.org/10.1175/jas-d-15-0267.1>
3. Sun, Y., G. Ramstein, C. Contoux, and T. Zhou, 2013: A comparative study of large-scale atmospheric circulation in the context of a future scenario (RCP4.5) and past warmth (mid-Pliocene). *Climate of the Past*, **9**, 1613-1627. <http://dx.doi.org/10.5194/cp-9-1613-2013>
4. Vallis, G.K., P. Zurita-Gotor, C. Cairns, and J. Kidston, 2015: Response of the large-scale structure of the atmosphere to global warming. *Quarterly Journal of the Royal Meteorological Society*, **141**, 1479-1501. <http://dx.doi.org/10.1002/qj.2456>
5. Feng, S. and Q. Fu, 2013: Expansion of global drylands under a warming climate. *Atmospheric Chemistry and Physics*, **13**, 10081-10094. <http://dx.doi.org/10.5194/acp-13-10081-2013>
6. Seidel, D.J., Q. Fu, W.J. Randel, and T.J. Reichler, 2008: Widening of the tropical belt in a changing climate. *Nature Geoscience*, **1**, 21-24. <http://dx.doi.org/10.1038/ngeo.2007.38>
7. Hurrell, J.W. and C. Deser, 2009: North Atlantic climate variability: The role of the North Atlantic oscillation. *Journal of Marine Systems*, **78**, 28-41. <http://dx.doi.org/10.1016/j.jmarsys.2008.11.026>
8. Linkin, M.E. and S. Nigam, 2008: The North Pacific Oscillation–West Pacific teleconnection pattern: Mature-phase structure and winter impacts. *Journal of Climate*, **21**, 1979-1997. <http://dx.doi.org/10.1175/2007JCLI2048.1>
9. Ning, L. and R.S. Bradley, 2016: NAO and PNA influences on winter temperature and precipitation over the eastern United States in CMIP5 GCMs. *Climate Dynamics*, **46**, 1257-1276. <http://dx.doi.org/10.1007/s00382-015-2643-9>
10. Grotjahn, R., R. Black, R. Leung, M.F. Wehner, M. Barlow, M. Bosilovich, A. Gershunov, W.J. Gutowski, J.R. Gyakum, R.W. Katz, Y.-Y. Lee, Y.-K. Lim, and Prabhat, 2016: North American extreme temperature events and related large scale meteorological patterns: A review of statistical methods, dynamics, modeling, and trends. *Climate Dynamics*, **46**, 1151-1184. <http://dx.doi.org/10.1007/s00382-015-2638-6>
11. Halpert, M.S. and C.F. Ropelewski, 1992: Surface temperature patterns associated with the Southern Oscillation. *Journal of Climate*, **5**, 577-593. [http://dx.doi.org/10.1175/1520-0442\(1992\)005<0577:STPAWT>2.0.CO;2](http://dx.doi.org/10.1175/1520-0442(1992)005<0577:STPAWT>2.0.CO;2)
12. Enfield, D.B., A.M. Mestas-Nuñez, and P.J. Trimble, 2001: The Atlantic Multidecadal Oscillation and its relation to rainfall and river flows in the continental U.S. *Geophysical Research Letters*, **28**, 2077-2080. <http://dx.doi.org/10.1029/2000GL012745>
13. Goldenberg, S.B., C.W. Landsea, A.M. Mestas-Nuñez, and W.M. Gray, 2001: The recent increase in Atlantic hurricane activity: Causes and implications. *Science*, **293**, 474-479. <http://dx.doi.org/10.1126/science.1060040>
14. Newman, M., M.A. Alexander, T.R. Ault, K.M. Cobb, C. Deser, E.D. Lorenzo, N.J. Mantua, A.J. Miller, S. Minobe, H. Nakamura, N. Schneider, D.J. Vimont, A.S. Phillips, J.D. Scott, and C.A. Smith, 2016: The Pacific Decadal Oscillation, revisited. *Journal of Climate*, **29**, 4399-4427. <http://dx.doi.org/10.1175/JCLI-D-15-0508.1>
15. Perlwitz, J., S. Pawson, R.L. Fogt, J.E. Nielsen, and W.D. Neff, 2008: Impact of stratospheric ozone hole recovery on Antarctic climate. *Geophysical Research Letters*, **35**, L08714. <http://dx.doi.org/10.1029/2008GL033317>
16. Palmer, T.N., F.J. Doblas-Reyes, A. Weisheimer, and M.J. Rodwell, 2008: Toward seamless prediction: Calibration of climate change projections using seasonal forecasts. *Bulletin of the American Meteorological Society*, **89**, 459-470. <http://dx.doi.org/10.1175/bams-89-4-459>
17. Deser, C., L. Terray, and A.S. Phillips, 2016: Forced and internal components of winter air temperature trends over North America during the past 50 years: Mechanisms and implications. *Journal of Climate*, **29**, 2237-2258. <http://dx.doi.org/10.1175/JCLI-D-15-0304.1>
18. Shepherd, T.G., 2014: Atmospheric circulation as a source of uncertainty in climate change projections. *Nature Geoscience*, **7**, 703-708. <http://dx.doi.org/10.1038/ngeo2253>



19. Christensen, J.H., K. Krishna Kumar, E. Aldrian, S.-I. An, I.F.A. Cavalcanti, M. de Castro, W. Dong, P. Goswami, A. Hall, J.K. Kanyanga, A. Kitoh, J. Kossin, N.-C. Lau, J. Renwick, D.B. Stephenson, S.-P. Xie, and T. Zhou, 2013: Climate phenomena and their relevance for future regional climate change. *Climate Change 2013: The Physical Science Basis. Contribution of Working Group I to the Fifth Assessment Report of the Intergovernmental Panel on Climate Change*. Stocker, T.F., D. Qin, G.-K. Plattner, M. Tignor, S.K. Allen, J. Boschung, A. Nauels, Y. Xia, V. Bex, and P.M. Midgley, Eds. Cambridge University Press, Cambridge, United Kingdom and New York, NY, USA, 1217-1308. <http://www.climatechange2013.org/report/full-report/>
20. Birner, T., S.M. Davis, and D.J. Seidel, 2014: The changing width of Earth's tropical belt. *Physics Today*, **67**, 38-44. <http://dx.doi.org/10.1063/PT.3.2620>
21. Brönnimann, S., A.M. Fischer, E. Rozanov, P. Poli, G.P. Compo, and P.D. Sardeshmukh, 2015: Southward shift of the northern tropical belt from 1945 to 1980. *Nature Geoscience*, **8**, 969-974. <http://dx.doi.org/10.1038/ngeo2568>
22. Davis, N.A. and T. Birner, 2013: Seasonal to multidecadal variability of the width of the tropical belt. *Journal of Geophysical Research Atmospheres*, **118**, 7773-7787. <http://dx.doi.org/10.1002/jgrd.50610>
23. Garfinkel, C.I., D.W. Waugh, and L.M. Polvani, 2015: Recent Hadley cell expansion: The role of internal atmospheric variability in reconciling modeled and observed trends. *Geophysical Research Letters*, **42**, 10,824-10,831. <http://dx.doi.org/10.1002/2015GL066942>
24. Hartmann, D.L., A.M.G. Klein Tank, M. Rusticucci, L.V. Alexander, S. Brönnimann, Y. Charabi, F.J. Dentener, E.J. Dlugokencky, D.R. Easterling, A. Kaplan, B.J. Soden, P.W. Thorne, M. Wild, and P.M. Zhai, 2013: Observations: Atmosphere and surface. *Climate Change 2013: The Physical Science Basis. Contribution of Working Group I to the Fifth Assessment Report of the Intergovernmental Panel on Climate Change*. Stocker, T.F., D. Qin, G.-K. Plattner, M. Tignor, S.K. Allen, J. Boschung, A. Nauels, Y. Xia, V. Bex, and P.M. Midgley, Eds. Cambridge University Press, Cambridge, United Kingdom and New York, NY, USA, 159-254. <http://www.climatechange2013.org/report/full-report/>
25. Karauskas, K.B. and C.C. Ummerhofer, 2014: On the dynamics of the Hadley circulation and subtropical drying. *Climate Dynamics*, **42**, 2259-2269. <http://dx.doi.org/10.1007/s00382-014-2129-1>
26. Lucas, C., B. Timbal, and H. Nguyen, 2014: The expanding tropics: A critical assessment of the observational and modeling studies. *Wiley Interdisciplinary Reviews: Climate Change*, **5**, 89-112. <http://dx.doi.org/10.1002/wcc.251>
27. Norris, J.R., R.J. Allen, A.T. Evan, M.D. Zelinka, C.W. O'Dell, and S.A. Klein, 2016: Evidence for climate change in the satellite cloud record. *Nature*, **536**, 72-75. <http://dx.doi.org/10.1038/nature18273>
28. Quan, X.-W., M.P. Hoerling, J. Perlwitz, H.F. Diaz, and T. Xu, 2014: How fast are the tropics expanding? *Journal of Climate*, **27**, 1999-2013. <http://dx.doi.org/10.1175/JCLI-D-13-00287.1>
29. Reichler, T., 2016: Chapter 6 - Poleward expansion of the atmospheric circulation *Climate Change (Second Edition)*. Letcher, T.M., Ed. Elsevier, Boston, 79-104. <http://dx.doi.org/10.1016/B978-0-444-63524-2.00006-3>
30. Bindoff, N.L., P.A. Stott, K.M. AchutaRao, M.R. Allen, N. Gillett, D. Gutzler, K. Hansingo, G. Hegerl, Y. Hu, S. Jain, I.I. Mokhov, J. Overland, J. Perlwitz, R. Sebbari, and X. Zhang, 2013: Detection and attribution of climate change: From global to regional. *Climate Change 2013: The Physical Science Basis. Contribution of Working Group I to the Fifth Assessment Report of the Intergovernmental Panel on Climate Change*. Stocker, T.F., D. Qin, G.-K. Plattner, M. Tignor, S.K. Allen, J. Boschung, A. Nauels, Y. Xia, V. Bex, and P.M. Midgley, Eds. Cambridge University Press, Cambridge, United Kingdom and New York, NY, USA, 867-952. <http://www.climatechange2013.org/report/full-report/>
31. Waugh, D.W., C.I. Garfinkel, and L.M. Polvani, 2015: Drivers of the recent tropical expansion in the Southern Hemisphere: Changing SSTs or ozone depletion? *Journal of Climate*, **28**, 6581-6586. <http://dx.doi.org/10.1175/JCLI-D-15-0138.1>
32. Allen, R.J., S.C. Sherwood, J.R. Norris, and C.S. Zender, 2012: Recent Northern Hemisphere tropical expansion primarily driven by black carbon and tropospheric ozone. *Nature*, **485**, 350-354. <http://dx.doi.org/10.1038/nature11097>
33. Kovilakam, M. and S. Mahajan, 2015: Black carbon aerosol-induced Northern Hemisphere tropical expansion. *Geophysical Research Letters*, **42**, 4964-4972. <http://dx.doi.org/10.1002/2015GL064559>
34. Adam, O., T. Schneider, and N. Harnik, 2014: Role of changes in mean temperatures versus temperature gradients in the recent widening of the Hadley circulation. *Journal of Climate*, **27**, 7450-7461. <http://dx.doi.org/10.1175/JCLI-D-14-00140.1>

35. Allen, R.J., J.R. Norris, and M. Kovilakam, 2014: Influence of anthropogenic aerosols and the Pacific Decadal Oscillation on tropical belt width. *Nature Geoscience*, **7**, 270-274. <http://dx.doi.org/10.1038/ngeo2091>
36. Chen, S., K. Wei, W. Chen, and L. Song, 2014: Regional changes in the annual mean Hadley circulation in recent decades. *Journal of Geophysical Research Atmospheres*, **119**, 7815-7832. <http://dx.doi.org/10.1002/2014JD021540>
37. Lucas, C. and H. Nguyen, 2015: Regional characteristics of tropical expansion and the role of climate variability. *Journal of Geophysical Research Atmospheres*, **120**, 6809-6824. <http://dx.doi.org/10.1002/2015JD023130>
38. Schwendike, J., G.J. Berry, M.J. Reeder, C. Jakob, P. Govekar, and R. Wardle, 2015: Trends in the local Hadley and local Walker circulations. *Journal of Geophysical Research Atmospheres*, **120**, 7599-7618. <http://dx.doi.org/10.1002/2014JD022652>
39. Prein, A.F., G.J. Holland, R.M. Rasmussen, M.P. Clark, and M.R. Tye, 2016: Running dry: The U.S. Southwest's drift into a drier climate state. *Geophysical Research Letters*, **43**, 1272-1279. <http://dx.doi.org/10.1002/2015GL066727>
40. Barnes, E.A. and L. Polvani, 2013: Response of the midlatitude jets, and of their variability, to increased greenhouse gases in the CMIP5 models. *Journal of Climate*, **26**, 7117-7135. <http://dx.doi.org/10.1175/JCLI-D-12-00536.1>
41. Collins, M., R. Knutti, J. Arblaster, J.-L. Dufresne, T. Fichefet, P. Friedlingstein, X. Gao, W.J. Gutowski, T. Johns, G. Krinner, M. Shongwe, C. Tebaldi, A.J. Weaver, and M. Wehner, 2013: Long-term climate change: Projections, commitments and irreversibility. *Climate Change 2013: The Physical Science Basis. Contribution of Working Group I to the Fifth Assessment Report of the Intergovernmental Panel on Climate Change*. Stocker, T.F., D. Qin, G.-K. Plattner, M. Tignor, S.K. Allen, J. Boschung, A. Nauels, Y. Xia, V. Bex, and P.M. Midgley, Eds. Cambridge University Press, Cambridge, United Kingdom and New York, NY, USA, 1029-1136. <http://www.climatechange2013.org/report/full-report/>
42. Scheff, J. and D. Frierson, 2012: Twenty-first-century multimodel subtropical precipitation declines are mostly midlatitude shifts. *Journal of Climate*, **25**, 4330-4347. <http://dx.doi.org/10.1175/JCLI-D-11-00393.1>
43. Scheff, J. and D.M.W. Frierson, 2012: Robust future precipitation declines in CMIP5 largely reflect the poleward expansion of model subtropical dry zones. *Geophysical Research Letters*, **39**, L18704. <http://dx.doi.org/10.1029/2012GL052910>
44. Simpson, I.R., R. Seager, M. Ting, and T.A. Shaw, 2016: Causes of change in Northern Hemisphere winter meridional winds and regional hydroclimate. *Nature Climate Change*, **6**, 65-70. <http://dx.doi.org/10.1038/nclimate2783>
45. Simpson, I.R., T.A. Shaw, and R. Seager, 2014: A diagnosis of the seasonally and longitudinally varying midlatitude circulation response to global warming. *Journal of the Atmospheric Sciences*, **71**, 2489-2515. <http://dx.doi.org/10.1175/JAS-D-13-0325.1>
46. Barnes, E.A. and L.M. Polvani, 2015: CMIP5 projections of Arctic amplification, of the North American/North Atlantic circulation, and of their relationship. *Journal of Climate*, **28**, 5254-5271. <http://dx.doi.org/10.1175/JCLI-D-14-00589.1>
47. Cattiaux, J. and C. Cassou, 2013: Opposite CMIP3/CMIP5 trends in the wintertime Northern Annular Mode explained by combined local sea ice and remote tropical influences. *Geophysical Research Letters*, **40**, 3682-3687. <http://dx.doi.org/10.1002/grl.50643>
48. Karpechko, A.Y. and E. Manzini, 2012: Stratospheric influence on tropospheric climate change in the Northern Hemisphere. *Journal of Geophysical Research*, **117**, D05133. <http://dx.doi.org/10.1029/2011JD017036>
49. Scaife, A.A., T. Spanghel, D.R. Fereday, U. Cubasch, U. Langematz, H. Akiyoshi, S. Bekki, P. Braesicke, N. Butchart, M.P. Chipperfield, A. Gettelman, S.C. Hardiman, M. Michou, E. Rozanov, and T.G. Shepherd, 2012: Climate change projections and stratosphere-troposphere interaction. *Climate Dynamics*, **38**, 2089-2097. <http://dx.doi.org/10.1007/s00382-011-1080-7>
50. Hoerling, M.P., A. Kumar, and T. Xu, 2001: Robustness of the nonlinear climate response to ENSO's extreme phases. *Journal of Climate*, **14**, 1277-1293. [http://dx.doi.org/10.1175/1520-0442\(2001\)014<1277:ROTNCR>2.0.CO;2](http://dx.doi.org/10.1175/1520-0442(2001)014<1277:ROTNCR>2.0.CO;2)
51. Kiladis, G.N. and H.F. Diaz, 1989: Global climatic anomalies associated with extremes in the Southern Oscillation. *Journal of Climate*, **2**, 1069-1090. [http://dx.doi.org/10.1175/1520-0442\(1989\)002<1069:G-CAAWE>2.0.CO;2](http://dx.doi.org/10.1175/1520-0442(1989)002<1069:G-CAAWE>2.0.CO;2)
52. Ropelewski, C.F. and M.S. Halpert, 1987: Global and regional scale precipitation patterns associated with the El Niño/Southern Oscillation. *Monthly Weather Review*, **115**, 1606-1626. [http://dx.doi.org/10.1175/1520-0493\(1987\)115<1606:GARSPP>2.0.CO;2](http://dx.doi.org/10.1175/1520-0493(1987)115<1606:GARSPP>2.0.CO;2)



53. Zhang, T., M.P. Hoerling, J. Perlwitz, and T. Xu, 2016: Forced atmospheric teleconnections during 1979–2014. *Journal of Climate*, **29**, 2333–2357. <http://dx.doi.org/10.1175/jcli-d-15-0226.1>
54. Hoerling, M., J. Eischeid, and J. Perlwitz, 2010: Regional precipitation trends: Distinguishing natural variability from anthropogenic forcing. *Journal of Climate*, **23**, 2131–2145. <http://dx.doi.org/10.1175/2009jcli3420.1>
55. Hoerling, M., J. Eischeid, J. Perlwitz, X.-W. Quan, K. Wolter, and L. Cheng, 2016: Characterizing recent trends in U.S. heavy precipitation. *Journal of Climate*, **29**, 2313–2332. <http://dx.doi.org/10.1175/jcli-d-15-0441.1>
56. Yu, J.-Y., Y. Zou, S.T. Kim, and T. Lee, 2012: The changing impact of El Niño on US winter temperatures. *Geophysical Research Letters*, **39**, L15702. <http://dx.doi.org/10.1029/2012GL052483>
57. Yu, J.-Y. and Y. Zou, 2013: The enhanced drying effect of Central-Pacific El Niño on US winter. *Environmental Research Letters*, **8**, 014019. <http://dx.doi.org/10.1088/1748-9326/8/1/014019>
58. Li, J., S.-P. Xie, E.R. Cook, G. Huang, R. D'Arrigo, F. Liu, J. Ma, and X.-T. Zheng, 2011: Interdecadal modulation of El Niño amplitude during the past millennium. *Nature Climate Change*, **1**, 114–118. <http://dx.doi.org/10.1038/nclimate1086>
59. Lee, T. and M.J. McPhaden, 2010: Increasing intensity of El Niño in the central-equatorial Pacific. *Geophysical Research Letters*, **37**, L14603. <http://dx.doi.org/10.1029/2010GL044007>
60. Yeh, S.-W., J.-S. Kug, B. Dewitte, M.-H. Kwon, B.P. Kirtman, and F.-F. Jin, 2009: El Niño in a changing climate. *Nature*, **461**, 511–514. <http://dx.doi.org/10.1038/nature08316>
61. Deser, C., I.R. Simpson, K.A. McKinnon, and A.S. Phillips, 2017: The Northern Hemisphere extratropical atmospheric circulation response to ENSO: How well do we know it and how do we evaluate models accordingly? *Journal of Climate*, **30**, 5059–5082. <http://dx.doi.org/10.1175/jcli-d-16-0844.1>
62. Garfinkel, C.I., M.M. Hurwitz, D.W. Waugh, and A.H. Butler, 2013: Are the teleconnections of Central Pacific and Eastern Pacific El Niño distinct in boreal wintertime? *Climate Dynamics*, **41**, 1835–1852. <http://dx.doi.org/10.1007/s00382-012-1570-2>
63. Capotondi, A., A.T. Wittenberg, M. Newman, E.D. Lorenz, J.-Y. Yu, P. Braconnot, J. Cole, B. Dewitte, B. Giese, E. Guilyardi, F.-F. Jin, K. Karnauskas, B. Kirtman, T. Lee, N. Schneider, Y. Xue, and S.-W. Yeh, 2015: Understanding ENSO diversity. *Bulletin of the American Meteorological Society*, **96** (12), 921–938. <http://dx.doi.org/10.1175/BAMS-D-13-00117.1>
64. Bellenger, H., E. Guilyardi, J. Leloup, M. Lengaigne, and J. Vialard, 2014: ENSO representation in climate models: From CMIP3 to CMIP5. *Climate Dynamics*, **42**, 1999–2018. <http://dx.doi.org/10.1007/s00382-013-1783-z>
65. Flato, G., J. Marotzke, B. Abiodun, P. Braconnot, S.C. Chou, W. Collins, P. Cox, F. Driouech, S. Emori, V. Eyring, C. Forest, P. Gleckler, E. Guilyardi, C. Jakob, V. Kattsov, C. Reason, and M. Rummukainen, 2013: Evaluation of climate models. *Climate Change 2013: The Physical Science Basis. Contribution of Working Group I to the Fifth Assessment Report of the Intergovernmental Panel on Climate Change*. Stocker, T.F., D. Qin, G.-K. Plattner, M. Tignor, S.K. Allen, J. Boschung, A. Nauels, Y. Xia, V. Bex, and P.M. Midgley, Eds. Cambridge University Press, Cambridge, United Kingdom and New York, NY, USA, 741–866. <http://www.climatechange2013.org/report/full-report/>
66. Sheffield, J., S.J. Camargo, R. Fu, Q. Hu, X. Jiang, N. Johnson, K.B. Karnauskas, S.T. Kim, J. Kinter, S. Kumar, B. Langenbrunner, E. Maloney, A. Mariotti, J.E. Meyerson, J.D. Neelin, S. Nigam, Z. Pan, A. Ruiz-Barradas, R. Seager, Y.L. Serra, D.-Z. Sun, C. Wang, S.-P. Xie, J.-Y. Yu, T. Zhang, and M. Zhao, 2013: North American climate in CMIP5 experiments. Part II: Evaluation of historical simulations of intraseasonal to decadal variability. *Journal of Climate*, **26**, 9247–9290. <http://dx.doi.org/10.1175/jcli-d-12-00593.1>
67. Coats, S., J.E. Smerdon, B.I. Cook, and R. Seager, 2013: Stationarity of the tropical Pacific teleconnection to North America in CMIP5/PMIP3 model simulations. *Geophysical Research Letters*, **40**, 4927–4932. <http://dx.doi.org/10.1002/grl.50938>
68. Langenbrunner, B. and J.D. Neelin, 2013: Analyzing ENSO teleconnections in CMIP models as a measure of model fidelity in simulating precipitation. *Journal of Climate*, **26**, 4431–4446. <http://dx.doi.org/10.1175/jcli-d-12-00542.1>
69. Kug, J.-S., S.-I. An, Y.-G. Ham, and I.-S. Kang, 2010: Changes in El Niño and La Niña teleconnections over North Pacific–America in the global warming simulations. *Theoretical and Applied Climatology*, **100**, 275–282. <http://dx.doi.org/10.1007/s00704-009-0183-0>

70. Meehl, G.A. and H. Teng, 2007: Multi-model changes in El Niño teleconnections over North America in a future warmer climate. *Climate Dynamics*, **29**, 779-790. <http://dx.doi.org/10.1007/s00382-007-0268-3>
71. Stevenson, S.L., 2012: Significant changes to ENSO strength and impacts in the twenty-first century: Results from CMIP5. *Geophysical Research Letters*, **39**, L17703. <http://dx.doi.org/10.1029/2012GL052759>
72. Zhou, Z.-Q., S.-P. Xie, X.-T. Zheng, Q. Liu, and H. Wang, 2014: Global warming-induced changes in El Niño teleconnections over the North Pacific and North America. *Journal of Climate*, **27**, 9050-9064. <http://dx.doi.org/10.1175/JCLI-D-14-00254.1>
73. Seager, R., N. Naik, and L. Vogel, 2012: Does global warming cause intensified interannual hydroclimate variability? *Journal of Climate*, **25**, 3355-3372. <http://dx.doi.org/10.1175/JCLI-D-11-00363.1>
74. Thompson, D.W.J. and J.M. Wallace, 2001: Regional climate impacts of the Northern Hemisphere annular mode. *Science*, **293**, 85-89. <http://dx.doi.org/10.1126/science.1058958>
75. Archambault, H.M., L.F. Bosart, D. Keyser, and A.R. Aiyyer, 2008: Influence of large-scale flow regimes on cool-season precipitation in the northeastern United States. *Monthly Weather Review*, **136**, 2945-2963. <http://dx.doi.org/10.1175/2007MWR2308.1>
76. Durkee, J.D., J.D. Frye, C.M. Fuhrmann, M.C. Lacke, H.G. Jeong, and T.L. Mote, 2008: Effects of the North Atlantic Oscillation on precipitation-type frequency and distribution in the eastern United States. *Theoretical and Applied Climatology*, **94**, 51-65. <http://dx.doi.org/10.1007/s00704-007-0345-x>
77. Thompson, D.W.J. and J.M. Wallace, 1998: The Arctic oscillation signature in the wintertime geopotential height and temperature fields. *Geophysical Research Letters*, **25**, 1297-1300. <http://dx.doi.org/10.1029/98GL00950>
78. Thompson, D.W.J. and J.M. Wallace, 2000: Annular modes in the extratropical circulation. Part I: Month-to-month variability. *Journal of Climate*, **13**, 1000-1016. [http://dx.doi.org/10.1175/1520-0442\(2000\)013<1000:AMITEC>2.0.CO;2](http://dx.doi.org/10.1175/1520-0442(2000)013<1000:AMITEC>2.0.CO;2)
79. Deser, C., 2000: On the teleconnectivity of the "Arctic Oscillation". *Geophysical Research Letters*, **27**, 779-782. <http://dx.doi.org/10.1029/1999GL010945>
80. Feldstein, S.B. and C. Franzke, 2006: Are the North Atlantic Oscillation and the Northern Annular Mode distinguishable? *Journal of the Atmospheric Sciences*, **63**, 2915-2930. <http://dx.doi.org/10.1175/JAS3798.1>
81. Cohen, J. and M. Barlow, 2005: The NAO, the AO, and global warming: How closely related? *Journal of Climate*, **18**, 4498-4513. <http://dx.doi.org/10.1175/jcli3530.1>
82. Hurrell, J.W., 1995: Decadal trends in the North Atlantic oscillation: Regional temperatures and precipitation. *Science*, **269**, 676-679. <http://dx.doi.org/10.1126/science.269.5224.676>
83. Overland, J., J.A. Francis, R. Hall, E. Hanna, S.-J. Kim, and T. Vihma, 2015: The melting Arctic and midlatitude weather patterns: Are they connected? *Journal of Climate*, **28**, 7917-7932. <http://dx.doi.org/10.1175/JCLI-D-14-00822.1>
84. Overland, J.E. and M. Wang, 2015: Increased variability in the early winter subarctic North American atmospheric circulation. *Journal of Climate*, **28**, 7297-7305. <http://dx.doi.org/10.1175/jcli-d-15-0395.1>
85. Delworth, T.L., F. Zeng, G.A. Vecchi, X. Yang, L. Zhang, and R. Zhang, 2016: The North Atlantic Oscillation as a driver of rapid climate change in the Northern Hemisphere. *Nature Geoscience*, **9**, 509-512. <http://dx.doi.org/10.1038/ngeo2738>
86. Peings, Y. and G. Magnusdottir, 2014: Forcing of the wintertime atmospheric circulation by the multidecadal fluctuations of the North Atlantic ocean. *Environmental Research Letters*, **9**, 034018. <http://dx.doi.org/10.1088/1748-9326/9/3/034018>
87. Yang, Q., T.H. Dixon, P.G. Myers, J. Bonin, D. Chambers, and M.R. van den Broeke, 2016: Recent increases in Arctic freshwater flux affects Labrador Sea convection and Atlantic overturning circulation. *Nature Communications*, **7**, 10525. <http://dx.doi.org/10.1038/ncomms10525>
88. Gong, H., L. Wang, W. Chen, X. Chen, and D. Nath, 2017: Biases of the wintertime Arctic Oscillation in CMIP5 models. *Environmental Research Letters*, **12**, 014001. <http://dx.doi.org/10.1088/1748-9326/12/1/014001>
89. Davini, P. and C. Cagnazzo, 2014: On the misinterpretation of the North Atlantic Oscillation in CMIP5 models. *Climate Dynamics*, **43**, 1497-1511. <http://dx.doi.org/10.1007/s00382-013-1970-y>
90. Shaw, T.A., J. Perlwitz, and O. Weiner, 2014: Troposphere-stratosphere coupling: Links to North Atlantic weather and climate, including their representation in CMIP5 models. *Journal of Geophysical Research Atmospheres*, **119**, 5864-5880. <http://dx.doi.org/10.1002/2013JD021191>



91. Lee, Y.-Y. and R.X. Black, 2013: Boreal winter low-frequency variability in CMIP5 models. *Journal of Geophysical Research Atmospheres*, **118**, 6891-6904. <http://dx.doi.org/10.1002/jgrd.50493>
92. Gillett, N.P. and J.C. Fyfe, 2013: Annular mode changes in the CMIP5 simulations. *Geophysical Research Letters*, **40**, 1189-1193. <http://dx.doi.org/10.1002/grl.50249>
93. Deser, C., A. Phillips, V. Bourdette, and H. Teng, 2012: Uncertainty in climate change projections: The role of internal variability. *Climate Dynamics*, **38**, 527-546. <http://dx.doi.org/10.1007/s00382-010-0977-x>
94. Manzini, E., A.Y. Karpechko, J. Anstey, M.P. Baldwin, R.X. Black, C. Cagnazzo, N. Calvo, A. Charlton-Perez, B. Christiansen, P. Davini, E. Gerber, M. Giorgetta, L. Gray, S.C. Hardiman, Y.Y. Lee, D.R. Marsh, B.A. McDaniel, A. Purich, A.A. Scaife, D. Shindell, S.W. Son, S. Watanabe, and G. Zappa, 2014: Northern winter climate change: Assessment of uncertainty in CMIP5 projections related to stratosphere-troposphere coupling. *Journal of Geophysical Research Atmospheres*, **119**, 7979-7998. <http://dx.doi.org/10.1002/2013JD021403>
95. Alexander, M.A., D.J. Vimont, P. Chang, and J.D. Scott, 2010: The impact of extratropical atmospheric variability on ENSO: Testing the seasonal footprinting mechanism using coupled model experiments. *Journal of Climate*, **23**, 2885-2901. <http://dx.doi.org/10.1175/2010jcli3205.1>
96. Vimont, D.J., J.M. Wallace, and D.S. Battisti, 2003: The seasonal footprinting mechanism in the Pacific: Implications for ENSO. *Journal of Climate*, **16**, 2668-2675. [http://dx.doi.org/10.1175/1520-0442\(2003\)016<2668:tsfmit>2.0.co;2](http://dx.doi.org/10.1175/1520-0442(2003)016<2668:tsfmit>2.0.co;2)
97. Di Lorenzo, E., K.M. Cobb, J.C. Furtado, N. Schneider, B.T. Anderson, A. Bracco, M.A. Alexander, and D.J. Vimont, 2010: Central Pacific El Niño and decadal climate change in the North Pacific Ocean. *Nature Geoscience*, **3**, 762-765. <http://dx.doi.org/10.1038/ngeo984>
98. Furtado, J.C., E.D. Lorenzo, N. Schneider, and N.A. Bond, 2011: North Pacific decadal variability and climate change in the IPCC AR4 models. *Journal of Climate*, **24**, 3049-3067. <http://dx.doi.org/10.1175/2010JCLI3584.1>
99. Leathers, D.J., B. Yarnal, and M.A. Palecki, 1991: The Pacific/North American teleconnection pattern and United States climate. Part I: Regional temperature and precipitation associations. *Journal of Climate*, **4**, 517-528. [http://dx.doi.org/10.1175/1520-0442\(1991\)004<0517:TPAT-PA>2.0.CO;2](http://dx.doi.org/10.1175/1520-0442(1991)004<0517:TPAT-PA>2.0.CO;2)
100. Loikith, P.C. and A.J. Broccoli, 2012: Characteristics of observed atmospheric circulation patterns associated with temperature extremes over North America. *Journal of Climate*, **25**, 7266-7281. <http://dx.doi.org/10.1175/JCLI-D-11-00709.1>
101. Coleman, J.S.M. and J.C. Rogers, 2003: Ohio River valley winter moisture conditions associated with the Pacific-North American teleconnection pattern. *Journal of Climate*, **16**, 969-981. [http://dx.doi.org/10.1175/1520-0442\(2003\)016<0969:ORVWMC>2.0.CO;2](http://dx.doi.org/10.1175/1520-0442(2003)016<0969:ORVWMC>2.0.CO;2)
102. Nigam, S., 2003: Teleconnections. *Encyclopedia of Atmospheric Sciences*. Holton, J.R., Ed. Academic Press, 2243-2269.
103. Li, Y. and N.-C. Lau, 2012: Impact of ENSO on the atmospheric variability over the North Atlantic in late winter – Role of transient eddies. *Journal of Climate*, **25**, 320-342. <http://dx.doi.org/10.1175/JCLI-D-11-00037.1>
104. Petoukhov, V., S. Rahmstorf, S. Petri, and H.J. Schellnhuber, 2013: Quasiresonant amplification of planetary waves and recent Northern Hemisphere weather extremes. *Proceedings of the National Academy of Sciences*, **110**, 5336-5341. <http://dx.doi.org/10.1073/pnas.1222000110>
105. Whan, K., F. Zwiers, and J. Sillmann, 2016: The influence of atmospheric blocking on extreme winter minimum temperatures in North America. *Journal of Climate*, **29**, 4361-4381. <http://dx.doi.org/10.1175/JCLI-D-15-0493.1>
106. Seager, R., M. Hoerling, S. Schubert, H. Wang, B. Lyon, A. Kumar, J. Nakamura, and N. Henderson, 2015: Causes of the 2011-14 California drought. *Journal of Climate*, **28**, 6997-7024. <http://dx.doi.org/10.1175/JCLI-D-14-00860.1>
107. Swain, D., M. Tsiang, M. Haughen, D. Singh, A. Charland, B. Rajarthan, and N.S. Diffenbaugh, 2014: The extraordinary California drought of 2013/14: Character, context and the role of climate change [in "Explaining Extreme Events of 2013 from a Climate Perspective"]. *Bulletin of the American Meteorological Society*, **95** (9), S3-S6. <http://dx.doi.org/10.1175/1520-0477-95.9.S1.1>
108. Teng, H. and G. Branstator, 2017: Causes of extreme ridges that induce California droughts. *Journal of Climate*, **30**, 1477-1492. <http://dx.doi.org/10.1175/jcli-d-16-0524.1>
109. Renwick, J.A. and J.M. Wallace, 1996: Relationships between North Pacific wintertime blocking, El Niño, and the PNA pattern. *Monthly Weather Review*, **124**, 2071-2076. [http://dx.doi.org/10.1175/1520-0493\(1996\)124<2071:RBNP-WB>2.0.CO;2](http://dx.doi.org/10.1175/1520-0493(1996)124<2071:RBNP-WB>2.0.CO;2)

110. Carrera, M.L., R.W. Higgins, and V.E. Kousky, 2004: Downstream weather impacts associated with atmospheric blocking over the northeast Pacific. *Journal of Climate*, **17**, 4823-4839. <http://dx.doi.org/10.1175/JCLI-3237.1>
111. Guirguis, K., A. Gershunov, R. Schwartz, and S. Bennett, 2011: Recent warm and cold daily winter temperature extremes in the Northern Hemisphere. *Geophysical Research Letters*, **38**, L17701. <http://dx.doi.org/10.1029/2011GL048762>
112. Wang, H., S. Schubert, R. Koster, Y.-G. Ham, and M. Suarez, 2014: On the role of SST forcing in the 2011 and 2012 extreme U.S. heat and drought: A study in contrasts. *Journal of Hydrometeorology*, **15**, 1255-1273. <http://dx.doi.org/10.1175/JHM-D-13-069.1>
113. Francis, J.A. and S.J. Vavrus, 2012: Evidence linking Arctic amplification to extreme weather in mid-latitudes. *Geophysical Research Letters*, **39**, L06801. <http://dx.doi.org/10.1029/2012GL051000>
114. Francis, J.A., S.J. Vavrus, and J. Cohen, 2017: Amplified Arctic warming and mid-latitude weather: Emerging connections. *Wiley Interdisciplinary Review: Climate Change*, **8**, e474. <http://dx.doi.org/10.1002/wcc.474>
115. Hanna, E., T.E. Cropper, R.J. Hall, and J. Cappel, 2016: Greenland blocking index 1851–2015: A regional climate change signal. *International Journal of Climatology*, **36**, 4847-4861. <http://dx.doi.org/10.1002/joc.4673>
116. Barnes, E.A., 2013: Revisiting the evidence linking Arctic amplification to extreme weather in midlatitudes. *Geophysical Research Letters*, **40**, 4734-4739. <http://dx.doi.org/10.1002/grl.50880>
117. Barnes, E.A., E. Dunn-Sigouin, G. Masato, and T. Woollings, 2014: Exploring recent trends in Northern Hemisphere blocking. *Geophysical Research Letters*, **41**, 638-644. <http://dx.doi.org/10.1002/2013GL058745>
118. Screen, J.A. and I. Simmonds, 2013: Exploring links between Arctic amplification and mid-latitude weather. *Geophysical Research Letters*, **40**, 959-964. <http://dx.doi.org/10.1002/grl.50174>
119. Hoskins, B. and T. Woollings, 2015: Persistent extratropical regimes and climate extremes. *Current Climate Change Reports*, **1**, 115-124. <http://dx.doi.org/10.1007/s40641-015-0020-8>
120. Kennedy, D., T. Parker, T. Woollings, B. Harvey, and L. Shaffrey, 2016: The response of high-impact blocking weather systems to climate change. *Geophysical Research Letters*, **43**, 7250-7258. <http://dx.doi.org/10.1002/2016GL069725>
121. Brandefelt, J. and H. Körnich, 2008: Northern Hemisphere stationary waves in future climate projections. *Journal of Climate*, **21**, 6341-6353. <http://dx.doi.org/10.1175/2008JCLI2373.1>
122. Haarsma, R.J. and F. Selten, 2012: Anthropogenic changes in the Walker circulation and their impact on the extra-tropical planetary wave structure in the Northern Hemisphere. *Climate Dynamics*, **39**, 1781-1799. <http://dx.doi.org/10.1007/s00382-012-1308-1>
123. Mantua, N.J., S.R. Hare, Y. Zhang, J.M. Wallace, and R.C. Francis, 1997: A Pacific interdecadal climate oscillation with impacts on salmon production. *Bulletin of the American Meteorological Society*, **78**, 1069-1080. [http://dx.doi.org/10.1175/1520-0477\(1997\)078<1069:APICOW>2.0.CO;2](http://dx.doi.org/10.1175/1520-0477(1997)078<1069:APICOW>2.0.CO;2)
124. Hartmann, B. and G. Wendler, 2005: The significance of the 1976 Pacific climate shift in the climatology of Alaska. *Journal of Climate*, **18**, 4824-4839. <http://dx.doi.org/10.1175/JCLI3532.1>
125. McAfee, S.A., 2014: Consistency and the lack thereof in Pacific Decadal Oscillation impacts on North American winter climate. *Journal of Climate*, **27**, 7410-7431. <http://dx.doi.org/10.1175/JCLI-D-14-00143.1>
126. Wang, T., O.H. Otterå, Y. Gao, and H. Wang, 2012: The response of the North Pacific Decadal Variability to strong tropical volcanic eruptions. *Climate Dynamics*, **39**, 2917-2936. <http://dx.doi.org/10.1007/s00382-012-1373-5>
127. Boo, K.-O., B.B.B. Booth, Y.-H. Byun, J. Lee, C. Cho, S. Shim, and K.-T. Kim, 2015: Influence of aerosols in multidecadal SST variability simulations over the North Pacific. *Journal of Geophysical Research Atmospheres*, **120**, 517-531. <http://dx.doi.org/10.1002/2014JD021933>
128. Yeh, S.-W., W.-M. Kim, Y.H. Kim, B.-K. Moon, R.J. Park, and C.-K. Song, 2013: Changes in the variability of the North Pacific sea surface temperature caused by direct sulfate aerosol forcing in China in a coupled general circulation model. *Journal of Geophysical Research Atmospheres*, **118**, 1261-1270. <http://dx.doi.org/10.1029/2012JD017947>
129. Meehl, G.A., A. Hu, J.M. Arblaster, J. Fasullo, and K.E. Trenberth, 2013: Externally forced and internally generated decadal climate variability associated with the Interdecadal Pacific Oscillation. *Journal of Climate*, **26**, 7298-7310. <http://dx.doi.org/10.1175/JCLI-D-12-00548.1>
130. Meehl, G.A., A. Hu, B.D. Santer, and S.-P. Xie, 2016: Contribution of the Interdecadal Pacific Oscillation to twentieth-century global surface temperature trends. *Nature Climate Change*, **6**, 1005-1008. <http://dx.doi.org/10.1038/nclimate3107>

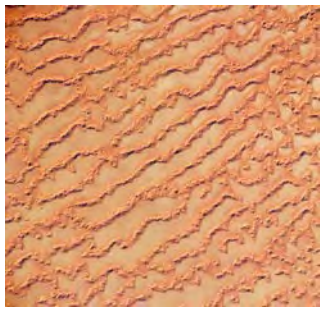
131. Lapp, S.L., J.-M. St. Jacques, E.M. Barrow, and D.J. Sauchyn, 2012: GCM projections for the Pacific Decadal Oscillation under greenhouse forcing for the early 21st century. *International Journal of Climatology*, **32**, 1423-1442. <http://dx.doi.org/10.1002/joc.2364>
132. Newman, M., 2007: Interannual to decadal predictability of tropical and North Pacific sea surface temperatures. *Journal of Climate*, **20**, 2333-2356. <http://dx.doi.org/10.1175/jcli4165.1>
133. Feng, S., Q. Hu, and R.J. Oglesby, 2011: Influence of Atlantic sea surface temperatures on persistent drought in North America. *Climate Dynamics*, **37**, 569-586. <http://dx.doi.org/10.1007/s00382-010-0835-x>
134. Kavvada, A., A. Ruiz-Barradas, and S. Nigam, 2013: AMO's structure and climate footprint in observations and IPCC AR5 climate simulations. *Climate Dynamics*, **41**, 1345-1364. <http://dx.doi.org/10.1007/s00382-013-1712-1>
135. Seager, R., Y. Kushnir, M. Ting, M. Cane, N. Naik, and J. Miller, 2008: Would advance knowledge of 1930s SSTs have allowed prediction of the Dust Bowl drought? *Journal of Climate*, **21**, 3261-3281. <http://dx.doi.org/10.1175/2007JCLI2134.1>
136. Chylek, P. and G. Lesins, 2008: Multidecadal variability of Atlantic hurricane activity: 1851-2007. *Journal of Geophysical Research*, **113**, D22106. <http://dx.doi.org/10.1029/2008JD010036>
137. Gray, W.M., J.D. Sheaffer, and C.W. Landsea, 1997: Climate trends associated with multidecadal variability of Atlantic hurricane activity. *Hurricanes: Climate and Socioeconomic Impacts*. Diaz, H.F. and R.S. Pulwarty, Eds. Springer, Berlin, Heidelberg, 15-53. http://dx.doi.org/10.1007/978-3-642-60672-4_2
138. Kossin, J.P., 2017: Hurricane intensification along U. S. coast suppressed during active hurricane periods. *Nature*, **541**, 390-393. <http://dx.doi.org/10.1038/nature20783>
139. Landsea, C.W., R.A. Pielke Jr., A.M. Messtas-Nuñez, and J.A. Knaff, 1999: Atlantic basin hurricanes: Indices of climatic changes. *Climatic Change*, **42**, 89-129. <http://dx.doi.org/10.1023/a:1005416332322>
140. Zhang, R. and T.L. Delworth, 2009: A new method for attributing climate variations over the Atlantic hurricane basin's main development region. *Geophysical Research Letters*, **36**, L06701. <http://dx.doi.org/10.1029/2009GL037260>
141. Caron, L.-P., M. Boudreault, and C.L. Bruyère, 2015: Changes in large-scale controls of Atlantic tropical cyclone activity with the phases of the Atlantic Multidecadal Oscillation. *Climate Dynamics*, **44**, 1801-1821. <http://dx.doi.org/10.1007/s00382-014-2186-5>
142. Delworth, L.T. and E.M. Mann, 2000: Observed and simulated multidecadal variability in the Northern Hemisphere. *Climate Dynamics*, **16**, 661-676. <http://dx.doi.org/10.1007/s003820000075>
143. Delworth, T.L., F. Zeng, L. Zhang, R. Zhang, G.A. Vecchi, and X. Yang, 2017: The central role of ocean dynamics in connecting the North Atlantic Oscillation to the extratropical component of the Atlantic Multidecadal Oscillation. *Journal of Climate*, **30**, 3789-3805. <http://dx.doi.org/10.1175/jcli-d-16-0358.1>
144. Frankcombe, L.M., A.v.d. Heydt, and H.A. Dijkstra, 2010: North Atlantic multidecadal climate variability: An investigation of dominant time scales and processes. *Journal of Climate*, **23**, 3626-3638. <http://dx.doi.org/10.1175/2010jcli3471.1>
145. Knight, J.R., C.K. Folland, and A.A. Scaife, 2006: Climate impacts of the Atlantic Multidecadal Oscillation. *Geophysical Research Letters*, **33**, L17706. <http://dx.doi.org/10.1029/2006GL026242>
146. Mann, M.E., B.A. Steinman, and S.K. Miller, 2014: On forced temperature changes, internal variability, and the AMO. *Geophysical Research Letters*, **41**, 3211-3219. <http://dx.doi.org/10.1002/2014GL059233>
147. Moore, G.W.K., J. Halfar, H. Majeed, W. Adey, and A. Kronz, 2017: Amplification of the Atlantic Multidecadal Oscillation associated with the onset of the industrial-era warming. *Scientific Reports*, **7**, 40861. <http://dx.doi.org/10.1038/srep40861>
148. Terray, L., 2012: Evidence for multiple drivers of North Atlantic multi-decadal climate variability. *Geophysical Research Letters*, **39**, L19712. <http://dx.doi.org/10.1029/2012GL053046>
149. Miles, M.W., D.V. Divine, T. Furevik, E. Jansen, M. Moros, and A.E.J. Ogilvie, 2014: A signal of persistent Atlantic multidecadal variability in Arctic sea ice. *Geophysical Research Letters*, **41**, 463-469. <http://dx.doi.org/10.1002/2013GL058084>
150. Trenary, L. and T. DelSole, 2016: Does the Atlantic Multidecadal Oscillation get its predictability from the Atlantic Meridional Overturning Circulation? *Journal of Climate*, **29**, 5267-5280. <http://dx.doi.org/10.1175/jcli-d-16-0030.1>



151. Clement, A., K. Bellomo, L.N. Murphy, M.A. Cane, T. Mauritsen, G. Rädcl, and B. Stevens, 2015: The Atlantic Multidecadal Oscillation without a role for ocean circulation. *Science*, **350**, 320-324. <http://dx.doi.org/10.1126/science.aab3980>
152. Clement, A., M.A. Cane, L.N. Murphy, K. Bellomo, T. Mauritsen, and B. Stevens, 2016: Response to Comment on "The Atlantic Multidecadal Oscillation without a role for ocean circulation". *Science*, **352**, 1527-1527. <http://dx.doi.org/10.1126/science.aaf2575>
153. Srivastava, A. and T. DelSole, 2017: Decadal predictability without ocean dynamics. *Proceedings of the National Academy of Sciences*, **114**, 2177-2182. <http://dx.doi.org/10.1073/pnas.1614085114>
154. Zhang, R., R. Sutton, G. Danabasoglu, T.L. Delworth, W.M. Kim, J. Robson, and S.G. Yeager, 2016: Comment on "The Atlantic Multidecadal Oscillation without a role for ocean circulation". *Science*, **352**, 1527-1527. <http://dx.doi.org/10.1126/science.aaf1660>
155. Canty, T., N.R. Mascioli, M.D. Smarte, and R.J. Salawitch, 2013: An empirical model of global climate - Part 1: A critical evaluation of volcanic cooling. *Atmospheric Chemistry and Physics*, **13**, 3997-4031. <http://dx.doi.org/10.5194/acp-13-3997-2013>
156. Evan, A.T., 2012: Atlantic hurricane activity following two major volcanic eruptions. *Journal of Geophysical Research*, **117**, D06101. <http://dx.doi.org/10.1029/2011JD016716>
157. Evan, A.T., D.J. Vimont, A.K. Heidinger, J.P. Kossin, and R. Bennartz, 2009: The role of aerosols in the evolution of tropical North Atlantic Ocean temperature anomalies. *Science*, **324**, 778-781. <http://dx.doi.org/10.1126/science.1167404>
158. Booth, B.B.B., N.J. Dunstone, P.R. Halloran, T. Andrews, and N. Bellouin, 2012: Aerosols implicated as a prime driver of twentieth-century North Atlantic climate variability. *Nature*, **484**, 228-232. <http://dx.doi.org/10.1038/nature10946>
159. Dunstone, N.J., D.M. Smith, B.B.B. Booth, L. Hermanson, and R. Eade, 2013: Anthropogenic aerosol forcing of Atlantic tropical storms. *Nature Geoscience*, **6**, 534-539. <http://dx.doi.org/10.1038/ngeo1854>
160. Mann, M.E. and K.A. Emanuel, 2006: Atlantic hurricane trends linked to climate change. *Eos, Transactions, American Geophysical Union*, **87**, 233-244. <http://dx.doi.org/10.1029/2006EO240001>
161. Sobel, A.H., S.J. Camargo, T.M. Hall, C.-Y. Lee, M.K. Tippett, and A.A. Wing, 2016: Human influence on tropical cyclone intensity. *Science*, **353**, 242-246. <http://dx.doi.org/10.1126/science.aaf6574>
162. Carslaw, K.S., L.A. Lee, C.L. Reddington, K.J. Pringle, A. Rap, P.M. Forster, G.W. Mann, D.V. Spracklen, M.T. Woodhouse, L.A. Regayre, and J.R. Pierce, 2013: Large contribution of natural aerosols to uncertainty in indirect forcing. *Nature*, **503**, 67-71. <http://dx.doi.org/10.1038/nature12674>
163. Stevens, B., 2015: Rethinking the lower bound on aerosol radiative forcing. *Journal of Climate*, **28**, 4794-4819. <http://dx.doi.org/10.1175/jcli-d-14-00656.1>
164. Ting, M., Y. Kushnir, R. Seager, and C. Li, 2009: Forced and internal twentieth-century SST trends in the North Atlantic. *Journal of Climate*, **22**, 1469-1481. <http://dx.doi.org/10.1175/2008jcli2561.1>
165. Tung, K.-K. and J. Zhou, 2013: Using data to attribute episodes of warming and cooling in instrumental records. *Proceedings of the National Academy of Sciences*, **110**, 2058-2063. <http://dx.doi.org/10.1073/pnas.1212471110>
166. Zhang, R., T.L. Delworth, R. Sutton, D.L.R. Hodson, K.W. Dixon, I.M. Held, Y. Kushnir, J. Marshall, Y. Ming, R. Msadek, J. Robson, A.J. Rosati, M. Ting, and G.A. Vecchi, 2013: Have aerosols caused the observed Atlantic multidecadal variability? *Journal of the Atmospheric Sciences*, **70**, 1135-1144. <http://dx.doi.org/10.1175/jas-d-12-0331.1>
167. Vincze, M. and I.M. Jánosi, 2011: Is the Atlantic Multidecadal Oscillation (AMO) a statistical phantom? *Nonlinear Processes in Geophysics*, **18**, 469-475. <http://dx.doi.org/10.5194/npg-18-469-2011>
168. Dima, M. and G. Lohmann, 2007: A hemispheric mechanism for the Atlantic Multidecadal Oscillation. *Journal of Climate*, **20**, 2706-2719. <http://dx.doi.org/10.1175/jcli4174.1>
169. Chylek, P., C.K. Folland, H.A. Dijkstra, G. Lesins, and M.K. Dubey, 2011: Ice-core data evidence for a prominent near 20 year time-scale of the Atlantic Multidecadal Oscillation. *Geophysical Research Letters*, **38**, L13704. <http://dx.doi.org/10.1029/2011GL047501>
170. Gray, S.T., L.J. Graumlich, J.L. Betancourt, and G.T. Pederson, 2004: A tree-ring based reconstruction of the Atlantic Multidecadal Oscillation since 1567 A.D. *Geophysical Research Letters*, **31**, L12205. <http://dx.doi.org/10.1029/2004GL019932>

171. Knudsen, M.F., B.H. Jacobsen, M.-S. Seidenkrantz, and J. Olsen, 2014: Evidence for external forcing of the Atlantic Multidecadal Oscillation since termination of the Little Ice Age. *Nature Communications*, **5**, 3323. <http://dx.doi.org/10.1038/ncomms4323>
172. Mann, M.E., J.D. Woodruff, J.P. Donnelly, and Z. Zhang, 2009: Atlantic hurricanes and climate over the past 1,500 years. *Nature*, **460**, 880-883. <http://dx.doi.org/10.1038/nature08219>
173. Deser, C., A.S. Phillips, M.A. Alexander, and B.V. Smoliak, 2014: Projecting North American climate over the next 50 years: Uncertainty due to internal variability. *Journal of Climate*, **27**, 2271-2296. <http://dx.doi.org/10.1175/JCLI-D-13-00451.1>
174. Wettstein, J.J. and C. Deser, 2014: Internal variability in projections of twenty-first-century Arctic sea ice loss: Role of the large-scale atmospheric circulation. *Journal of Climate*, **27**, 527-550. <http://dx.doi.org/10.1175/JCLI-D-12-00839.1>
175. Thompson, D.W.J., E.A. Barnes, C. Deser, W.E. Foust, and A.S. Phillips, 2015: Quantifying the role of internal climate variability in future climate trends. *Journal of Climate*, **28**, 6443-6456. <http://dx.doi.org/10.1175/JCLI-D-14-00830.1>
176. Knutson, T.R., F. Zeng, and A.T. Wittenberg, 2013: Multimodel assessment of regional surface temperature trends: CMIP3 and CMIP5 twentieth-century simulations. *Journal of Climate*, **26**, 8709-8743. <http://dx.doi.org/10.1175/JCLI-D-12-00567.1>
177. NWS, 2016: Global Circulations in NWS Jet Stream: An Online School for Weather. National Weather Service. <http://www.srh.noaa.gov/jetstream/global/circ.html>
178. Lindsey, R., 2016: How El Niño and La Niña affect the winter jet stream and U.S. climate. Climate.gov. <https://www.climate.gov/news-features/featured-images/how-el-ni%C3%B1o-and-la-ni%C3%B1a-affect-winter-jet-stream-and-us-climate>
179. Vose, R.S., S. Applequist, M. Squires, I. Durre, M.J. Menne, C.N. Williams, Jr., C. Fenimore, K. Gleason, and D. Arndt, 2014: Improved historical temperature and precipitation time series for U.S. climate divisions. *Journal of Applied Meteorology and Climatology*, **53**, 1232-1251. <http://dx.doi.org/10.1175/JAMC-D-13-0248.1>





6

Temperature Changes in the United States

KEY FINDINGS

1. Annual average temperature over the contiguous United States has increased by 1.2°F (0.7°C) for the period 1986–2016 relative to 1901–1960 and by 1.8°F (1.0°C) based on a linear regression for the period 1895–2016 (*very high confidence*). Surface and satellite data are consistent in their depiction of rapid warming since 1979 (*high confidence*). Paleo-temperature evidence shows that recent decades are the warmest of the past 1,500 years (*medium confidence*).
2. There have been marked changes in temperature extremes across the contiguous United States. The frequency of cold waves has decreased since the early 1900s, and the frequency of heat waves has increased since the mid-1960s. The Dust Bowl era of the 1930s remains the peak period for extreme heat. The number of high temperature records set in the past two decades far exceeds the number of low temperature records. (*Very high confidence*)
3. Annual average temperature over the contiguous United States is projected to rise (*very high confidence*). Increases of about 2.5°F (1.4°C) are projected for the period 2021–2050 relative to 1976–2005 in all RCP scenarios, implying recent record-setting years may be “common” in the next few decades (*high confidence*). Much larger rises are projected by late century (2071–2100): 2.8°–7.3°F (1.6°–4.1°C) in a lower scenario (RCP4.5) and 5.8°–11.9°F (3.2°–6.6°C) in the higher scenario (RCP8.5) (*high confidence*).
4. Extreme temperatures in the contiguous United States are projected to increase even more than average temperatures. The temperatures of extremely cold days and extremely warm days are both expected to increase. Cold waves are projected to become less intense while heat waves will become more intense. The number of days below freezing is projected to decline while the number above 90°F will rise. (*Very high confidence*)

Recommended Citation for Chapter

Vose, R.S., D.R. Easterling, K.E. Kunkel, A.N. LeGrande, and M.F. Wehner, 2017: Temperature changes in the United States. In: *Climate Science Special Report: Fourth National Climate Assessment, Volume I* [Wuebbles, D.J., D.W. Fahey, K.A. Hibbard, D.J. Dokken, B.C. Stewart, and T.K. Maycock (eds.)]. U.S. Global Change Research Program, Washington, DC, USA, pp. 185-206, doi: 10.7930/J0N29V45.

Introduction

Temperature is among the most important climatic elements used in decision-making. For example, builders and insurers use temperature data for planning and risk management while energy companies and regulators use temperature data to predict demand and set utility rates. Temperature is also a key indicator of climate change: recent increases are apparent over the land, ocean, and troposphere, and substantial changes are expected for this century. This chapter summarizes the major observed and projected changes in near-surface air temperature over the United States, emphasizing new data sets and model projections since the Third National Climate Assessment (NCA3). Changes are depicted using a spectrum of observations, including surface weather stations, moored ocean buoys, polar-orbiting satellites, and temperature-sensitive proxies. Projections are based on global models and downscaled products from CMIP5 (Coupled Model Intercomparison Project Phase 5) using a suite of Representative Concentration Pathways (RCPs; see Ch. 4: Projections for more on RCPs and future scenarios).

6.1 Historical Changes

6.1.1 Average Temperatures

Changes in average temperature are described using a suite of observational datasets. As in NCA3, changes in land temperature are assessed using the nClimGrid dataset.^{1,2} Along U.S. coastlines, changes in sea surface temperatures are quantified using a new reconstruction³ that forms the ocean component of the NOAA Global Temperature dataset.⁴ Changes in middle tropospheric temperature are examined using updated versions of multiple satellite datasets.^{5,6,7}

The annual average temperature of the contiguous United States has risen since the start of the 20th century. In general, temperature increased until about 1940, decreased until

about 1970, and increased rapidly through 2016. Because the increase was not constant over time, multiple methods were evaluated in this report (as in NCA3) to quantify the trend. All methods yielded rates of warming that were significant at the 95% level. The lowest estimate of 1.2°F (0.7°C) was obtained by computing the difference between the average for 1986–2016 (i.e., present-day) and the average for 1901–1960 (i.e., the first half of the last century). The highest estimate of 1.8°F (1.0°C) was obtained by fitting a linear (least-squares) regression line through the period 1895–2016. Thus, the temperature increase cited in this assessment is 1.2°–1.8°F (0.7°–1.0°C).

This increase is about 0.1°F (0.06°C) less than presented in NCA3, and it results from the use of slightly different periods in each report. In particular, the decline in the lower bound stems from the use of different time periods to represent present-day climate (NCA3 used 1991–2012, which was slightly warmer than the 1986–2016 period used here). The decline in the upper bound stems mainly from temperature differences late in the record (e.g., the last year of data available for NCA3 was 2012, which was the warmest year on record for the contiguous United States).

Each NCA region experienced a net warming through 2016 (Table 6.1). The largest changes were in the western United States, where average temperature increased by more than 1.5°F (0.8°C) in Alaska, the Northwest, the Southwest, and also in the Northern Great Plains. As noted in NCA3, the Southeast had the least warming, driven by a combination of natural variations and human influences.⁸ In most regions, average minimum temperature increased at a slightly higher rate than average maximum temperature, with the Midwest having the largest discrepancy, and the Southwest and Northwest having the smallest. This differential rate of warming resulted in a continuing



Table 6.1. Observed changes in annual average temperature (°F) for each National Climate Assessment region. Changes are the difference between the average for present-day (1986–2016) and the average for the first half of the last century (1901–1960 for the contiguous United States, 1925–1960 for Alaska, Hawai’i, and the Caribbean). Estimates are derived from the nClimDiv dataset^{1,2}.

NCA Region	Change in Annual Average Temperature	Change in Annual Average Maximum Temperature	Change in Annual Average Minimum Temperature
Contiguous U.S.	1.23°F	1.06°F	1.41°F
Northeast	1.43°F	1.16°F	1.70°F
Southeast	0.46°F	0.16°F	0.76°F
Midwest	1.26°F	0.77°F	1.75°F
Great Plains North	1.69°F	1.66°F	1.72°F
Great Plains South	0.76°F	0.56°F	0.96°F
Southwest	1.61°F	1.61°F	1.61°F
Northwest	1.54°F	1.52°F	1.56°F
Alaska	1.67°F	1.43°F	1.91°F
Hawaii	1.26°F	1.01°F	1.49°F
Caribbean	1.35°F	1.08°F	1.60°F

decrease in the diurnal temperature range that is consistent with other parts of the globe.⁹ Annual average sea surface temperature also increased along all regional coastlines (see Figure 1.3), though changes were generally smaller than over land owing to the higher heat capacity of water. Increases were largest in Alaska (greater than 1.0°F [0.6°C]) while increases were smallest (less than 0.5°F [0.3°C]) in coastal areas of the Southeast.

More than 95% of the land surface of the contiguous United States had an increase in annual average temperature (Figure 6.1). In contrast, only small (and somewhat dispersed) parts of the Southeast and Southern Great Plains experienced cooling. From a seasonal perspective, warming was greatest and most widespread in winter, with increases of over 1.5°F (0.8°C) in most areas. In summer, warming was less extensive (mainly along the East Coast and in the western third of the Nation), while cooling was evident in parts of the Southeast, Midwest, and Great Plains.

There has been a rapid increase in the average temperature of the contiguous United States over the past several decades. There is general consistency on this point between the surface thermometer record from NOAA¹ and the middle tropospheric satellite records from Remote Sensing Systems (RSS),⁵ NOAA’s Center for Satellite Applications and Research (STAR),⁷ and the University of Alabama in Huntsville (UAH).⁶ In particular, for the period 1979–2016, the rate of warming in the surface record was 0.512°F (0.284°C) per decade, versus trends of 0.455°F (0.253°C), 0.421°F (0.234°C), and 0.289°F (0.160°C) per decade for RSS version 4, STAR version 3, and UAH version 6, respectively (after accounting for stratospheric influences). All trends are statistically significant at the 95% level. For the contiguous United States, the year 2016 was the second-warmest on record at the surface and in the middle troposphere (2012 was the warmest year at the surface, and 2015 was the warmest in the middle troposphere). Generally speaking, surface and satellite records

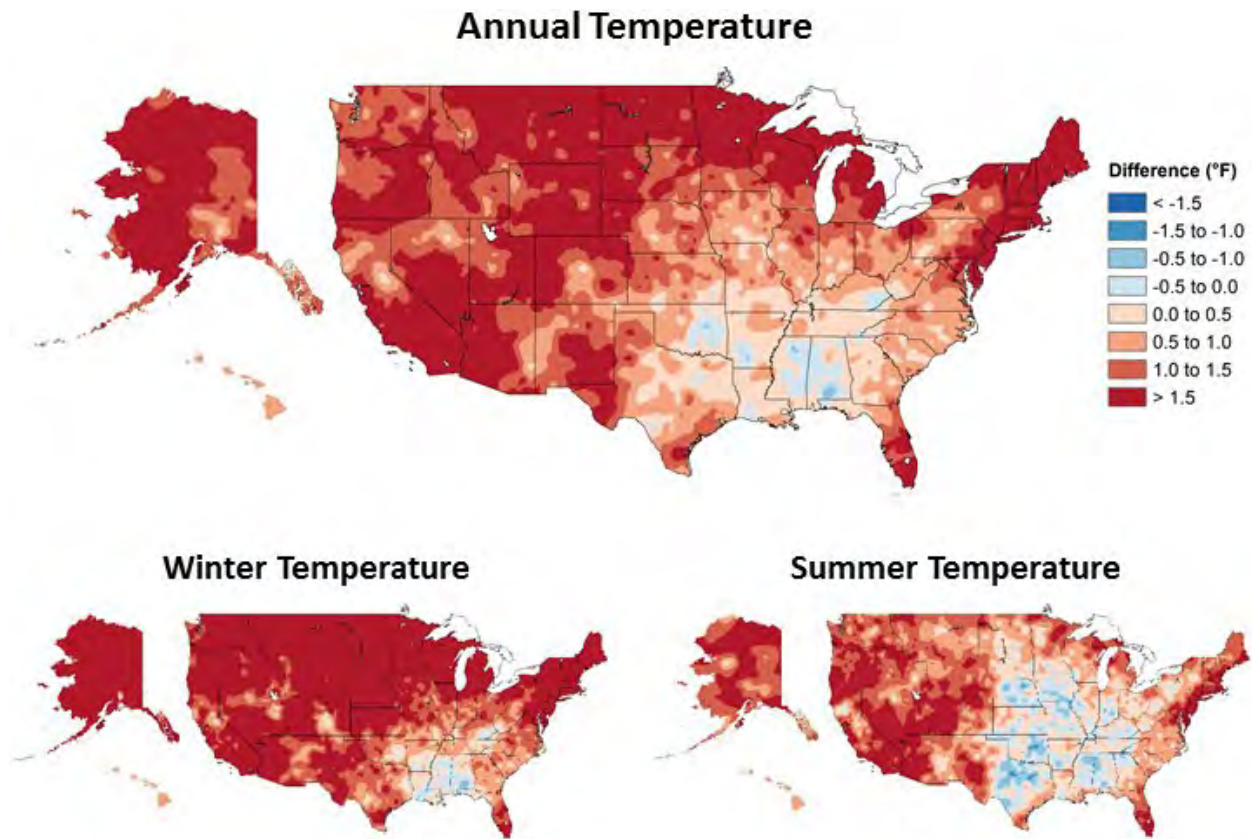


Figure 6.1. Observed changes in annual, winter, and summer temperature (°F). Changes are the difference between the average for present-day (1986–2016) and the average for the first half of the last century (1901–1960 for the contiguous United States, 1925–1960 for Alaska and Hawai’i). Estimates are derived from the nClimDiv dataset.^{1,2} (Figure source: NOAA/NCEI).

do not have identical trends because they do not represent the same physical quantity; surface measurements are made using thermometers in shelters about 1.5 meters above the ground whereas satellite measurements are mass-weighted averages of microwave emissions from deep atmospheric layers. The UAH record likely has a lower trend because it differs from the other satellite products in the treatment of target temperatures from the NOAA-9 satellite as well as in the correction for diurnal drift.¹⁰

Recent paleo-temperature evidence confirms the unusual character of wide-scale warming during the past few decades as determined from the instrumental record. The most important new paleoclimate study since NCA3 showed that for each of the seven continental regions, the reconstructed area-weighted

average temperature for 1971–2000 was higher than for any other time in nearly 1,400 years,¹¹ although with significant uncertainty around the central estimate that leads to this conclusion. Recent (up to 2006) 30-year smoothed temperatures across temperate North America (including most of the continental United States) are similarly reconstructed as the warmest over the past 1,500 years¹² (Figure 6.2). Unlike the PAGES 2k seven-continent result mentioned above, this conclusion for North America is robust in relation to the estimated uncertainty range. Reconstruction data since 1500 for western temperate North America show the same conclusion at the annual time scale for 1986–2005. This time period and the running 20-year periods thereafter are warmer than all possible continuous 20-year sequences in a 1,000-member statistical reconstruction ensemble.¹³

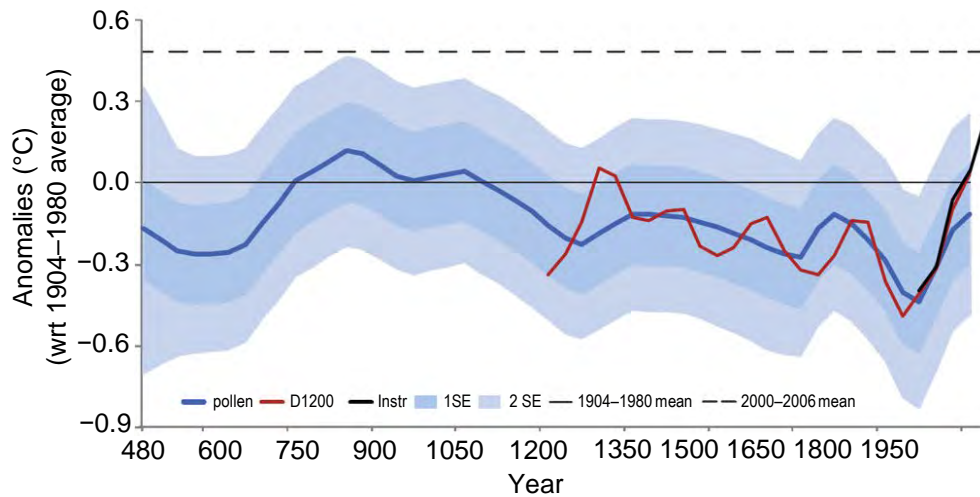


Figure 6.2. Pollen-based temperature reconstruction for temperate North America. The blue curve depicts the pollen-based reconstruction of 30-year averages (as anomalies from 1904 to 1980) for the temperate region (30°–55°N, 75°–130°W). The red curve shows the corresponding tree ring-based decadal average reconstruction, which was smoothed and used to calibrate the lower-frequency pollen-based estimate. Light (medium) blue zones indicate 2 standard error (1 standard error) uncertainty estimations associated with each 30-year value. The black curve shows comparably smoothed instrumental temperature values up to 1980. The dashed black line represents the average temperature anomaly of comparably smoothed instrumental data for the period 2000–2006. (Figure source: NOAA NCEI).

6.1.2 Temperature Extremes

Shifts in temperature extremes are examined using a suite of societally relevant climate change indices^{14, 15} derived from long-term observations of daily surface temperature.¹⁶ The coldest and warmest temperatures of the year are of particular relevance given their widespread use in engineering, agricultural, and other sectoral applications (for example, extreme annual design conditions by the American Society of Heating, Refrigeration, and Air Conditioning; plant hardiness zones by the U.S. Department of Agriculture). Cold waves and heat waves (that is, extended periods of below or above normal temperature) are likewise of great importance because of their numerous societal and environmental impacts, which span from human health to plant and animal phenology. Changes are considered for a spectrum of event frequencies and intensities, ranging from the typical annual extreme to the 1-in-10 year event (an extreme that only has a 10% chance of occurrence in any given year). The discussion focuses on the contiguous United States; Alaska, Hawai'i, and the Caribbean

do not have a sufficient number of long-term stations for a century-scale analysis.

Cold extremes have become less severe over the past century. For example, the coldest daily temperature of the year has increased at most locations in the contiguous United States (Figure 6.3). All regions experienced net increases (Table 6.2), with the largest rises in the Northern Great Plains and the Northwest (roughly 4.5°F [2.5°C]), and the smallest in the Southeast (about 1.0°F [0.6°C]). In general, there were increases throughout the record, with a slight acceleration in recent decades (Figure 6.3). The temperature of extremely cold days (1-in-10 year events) generally exhibited the same pattern of increases as the coldest daily temperature of the year. Consistent with these increases, the number of cool nights per year (those with a minimum temperature below the 10th percentile for 1961–1990) declined in all regions, with much of the West having decreases of roughly two weeks. The frequency of cold waves (6-day periods with a minimum temperature below the

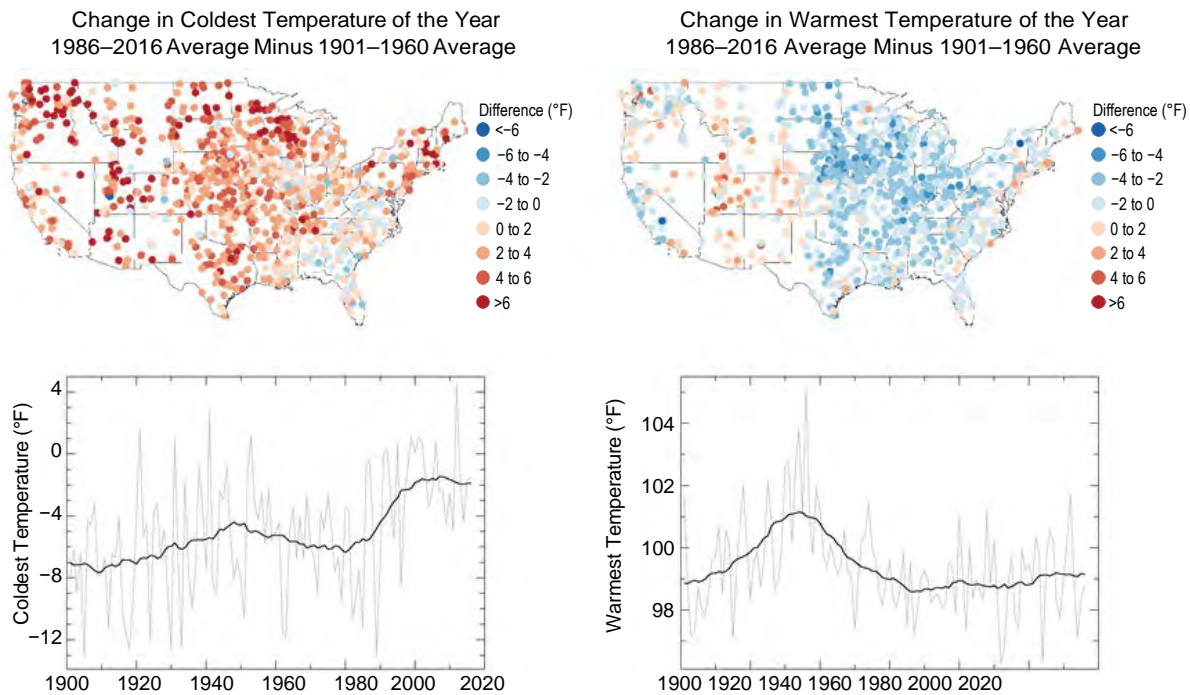


Figure 6.3. Observed changes in the coldest and warmest daily temperatures (°F) of the year in the contiguous United States. Maps (top) depict changes at stations; changes are the difference between the average for present-day (1986–2016) and the average for the first half of the last century (1901–1960). Time series (bottom) depict the area-weighted average for the contiguous United States. Estimates are derived from long-term stations with minimal missing data in the Global Historical Climatology Network–Daily dataset.¹⁶ (Figure source: NOAA/NCEI).

Table 6.2. Observed changes in the coldest and warmest daily temperatures (°F) of the year for each National Climate Assessment region in the contiguous United States. Changes are the difference between the average for present-day (1986–2016) and the average for the first half of the last century (1901–1960). Estimates are derived from long-term stations with minimal missing data in the Global Historical Climatology Network–Daily dataset.¹⁶

NCA Region	Change in Coldest Day of the Year	Change in Warmest Day of the Year
Northeast	2.83°F	-0.92°F
Southeast	1.13°F	-1.49°F
Midwest	2.93°F	-2.22°F
Great Plains North	4.40°F	-1.08°F
Great Plains South	3.25°F	-1.07°F
Southwest	3.99°F	0.50°F
Northwest	4.78°F	-0.17°F

10th percentile for 1961–1990) has fallen over the past century (Figure 6.4). The frequency of intense cold waves (4-day, 1-in-5 year events) peaked in the 1980s and then reached record-low levels in the 2000s.¹⁷

Changes in warm extremes are more nuanced than changes in cold extremes. For instance, the warmest daily temperature of the year increased in some parts of the West over the past century (Figure 6.3), but there were decreases in almost all locations east of the Rocky Mountains. In fact, all eastern regions experienced a net decrease (Table 6.2), most notably the Midwest (about 2.2°F [1.2°C]) and the Southeast (roughly 1.5°F [0.8°C]). The decreases in the eastern half of Nation, particularly in the Great Plains, are mainly tied to the unprecedented summer heat of the 1930s Dust Bowl era, which was exacerbated by land-surface feedbacks driven by springtime

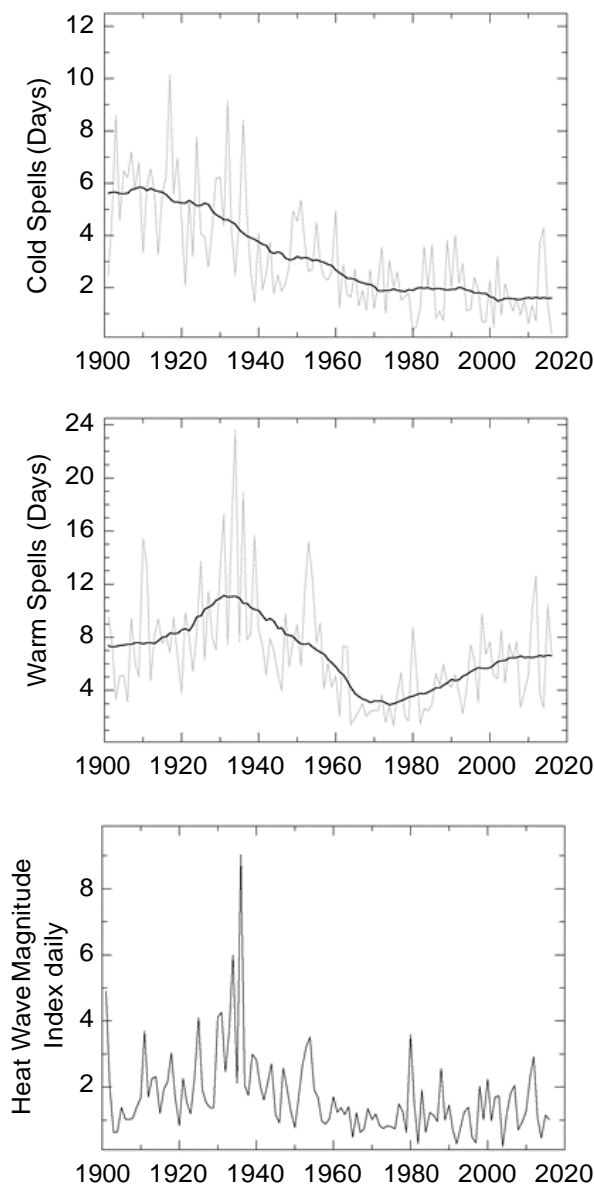


Figure 6.4. Observed changes in cold and heat waves in the contiguous United States. The top panel depicts changes in the frequency of cold waves; the middle panel depicts changes in the frequency of heat waves; and the bottom panel depicts changes in the intensity of heat waves. Cold and heat wave frequency indices are defined in Zhang et al.,¹⁵ and the heat wave intensity index is defined in Russo et al.¹⁴ Estimates are derived from long-term stations with minimal missing data in the Global Historical Climatology Network–Daily dataset.¹⁶ (Figure source: NOAA/NCEI).

precipitation deficits and land mismanagement.¹⁸ However, anthropogenic aerosol forcing may also have reduced summer temperatures in the Northeast and Southeast from the early 1950s to the mid-1970s,¹⁹ and agricultural intensification may have suppressed the hottest extremes in the Midwest.²⁰ Since the mid-1960s, there has been only a very slight increase in the warmest daily temperature of the year (amidst large interannual variability). Heat waves (6-day periods with a

maximum temperature above the 90th percentile for 1961–1990) increased in frequency until the mid-1930s, became considerably less common through the mid-1960s, and increased in frequency again thereafter (Figure 6.4). As with warm daily temperatures, heat wave magnitude reached a maximum in the 1930s. The frequency of intense heat waves (4-day, 1-in-5 year events) has generally increased since the 1960s in most regions except the Midwest and the Great

Plains.^{17,21} Since the early 1980s (Figure 6.4), there is suggestive evidence of a slight increase in the intensity of heat waves nationwide¹⁴ as well as an increase in the concurrence of droughts and heat waves.²²

Changes in the occurrence of record-setting daily temperatures are also apparent. Very generally, the number of record lows has been declining since the late-1970s while the number of record highs has been rising.²³ By extension, there has been an increase in the ratio of the number of record highs to record lows (Figure 6.5). Over the past two decades, the average of this ratio exceeds two (meaning that twice as many high-temperature records have been set as low-temperature records). The number of new highs has surpassed the number of new lows in 15 of the last 20 years, with 2012 and 2016 being particularly extreme (ratios of seven and five, respectively).

6.2 Detection and Attribution

6.2.1 Average Temperatures

While a confident attribution of global temperature increases to anthropogenic forcing has been made,²⁴ detection and attribution assessment statements for smaller regions are generally much weaker. Nevertheless, some detectable anthropogenic influences on average temperature have been reported for North America and parts of the United States (e.g., Christidis et al. 2010;²⁵ Bonfils et al. 2008;²⁶ Pierce et al. 2009²⁷). Figure 6.6 shows an example for linear trends for 1901–2015, indicating a detectable anthropogenic warming since 1901 over the western and northern regions of the contiguous United States for the CMIP5 multimodel ensemble—a condition that was also met for most of the individual models.²⁸ The Southeast stands out as the only region with no “detectable” warming since 1901; observed trends there were inconsistent with CMIP5 All Forcing historical runs.²⁸ The cause

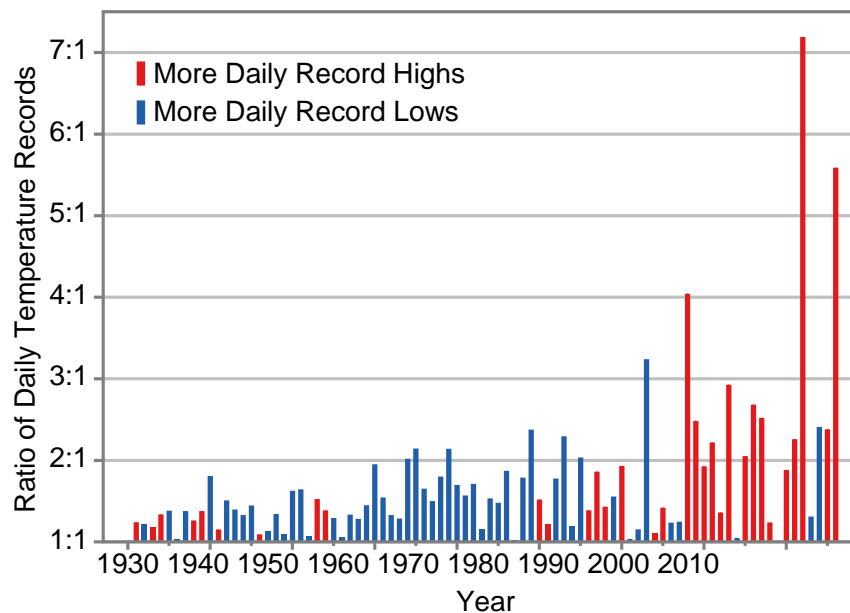


Figure 6.5. Observed changes in the occurrence of record-setting daily temperatures in the contiguous United States. Red bars indicate a year with more daily record highs than daily record lows, while blue bars indicate a year with more record lows than highs. The height of the bar indicates the ratio of record highs to lows (red) or of record lows to highs (blue). For example, a ratio of 2:1 for a blue bar means that there were twice as many record daily lows as daily record highs that year. Estimates are derived from long-term stations with minimal missing data in the Global Historical Climatology Network–Daily dataset.¹⁶ (Figure source: NOAA/NCEI).

Assessment of Annual Surface Temperature Trends (1901–2015)

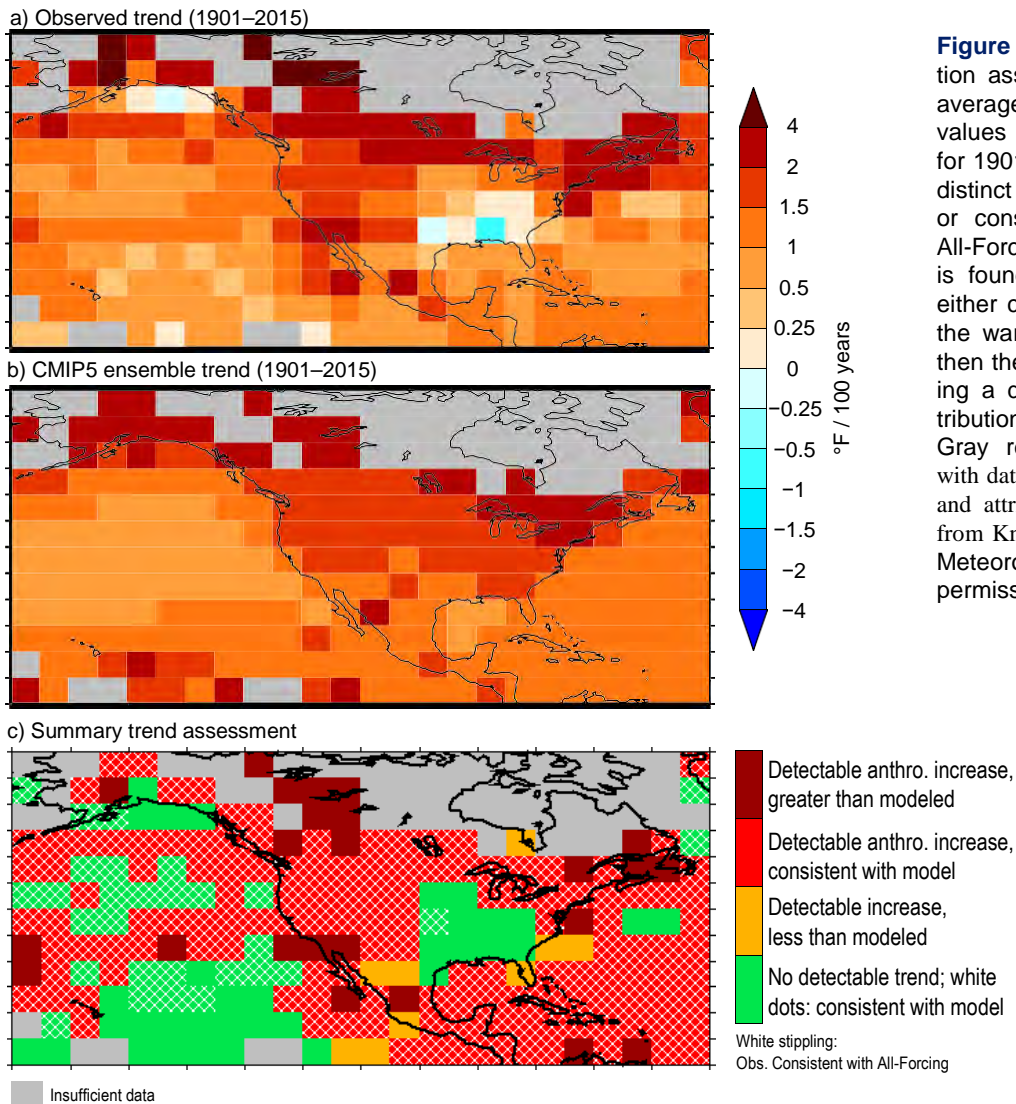


Figure 6.6. Detection and attribution assessment of trends in annual average temperature (°F). Grid-box values indicate whether linear trends for 1901–2015 are detectable (that is, distinct from natural variability) and/or consistent with CMIP5 historical All-Forcing runs. If the grid-box trend is found to be both detectable and either consistent with or greater than the warming in the All-Forcing runs, then the grid box is assessed as having a detectable anthropogenic contribution to warming over the period. Gray regions represent grid boxes with data that are too sparse for detection and attribution. (Figure source: updated from Knutson et al. 2013;²⁸ © American Meteorological Society. Used with permission.)

of this “warming hole,” or lack of a long-term warming trend, remains uncertain, though it is likely a combination of natural and human causes. Some studies conclude that changes in anthropogenic aerosols have played a crucial role (e.g., Leibensperger et al. 2012;^{29,30} Yu et al. 2014³¹), whereas other studies infer a possible large role for atmospheric circulation,³² internal climate variability (e.g., Meehl et al. 2012;⁸ Knutson et al. 2013²⁸), and changes in land use (e.g., Goldstein et al. 2009;³³ Xu et al. 2015³⁴). Notably, the Southeast has been warming rapidly since the early 1960s.^{35,36} In summary, there is medium confidence for detectable anthropogenic warming over the western and northern regions of the contiguous United States.

6.2.2 Temperature Extremes

The Intergovernmental Panel on Climate Change’s (IPCC’s) Fifth Assessment Report (AR5)²⁴ concluded that it is very likely that human influence has contributed to the observed changes in frequency and intensity of temperature extremes on the global scale since the mid-20th century. The combined influence of anthropogenic and natural forcings was also detectable (medium confidence) over large subregions of North America (e.g., Zwiers et al. 2011;³⁷ Min et al. 2013³⁸). In general, however, results for the contiguous United States are not as compelling as for global land areas, in part because detection of changes in U.S. regional temperature extremes is affected by

extreme temperature in the 1930s.¹⁷ Table 6.3 summarizes available attribution statements for recent extreme U.S. temperature events. As an example, the recent record or near-record high March–May average temperatures occurring in 2012 over the eastern United States were attributed in part to external (natural plus anthropogenic) forcing;³⁹ the century-scale trend response of temperature to external forcing is typically a close approximation to the anthropogenic forcing response alone. Another study found that although the extreme March 2012 warm anomalies over the United States were mostly due to natural variability, anthropogenic warming contributed to the severity.⁴⁰ Such statements reveal that both natural and anthropogenic factors influence the severity of extreme temperature events. Nearly every modern analysis of current extreme hot and cold events reveals some degree of attributable human influence.

6.3 Projected Changes

6.3.1 Average Temperatures

Temperature projections are based on global model results and associated downscaled products from CMIP5 using a suite of Representative Concentration Pathways (RCPs). In contrast to NCA3, model weighting is employed to refine projections of temperature for each RCP (Ch. 4: Projections; Appendix B: Model Weighting). Weighting parameters are based on model independence and skill over North America for seasonal temperature and annual extremes. Unless stated otherwise, all changes presented here represent the weighted multimodel mean. The weighting scheme helps refine confidence and likelihood statements, but projections of U.S. surface air temperature remain very similar to those in NCA3. Generally speaking, extreme temperatures are projected to increase even more than average temperatures.⁴¹

Table 6.3. Extreme temperature events in the United States for which attribution statements have been made. There are three possible attribution statements: “+” shows an attributable human-induced increase in frequency or intensity, “–” shows an attributable human-induced decrease in frequency or intensity, “0” shows no attributable human contribution.

Study	Period	Region	Type	Statement
Rupp et al. 2012 ⁵²	Spring/Summer 2011	Texas	Hot	+
Angéilil et al. 2017 ⁵³				+
Hoerling et al. 2013 ⁵⁴	Summer 2011	Texas	Hot	+
Diffenbaugh and Scherer 2013 ⁵⁵	July 2012	Northcentral and Northeast	Hot	+
Angéilil et al. 2017 ⁵³				+
Cattiaux and Yiou 2013 ⁵⁶	Spring 2012	East	Hot	0
Angéilil et al. 2017 ⁵³				+
Knutson et al. 2013b ³⁹	Spring 2012	East	Hot	+
Angéilil et al. 2017 ⁵³				+
Jeon et al 2016 ⁵⁷	Summer 2011	Texas/ Oklahoma	Hot	+
Dole et al. 2014 ⁴⁰	March 2012	Upper Midwest	Hot	+
Seager et al. 2014 ⁵⁸	2011–2014	California	Hot	+
Wolter et al. 2015 ⁵⁹	Winter 2014	Midwest	Cold	–
Trenary et al. 2015 ⁶⁰	Winter 2014	East	Cold	0

The annual average temperature of the contiguous United States is projected to rise throughout the century. Increases for the period 2021–2050 relative to 1976–2005 are projected to be about 2.5°F (1.4°C) for a lower scenario (RCP4.5) and 2.9°F (1.6°C) for the higher scenario (RCP8.5); the similarity in warming reflects the similarity in greenhouse gas concentrations during this period (Figure 4.1). Notably, a 2.5°F (1.4°C) increase makes the near-term average comparable to the hottest year in the historical record (2012). In other words, recent record-breaking years may be “common” in the next few decades. By late-century (2071–2100), the RCPs diverge significantly, leading to different rates of warming: approximately 5.0°F (2.8°C) for RCP4.5 and 8.7°F (4.8°C) for RCP8.5. Likewise, there are different ranges of warming for each scenario: 2.8°–7.3°F (1.6°–4.1°C) for RCP4.5 and 5.8°–11.9°F (3.2°–6.6°C) for RCP8.5. (The range is defined here as the difference between the average increase in the three coolest models and the average increase in the three warmest models.) For both RCPs, slightly greater increases are projected in summer than winter (except for Alaska), and average maximums will rise slightly faster than average minimums (except in the Southeast and Southern Great Plains).

Statistically significant warming is projected for all parts of the United States throughout the century (Figure 6.7). Consistent with polar amplification, warming rates (and spatial gradients) are greater at higher latitudes. For example, warming is largest in Alaska (more than 12.0°F [6.7°C] in the northern half of the state by late-century under RCP8.5), driven in part by a decrease in snow cover and thus surface albedo. Similarly, northern regions of the contiguous United States have slightly more warming than other regions (roughly 9.0°F [5.5°C] in the Northeast, Midwest, and Northern Great Plains by late-century under RCP8.5; Table 6.4). The Southeast has slightly less warming because of latent heat release from increases in evapotranspiration (as is already evident in the observed record). Warming is smallest in Hawai’i and the Caribbean (roughly 4.0°–6.0°F [2.2°–3.3°C] by late century under RCP8.5) due to the moderating effects of surrounding oceans. From a sub-regional perspective, less warming is projected along the coasts of the contiguous United States, again due to maritime influences, although increases are still substantial. Warming at higher elevations may be underestimated because the resolution of the CMIP5 models does not capture orography in detail.



Projected Changes in Annual Average Temperature

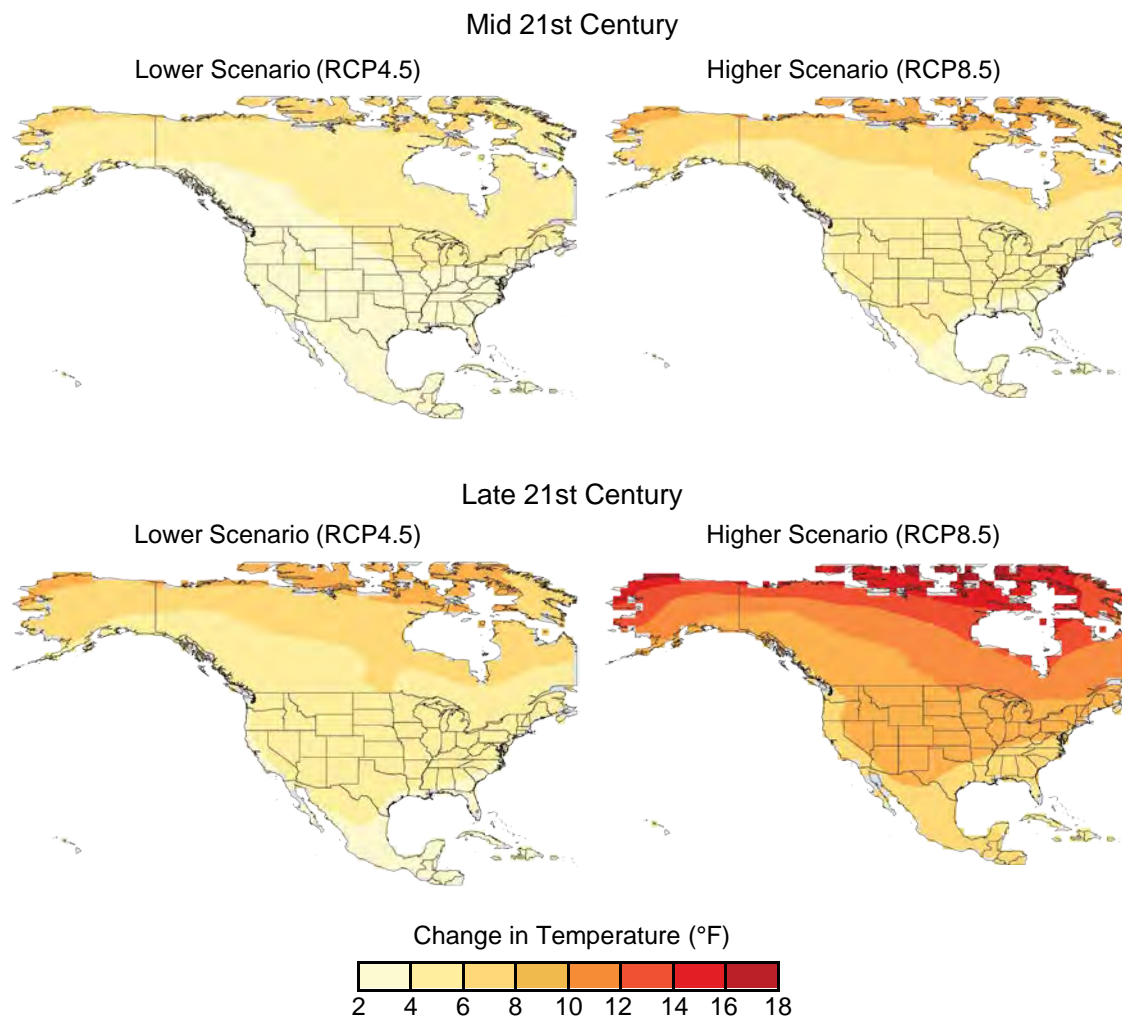


Figure 6.7. Projected changes in annual average temperatures (°F). Changes are the difference between the average for mid-century (2036–2065; top) or late-century (2070–2099, bottom) and the average for near-present (1976–2005). Each map depicts the weighted multimodel mean. Increases are statistically significant in all areas (that is, more than 50% of the models show a statistically significant change, and more than 67% agree on the sign of the change⁴⁵). (Figure source: CICS-NC and NOAA NCEI).

Table 6.4. Projected changes in annual average temperature (°F) for each National Climate Assessment region in the contiguous United States. Changes are the difference between the average for mid-century (2036–2065) or late-century (2071–2100) and the average for near-present (1976–2005) under the higher scenario (RCP8.5) and a lower scenario (RCP4.5). Estimates are derived from 32 climate models that were statistically downscaled using the Localized Constructed Analogs technique.⁵¹ Increases are statistically significant in all areas (that is, more than 50% of the models show a statistically significant change, and more than 67% agree on the sign of the change⁴⁵).

NCA Region	RCP4.5 Mid-Century (2036–2065)	RCP8.5 Mid-Century (2036–2065)	RCP4.5 Late-Century (2071–2100)	RCP8.5 Late-Century (2071–2100)
Northeast	3.98°F	5.09°F	5.27°F	9.11°F
Southeast	3.40°F	4.30°F	4.43°F	7.72°F
Midwest	4.21°F	5.29°F	5.57°F	9.49°F
Great Plains North	4.05°F	5.10°F	5.44°F	9.37°F
Great Plains South	3.62°F	4.61°F	4.78°F	8.44°F
Southwest	3.72°F	4.80°F	4.93°F	8.65°F
Northwest	3.66°F	4.67°F	4.99°F	8.51°F

6.3.2 Temperature Extremes

Daily extreme temperatures are projected to increase substantially in the contiguous United States, particularly under the higher scenario (RCP8.5). For instance, the coldest and warmest daily temperatures of the year are expected to increase at least 5°F (2.8°C) in most areas by mid-century,⁴² rising to 10°F (5.5°C) or more by late-century.⁴³ In general, there will be larger increases in the coldest temperatures of the year, especially in the northern half of the Nation, whereas the warmest temperatures will exhibit somewhat more uniform changes geographically (Figure 6.8). By mid-century, the upper bound for projected changes (i.e., the average of the three warmest models) is about 2°F (1.1°C) greater than the weighted multimodel mean. On a regional basis, annual extremes (Table 6.5) are consistently projected to rise faster than annual averages (Table 6.4). Future changes in “very rare” extremes are also striking; by late century, current 1-in-20 year maximums are projected to occur every year, while current 1-in-20 year minimums are not expected to occur at all.⁴⁴

The frequency and intensity of cold waves is projected to decrease while the frequency and

intensity of heat waves is projected to increase throughout the century. The frequency of cold waves (6-day periods with a minimum temperature below the 10th percentile) will decrease the most in Alaska and the least in the Northeast while the frequency of heat waves (6-day periods with a maximum temperature above the 90th percentile) will increase in all regions, particularly the Southeast, Southwest, and Alaska. By mid-century, decreases in the frequency of cold waves are similar across RCPs whereas increases in the frequency of heat waves are about 50% greater in the higher scenario (RCP8.5) than the lower scenario (RCP4.5).⁴⁵ The intensity of cold waves is projected to decrease while the intensity of heat waves is projected to increase, dramatically so under RCP8.5. By mid-century, both extreme cold waves and extreme heat waves (5-day, 1-in-10 year events) are projected to have temperature increases of at least 11.0°F (6.1°C) nationwide, with larger increases in northern regions (the Northeast, Midwest, Northern Great Plains, and Northwest; Table 6.5).

There are large projected changes in the number of days exceeding key temperature thresholds throughout the contiguous United States.



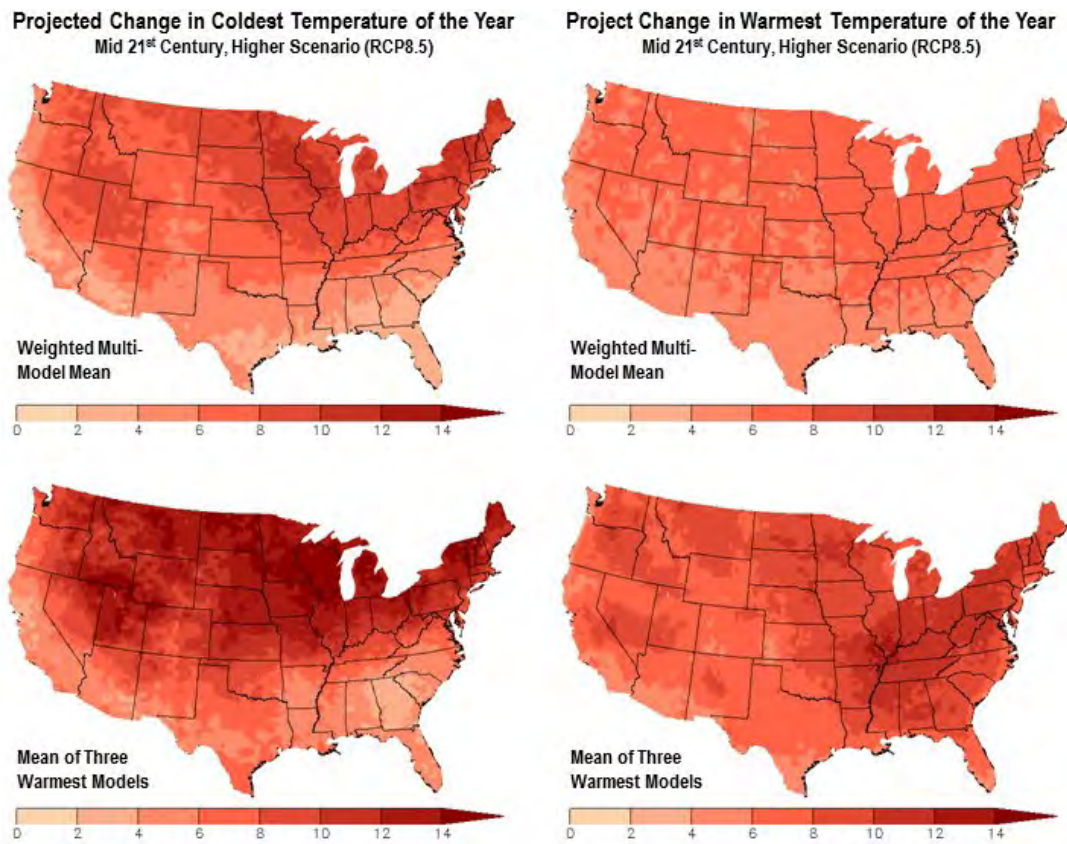


Figure 6.8. Projected changes in the coldest and warmest daily temperatures (°F) of the year in the contiguous United States. Changes are the difference between the average for mid-century (2036–2065) and the average for near-present (1976–2005) under the higher scenario (RCP8.5). Maps in the top row depict the weighted multimodel mean whereas maps on the bottom row depict the mean of the three warmest models (that is, the models with the largest temperature increase). Maps are derived from 32 climate model projections that were statistically down-scaled using the Localized Constructed Analogs technique.⁵¹ Increases are statistically significant in all areas (that is, more than 50% of the models show a statistically significant change, and more than 67% agree on the sign of the change⁴⁵). (Figure source: CICS-NC and NOAA NCEI).

Table 6.5. Projected changes in temperature extremes (°F) for each National Climate Assessment region in the contiguous United States. Changes are the difference between the average for mid-century (2036–2065) and the average for near-present (1976–2005) under the higher scenario (RCP8.5). Estimates are derived from 32 climate models that were statistically down-scaled using the Localized Constructed Analogs technique.⁵¹ Increases are statistically significant in all areas (that is, more than 50% of the models show a statistically significant change, and more than 67% agree on the sign of the change⁴⁵).

NCA Region	Change in Coldest Day of the Year	Change in Coldest 5-Day 1-in-10 Year Event	Change in Warmest Day of the Year	Change in Warmest 5-Day 1-in-10 Year Event
Northeast	9.51°F	15.93°F	6.51°F	12.88°F
Southeast	4.97°F	8.84°F	5.79°F	11.09°F
Midwest	9.44°F	15.52°F	6.71°F	13.02°F
Great Plains North	8.01°F	12.01°F	6.48°F	12.00°F
Great Plains South	5.49°F	9.41°F	5.70°F	10.73°F
Southwest	6.13°F	10.20°F	5.85°F	11.17°F
Northwest	7.33°F	10.95°F	6.25°F	12.31°F

For instance, there are about 20–30 more days per year with a maximum over 90°F (32°C) in most areas by mid-century under RCP8.5, with increases of 40–50 days in much of the Southeast (Figure 6.9). The upper bound for projected changes is very roughly 10 days greater than the weighted multimodel mean. Consistent with widespread warming, there

are 20–30 fewer days per year with a minimum temperature below freezing in the northern and eastern parts of the nation, with decreases of more than 40–50 days in much the West. The upper bound for projected changes in freezing events is very roughly 10–20 days fewer than the weighted multimodel mean in many areas.

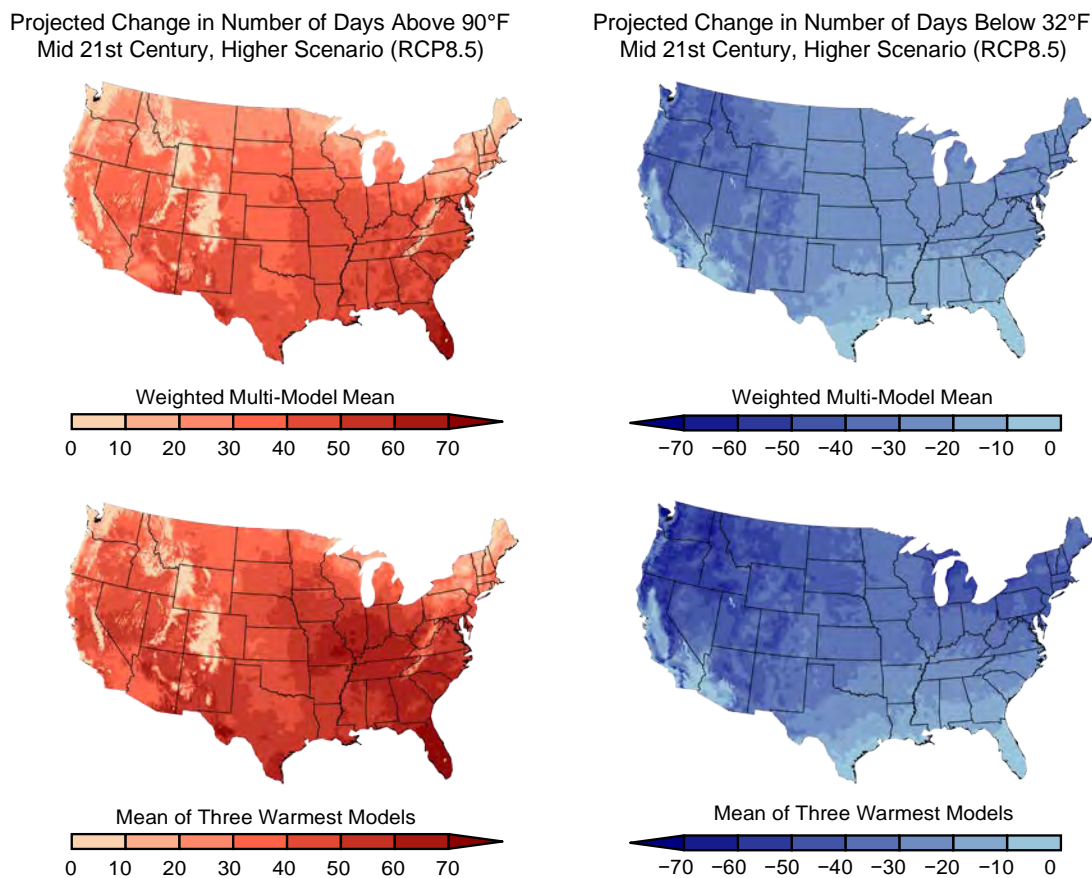


Figure 6.9. Projected changes in the number of days per year with a maximum temperature above 90°F and a minimum temperature below 32°F in the contiguous United States. Changes are the difference between the average for mid-century (2036–2065) and the average for near-present (1976–2005) under the higher scenario (RCP8.5). Maps in the top row depict the weighted multimodel mean whereas maps on the bottom row depict the mean of the three warmest models (that is, the models with the largest temperature increase). Maps are derived from 32 climate model projections that were statistically downscaled using the Localized Constructed Analogs technique.⁵¹ Changes are statistically significant in all areas (that is, more than 50% of the models show a statistically significant change, and more than 67% agree on the sign of the change⁴⁵). (Figure source: CICS-NC and NOAA NCEI).

TRACEABLE ACCOUNTS

Key Finding 1 Annual average temperature over the contiguous United States has increased by 1.2°F (0.7°C) for the period 1986–2016 relative to 1901–1960 and by 1.8°F (1.0°C) based on a linear regression for the period 1895–2016 (*very high confidence*). Surface and satellite data are consistent in their depiction of rapid warming since 1979 (*high confidence*). Paleo-temperature evidence shows that recent decades are the warmest of the past 1,500 years (*medium confidence*).

Description of Evidence Base

The key finding and supporting text summarize extensive evidence documented in the climate science literature. Similar statements about changes exist in other reports (e.g., NCA3;⁴⁶ Global Climate Change Impacts in the United States;⁴⁷ SAP 1.1: Temperature trends in the lower atmosphere⁴⁸).

Evidence for changes in U.S. climate arises from multiple analyses of data from in situ, satellite, and other records undertaken by many groups over several decades. The primary dataset for surface temperatures in the United States is nClimGrid,^{1, 2} though trends are similar in the U.S. Historical Climatology Network, the Global Historical Climatology Network, and other datasets. Several atmospheric reanalyses (e.g., 20th Century Reanalysis, Climate Forecast System Reanalysis, ERA-Interim, Modern Era Reanalysis for Research and Applications) confirm rapid warming at the surface since 1979, with observed trends closely tracking the ensemble mean of the reanalyses. Several recently improved satellite datasets document changes in middle tropospheric temperatures.^{5, 6, 7} Longer-term changes are depicted using multiple paleo analyses (e.g., Wahl and Smerdon 2012;¹³ Trouet et al. 2013¹²).

Major Uncertainties

The primary uncertainties for surface data relate to historical changes in station location, temperature instrumentation, observing practice, and spatial sampling (particularly in areas and periods with low station density, such as the intermountain West in the early 20th century). Satellite records are similarly impacted by non-climatic changes such as orbital decay, diurnal

sampling, and instrument calibration to target temperatures. Several uncertainties are inherent in temperature-sensitive proxies, such as dating techniques and spatial sampling.

Assessment of confidence based on evidence and agreement, including short description of nature of evidence and level of agreement

Very high (since 1895), *High* (for surface/satellite agreement since 1979), *Medium* (for paleo)

Likelihood of Impact

Extremely Likely

Summary sentence or paragraph that integrates the above information

There is *very high confidence* in observed changes in average temperature over the United States based upon the convergence of evidence from multiple data sources, analyses, and assessments.

Key Finding 2

There have been marked changes in temperature extremes across the contiguous United States. The frequency of cold waves has decreased since the early 1900s, and the frequency of heat waves has increased since the mid-1960s. The Dust Bowl era of the 1930s remains the peak period for extreme heat. The number of high temperature records set in the past two decades far exceeds the number of low temperature records. (*Very high confidence*)

Description of Evidence Base

The key finding and supporting text summarize extensive evidence documented in the climate science literature. Similar statements about changes have also been made in other reports (e.g., NCA3;⁴⁶ SAP 3.3: Weather and Climate Extremes in a Changing Climate;⁴⁹ IPCC Special Report on Managing the Risks of Extreme Events and Disasters to Advance Climate Change Adaptation⁵⁰).

Evidence for changes in U.S. climate arises from multiple analyses of in situ data using widely published climate extremes indices. For the analyses presented



here, the source of in situ data is the Global Historical Climatology Network–Daily dataset,¹⁶ with changes in extremes being assessed using long-term stations with minimal missing data to avoid network-induced variability on the long-term time series. Cold wave frequency was quantified using the Cold Spell Duration Index,¹⁵ heat wave frequency was quantified using the Warm Spell Duration Index,¹⁵ and heat wave intensity were quantified using the Heat Wave Magnitude Index Daily.¹⁴ Station-based index values were averaged into 4° grid boxes, which were then area-averaged into a time series for the contiguous United States. Note that a variety of other threshold and percentile-based indices were also evaluated, with consistent results (e.g., the Dust Bowl was consistently the peak period for extreme heat). Changes in record-setting temperatures were quantified as in Meehl et al. (2016).²³

Major Uncertainties

The primary uncertainties for in situ data relate to historical changes in station location, temperature instrumentation, observing practice, and spatial sampling (particularly the precision of estimates of change in areas and periods with low station density, such as the intermountain West in the early 20th century).

Assessment of confidence based on evidence and agreement, including short description of nature of evidence and level of agreement

Very high

Likelihood of Impact

Extremely likely

Summary sentence or paragraph that integrates the above information

There is *very high confidence* in observed changes in temperature extremes over the United States based upon the convergence of evidence from multiple data sources, analyses, and assessments.

Key Finding 3

Annual average temperature over the contiguous United States is projected to rise (*very high confidence*). Increases of about 2.5°F (1.4°C) are projected

for the period 2021–2050 relative to 1976–2005 in all RCP scenarios, implying recent record-setting years may be “common” in the next few decades (*high confidence*). Much larger rises are projected by late century (2071–2100): 2.8°–7.3°F (1.6°–4.1°C) in a lower scenario (RCP4.5) and 5.8°–11.9°F (3.2°–6.6°C) in a higher scenario (RCP8.5) (*high confidence*).

Description of Evidence Base

The key finding and supporting text summarize extensive evidence documented in the climate science literature. Similar statements about changes have also been made in other reports (e.g., NCA3;⁴⁶ Global Climate Change Impacts in the United States⁴⁷). The basic physics underlying the impact of human emissions on climate has also been documented in every IPCC assessment.

Projections are based on global model results and associated downscaled products from CMIP5 for RCP4.5 (lower scenario) and RCP8.5 (higher scenario). Model weighting is employed to refine projections for each RCP. Weighting parameters are based on model independence and skill over North America for seasonal temperature and annual extremes. The multimodel mean is based on 32 model projections that were statistically downscaled using the Localized Constructed Analogs technique.⁵¹ The range is defined as the difference between the average increase in the three coolest models and the average increase in the three warmest models. All increases are significant (i.e., more than 50% of the models show a statistically significant change, and more than 67% agree on the sign of the change⁴⁵).

Major Uncertainties

Global climate models are subject to structural and parametric uncertainty, resulting in a range of estimates of future changes in average temperature. This is partially mitigated through the use of model weighting and pattern scaling. Furthermore, virtually every ensemble member of every model projection contains an increase in temperature by mid- and late-century. Empirical downscaling introduces additional uncertainty (e.g., with respect to stationarity).



Assessment of confidence based on evidence and agreement, including short description of nature of evidence and level of agreement

Very high for projected change in annual average temperature; *high confidence* for record-setting years becoming the norm in the near future; *high confidence* for much larger temperature increases by late century under a higher scenario (RCP8.5).

Likelihood of Impact

Extremely likely

Summary sentence or paragraph that integrates the above information

There is *very high confidence* in projected changes in average temperature over the United States based upon the convergence of evidence from multiple model simulations, analyses, and assessments.

Key Finding 4

Extreme temperatures in the contiguous United States are projected to increase even more than average temperatures. The temperatures of extremely cold days and extremely warm days are both expected to increase. Cold waves are projected to become less intense while heat waves will become more intense. The number of days below freezing is projected to decline while the number above 90°F will rise. (*Very high confidence*)

Description of Evidence Base

The key finding and supporting text summarize extensive evidence documented in the climate science literature (e.g., Fischer et al. 2013;⁴² Sillmann et al. 2013;⁴³ Wuebbles et al. 2014;⁴⁴ Sun et al. 2015⁴⁵). Similar statements about changes have also been made in other national assessments (such as NCA3) and in reports by the Climate Change Science Program (such as SAP 3.3: Weather and Climate Extremes in a Changing Climate⁴⁹).

Projections are based on global model results and associated downscaled products from CMIP5 for RCP4.5 (lower scenario) and RCP8.5 (higher scenario). Model weighting is employed to refine projections for each RCP. Weighting parameters are based on model independence and skill over North America for seasonal

temperature and annual extremes. The multimodel mean is based on 32 model projections that were statistically downscaled using the Localized Constructed Analogs technique.⁵¹ Downscaling improves on the coarse model output, establishing a more geographically accurate baseline for changes in extremes and the number of days per year over key thresholds. The upper bound for projected changes is the average of the three warmest models. All increases are significant (i.e., more than 50% of the models show a statistically significant change, and more than 67% agree on the sign of the change⁴⁵).

Major Uncertainties

Global climate models are subject to structural and parametric uncertainty, resulting in a range of estimates of future changes in temperature extremes. This is partially mitigated through the use of model weighting and pattern scaling. Furthermore, virtually every ensemble member of every model projection contains an increase in temperature by mid- and late-century. Empirical downscaling introduces additional uncertainty (e.g., with respect to stationarity).

Assessment of confidence based on evidence and agreement, including short description of nature of evidence and level of agreement

Very high

Likelihood of Impact

Extremely likely

Summary Sentence

There is *very high confidence* in projected changes in temperature extremes over the United States based upon the convergence of evidence from multiple model simulations, analyses, and assessments.



REFERENCES

1. Vose, R.S., S. Applequist, M. Squires, I. Durre, M.J. Menne, C.N. Williams, Jr., C. Fenimore, K. Gleason, and D. Arndt, 2014: Improved historical temperature and precipitation time series for U.S. climate divisions. *Journal of Applied Meteorology and Climatology*, **53**, 1232-1251. <http://dx.doi.org/10.1175/JAMC-D-13-0248.1>
2. Vose, R.S., M. Squires, D. Arndt, I. Durre, C. Fenimore, K. Gleason, M.J. Menne, J. Partain, C.N. Williams Jr., P.A. Bieniek, and R.L. Thoman, 2017: Deriving historical temperature and precipitation time series for Alaska climate divisions via climatologically aided interpolation. *Journal of Service Climatology* **10**, 20. <https://www.stateclimate.org/sites/default/files/upload/pdf/journal-articles/2017-Ross-et-al.pdf>
3. Huang, B., V.F. Banzon, E. Freeman, J. Lawrimore, W. Liu, T.C. Peterson, T.M. Smith, P.W. Thorne, S.D. Woodruff, and H.-M. Zhang, 2015: Extended Reconstructed Sea Surface Temperature Version 4 (ERSST.v4). Part I: Upgrades and intercomparisons. *Journal of Climate*, **28**, 911-930. <http://dx.doi.org/10.1175/JCLI-D-14-00006.1>
4. Vose, R.S., D. Arndt, V.F. Banzon, D.R. Easterling, B. Gleason, B. Huang, E. Kearns, J.H. Lawrimore, M.J. Menne, T.C. Peterson, R.W. Reynolds, T.M. Smith, C.N. Williams, and D.L. Wuertz, 2012: NOAA's merged land-ocean surface temperature analysis. *Bulletin of the American Meteorological Society*, **93**, 1677-1685. <http://dx.doi.org/10.1175/BAMS-D-11-00241.1>
5. Mears, C.A. and F.J. Wentz, 2016: Sensitivity of satellite-derived tropospheric temperature trends to the diurnal cycle adjustment. *Journal of Climate*, **29**, 3629-3646. <http://dx.doi.org/10.1175/JCLI-D-15-0744.1>
6. Spencer, R.W., J.R. Christy, and W.D. Braswell, 2017: UAH Version 6 global satellite temperature products: Methodology and results. *Asia-Pacific Journal of Atmospheric Sciences*, **53**, 121-130. <http://dx.doi.org/10.1007/s13143-017-0010-y>
7. Zou, C.-Z. and J. Li, 2014: NOAA MSU Mean Layer Temperature. National Oceanic and Atmospheric Administration, Center for Satellite Applications and Research, 35 pp. http://www.star.nesdis.noaa.gov/smcd/emb/mscat/documents/MSU_TCDR_CATBD_Zou_Li.pdf
8. Meehl, G.A., J.M. Arblaster, and G. Branstator, 2012: Mechanisms contributing to the warming hole and the consequent US east-west differential of heat extremes. *Journal of Climate*, **25**, 6394-6408. <http://dx.doi.org/10.1175/JCLI-D-11-00655.1>
9. Thorne, P.W., M.G. Donat, R.J.H. Dunn, C.N. Williams, L.V. Alexander, J. Caesar, I. Durre, I. Harris, Z. Hausfather, P.D. Jones, M.J. Menne, R. Rohde, R.S. Vose, R. Davy, A.M.G. Klein-Tank, J.H. Lawrimore, T.C. Peterson, and J.J. Rennie, 2016: Reassessing changes in diurnal temperature range: Intercomparison and evaluation of existing global data set estimates. *Journal of Geophysical Research Atmospheres*, **121**, 5138-5158. <http://dx.doi.org/10.1002/2015JD024584>
10. Po-Chedley, S., T.J. Thorsen, and Q. Fu, 2015: Removing diurnal cycle contamination in satellite-derived tropospheric temperatures: Understanding tropical tropospheric trend discrepancies. *Journal of Climate*, **28**, 2274-2290. <http://dx.doi.org/10.1175/JCLI-D-13-00767.1>
11. PAGES 2K Consortium, 2013: Continental-scale temperature variability during the past two millennia. *Nature Geoscience*, **6**, 339-346. <http://dx.doi.org/10.1038/ngeo1797>
12. Trouet, V., H.F. Diaz, E.R. Wahl, A.E. Viau, R. Graham, N. Graham, and E.R. Cook, 2013: A 1500-year reconstruction of annual mean temperature for temperate North America on decadal-to-multidecadal time scales. *Environmental Research Letters*, **8**, 024008. <http://dx.doi.org/10.1088/1748-9326/8/2/024008>
13. Wahl, E.R. and J.E. Smerdon, 2012: Comparative performance of paleoclimate field and index reconstructions derived from climate proxies and noise-only predictors. *Geophysical Research Letters*, **39**, L06703. <http://dx.doi.org/10.1029/2012GL051086>
14. Russo, S., A. Dosio, R.G. Graversen, J. Sillmann, H. Carrao, M.B. Dunbar, A. Singleton, P. Montagna, P. Barbola, and J.V. Vogt, 2014: Magnitude of extreme heat waves in present climate and their projection in a warming world. *Journal of Geophysical Research Atmospheres*, **119**, 12,500-12,512. <http://dx.doi.org/10.1002/2014JD022098>
15. Zhang, X., L. Alexander, G.C. Hegerl, P. Jones, A.K. Tank, T.C. Peterson, B. Trewin, and F.W. Zwiers, 2011: Indices for monitoring changes in extremes based on daily temperature and precipitation data. *Wiley Interdisciplinary Reviews: Climate Change*, **2**, 851-870. <http://dx.doi.org/10.1002/wcc.147>
16. Menne, M.J., I. Durre, R.S. Vose, B.E. Gleason, and T.G. Houston, 2012: An overview of the global historical climatology network-daily database. *Journal of Atmospheric and Oceanic Technology*, **29**, 897-910. <http://dx.doi.org/10.1175/JTECH-D-11-00103.1>



17. Peterson, T.C., R.R. Heim, R. Hirsch, D.P. Kaiser, H. Brooks, N.S. Diffenbaugh, R.M. Dole, J.P. Giannantonio, K. Guirguis, T.R. Karl, R.W. Katz, K. Kunkel, D. Lettenmaier, G.J. McCabe, C.J. Paciorek, K.R. Ryberg, S. Schubert, V.B.S. Silva, B.C. Stewart, A.V. Vecchia, G. Villarini, R.S. Vose, J. Walsh, M. Wehner, D. Wollock, K. Wolter, C.A. Woodhouse, and D. Wuebbles, 2013: Monitoring and understanding changes in heat waves, cold waves, floods and droughts in the United States: State of knowledge. *Bulletin of the American Meteorological Society*, **94**, 821-834. <http://dx.doi.org/10.1175/BAMS-D-12-00066.1>
18. Donat, M.G., A.D. King, J.T. Overpeck, L.V. Alexander, I. Durre, and D.J. Karoly, 2016: Extraordinary heat during the 1930s US Dust Bowl and associated large-scale conditions. *Climate Dynamics*, **46**, 413-426. <http://dx.doi.org/10.1007/s00382-015-2590-5>
19. Mascioli, N.R., M. Previdi, A.M. Fiore, and M. Ting, 2017: Timing and seasonality of the United States 'warming hole'. *Environmental Research Letters*, **12**, 034008. <http://dx.doi.org/10.1088/1748-9326/aa5ef4>
20. Mueller, N.D., E.E. Butler, K.A. McKinnon, A. Rhines, M. Tingley, N.M. Holbrook, and P. Huybers, 2016: Cooling of US Midwest summer temperature extremes from cropland intensification. *Nature Climate Change*, **6**, 317-322. <http://dx.doi.org/10.1038/nclimate2825>
21. Smith, T.T., B.F. Zaitchik, and J.M. Gohlke, 2013: Heat waves in the United States: Definitions, patterns and trends. *Climatic Change*, **118**, 811-825. <http://dx.doi.org/10.1007/s10584-012-0659-2>
22. Mazdiyasn, O. and A. AghaKouchak, 2015: Substantial increase in concurrent droughts and heatwaves in the United States. *Proceedings of the National Academy of Sciences*, **112**, 11484-11489. <http://dx.doi.org/10.1073/pnas.1422945112>
23. Meehl, G.A., C. Tebaldi, and D. Adams-Smith, 2016: US daily temperature records past, present, and future. *Proceedings of the National Academy of Sciences*, **113**, 13977-13982. <http://dx.doi.org/10.1073/pnas.1606117113>
24. Bindoff, N.L., P.A. Stott, K.M. AchutaRao, M.R. Allen, N. Gillett, D. Gutzler, K. Hansingo, G. Hegerl, Y. Hu, S. Jain, I.I. Mokhov, J. Overland, J. Perlwitz, R. Sebbani, and X. Zhang, 2013: Detection and attribution of climate change: From global to regional. *Climate Change 2013: The Physical Science Basis. Contribution of Working Group I to the Fifth Assessment Report of the Intergovernmental Panel on Climate Change*. Stocker, T.F., D. Qin, G.-K. Plattner, M. Tignor, S.K. Allen, J. Boschung, A. Nauels, Y. Xia, V. Bex, and P.M. Midgley, Eds. Cambridge University Press, Cambridge, United Kingdom and New York, NY, USA, 867-952. <http://www.climatechange2013.org/report/full-report/>
25. Christidis, N., P.A. Stott, F.W. Zwiers, H. Shiogama, and T. Nozawa, 2010: Probabilistic estimates of recent changes in temperature: A multi-scale attribution analysis. *Climate Dynamics*, **34**, 1139-1156. <http://dx.doi.org/10.1007/s00382-009-0615-7>
26. Bonfils, C., P.B. Duffy, B.D. Santer, T.M.L. Wigley, D.B. Lobell, T.J. Phillips, and C. Doutriaux, 2008: Identification of external influences on temperatures in California. *Climatic Change*, **87**, 43-55. <http://dx.doi.org/10.1007/s10584-007-9374-9>
27. Pierce, D.W., T.P. Barnett, B.D. Santer, and P.J. Gleckler, 2009: Selecting global climate models for regional climate change studies. *Proceedings of the National Academy of Sciences*, **106**, 8441-8446. <http://dx.doi.org/10.1073/pnas.0900094106>
28. Knutson, T.R., F. Zeng, and A.T. Wittenberg, 2013: Multimodel assessment of regional surface temperature trends: CMIP3 and CMIP5 twentieth-century simulations. *Journal of Climate*, **26**, 8709-8743. <http://dx.doi.org/10.1175/JCLI-D-12-00567.1>
29. Leibensperger, E.M., L.J. Mickley, D.J. Jacob, W.T. Chen, J.H. Seinfeld, A. Nenes, P.J. Adams, D.G. Streets, N. Kumar, and D. Rind, 2012: Climatic effects of 1950-2050 changes in US anthropogenic aerosols - Part 1: Aerosol trends and radiative forcing. *Atmospheric Chemistry and Physics*, **12**, 3333-3348. <http://dx.doi.org/10.5194/acp-12-3333-2012>
30. Leibensperger, E.M., L.J. Mickley, D.J. Jacob, W.T. Chen, J.H. Seinfeld, A. Nenes, P.J. Adams, D.G. Streets, N. Kumar, and D. Rind, 2012: Climatic effects of 1950-2050 changes in US anthropogenic aerosols - Part 2: Climate response. *Atmospheric Chemistry and Physics*, **12**, 3349-3362. <http://dx.doi.org/10.5194/acp-12-3349-2012>
31. Yu, S., K. Alapaty, R. Mathur, J. Pleim, Y. Zhang, C. Nolte, B. Eder, K. Foley, and T. Nagashima, 2014: Attribution of the United States "warming hole": Aerosol indirect effect and precipitable water vapor. *Scientific Reports*, **4**, 6929. <http://dx.doi.org/10.1038/srep06929>
32. Abatzoglou, J.T. and K.T. Redmond, 2007: Asymmetry between trends in spring and autumn temperature and circulation regimes over western North America. *Geophysical Research Letters*, **34**, L18808. <http://dx.doi.org/10.1029/2007GL030891>
33. Goldstein, A.H., C.D. Koven, C.L. Heald, and I.Y. Fung, 2009: Biogenic carbon and anthropogenic pollutants combine to form a cooling haze over the southeastern United States. *Proceedings of the National Academy of Sciences*, **106**, 8835-8840. <http://dx.doi.org/10.1073/pnas.0904128106>



34. Xu, L., H. Guo, C.M. Boyd, M. Klein, A. Bougiatioti, K.M. Cerully, J.R. Hite, G. Isaacman-VanWertz, N.M. Kreisberg, C. Knote, K. Olson, A. Koss, A.H. Goldstein, S.V. Hering, J. de Gouw, K. Baumann, S.-H. Lee, A. Nenes, R.J. Weber, and N.L. Ng, 2015: Effects of anthropogenic emissions on aerosol formation from isoprene and monoterpenes in the southeastern United States. *Proceedings of the National Academy of Sciences*, **112**, 37-42. <http://dx.doi.org/10.1073/pnas.1417609112>
35. Pan, Z., X. Liu, S. Kumar, Z. Gao, and J. Kinter, 2013: Intermodel variability and mechanism attribution of central and southeastern U.S. anomalous cooling in the twentieth century as simulated by CMIP5 models. *Journal of Climate*, **26**, 6215-6237. <http://dx.doi.org/10.1175/JCLI-D-12-00559.1>
36. Walsh, J., D. Wuebbles, K. Hayhoe, J. Kossin, K. Kunkel, G. Stephens, P. Thorne, R. Vose, M. Wehner, J. Willis, D. Anderson, S. Doney, R. Feely, P. Hennon, V. Kharin, T. Knutson, F. Landerer, T. Lenton, J. Kennedy, and R. Somerville, 2014: Ch. 2: Our changing climate. *Climate Change Impacts in the United States: The Third National Climate Assessment*. Melillo, J.M., T.C. Richmond, and G.W. Yohe, Eds. U.S. Global Change Research Program, Washington, D.C., 19-67. <http://dx.doi.org/10.7930/J0KW5CXT>
37. Zwiers, F.W., X.B. Zhang, and Y. Feng, 2011: Anthropogenic influence on long return period daily temperature extremes at regional scales. *Journal of Climate*, **24**, 881-892. <http://dx.doi.org/10.1175/2010jcli3908.1>
38. Min, S.-K., X. Zhang, F. Zwiers, H. Shioyama, Y.-S. Tung, and M. Wehner, 2013: Multimodel detection and attribution of extreme temperature changes. *Journal of Climate*, **26**, 7430-7451. <http://dx.doi.org/10.1175/JCLI-D-12-00551.1>
39. Knutson, T.R., F. Zeng, and A.T. Wittenberg, 2013: The extreme March-May 2012 warm anomaly over the eastern United States: Global context and multimodel trend analysis [in "Explaining Extreme Events of 2012 from a Climate Perspective"]. *Bulletin of the American Meteorological Society*, **94** (9), S13-S17. <http://dx.doi.org/10.1175/BAMS-D-13-00085.1>
40. Dole, R., M. Hoerling, A. Kumar, J. Eischeid, J. Perlwitz, X.-W. Quan, G. Kiladis, R. Webb, D. Murray, M. Chen, K. Wolter, and T. Zhang, 2014: The making of an extreme event: Putting the pieces together. *Bulletin of the American Meteorological Society*, **95**, 427-440. <http://dx.doi.org/10.1175/BAMS-D-12-00069.1>
41. Collins, M., R. Knutti, J. Arblaster, J.-L. Dufresne, T. Fichefet, P. Friedlingstein, X. Gao, W.J. Gutowski, T. Johns, G. Krinner, M. Shongwe, C. Tebaldi, A.J. Weaver, and M. Wehner, 2013: Long-term climate change: Projections, commitments and irreversibility. *Climate Change 2013: The Physical Science Basis. Contribution of Working Group I to the Fifth Assessment Report of the Intergovernmental Panel on Climate Change*. Stocker, T.F., D. Qin, G.-K. Plattner, M. Tignor, S.K. Allen, J. Boschung, A. Nauels, Y. Xia, V. Bex, and P.M. Midgley, Eds. Cambridge University Press, Cambridge, United Kingdom and New York, NY, USA, 1029-1136. <http://www.climatechange2013.org/report/full-report/>
42. Fischer, E.M., U. Beyerle, and R. Knutti, 2013: Robust spatially aggregated projections of climate extremes. *Nature Climate Change*, **3**, 1033-1038. <http://dx.doi.org/10.1038/nclimate2051>
43. Sillmann, J., V.V. Kharin, F.W. Zwiers, X. Zhang, and D. Bronaugh, 2013: Climate extremes indices in the CMIP5 multimodel ensemble: Part 2. Future climate projections. *Journal of Geophysical Research Atmospheres*, **118**, 2473-2493. <http://dx.doi.org/10.1002/jgrd.50188>
44. Wuebbles, D., G. Meehl, K. Hayhoe, T.R. Karl, K. Kunkel, B. Santer, M. Wehner, B. Colle, E.M. Fischer, R. Fu, A. Goodman, E. Janssen, V. Kharin, H. Lee, W. Li, L.N. Long, S.C. Olsen, Z. Pan, A. Seth, J. Sheffield, and L. Sun, 2014: CMIP5 climate model analyses: Climate extremes in the United States. *Bulletin of the American Meteorological Society*, **95**, 571-583. <http://dx.doi.org/10.1175/BAMS-D-12-00172.1>
45. Sun, L., K.E. Kunkel, L.E. Stevens, A. Buddenberg, J.G. Dobson, and D.R. Easterling, 2015: Regional Surface Climate Conditions in CMIP3 and CMIP5 for the United States: Differences, Similarities, and Implications for the U.S. National Climate Assessment. NOAA Technical Report NESDIS 144. National Oceanic and Atmospheric Administration, National Environmental Satellite, Data, and Information Service, 111 pp. <http://dx.doi.org/10.7289/V5RB72KG>
46. Melillo, J.M., T.C. Richmond, and G.W. Yohe, eds., 2014: *Climate Change Impacts in the United States: The Third National Climate Assessment*. U.S. Global Change Research Program: Washington, D.C., 841 pp. <http://dx.doi.org/10.7930/J0Z31WJ2>
47. Karl, T.R., J.T. Melillo, and T.C. Peterson, eds., 2009: *Global Climate Change Impacts in the United States*. Cambridge University Press: New York, NY, 189 pp. <http://downloads.globalchange.gov/usimpacts/pdfs/climate-impacts-report.pdf>



48. CCSP, 2006: *Temperature Trends in the Lower Atmosphere: Steps for Understanding and Reconciling Differences. A Report by the U.S. Climate Change Science Program and the Subcommittee on Global Change Research*. National Oceanic and Atmospheric Administration, Washington, D.C., 164 pp. <http://www.globalchange.gov/browse/reports/sap-11-temperature-trends-lower-atmosphere-steps-understanding-reconciling>
49. CCSP, 2008: *Weather and Climate Extremes in a Changing Climate - Regions of Focus - North America, Hawaii, Caribbean, and U.S. Pacific Islands. A Report by the U.S. Climate Change Science Program and the Subcommittee on Global Change Research*. Karl, T.R., G.A. Meehl, C.D. Miller, S.J. Hassol, A.M. Waple, and W.L. Murray, Eds. Department of Commerce, NOAA's National Climatic Data Center, Washington, D.C., 164 pp. <http://downloads.globalchange.gov/sap/sap3-3/sap3-3-final-all.pdf>
50. IPCC, 2012: *Managing the Risks of Extreme Events and Disasters to Advance Climate Change Adaptation. A Special Report of Working Groups I and II of the Intergovernmental Panel on Climate Change*. Field, C.B., V. Barros, T.F. Stocker, D. Qin, D.J. Dokken, K.L. Ebi, M.D. Mastrandrea, K.J. Mach, G.-K. Plattner, S.K. Allen, M. Tignor, and P.M. Midgley (Eds.). Cambridge University Press, Cambridge, UK and New York, NY. 582 pp. https://www.ipcc.ch/pdf/special-reports/srex/SREX_Full_Report.pdf
51. Pierce, D.W., D.R. Cayan, and B.L. Thrasher, 2014: Statistical downscaling using Localized Constructed Analogs (LOCA). *Journal of Hydrometeorology*, **15**, 2558-2585. <http://dx.doi.org/10.1175/jhm-d-14-0082.1>
52. Rupp, D.E., P.W. Mote, N. Massey, C.J. Rye, R. Jones, and M.R. Allen, 2012: Did human influence on climate make the 2011 Texas drought more probable? [in "Explaining Extreme Events of 2011 from a Climate Perspective"]. *Bulletin of the American Meteorological Society*, **93**, 1052-1054. <http://dx.doi.org/10.1175/BAMS-D-12-00021.1>
53. Angéilil, O., D. Stone, M. Wehner, C.J. Paciorek, H. Krishnan, and W. Collins, 2017: An independent assessment of anthropogenic attribution statements for recent extreme temperature and rainfall events. *Journal of Climate*, **30**, 5-16. <http://dx.doi.org/10.1175/JCLI-D-16-0077.1>
54. Hoerling, M., M. Chen, R. Dole, J. Eischeid, A. Kumar, J.W. Nielsen-Gammon, P. Pegion, J. Perlwitz, X.-W. Quan, and T. Zhang, 2013: Anatomy of an extreme event. *Journal of Climate*, **26**, 2811-2832. <http://dx.doi.org/10.1175/JCLI-D-12-00270.1>
55. Diffenbaugh, N.S. and M. Scherer, 2013: Likelihood of July 2012 U.S. temperatures in pre-industrial and current forcing regimes [in "Explaining Extreme Events of 2013 from a Climate Perspective"]. *Bulletin of the American Meteorological Society*, **94** (9), S6-S9. <http://dx.doi.org/10.1175/BAMS-D-13-00085.1>
56. Cattiaux, J. and P. Yiou, 2013: U.S. heat waves of spring and summer 2012 from the flow analogue perspective [in "Explaining Extreme Events of 2012 from a Climate Perspective"]. *Bulletin of the American Meteorological Society*, **94** (9), S10-S13. <http://dx.doi.org/10.1175/BAMS-D-13-00085.1>
57. Jeon, S., C.J. Paciorek, and M.F. Wehner, 2016: Quantile-based bias correction and uncertainty quantification of extreme event attribution statements. *Weather and Climate Extremes*, **12**, 24-32. <http://dx.doi.org/10.1016/j.wace.2016.02.001>
58. Seager, R., M. Hoerling, D.S. Siegfried, h. Wang, B. Lyon, A. Kumar, J. Nakamura, and N. Henderson, 2014: Causes and Predictability of the 2011-14 California Drought. National Oceanic and Atmospheric Administration, Drought Task Force Narrative Team, 40 pp. <http://dx.doi.org/10.7289/V58K771F>
59. Wolter, K., J.K. Eischeid, X.-W. Quan, T.N. Chase, M. Hoerling, R.M. Dole, G.J.V. Oldenborgh, and J.E. Walsh, 2015: How unusual was the cold winter of 2013/14 in the Upper Midwest? [in "Explaining Extreme Events of 2014 from a Climate Perspective"]. *Bulletin of the American Meteorological Society*, **96** (12), S10-S14. <http://dx.doi.org/10.1175/bams-d-15-00126.1>
60. Trenary, L., T. DelSole, B. Doty, and M.K. Tippett, 2015: Was the cold eastern US Winter of 2014 due to increased variability? *Bulletin of the American Meteorological Society*, **96** (12), S15-S19. <http://dx.doi.org/10.1175/bams-d-15-00138.1>





7

Precipitation Change in the United States

KEY FINDINGS

1. Annual precipitation has decreased in much of the West, Southwest, and Southeast and increased in most of the Northern and Southern Plains, Midwest, and Northeast. A national average increase of 4% in annual precipitation since 1901 is mostly a result of large increases in the fall season. (*Medium confidence*)
2. Heavy precipitation events in most parts of the United States have increased in both intensity and frequency since 1901 (*high confidence*). There are important regional differences in trends, with the largest increases occurring in the northeastern United States (*high confidence*). In particular, mesoscale convective systems (organized clusters of thunderstorms) – the main mechanism for warm season precipitation in the central part of the United States – have increased in occurrence and precipitation amounts since 1979 (*medium confidence*).
3. The frequency and intensity of heavy precipitation events are projected to continue to increase over the 21st century (*high confidence*). Mesoscale convective systems in the central United States are expected to continue to increase in number and intensity in the future (*medium confidence*). There are, however, important regional and seasonal differences in projected changes in total precipitation: the northern United States, including Alaska, is projected to receive more precipitation in the winter and spring, and parts of the southwestern United States are projected to receive less precipitation in the winter and spring (*medium confidence*).
4. Northern Hemisphere spring snow cover extent, North America maximum snow depth, snow water equivalent in the western United States, and extreme snowfall years in the southern and western United States have all declined, while extreme snowfall years in parts of the northern United States have increased (*medium confidence*). Projections indicate large declines in snowpack in the western United States and shifts to more precipitation falling as rain than snow in the cold season in many parts of the central and eastern United States (*high confidence*).

Recommended Citation for Chapter

Easterling, D.R., K.E. Kunkel, J.R. Arnold, T. Knutson, A.N. LeGrande, L.R. Leung, R.S. Vose, D.E. Waliser, and M.F. Wehner, 2017: Precipitation change in the United States. In: *Climate Science Special Report: Fourth National Climate Assessment, Volume I* [Wuebbles, D.J., D.W. Fahey, K.A. Hibbard, D.J. Dokken, B.C. Stewart, and T.K. Maycock (eds.)]. U.S. Global Change Research Program, Washington, DC, USA, pp. 207-230, doi: 10.7930/J0H993CC.

Introduction

Changes in precipitation are one of the most important potential outcomes of a warming world because precipitation is integral to the very nature of society and ecosystems. These systems have developed and adapted to the past envelope of precipitation variations. Any large changes beyond the historical envelope may have profound societal and ecological impacts.

Historical variations in precipitation, as observed from both instrumental and proxy records, establish the context around which future projected changes can be interpreted, because it is within that context that systems have evolved. Long-term station observations from core climate networks serve as a primary source to establish observed changes in both means and extremes. Proxy records, which are used to reconstruct past climate conditions, are varied and include sources such as tree ring and ice core data. Projected changes are examined using the Coupled Model Inter-comparison Project Phase 5 (CMIP5) suite of model simulations. They establish the likelihood of distinct regional and seasonal patterns of change.

7.1 Historical Changes

7.1.1 Mean Changes

Annual precipitation averaged across the United States has increased approximately 4% over the 1901–2015 period, slightly less than the 5% increase reported in the Third National Climate Assessment (NCA3) over the 1901–2012 period.¹ There continue to be important regional and seasonal differences in precipitation changes (Figure 7.1). Seasonally, national increases are largest in the fall, while little change is observed for winter. Regional differences are apparent, as the Northeast, Midwest, and Great Plains have had increases

while parts of the Southwest and Southeast have had decreases. The slight decrease in the change in annual precipitation across the United States since NCA3 appears to be the result of the recent lingering droughts in the western and southwestern United States.^{2,3} However, the recent meteorological drought in California that began in late 2011^{4,5} now appears to be largely over, due to the substantial precipitation and snowpack the state received in the winter of 2016–2017. The year 2015 was the third wettest on record, just behind 1973 and 1983 (all of which were years marked by El Niño events). Interannual variability is substantial, as evidenced by large multiyear meteorological and agricultural droughts in the 1930s and 1950s.

Changes in precipitation differ markedly across the seasons, as do regional patterns of increases and decreases. For the contiguous United States, fall exhibits the largest (10%) and most widespread increase, exceeding 15% in much of the Northern Great Plains, Southeast, and Northeast. Winter average for the United States has the smallest increase (2%), with drying over most of the western United States as well as parts of the Southeast. In particular, a reduction in streamflow in the northwestern United States has been linked to a decrease in orographic enhancement of precipitation since 1950.⁶ Spring and summer have comparable increases (about 3.5%) but substantially different patterns. In spring, the northern half of the contiguous United States has become wetter, and the southern half has become drier. In summer, there is a mixture of increases and decreases across the Nation. Alaska shows little change in annual precipitation (+1.5%); however, in all seasons, central Alaska shows declines and the panhandle shows increases. Hawai'i shows a decline of more than 15% in annual precipitation.



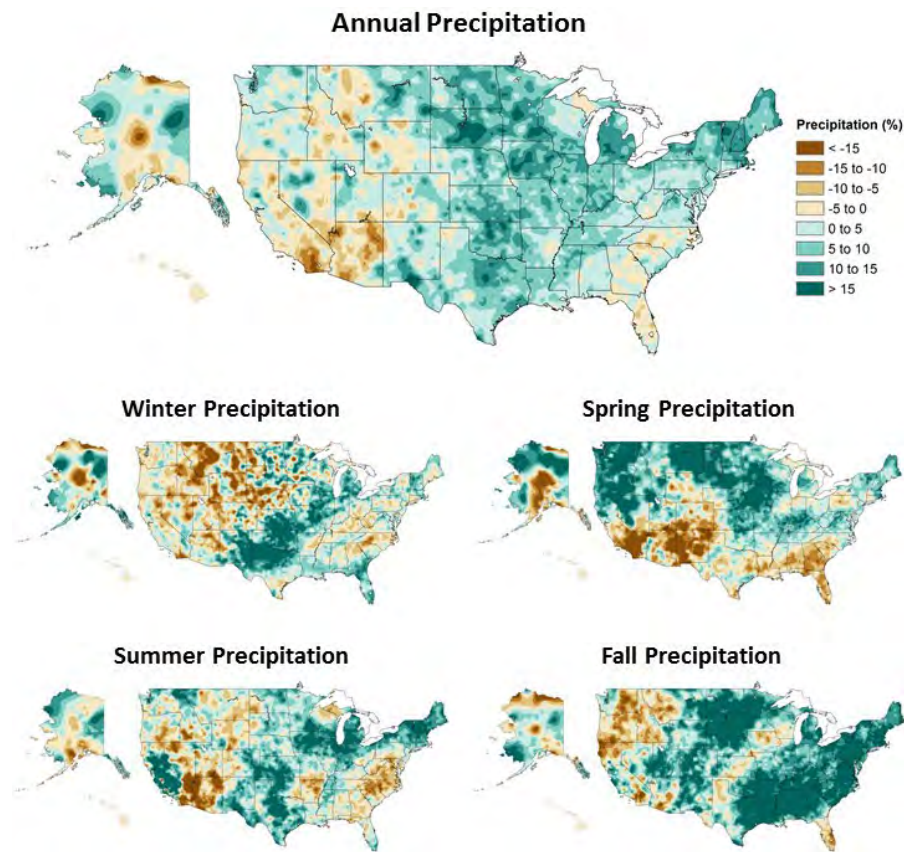


Figure 7.1: Annual and seasonal changes in precipitation over the United States. Changes are the average for present-day (1986–2015) minus the average for the first half of the last century (1901–1960 for the contiguous United States, 1925–1960 for Alaska and Hawai‘i) divided by the average for the first half of the century. (Figure source: [top panel] adapted from Peterson et al. 2013,⁷⁸ © American Meteorological Society. Used with permission; [bottom four panels] NOAA NCEI, data source: nCLIMDiv].

7.1.2 Snow

Changes in snow cover extent (SCE) in the Northern Hemisphere exhibit a strong seasonal dependence.⁷ There has been little change in winter SCE since the 1960s (when the first satellite records became available), while fall SCE has increased. However, the decline in spring SCE is larger than the increase in fall and is due in part to higher temperatures that shorten the time snow spends on the ground in the spring. This tendency is highlighted by the recent occurrences of both unusually high and unusually low monthly (October–June) SCE values, including the top 5 highest and top 5 lowest values in the 48 years of data. From 2010 onward, 7 of the 45 highest monthly SCE values occurred, all in the fall or winter (mostly in November and December), while 9 of the 10 lowest May and June values occurred.

This reflects the trend toward earlier spring snowmelt, particularly at high latitudes.⁸ An analysis of seasonal maximum snow depth for 1961–2015 over North America indicates a statistically significant downward trend of 0.11 standardized anomalies per decade and a trend toward the seasonal maximum snow depth occurring earlier—approximately one week earlier on average since the 1960s.⁸ There has been a statistically significant decrease over the period of 1930–2007 in the frequency of years with a large number of snowfall days (years exceeding the 90th percentile) in the southern United States and the U.S. Pacific Northwest and an increase in the northern United States.⁹ In the snow belts of the Great Lakes, lake effect snowfall has increased overall since the early 20th century for Lakes Superior, Michigan-Huron, and Erie.¹⁰ However, individual studies for

Lakes Michigan¹¹ and Ontario¹² indicate that this increase has not been continuous. In both cases, upward trends were observed until the 1970s/early 1980s. Since then, however, lake effect snowfall has decreased in these regions. Lake effect snows along the Great Lakes are affected greatly by ice cover extent and lake water temperatures. As ice cover diminishes in winter, the expectation is for more lake effect snow until temperatures increase enough such that much of what now falls as snow instead falls as rain.^{13, 14}

End-of-season snow water equivalent (SWE)—especially important where water supply is dominated by spring snow melt (for example, in much of the American West)—has declined since 1980 in the western United States, based on analysis of in situ observations, and is associated with springtime warming.¹⁵ Satellite measurements of SWE based on brightness temperature also show a decrease over this period.¹⁶ The variability of western United States SWE is largely driven by the most extreme events, with the top decile of events explaining 69% of the variability.¹⁷ The recent drought in the western United States was highlighted by the extremely dry 2014–2015 winter that followed three previous dry winters. At Donner Summit, CA, (approximate elevation of 2,100 meters) in the Sierra Nevada Mountains, end-of-season SWE on April 1, 2015, was the lowest on record, based on survey measurements back to 1910, at only 0.51 inches (1.3 cm), or less than 2% of the long-term average. This followed the previous record low in 2014. The estimated return period of this drought is at least 500 years based on paleoclimatic reconstructions.¹⁸

7.1.3 Observed changes in U.S. seasonal extreme precipitation.

Extreme precipitation events occur when the air is nearly completely saturated. Hence, extreme precipitation events are generally

observed to increase in intensity by about 6% to 7% for each degree Celsius of temperature increase, as dictated by the Clausius–Clapeyron relation. Figure 7.2 shows the observed change in the 20-year return value of the seasonal maximum 1-day precipitation totals over the period 1948–2015. A mix of increases and decreases is shown, with the Northwest showing very small changes in all seasons, the southern Great Plains showing a large increase in winter, and the Southeast showing a large increase in the fall.

A U.S. index of extreme precipitation from NCA3 was updated (Figure 7.3) through 2016. This is the number of 2-day precipitation events exceeding the threshold for a 5-year recurrence. The values were calculated by first arithmetically averaging the station data for all stations within each 1° by 1° latitude/longitude grid for each year and then averaging over the grid values across the contiguous United States for each year during the period of 1896–2015. The number of events has been well above average for the last three decades. The slight drop from 2006–2010 to 2011–2016 reflects a below-average number during the widespread severe meteorological drought year of 2012, while the other years in this pentad were well above average. The index value for 2015 was 80% above the 1901–1960 reference period average and the third highest value in the 120 years of record (after 1998 and 2008).

Maximum daily precipitation totals were calculated for consecutive 5-year blocks from 1901 (1901–1905, 1906–1910, 1911–1915, ..., 2011–2016) for individual long-term stations. For each 5-year block, these values were aggregated to the regional scale by first arithmetically averaging the station 5-year maximum for all stations within each 2° by 2° latitude/longitude grid and then averaging across all grids within each region to



Observed Change in Daily, 20-year Return Level Precipitation

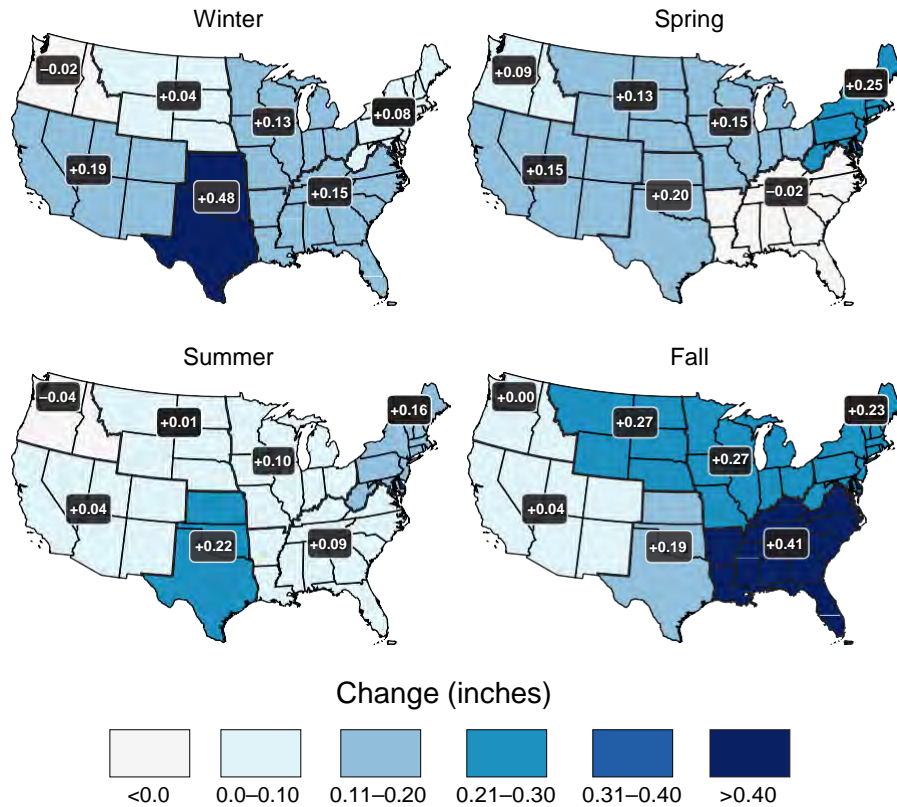


Figure 7.2: Observed changes in the 20-year return value of the seasonal daily precipitation totals for the contiguous United States over the period 1948 to 2015 using data from the Global Historical Climatology Network (GHCN) dataset. (Figure source: adapted from Kunkel et al. 2013;⁶¹ © American Meteorological Society. Used with permission.)

2-Day Precipitation Events Exceeding 5-Year Recurrence Interval

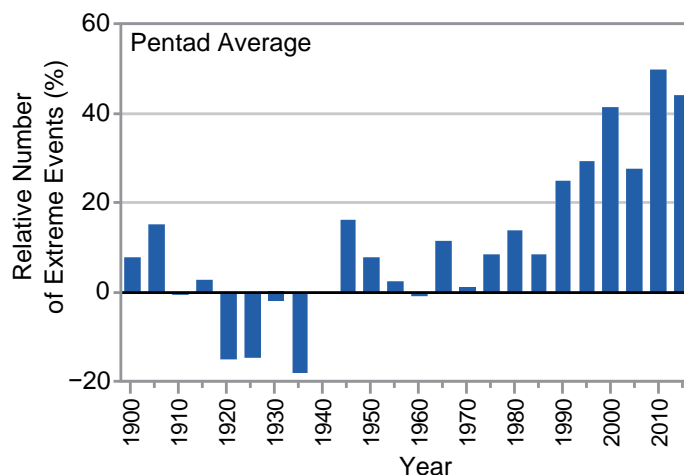


Figure 7.3: Index of the number of 2-day precipitation events exceeding the station-specific threshold for a 5-year recurrence interval in the contiguous United States, expressed as a percentage difference from the 1901–1960 mean. The annual values are averaged over 5-year periods, with the pentad label indicating the ending year of the period. Annual time series of the number of events are first calculated at individual stations. Next, the grid box time series are calculated as the average of all stations in the grid box. Finally, a national time series is calculated as the average of the grid box time series. Data source: GHCN-Daily. (Figure source: CICS-NC and NOAA NCEI).

create a regional time series. Finally, a trend was computed for the resulting regional time series. The difference between these two periods (Figure 7.4, upper left panel) indicates substantial increases over the eastern United States, particularly the northeastern United States with an increase of 27% since 1901. The increases are much smaller over the western United States, with the southwestern and northwestern United States showing little increase.

Another index of extreme precipitation from NCA3 (the total precipitation falling in the top 1% of all days with precipitation) was updated through 2016 (Figure 7.4, upper right panel). This analysis is for 1958–2016. There are increases in all regions, with the largest increases again in the northeastern United States. There are some changes in the values compared to NCA3, with small increases in some regions such as the Midwest and Southwest and small decreases in others such as the Northeast, but the overall picture of changes is the same.

Observed Change in Heavy Precipitation

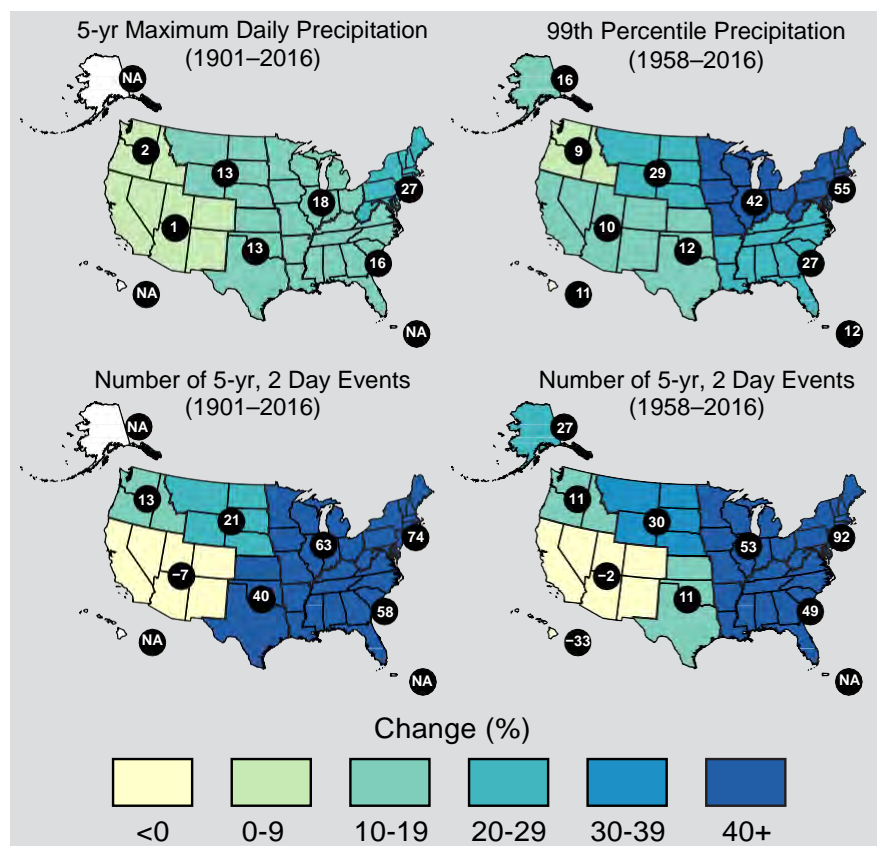


Figure 7.4: These maps show the change in several metrics of extreme precipitation by NCA4 region, including (upper left) the maximum daily precipitation in consecutive 5-year blocks, (upper right) the amount of precipitation falling in daily events that exceed the 99th percentile of all non-zero precipitation days, (lower left) the number of 2-day events with a precipitation total exceeding the largest 2-day amount that is expected to occur, on average, only once every 5 years, as calculated over 1901–2016, and (lower right) the number of 2-day events with a precipitation total exceeding the largest 2-day amount that is expected to occur, on average, only once every 5 years, as calculated over 1958–2016. The numerical value is the percent change over the entire period, either 1901–2016 or 1958–2016. The percentages are first calculated for individual stations, then averaged over 2° latitude by 2° longitude grid boxes, and finally averaged over each NCA4 region. Note that Alaska and Hawai'i are not included in the 1901–2016 maps owing to a lack of observations in the earlier part of the 20th century. (Figure source: CICS-NC and NOAA/NCCEI).

The national results shown in Figure 7.3 were disaggregated into regional values for two periods: 1901–2016 (Figure 7.4, lower left panel) and 1958–2016 (Figure 7.4, lower right panel) for comparison with Figure 7.4, upper right panel. As with the other metrics, there are large increases over the eastern half of the United States while the increases in the western United States are smaller and there are actually small decreases in the Southwest.

There are differences in the magnitude of changes among the four different regional metrics in Figure 7.4, but the overall picture is the same: large increases in the eastern half of the United States and smaller increases, or slight decreases, in the western United States.

7.1.4 Extratropical Cyclones and Mesoscale Convective Systems

As described in Chapter 9: Extreme Storms, there is uncertainty about future changes in winter extratropical cyclones (ETCs).¹⁹ Thus, the potential effects on winter extreme precipitation events is also uncertain. Summertime ETC activity across North America has decreased since 1979, with a reduction of more than 35% in the number of strong summertime ETCs.²⁰ Most climate models simulate little change over this same historical period, but they project a decrease in summer ETC activity during the remainder of the 21st century.²⁰ This is potentially relevant to extreme precipitation in the northeastern quadrant of the United States because a large percentage of the extreme precipitation events in this region are caused by ETCs and their associated fronts.²¹ This suggests that in the future there may be fewer opportunities in the summer for extreme precipitation, although increases in water vapor are likely to overcompensate for any decreases in ETCs by increasing the likelihood that an ETC will produce excessive rainfall amounts. A very idealized set of climate simulations²² suggests that substantial projected

warming will lead to a decrease in the number of ETCs but an increase in the intensity of the strongest ETCs. One factor potentially causing this model ETC intensification is an increase in latent heat release in these storms related to a moister atmosphere. Because of the idealized nature of these simulations, the implications of these results for the real earth–atmosphere system is uncertain. However, the increased latent heat mechanism is likely to occur given the high confidence in a future moister atmosphere. For eastern North America, CMIP5 simulations of the future indicate an increase in strong ETCs.¹⁹ Thus, it is possible that the most extreme precipitation events associated with ETCs may increase in the future.

Mesoscale convective systems (MCSs), which contribute substantially to warm season precipitation in the tropics and subtropics,²³ account for about half of rainfall in the central United States.²⁴ Schumacher and Johnson²⁵ reported that 74% of all warm season extreme rain events over the eastern two-thirds of the United States during the period 1999–2003 were associated with an MCS. Feng et al.²⁶ found that large regions of the central United States experienced statistically significant upward trends in April–June MCS rainfall of 0.4–0.8 mm per day (approximately 20%–40%) per decade from 1979 to 2014. They further found upward trends in MCS frequency of occurrence, lifetime, and precipitation amount, which they attribute to an enhanced west-to-east pressure gradient (enhanced Great Plains low-level jet) and enhanced specific humidity throughout the eastern Great Plains.

7.1.5 Detection and Attribution

Trends

Detectability of trends (compared to internal variability) for a number of precipitation metrics over the continental United States has been examined; however, trends identified for the U.S. regions have not been clearly attribut-



ed to anthropogenic forcing.^{27, 28} One study concluded that increasing precipitation trends in some north-central U.S. regions and the extreme annual anomalies there in 2013 were at least partly attributable to the combination of anthropogenic and natural forcing.²⁹

There is *medium confidence* that anthropogenic forcing has contributed to global-scale intensification of heavy precipitation over land regions with sufficient data coverage.³⁰ Global changes in extreme precipitation have been attributed to anthropogenically forced climate change,^{31, 32} including annual maximum 1-day and 5-day accumulated precipitation over Northern Hemisphere land regions and (relevant to this report) over the North American continent.³³ Although the United States was not separately assessed, the parts of North America with sufficient data for analysis included the continental United States and parts of southern Canada, Mexico, and Central America. Since the covered region was predominantly over the United States, these detection/attribution findings are applicable to the continental United States.

Analyses of precipitation extreme changes over the United States by region (20-year return values of seasonal daily precipitation over 1948–2015, Figure 7.2) show statistically significant increases consistent with theoretical expectations and previous analyses.³⁴ Further, a significant increase in the area affected by precipitation extremes over North America has also been detected.³⁵ There is likely an anthropogenic influence on the upward trend in heavy precipitation,³⁶ although models underestimate the magnitude of the trend. Extreme rainfall from U.S. landfalling tropical cyclones has been higher in recent years (1994–2008) than the long-term historical average, even accounting for temporal changes in storm frequency.¹⁰

Based on current evidence, it is concluded that detectable but not attributable increases in mean precipitation have occurred over parts of the central United States. Formal detection-attribution studies indicate a human contribution to extreme precipitation increases over the continental United States, but confidence is *low* based on those studies alone due to the short observational period, high natural variability, and model uncertainty.

In summary, based on available studies, it is concluded that for the continental United States there is *high confidence* in the detection of extreme precipitation increases, while there is *low confidence* in attributing the extreme precipitation changes purely to anthropogenic forcing. There is stronger evidence for a human contribution (*medium confidence*) when taking into account process-based understanding (increased water vapor in a warmer atmosphere), evidence from weather and climate models, and trends in other parts of the world.

Event Attribution

A number of recent heavy precipitation events have been examined to determine the degree to which their occurrence and severity can be attributed to human-induced climate change. Table 7.1 summarizes available attribution statements for recent extreme U.S. precipitation events. Seasonal and annual precipitation extremes occurring in the north-central and eastern U.S. regions in 2013 were examined for evidence of an anthropogenic influence on their occurrence.²⁹ Increasing trends in annual precipitation were detected in the northern tier of states, March–May precipitation in the upper Midwest, and June–August precipitation in the eastern United States since 1900. These trends are attributed to external forcing (anthropogenic and natural) but could not be directly attributed to anthropogenic forcing alone. However, based on this analysis, it is



Table 7.1. A list of U.S. extreme precipitation events for which attribution statements have been made. In the far right column, “+” indicates that an attributable human-induced increase in frequency and/or magnitude was found, “-” indicates that an attributable human-induced decrease in frequency and/or magnitude was found, “0” indicates no attributable human contribution was identified. As in Tables 6.1 and 8.2, several of the events were originally examined in the *Bulletin of the American Meteorological Society’s* (BAMS) State of the Climate Reports and reexamined by Angéilil et al.⁷⁶ In these cases, both attribution statements are listed with the original authors first. Source: M. Wehner.

Authors	Event year and duration	Region	Type	Attribution statement
Knutson et al. 2014 ²⁹ / Angéilil et al. 2017 ⁷⁶	ANN 2013	U.S. Northern Tier	Wet	+/0
Knutson et al. 2014 ²⁹ / Angéilil et al. 2017 ⁷⁶	MAM 2013	U.S. Upper Midwest	Wet	+/+
Knutson et al. 2014 ²⁹ / Angéilil et al. 2017 ⁷⁶	JJA 2013	Eastern U.S. Region	Wet	+/-
Edwards et al. 2014 ⁷⁷	October 4–5, 2013	South Dakota	Blizzard	0
Hoerling et al. 2014 ³⁷	September 10–14, 2013	Colorado	Wet	0
Pall et al. 2017 ³⁸	September 10–14, 2013	Colorado	Wet	+
Northwest	3.66°F	4.67°F	4.99°F	8.51°F

concluded that the probability of these kinds of extremes has increased due to anthropogenic forcing.

The human influence on individual storms has been investigated with conflicting results. For example, in examining the attribution of the 2013 Colorado floods, one study finds that despite the expected human-induced increase in available moisture, the GEOS-5 model produces fewer extreme storms in the 1983–2012 period compared to the 1871–1900 period in Colorado during the fall season; the study attributes that behavior to changes in the large-scale circulation.³⁷ However, another study finds that such coarse models cannot produce the observed magnitude of precipitation due to resolution constraints.³⁸ Based on a highly conditional set of hindcast simulations

imposing the large-scale meteorology and a substantial increase in both the probability and magnitude of the observed precipitation accumulation magnitudes in that particular meteorological situation, the study could not address the question of whether such situations have become more or less probable. Extreme precipitation event attribution is inherently limited by the rarity of the necessary meteorological conditions and the limited number of model simulations that can be performed to examine rare events. This remains an open and active area of research. However, based on these two studies, the anthropogenic contribution to the 2013 Colorado heavy rainfall-flood event is unclear.

An event attribution study of the potential influence of anthropogenic climate change on



the extreme 3-day rainfall event associated with flooding in Louisiana in August 2016³⁹ finds that such extreme rainfall events have become more likely since 1900. Model simulations of extreme rainfall suggest that anthropogenic forcing has increased the odds of such a 3-day extreme precipitation event by 40% or more.

7.2 Projections

Changes in precipitation in a warmer climate are governed by many factors. Although energy constraints can be used to understand global changes in precipitation, projecting regional changes is much more difficult because of uncertainty in projecting changes in the large-scale circulation that plays an important role in the formation of clouds and precipitation.⁴⁰ For the contiguous United States (CONUS), future changes in seasonal average precipitation will include a mix of increases, decreases, or little change, depending on location and season (Figure 7.5). High-latitude regions are generally projected to become wetter while the subtropical zone is projected to become drier. As the CONUS lies between these two regions, there is significant uncertainty about the sign and magnitude of future anthropogenic changes to seasonal precipitation in much of the region, particularly in the middle latitudes of the Nation. However, because the physical mechanisms controlling extreme precipitation differ from those controlling seasonal average precipitation (Section 7.1.4), in particular atmospheric water vapor will increase with increasing temperatures, confidence is *high* that precipitation extremes will increase in frequency and intensity in the future throughout the CONUS.

Global climate models used to project precipitation changes exhibit varying degrees of fidelity in capturing the observed climatology and seasonal variations of precipitation across the United States. Global or regional climate

models with higher horizontal resolution generally achieve better skill than the CMIP5 models in capturing the spatial patterns and magnitude of winter precipitation in the western and southeastern United States (e.g., Mearns et al. 2012;⁴¹ Wehner 2013;⁴² Bacmeister et al. 2014;⁴³ Wehner et al. 2014⁴⁴), leading to improved simulations of snowpack and runoff (e.g., Rauscher et al. 2008;⁴⁵ Rasmussen et al. 2011⁴⁶). Simulation of present and future summer precipitation remains a significant challenge, as current convective parameterizations fail to properly represent the statistics of mesoscale convective systems.⁴⁷ As a result, high-resolution models that still require the parameterization of deep convection exhibit mixed results.^{44,48} Advances in computing technology are beginning to enable regional climate modeling at the higher resolutions (1–4 km), permitting the direct simulation of convective clouds systems (e.g., Ban et al. 2014⁴⁹) and eliminating the need for this class of parameterization. However, projections from such models are not yet ready for inclusion in this report.

Important progress has been made by the climate modeling community in providing multimodel ensembles such as CMIP5⁵⁰ and NARCCAP⁴¹ to characterize projection uncertainty arising from model differences and large ensemble simulations such as CESM-LE⁵¹ to characterize uncertainty inherent in the climate system due to internal variability. These ensembles provide an important resource for examining the uncertainties in future precipitation projections.



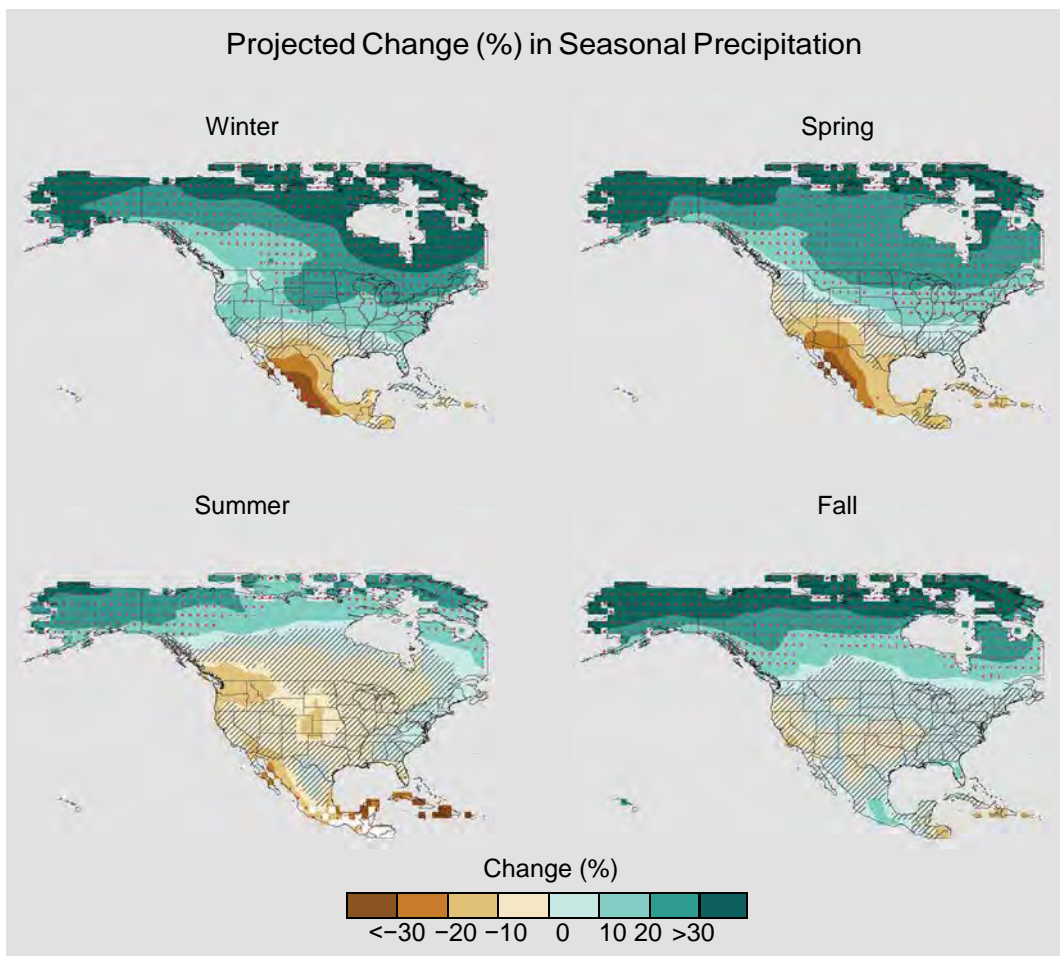


Figure 7.5: Projected change (%) in total seasonal precipitation from CMIP5 simulations for 2070–2099. The values are weighted multimodel means and expressed as the percent change relative to the 1976–2005 average. These are results for the higher scenario (RCP8.5). Stippling indicates that changes are assessed to be large compared to natural variations. Hatching indicates that changes are assessed to be small compared to natural variations. Blank regions (if any) are where projections are assessed to be inconclusive. Data source: World Climate Research Program’s (WCRP’s) Coupled Model Intercomparison Project. (Figure source: NOAA NCEI).

7.2.1 Future Changes in U.S. Seasonal Mean Precipitation

In the United States, projected changes in seasonal mean precipitation span the range from profound decreases to profound increases. In many regions and seasons, projected changes in precipitation are not large compared to natural variations. The general pattern of change is clear and consistent with theoretical expectations. Figure 7.5 shows the weighted CMIP5 multimodel average seasonal change at the end of the century compared to the present under the higher scenario (RCP8.5; see Ch. 4: Projections for discussion of RCPs).

In this figure, changes projected with high confidence to be larger than natural variations are stippled. Regions where future changes are projected with high confidence to be smaller than natural variations are hatched. In winter and spring, the northern part of the country is projected to become wetter as the global climate warms. In the early to middle parts of this century, this will likely be manifested as increases in snowfall.⁵² By the latter half of the century, as temperature continues to increase, it will be too warm to snow in many current snow-producing situations, and precipitation will mostly be rainfall. In the southwestern

United States, precipitation will decrease in the spring but the changes are only a little larger than natural variations. Many other regions of the country will not experience significant changes in average precipitation. This is also the case over most of the country in the summer and fall.

This pattern of projected precipitation change arises because of changes in locally available water vapor and weather system shifts. In the northern part of the continent, increases in water vapor, together with changes in circulation that are the result of expansion of the Hadley cell, bring more moisture to these latitudes while maintaining or increasing the frequency of precipitation-producing weather systems. This change in the Hadley circulation (see Ch. 5: Circulation and Variability for discussion of circulation changes) also causes the subtropics, the region between the northern and southern edges of the tropics and the midlatitudes (about 35° of latitude), to be drier in warmer climates as well as moving the mean storm track northward and away from the subtropics, decreasing the frequency of precipitation-producing systems. The combination of these two factors results in precipitation decreases in the southwestern United States, Mexico, and the Caribbean.⁵³

Projected Changes In Snow

The Third National Climate Assessment⁵⁴ projected reductions in annual snowpack of up to 40% in the western United States based on the SRES A2 emissions scenario in the CMIP3 suite of climate model projections. Recent research using the CMIP5 suite of climate model projections forced with a higher scenario (RCP8.5) and statistically downscaled for the western United States continues to show the expected declines in various snow metrics, including snow water equivalent, the number of extreme snowfall events, and number of snowfall days.⁵⁵ A northward shift in the rain-snow transition zone in the central and

eastern United States was found using statistically downscaled CMIP5 simulations forced with RCP8.5. By the end of the 21st century, large areas that are currently snow dominated in the cold season are expected to be rainfall dominated.⁵⁶

The Variable Infiltration Capacity (VIC) model has been used to investigate the potential effects of climate change on SWE. Declines in SWE are projected in all western U.S. mountain ranges during the 21st century with the virtual disappearance of snowpack in the southernmost mountains by the end of the 21st century under both the lower (RCP4.5) and higher (RCP8.5) scenarios.⁵⁷ The projected decreases are most robust at the lower elevations of areas where snowpack accumulation is now reliable (for example, the Cascades and northern Sierra Nevada ranges). In these areas, future decreases in SWE are largely driven by increases in temperature. At higher (colder) elevations, projections are driven more by precipitation changes and are thus more uncertain.

7.2.2 Extremes

Heavy Precipitation Events

Studies project that the observed increase in heavy precipitation events will continue in the future (e.g. Janssen et al. 2014,⁵⁸ 2016⁵⁹). Similar to observed changes, increases are expected in all regions, even those regions where total precipitation is projected to decline, such as the southwestern United States. Under the higher scenario (RCP8.5) the number of extreme events (exceeding a 5-year return period) increases by two to three times the historical average in every region (Figure 7.6) by the end of the 21st century, with the largest increases in the Northeast. Under the lower scenario (RCP4.5), increases are 50%–100%. Research shows that there is strong evidence, both from the observed record and modeling studies, that increased water vapor resulting from high-



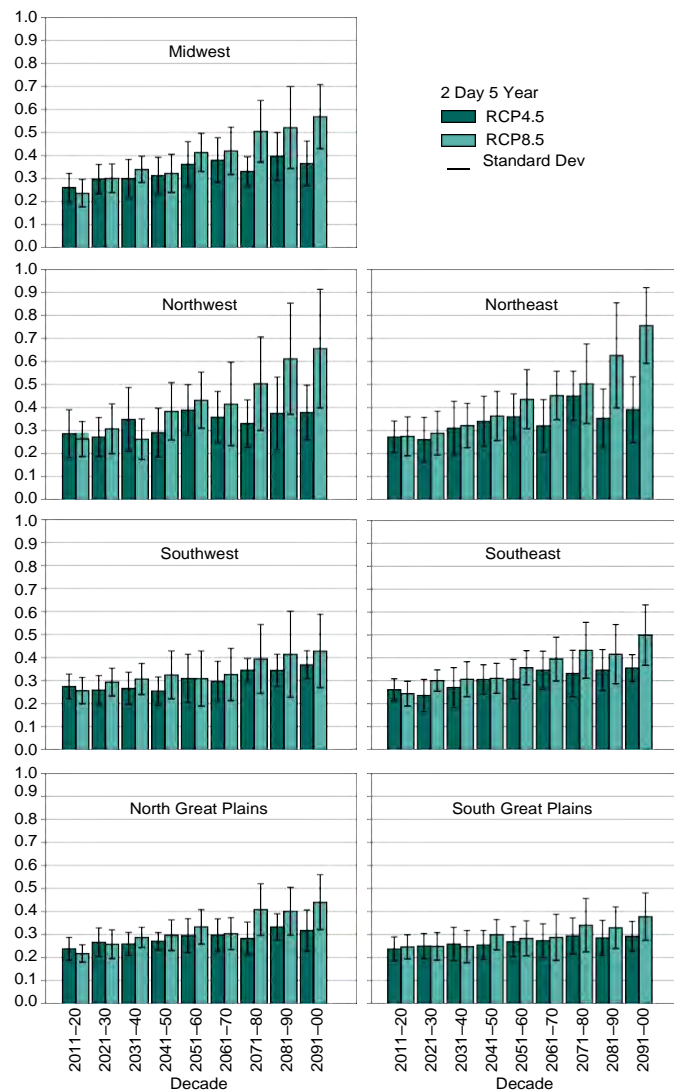


Figure 7.6: Regional extreme precipitation event frequency for a lower scenario (RCP4.5) (green; 16 CMIP5 models) and the higher scenario (RCP8.5) (blue; 14 CMIP5 models) for a 2-day duration and 5-year return. Calculated for 2006–2100 but decadal anomalies begin in 2011. Error bars are ± 1 standard deviation; standard deviation is calculated from the 14 or 16 model values that represent the aggregated average over the regions, over the decades, and over the ensemble members of each model. The average frequency for the historical reference period is 0.2 by definition and the values in this graph should be interpreted with respect to a comparison with this historical average value. (Figure source: Janssen et al. 2014⁵⁸).

er temperatures is the primary cause of the increases.^{42, 60, 61} Additional effects on extreme precipitation due to changes in dynamical processes are poorly understood. However, atmospheric rivers (ARs), especially along the West Coast of the United States, are projected to increase in number and water vapor transport⁶² and experience landfall at lower latitudes⁶³ by the end of the 21st century.

Projections of changes in the 20-year return period amount for daily precipitation (Figure 7.7) using LOcally Constructed Analogs (LOCA) downscaled data also show large percentage increases for both the middle and late 21st century. A lower scenario (RCP4.5) show increases of around 10% for mid-century and up to 14% for the late century projections. A higher scenario (RCP8.5) shows even larger increases for both mid- and late-century

Projected Change in Daily, 20-year Extreme Precipitation

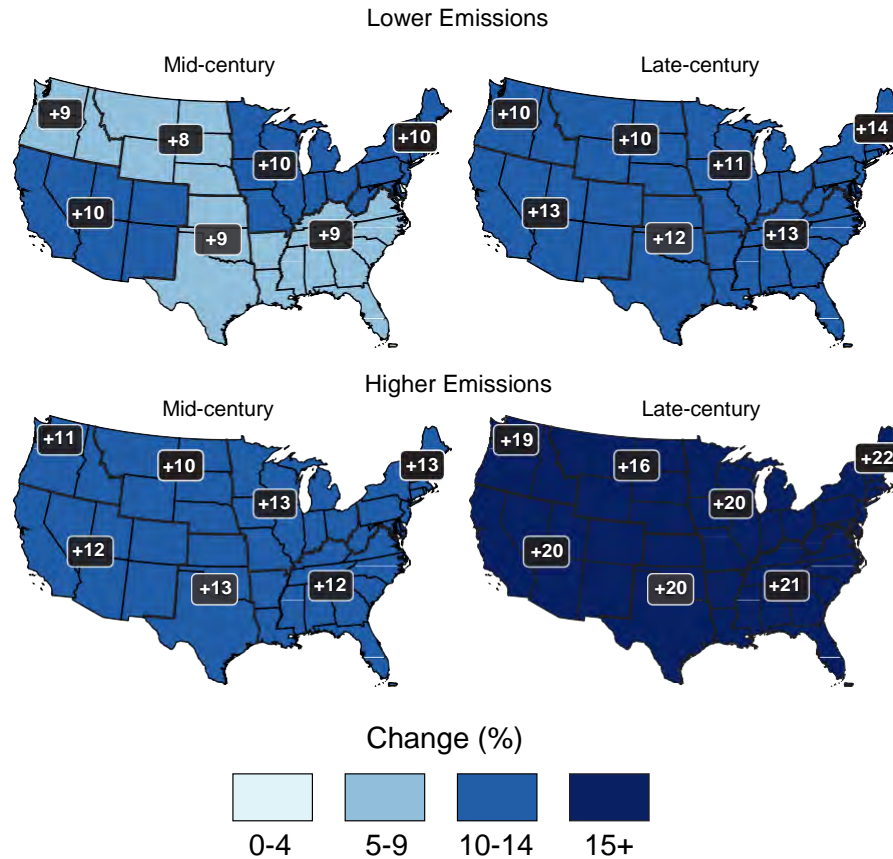


Figure 7.7: Projected change in the 20-year return period amount for daily precipitation for mid- (left maps) and late-21st century (right maps). Results are shown for a lower scenario (top maps; RCP4.5) and for a higher scenario (bottom maps, RCP8.5). These results are calculated from the LOCA downscaled data. (Figure source: CICS-NC and NOAA NCEI).

projections, with increases of around 20% by late 21st century. No region in either scenario shows a decline in heavy precipitation. The increases in extreme precipitation tend to increase with return level, such that increases for the 100-year return level are about 30% by the end of the century under a higher scenario (RCP8.5).

Projections of changes in the distribution of daily precipitation amounts (Figure 7.8) indicate an overall more extreme precipitation climate. Specifically, the projections indicate a slight increase in the numbers of dry days and the very lightest precipitation days and a large increase in the heaviest days. The number of days with precipitation amounts greater than the 95th percentile of all non-zero precipita-

tion days increases by more than 25%. At the same time, the number of days with precipitation amounts in the 10th–80th percentile range decreases.

Most global climate models lack sufficient resolution to project changes in mesoscale convective systems (MCSs) in a changing climate.⁶⁴ However, research by Cook et al.⁶⁵ attempted to identify clues to changes in dynamical forcing that create MCSs. To do this, they examined the ability of 18 coupled ocean–atmosphere global climate models (GCMs) to simulate potential 21st century changes in warm-season flow and the associated U.S. Midwest hydrology resulting from increases in greenhouse gases. They selected a subset of six models that best captured the

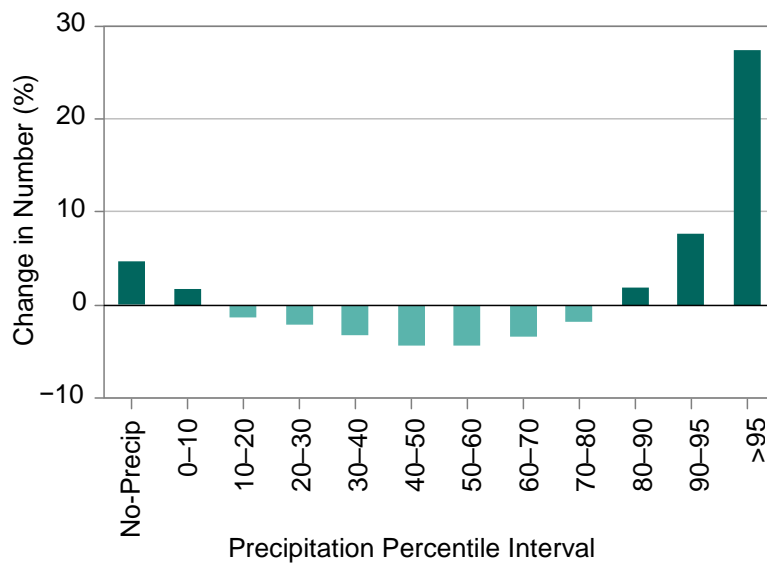


Figure 7.8: Projected change (percentage change relative to the 1976–2005 reference period average) in the number of daily zero (“No-Precip”) and non-zero precipitation days (by percentile bins) for late-21st century under a higher scenario (RCP8.5). The precipitation percentile bin thresholds are based on daily non-zero precipitation amounts from the 1976–2005 reference period that have been ranked from low to high. These results are calculated from the LOCA downscaled data. (Figure source: CICS-NC and NOAA NCEI).

low-level flow and associated dynamics of the present-day climate of the central United States and then analyzed these models for changes due to enhanced greenhouse gas forcing. In each of these models, spring-time precipitation increases significantly (by 20%–40%) in the upper Mississippi Valley and decreases to the south. The enhanced moisture convergence leading to modeled future climate rainfall increases in the U.S. Midwest is caused by meridional convergence at 850 hPa, connecting the rainfall changes with the Great Plains Low-Level Jet intensification.⁶⁶ This is consistent with findings from Feng et al.²⁶ in the observational record for the period 1979–2014 and by Pan et al.⁶⁷ by use of a regional climate model.

Changes in intense hourly precipitation events were simulated by Prein et al.⁶⁸ where they found the most intense hourly events (99.9 percentile) in the central United States increase at the expense of moderately intense (97.5 percentile) hourly events in the warm season. They also found the frequency of seasonal hourly precipitation extremes is expected to

increase in all regions by up to five times in the same areas that show the highest increases in extreme precipitation rates.

Hurricane Precipitation

Regional model projections of precipitation from landfalling tropical cyclones over the United States, based on downscaling of CMIP5 model climate changes, suggest that the occurrence frequency of post-landfall tropical cyclones over the United States will change little compared to present day during the 21st century, as the reduced frequency of tropical cyclones over the Atlantic domain is mostly offset by a greater landfalling fraction. However, when downscaling from CMIP3 model climate changes, projections show a reduced occurrence frequency over U.S. land, indicating uncertainty about future outcomes. The average tropical cyclone rainfall rates within 500 km (about 311 miles) of the storm center increased by 8% to 17% in the simulations, which was at least as much as expected from the water vapor content increase factor alone.

Several studies have projected increases of precipitation rates within hurricanes over ocean regions,⁶⁹ particularly for the Atlantic basin.⁷⁰ The primary physical mechanism for this increase is the enhanced water vapor content in the warmer atmosphere, which enhances moisture convergence into the storm for a given circulation strength, although a more intense circulation can also contribute.⁷¹ Since hurricanes are responsible for many of the most extreme precipitation events in the southeastern United States,^{10, 21} such events are likely to be even heavier in the future. In a set of idealized forcing experiments, this effect was partly offset by differences in warming rates at the surface and at altitude.⁷²



TRACEABLE ACCOUNTS

Key Finding 1

Annual precipitation has decreased in much of the West, Southwest, and Southeast and increased in most of the Northern and Southern Plains, Midwest, and Northeast. A national average increase of 4% in annual precipitation since 1901 is mostly a result of large increases in the fall season. (*Medium confidence*)

Description of evidence base

The key finding and supporting text summarizes extensive evidence documented in the climate science peer-reviewed literature. Evidence of long-term changes in precipitation is based on analysis of daily precipitation observations from the U.S. Cooperative Observer Network (<http://www.nws.noaa.gov/om/coop/>) and shown in Figure 7.1. Published work, such as the Third National Climate Assessment,⁷³ and Figure 7.1 show important regional and seasonal differences in U.S. precipitation change since 1901.

Major uncertainties

The main source of uncertainty is the sensitivity of observed precipitation trends to the spatial distribution of observing stations and to historical changes in station location, rain gauges, the local landscape, and observing practices. These issues are mitigated somewhat by new methods to produce spatial grids through time.⁷⁴

Assessment of confidence based on evidence and agreement, including short description of nature of evidence and level of agreement

Based on the evidence and understanding of the issues leading to uncertainties, confidence is *medium* that average annual precipitation has increased in the United States. Furthermore, confidence is also *medium* that the important regional and seasonal differences in changes documented in the text and in Figure 7.1 are robust.

Summary sentence or paragraph that integrates the above information

Based on the patterns shown in Figure 7.1 and numerous additional studies of precipitation changes in the United States, there is *medium confidence* in the ob-

served changes in annual and seasonal precipitation over the various regions and the United States as a whole.

Key Finding 2

Heavy precipitation events in most parts of the United States have increased in both intensity and frequency since 1901 (*high confidence*). There are important regional differences in trends, with the largest increases occurring in the northeastern United States (*high confidence*). In particular, mesoscale convective systems (organized clusters of thunderstorms)—the main mechanism for warm season precipitation in the central part of the United States—have increased in occurrence and precipitation amounts since 1979 (*medium confidence*).

Description of evidence base

The key finding and supporting text summarize extensive evidence documented in the climate science peer-reviewed literature. Numerous papers have been written documenting observed changes in heavy precipitation events in the United States, including those cited in the Third National Climate Assessment and in this assessment. Although station-based analyses (e.g., Westra et al. 2013³⁴) do not show large numbers of statistically significant station-based trends, area averaging reduces the noise inherent in station-based data and produces robust increasing signals (see Figures 7.2 and 7.3). Evidence of long-term changes in precipitation is based on analysis of daily precipitation observations from the U.S. Cooperative Observer Network (<http://www.nws.noaa.gov/om/coop/>) and shown in Figures 7.2, 7.3, and 7.4.

Major uncertainties

The main source of uncertainty is the sensitivity of observed precipitation trends to the spatial distribution of observing stations and to historical changes in station location, rain gauges, and observing practices. These issues are mitigated somewhat by methods used to produce spatial grids through gridbox averaging.



Assessment of confidence based on evidence and agreement, including short description of nature of evidence and level of agreement

Based on the evidence and understanding of the issues leading to uncertainties, confidence is *high* that heavy precipitation events have increased in the United States. Furthermore, confidence is also *high* that the important regional and seasonal differences in changes documented in the text and in Figures 7.2, 7.3, and 7.4 are robust.

Summary sentence or paragraph that integrates the above information

Based on numerous analyses of the observed record in the United States there is *high confidence* in the observed changes in heavy precipitation events, and *medium confidence* in observed changes in mesoscale convective systems.

Key Finding 3

The frequency and intensity of heavy precipitation events are projected to continue to increase over the 21st century (*high confidence*). Mesoscale convective systems in the central United States are expected to continue to increase in number and intensity in the future (*medium confidence*). There are, however, important regional and seasonal differences in projected changes in total precipitation: the northern United States, including Alaska, is projected to receive more precipitation in the winter and spring, and parts of the southwestern United States are projected to receive less precipitation in the winter and spring (*medium confidence*).

Description of evidence base

Evidence for future changes in precipitation is based on climate model projections and our understanding of the climate system's response to increasing greenhouse gases and of regional mechanisms behind the projected changes. In particular, Figure 7.7 documents projected changes in the 20-year return period amount using the LOCA data, and Figure 7.6 shows changes in 2 day totals for the 5-year return period using the CMIP5 suite of models. Each figure shows robust changes in extreme precipitation events as they are defined in

the figure. However, Figure 7.5, which shows changes in seasonal and annual precipitation, indicates where confidence in the changes is higher based on consistency between the models and that there are large areas where the projected change is uncertain.

Major uncertainties

A key issue is how well climate models simulate precipitation, which is one of the more challenging aspects of weather and climate simulation. In particular, comparisons of model projections for total precipitation (from both CMIP3 and CMIP5, see Sun et al. 2015⁷⁵) by NCA3 region show a spread of responses in some regions (for example, the Southwest) such that they are opposite from the ensemble average response. The continental United States is positioned in the transition zone between expected drying in the subtropics and wetting in the mid- and higher-latitudes. There are some differences in the location of this transition between CMIP3 and CMIP5 models and thus there remains uncertainty in the exact location of the transition zone.

Assessment of confidence based on evidence and agreement, including short description of nature of evidence and level of agreement

Based on evidence from climate model simulations and our fundamental understanding of the relationship of water vapor to temperature, confidence is *high* that extreme precipitation will increase in all regions of the United States. However, based on the evidence and understanding of the issues leading to uncertainties, confidence is *medium* that that more total precipitation is projected for the northern U.S. and less for the Southwest.

Summary sentence or paragraph that integrates the above information

Based on numerous analyses of model simulations and our understanding of the climate system there is *high confidence* in the projected changes in precipitation extremes and *medium confidence* in projected changes in total precipitation over the United States.



Key Finding 4

Northern Hemisphere spring snow cover extent, North America maximum snow depth, snow water equivalent in the western United States, and extreme snowfall years in the southern and western United States have all declined, while extreme snowfall years in parts of the northern United States have increased (*medium confidence*). Projections indicate large declines in snowpack in the western United States and shifts to more precipitation falling as rain than snow in the cold season in many parts of the central and eastern United States (*high confidence*).

Description of evidence base

Evidence of historical changes in snow cover extent and a reduction in extreme snowfall years is consistent with our understanding of the climate system's response to increasing greenhouse gases. Furthermore, climate models continue to consistently show future declines in snowpack in the western United States. Recent model projections for the eastern United States also confirm a future shift from snowfall to rainfall during the cold season in colder portions of the central and eastern United States. Each of these changes is documented in the peer-reviewed literature and are cited in the main text of this chapter.

Major uncertainties

The main source of uncertainty is the sensitivity of observed snow changes to the spatial distribution of observing stations and to historical changes in station location, rain gauges, and observing practices, particularly for snow. Another key issue is the ability of climate models to simulate precipitation, particularly snow. Future changes in the frequency and intensity of meteorological systems causing heavy snow are less certain than temperature changes.

Assessment of confidence based on evidence and agreement, including short description of nature of evidence and level of agreement

Given the evidence base and uncertainties, confidence is *medium* that snow cover extent has declined in the United States and *medium* that extreme snowfall years have declined in recent years. Confidence is *high* that western United States snowpack will decline in the future, and confidence is *medium* that a shift from snow domination to rain domination will occur in the parts of the central and eastern United States cited in the text.

Summary sentence or paragraph that integrates the above information

Based on observational analyses of snow cover, depth, and water equivalent there is *medium confidence* in the observed changes, and based on model simulations for the future there is *high confidence* in snowpack declines in the western United States and *medium confidence* in the shift to rain from snow in the eastern United States.



REFERENCES

1. Walsh, J., D. Wuebbles, K. Hayhoe, J. Kossin, K. Kunkel, G. Stephens, P. Thorne, R. Vose, M. Wehner, J. Willis, D. Anderson, S. Doney, R. Feely, P. Hennon, V. Kharin, T. Knutson, F. Landerer, T. Lenton, J. Kennedy, and R. Somerville, 2014: Ch. 2: Our changing climate. *Climate Change Impacts in the United States: The Third National Climate Assessment*. Melillo, J.M., T.C. Richmond, and G.W. Yohe, Eds. U.S. Global Change Research Program, Washington, D.C., 19-67. <http://dx.doi.org/10.7930/J0KW5CXT>
2. NOAA, 2016: Climate at a Glance: Southwest PDSI. http://www.ncdc.noaa.gov/cag/time-series/us/107/0/pdsi/12/12/1895-2016?base_prd=true&firstbaseyear=1901&lastbaseyear=2000
3. Barnston, A.G. and B. Lyon, 2016: Does the NMME capture a recent decadal shift toward increasing drought occurrence in the southwestern United States? *Journal of Climate*, **29**, 561-581. <http://dx.doi.org/10.1175/JCLI-D-15-0311.1>
4. Seager, R., M. Hoerling, S. Schubert, H. Wang, B. Lyon, A. Kumar, J. Nakamura, and N. Henderson, 2015: Causes of the 2011-14 California drought. *Journal of Climate*, **28**, 6997-7024. <http://dx.doi.org/10.1175/JCLI-D-14-00860.1>
5. NOAA, 2016: Climate at a Glance: California PDSI. http://www.ncdc.noaa.gov/cag/time-series/us/4/0/pdsi/12/9/1895-2016?base_prd=true&firstbaseyear=1901&lastbaseyear=2000
6. Luce, C.H., J.T. Abatzoglou, and Z.A. Holden, 2013: The missing mountain water: Slower westerlies decrease orographic enhancement in the Pacific Northwest USA. *Science*, **342**, 1360-1364. <http://dx.doi.org/10.1126/science.1242335>
7. Vaughan, D.G., J.C. Comiso, I. Allison, J. Carrasco, G. Kaser, R. Kwok, P. Mote, T. Murray, F. Paul, J. Ren, E. Rignot, O. Solomina, K. Steffen, and T. Zhang, 2013: Observations: Cryosphere. *Climate Change 2013: The Physical Science Basis. Contribution of Working Group I to the Fifth Assessment Report of the Intergovernmental Panel on Climate Change*. Stocker, T.F., D. Qin, G.-K. Plattner, M. Tignor, S.K. Allen, J. Boschung, A. Nauels, Y. Xia, V. Bex, and P.M. Midgley, Eds. Cambridge University Press, Cambridge, United Kingdom and New York, NY, USA, 317-382. <http://www.climatechange2013.org/report/full-report/>
8. Kunkel, K.E., D.A. Robinson, S. Champion, X. Yin, T. Estilow, and R.M. Frankson, 2016: Trends and extremes in Northern Hemisphere snow characteristics. *Current Climate Change Reports*, **2**, 65-73. <http://dx.doi.org/10.1007/s40641-016-0036-8>
9. Kluver, D. and D. Leathers, 2015: Regionalization of snowfall frequency and trends over the contiguous United States. *International Journal of Climatology*, **35**, 4348-4358. <http://dx.doi.org/10.1002/joc.4292>
10. Kunkel, K.E., D.R. Easterling, D.A.R. Kristovich, B. Gleason, L. Stoecker, and R. Smith, 2010: Recent increases in U.S. heavy precipitation associated with tropical cyclones. *Geophysical Research Letters*, **37**, L24706. <http://dx.doi.org/10.1029/2010GL045164>
11. Bard, L. and D.A.R. Kristovich, 2012: Trend reversal in Lake Michigan contribution to snowfall. *Journal of Applied Meteorology and Climatology*, **51**, 2038-2046. <http://dx.doi.org/10.1175/jamc-d-12-064.1>
12. Hartnett, J.J., J.M. Collins, M.A. Baxter, and D.P. Chambers, 2014: Spatiotemporal snowfall trends in central New York. *Journal of Applied Meteorology and Climatology*, **53**, 2685-2697. <http://dx.doi.org/10.1175/jamc-d-14-0084.1>
13. Wright, D.M., D.J. Posselt, and A.L. Steiner, 2013: Sensitivity of lake-effect snowfall to lake ice cover and temperature in the Great Lakes region. *Monthly Weather Review*, **141**, 670-689. <http://dx.doi.org/10.1175/mwr-d-12-00038.1>
14. Vavrus, S., M. Notaro, and A. Zarrin, 2013: The role of ice cover in heavy lake-effect snowstorms over the Great Lakes Basin as simulated by RegCM4. *Monthly Weather Review*, **141**, 148-165. <http://dx.doi.org/10.1175/mwr-d-12-00107.1>
15. Pederson, G.T., J.L. Betancourt, and G.J. McCabe, 2013: Regional patterns and proximal causes of the recent snowpack decline in the Rocky Mountains, U.S. *Geophysical Research Letters*, **40**, 1811-1816. <http://dx.doi.org/10.1002/grl.50424>
16. Gan, T.Y., R.G. Barry, M. Gizaw, A. Gobena, and R. Balaji, 2013: Changes in North American snowpacks for 1979-2007 detected from the snow water equivalent data of SMMR and SSM/I passive microwave and related climatic factors. *Journal of Geophysical Research Atmospheres*, **118**, 7682-7697. <http://dx.doi.org/10.1002/jgrd.50507>
17. Lute, A.C. and J.T. Abatzoglou, 2014: Role of extreme snowfall events in interannual variability of snowfall accumulation in the western United States. *Water Resources Research*, **50**, 2874-2888. <http://dx.doi.org/10.1002/2013WR014465>
18. Belmecheri, S., F. Babst, E.R. Wahl, D.W. Stahle, and V. Trouet, 2016: Multi-century evaluation of Sierra Nevada snowpack. *Nature Climate Change*, **6**, 2-3. <http://dx.doi.org/10.1038/nclimate2809>
19. Colle, B.A., Z. Zhang, K.A. Lombardo, E. Chang, P. Liu, and M. Zhang, 2013: Historical evaluation and future prediction of eastern North American and western Atlantic extratropical cyclones in the CMIP5 models during the cool season. *Journal of Climate*, **26**, 6882-6903. <http://dx.doi.org/10.1175/JCLI-D-12-00498.1>



20. Chang, E.K.M., C.-G. Ma, C. Zheng, and A.M.W. Yau, 2016: Observed and projected decrease in Northern Hemisphere extratropical cyclone activity in summer and its impacts on maximum temperature. *Geophysical Research Letters*, **43**, 2200-2208. <http://dx.doi.org/10.1002/2016GL068172>
21. Kunkel, K.E., D.R. Easterling, D.A. Kristovich, B. Gleason, L. Stoecker, and R. Smith, 2012: Meteorological causes of the secular variations in observed extreme precipitation events for the conterminous United States. *Journal of Hydrometeorology*, **13**, 1131-1141. <http://dx.doi.org/10.1175/JHM-D-11-0108.1>
22. Pfahl, S., P.A. O’Gorman, and M.S. Singh, 2015: Extratropical cyclones in idealized simulations of changed climates. *Journal of Climate*, **28**, 9373-9392. <http://dx.doi.org/10.1175/JCLI-D-14-00816.1>
23. Nesbitt, S.W., R. Cifelli, and S.A. Rutledge, 2006: Storm morphology and rainfall characteristics of TRMM precipitation features. *Monthly Weather Review*, **134**, 2702-2721. <http://dx.doi.org/10.1175/mwr3200.1>
24. Fritsch, J.M., R.J. Kane, and C.R. Chelius, 1986: The contribution of mesoscale convective weather systems to the warm-season precipitation in the United States. *Journal of Climate and Applied Meteorology*, **25**, 1333-1345. [http://dx.doi.org/10.1175/1520-0450\(1986\)025<1333:tcomcw>2.0.co;2](http://dx.doi.org/10.1175/1520-0450(1986)025<1333:tcomcw>2.0.co;2)
25. Schumacher, R.S. and R.H. Johnson, 2006: Characteristics of U.S. extreme rain events during 1999–2003. *Weather and Forecasting*, **21**, 69-85. <http://dx.doi.org/10.1175/waf900.1>
26. Feng, Z., L.R. Leung, S. Hagos, R.A. Houze, C.D. Burleyson, and K. Balaguru, 2016: More frequent intense and long-lived storms dominate the springtime trend in central US rainfall. *Nature Communications*, **7**, 13429. <http://dx.doi.org/10.1038/ncomms13429>
27. Anderson, B.T., D.J. Gianotti, and G.D. Salvucci, 2015: Detectability of historical trends in station-based precipitation characteristics over the continental United States. *Journal of Geophysical Research Atmospheres*, **120**, 4842-4859. <http://dx.doi.org/10.1002/2014JD022960>
28. Easterling, D.R., K.E. Kunkel, M.F. Wehner, and L. Sun, 2016: Detection and attribution of climate extremes in the observed record. *Weather and Climate Extremes*, **11**, 17-27. <http://dx.doi.org/10.1016/j.wace.2016.01.001>
29. Knutson, T.R., F. Zeng, and A.T. Wittenberg, 2014: Seasonal and annual mean precipitation extremes occurring during 2013: A U.S. focused analysis [in “Explaining Extreme Events of 2013 from a Climate Perspective”]. *Bulletin of the American Meteorological Society*, **95** (9), S19-S23. <http://dx.doi.org/10.1175/1520-0477-95.9.S1.1>
30. Bindoff, N.L., P.A. Stott, K.M. AchutaRao, M.R. Allen, N. Gillett, D. Gutzler, K. Hansingo, G. Hegerl, Y. Hu, S. Jain, I.I. Mokhov, J. Overland, J. Perlwitz, R. Sebbari, and X. Zhang, 2013: Detection and attribution of climate change: From global to regional. *Climate Change 2013: The Physical Science Basis. Contribution of Working Group I to the Fifth Assessment Report of the Intergovernmental Panel on Climate Change*. Stocker, T.F., D. Qin, G.-K. Plattner, M. Tignor, S.K. Allen, J. Boschung, A. Nauels, Y. Xia, V. Bex, and P.M. Midgley, Eds. Cambridge University Press, Cambridge, United Kingdom and New York, NY, USA, 867-952. <http://www.climatechange2013.org/report/full-report/>
31. Min, S.K., X. Zhang, F.W. Zwiers, and G.C. Hegerl, 2011: Human contribution to more-intense precipitation extremes. *Nature*, **470**, 378-381. <http://dx.doi.org/10.1038/nature09763>
32. Min, S.-K., X. Zhang, F. Zwiers, H. Shiogama, Y.-S. Tung, and M. Wehner, 2013: Multimodel detection and attribution of extreme temperature changes. *Journal of Climate*, **26**, 7430-7451. <http://dx.doi.org/10.1175/JCLI-D-12-00551.1>
33. Zhang, X., H. Wan, F.W. Zwiers, G.C. Hegerl, and S.-K. Min, 2013: Attributing intensification of precipitation extremes to human influence. *Geophysical Research Letters*, **40**, 5252-5257. <http://dx.doi.org/10.1002/grl.51010>
34. Westra, S., L.V. Alexander, and F.W. Zwiers, 2013: Global increasing trends in annual maximum daily precipitation. *Journal of Climate*, **26**, 3904-3918. <http://dx.doi.org/10.1175/JCLI-D-12-00502.1>
35. Dittus, A.J., D.J. Karoly, S.C. Lewis, and L.V. Alexander, 2015: A multiregion assessment of observed changes in the areal extent of temperature and precipitation extremes. *Journal of Climate*, **28**, 9206-9220. <http://dx.doi.org/10.1175/JCLI-D-14-00753.1>
36. Dittus, A.J., D.J. Karoly, S.C. Lewis, L.V. Alexander, and M.G. Donat, 2016: A multiregion model evaluation and attribution study of historical changes in the area affected by temperature and precipitation extremes. *Journal of Climate*, **29**, 8285-8299. <http://dx.doi.org/10.1175/jcli-d-16-0164.1>
37. Hoerling, M., K. Wolter, J. Perlwitz, X. Quan, J. Eischeid, H. Want, S. Schubert, H. Diaz, and R. Dole, 2014: Northeast Colorado extreme rains interpreted in a climate change context [in “Explaining Extreme Events of 2013 from a Climate Perspective”]. *Bulletin of the American Meteorological Society*, **95** (9), S15-S18. <http://dx.doi.org/10.1175/1520-0477-95.9.S1.1>
38. Pall, P.C.M.P., M.F. Wehner, D.A. Stone, C.J. Paciorek, and W.D. Collins, 2017: Diagnosing anthropogenic contributions to heavy Colorado rainfall in September 2013. *Weather and Climate Extremes*, **17**, 1-6. <http://dx.doi.org/10.1016/j.wace.2017.03.004>



39. van der Wiel, K., S.B. Kapnick, G.J. van Oldenborgh, K. Whan, S. Philip, G.A. Vecchi, R.K. Singh, J. Arrighi, and H. Cullen, 2017: Rapid attribution of the August 2016 flood-inducing extreme precipitation in south Louisiana to climate change. *Hydrology and Earth System Sciences*, **21**, 897-921. <http://dx.doi.org/10.5194/hess-21-897-2017>
40. Shepherd, T.G., 2014: Atmospheric circulation as a source of uncertainty in climate change projections. *Nature Geoscience*, **7**, 703-708. <http://dx.doi.org/10.1038/ngeo2253>
41. Mearns, L.O., R. Arritt, S. Biner, M.S. Bukovsky, S. Stain, S. Sain, D. Caya, J. Correia, Jr., D. Flory, W. Gutowski, E.S. Takle, R. Jones, R. Leung, W. Moufouma-Okia, L. McDaniel, A.M.B. Nunes, Y. Qian, J. Roads, L. Sloan, and M. Snyder, 2012: The North American regional climate change assessment program: Overview of phase I results. *Bulletin of the American Meteorological Society*, **93**, 1337-1362. <http://dx.doi.org/10.1175/BAMS-D-11-00223.1>
42. Wehner, M.F., 2013: Very extreme seasonal precipitation in the NARCCAP ensemble: Model performance and projections. *Climate Dynamics*, **40**, 59-80. <http://dx.doi.org/10.1007/s00382-012-1393-1>
43. Bacmeister, J.T., M.F. Wehner, R.B. Neale, A. Gettelman, C. Hannay, P.H. Lauritzen, J.M. Caron, and J.E. Truesdale, 2014: Exploratory high-resolution climate simulations using the Community Atmosphere Model (CAM). *Journal of Climate*, **27**, 3073-3099. <http://dx.doi.org/10.1175/JCLI-D-13-00387.1>
44. Wehner, M.F., K.A. Reed, F. Li, Prabhat, J. Bacmeister, C.-T. Chen, C. Paciorek, P.J. Gleckler, K.R. Sperber, W.D. Collins, A. Gettelman, and C. Jablonowski, 2014: The effect of horizontal resolution on simulation quality in the Community Atmospheric Model, CAM5.1. *Journal of Advances in Modeling Earth Systems*, **6**, 980-997. <http://dx.doi.org/10.1002/2013MS000276>
45. Rauscher, S.A., J.S. Pal, N.S. Diffenbaugh, and M.M. Benedetti, 2008: Future changes in snowmelt-driven runoff timing over the western US. *Geophysical Research Letters*, **35**, L16703. <http://dx.doi.org/10.1029/2008GL034424>
46. Rasmussen, R., C. Liu, K. Ikeda, D. Gochis, D. Yates, F. Chen, M. Tewari, M. Barlage, J. Dudhia, W. Yu, K. Miller, K. Arsenaault, V. Grubišić, G. Thompson, and E. Gutmann, 2011: High-resolution coupled climate runoff simulations of seasonal snowfall over Colorado: A process study of current and warmer climate. *Journal of Climate*, **24**, 3015-3048. <http://dx.doi.org/10.1175/2010JCLI3985.1>
47. Boyle, J. and S.A. Klein, 2010: Impact of horizontal resolution on climate model forecasts of tropical precipitation and diabatic heating for the TWP-ICE period. *Journal of Geophysical Research*, **115**, D23113. <http://dx.doi.org/10.1029/2010JD014262>
48. Sakaguchi, K., L.R. Leung, C. Zhao, Q. Yang, J. Lu, S. Hagos, S.A. Rauscher, L. Dong, T.D. Ringler, and P.H. Lauritzen, 2015: Exploring a multiresolution approach using AMIP simulations. *Journal of Climate*, **28**, 5549-5574. <http://dx.doi.org/10.1175/JCLI-D-14-00729.1>
49. Ban, N., J. Schmidli, and C. Schär, 2014: Evaluation of the convection-resolving regional climate modeling approach in decade-long simulations. *Journal of Geophysical Research Atmospheres*, **119**, 7889-7907. <http://dx.doi.org/10.1002/2014JD021478>
50. Taylor, K.E., R.J. Stouffer, and G.A. Meehl, 2012: An overview of CMIP5 and the experiment design. *Bulletin of the American Meteorological Society*, **93**, 485-498. <http://dx.doi.org/10.1175/BAMS-D-11-00094.1>
51. Kay, J.E., C. Deser, A. Phillips, A. Mai, C. Hannay, G. Strand, J.M. Arblaster, S.C. Bates, G. Danabasoglu, J. Edwards, M. Holland, P. Kushner, J.-F. Lamarque, D. Lawrence, K. Lindsay, A. Middleton, E. Munoz, R. Neale, K. Oleson, L. Polvani, and M. Vertenstein, 2015: The Community Earth System Model (CESM) large ensemble project: A community resource for studying climate change in the presence of internal climate variability. *Bulletin of the American Meteorological Society*, **96** (12), 1333-1349. <http://dx.doi.org/10.1175/BAMS-D-13-00255.1>
52. O'Gorman, P.A., 2014: Contrasting responses of mean and extreme snowfall to climate change. *Nature*, **512**, 416-418. <http://dx.doi.org/10.1038/nature13625>
53. Collins, M., R. Knutti, J. Arblaster, J.-L. Dufresne, T. Fichet, P. Friedlingstein, X. Gao, W.J. Gutowski, T. Johns, G. Krinner, M. Shongwe, C. Tebaldi, A.J. Weaver, and M. Wehner, 2013: Long-term climate change: Projections, commitments and irreversibility. *Climate Change 2013: The Physical Science Basis. Contribution of Working Group I to the Fifth Assessment Report of the Intergovernmental Panel on Climate Change*. Stocker, T.F., D. Qin, G.-K. Plattner, M. Tignor, S.K. Allen, J. Boschung, A. Nauels, Y. Xia, V. Bex, and P.M. Midgley, Eds. Cambridge University Press, Cambridge, United Kingdom and New York, NY, USA, 1029-1136. <http://www.climatechange2013.org/report/full-report/>
54. Georgakakos, A., P. Fleming, M. Dettinger, C. Peters-Lidard, T.C. Richmond, K. Reckhow, K. White, and D. Yates, 2014: Ch. 3: Water resources. *Climate Change Impacts in the United States: The Third National Climate Assessment*. Melillo, J.M., T.C. Richmond, and G.W. Yohe, Eds. U.S. Global Change Research Program, Washington, D.C., 69-112. <http://dx.doi.org/10.7930/JOG44N6T>
55. Lute, A.C., J.T. Abatzoglou, and K.C. Hegewisch, 2015: Projected changes in snowfall extremes and interannual variability of snowfall in the western United States. *Water Resources Research*, **51**, 960-972. <http://dx.doi.org/10.1002/2014WR016267>



56. Ning, L. and R.S. Bradley, 2015: Snow occurrence changes over the central and eastern United States under future warming scenarios. *Scientific Reports*, **5**, 17073. <http://dx.doi.org/10.1038/srep17073>
57. Gergel, D.R., B. Nijssen, J.T. Abatzoglou, D.P. Lettenmaier, and M.R. Stumbaugh, 2017: Effects of climate change on snowpack and fire potential in the western USA. *Climatic Change*, **141**, 287-299. <http://dx.doi.org/10.1007/s10584-017-1899-y>
58. Janssen, E., D.J. Wuebbles, K.E. Kunkel, S.C. Olsen, and A. Goodman, 2014: Observational- and model-based trends and projections of extreme precipitation over the contiguous United States. *Earth's Future*, **2**, 99-113. <http://dx.doi.org/10.1002/2013EF000185>
59. Janssen, E., R.L. Sriver, D.J. Wuebbles, and K.E. Kunkel, 2016: Seasonal and regional variations in extreme precipitation event frequency using CMIP5. *Geophysical Research Letters*, **43**, 5385-5393. <http://dx.doi.org/10.1002/2016GL069151>
60. Kunkel, K.E., T.R. Karl, H. Brooks, J. Kossin, J. Lawrimore, D. Arndt, L. Bosart, D. Changnon, S.L. Cutter, N. Doesken, K. Emanuel, P.Y. Groisman, R.W. Katz, T. Knutson, J. O'Brien, C.J. Paciorek, T.C. Peterson, K. Redmond, D. Robinson, J. Trapp, R. Vose, S. Weaver, M. Wehner, K. Wolter, and D. Wuebbles, 2013: Monitoring and understanding trends in extreme storms: State of knowledge. *Bulletin of the American Meteorological Society*, **94**, 499-514. <http://dx.doi.org/10.1175/BAMS-D-11-00262.1>
61. Kunkel, K.E., T.R. Karl, D.R. Easterling, K. Redmond, J. Young, X. Yin, and P. Hennon, 2013: Probable maximum precipitation and climate change. *Geophysical Research Letters*, **40**, 1402-1408. <http://dx.doi.org/10.1002/grl.50334>
62. Dettinger, M., 2011: Climate change, atmospheric rivers, and floods in California—a multimodel analysis of storm frequency and magnitude changes. *Journal of the American Water Resources Association*, **47**, 514-523. <http://dx.doi.org/10.1111/j.1752-1688.2011.00546.x>
63. Shields, C.A. and J.T. Kiehl, 2016: Atmospheric river landfall-latitude changes in future climate simulations. *Geophysical Research Letters*, **43**, 8775-8782. <http://dx.doi.org/10.1002/2016GL070470>
64. Kooperman, G.J., M.S. Pritchard, and R.C.J. Somerville, 2013: Robustness and sensitivities of central U.S. summer convection in the super-parameterized CAM: Multi-model intercomparison with a new regional EOF index. *Geophysical Research Letters*, **40**, 3287-3291. <http://dx.doi.org/10.1002/grl.50597>
65. Cook, K.H., E.K. Vizy, Z.S. Launer, and C.M. Patricola, 2008: Springtime intensification of the Great Plains low-level jet and midwest precipitation in GCM simulations of the twenty-first century. *Journal of Climate*, **21**, 6321-6340. <http://dx.doi.org/10.1175/2008jcli2355.1>
66. Higgins, R.W., Y. Yao, E.S. Yarosh, J.E. Janowiak, and K.C. Mo, 1997: Influence of the Great Plains low-level jet on summertime precipitation and moisture transport over the central United States. *Journal of Climate*, **10**, 481-507. [http://dx.doi.org/10.1175/1520-0442\(1997\)010<0481:iotgpl>2.0.co;2](http://dx.doi.org/10.1175/1520-0442(1997)010<0481:iotgpl>2.0.co;2)
67. Pan, Z., R.W. Arritt, E.S. Takle, W.J. Gutowski, Jr., C.J. Anderson, and M. Segal, 2004: Altered hydrologic feedback in a warming climate introduces a “warming hole”. *Geophysical Research Letters*, **31**, L17109. <http://dx.doi.org/10.1029/2004GL020528>
68. Prein, A.F., R.M. Rasmussen, K. Ikeda, C. Liu, M.P. Clark, and G.J. Holland, 2017: The future intensification of hourly precipitation extremes. *Nature Climate Change*, **7**, 48-52. <http://dx.doi.org/10.1038/nclimate3168>
69. Knutson, T.R., J.L. McBride, J. Chan, K. Emanuel, G. Holland, C. Landsea, I. Held, J.P. Kossin, A.K. Srivastava, and M. Sugi, 2010: Tropical cyclones and climate change. *Nature Geoscience*, **3**, 157-163. <http://dx.doi.org/10.1038/ngeo779>
70. Knutson, T.R., J.J. Sirutis, G.A. Vecchi, S. Garner, M. Zhao, H.-S. Kim, M. Bender, R.E. Tuleya, I.M. Held, and G. Villarini, 2013: Dynamical downscaling projections of twenty-first-century Atlantic hurricane activity: CMIP3 and CMIP5 model-based scenarios. *Journal of Climate*, **27**, 6591-6617. <http://dx.doi.org/10.1175/jcli-d-12-00539.1>
71. Wang, C.-C., B.-X. Lin, C.-T. Chen, and S.-H. Lo, 2015: Quantifying the effects of long-term climate change on tropical cyclone rainfall using a cloud-resolving model: Examples of two landfall typhoons in Taiwan. *Journal of Climate*, **28**, 66-85. <http://dx.doi.org/10.1175/JCLI-D-14-00044.1>
72. Villarini, G., D.A. Lavers, E. Scoccimarro, M. Zhao, M.F. Wehner, G.A. Vecchi, T.R. Knutson, and K.A. Reed, 2014: Sensitivity of tropical cyclone rainfall to idealized global-scale forcings. *Journal of Climate*, **27**, 4622-4641. <http://dx.doi.org/10.1175/JCLI-D-13-00780.1>
73. Melillo, J.M., T.C. Richmond, and G.W. Yohe, eds., 2014: *Climate Change Impacts in the United States: The Third National Climate Assessment*. U.S. Global Change Research Program: Washington, D.C., 841 pp. <http://dx.doi.org/10.7930/J0Z31WJ2>
74. Vose, R.S., S. Applequist, M. Squires, I. Durre, M.J. Menne, C.N. Williams, Jr., C. Fenimore, K. Gleason, and D. Arndt, 2014: Improved historical temperature and precipitation time series for U.S. climate divisions. *Journal of Applied Meteorology and Climatology*, **53**, 1232-1251. <http://dx.doi.org/10.1175/JAMC-D-13-0248.1>



75. Sun, L., K.E. Kunkel, L.E. Stevens, A. Buddenberg, J.G. Dobson, and D.R. Easterling, 2015: Regional Surface Climate Conditions in CMIP3 and CMIP5 for the United States: Differences, Similarities, and Implications for the U.S. National Climate Assessment. NOAA Technical Report NESDIS 144. National Oceanic and Atmospheric Administration, National Environmental Satellite, Data, and Information Service, 111 pp. <http://dx.doi.org/10.7289/V5RB72KG>
76. Angéilil, O., D. Stone, M. Wehner, C.J. Paciorek, H. Krishnan, and W. Collins, 2017: An independent assessment of anthropogenic attribution statements for recent extreme temperature and rainfall events. *Journal of Climate*, **30**, 5-16. <http://dx.doi.org/10.1175/JCLI-D-16-0077.1>
77. Edwards, L.M., M. Bunkers, J.T. Abatzoglou, D.P. Todey, and L.E. Parker, 2014: October 2013 blizzard in western South Dakota [in "Explaining Extreme Events of 2013 from a Climate Perspective"]. *Bulletin of the American Meteorological Society*, **95 (9)**, S23-S26. <http://dx.doi.org/10.1175/1520-0477-95.9.S1.1>
78. Peterson, T.C., R.R. Heim, R. Hirsch, D.P. Kaiser, H. Brooks, N.S. Diffenbaugh, R.M. Dole, J.P. Giovannetone, K. Guirguis, T.R. Karl, R.W. Katz, K. Kunkel, D. Lettenmaier, G.J. McCabe, C.J. Paciorek, K.R. Ryberg, S. Schubert, V.B.S. Silva, B.C. Stewart, A.V. Vecchia, G. Villarini, R.S. Vose, J. Walsh, M. Wehner, D. Wollock, K. Wolter, C.A. Woodhouse, and D. Wuebbles, 2013: Monitoring and understanding changes in heat waves, cold waves, floods and droughts in the United States: State of knowledge. *Bulletin of the American Meteorological Society*, **94**, 821-834. <http://dx.doi.org/10.1175/BAMS-D-12-00066.1>





8

Droughts, Floods, and Wildfires

KEY FINDINGS

1. Recent droughts and associated heat waves have reached record intensity in some regions of the United States; however, by geographical scale and duration, the Dust Bowl era of the 1930s remains the benchmark drought and extreme heat event in the historical record (*very high confidence*). While by some measures drought has decreased over much of the continental United States in association with long-term increases in precipitation, neither the precipitation increases nor inferred drought decreases have been confidently attributed to anthropogenic forcing.
2. The human effect on recent major U.S. droughts is complicated. Little evidence is found for a human influence on observed precipitation deficits, but much evidence is found for a human influence on surface soil moisture deficits due to increased evapotranspiration caused by higher temperatures. (*High confidence*)
3. Future decreases in surface (top 10 cm) soil moisture from anthropogenic forcing over most of the United States are *likely* as the climate warms under higher scenarios. (*Medium confidence*)
4. Substantial reductions in western U.S. winter and spring snowpack are projected as the climate warms. Earlier spring melt and reduced snow water equivalent have been formally attributed to human-induced warming (*high confidence*) and will *very likely* be exacerbated as the climate continues to warm (*very high confidence*). Under higher scenarios, and assuming no change to current water resources management, chronic, long-duration hydrological drought is increasingly possible by the end of this century (*very high confidence*).
5. Detectable changes in some classes of flood frequency have occurred in parts of the United States and are a mix of increases and decreases. Extreme precipitation, one of the controlling factors in flood statistics, is observed to have generally increased and is projected to continue to do so across the United States in a warming atmosphere. However, formal attribution approaches have not established a significant connection of increased riverine flooding to human-induced climate change, and the timing of any emergence of a future detectable anthropogenic change in flooding is unclear. (*Medium confidence*)
6. The incidence of large forest fires in the western United States and Alaska has increased since the early 1980s (*high confidence*) and is projected to further increase in those regions as the climate warms, with profound changes to certain ecosystems (*medium confidence*).

Recommended Citation for Chapter

Wehner, M.F., J.R. Arnold, T. Knutson, K.E. Kunkel, and A.N. LeGrande, 2017: Droughts, floods, and wildfires. In: *Climate Science Special Report: Fourth National Climate Assessment, Volume I* [Wuebbles, D.J., D.W. Fahey, K.A. Hibbard, D.J. Dokken, B.C. Stewart, and T.K. Maycock (eds.)]. U.S. Global Change Research Program, Washington, DC, USA, pp. 231-256 doi: 10.7930/J0CJ8BNN.

8.1 Drought

The word “drought” brings to mind abnormally dry conditions. However, the meaning of “dry” can be ambiguous and lead to confusion in how drought is actually defined. Three different classes of droughts are defined by NOAA and describe a useful hierarchical set of water deficit characterization, each with different impacts. “Meteorological drought” describes conditions of precipitation deficit. “Agricultural drought” describes conditions of soil moisture deficit. “Hydrological drought” describes conditions of deficit in runoff.¹ Clearly these three characterizations of drought are related but are also different descriptions of water shortages with different target audiences and different time scales. In particular, agricultural drought is of concern to producers of food while hydrological drought is of concern to water system managers. Soil moisture is a function of both precipitation and evapotranspiration. Because potential evapotranspiration increases with temperature, anthropogenic climate change generally results in drier soils and often less runoff in the long term. In fact, under the higher scenario (RCP8.5; see Ch. 4: Projections for a description of the RCP scenarios) at the end of the 21st century, no region of the planet is projected to experience significantly higher levels of annual average surface soil moisture due to the sensitivity of evapotranspiration to temperature, even though much higher precipitation is projected in some regions.² Seasonal and annual total runoff, on the other hand, are projected to either increase or decrease, depending on location and season under the same conditions,² illustrating the complex relationships between the various components of the hydrological system. Meteorological drought can occur on a range of time scales, in addition to seasonal or annual time scales. “Flash droughts” can result from just a few weeks of dry weather,³ and the paleoclimate record contains droughts of several

decades. Hence, it is vital to describe precisely the definition of drought in any public discussion to avoid confusion due to this complexity. As the climate changes, conditions currently considered “abnormally” dry may become relatively “normal” in those regions undergoing aridification, or extremely unlikely in those regions becoming wetter. Hence, the reference conditions defining drought may need to be modified from those currently in practice.

8.1.1 Historical Context

The United States has experienced all three types of droughts in the past, always driven, at least in some part, by natural variations in seasonal and/or annual precipitation amounts. As the climate changes, we can expect that human activities will alter the effect of these natural variations. The “Dust Bowl” drought of the 1930s is still the most significant meteorological and agricultural drought experienced in the United States in terms of its geographic and temporal extent. However, even though it happened prior to most of the current global warming, human activities exacerbated the dryness of the soil by the farming practices of the time.⁴ Tree ring archives reveal that such droughts (in the agricultural sense) have occurred occasionally over the last 1,000 years.⁵ Climate model simulations suggest that droughts lasting several years to decades occur naturally in the southwestern United States.⁶ The Intergovernmental Panel on Climate Change Fifth Assessment Report (IPCC AR5)⁷ concluded “there is low confidence in detection and attribution of changes in (meteorological) drought over global land areas since the mid-20th century, owing to observational uncertainties and difficulties in distinguishing decadal-scale variability in drought from long-term trends.” As they noted, this was a weaker attribution statement than in the Fourth Assessment Report,⁸ which had concluded “that an increased risk of drought was *more likely than not* due to

